frontiers | Research Topics

Tumor microenvironment and metabolic reprogramming in cancer

Edited by
Wei Chong, Hao Chen, Houjuan Zhu, Asif Raza and Yiju Wei

Published in
Frontiers in Immunology
Frontiers in Oncology

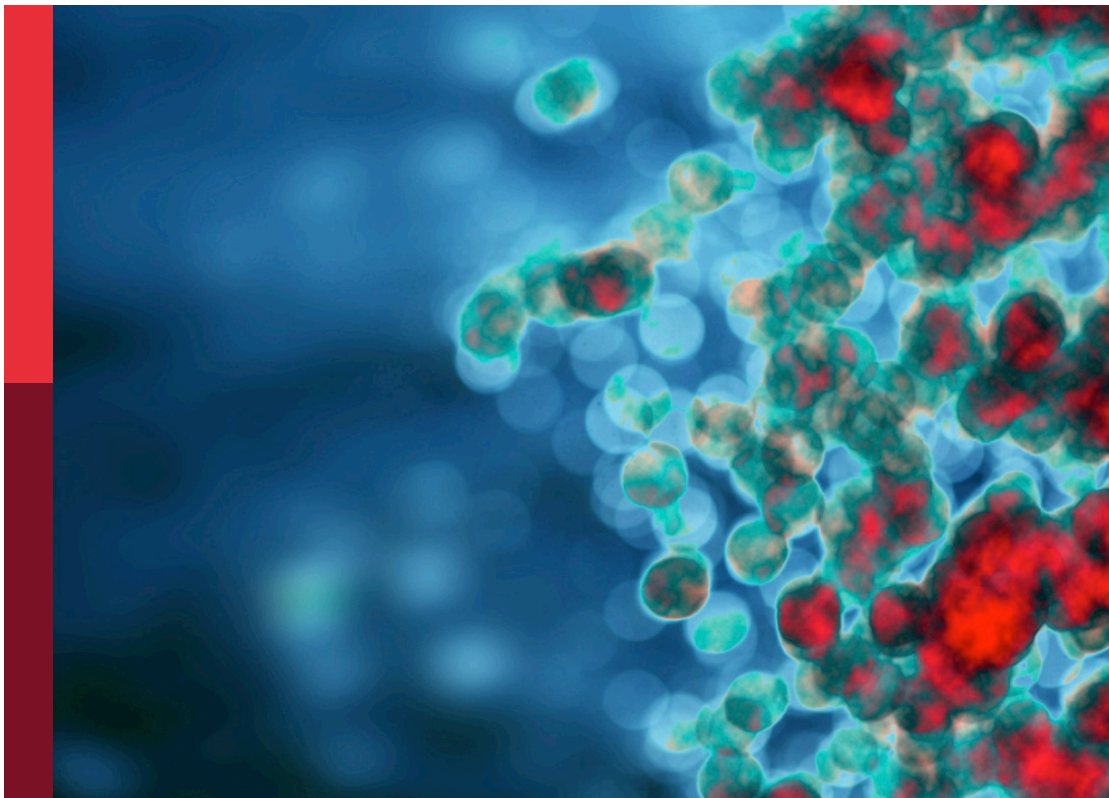

ISSN 1664-8714
ISBN 978-2-8325-5578-1
DOI 10.3389/978-2-8325-5578-1

About Frontiers

Frontiers is more than just an open access publisher of scholarly articles: it is a pioneering approach to the world of academia, radically improving the way scholarly research is managed. The grand vision of Frontiers is a world where all people have an equal opportunity to seek, share and generate knowledge. Frontiers provides immediate and permanent online open access to all its publications, but this alone is not enough to realize our grand goals.

Frontiers journal series

The Frontiers journal series is a multi-tier and interdisciplinary set of open-access, online journals, promising a paradigm shift from the current review, selection and dissemination processes in academic publishing. All Frontiers journals are driven by researchers for researchers; therefore, they constitute a service to the scholarly community. At the same time, the *Frontiers journal series* operates on a revolutionary invention, the tiered publishing system, initially addressing specific communities of scholars, and gradually climbing up to broader public understanding, thus serving the interests of the lay society, too.

Dedication to quality

Each Frontiers article is a landmark of the highest quality, thanks to genuinely collaborative interactions between authors and review editors, who include some of the world's best academicians. Research must be certified by peers before entering a stream of knowledge that may eventually reach the public - and shape society; therefore, Frontiers only applies the most rigorous and unbiased reviews. Frontiers revolutionizes research publishing by freely delivering the most outstanding research, evaluated with no bias from both the academic and social point of view. By applying the most advanced information technologies, Frontiers is catapulting scholarly publishing into a new generation.

What are Frontiers Research Topics?

Frontiers Research Topics are very popular trademarks of the *Frontiers journals series*: they are collections of at least ten articles, all centered on a particular subject. With their unique mix of varied contributions from Original Research to Review Articles, Frontiers Research Topics unify the most influential researchers, the latest key findings and historical advances in a hot research area.

Find out more on how to host your own Frontiers Research Topic or contribute to one as an author by contacting the Frontiers editorial office: frontiersin.org/about/contact

Tumor microenvironment and metabolic reprogramming in cancer

Topic editors

Wei Chong — Shandong Provincial Hospital, China
Hao Chen — Shandong University, China
Houjuan Zhu — Institute of Materials Research and Engineering (A*STAR), Singapore
Asif Raza — Penn State Milton S. Hershey Medical Center, United States
Yiju Wei — Shandong First Medical University, China

Citation

Chong, W., Chen, H., Zhu, H., Raza, A., Wei, Y., eds. (2024). *Tumor microenvironment and metabolic reprogramming in cancer*. Lausanne: Frontiers Media SA.
doi: 10.3389/978-2-8325-5578-1

Table of contents

frontiers | Frontiers in Immunology

TYPE Editorial
PUBLISHED 08 October 2024
DOI 10.3389/fimmu.2024.1497966

OPEN ACCESS

EDITED AND REVIEWED BY
Peter Brossart,
University of Bonn, Germany

*CORRESPONDENCE
Wei Chong
chongwei.good@163.com
Hao Chen
chenhao6938@163.com
Xingyu Zhu
zhuxingyu1996@126.com

†These authors have contributed equally to this work

RECEIVED 18 September 2024
ACCEPTED 20 September 2024
PUBLISHED 08 October 2024

CITATION
Cui X, Liu X, Feng R, Wang X, Wei Y, Zhu H, Raza A, Zhu X, Chen H and Chong W (2024) Editorial: Tumor microenvironment and metabolic reprogramming in cancer. *Front. Immunol.* 15:1497966. doi: 10.3389/fimmu.2024.1497966

Editorial: Tumor microenvironment and metabolic reprogramming in cancer

Xiaoling Cui[1,2,3†], Xinyu Liu[1,2,3†], Rongjie Feng[4†], Xiaohan Wang[1,2,3], Yiju Wei[3,5], Houjuan Zhu[6], Asif Raza[7], Xingyu Zhu[1,2,3*], Hao Chen[8*] and Wei Chong[1,2,3*]

[1]Department of Gastrointestinal Surgery, Shandong Provincial Hospital Affiliated to Shandong First Medical University, Jinan, China, [2]Shandong Provincial Laboratory of Translational Medicine Engineering for Digestive Tumors, Shandong Provincial Hospital, Jinan, China, [3]Medical Science and Technology Innovation Center, Shandong First Medical University & Shandong Academy of Medical Sciences, Jinan, China, [4]Department of Orthopedics, Shandong Provincial Hospital Affiliated to Shandong First Medical University, Jinan, Shandong, China, [5]School of Life Science, Shandong First Medical University & Shandong Academy of Medical Sciences, Jinan, Shandong, China, [6]Institute of Materials Research and Engineering (IMRE), Agency for Science, Technology and Research (ASTAR), Singapore, Singapore, [7]Department of Pharmacology, Penn State Cancer Institute, The Pennsylvania State University College of Medicine, Hershey, PA, United States, [8]Clinical Research Center of Shandong University, Clinical Epidemiology Unit, Qilu Hospital of Shandong University, Jinan, China

KEYWORDS

cancer, metabolic reprogramming, TME (tumor microenvironment), tumor, multi omics

Editorial on the Research Topic
Tumor microenvironment and metabolic reprogramming in cancer

The tumor microenvironment (TME) is a complex and dynamic entity that plays a crucial role in cancer progression, treatment resistance, and metastasis (1). One of the most significant aspects of the TME is the metabolic reprogramming that occurs in both cancer cells and the surrounding stromal and immune cells (2). The following editorial synthesizes insights from eleven recent studies that highlight the intricate relationship between the TME, metabolic pathways, and cancer development, offering new avenues for therapeutic intervention.

A recent review by Long et al. explores how tumor metabolism affects immune cells in the TME. Metabolic byproducts like lactate and reactive oxygen species can impair the function of immune cells, creating an immunosuppressive environment that shields the tumor from immune attack. Understanding these interactions is key to developing strategies to restore immune function and enhance immunotherapy efficacy. In addition, the role of specific metabolic pathways in cancer progression is researched by Zhou et al. The identification of key genes related to tryptophan metabolism, such as NAMPT, IDO1, and ACAT1, as significant biomarkers in BLCA, points to the potential of these pathways as targets for therapy. Similarly, Li et al. find that using machine learning to identify genes related to glutamine metabolism in breast cancer patients provides a new approach for prognostic modeling, which has the potential to guide more effective and less toxic personalized treatment strategies.

A recent review by Li et al. emphasizes the importance of glycolysis, often upregulated in cancer cells to meet energy demands. Key enzymes like hexokinase, phosphofructokinase, and pyruvate kinase are highlighted for their role in cancer progression, along with related signaling pathways and transcription factors as potential therapeutic targets. The review suggests targeting glycolysis could provide new therapeutic strategies for improving ovarian cancer treatment and prognosis.

The TME is also influenced by hormonal and inflammatory factors, which can significantly impact cancer progression (3). A recent review by Wenxuan et al. discusses how steroid hormones like androgens, estrogens, and progestins influence colorectal cancer growth and therapy response, suggesting targets for hormone-based treatments. Additionally, Habanjar et al. highlights that the pro-inflammatory environment in obese patients can impair the protective role of myoepithelial cells, promoting cancer progression, and underscores the importance of considering obesity in breast cancer treatment and prognosis.

Peng et al. identify circ_BBS9 as a potential biomarker and therapeutic target in lung adenocarcinoma (LUAD), noting its downregulation in LUAD tissues and association with poor prognosis. Circ_BBS9 interacts with IFIT3, influencing immune infiltration in the tumor microenvironment. Similarly, Fan et al. find that increased CD8+ T cell infiltration is linked to poorer prognosis in prostate cancer, suggesting that targeting MLXIPL, related to these T cells, could improve outcomes, particularly in immunotherapy.

The influence of the TME on cancer progression is further explored in the context of different cancer types. For instance, Kim et al. studies the aryl hydrocarbon receptor (AhR) in various solid tumors and reveales its differential expression in cancer cells and immune cells within the TME. These findings suggest that AhR could serve as a therapeutic target, particularly in cancers where its expression is associated with poor prognosis.

Moreover, the emerging role of extracellular vesicles (EVs) in the metastatic process, particularly in brain metastases (4), underscores the complexity of the TME. The recent research by Li et al. highlights the potential of EVs as biomarkers for early detection and as targets for therapeutic intervention, particularly in enhancing the delivery and efficacy of drugs targeting brain metastases.

As research advances, natural agents like epigallocatechin gallate (EGCG) show promise for more effective and less toxic cancer therapies. Li et al.'s review highlights how EGCG impacts the tumor microenvironment, metabolism, and immunotherapy efficacy, enhancing immune responses and suppressing immunosuppressive cells, making it a potential boost for cancer immunotherapy and treatment outcomes.

In conclusion, the studies discussed in this editorial provide a comprehensive overview of the dynamic interplay between tumor metabolism and the microenvironment, highlighting the potential of targeting these interactions to improve cancer treatment. As our understanding of these processes deepens, it opens the door to more effective, personalized therapies that not only target the cancer cells but also modulate the TME to enhance immune responses and overcome therapeutic resistance. The future of cancer therapy lies in the integration of metabolic and immunological insights, paving the way for innovative approaches that could transform patient outcomes.

Author contributions

XC: Writing – original draft. XL: Writing – original draft. RF: Writing – original draft. XW: Writing – original draft. YW: Writing – review & editing. HZ: Writing – review & editing. AR: Writing – review & editing. XZ: Writing – review & editing. HC: Writing – review & editing. WC: Writing – review & editing.

Funding

The author(s) declare financial support was received for the research, authorship, and/or publication of this article. This work was supported by National Natural Science Foundation of China (82102702, 82103322, and 82473112), Natural Science Foundation of Shandong Province of China (ZR2021QH141), Special Foundation for Taishan Scholars Program of Shandong Province (no. tsqn202306373).

Conflict of interest

The authors declare that the research was conducted in the absence of any commercial or financial relationships that could be construed as a potential conflict of interest.

Publisher's note

References

1. Tong X, Tang R, Xiao M, Xu J, Wang W, Zhang B, et al. Targeting cell death pathways for cancer therapy: recent developments in necroptosis, pyroptosis, ferroptosis, and cuproptosis research. *J Hematol Oncol.* (2022) 15:174. doi: 10.1186/s13045-022-01392-3

2. Yang K, Wang X, Song C, He Z, Wang R, Xu Y, et al. The role of lipid metabolic reprogramming in tumor microenvironment. *Theranostics.* (2023) 13:1774–808. doi: 10.7150/thno.82920

3. Wang H, Li N, Liu Q, Guo J, Pan Q, Cheng B, et al. Antiandrogen treatment induces stromal cell reprogramming to promote castration resistance in prostate cancer. *Cancer Cell*. (2023) 41:1345–1362.e9. doi: 10.1016/j.ccell.2023.05.016

4. Yang E, Wang X, Gong Z, Yu M, Wu H, Zhang D, et al. Exosome-mediated metabolic reprogramming: the emerging role in tumor microenvironment remodeling and its influence on cancer progression. *Signal Transduct Target Ther*. (2020) 5:242. doi: 10.1038/s41392-020-00359-5

frontiers | Frontiers in Immunology

TYPE Original Research
PUBLISHED 26 October 2023
DOI 10.3389/fimmu.2023.1283792

OPEN ACCESS

EDITED BY
Wei Chong,
Shandong Provincial Hospital, China

REVIEWED BY
Liang Zhao,
Johns Hopkins Medicine, United States
Fan Chao,
Fudan University, China
Ning Zhang,
Kyoto University, Japan

*CORRESPONDENCE
Linlin Xue
13127136560@163.com

RECEIVED 27 August 2023
ACCEPTED 12 October 2023
PUBLISHED 26 October 2023

CITATION
Zhou G, Qin G, Zhang Z, Zhao H and Xue L (2023) Identification of tryptophan metabolism- and immune-related genes signature and prediction of immune infiltration landscape in bladder urothelial carcinoma. *Front. Immunol.* 14:1283792. doi: 10.3389/fimmu.2023.1283792

Identification of tryptophan metabolism- and immune-related genes signature and prediction of immune infiltration landscape in bladder urothelial carcinoma

Guanwen Zhou[1], Guoliang Qin[1], Zhaocun Zhang[1], Haifeng Zhao[1] and Linlin Xue[2*]

[1]Department of Urology, Qilu Hospital of Shandong University, Jinan, China, [2]Department of Clinical Laboratory, Shandong Cancer Hospital and Institute, Shandong First Medical University and Shandong Academy of Medical Sciences, Jinan, China

Introduction: Tryptophan metabolism is indirectly involved in immune tolerance and promotes response to anticancer drugs. However, the mechanisms underlying tryptophan metabolism and immune landscape in bladder urothelial carcinoma (BLCA) are not fully understood.

Methods: A BLCA dataset containing 406 tumor samples with clinical survival information and 19 normal samples were obtained from the Cancer Genome Atlas database. The validation set, GSE32894, contained 223 BLCA tumor samples with survival information, and the single-cell dataset, GSE135337, included seven BLCA tumor samples; both were obtained from the gene expression omnibus database. Univariate and multivariate Cox regression analyses were conducted to evaluate clinical parameters and risk scores. Immune infiltration and checkpoint analyses were performed to explore the immune landscape of BLCA. Single-cell analysis was conducted to further identify the roles of model genes in BLCA. Finally, NAMPT expression in BLCA and adjacent tissues was detected using RT-qPCR, CCK-8 and Transwell assays were conducted to determine the role of NAMPT in BLCA cells.

Results: Six crossover genes (TDO2, ACAT1, IDO1, KMO, KYNU, and NAMPT) were identified by overlap analysis of tryptophan metabolism-related genes, immune-related genes, and differentially expressed genes (DEGs). Three biomarkers, NAMPT, IDO1, and ACAT1, were identified using Cox regression analysis. Accordingly, a tryptophan metabolism- and immune-related gene risk model was constructed, and the patients were divided into high- and low-risk groups. There were significant differences in the clinical parameters, prognosis, immune infiltration, and immunotherapy response between the risk groups. RT-

qPCR revealed that NAMPT was upregulated in BLCA samples. Knocking down NAMPT significantly inhibited BLCA cell proliferation, migration, and invasion.

Discussion: In our study, we constructed a tryptophan metabolism- and immune-related gene risk model based on three biomarkers, namely NAMPT, IDO1, and ACAT1, that were significantly associated with the progression and immune landscape of BLCA. The risk model could effectively predict patient prognosis and immunotherapy response and can guide individualized immunotherapy.

KEYWORDS

Bladder urothelial carcinoma, immune, tryptophan metabolism, prognosis, biomarkers

1 Introduction

Bladder urothelial carcinoma (BLCA) is the most prevalent malignancy of the urinary system, with an estimated 573,000 new cases and 213,000 deaths in 2020, making it the tenth most common malignancy worldwide (1). Despite early diagnosis and advanced treatment, BLCA remains the main cause of tumor-related deaths due to its high recurrence and invasiveness (1, 2). Therefore, further research on the complex pathogenesis of BLCA is urgently required.

As an essential amino acid in the human body, tryptophan participates in the regulation of inflammatory responses, oxidative stress, and immune activation through kynurenine metabolism, and plays an important role in the tumor microenvironment and tumor metabolism (3–5). Aberrant regulation of tryptophan metabolism is closely associated with the occurrence and progression of various tumors, including BLCA (6–9). Abnormal regulation of the immune microenvironment also occurs in BLCA (10, 11). An abnormal immune microenvironment can induce the immune escape of BLCA cells by inhibiting the activity of T cells and natural killer cells (10). In recent years, the rapid development of tumor immunotherapy has provided a new method for the treatment of BLCA. Tumor immunotherapy can regulate immune system function and reactivate the ability of the immune system to kill cancer cells, thereby suppressing tumor cell proliferation and invasion. Immune checkpoint inhibitors (ICIs) are new methods for tumor treatment in addition to surgery, chemotherapy, and radiotherapy, and have been approved for the treatment of melanoma, lung cancer, colorectal cancer, and BLCA (12, 13). Abnormal tryptophan metabolism leads to apoptosis and dysfunction of immune cells and induce the formation of an immunosuppressive microenvironment, thereby weakening the therapeutic effect of ICIs (6). Therefore, it is important to elucidate the role of tryptophan metabolism in the progression and the immune landscape of BLCA.

Our study aimed to explore the mechanisms of tryptophan metabolism and immune-related genes in BLCA and construct a risk model. We found that three biomarkers, NAMPT, IDO1, and ACAT1, were significantly associated with the progression and the immune landscape of BLCA. Accordingly, we constructed a tryptophan metabolism- and immune-related gene risk model and divided the patients into high- and low-risk groups. The risk model could effectively predict patient prognosis and immunotherapy response and guide individualized immunotherapy.

2 Materials and methods

2.1 Data sources

A BLCA dataset was obtained from the Cancer Genome Atlas (TCGA) database, namely the TCGA-BLCA dataset (training set), containing 406 BLCA (tumor) samples with clinical survival information and 19 normal samples. The validation set, GSE32894, containing 223 BLCA samples with survival information, and the single-cell dataset GSE135337, including seven BLCA tumor samples, were obtained from the GEO online database. Furthermore, 61-tryptophan metabolism-related genes were obtained after removing repetitive data using the MsigDB online database (https://www.gsea-msigdb.org/gsea/msigdb/index.jsp). A total of 2991 immune-related genes were retrieved after removing the repetition data based on the ImmPort (http://www.immport.org/), TISIDB (http://cis.hku.hk/TISIDB), and InnateDB (http://www.innatedb.com) databases.

2.2 Screening and enrichment analysis of crossover genes

Differentially expressed genes (DEGs) between the BLCA and normal groups in the TCGA-BLCA dataset were acquired using the DESeq2 (v. 1.34.0) (14) package ($|Log2FC| > 1$ and P. adj< 0.05). Heat and volcano maps of these DEGs were plotted using the pheatmap (v 1.0.12) and ggplot2 (v 3.3.5) (15) packages, respectively. Furthermore, 61 tryptophan metabolism-related genes, 2991 immune-related genes, and DEGs were subject to overlapping analysis to achieve gene crossover. To study the related signaling pathways and biological functions of these crossover genes, KEGG and GO enrichment analyses (P. adj< 0.05) were conducted using the ClusterProfiler (v. 4.6.0) package (16).

2.3 The construction, evaluation, and verification of the risk model

Univariate Cox analysis was performed on the above crossover genes to identify the candidate genes related to prognosis (HR ≠ 1, P< 0.2) (17, 18). Subsequently, the LASSO algorithm was implemented for the candidate genes to identify biomarkers (model genes). Based on the expression of the above biomarkers, a risk model was created and the samples in the training set, TCGA-BLCA, and validation set, GSE32894, were classified into high- and low-risk groups, respectively, using the optimum cut-off value of the risk score.

$$Riskscore_{sample} = \sum_{n=1}^{n} (Coef_i \star x_i)$$

Kaplan-Meier (K-M) survival curves and receiver operating characteristic (ROC) curves (1-, 3-, and 5-year) were plotted. Differences in risk scores between the different clinical indicator subgroups (invasion, sex, T stage, M stage, N stage, Age, Grade, and Stage) were analyzed using the Wilcoxon test (P< 0.05).

2.4 Independent prognostic analysis

The prognostic value of clinical survival prediction was evaluated by combining risk scores with other clinical features. Clinical features (invasion, age, etc.) and risk scores were included in univariate Cox analysis. Multivariate Cox analysis was implemented for clinical features acquired by univariate Cox analysis to determine independent prognostic factors (P< 0.05). Furthermore, a nomogram was created to predict the survival rates of patients with BLCA (1-, 3-, and 5-year survival rates). Calibration curves and decision curve analysis (DCA) were used to verify the nomogram's validity.

2.5 Immune microenvironment analysis

The CIBERSORT algorithm was used to determine the proportions of immune cell infiltrates in each sample. Differential immune cells between the two subgroups were compared (P< 0.05). The relationships between the differentially expressed immune cells were analyzed using Spearman's method. The relationships between biomarkers and differential immune cells were computed using the Spearman method. Moreover, the expression differences of 48 immune checkpoints (IDO1, CD27, PDCD1, etc.) between the two risk subgroups were compared. Associations between differential immune checkpoints and biomarkers were computed using Spearman's method. The Tumor Immune Dysfunction and Exclusion (TIDE) algorithm was used from the TIDE online database (http://tide.dfci.harvard.edu/) to detect dysfunction and exclusion scores. Immunophenoscore (IPS) was calculated based on the gene expression of representative cell types using the TCIA database (https://tcia.at/). Moreover, the differences in the TIDE and IPS scores between the two subgroups were compared.

2.6 Mutation analysis

In this study, we used the maftools (v 2.10.5) package (19) to analyze the tumor mutation burden (TMB) in the two risk subgroups. In TCGA-BLCA dataset, mutations in IDO1, IDO2, and TDO2 between the two risk subgroups were analyzed. Furthermore, the BLCA samples in TCGA-BLCA dataset were divided into four groups: high TMB-high-risk, low TMB-high-risk, high TMB-low-risk, and low TMB-low-risk. K-M survival curves for the four subgroups were plotted.

2.7 Single-cell analysis

In this study, we used the Seurat (v 4.1.0) package for the quality control of the GSE135337 dataset. First, cells with less than 200 genes, genes included in less than three cells, and cells with expressed genes fewer than 100 or more than 5000 were excluded, the proportion of mitochondria genes was limited to less than 5%. The 'Normalize Data' and 'Find Variable Features' functions were used to standardize the data. Principal components analysis (PCA) was conducted using the 'JackStrawPlot' function. The cells were clustered using uniform manifold approximation and projection (UMAP) (resolution = 0.4). The cell groups were annotated using marker genes (PDPN, TAGLN, PECAM1, EPCAM, CD3E, DCN, KRT8, CD2, KRT18, CD14, CSF1R, AIF1, VWF, CD3D, and CLDN5) (20). Subsequently, the expression levels of the three biomarkers in different cell groups were analyzed and visualized.

2.8 Patient samples

BLCA and paracancerous tissues were obtained from patients with BLCA at the Qilu Hospital of Shandong University between 2021 and 2022. All participants were informed of the study before surgery and provided consent. This study was approved by the Institutional Review Board of the Qilu Hospital of Shandong University (No.2020046).

2.9 Cell culture

BLCA cell lines, T24 and 5637, were purchased from the Type Culture Collection of the Chinese Academy of Sciences (Shanghai, China). All cell lines were tested for mycoplasma and resulted negative. T24 and 5637 were cultured in 1640 medium (Gibco, USA) supplemented with 10% fetal bovine serum (FBS, Gibco, USA). All cell lines were cultured in a 5% CO2 incubator at 37°C.

2.10 siRNA transfection

Cells were plated in six-well dishes and transfected with siRNA-NAMPT or negative control using Lipofectamine 3000 (Invitrogen, USA). All siRNA sequences are listed in Supplementary Table 1.

2.11 RNA isolation and quantitative reverse transcription polymerase chain reaction (RT-qPCR)

Total RNA was extracted from tissues and cell lines using the TRIzol reagent (Invitrogen, USA). cDNA was synthesized from the

total RNA using Evo M-MLV RT Premix (Accurate Biology, China). RT-qPCR was performed using a Premix Pro Taq HS qPCR Kit (Accurate Biology, China) on a LightCycler 96 instrument (Roche, Basel, Switzerland). β-actin was used as an internal control. All assays were replicated three times, and the data were analyzed using the 2−ΔΔCT method. All PCR primers were purchased from Accurate Biology (Shanghai, China), and sequences are listed in Supplementary Table 2.

2.12 Cell Counting kit-8 (CCK-8) and transwell assays

Cells were seeded in 96 well plates at a density of approximately 2000 cells per well. Cell Counting kit-8 (CCK-8) (Bioss, China) was used to detect cell proliferation at 0, 24, 48, 72, and 96 h after culture. Absorbance was measured at 450 nm using a spectrophotometer (Tecan, Switzerland).

For Transwell assay, cells were seeded into an 8.0 Corning™ 24-well Transwell assay plate (Corning, USA) at a density of approximately 20,000 cells per well. After 24 h in an incubator with 5% CO2 at 37°C, the cells below the membrane were fixed with methanol and stained with crystal violet. The cell numbers in three random fields were counted.

3 Results

3.1 A total of six crossover genes were acquired by crossing tryptophan metabolism-related genes, immune-related genes, and DEGs

There were 8867 DEGs between BLCA and normal samples (Figure 1A; Supplementary Table 3). The expression heatmap of the top 10 upregulated and downregulated DEGs is shown in Figure 1B. Through an intersection analysis, using the Venn diagram, six genes (TDO2, ACAT1, IDO1, KMO, KYNU, and NAMPT) were identified (Figure 1C). The enrichment analysis results showed that the crossover genes were mainly associated with 'alpha-amino acid catabolic process', 'dioxygenase activity' GO terms, and 'Tryptophan metabolism', 'Biosynthesis of cofactors' KEGG pathways (Figures 1D, E; Supplementary Tables 4, 5).

3.2 NAMPT, IDO1, and ACAT1 are tryptophan metabolism- and immune-related biomarkers for BLCA

Three candidate prognostic genes, NAMPT, IDO1, and ACAT1, were identified by univariate Cox regression analysis (Figure 2A). Three biomarkers (NAMPT, IDO1, and ACAT1) were identified using the LASSO algorithm (lambda = 0.001919658) (Figure 2B). In the TCGA-BLCA dataset, BLCA samples were classified into two risk subgroups using the best cut-off value of risk score at 1.933147; the proportion of deaths in the high-risk group was significantly higher than that in the low-risk group (Figures 2C–E). With an increase in the risk score, we found that the expression of IDO1 was downregulated, while those of NAMPT and ACAT1 were upregulated (Figure 2F). We found a distinct survival difference between these two subgroups (P< 0.05), with patients in the high-risk group usually having a poorer prognosis than those in the low-risk group (Figure 2G). Moreover, the area under the ROC curve (AUC) values (1-, 3-, and 5-year) were all above or equal to 0.6, suggesting that the risk score could better predict the survival status of BLCA patients (Figure 2H).

3.3 Accuracy of the predictive model was confirmed using the validation set

We verified the risk model's utility using the validation set GSE32894 and found that the results were consistent with those of the training set (Figures 3A–E). Furthermore, there were significant differences in the corresponding risk scores for invasion (YES and NO), tumor stage (Stage 1/2 and Stage 3, Stage 1/2, and Stage 4), grade (High and Low), T stage (T0/1/2 and T3, T0/1/2, and T4), and M stage (M0 and M1) (Figure 3F).

3.4 Construction of a nomogram comprising independent prognostic factors (risk score and invasion)

Univariate and multivariate Cox regression analyses were conducted to evaluate the clinical parameters and risk score to assess their prognostic value. The results demonstrated that risk score, age, invasion, T stage, N stage, and M stage were significant prognostic factors (Figure 4A). Multivariate Cox analysis was implemented for clinical features acquired by univariate Cox analysis to determine independent prognostic factors, the results demonstrated that risk score and invasion remained independent prognostic factors for BLCA (Figure 4B). Subsequently, a nomogram for predicting survival in patients with BLCA (1, 3- and 5-year) was created based on risk score and invasion (Figure 4C). Calibration curves and DCA indicated that the nomogram had a favorable predictive ability for BLCA (Figures 4D, E).

3.5 Immune infiltration and immune checkpoint analyses for tryptophan metabolism and immune-related biomarkers in BLCA

To clarify the relationship between our prognostic risk model and the tumor immune microenvironment, we investigated the differences in immune cell infiltration between the high- and low-risk groups using the CIBERSORT algorithm (Figure 5A). Furthermore, we found five immune cells [CD8+ T cells, macrophage with M1 phenotype, and regulatory T cells (Tregs)] that were differentially expressed between the two risk subgroups (Figure 5B). In the BLCA samples, we analyzed the Spearman

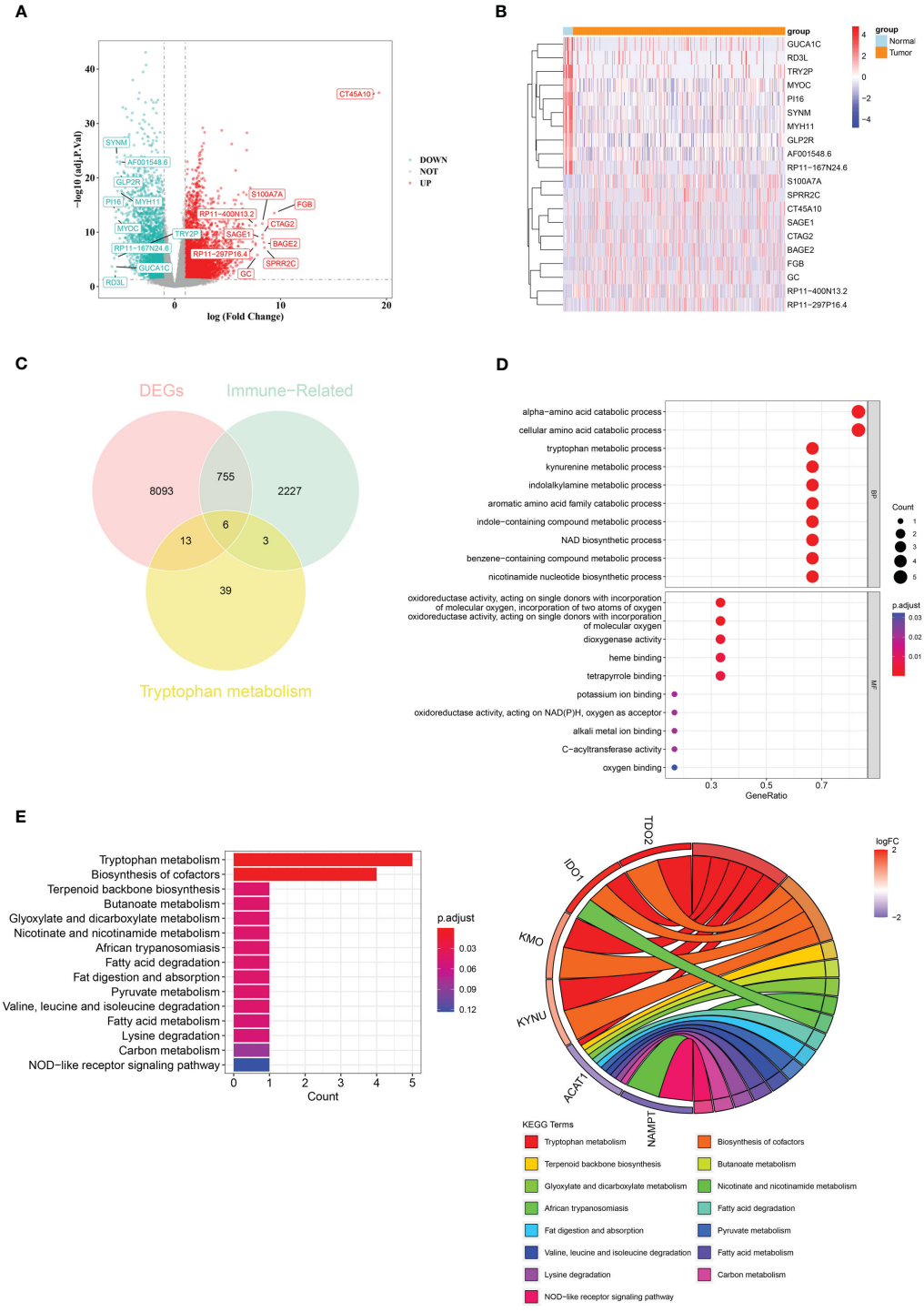

FIGURE 1
A total of six crossover genes were acquired through the overlap of tryptophan metabolism-related genes, immune-related genes, and DEGs. **(A)** Differentially expressed genes (DEGs) between the BLCA and normal groups. **(B)** The expressional heat map of the top 10 up- and down-regulated DEGs. **(C)** Six crossover genes achieved by intersection analysis. **(D, E)** GO and KEGG analyses of crossover genes.

correlation between differentially infiltrating immune cells and found a significant correlation between CD8 + T cells and macrophage with M1 phenotype (macrophage M1) (|Cor| > 0.3) (Figure 5C). Moreover, NAMPT was significantly negatively correlated with regulatory T cells (Tregs) (Cor = -0.307), and there was a significant positive relationship between macrophages M1 and IDO1 (Cor = 0.626) (Figure 5D). We found that 15 immune checkpoints (including IDO1, CD27, PDCD1, etc.) were differentially expressed between the two risk subgroups (P< 0.05) (Figure 5E). Among these, IDO1 was positively correlated with most differential immune checkpoints and highly positively associated with PDCD1, CTLA4, CD27, LAG3, and TIGIT (Cor > 0.6) (Figure 5F).

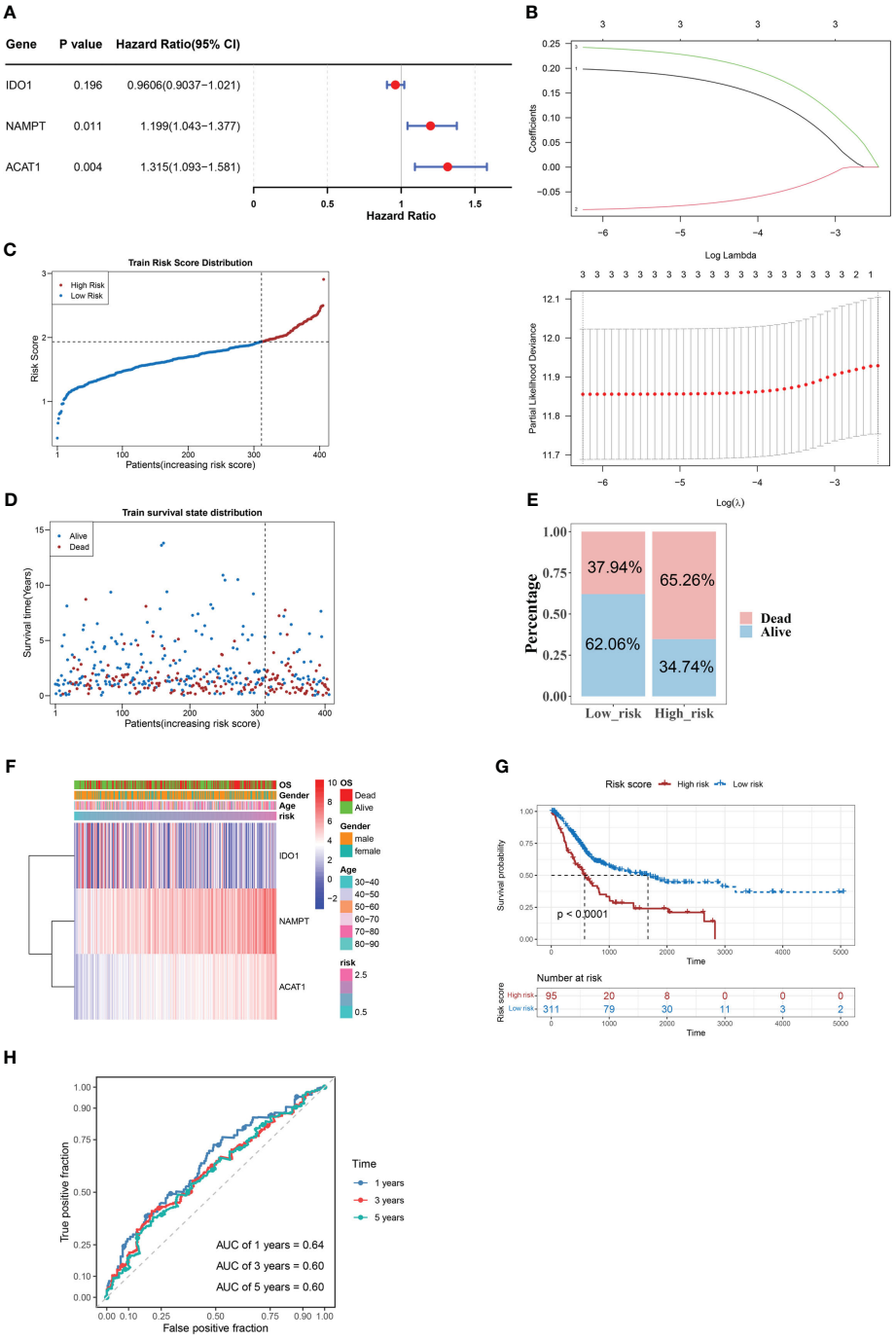

FIGURE 2
NAMPT, IDO1, and ACAT1 are tryptophan metabolism and immune-related biomarkers for BLCA. **(A)** Univariate Cox analysis of the prognostic candidate genes. **(B)** Average of coefficients of the three biomarkers (NAMPT, IDO1, and ACAT1) in the LASSO Cox regression at each lambda value (above). The partial likelihood deviance varies in accordance with the trend of the log lambda (below). **(C–E)** The distribution of risk scores **(C)**, the distribution of survival status **(D)**, and the proportion of people with different survival statuses **(E)** in the training set. **(F)** Heatmap of the three biomarkers. **(G)** Kaplan Meier curve for the training set. **(H)** 1-, 3-, and 5-year ROC curves for the training set.

3.6 Analysis of TIDE, IPS, and mutations between the two risk score groups

To explore the guiding value of the risk model for tumor immune exclusion and dysfunction, we used the TIDE algorithm to predict the response to ICIs. The results revealed that the high-risk group had higher exclusion scores but significantly lower dysfunction scores than the low-risk group, suggesting that the high-risk group was more likely to experience T cell exhaustion than the low-risk group, while the low-risk group was more likely to experience immune cell dysfunction (Figure 6A). Subsequently, we used IPS to predict the immunotherapeutic response of BLCA

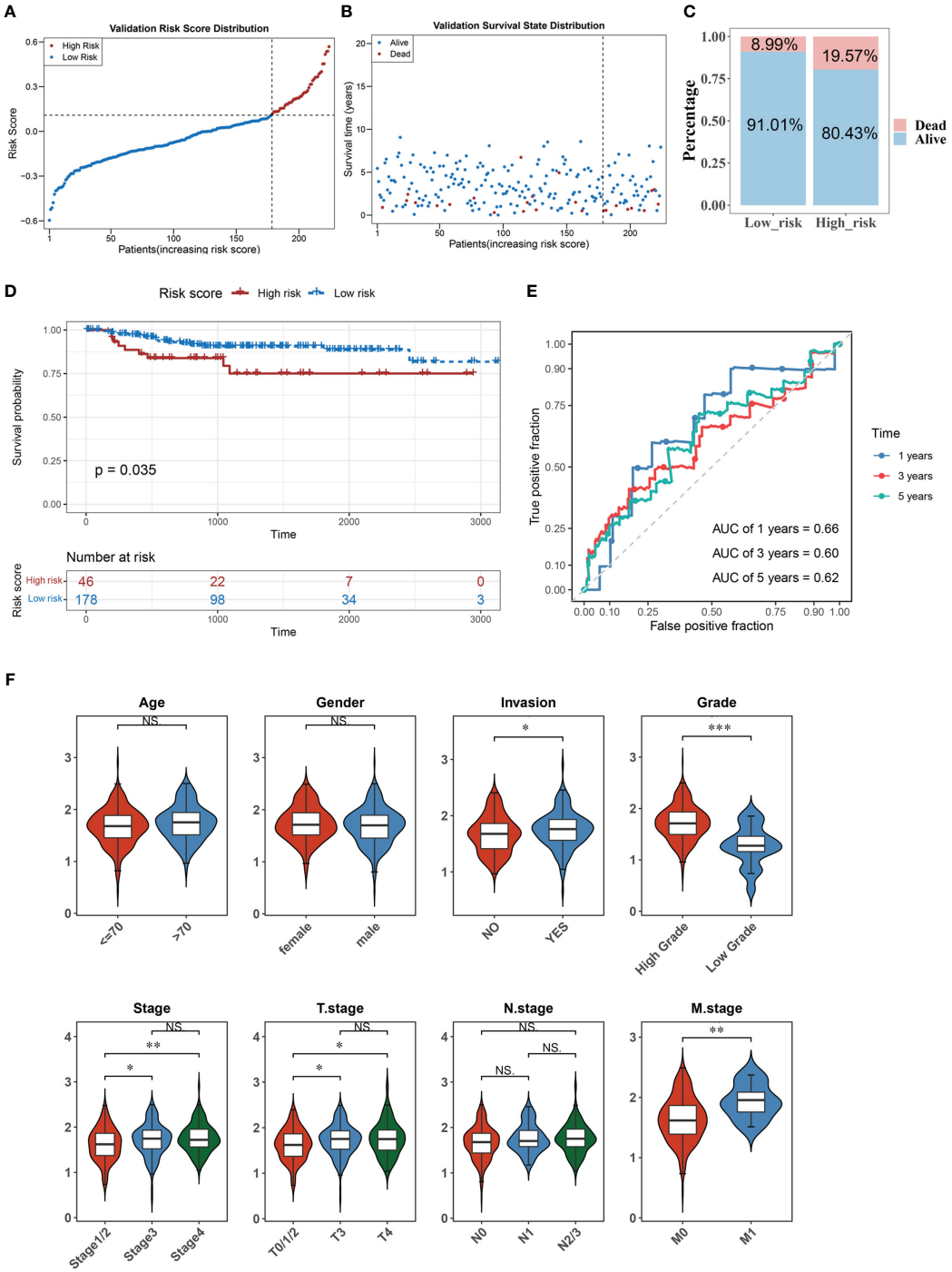

FIGURE 3
The accuracy of the predictive model was confirmed in the validation set. **(A–C)** The distribution of risk scores **(A)**, the distribution of survival status **(B)**, and the proportion of people with different survival statuses **(C)** in the validation set. **(D)** Kaplan Meier curve for the validation set. **(E)** 1-, 3-, and 5-year ROC curves for the validation set. **(F)** Distribution of risk scores for different clinical features. *P< 0.05, **P< 0.01, ***P< 0.001. . ns, No significance.

patients who received different treatment modalities (such as no treatment, anti-CTLA4, anti-PD1/PD-L1/PD-L2, or combination therapy). We found that patients in the low-risk group had a higher IPS, indicating better immunotherapy efficacy. Thus, these patients were more likely to benefit from immunotherapy (Figure 6B).

By analyzing the tumor mutation burden (TMB), we found that only the IDO1 gene was mutated (missense mutation) in the high-risk group, whereas in the low-risk group, NAMTP, ACAT1, and IDO1 were all mutated, most of which were missense mutations and a small fraction were insertion frameshift mutations (Figures 6C, D). Three

10.3389/fimmu.2023.1283792

genes (IDO2, IDO1, and TDO2) in the high-risk group were mutated in five samples, whereas these genes in the low-risk group were mutated in seven samples (Figures 6E, F). Based on the mutation data from TCGA-BLCA dataset, the BLCA samples in TCGA-BLCA were divided into high TMB-high-risk, high TMB-low-risk, low TMB-high-risk, and low TMB-low-risk groups. K-M curves of the four groups were then analyzed. We found a significant difference in survival among the four groups (P< 0.05), and the survival status was the worst in the low-TMB-high-risk group (Figure 6G).

3.7 Single-cell analysis for tryptophan metabolism- and immune-related biomarkers in BLCA

Based on the single-cell sequencing dataset (GSE135337), 18,718 core cells were acquired after quality control (Figure 7A). After normalizing the data, the top 2000 highly variable genes were screened for downstream analysis (Figure 7B). According to PCA results, 20 principal

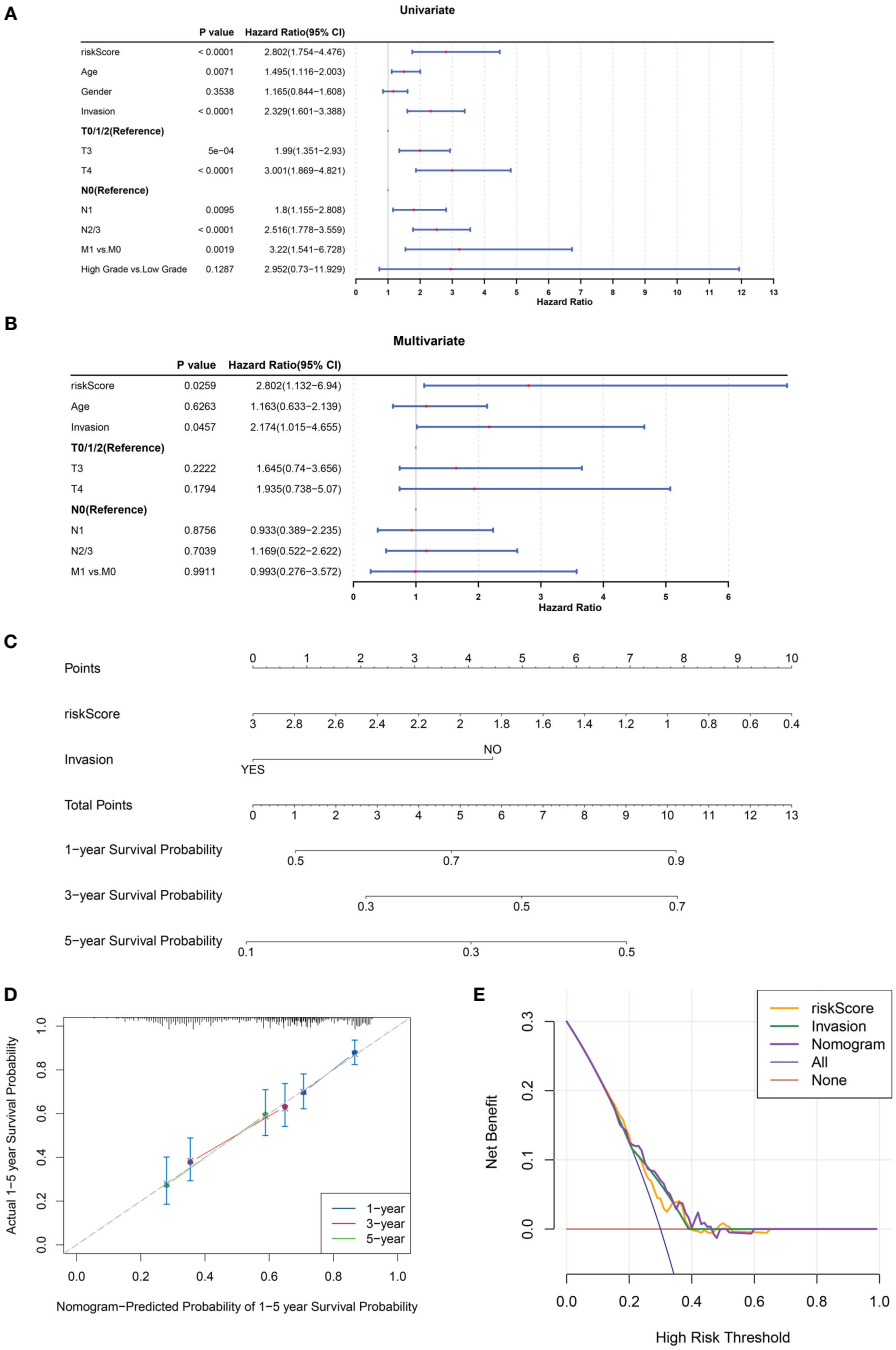

FIGURE 4
A nomogram comprising independent prognostic factors (risk score and invasion) was created. **(A, B)** Univariate **(A)** and multivariate **(B)** Cox regression analyses of potential prognostic factors for overall survival. **(C)** The nomogram for predicting survival in BLCA patients (1-, 3- and 5-year). **(D, E)** Evaluation of the accuracy of prediction using the calibration curve **(D)** and DCA curve **(E)**.

10.3389/fimmu.2023.1283792

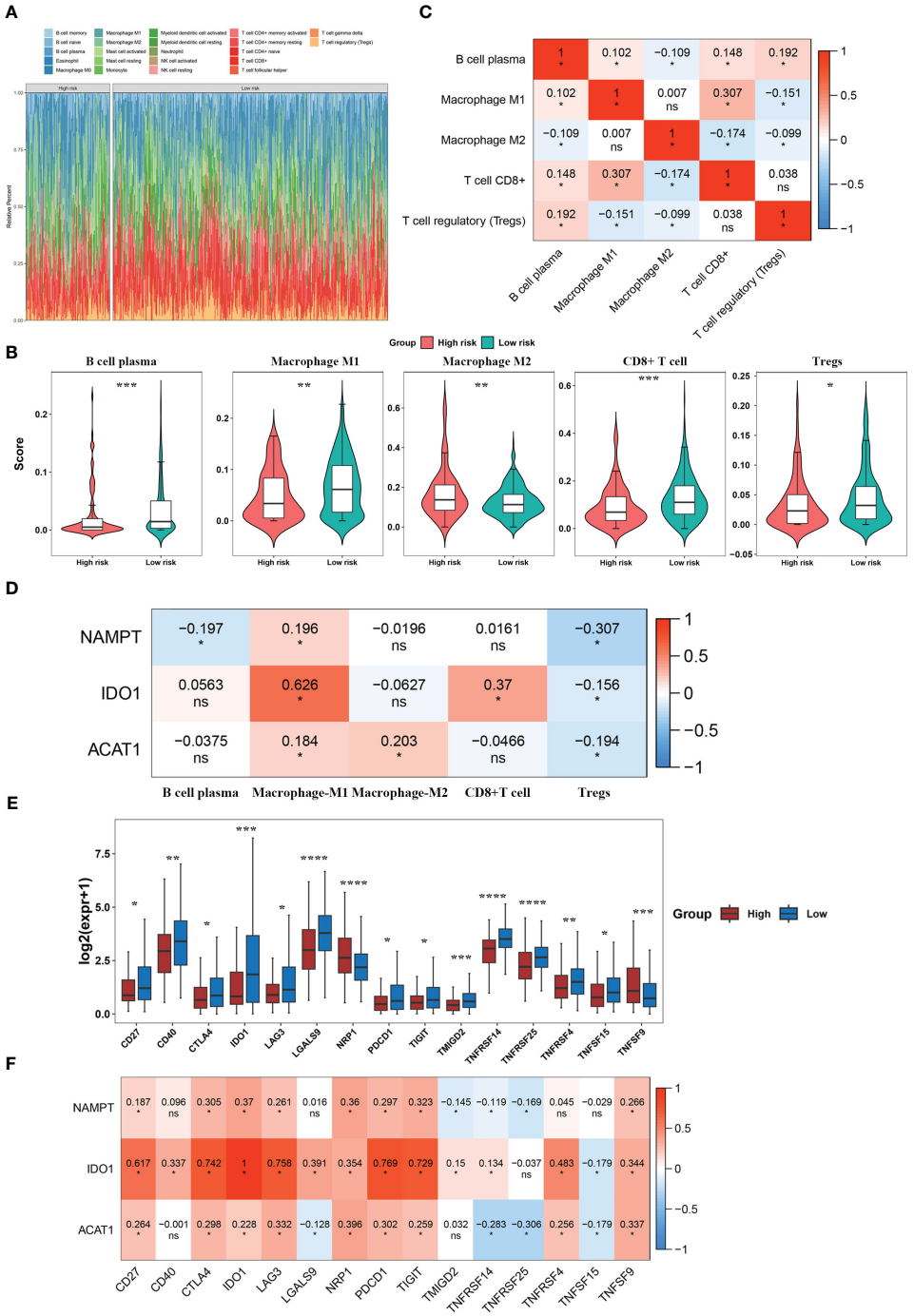

FIGURE 5
Immune infiltration and immune checkpoint analyses for tryptophan metabolism and immune-related biomarkers for BLCA. **(A)** Immune cell infiltration levels in BLCA patients. **(B)** Differential immune cells between the two risk subgroups. **(C)** Correlation heatmap of differential immune cells. **(D)** Correlation heatmap between model genes and differential immune cells. **(E)** Immune checkpoints with differential expression. **(F)** Correlation heatmap between model genes and differential immune checkpoints. *P< 0.05, **P< 0.01, ***P< 0.001, ****P< 0.0001. ns, No significance.

components (P< 0.05) were selected for subsequent analyses (Figure 7C). Using UMAP, the core cells were clustered into 15 classes (Figure 7D). The main annotations included five cell types: endothelial cells, epithelial cells, myeloid/macrophages, fibroblasts, and T cells. We found that NAMPT was expressed in all five cell groups; IDO1 was partially expressed in epithelial cells, myeloid/macrophages, and T cells, and ACAT1 was highly expressed in endothelial cells, epithelial cells, and fibroblasts and partially expressed in myeloid/macrophages and T cells (Figures 7E–G).

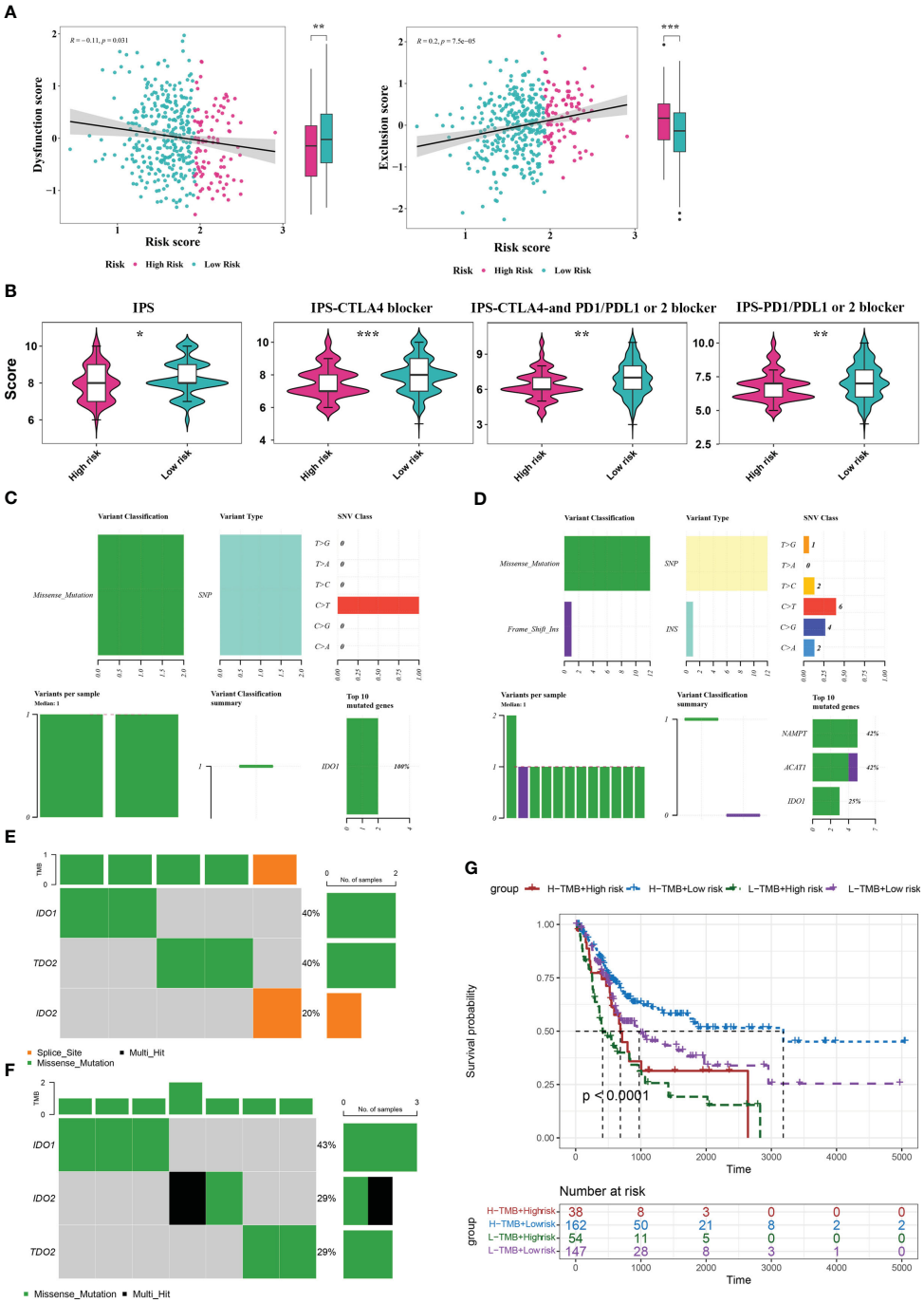

FIGURE 6
Analysis of TIDE, IPS, and mutations between the two risk score groups. **(A)** TIDE analysis between high- and low-risk groups. **(B)** IPS scores between high- and low-risk groups. **(C, D)** Mutation analysis for genes in the model in the high- **(C)** and low-risk **(D)** groups. **(E, F)** Mutation analysis for IDO1, IDO2, and TDO2 in the high- **(E)** and low-risk **(F)** groups. **(G)** Kaplan Meier curve analysis for the four different groups. *P< 0.05, **P< 0.01, ***P< 0.001.

3.8 NAMPT was upregulated in BLCA tissues and could regulate BLCA cell proliferation and invasion *in vitro*

NAMPT expression was significantly higher in cancer tissues than in adjacent tissues (Figure 8A). The effects of NAMPT on cell proliferation and invasion were explored to determine its role in BLCA cells. The efficiency of NAMPT knockdown was verified using RT-qPCR (Figure 8B). CCK-8 assay demonstrated that NAMPT knockdown significantly inhibited the proliferation of T24 and 5637 cells (Figure 8C). Moreover, the migration and invasion abilities of T24 and 5637 cells were significantly decreased after NAMPT knockdown (Figure 8D).

10.3389/fimmu.2023.1283792

4 Discussion

BLCA is a common malignancy of the urine system. The incidence and mortality rates of BLCA have increased recently. The 5-year survival rate of muscle-invasive BLCA (MIBC) is less than 50%, and the prognosis of metastatic BLCA is even worse, with a 5-year survival rate of less than 15% (2). Ultrasonography and cystoscopy are traditional methods for diagnosing bladder cancer. In recent years, the researches on bladder cancer biomarkers have received significant attention in order to improve the accuracy of non-invasive detection of bladder cancer. Many cancer-associated molecules have been identified over the recent years which include

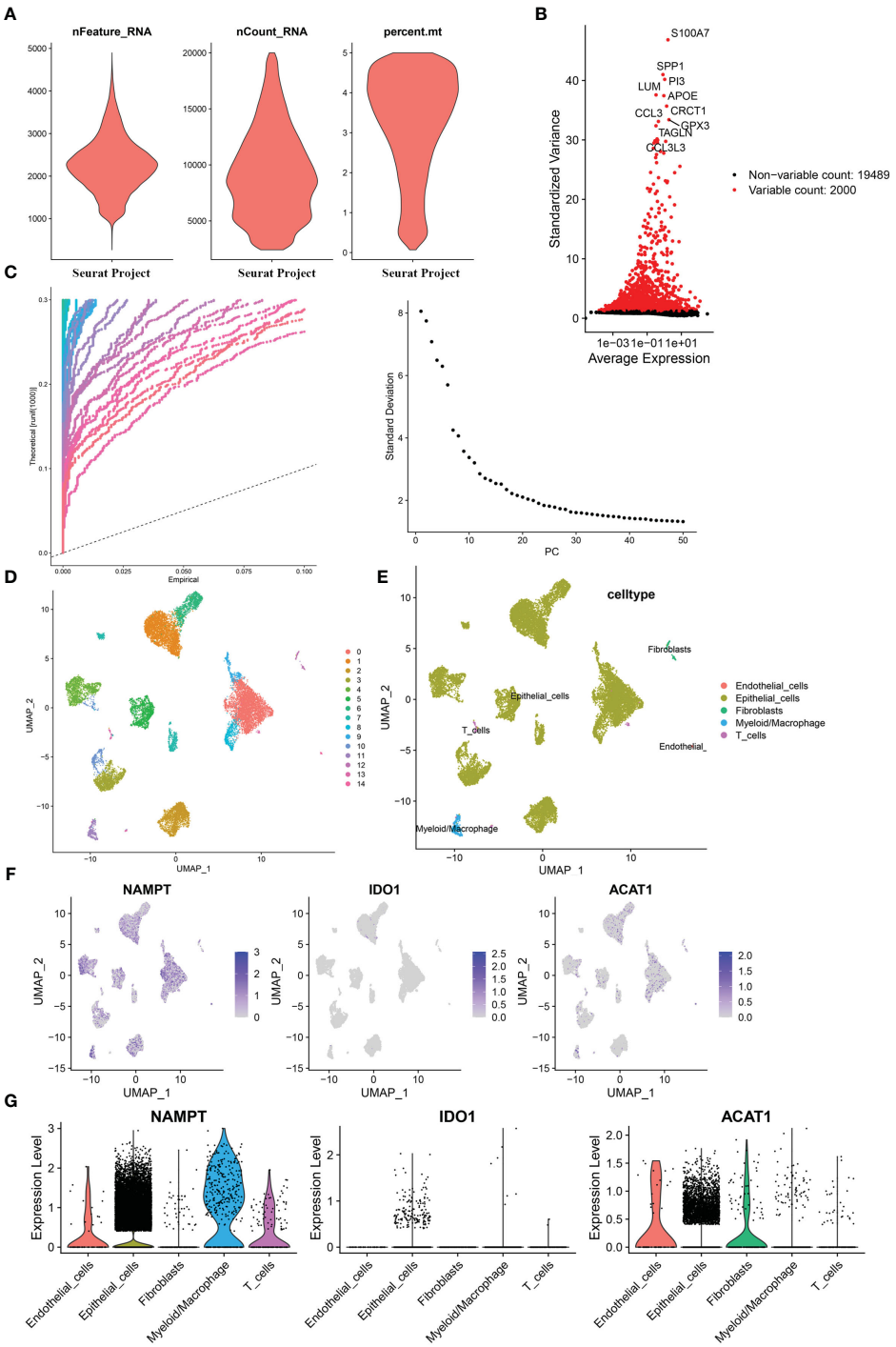

FIGURE 7
Single-cell analysis for the model genes. **(A)** A total of 18,718 core cells were analyzed after quality control. **(B)** Screening for highly variable gene expression. **(C)** Scatter plots (left) and gravel plots (right) of principal components according to PCA results. **(D)** After UMAP dimensionality reduction, cells were divided into 15 groups. **(E)** Annotation of cell populations using marker genes. **(F)** Expression of model genes in different cell populations. **(G)** Violin plot for expression of model genes in different cell populations.

EGFR, NMP22, FGFR3, p53 etc. (21–23). However, due to the lack of sufficient sensitivity and specificity in most biomarkers, there is still no ideal biomarker in clinical practice that can replace cystoscopy for the diagnosis, treatment, and prognostic evaluation of bladder cancer.

Due to the heterogeneity of BLCA, the response to different molecular subtypes of bladder cancer varies greatly with chemotherapy and targeted therapy. Therefore, there is an urgent need to develop new therapeutic drugs that can significantly inhibit tumor proliferation and effectively improve the prognosis of patients with locally advanced and metastatic BLCA. In recent years, immunotherapy has led to significant breakthroughs in BLCA treatment. Immunotherapeutic drugs such as ICIs have been widely used in BLCA (24). Immune checkpoints are a class of immune regulatory molecules comprising receptors expressed on the surface of immune cells and ligands expressed on the surface of tumor cells. The interaction between these two components can regulate the immune system activity and affect tumor immunity.

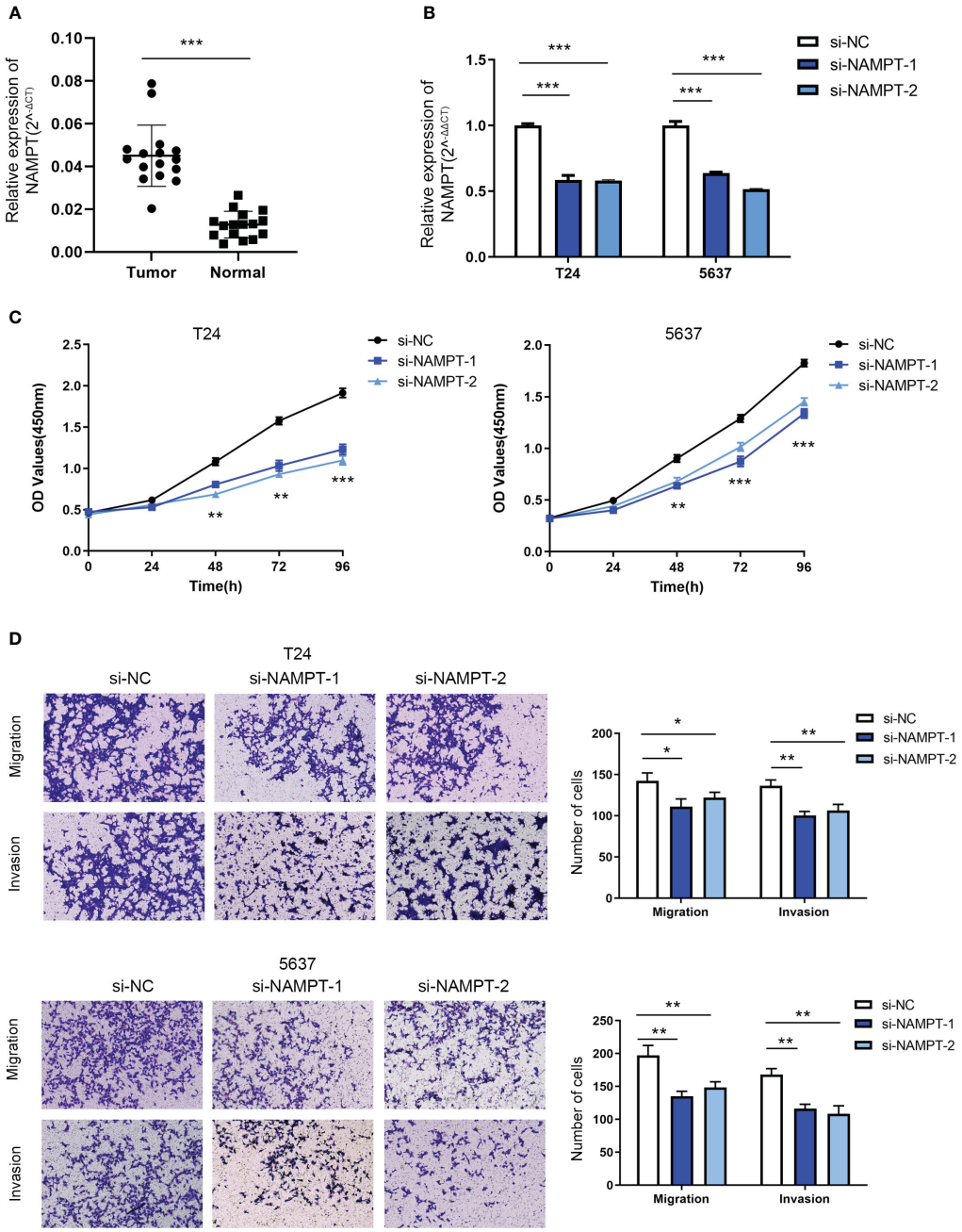

FIGURE 8
NAMPT was upregulated in BLCA tissues and could regulate BLCA cell proliferation and invasion *in vitro*. **(A)** NAMPT expression in BLCA and matched adjacent normal tissues detected by RT-qPCR. **(B)** Efficiency of NAMPT knockdown was verified by RT-qPCR. **(C)** The proliferative ability of NAMPT knockdown cells was determined using CCK-8 assay. **(D)** Transwell assay was used to detect the migration and invasion abilities of cells with NAMPT knockdown. *P< 0.05, **P< 0.01, ***P< 0.001.

However, owing to the complexity of the tumor immune microenvironment, the overall effective rate of immunotherapy is only 10– 30%, and most patients cannot benefit from immunotherapy (25). Therefore, improving the responsiveness of patients to immunotherapy and restoring the body's antitumor immune response are important problems that urgently need to be solved.

In order to adapt to the hypoxic and nutrient-poor microenvironment to achieve rapid growth, tumor cells change their energy metabolism behavior, referred to as "metabolic reprogramming," basic characteristics of tumors (26). In addition to participating in protein synthesis, tryptophan is an important energy source for the immune system (27). Disorders in tryptophan metabolism can lead to apoptosis and dysfunction of immune cells, induce the formation of an immunosuppressive microenvironment, and affect the efficacy of ICIs. Specifically, abnormal tryptophan metabolism leads to tryptophan depletion, which leads to insufficient energy in immune cells and affects the activity of the immune system (5, 6, 28). Tryptophan depletion leads to increased levels of free tRNAs, which directly activate regulatory T cells (Tregs) through the General Control Non-derepressible-2 (GCN2) pathway, thus inhibiting the activity of antigen-presenting cells and the proliferation of CD8+ T cells (29, 30). Furthermore, the accumulation of tryptophan metabolites enhances IDO1 activity and creates an inhibitory immune microenvironment (6, 31). Therefore, inhibiting the activity of key enzymes (IDO1, IDO2, and TDO) in the tryptophan metabolism pathway can restore the activity of immune cells, which has been investigated as a potential strategy to restore immune function and improve the response to immunotherapy.

Unlike single-gene biomarkers, risk scoring models analyze different model genes together, resulting in higher sensitivity and specificity. Therefore, risk scoring models can be used for early diagnosis, treatment decisions, individual monitoring and follow-up of bladder cancer. Using univariate and multivariate Cox regression analyses, we constructed a risk model that included the NAMPT, ACAT1, and IDO1 genes. The K-M survival and ROC curves were used to verify the validity of the risk model, and the results showed that there was a significant survival difference between the high- and low-risk groups, indicating that the risk model had good predictive ability. NAMPT plays a significant role in various cellular processes, including energy metabolism, nicotinamide adenine dinucleotide (NAD+) biosynthesis, and cell survival (32). High NAMPT expression is associated with enhanced NAD+ biosynthesis, which may lead to advantages in tumor cell proliferation and survival (32, 33). Moreover, an upregulated expression of NAMPT has been associated with chemoresistance and reduced chemotherapy efficacy (34). In this study, we verified that NAMPT knockdown significantly inhibited BLCA cell proliferation, migration and invasion. ACAT1 plays a crucial role in cellular lipid metabolism (35), and several studies have investigated the roles of lipid metabolism and related enzymes in BLCA (36, 37). As a result, there may have potential implications for ACAT1 action in BLCA, although more research is needed to understand its precise role in this context.

Single-cell sequencing allows researchers to study the genetic and genomic characteristics of individual cells, revealing the cellular heterogeneity in tissues and organs. Using a single-cell sequencing dataset, we found that NAMPT and ACAT1 were expressed in various cell types, whereas IDO1 was mainly expressed in immune cells. This further verified that NAMPT and ACAT1 play biological roles mainly by regulating the energy metabolism of various cell types, whereas IDO1 affects tumor progression by regulating the activity of immune cells.

In addition to the tryptophan metabolism pathway, KEGG pathway analysis suggested the enrichment of the NOD-like receptor signaling pathway. NOD-like receptors (NLRs) are a class of signaling receptors found in immune cells that are involved in biological processes such as apoptosis, inflammation, and immune responses (38, 39). Moreover, the NLR signaling pathway can regulate tryptophan metabolism (40), which is involved in the immune response and plays a critical role in tumor immune evasion.

Abnormalities in the tumor microenvironment (TME) are important factors that induce tumor metabolic reprogramming (41, 42). The TME is a complex network composed of the extracellular matrix, hematopoietic cells, and mesenchymal cells. An aberrant tumor immune microenvironment is conducive to the differentiation of tumor cells into highly aggressive cell subtypes and suppression of antitumor immune responses, leading to tumor progression (43). In this study, we further explored the relationship between tryptophan metabolism and the tumor immune microenvironment in BLCA. The CIBERSORT algorithm demonstrated that five immune cells (CD8+ T cells, macrophages M1 and M2, regulatory T cells (Tregs), and B cells) were differentially expressed between the two risk subgroups. The low-risk group was associated with a higher level of CD8+ T cell infiltration, indicating that the immune system in the low-risk group exerted a more effective response against tumor proliferation. Moreover, the infiltration of macrophages M1 was negatively associated with risk scores, whereas macrophage M2 was positively associated with risk scores. Macrophages M1 inhibit tumor growth by directly killing tumor cells or stimulating other immune cells to enhance the host antitumor immune response, whereas macrophages M2 suppress immune system activity, thereby weakening antitumor immunity. IPS analysis revealed that patients in the low-risk groups had better immunotherapy efficacy and were more likely to benefit from immunotherapy. These results indicate that differences in tryptophan metabolism between the high- and low-risk groups could affect the TME. The high-risk group, which represents higher tryptophan metabolism, is more likely to form an immunosuppressive microenvironment, induce immune escape of tumor cells, and result in a worse immunotherapy response and prognosis.

In conclusion, the tryptophan metabolism- and immune-related gene risk model can effectively predict patient prognosis and immunotherapy response and is an effective prognostic model for BLCA. Our study further explored the potential applications of tryptophan metabolism in improving the response to immunotherapy and has crucial implications for individualized therapy to improve the prognosis of patients with BLCA.

However, further validation using basic experiments is required to confirm our findings.

Data availability statement

The datasets presented in this study can be found in online repositories. The names of the repository/repositories and accession number(s) can be found in the article/Supplementary Material.

Ethics statement

The studies involving humans were approved by Institutional Review Board of Qilu Hospital. The studies were conducted in accordance with the local legislation and institutional requirements. The participants provided their written informed consent to participate in this study.

Author contributions

LX: Formal Analysis, Investigation, Methodology, Software, Validation, Writing – review & editing. GQ: Data curation, Resources, Writing – original draft. ZZ: Conceptualization, Project administration, Resources, Software, Writing – original draft. HZ: Data curation, Resources, Validation, Writing – review & editing. GZ: Funding acquisition, Project administration, Supervision, Validation, Visualization, Writing – original draft.

Funding

The author(s) declare financial support was received for the research, authorship, and/or publication of this article. This research was supported by the Natural Science Foundation of Shandong Province (ZR2020MH082 and ZR2023QH047).

Acknowledgments

We sincerely thank the editor and reviewers whose comments and suggestions helped improve this article.

Conflict of interest

The authors declare that the research was conducted in the absence of any commercial or financial relationships that could be construed as a potential conflict of interest.

The handling editor WC declared a shared parent affiliation with the authors at the time of review.

Publisher's note

Supplementary material

The Supplementary Material for this article can be found online at: https://www.frontiersin.org/articles/10.3389/fimmu.2023.1283792/full#supplementary-material

References

1. Sung H, Ferlay J, Siegel RL, Laversanne M, Soerjomataram I, Jemal A, et al. Global cancer statistics 2020: GLOBOCAN estimates of incidence and mortality worldwide for 36 cancers in 185 countries. *CA Cancer J Clin* (2021) 71(3):209–49. doi: 10.3322/caac.21660

2. Patel VG, Oh WK, Galsky MD. Treatment of muscle-invasive and advanced bladder cancer in 2020. *CA Cancer J Clin* (2020) 70(5):404–23. doi: 10.3322/caac.21631

3. Perez-Castro L, Garcia R, Venkateswaran N, Barnes S, Conacci-Sorrell M. Tryptophan and its metabolites in normal physiology and cancer etiology. *FEBS J* (2023) 290(1):7–27. doi: 10.1111/febs.16245

4. Hezaveh K, Shinde RS, Klotgen A, Halaby MJ, Lamorte S, Ciudad MT, et al. Tryptophan-derived microbial metabolites activate the aryl hydrocarbon receptor in tumor-associated macrophages to suppress anti-tumor immunity. *Immunity* (2022) 55 (2):324–40 e8. doi: 10.1016/j.immuni.2022.01.006

5. Fiore A, Murray PJ. Tryptophan and indole metabolism in immune regulation. *Curr Opin Immunol* (2021) 70:7–14. doi: 10.1016/j.coi.2020.12.001

6. Platten M, Nollen EAA, Rohrig UF, Fallarino F, Opitz CA. Tryptophan metabolism as a common therapeutic target in cancer, neurodegeneration and beyond. *Nat Rev Drug Discovery* (2019) 18(5):379–401. doi: 10.1038/s41573-019-0016-5

7. Chen W, Wen L, Bao Y, Tang Z, Zhao J, Zhang X, et al. Gut flora disequilibrium promotes the initiation of liver cancer by modulating tryptophan metabolism and up-regulating SREBP2. *Proc Natl Acad Sci USA* (2022) 119(52):e2203894119. doi: 10.1073/pnas.2203894119

8. Santhanam S, Alvarado DM, Ciorba MA. Therapeutic targeting of inflammation and tryptophan metabolism in colon and gastrointestinal cancer. *Transl Res* (2016) 167 (1):67–79. doi: 10.1016/j.trsl.2015.07.003

9. Lee SH, Mahendran R, Tham SM, Thamboo TP, Chionh BJ, Lim YX, et al. Tryptophan-kynurenine ratio as a biomarker of bladder cancer. *BJU Int* (2021) 127 (4):445–53. doi: 10.1111/bju.15205

10. Tran L, Xiao JF, Agarwal N, Duex JE, Theodorescu D. Advances in bladder cancer biology and therapy. *Nat Rev Cancer* (2021) 21(2):104–21. doi: 10.1038/s41568-020-00313-1

11. Lee HW, Chung W, Lee HO, Jeong DE, Jo A, Lim JE, et al. Single-cell RNA sequencing reveals the tumor microenvironment and facilitates strategic choices to circumvent treatment failure in a chemorefractory bladder cancer patient. *Genome Med* (2020) 12(1):47. doi: 10.1186/s13073-020-00741-6

12. Topalian SL, Taube JM, Anders RA, Pardoll DM. Mechanism-driven biomarkers to guide immune checkpoint blockade in cancer therapy. *Nat Rev Cancer* (2016) 16 (5):275–87. doi: 10.1038/nrc.2016.36

13. Galluzzi L, Humeau J, Buque A, Zitvogel L, Kroemer G. Immunostimulation with chemotherapy in the era of immune checkpoint inhibitors. *Nat Rev Clin Oncol* (2020) 17(12):725–41. doi: 10.1038/s41571-020-0413-z

14. Robinson MD, McCarthy DJ, Smyth GK. edgeR: a Bioconductor package for differential expression analysis of digital gene expression data. *Bioinformatics* (2010) 26 (1):139–40. doi: 10.1093/bioinformatics/btp616

15. Ito K, Murphy D. Application of ggplot2 to pharmacometric graphics. *CPT Pharmacometrics Syst Pharmacol* (2013) 2(10):e79. doi: 10.1038/psp.2013.56

16. Wu T, Hu E, Xu S, Chen M, Guo P, Dai Z, et al. clusterProfiler 4.0: A universal enrichment tool for interpreting omics data. *Innovation (Camb)* (2021) 2(3):100141. doi: 10.1016/j.xinn.2021.100141

17. Aloia TA, Harpole DHJr., Reed CE, Allegra C, Moore MB, Herndon JE2nd, et al. Tumor marker expression is predictive of survival in patients with esophageal cancer. *Ann Thorac Surg* (2001) 72(3):859–66. doi: 10.1016/S0003-4975(01)02838-7

18. Koldingsnes W, Nossent H. Predictors of survival and organ damage in Wegener's granulomatosis. *Rheumatol (Oxford)* (2002) 41(5):572–81. doi: 10.1093/rheumatology/41.5.572

19. Mayakonda A, Lin DC, Assenov Y, Plass C, Koeffler HP. Maftools: efficient and comprehensive analysis of somatic variants in cancer. *Genome Res* (2018) 28(11):1747–56. doi: 10.1101/gr.239244.118

20. Lai H, Cheng X, Liu Q, Luo W, Liu M, Zhang M, et al. Single-cell RNA sequencing reveals the epithelial cell heterogeneity and invasive subpopulation in human bladder cancer. *Int J Cancer* (2021) 149(12):2099–115. doi: 10.1002/ijc.33794

21. Sharma B, Kanwar SS. Phosphatidylserine: A cancer cell targeting biomarker. *Semin Cancer Biol* (2018) 52(Pt 1):17–25. doi: 10.1016/j.semcancer.2017.08.012

22. Ascione CM, Napolitano F, Esposito D, Servetto A, Belli S, Santaniello A, et al. Role of FGFR3 in bladder cancer: Treatment landscape and future challenges. *Cancer Treat Rev* (2023) 115:102530. doi: 10.1016/j.ctrv.2023.102530

23. Daizumoto K, Yoshimaru T, Matsushita Y, Fukawa T, Uehara H, Ono M, et al. A DDX31/mutant-p53/EGFR axis promotes multistep progression of muscle-invasive bladder cancer. *Cancer Res* (2018) 78(9):2233–47. doi: 10.1158/0008-5472.CAN-17-2528

24. Cathomas R, Lorch A, Bruins HM, Comperat EM, Cowan NC, Efstathiou JA, et al. The 2021 updated European association of urology guidelines on metastatic urothelial carcinoma. *Eur Urol* (2022) 81(1):95–103. doi: 10.1016/j.eururo.2021.09.026

25. Bagchi S, Yuan R, Engleman EG. Immune checkpoint inhibitors for the treatment of cancer: clinical impact and mechanisms of response and resistance. *Annu Rev Pathol* (2021) 16:223–49. doi: 10.1146/annurev-pathol-042020-042741

26. Hanahan D, Weinberg RA. Hallmarks of cancer: the next generation. *Cell* (2011) 144(5):646–74. doi: 10.1016/j.cell.2011.02.013

27. Agus A, Planchais J, Sokol H. Gut microbiota regulation of tryptophan metabolism in health and disease. *Cell Host Microbe* (2018) 23(6):716–24. doi: 10.1016/j.chom.2018.05.003

28. Cervenka I, Agudelo LZ, Ruas JL. Kynurenines: Tryptophan's metabolites in exercise, inflammation, and mental health. *Science* (2017) 357(6349):eaaf9794. doi: 10.1126/science.aaf9794

29. Munn DH, Mellor AL. IDO in the tumor microenvironment: inflammation, counter-regulation, and tolerance. *Trends Immunol* (2016) 37(3):193–207. doi: 10.1016/j.it.2016.01.002

30. Munn DH, Sharma MD, Baban B, Harding HP, Zhang Y, Ron D, et al. GCN2 kinase in T cells mediates proliferative arrest and anergy induction in response to indoleamine 2,3-dioxygenase. *Immunity* (2005) 22(5):633–42. doi: 10.1016/j.immuni.2005.03.013

31. Newman AC, Falcone M, Huerta Uribe A, Zhang T, Athineos D, Pietzke M, et al. Immune-regulated IDO1-dependent tryptophan metabolism is source of one-carbon units for pancreatic cancer and stellate cells. *Mol Cell* (2021) 81(11):2290–302 e7. doi: 10.1016/j.molcel.2021.03.019

32. Garten A, Schuster S, Penke M, Gorski T, de Giorgis T, Kiess W. Physiological and pathophysiological roles of NAMPT and NAD metabolism. *Nat Rev Endocrinol* (2015) 11(9):535–46. doi: 10.1038/nrendo.2015.117

33. Navas LE, Carnero A. NAD(+) metabolism, stemness, the immune response, and cancer. *Signal Transduct Target Ther* (2021) 6(1):2. doi: 10.1038/s41392-020-00354-w

34. Nacarelli T, Fukumoto T, Zundell JA, Fatkhutdinov N, Jean S, Cadungog MG, et al. NAMPT inhibition suppresses cancer stem-like cells associated with therapy-induced senescence in ovarian cancer. *Cancer Res* (2020) 80(4):890–900. doi: 10.1158/0008-5472.CAN-19-2830

35. Gu L, Zhu Y, Lin X, Tan X, Lu B, Li Y. Stabilization of FASN by ACAT1-mediated GNPAT acetylation promotes lipid metabolism and hepatocarcinogenesis. *Oncogene* (2020) 39(11):2437–49. doi: 10.1038/s41388-020-1156-0

36. Liu P, Fan B, Othmane B, Hu J, Li H, Cui Y, et al. m(6)A-induced lncDBET promotes the Malignant progression of bladder cancer through FABP5-mediated lipid metabolism. *Theranostics* (2022) 12(14):6291–307. doi: 10.7150/thno.71456

37. Yang YY, Hong SY, Xun Y, Liu CQ, Sun JX, Xu JZ, et al. Characterization of the lipid metabolism in bladder cancer to guide clinical therapy. *J Oncol* (2022) 2022:7679652. doi: 10.1155/2022/7679652

38. Saxena M, Yeretssian G. NOD-like receptors: master regulators of inflammation and cancer. *Front Immunol* (2014) 5:327. doi: 10.3389/fimmu.2014.00327

39. Kent A, Blander JM. Nod-like receptors: key molecular switches in the conundrum of cancer. *Front Immunol* (2014) 5:185. doi: 10.3389/fimmu.2014.00185

40. Li T, Fu B, Zhang X, Zhou Y, Yang M, Cao M, et al. Overproduction of gastrointestinal 5-HT promotes colitis-associated colorectal cancer progression *via* enhancing NLRP3 inflammasome activation. *Cancer Immunol Res* (2021) 9(9):1008–23. doi: 10.1158/2326-6066.CIR-20-1043

41. Dey P, Kimmelman AC, DePinho RA. Metabolic codependencies in the tumor microenvironment. *Cancer Discovery* (2021) 11(5):1067–81. doi: 10.1158/2159-8290.CD-20-1211

42. Xia L, Oyang L, Lin J, Tan S, Han Y, Wu N, et al. The cancer metabolic reprogramming and immune response. *Mol Cancer* (2021) 20(1):28. doi: 10.1186/s12943-021-01316-8

43. Riaz N, Havel JJ, Makarov V, Desrichard A, Urba WJ, Sims JS, et al. Tumor and microenvironment evolution during immunotherapy with nivolumab. *Cell* (2017) 171 (4):934–49 e16. doi: 10.1016/j.cell.2017.09.028

frontiers | Frontiers in Immunology

TYPE Review
PUBLISHED 28 November 2023
DOI 10.3389/fimmu.2023.1284853

OPEN ACCESS

EDITED BY
Houjuan Zhu,
Institute of Materials Research and Engineering (A*STAR), Singapore

REVIEWED BY
Fanrong Liu,
Second Affiliated Hospital of Nanchang University, China
Siu Hong Dexter Wong,
Hong Kong Polytechnic University, Hong Kong SAR, China

*CORRESPONDENCE
Feng-Juan Han
hanfengjuan2004@163.com

RECEIVED 29 August 2023
ACCEPTED 10 November 2023
PUBLISHED 28 November 2023

CITATION
Li C, Liu F-Y, Shen Y, Tian Y and Han F-J (2023) Research progress on the mechanism of glycolysis in ovarian cancer. *Front. Immunol.* 14:1284853. doi: 10.3389/fimmu.2023.1284853

Research progress on the mechanism of glycolysis in ovarian cancer

Chan Li[1], Fang-Yuan Liu[1], Ying Shen[1,2], Yuan Tian[3] and Feng-Juan Han[2*]

[1]Heilongjiang University of Traditional Chinese Medicine (TCM), Harbin, Heilongjiang, China, [2]The First Affiliated Hospital of Heilongjiang University of Traditional Chinese Medicine (TCM), Harbin, Heilongjiang, China, [3]Zhejiang University of Chinese Medicine, Hangzhou, Zhejiang, China

Glycolysis is the preferred energy metabolism pathway in cancer cells even when the oxygen content is sufficient. Through glycolysis, cancer cells convert glucose into pyruvic acid and then lactate to rapidly produce energy and promote cancer progression. Changes in glycolysis activity play a crucial role in the biosynthesis and energy requirements of cancer cells needed to maintain growth and metastasis. This review focuses on ovarian cancer and the significance of key rate-limiting enzymes (hexokinase, phosphofructokinase, and pyruvate kinase, related signaling pathways (PI3K-AKT, Wnt, MAPK, AMPK), transcription regulators (HIF-1a), and non-coding RNA in the glycolytic pathway. Understanding the relationship between glycolysis and these different mechanisms may provide new opportunities for the future treatment of ovarian cancer.

KEYWORDS

ovarian cancer, glycolysis, hexokinase, phosphofructokinase, pyruvate kinase

1 Introduction

Ovarian cancer (OC) is a common malignancy in gynecology, with approximately 310,000 women diagnosed and 200,000 deaths each year worldwide (1). The insidious nature of the early stage of the disease means that most patients have an advanced form of the disease at the time of diagnosis, and consequently, the disease has an extremely high mortality rate. Risk factors for OC include a family history of ovarian or breast cancer, age,

Abbreviations: AKT, protein kinase B; AMPK, AMP-activated protein kinase; CAF, Cancer-associated fibroblast; EMT, epithelial–mesenchymal transition; HK, Hexokinase; LDH, lactate dehydrogenase; LDHA, lactate dehydrogenase A; MAPK, mitogen-activated protein kinase; MiRNA, microRNA; NK, Natural killer cells; NKT, Natural killer T cells; HIF-1α, hypoxia-inducible factors; OC, Ovarian cancer; OXPHOS oxidative phosphorylation; PDK, Pyruvate dehydrogenase kinase; PDH, pyruvate dehydrogenase; PFK, phosphofructokinase; PK, Pyruvate kinase; ROS, Reactive oxygen species; TAM, Tumor-associated macrophages; TCM, Traditional Chinese medicine; TME, The tumor microenvironment; VEGF, vascular endothelial growth factor.

endometriosis, obesity, early menarche, and menopausal hormone therapy (2). The main treatment methods for OC include surgery, radiotherapy, chemotherapy, and immunotherapy, but more than half of patients will have adverse outcomes such as recurrence, metastasis, and chemotherapy resistance.

Metabolic reprogramming is a distinguishing hallmark of cancer, and glycolysis is a central factor in cancer progression (3). In normal cells, glucose maintains a state of homeostasis. In the 1920s, Warburg proposed that cancer cells preferentially rely on the conversion of glucose to pyruvate, and then to lactate, to produce large amounts of energy, even if the oxygen content is normal (4). This transformation of glucose utilization from oxidative phosphorylation (OXPHOS) is called glycolysis and is predominantly characterized by increased rates of glucose uptake and lactate production. Glycolysis produces ATP in quantities smaller than those of OXPHOS but may be up to 100 times more efficient, which, in turn, promotes higher glycolytic activity (5). This low-yield and high-rate glycolysis mode not only generates the ATP required, but also produces more substances such as nicotinamide adenine dinucleotide (NADPH), which are required for glycogen, protein, and nucleotide synthesis, thereby allowing cells to quickly adapt to energy- and nutrient-deficient microenvironments.

2 OC tumor microenvironment

The tumor microenvironment (TME) is ecologically complex because it contains various growth factors, chemokines, cytokines, and angiogenic factors, and it plays a crucial role in cancer. In the TME, cancer cells require increased glycolytic activity to compensate for the large amounts of energy and nutrients that their abnormal metabolism requires.

Lactate, which is the end product of glycolysis, is an immunomodulatory compound that can be absorbed by endothelial cells (6) and related fibroblasts, triggering the production of multiple cytokines and vascular endothelial growth factor and promoting OC invasion, metastasis, and drug resistance (Figure 1). The overproduction of lactic acid leads to acidification of the TME, forming an immunosuppressive microenvironment, which is a key mechanism of cellular immune escape. Lactate is also the main energy source of mitochondrial metabolism, which is involved in inhibiting the proliferation of immune effector cells and inducing immune cell dedifferentiation (7, 8). In addition, lactate has been reported to not only reduce the activity of natural killer (NK) cells and natural killer T (NKT) cells (9), but also promote the proliferation of T lymphocytes and accelerate the establishment of immunosuppressive microenvironment. Furthermore, lactate can affect the growth and apoptosis of cancer cells by regulating the function of tumor-associated macrophages (TAM). TAM can be divided into two subtypes—M1 and M2—according to their activated phenotype. The M1 TAM are proinflammatory macrophages that are dependent on glycolysis and inhibit the proliferation of cancer cells; the M2 type are anti-inflammatory macrophages that rely on oxidative phosphorylation to promote the proliferation and metastasis of cancer cells. Lactate was found to induce TAM polarization to the M2 phenotype and promote tumor growth in the TME (10).

Numerous studies have shown that glycolysis (11) can participate in multiple stages of OC development by promoting cancer cell proliferation, invasion, metastasis, and chemoresistance, and thus influencing prognosis. Liu et al. (12) found that enhanced glycolytic activity was linked to poor prognosis in OC and a low survival rate. Inhibitors of phosphoglycerate kinase (PGK1), which can serve as an independent risk factor for OC survival and prognosis (13), reduce epithelial–mesenchymal transition (EMT) and reverse the glycolytic effect, which, in turn, reduces the capacity of OC cells to migrate and invade. Phosphoglycerate mutase (PGAM1) can mediate the synthesis of lactate and pyruvate and participate in regulating the resistance of OC cells to the chemotherapy drug paclitaxel (14). In addition, Bi et al. (15) finding in constructing a prognostic model of OC associated with glycolysis that gene characteristics are related to the TME, especially immune cell infiltration and expression of immune-related genes, which can be used as a potential therapeutic target for OC. Overexpression of mitochondrial elongation factor 2 (MIEF2) can promote the transformation of OC from OXPHOS to glycolysis (16), whereas inhibiting the expression of MIEF2 may induce cell cycle arrest and apoptosis. In addition, metabolic intermediates produced during glycolysis can be used for macromolecular biosynthesis in cancer progression. It was reported (17) that downregulation of glucose-6-phosphate isomerase, fructose-bisphosphate aldolase, lactate dehydrogenase (LDH), and phosphoglycerate kinase (PGK1) expression was directly correlated with drug resistance in the established OC cisplatin-resistant cell line A2780-DR, and overexpression of Ras-related proteins enhanced the sensitivity of these cells to cisplatin therapy. The long-chain coding RNA NRCP (18) leads to the overexpression of downstream glucose-6-phosphate isomerase, which increases sensitivity to cisplatin when targeting siRNAs with NRCP using DOPC nanoliposomes. In the OC A2780 cell line, sphingosine kinase-1 (SK1) is a crucial enzyme in a metabolic pathway that supports macromolecular biosynthesis (19). This finding was demonstrated by upregulated expression of the proton/monocarboxylic acid transporter MCT1 and GLUT3, increased lactate production, and activation of the AKT pathway.

Recently, the role of glycolysis in OC has received much attention, with glycolysis being a marker of OC progression and a potential therapeutic target. Glycolysis inhibitors, traditional Chinese medicine (TCM) ingredients, and chemotherapy drugs have been reported to affect the incidence and progression of OC by knocking down or reversing glycolysis activity. However, there are no systematic studies and discussions on how glycolysis regulates and influences the progression and treatment of OC. Therefore, we summarize the roles of several key enzymes, signaling pathways, cellular transcription factors, and non-coding RNAs (ncRNAs) involved in glycolysis in OC to supply novel insights for the treatment of this malignancy.

3 Key enzymes of glycolysis as potential targets for OC

During the progression of cancer, the increase of glycolysis enzyme activity is proportional to the rate of glycolysis. The rate-limiting enzymes of the glycolysis pathway are HK, PFK, and PKM

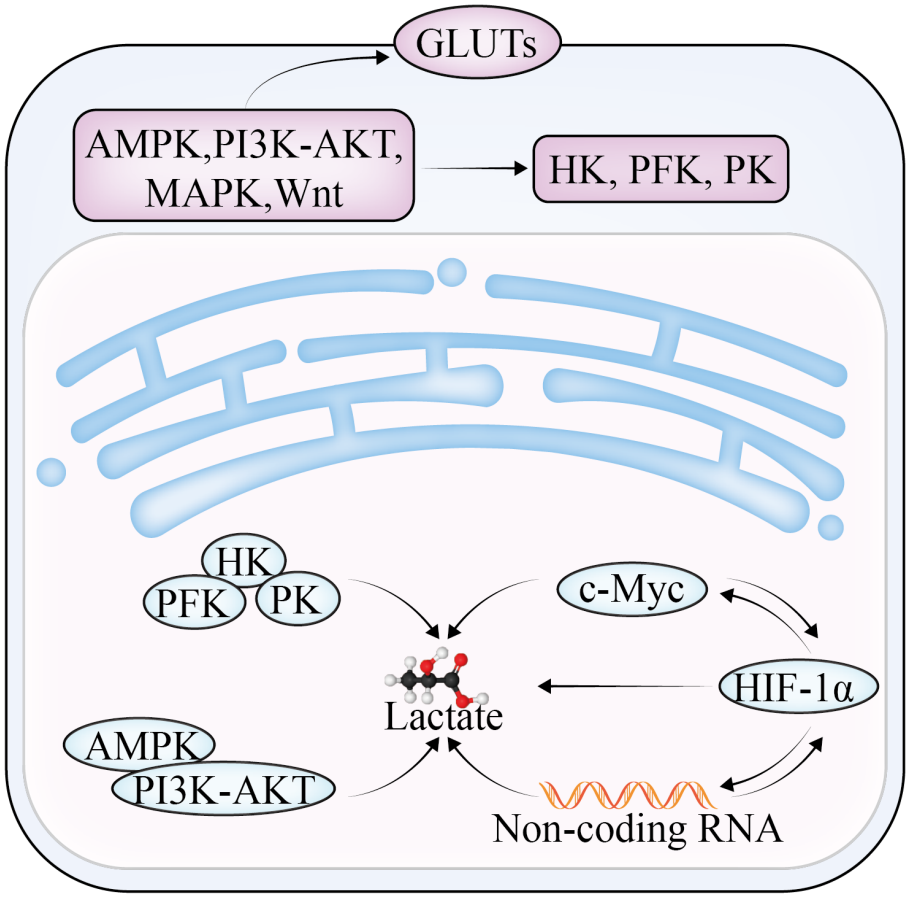

FIGURE 1
The regulatory mechanism of lactate in glycolysis in OC.

(Figure 2). Changes in the activities of these enzymes play a key role in the pathogenesis of OC consequently, the enzymes can be used as prognostic indicators and therapeutic targets of OC.

3.1 Hexokinase

The first rate-limiting enzyme in the glycolytic pathway is HK, which converts glucose into glucose 6-phosphate (G-6-P) through phosphorylation and is a key molecule regulating cell energy metabolism.HK consists of five major isoforms: HK1, HK2, HK3, HK4, and HKDC1. HK1 is mainly found in the brain. HK2 predominantly exists in insulin-sensitive tissues and tumor cells, and its functions include metabolic rewiring of glycolysis, regulation of autophagy, and shielding from cell death stimulation. HK3 is mainly distributed in the bone marrow, lungs, and spleen. HK4 can regulate insulin secretion, glucose uptake, and glycogen synthesis and decomposition in the liver. HKDC1, a recently discovered isozyme, is adjacent to the HK1 gene.

In OC, the increase in HK activity is related to the overexpression of HK2, especially in ascites (20) and metastatic foci. HK2 can control lactate production and promote OC metastasis through the expression of MMP9/NANOG/SOX9 mediated by the FAK/ERK1/2 signaling pathway. The increased activity of HK2 can also participate in angiogenesis. HK2 (21) is influenced by several signaling pathways and transcription factors, including PI3K/AKT, FAK/ERK1/2, HIF-1, RAS, and STAT2. Zhang et al. (22) found that DNMT3A can promote glucose consumption and lactate production by upregulating the expression of HK2 and PKM2. CRMP2 (23) can affect angiogenesis by activating the expression of HIF-1 and HK2. Lysophosphatidic acid, a blood-derived lipid medium, is abundant in the ascites of patients with OC, and was found to selectively upregulate HK2 (24), subsequently inducing cell proliferation and enhancing the glycolysis rate and lactate production. HK2 levels are also regulated by microRNA (miRNA) after transcription. Tuo et al. (25) reported that miR-532-3p inhibited OC cell proliferation and invasion through the GPNMB/HIF-1α/HK2 axis. In addition, BRCA1 (26) deficiency can increase glycolytic activity by inducing the transcription factors MYC and STAT3 to activate HK2 expression. Meanwhile, BRCA1 deficiency decreases fatty acid oxidation, enhances triphosphopyridine nucleotide generation, and participates in the upregulation of OXPHOS via the pentose phosphate pathway. This upregulation of HK2 induced by BRCA1 deficiency could be partially reversed by aspirin.

In summary, HK2 is closely related to the energy metabolism, proliferation and invasion, lactate production, and angiogenesis of OC cells, and may be an OC prognostic indicator and treatment target.

10.3389/fimmu.2023.1284853

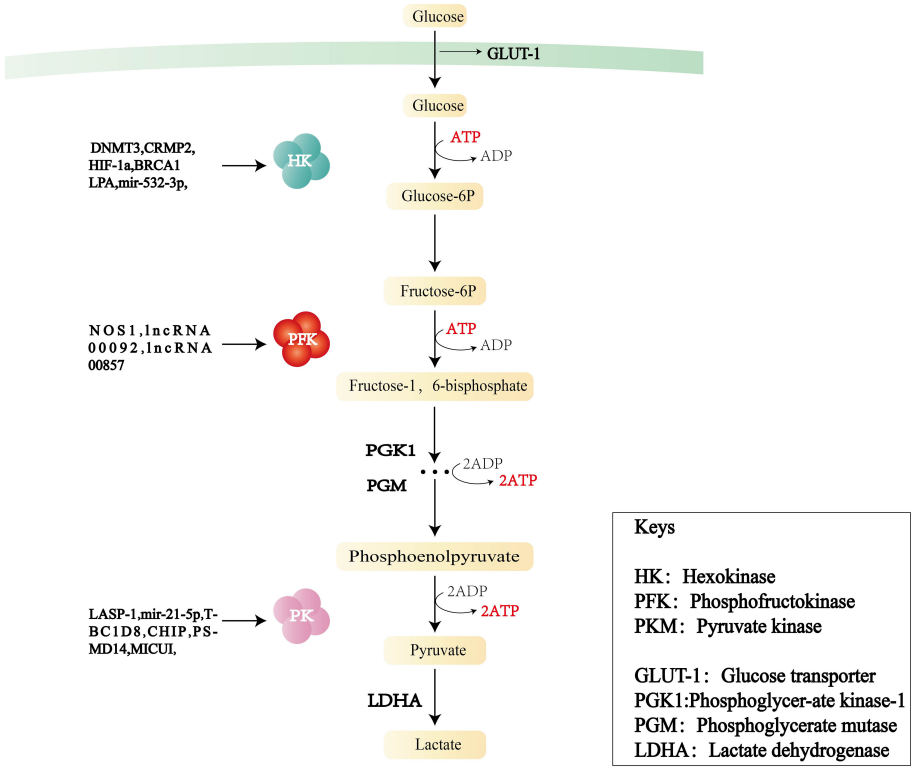

FIGURE 2
Flowchart of glycolysis and the role of three key enzymes—hexokinase (HK), phosphofructokinase (PFK), and pyruvate kinase (PKM)—in OC.

3.2 Phosphofructokinase

Fructose-6-phosphate kinase 1 (PFK1) is the second rate-limiting enzyme of the glycolytic pathway. It catalyzes the conversion of fructose 6-phosphate to fructose-1,6-fructose diphosphate. This irreversible step determines the rate and level of glycolysis and is the critical regulation point in the glycolysis process. PFK1 acts in the form of a homomeric or heteromorphic tetramer, including catalytic sites and regulatory sites of allosteric effectors. When the concentration of ATP is high, it can bind to the regulatory site, change the conformation of the enzyme, and prevent ATP from binding to the catalytic site, resulting in a decrease in enzyme activity. PFK2 is a bifunctional protein: in the non-phosphorylated state, it has the function of a kinase, phosphorylating fructose 6-phosphate(f-6p) to produce fructose-2,6-bisphosphate (F-2,6-BP), whereas in the phosphorylated state, it transforms into a phosphatase and catalyzes the conversion of 2-6 diphosphate fructose to 6-phosphate fructose. In addition, F-2,6-BP —a key activator of PFK1–is produced by PFKB2 (27); it is a product of f-6p catalyzed by PFKB3 (28), participates in the glycolytic process, and is also regulated and maintained by the dual action of phosphorylation and dephosphorylation by PFKB4.

The PFK family and its metabolites are instrumental in the regulation of glycolysis. High PFK activity is associated with poor metastasis or poorer survival. Jiang (29) et al. demonstrated that PFKB3 was associated with advanced/graded OC and adverse outcomes in experiments conducted both *in vivo* and *in vitro*. PFKM (muscle type) is one of the three isoforms of PFK expressed in most mammals. Endogenous nitride NOS1 (30) has been confirmed to engage in OC metabolic reprogramming by inducing the s-nitrosylation of PFKM at Cys351 to stabilize the tetramerization of PFKM, thereby resisting the negative feedback of downstream metabolic intermediates, leading to an increase in glycolysis and the tricarboxylic acid cycle. Long non-coding RNA (LINC RNA)00092 (31) serves as a key node for cancer-associated fibroblast (CAF)-mediated metastasis. Further studies revealed that CXCL14, a pro-mediator secreted in CAF, induced LINC RNA00092 to bind to PFKFB2 to promote OC metastasis. Moreover, the PFK family has an impact on OC chemoresistance. The activity of PFKFB3 is positively correlated with OC chemoresistance and lipid droplet biogenesis (32), and its inhibitor, PFK-158, targets glycolytic and adipogenic pathways, making chemoresistant cells sensitive to drug-induced cytotoxicity. Yap is a transcriptional activator encoded by paralogous genes and regulated by the Hippo pathway. The lncRNA 00857 can upregulate YAP1 in the Hippo signaling pathway by competitively binding miR-486-5p, thereby enhancing glycolytic activity and promoting the proliferation and migration of OC cells (33). Research (34) has shown that PFK1 and F-1,6-BP can promote positive feedback loops in the phosphatidylinositol 3-kinase (PI3K) and/or YAP/TAZ signaling pathways. Targeting PFK1 and its product F-1,6-BP can improve the clinical efficacy of PI3K and/or YAP/TAZ inhibitors in practice.

3.3 Pyruvate kinase

PK is the final rate-limiting enzyme of the glycolytic pathway and catalyzes the conversion of phosphoenolpyruvate to pyruvate with concomitant production of ATP. PK comprises four isoforms: L, R, M1, and M2. PKM2 is the major isoform in proliferating cells and plays a key role in the direct regulation of gene expression and pre-cyclic cellular expression. PKM2 exists in tetrameric and dimeric forms. The tetramer has high catalytic activity and can rapidly convert phosphoenolpyruvate to pyruvate, increasing glycolytic yield and generating more ATP. The dimer has low catalytic activity and can be translocated into the nucleus, acting as a coactivator of HIF-1, NF-κB, STAT3, and PISK-AKT, and promoting the transcription of target genes, positive feedback regulation of glycolysis, and angiogenesis. The ratio between the tetrameric and dimeric forms determines PKM2 activity and the glycolysis flux of catabolism or anabolism. In addition, PKM2 mutants exist mainly as dimers, and their overexpression promotes cell proliferation.

PK affects tumor cell growth, invasion, and angiogenesis, and could be a potential therapeutic target for OC. Evidence suggests (35) that disruption of pyruvate dehydrogenase (PDH) phosphorylation to PDK (PDK–PDH axis) may affect OC progression and chemotherapy resistance. MICU1 regulates mitochondrial free Ca^{2+}, and its overexpression is a feature of many cancers. Silencing MICU1 (36) stimulates PDK to activate PDH, reduces lactate production, and increases cisplatin efficacy. When LIM and SH3 protein 1 (LASP-1) (37) is downregulated, it may affect zyxin proteins through the upregulation of PK, inducing G2 phase accumulation in SKOV3 cells (a human OC cell line) and thereby reducing tumor growth and invasion. Pyruvate dehydrogenase kinase 1 (PDK1) (38) blocking the trigger factor is a symbol of cancer cell metabolic changes *in vitro*. Furthermore, silencing PDK1 can reduce angiogenesis and increase tumor cell necrosis in OC316 and OVCAR3 tumor models. In addition, PDHA1 is a carrier gene for an important subunit of PDK1. Exosomal miR-21-5p (39) promotes cell viability and glycolysis and inhibits the chemical sensitivity of SKOV3 progenitor cells by inhibiting PDHA1. Follicle-stimulating hormone has been shown to regulate cellular metabolism in patients with OC, and further studies (40) found that follicle-stimulating hormone increased PKM2 expression in cells by promoting anabolism, which enhanced OC proliferation. CHIP (41), which is an E3 ligase that mediates PKM2 degradation, downregulates PKM2 by promoting its ubiquitination and degradation. Overexpression of CHIP reduces the production of pyruvate and lactate, and thus reduces glycolysis. CHIP can also affect glycolysis by influencing PKM2 nuclear translocation. TBC1D8 (42) reduces PK activity by binding to PKM2 and hindering PKM2 tetramerization while promoting PKM2 nuclear translocation, thereby inducing the expression of genes involved in glucose metabolism and the cell cycle. PSMD14 (43) downregulates PKM2 by decreasing ubiquitylation of the K63 connection on PKM2. This action downregulates the ratio of PKM2 tetramers to dimers and monomers to reduce PK activity while promoting nuclear translocation of PKM2 to enhance transcription of downstream oncogenes, which, in turn, stimulates malignant progression of OC. Moreover, the PSMD14 inhibitor O-phenanthroline inhibits the colony formation and growth of OC cells in a concentration-dependent manner.

4 Interplay of signaling pathway and OC

With the deepening of research on the pathogenesis of cancer at the molecular level, glycolysis is considered to be the main metabolic phenotype of cancer. In this section, we summarize the research on signaling pathways involved in glycolysis and OC, including PI3K/AKT, MAPK, Wnt, and AMPK signaling pathways (Figure 3).

4.1 AMPK

AMPK is a highly conserved serine/threonine kinase that regulates cellular homeostasis by modulating the ratio of ATP to ADP and plays a pivotal role in the regulation of cellular energy homeostasis, including glucose, protein, and lipid metabolism and autophagy. There are numerous AMPK-related proteins, including salt-inducible kinase (SIK1), QIK (also known as SIK2), QSK (also known as SIK3 kinase), and maternal embryonic leucine zipper kinase proteins. AMPK proteins participate in various reproductive physiological functions, including follicle maturation, menopause, embryogenesis, and oocyte maturation. As a cellular energy receptor, AMPK responds to low levels of ATP and, upon its activation, positively regulates signaling pathways that replenish cellular ATP supply. Glycolytic activity is also associated with the energy state of cells. When the intracellular ATP level is high, HK, PFK, and PKM are inhibited by excess glucose 6-phosphate, citrate, and ATP, respectively, which reduces glycolysis activity; conversely, when ATP is insufficient in the body, glycolysis can be activated through ADP to remove the inhibition of ATP on PFK-1, F-1,6-BP to activate PK, as well as on F-2,6-BP to activate PFK-1.

AMPK dysfunction has a critical role in growth, proliferation, metastasis, and invasion in OC. Gao et al. (44) reported that SIK2 not only promotes mitochondrial fission and inhibits mitochondrial OXPHOS by phosphorylating the serine 616 (Ser616) site of Drp1 but also upregulates HIF-1 by activating the PI3K/AKT signaling pathway. SIK2 can directly activate the transcription of major genes of glycolysis and promote glycolysis. In addition, transient receptor potential 7 (TRPM7) may be a potential interventional therapy target for OC (45). When TRPM7 is silenced, ubiquitination degradation of HIF-1α and AMPK activation are enhanced in OC, which results in the conversion of glycolysis to OXPHOS and consequently inhibits OC proliferation. For OC treatment, the herbal extract resveratrol upregulates AMPK expression, and reduces mTOR expression and activation to inhibit glycolysis in OC cells. AMPK activators (46) not only prevent cancer progression and metastasis but also have a significant effect in improving the efficacy of cisplatin in OC.

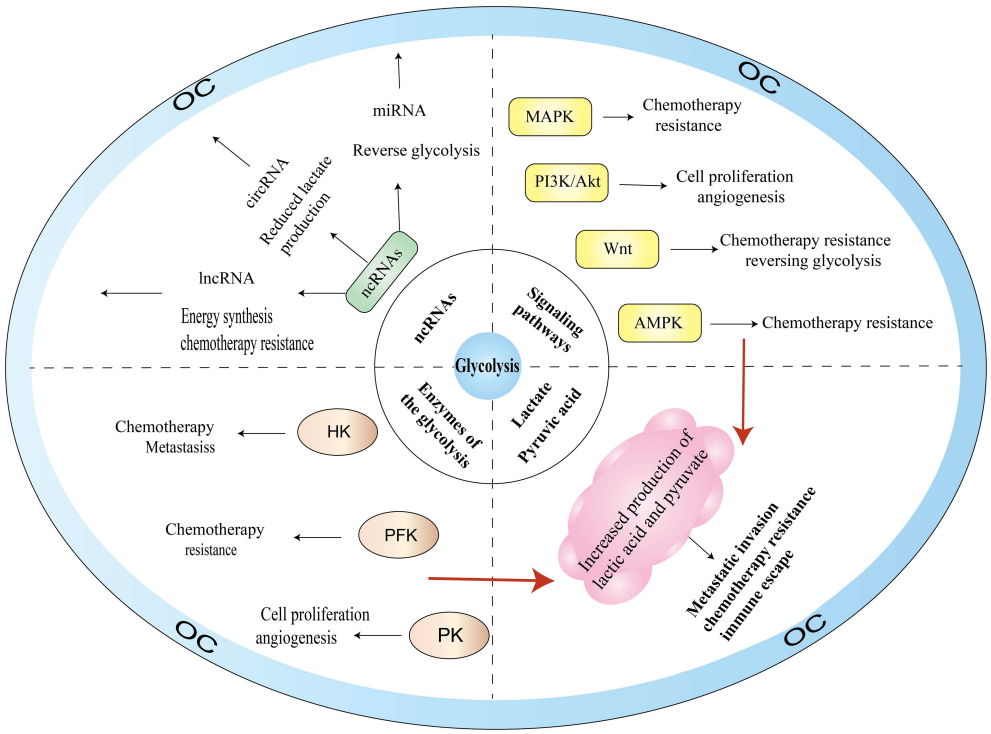

FIGURE 3
Glycolysis-related pathogenesis of OC.

4.2 PI3K-AKT

PI3K is a dimerized object complex consisting of catalytic and regulatory subunits and includes three major types of lipid kinases—class I (IA and IB), class II, and class III—plus a group of distant relatives that are sometimes referred to as class IV. The level of glycolysis can be affected by oncogenes or tumor suppressor genes directly or indirectly, regulating gene expression and enzyme activity. AKT, as a proto-oncogene, is a serine/threonine protein kinase that can be directly activated by PI3K and inhibits or enhances the activity of target proteins through phosphorylation. Thus, AKT regulates the downstream pathways of mTOR, VEGF, MAPK, and glycolysis, and plays an essential part in the proliferation and survival of the cells, transcription, and protein synthesis. PI3K-AKT signaling (47) is mediated by serine or threonine phosphorylation of a series of downstream substrates and affects cell proliferation and apoptosis, glucose homeostasis, angiogenesis, and invasive metastasis.

The PI3K-AKT signaling pathway regulates OC glycolysis through various mechanisms. First, the PI3K-AKT pathway can regulate the activity and expression of some glycolytic enzymes such as HK2, PFK, and PK. Jia et al. (48) found that the oncogene ACTL6A not only mediated glucose utilization, lactate generation, and pyruvate levels by regulating PGK1, but was also upregulated by follicle-stimulating hormone through the PI3K/AKT pathway, which promoted OC glycolysis. YWHAZ (also known as 14-3-3ζ) (49) affects the glucose uptake rate of OC by downregulating PI3K/AKT phosphorylation. Second, the regulation of glycolytic enzyme expression can be mediated by PI3K-AKT through its modulation of AMPK and HIF expression. Creatine kinase B is a cell membrane isoform of creatine kinase (50). Knockdown of creatine kinase B induces cell cycle G2 arrest by enhancing p21 expression and influencing the pathways of PI3K/AKT and AMPK. These actions decrease the generation of lactate and the consumption of glucose, enhance the generation of reactive oxygen species (ROS) and the consumption of oxygen, and thus inhibit OC cell growth and induce apoptosis, making the OC cells more sensitive to chemotherapeutic drugs. Third, PI3K-AKT activates downstream regulators such as mTOR and VEGF, thereby promoting glycolysis and angiogenesis in OC. AKT is one of the downstream targets of epidermal growth factor receptor, which is overexpressed in approximately 70% of OC cases. Epidermal growth factor receptor is closely linked to metastasis, angiogenesis, and pro-apoptotic and pro-survival signaling levels. FBN1 (51) activates its downstream AKT pathway by mediating the phosphorylation of vascular endothelial growth factor receptor 2 (VEGFR2) and induces the phosphorylation of STAT2 involved in glycolysis and angiogenesis, leading to OC cell chemotherapy tolerance. In addition, FBN1 treatment combined with apatinib enhances OC chemosensitivity.

4.3 MAPK

The MAPK signaling pathways are critical for cell proliferation, differentiation, apoptosis, and stress response under normal and pathological conditions. MAPKs consist of four subfamilies—ERK, p38, JNK, and BMK1—and are evolutionarily conserved serine-threonine kinases. Currently, the most widely studied pathway in

the MAPK family is the Ras-Raf-MEK-ERK signaling pathway. Ras activation can produce effects with several downstream proteins, including AF6, PI3K, PLCε, and Raf. For example, Ras-GTP causes RAF protein to be phosphorylated, and the activated RAF kinase binds to the downstream MEK1/2 and subsequently activates ERK1/2. Activated ERK1/2 induces the expression of genes related to the cell cycle and proliferation and phosphorylates various kinases for OC cell proliferation and adhesion.

ERK1/2 is the only downstream target of MEK kinase, and ERK inhibitors can effectively block the Ras-Raf-MEK-ERK signaling pathway while effectively reversing chemotherapy resistance caused by upstream BRAF and MEK mutations. Sirt6 (52), which is an important oncogenic factor, was found to regulate the ERK1/2-driven phosphorylation of Drp1at Ser616, regulating mitochondrial function, cell invasion, cell proliferation, and glycolysis in OC cells. In addition, the lncRNA AB073614, which is correlated with poor survival in patients with OC, may exert oncogenic effects on OC cells by modulating ERK1/2-mediated signaling pathways (53). Snail (54) is a key inducer of OC EMT and was found to enhance OC sensitivity to chemotherapy by inhibiting phosphorylated ERK and thus inhibiting the glycolytic pathway. Collectively, these findings provide further support for the glycolytic therapy of OC, wherein targeting MAPKs may become a therapeutic strategy.

4.4 Wnt

The Wnt signaling pathways are involved in cell growth, development, proliferation, stem cell renewal, angiogenesis, chemotherapy resistance, and immune escape, and are among the critical pathways for promoting OC progression. Wnt/β-catenin is the classical Wnt signaling pathway and consists of the transmembrane receptors of the Frizzled family, CK1, GSK3, and Axin, and the TCF/LEF family of transcription factors. This pathway flips β-catenin intracellularly, and when the cell is not stimulated by Wnt signaling, the cytoplasmic casein kinase CK1a, the glycogen synthase kinase GSK3β, the scaffolding protein Axin, and the adenomatous polyposis coli protein form a destructive complex, with β-catenin at serine residues 45, 33, and 37 (Ser45, Ser33, and Ser37) first by GSK3β phosphorylation and then by CK1a. β-Catenin is eventually degraded by ubiquitination modification via E3 ubiquitin ligase, preventing the nuclear translocation of Wnt/β-catenin.

The mechanism of Wnt signaling to regulate glycolysis in OC can be summarized as follows. First, Wnt regulates the transcription of multiple glycolytic enzymes, including lactate dehydrogenase A (LDHA), pyruvate carboxylase, HK2, PFKB3, and PKM. The lncRNA HOXB-AS3, which regulates glycolysis by downregulating miR-378a-3p targeting LDHA, also activates the Wnt/β-catenin pathway and enhances EMT, decreasing OC cell proliferation and enhancing cisplatin sensitivity (55). TNKS (56), an oncogenic regulator of OC, upregulates pyruvate carboxylase to promote aerobic glycolysis by activating Wnt/β-catenin/snail signaling. The inhibition of TNKS activity not only blocks the cell cycle and induces apoptosis, but also enhances the drug sensitivity of OC. Second, Wnt influences OC progression and therapeutic resistance by regulating the multifunctional differentiation and regeneration of cancer stem cells. Cancer stem cells are a class of tumor cells with self-renewal capacity and are considered to be a major source of drug resistance, cancer recurrence, and metastasis. The miR-1180 released by bone marrow stromal stem cells (57) enhances chemoresistance in OC by activating the downstream components of the Wnt signaling pathway (i.e., Wnt5a and β-linked proteins) and upregulating glycolysis levels. Third, Wnt affects the TME and EMT to promote tumor development. Intraperitoneal (58) delivery of 188Re liposome therapy has been reported to block EMT and reactivate p53 function, shifting the metabolic state from glycolysis to OXPHOS and controlling tumor cell growth.

5 Transcription factors and OC

5.1 c-Myc

Transcription factors play a key regulatory role in OC. Among them, c-Myc is involved in the regulation of cell proliferation, the cell cycle and metabolic reprogramming, and is a vital oncogene in glycolysis in OC. Many studies have shown that overexpression of c-Myc is significantly associated with poor prognosis in patients. c-Myc is a helix-loop-helix leucine zipper transcription factor that closely links cell metabolism with the occurrence and development of tumors. Under normal oxygen conditions, c-Myc (59) can directly promote glycolysis activity through LDHA. c-Myc can also promote the expression of Glut1, PKM, and HK2, and promote glycolytic activity. Furthermore, c-Myc can synergistically act with HIF-1 on PDK1 to promote the conversion of glucose to lactate. It has been reported that fructose-1,6-bisphosphatase 1 (FBP1) is an important target gene of c-Myc, and knockdown of FBP1 significantly reverses the low expression of c-Myc, increases glucose consumption and lactate production, and promotes OC progression and cisplatin resistance (60). The serine/threonine kinase PIM1 (61) activates the expression of PGK1 and LDHA by mediating c-Myc phosphorylation, which regulates glycolysis, and the PIM1 inhibitor SMI4a induces chemical sensitization of cisplatin. In addition, c-Myc is closely linked to other transcription factors and signaling pathways, such as HIF-1a, the Wnt signaling pathway, and the ERK signaling pathway. For example, HK2 (62) promotes OC cell proliferation and tumor formation through Wnt/β-catenin-mediated upregulation of c-Myc. MiR-1180 (57) also can upregulate glycolysis through the activation of Wnt/β-catenin and c-Myc, thus enhancing the chemotherapy resistance of OC cells. Based on the key role of c-Myc and glycolytic interactions in OC tumorigenesis, c-Myc may be a promising therapeutic target.

5.2 HIF-1a

Hypoxia (63) is a prominent feature of the TME and is positively correlated with tumor cell growth and metastasis, angiogenesis, and chemoresistance. HIF is a transcription factor in the nucleus that promotes cellular adaptation to hypoxic environments, and includes

HIF-1a, HIF-2a, and HIF-3a. HIF-1a is overexpressed in OC and holds a prominent position in multiple pathways of OC development. HIF-1a can regulate the transcription of various genes, including erythropoietin, Glut1, HK2, PFK1, PKM, and VEGF, which promotes the rate of glucose uptake or lactate production. In addition, intracellular ATP is a key determinant of chemoresistance. Under hypoxic conditions, glycolysis is the main energy production pathway, and sensitizing cancer cells requires depletion of intracellular ATP by inhibiting glycolysis.

HIF-1a is frequently upregulated in OC, and its inhibition is an effective strategy for treating OC, including inhibiting glycolysis and improving platinum resistance. After interacting with CAFs, OC cells can mobilize glycogen as an energy source, playing a crucial role in cancer progression, metastasis, and treatment resistance (64). Lysophosphatidic acid, which is a lipid growth factor and GPCR ligand, was found to stimulate aerobic glycolysis in cancer cells by inducing a pseudo-hypoxic response via upregulation of HIF1α levels (65); this response is involved in the transition of normal fibroblasts to a CAF phenotype. Another study found that lysophosphatidic acid (66) stimulates a pseudo-hypoxic response through Rac-mediated activation of triphosphopyridine nucleotide oxidase and ROS production, which activates HIF-1α, induces Glut1 and HKII expression, and affects the metabolic reprogramming of OC cells. Overexpression of the lncRNA GHET1 (67) promotes glucose uptake and lactate production in OC by blocking HIF-1α degradation and upregulating the protein level of HIF-1α, ultimately leading to proliferation and colony formation. Conversely, inhibiting GHET1 induces G1 cell cycle arrest and apoptosis. In addition, lactate has been shown to stabilize HIF1α in the stroma, leading to increased production of proangiogenic cytokines. Ai et al. (68) showed that degradation of HIF-1 converts aerobic glycolysis to mitochondrial OXPHOS in platinum-resistant cells, resulting in overproduction of ROS and induction of apoptosis. Cryptotanshinone (69) inhibits glucose uptake and lactate production by inhibiting the STAT3/SIRT3/HIF-1a signaling pathway. Ginsenoside (70) inhibits the HIF-1α-stimulated Warburg effect in OC via the regeneration of DNMT3A-mediated upregulation of miR-519a-5p by DNA methylation. The HIF-1α inhibitor EF24 (71) blocks the response to glucose uptake, the rate of glycolysis, and lactic acid production by downregulating GLUT-1 expression and thereby reversing the OC glycolytic effects. Therefore, targeting HIF-1α/cisplatin in combination with HIF-1α inhibitors or degraders could provide a new opportunity for the treatment of individuals with platinum-resistant cancers.

5.3 Non-coding RNA

Non-coding RNA (ncRNA) accounts for over 90% of the human genome, from which it is transcribed as protein-free RNA. NcRNAs engage in a variety of biological processes including development, proliferation, post-transcriptional modification, apoptosis, and cell metabolism. ncRNAs can be divided into lncRNA, miRNA, and circular RNA (circ RNA). LncRNAs, which are more than 200 nucleotides in length, have a broad variety of functions, such as transcriptional regulation and modulation of gene expression, and are considered potential targets for diagnosis and therapy. In addition, lncRNAs participate in the glycolytic pathway through HKII, PFK, PKM, Glut1, and c-Myc and associated signaling pathways to regulate energy metabolism in tumors. MiRNAs are approximately 22 to 23 nucleotides in length, and more than 60% of coding genes are potential regulatory targets for miRNAs. In terms of glycolysis, miRNAs can target key enzymes in glucose catabolism and ATP production in beta cells (72). CircRNAs are single-stranded circular RNA molecules involved in regulating transcription or influencing gene expression.

ncRNAs can regulate OC glycolysis through the glycolytic enzymes or various signaling pathways (Table 1). Overexpression or reduced expression of ncRNA molecules can affect OC energy synthesis, translocation, and the progression of drug resistance by regulating glycolytic activity. In addition, lncRNAs act as "sponges" that can competitively bind to miRNAs and reduce the inhibition of target genes by miRNAs. The lncRNA NEAT1 (73) can directly target BZW1 through the target mir-4500 to upregulate the glycolytic activity of OC cells *in vivo*, which can contribute to the proliferation and colony formation of OC. The lncRNA oiP5-aS1 (74) can upregulate CCNG1 by targeting mir-128 and plays a tumorigenic role in the development of OC. Decreased expression of lncRNA 00504 (75) simultaneously reduces the expression of PKM2, HK2, and PDK1, and alters aerobic glycolysis in OC. The circ_0025033 (76) inhibits glucose consumption and lactate generation by targeting miR-184 to upregulate LSM4 expression. Lin and colleagues found that the circRNA ITCH (77) regulates the level of CDH1 protein by targeting miR-106a to inhibit proliferation, invasion, and glycolysis and promote apoptosis of OC cells. Another study found that miRNA-195 (78) could increase Ca^{2+} uptake, reverse glycolysis, and improve OC survival time by inhibiting MICU1 expression in OC. Furthermore, miR-383 (79) can directly target LDHA to inhibit the aerobic glycolysis of OC cells and inhibit cell proliferation and invasion. Notch is another signaling pathway involved in OC cell proliferation, invasion, metastasis, and angiogenesis. Ezh2 (80) is a central target and sensor for glycolytic metabolism in the TME, with multifunctional and anti-apoptotic properties. It can be restricted by the high expression of miRNA101 and miRNA26a, and can directly bind to Notch signaling pathway inhibitors, activate the Notch pathway, stimulate the expression of multifunctional cytokines in T cells and promote their activation, and control effector T cell multifunctionality and survival through Bcl-2 signaling.

6 Treatment

Currently, there are various herbal components and chemotherapeutic agents that target glycolytic enzymes or regulatory factors for the treatment of OC. Ginsenoside (20(s)-Rg3) is an antitumor complex extracted from the TCM ginseng (81) and can be used to effectively inhibit glycolysis by inducing the STAT3/HK2 pathway in OC cells. Cardamonin (82) can participate in autophagy in OC cells, inhibit the glycolysis-mediated activation of AMPK, inhibit the activity of HK2 and LDHA, and reduce

TABLE 1 Target sites of ncRNAs in OC glycolysis.

ncRNA	Target	Involvement of other factors	Function	Reference
lncRNA NEAT1	mir-4500	BZW1	Upregulate	(75)
lncRNA 00504	PKM2, HK2, PDK1	miR-1244	Downregulate	(33)
lncRNA 00857	YAP1	miR-486-5p	Upregulate	(18)
lncRNA NRCP	PFKB3		Upregulate	(80)
miRNA101/miRNA26a	EZH2	Bcl-2	Downregulate	(36)
miR-532-3p	MICU1	HIF-1a	Downregulate	(78)
miRNA-195	LDHA	Ca^{2+}	Downregulate	(55)
lncRNA HOXB-AS3	LDHA	miR-378a-3p	Downregulate	(76)
circ_0025033	miR-184	LSM4	Downregulate	(73)
lncRNA GEHT1	HIF-1a	LDHA	Upregulate	(31)
lncRNA 00092	PFKB2		Upregulate	(53)
lncRNA AB073614	ERK1/2		Downregulate	(74)
lncRNA oiP5-aS1		Mir-128	Upregulate	(77)
circRNA ITCH		miR-106a	Downregulate	(79)
miRNA-383	LDHA		Downregulate	(80)

mTORC1 signaling activation and HK2 expression, which, in turn, reduces the secretion of lactic acid and the production of ATP. The coumarin compound DIC (83) was reported to effectively inhibit pyruvate dehydrogenase kinase (PDK) activity, shift glucose metabolism from glycolysis to OXPHOS, generate higher levels of reactive oxygen species (ROS), attenuate mitochondrial membrane potential, and induce apoptosis. Meanwhile, resveratrol (84) inhibits AKT and mTOR signaling, and decreases glucose uptake and lactic acid production. In addition, resveratrol (85) can activate AMPK and inhibit its phosphorylation, thereby inhibiting the proliferation, migration, and invasion of OC cells and promoting apoptosis of these cells. Baicalein can inhibit the rate of glycolysis by regulating the expression of PGM, HK2, and PDHK1, which are key genes downstream of p53. Heme (86) is an essential cofactor for the electron transport chain and the enzyme ATP synthase in mitochondrial OXPHOS. Enhancement of heme synthesis by exogenous supplementation with the heme precursor 5-aminolevulinic acid reduces HK2 transcription and inhibits glycolysis. The chemotherapy drug isoflurane (87) induces overexpression of HK2, PKM2, and LDHA by promoting the phosphorylation of AKT, leading to an increase in glucose uptake and lactate production, and enhancing the glycolysis rate. A novel PFKB3 inhibitor, 3PO, which enhances the cytotoxic effects of cisplatin on platinum-sensitive and platinum-resistant OC cells, may offer fresh ideas for how to treat OC (88). The PKM2 inhibitor shikonin (89) can inhibit the glycolysis rate, OC growth, and cell migration according to glucose consumption. The Bcl2 inhibitor ABT737 can reverse glycolysis and promote apoptosis through SIRT3-HIF. The receptor tyrosine kinase AXL (90) is thought to be associated with chemoresistance in OC, and studies have confirmed that inhibiting AXL through the phosphorylation of PKM2 not only reduces glucose uptake and lactate production in OC cells, but also enhances the efficacy of cisplatin on OC cells and even reverses cisplatin resistance. Rapamycin (91), which is a macrolide ester produced by *Streptomyces hygroscopicus*, prevents the progression of OC by inhibiting mTOR and blocking the cells in G1 phase. Isopropionolactone (92) effectively targets LDHA, PFK, and HK, glucose consumption and lactic acid production, and is sensitive to cisplatin-induced apoptosis. Thus, targeting glycolytic enzymes, regulatory factors, and signaling pathways may provide another therapeutic approach for OC patients and be a potential therapeutic target.

7 Discussion

Glycolysis is a recognized hallmark of tumorigenesis and has provided new therapeutic ideas in oncological research, especially playing a significant therapeutic role in liver cancer and breast cancer. In recent years, a plethora of studies have shown that aberrant expression of glycolytic enzyme activities can serve as a marker of poor prognosis in OC and is strongly associated with low survival. Among them, enhanced expression of three key enzymes in glycolysis—HK, PFK, and PK—can affect OC proliferation, invasion, and metastasis, angiogenesis, and chemoresistance, and can even reverse the glycolytic effect when their activities are inhibited. Glycolytic enzymes also interact with signaling pathways such as AMPK, MAPK, PI3K-AKT, Wnt to promote the malignant process of OC and increase cell proliferation and invasion, metastatic relapse, and chemoresistance of OC, which may be one of the reasons for the low survival rate of OC. In addition, the glycolytic end product lactate can participate in the

formation of an immunosuppressive microenvironment, which, in turn, affects chemoresistance and immunosuppression. This is consistent with Bi et al. (15) finding in constructing a prognostic model of OC associated with glycolysis that immune cell infiltration and expression of immune-related genes are related to the TME. HIF-1a can induce a hypoxic microenvironment in OC, and when the expression level of HIF-1a is elevated, it facilitates the cells to make full use of the oxygen when they are hypoxic, confirming that TME favors metabolic reprogramming in cancer. In addition, ncRNAs can regulate glycolytic activity to maintain and promote various malignant behaviors in OC, and some of these ncRNAs can also serve as prognostic markers and potential therapeutic targets for OC. However, for patients with early OC, glycolysis detection, diagnosis, and prognosis assessment are still insufficient. TCM monomers and key enzyme inhibitors may open a new window for the clinical treatment of OC. First, glycolysis activity is directly inhibited by targeting the key enzyme activity; second, it reduces glucose uptake and lactic acid production by inhibiting Glut or LDHA levels; and finally, the level of glycolysis can be indirectly regulated via signaling pathway involved in glycolysis. However, although the application of glycolysis inhibitors has been confirmed, there is no evidence suggesting that glycolysis inhibitors or a combination of classical chemotherapy drugs have been put into clinical use. Therefore, large-scale clinical trials of effective inhibitors and/or combination(s) of classical chemotherapeutic agents are needed. This article only reviews the mechanisms of action of key glycolytic enzymes, transcription factors, ncRNAs and signaling pathways in OC. The chemotherapy resistance, immune escape, and specific regulatory mechanisms still need to be explored in depth.

Author contributions

CL: Writing – original draft, Writing – review & editing. F-YL: Supervision, Writing – review & editing. YS: Supervision, Writing – review & editing. YT: Writing – review & editing. F-JH: Funding acquisition, Supervision, Writing – review & editing.

Funding

The author(s) declare financial support was received for the research, authorship, and/or publication of this article. The work was supported by National Natural Science Foundation of China (No. 82074484), National Natural Science Foundation of China (No. 82274566), National Natural Science Foundation of China (No. 82305301).

Acknowledgments

We acknowledge the Charlesworth Group for their expert language polishing services, enhancing the clarity and quality of our manuscript. Thanks to Adobe Illustrator.

Conflict of interest

The authors declare that the research was conducted in the absence of any commercial or financial relationships that could be construed as a potential conflict of interest.

Publisher's note

References

1. Sung H, Ferlay J, Siegel RL, Laversanne M, Soerjomataram I, Jemal A, et al. Global cancer statistics (2020): GLOBOCAN Estimates of Incidence and Mortality Worldwide for 36 Cancers in 185 Countries. *CA Cancer J Clin* (2021) 71:209–49. doi: 10.3322/caac.21660

2. Reid BM, Permuth JB, Sellers TA. Epidemiology of ovarian cancer: a review. *Cancer Biol Med* (2017) 14:9–32. doi: 10.20892/j.issn.2095-3941.2016.0084

3. Hanahan D. Hallmarks of cancer: new dimensions. *Cancer Discov* (2022) 12:31–46. doi: 10.1158/2159-8290.CD-21-1059

4. Locasale JW, Cantley LC. Altered metabolism in cancer. *BMC Biol* (2010) 8:88. doi: 10.1186/1741-7007-8-88

5. Koppenol WH, Bounds PL, Dang CV. Otto Warburg's contributions to current concepts of cancer metabolism. *Nat Rev Cancer* (2011) 11:325. doi: 10.1038/nrc3038

6. Vaupel P, Schmidberger H, Mayer A. The Warburg effect: essential part of metabolic reprogramming and central contributor to cancer progression. *Int J Radiat Biol* (2019) 95:912–9. doi: 10.1080/09553002.2019.1589653

7. Wang JX, Choi SYC, Niu X, Kang N, Xue H, Killam J, et al. Lactic acid and an acidic tumor microenvironment suppress anticancer immunity. *Int J Mol Sci* (2020) 21:8363. doi: 10.3390/ijms21218363:10/gr59gw

8. Choi SY, Collins CC, Gout PW, Wang Y. Cancer-generated lactic acid: a regulatory, immunosuppressive metabolite? *J Pathol vol* (2013) 230:350–5:4. doi: 10.1002/path.4218

9. Kumar A, Pyaram K, Yarosz EL, Hong H, Lyssiotis CA, Giri S, et al. Enhanced oxidative phosphorylation in NKT cells is essential for their survival and function. *Proc Natl Acad Sci USA* (2019) 116(15):7439–48. doi: 10.1073/pnas.1901376116

10. Colegio OR, Chu NQ, Szabo AL, Chu T, Rhebergen AM, Jairam V, et al. Functional polarization of tumour-associated macrophages by tumour-derived lactic acid. *Nature* (2014) 513(7519):559–63. doi: 10.1038/nature13490

11. Fabian C, Koetz L, Favaro E, Indraccolo S, Mueller-Klieser W, Sattler UG. Protein profiles in human ovarian cancer cell lines correspond to their metabolic activity and to metabolic profiles of respective tumor xenografts. *FEBS J* (2012) 279:882–91. doi: 10.1111/j.1742-4658.2012.08479.x

12. Liu YC, Lin P, Zhao YJ, Wu LY, Wu YQ, Peng JB, et al. Pan-cancer analysis of clinical significance and associated molecular features of glycolysis. *Bioengineered* (2021) 12:4233–46. doi: 10.1080/21655979.2021.1955510:10/gmghbw

13. Gou R, Hu Y, Liu O, Dong H, Gao L, Wang S, et al. PGK1 is a key target for anti-glycolytic therapy of ovarian cancer: based on the comprehensive analysis of glycolysis-related genes. *Front Oncol* (2021) 11:682461:10/gr7tqh. doi: 10.3389/fonc.2021.682461:10/gr7tqh

14. Feng Y, Zhang X, Zhang S, Xu S, Chen X, Zhou C, et al. Establishment of new prognostic gene markers related to glycolysis in ovarian cancer and its relationship with immune infiltration of tumor microenvironment PGAM1 promotes glycolytic metabolism and paclitaxel resistance via pyruvic acid production in ovarian cancer cells. *Front Biosci (Landmark Ed)* (2022) 27:262. doi: 10.31083/j.fbl2709262

15. Bi J, Bi F, Pan X, Yang Q. Establishment of a novel glycolysis-related prognostic gene signature for ovarian cancer and its relationships with immune infiltration of the tumor microenvironment. *J Transl Med* (2021) 19(1):382. doi: 10.1186/s12967-021-03057-0

16. Zhao S, Zhang X, Shi Y, Cheng L, Song T, Wu B, et al. MIEF2 over-expression promotes tumor growth and metastasis through reprogramming of glucose metabolism in ovarian cancer. *J Exp Clin Cancer Res CR* (2020) 39:286. doi: 10.1186/s13046-020-01802-9

17. Lixu J, Huo Y, Zheng Z, Jiang X, Deng H, Chen Y, et al. Down-regulation of ras-related protein rab5c-dependent endocytosis and glycolysis in cisplatin-resistant ovarian cancer cell lines. *Mol Cell Proteomics* (2014) 13:3138–51. doi: 10.1074/mcp.M113.033217

18. Rupaimoole R, Lee J, Haemmerle M, Ling H, Previs RA, Pradeep S, et al. Long noncoding RNA ceruloplasmin promotes cancer growth by altering glycolysis. *Cell Rep* (2015) 13:2395–402. doi: 10.1016/j.celrep.2015.11.047

19. Bernacchioni C, Ghini V, Cencetti F, Japtok L, Donati C, Bruni P, et al. NMR metabolomics highlights sphingosine kinase-1 as a new molecular switch in the orchestration of aberrant metabolic phenotype in cancer cells. *Mol Oncol* (2017) 11:517–33. doi: 10.1002/1878-0261.12048

20. Siu MKY, Jiang YX, Wang JJ, Leung THY, Han CY, Tsang BK, et al. Hexokinase 2 regulates ovarian cancer cell migration, invasion and stemness via FAK/ERK1/2/MMP9/NANOG/SOX9 signaling cascades. *Cancers* (2019) 11:813. doi: 10.3390/cancers11060813:10/ghczcr

21. Garcia SN, Guedes RC, Marques MM. Unlocking the potential of HK2 in cancer metabolism and therapeutics. *Curr Med Chem* (2019) 26:7285–322. doi: 10.2174/0929867326666181213092652

22. Zhang S, Pei M, Li Z, Li H, Liu Y, Li J. Double-negative feedback interaction between DNA methyltransferase 3A and microRNA-145 in the Warburg effect of ovarian cancer cells. *Cancer Sci* (2018) 109:2734–45. doi: 10.1111/cas.13734

23. Jin Y, Bian S, Wang H, Mo J, Fei H, Li L, et al. CRMP. *Cell Death Dis* (2022) 13:675. doi: 10.1038/s41419-022-05129-5

24. Mukherjee A, Ma Y, Yuan F, Gong Y, Fang Z, Mohamed EM, et al. Lysophosphatidic acid up-regulates hexokinase II and glycolysis to promote proliferation of ovarian cancer cells. *Neoplasia* (2015) 17:723–34. doi: 10.1016/j.neo.2015.09.003

25. Tuo X, Zhou Y, Yang X, Ma S, Liu D, Zhang X, et al. miR-532-3p suppresses proliferation and invasion of ovarian cancer cells via GPNMB/HIF-1α/HK2 axis. *Pathol Res Pract* (2022) 237:154032. doi: 10.1016/j.prp.2022.154032:10/gsdc5z

26. Chiyoda T, Hart PC, Eckert MA, McGregor SM, Lastra RR, Hamamoto R, et al. Loss of BRCA1 in the cells of origin of ovarian cancer induces glycolysis: a window of opportunity for ovarian cancer chemoprevention. *Cancer Prev Res (Phila)* (2017) 10:255–66. doi: 10.1158/1940-6207.CAPR-16-0281

27. Simula L, Alifano M, Icard P. How phosphofructokinase-1 promotes PI3K and YAP/TAZ in cancer: therapeutic perspectives. *Cancers (Basel)* (2022) 14(10):2478. doi: 10.3390/cancers14102478

28. Bartrons R, Rodríguez-García A, Simon-Molas H, Castaño E, Manzano A, Navarro-Sabaté À. The potential utility of PFKFB3 as a therapeutic target. *Expert Opin Ther Targets* (2018) 22:659–74. doi: 10.1080/14728222.2018.1498082:10/gsdmt4

29. Jiang YX, Siu MKY, Wang JJ, Leung THY, Chan DW, Cheung ANY, et al. PFKFB3 regulates chemoresistance, metastasis and stemness via IAP proteins and the NF-κB signaling pathway in ovarian cancer. *Front Oncol* (2022) 12:748403:10/gr7tmw. doi: 10.3389/fonc.2022.748403:10/gr7tmw

30. Gao W, Huang M, Chen X, Chen J, Zou Z, Li L. The role of S-nitrosylation of PFKM in regulation of glycolysis in ovarian cancer cells. *Cell Death Dis* (2021) 12:408. doi: 10.1038/s41419-021-03681-0

31. Zhao L, Ji G, Le X, Wang C, Xu L, Feng M, et al. Long noncoding RNA LINC00092 acts in cancer-associated fibroblasts to drive glycolysis and progression of ovarian cancer. *Cancer Res* (2017) 77:1369–82. doi: 10.1158/0008-5472.CAN-16-1615

32. Mondal S, Roy D, Bhattacharya S, Jin L, Jung D, Zhang S, et al. Therapeutic targeting of PFKFB3 with a novel glycolytic inhibitor PFK158 promotes lipophagy and chemosensitivity in gynecologic cancers. *Int J Cancer* (2019) 144:178–89. doi: 10.1002/ijc.31868

33. Lin X, Feng D, Li P. LncRNA LINC00857 regulates the progression and glycolysis in ovarian cancer by modulating the Hippo signaling pathway. *Cancer Med* (2020) 9:8122–32. doi: 10.1002/cam4.3322

34. Enzo E, Santinon G, Pocaterra A, Aragona M, Bresolin S, Forcato M, et al. Aerobic glycolysis tunes YAP/TAZ transcriptional activity. *EMBO J* (2015) 34:1349–70. doi: 10.15252/embj.201490379:10/f26sx7

35. Vaitheesvaran B, Xu J, Yee J, Q-Y L, Go VL, Xiao GG, et al. The Warburg effect: a balance of flux analysis. *Metab Off J Metabolomic Soc* (2015) 11:787–96. doi: 10.1007/s11306-014-0760-9:10/gsdnh2

36. Chakraborty PK, Mustafi SB, Xiong X, Dwivedi SKD, Nesin V, Saha S, et al. MICU1 drives glycolysis and chemoresistance in ovarian cancer. *Nat Commun* (2017) 8:14634. doi: 10.1038/ncomms14634

37. Grunewald TGP, Kammerer U, Winkler C, Schindler D, Sickmann A, Honig A, et al. Overexpression of LASP-1 mediates migration and proliferation of human ovarian cancer cells and influences zyxin localisation. *Br J Cancer* (2007) 96:296–305. doi: 10.1038/sj.bjc.6603545

38. Venturoli C, Piga I, Curtarello M, Verza M, Esposito G, Venuto S, et al. Genetic perturbation of pyruvate dehydrogenase kinase 1 modulates growth, angiogenesis and metabolic pathways in ovarian cancer xenografts. *Cells* (2021) 10:325. doi: 10.3390/cells10020325

39. Zhuang L, Zhang B, Liu X, Lin L, Wang L, Hong Z, et al. Exosomal miR-21-5p derived from cisplatin-resistant SKOV3 ovarian cancer cells promotes glycolysis and inhibits chemosensitivity of its progenitor SKOV3 cells by targeting PDHA1. *Cell Biol Int* (2021) 45:2140–9. doi: 10.1002/cbin.11671

40. Li S, Ji X, Wang R, Miao Y. Follicle-stimulating hormone promoted pyruvate kinase isozyme type M2-induced glycolysis and proliferation of ovarian cancer cells. *Arch Gynecol Obstet* (2019) 299:1443–51. doi: 10.1007/s00404-019-05100-4

41. Shang Y, He J, Wang Y, Feng Q, Zhang Y, Guo J, et al. CHIP/Stub1 regulates the Warburg effect by promoting degradation of PKM2 in ovarian carcinoma. *Oncogene* (2017) 36:4191–200. doi: 10.1038/onc.2017.31

42. Chen M, Sheng XJ, Qin YY, Zhu S, Wu QX, Jia L, et al. TBC1D8 amplification drives tumorigenesis through metabolism reprogramming in ovarian cancer. *Theranostics* (2019) 9:676–90. doi: 10.7150/thno.30224

43. Sun T, Liu Z, Bi F, Yang Q. Deubiquitinase PSMD14 promotes ovarian cancer progression by decreasing enzymatic activity of PKM2. *Mol Oncol* (2021) 15:3639–58. doi: 10.1002/1878-0261.13076

44. Gao T, Zhang X, Zhao J, Zhou F, Wang Y, Zhao Z, et al. SIK2 promotes reprogramming of glucose metabolism through PI3K/AKT/HIF-1α pathway and Drp1-mediated mitochondrial fission in ovarian cancer. *Cancer Lett* (2020) 469:89–101. doi: 10.1016/j.canlet.2019.10.029:Tumor

45. Chen Y, Liu L, Xia L, Wu N, Wang Y, Li H, et al. TRPM7 silencing modulates glucose metabolic reprogramming to inhibit the growth of ovarian cancer by enhancing AMPK activation to promote HIF-1α degradation. *J Exp Clin Cancer Res CR* (2022) 41:44. doi: 10.1186/s13046-022-02252-1

46. Yung MMH, Ngan HYS, Chan DW. Targeting AMPK signaling in combating ovarian cancers: opportunities and challenges. *Acta Biochim Biophys Sin (Shanghai)* (2016) 48:301–17. doi: 10.1093/abbs/gmv128

47. Ediriweera MK, Tennekoon KH, Samarakoon SR. Role of the PI3K/AKT/mTOR signaling pathway in ovarian cancer: biological and therapeutic significance. *Semin Cancer Biol* (2019) 59:147–60. doi: 10.1016/j.semcancer.2019.05.012

48. Zhang J, Zhang J, Wei Y, Li Q, Wang Q. ACTL6A regulates follicle-stimulating hormone-driven glycolysis in ovarian cancer cells via PGK1. *Cell Death Dis* (2019) 10:811. doi: 10.1038/s41419-019-2050-y

49. Shi J, Ye J, Fei H, Jiang SH, Wu ZY, Chen YP, et al. YWHAZ promotes ovarian cancer metastasis by modulating glycolysis. *Oncol Rep* (2019) 41:1101–12. doi: 10.3892/or.2018.6920

50. Li XH, Chen XJ, Ou WB, Zhang Q, Lv ZR, Zhan Y, et al. Knockdown of creatine kinase B inhibits ovarian cancer progression by decreasing glycolysis. *Int J Biochem Cell Biol* (2013) 45:979–86. doi: 10.1016/j.biocel.2013.02.003

51. Wang Z, Chen W, Zuo L, Xu M, Wu Y, Huang J, et al. The Fibrillin-1/VEGFR2/STAT2 signaling axis promotes chemoresistance via modulating glycolysis and angiogenesis in ovarian cancer organoids and cells. *Cancer Commun (Lond)* (2022) 42:245–65. doi: 10.1002/cac2.12274

52. Bandopadhyay S, Prasad P, Ray U, Das Ghosh D, Roy SS. SIRT6 promotes mitochondrial fission and subsequent cellular invasion in ovarian cancer. *FEBS Open Bio* (2022) 12:1657–76. doi: 10.1002/2211-5463.13452

53. Zeng S, Liu S, Feng J, Gao J, Xue F. Upregulation of lncRNA AB073614 functions as a predictor of epithelial ovarian cancer prognosis and promotes tumor growth in *vitro* and in *vivo*. *Cancer biomark* (2019) 24(4):421–8. doi: 10.3233/CBM-182160

54. Jia L, Zhou J, Zhao H, Jin H, Lv M, Zhao N. Corilagin sensitizes epithelial ovarian cancer to chemotherapy by inhibiting Snail-glycolysis pathways. *Oncol Rep* (2017) 38:2464–70. doi: 10.3892/or.2017.5886

55. Xu S, Jia G, Zhang H, Wang L, Cong Y, Lv M, et al. LncRNA HOXB-AS3 promotes growth, invasion and migration of epithelial ovarian cancer by altering glycolysis. *Life Sci* (2021) 264:118636. doi: 10.1016/j.lfs.2020.118636

56. Yang HY, Shen JX, Wang Y, Liu Y, Shen DY, Quan S. Tankyrase promotes aerobic glycolysis and proliferation of ovarian cancer through activation of Wnt/β-catenin signaling. *BioMed Res Int* (2019) 2019:2686340. doi: 10.1155/2019/2686340

57. Gu ZW, He YF, Wang WJ, Tian Q, Di W. MiR-1180 from bone marrow-derived mesenchymal stem cells induces glycolysis and chemoresistance in ovarian cancer cells by upregulating the Wnt signaling pathway. *J Zhejiang Univ Sci B* (2019) 20:219–37. doi: 10.1631/jzus.B1800190

58. Shen YA, Lan KL, Chang CH, Lin LT, He CL, Chen PH, et al. Intraperitoneal (188) Re-Liposome delivery switches ovarian cancer metabolism from glycolysis to oxidative phosphorylation and effectively controls ovarian tumour growth in mice. *Radiother Oncol J Eur Soc Ther Rad Oncol* (2016) 119:282–90. doi: 10.1016/j.radonc.2016.02.007

59. Dang CV, Le A, Gao P. MYC-induced cancer cell energy metabolism and therapeutic opportunities. *Clin Cancer Res* (2009) 15(21):6479–83. doi: 10.1158/1078-0432.CCR-09-0889

60. Li H, Qi Z, Niu Y, Yang Y, Li M, Pang Y, et al. FBP1 regulates proliferation, metastasis, and chemoresistance by participating in C-MYC/STAT3 signaling axis in ovarian cancer. *Oncogene* (2021) 40(40):5938–49. doi: 10.1038/s41388-021-01957-5

61. Wu Y, Deng Y, Zhu J, Duan Y, Weng W, Wu X. Pim1 promotes cell proliferation and regulates glycolysis via interaction with MYC in ovarian cancer. *Onco Targets Ther* (2018) 11:6647–56. doi: 10.2147/OTT.S180520

62. Liu X, Zuo X, Sun X, Tian X, Teng Y. Hexokinase 2 promotes cell proliferation and tumor formation through the Wnt/β-catenin pathway-mediated cyclin D1/c-myc upregulation in epithelial ovarian cancer. *J Cancer* (2022) 13(8):2559–69. doi: 10.7150/jca.71894

63. Harris AL. Hypoxia—a key regulatory factor in tumour growth. *Nat Rev Cancer* (2002) 2:38–47. doi: 10.1038/nrc704

64. Curtis M, Kenny HA, Ashcroft B, Mukherjee A, Johnson A, Zhang Y, et al. Fibroblasts mobilize tumor cell glycogen to promote proliferation and metastasis. *Cell Metab* (2019) 29:141–155.e9. doi: 10.1016/j.cmet.2018.08.007

65. Radhakrishnan R, Ha JH, Jayaraman M, Liu J, Moxley KM, Isidoro C, et al. Ovarian cancer cell-derived lysophosphatidic acid induces glycolytic shift and cancer-associated fibroblast-phenotype in normal and peritumoral fibroblasts. *Cancer Lett* (2019) 442:464–74. doi: 10.1016/j.canlet.2018.11.023

66. Ha JH, Radhakrishnan R, Jayaraman M, et al. LPA induces metabolic reprogramming in ovarian cancer via a pseudohypoxic response. *Cancer Res* (2018) 78:1923–34. doi: 10.1158/0008-5472.CAN-17-1624

67. Liu D, Li H. Long non-coding RNA GEHT1 promoted the proliferation of ovarian cancer cells via modulating the protein stability of HIF-1α. *Biosci Rep* (2019) 39:BSR20181650. doi: 10.1042/BSR20181650

68. Ai Z, Lu Y, Qiu S, Fan Z. Overcoming cisplatin resistance of ovarian cancer cells by targeting HIF-1-regulated cancer metabolism. *Cancer Lett* (2016) 373:36–44. doi: 10.1016/j.canlet.2016.01.009

69. Yang Y, Cao Y, Chen L, Liu F, Qi Z, Cheng X, et al. Cryptotanshinone suppresses cell proliferation and glucose metabolism via STAT3/SIRT3 signaling pathway in ovarian cancer cells. *Cancer Med* (2018) 7:4610–8. doi: 10.1002/cam4.1691

70. Zhang D, Wang Y, Dong L, Huang Y, Yuan J, Ben W, et al. Therapeutic role of EF24 targeting glucose transporter 1-mediated metabolism and metastasis in ovarian cancer cells. *Cancer Sci* (2013) 104:1690–6. doi: 10.1111/cas.12293

71. Lu J, Chen H, He F, et al. Ginsenoside 20(S)-Rg3 upregulates HIF-1α-targeting miR-519a-5p to inhibit the Warburg effect in ovarian cancer cells. *Clin Exp Pharmacol Physiol* (2020) 47(8):1455–63. doi: 10.1111/1440-1681.13321

72. Agbu P, Carthew RW. MicroRNA-mediated regulation of glucose and lipid metabolism. *Nat Rev Mol Cell Biol* (2021) 22(6):425–38. doi: 10.1038/s41580-021-00354-w

73. Xu H, Sun X, Huang Y, Si Q, Li M. Long non−coding RNA NEAT1 modifies cell proliferation, colony formation, apoptosis, migration and invasion *via* the miR−4500/BZW1 axis in ovarian cancer. *Mol Med Rep* (2020) 22:3347–57. doi: 10.3892/mmr.2020.11408

74. Liu Y, Fu X, Wang X, Liu Y, Song X. Long non−coding RNA OIP5−AS1 facilitates the progression of ovarian cancer *via* the miR−128−3p/CCNG1 axis. *Mol Med Rep* (2021) 23(5):388. doi: 10.3892/mmr.2021.12027

75. Liu Y, He X, Chen Y, Cao D. Long non-coding RNA LINC00504 regulates the Warburg effect in ovarian cancer through inhibition of miR-1244. *Mol Cell Biochem* (2020) 464:39–50. doi: 10.1007/s11010-019-03647-z

76. Hou W, Zhang Y. Circ_0025033 promotes the progression of ovarian cancer by activating the expression of LSM4 *via* targeting miR-184. *Pathol Res Pract* (2021) 217:153275. doi: 10.1016/j.prp.2020.153275

77. Lin C, Xu X, Yang Q, Liang L, Qiao S. Circular RNA ITCH suppresses proliferation, invasion, and glycolysis of ovarian cancer cells by up-regulating CDH1 *via* sponging miR-106a. *Cancer Cell Int* (2020) 20:336. doi: 10.1186/s12935-020-01420-7

78. Rao G, Dwivedi SKD, Zhang Y, Dey A, Shameer K, Karthik R, et al. MicroRNA-195 controls MICU1 expression and tumor growth in ovarian cancer. *EMBO Rep* (2020) 21:10e48483. doi: 10.15252/embr.201948483

79. Han RL, Wang FP, Zhang PA, Zhou XY, Li Y. miR-383 inhibits ovarian cancer cell proliferation, invasion and aerobic glycolysis by targeting LDHA. *Neoplasma* (2017) 64(2):244–52. doi: 10.4149/neo_2017_211

80. Zhao E, Maj T, Kryczek I, Li W, Wu K, Zhao L, et al. Cancer mediates effector T cell dysfunction by targeting microRNAs and EZH2 *via* glycolysis restriction. *Nat Immunol* (2016) 17:95–103. doi: 10.1038/ni.3313

81. Li J, Liu T, Zhao L, et al. Ginsenoside 20(S)−Rg3 inhibits the Warburg effect through STAT3 pathways in ovarian cancer cells. *Int J Oncol* (2015) 46:775–81. doi: 10.3892/ijo.2014.2767

82. Shi D, Zhao D, Niu P, Zhu Y, Zhou J, Chen H. Glycolysis inhibition *via* mTOR suppression is a key step in cardamonin-induced autophagy in SKOV3 cells. *BMC Complement Altern Med* (2018) 18:317. doi: 10.1186/s12906-018-2380-9

83. Zhang W, Su J, Xu H, Yu S, Liu Y, Zhang Y, et al. Dicumarol inhibits PDK1 and targets multiple malignant behaviors of ovarian cancer cells. *PloS One* (2017) 12:e0179672. doi: 10.1371/journal.pone.0179672

84. Kueck A, Opipari AW Jr, Griffith KA, Tan L, Choi M, Huang J, et al. Resveratrol inhibits glucose metabolism in human ovarian cancer cells. *Gynecol Oncol* (2007) 107(3):450–7. doi: 10.1016/j.ygyno.2007.07.065

85. Liu Y, Tong L, Luo Y, Li X, Chen G, Wang Y, et al. Resveratrol inhibits the proliferation and induces the apoptosis in ovarian cancer cells via inhibiting glycolysis and targeting AMPK/mTOR signaling pathway. *J Cell Biochem* (2018) 119(7):6162–72. doi: 10.1002/jcb.26822

86. Kaur P, Nagar S, Bhagwat M, Uddin M, Zhu Y, Vancurova I, et al. Activated heme synthesis regulates glycolysis and oxidative metabolism in breast and ovarian cancer cells. *PloS One* (2021) 16:e0260400. doi: 10.1371/journal.pone.0260400

87. Guo NL, Zhang JX, Wu JP, Xu YH. Isoflurane promotes glucose metabolism through up-regulation of miR-21 and suppresses mitochondrial oxidative phosphorylation in ovarian cancer cells. *Biosci Rep* (2017) 37:BSR20170818. doi: 10.1042/BSR20170818

88. Xintaropoulou C, Ward C, Wise A, Queckborner S, Turnbull A, Michie CO, et al. Expression of glycolytic enzymes in ovarian cancers and evaluation of the glycolytic pathway as a strategy for ovarian cancer treatment. *BMC Cancer* (2018) 18:636. doi: 10.1186/s12885-018-4521-4

89. Chao TK, Huang TS, Liao YP, Huang RL, Su PH, Shen HY, et al. Pyruvate kinase M2 is a poor prognostic marker of and a therapeutic target in ovarian cancer. *PloS One* (2017) 12:e0182166. doi: 10.1371/journal.pone.0182166:10/gbp2fg

90. Tian M, Chen XS, Li LY, Wu HZ, Zeng D, Wang XL, et al. Inhibition of AXL enhances chemosensitivity of human ovarian cancer cells to cisplatin via decreasing glycolysis. *Acta Pharmacol Sin* (2021) 42:1180–9. doi: 10.1038/s41401-020-00546-8

91. Loar P, Wahl H, Kshirsagar M, Gossner G, Griffith K, Liu JR. Inhibition of glycolysis enhances cisplatin-induced apoptosis in ovarian cancer cells. *Am J Obstet Gynecol* (2010) 202:–371.e8. doi: 10.1016/j.ajog.2009.10.883

92. Chun J. Isoalantolactone suppresses glycolysis and resensitizes cisplatin-based chemotherapy in cisplatin-resistant ovarian cancer cells. *Int J Mol Sci* (2023) 24(15):12397. doi: 10.3892/or.2017.5886

frontiers | Frontiers in Oncology

TYPE Review
PUBLISHED 05 December 2023
DOI 10.3389/fonc.2023.1323826

OPEN ACCESS

EDITED BY
Asif Raza,
Penn State Milton S. Hershey Medical Center, United States

REVIEWED BY
Kousalya Lavudi,
KIIT University, India
Venugopal Vangala,
The Pennsylvania State University, United States

*CORRESPONDENCE
Wenhong Deng
wenhongdeng@whu.edu.cn

†These authors have contributed equally to this work

RECEIVED 18 October 2023
ACCEPTED 15 November 2023
PUBLISHED 05 December 2023

CITATION
Wenxuan L, Liu L, Zhang L, Qiu Z, Wu Z and Deng W (2023) Role of gonadally synthesized steroid hormones in the colorectal cancer microenvironment. *Front. Oncol.* 13:1323826. doi: 10.3389/fonc.2023.1323826

Role of gonadally synthesized steroid hormones in the colorectal cancer microenvironment

Liu Wenxuan†, Li Liu†, Lilong Zhang, Zhendong Qiu, Zhongkai Wu and Wenhong Deng*

Department of General Surgery, Renmin Hospital of Wuhan University, Wuhan, Hubei, China

Objective: To understand the relationship between steroid hormones synthesized by the gonads and colorectal cancer as well as its tumor microenvironment, in the expectation of providing new ideas in order to detect and treat colorectal cancer.

Methods: Through reviewing the relevant literature at home and abroad, we summarized that androgens promote the growth of colorectal cancer, and estrogens and progesterone help prevent bowel cancer from developing; these three hormones also have a relevant role in the cellular and other non-cellular components of the tumor microenvironment of colorectal cancer.

Conclusion: The current literature suggests that androgens, estrogens, and progesterone are valuable in diagnosing and treating colorectal cancer, and that androgens promote the growth of colorectal cancer whereas estrogens and progesterone inhibit colorectal cancer, and that, in addition, the receptors associated with them are implicated in the modulation of a variety of cellular components of the microenvironment of colorectal cancer.

KEYWORDS

estrogens, progesterone, androgens, tumor microenvironment, colorectal cancer

1 Introduction

Colorectal cancer (CRC) is a global disease that represents a serious threat to the lives and health of people around the world, and is a widespread malignant tumor of the gastrointestinal tract. In accordance with the most recent statistics on cancer, colorectal cancer is the third most common cancer in the world, after lung cancer, and the second most common cause of death (1). The cause of this disease, like other malignant tumors, remains unclear and may be related to a number of precancerous lesions and genetic factors.

Several reports suggest that colorectal cancer is considered a steroid hormone-sensitive tumor (2). Steroid hormones include two major groups of sex hormones and adrenocortical hormones, the main ones synthesized in the gonads are estrogens, androgens and progesterone (3). They are cholesterol derivatives that are fat-soluble, thus, they can traverse across the plasma membrane and attach to intracellular receptors(also known as nuclear receptors, NRs), regulating gene expression. Hormones have a significant impact on the progression of colorectal cancer either through a specific target organ or by regulating a metabolic process (4).

Recently, it has been discovered that the tumor microenvironment plays a crucial part in regulating tumor growth and shaping the tumor's responsiveness to treatment. The microenvironment of tumor is a multifaceted milieu essential for the sustenance and growth of malignant cells, constituted by neighboring vasculature, immune cells, fibroblasts, bone marrow-derived inflammatory cells, diverse signal biomolecules, and extracellular matrix (5). Steroid hormones synthesized by gonads in tumors are closely associated with the tumor microenvironment, and can have an impact on the tumor microenvironment through the release of cell-signaling molecules, which in turn affect cancer cell growth and development.

In this paper, we will discuss the impacts of steroid hormones synthesized by the gonads on colorectal cancer and its tumor microenvironment in order to improve the understanding of the tumor microenvironment and seek new therapeutic targets.

2 Steroid hormones synthesized by the gonads

Androgens are steroid hormones that are synthesized mainly by testicular interstitial cells. Androgen production, mediated by the androgen receptor (AR), is the principal function of androgens (6). AR belongs to the nuclear receptor superfamily and is a ligand-dependent transcription factor. AR is transcriptionally activated mainly through a ligand-dependent manner, and the activating ligands are mainly testosterone and dihydrotestosterone. When activated, Dissociation from heat shock protein 90 (HSP90), translocation to the nucleus, binding to AR on target genes and ultimately induces transcription of the androgen response (7).

Estrogen mainly facilitates the development of female secondary sex characteristics and maturation of sex organs. Natural estrogens are mainly estradiol, estrone and estriol. Estrogen exerts various biological effects by combining with the estrogen receptor (ER) and regulating the expression of a series of downstream genes, which is the classical estrogen signaling pathway (8). Estrogen receptors include the traditional nuclear receptors ERα and ERβ, which mediate the genotypic effects of estrogen, i.e., "genotypic" regulation through the regulation of the transcription of specific target genes, and the membranous G protein-coupled estrogen receptor (GPER), which mediates the rapid nongenotypic effects of estrogen and exerts indirect transcriptional regulation through the second messenger system (9, 10).

Progesterone is a steroid hormone which is synthesized by the placenta, the ovaries and the adrenal glands, progesterone is supposed to refer to the natural hormone, while progesterone is a general term that includes progesterone and synthetic progesterone (11). Progesterone hormone and estrogen are inextricably linked, and progesterone hormone builds on estrogen's actions (12).

3 Hormones and their receptors in colorectal cancer cells

3.1 Androgens and their receptors and colorectal cancer

Epidemiologic and experimental studies have shown androgens and their influence in developing colorectal cancer. Testosterone treatment accelerates the proliferation of small intestinal and colon tumor cells, which is inhibited after depopulation of colon tumor cells (13). Exogenous testosterone alters tumor distribution and characteristics and inhibits abnormal epithelial cell proliferation (14). Interaction of androgens with the nerve growth factor receptor NGF receptor affects colorectal cancer cells (15). Radiotherapy (46-50Gy) for rectal cancer was associated with markedly elevated serum FSH and LH and markedly lowered testosterone levels (16). Involving androgens in the TUBB3 pathway opens the door to clinical trials evaluating antiandrogens to increase the efficacy of chemotherapy in male colorectal cancer patients (17). The antiandrogen drug flutamide also inhibits colon tumor cell proliferation (13). Activation of the androgen receptor increases the expression of bone morphogenetic protein (BMP) inhibitors but decreases the expression of BMP4 and Wnt inhibitors in primary stromal cells, which promotes the growth of intestinal organoids.Overall, this study reveals the role of androgens in promoting proliferation and inhibiting differentiation, suggesting that stromal cells constitute the microenvironment of intestinal stem cells, it provides a possible explanation for the high incidence of colorectal cancer in men (18).

ERα and AR proteins were elevated in malignant tumor tissues, and ERβ and progesterone receptor (PR) were significantly decreased. AR expression was highest in male tumor tissues, where AR receptor blockers induced apoptosis and testosterone co-treatment impeded the effect (19). Furthermore, AR has been shown to be expressed at both the mRNA and protein levels on both healthy and cancerous colon mucosa (20). Abdulkader M Albasri et al. examined the androgen receptor status in colon cancer patients using immunohistochemistry and correlating the results with all available clinicopathological parameters that predict prognosis. Patients with higher levels of AR expression had significantly worse survival and AR expression may be a prognostic marker for colorectal cancer (21).

ARA54 is an androgen receptor coactivator that enhances AR-dependent activation of transcription. Hirotoshi Kikuchi et al. demonstrated that ARA54 may be involved in promoting cell cycle progression and cell proliferation through the induction of

cell cycle protein D1 (22). The human androgen receptor gene contains a polymorphic CAG repeat region that varies from 8 to 35 repeats in the average population. The length of the repeat sequence is negatively correlated with the trans-activation potential of the receptor (23). Long CAG repeats and negative AR expression were both associated with poor 5-year overall survival in colorectal cancer, according to Rui Huang et al. (24). Androgens are known to be expressed on the mucous membranes of the bowel, AR CAG repeat sequences undergo a variety of unique somatic mutations that primarily result in the case of shorter alleles. Colorectal epithelial cells that carry AR alleles with shorter CAG repeat sequences are more sensitive to androgens and are favored to grow (25). Coactivator-associated arginine methyltransferase 1 (CARM1) functions as a transcriptional co-activator of AR-mediated signaling. Young-Rang Kim et al. found that CARM1 is particularly highly expressed in colorectal cancer through tissue microarrays, which was demonstrated by further investigation using surgery specimens. Transcriptional regulator CARM1 by altering the activity of P53 and NF-κB, especially in colorectal cancer (26).

Shuchen Gu et al. were the first to demonstrated that mAR are primarily expressed in colorectal tumors and showed that their activation induces an anti-tumor response *in vitro* and reduces tumorigenicity *in vivo* (27). Vinculin is a protein that controls cell adhesion and actin reorganization. It is efficiently phosphorylated upon mAR activation. mAR activation inhibits the pro-survival signaling Akt/Bad signal pathway *in vitro* and *in vivo* and blocks colon cancer cell migration by regulating neuregulin signaling and actin reorganization, supporting the potent tumorigenic effects of these receptors (28). Gu et al. went on to discover in colon tumor cells the regulation of FAK/mTOR/p70S6K/PAK1 signaling pathway by testosterone-coupled receptors through activation of mAR, which controls early testosterone-induced actin rearrangement in colorectal cancer cells (29). Then mAR was found to be downregulated by specific testosterone albumin coupling (TAC) to regulate the late expression and/or activity of the oncogenic gene products c-Src, GSK-3β, and β-linker proteins, which promotes a pro-apoptotic response in colorectal tumor cells (30).

In summary, androgens and their receptors promote tumor growth in most cases in colorectal cancer, but the related signaling pathways are still not well understood, so more research is needed into the role of androgens and their receptors in colorectal cancer.

3.2 Estrogen and its receptors and colorectal cancer

Estrogen and its receptor are essential for CRC tumorigenesis and progression. Ryuichiro Sato et al. used liquid chromatography-electrospray ionization tandem mass spectrometry (LC-ESI-MS) and immunohistochemistry to show that the STS (steroid sulfatase)/EST (estrogen sulfotransferase) status of the cancerous tissues determines the level of estrogen in the tumors, which proves that estrogen is mainly produced locally via the sulfatase pathway and plays an essential role in the progression of the disease progression (31). Estradiol regulates colorectal cancer stem cell bioactivity and interaction with endothelial cells (32). Estrogen promotes the development of inflammation-associated cancers by impairing mucosal responses to inflammatory injury (33). Nrf2 inhibits macrophage inflammatory responses by blocking pro-inflammatory factor transcription (34), and estradiol inhibits CRC by modulating the Nrf2-related pathway (35) Estrogen further inhibits CRC in the absence of Nrf2 by upregulating ERβ-related alternative pathways (36). Estrogen prevents the sustained growth of COLO-205 human colon cancer cells through induction of apoptosis, reduction of c-myb protein and reduction of transcription of the anti-apoptotic protein bcl-2 (37).

Many studies have shown that estrogen action under physiological and pathophysiological circumstances is mediated by estrogen receptors ERα and ERβ as well as membrane-bound GPER (10). Asmaa Abd ElGhany Abd ElLateef et al. reported that lower levels of ER/PR expression were associated with a more extensive CRC primary tumors and poorer prognosis (38). Nancy L Cho et al. also reported that ERα and ERβ are inhibitory modulators of antigen presenting cell (APC)-dependent colon tumorigenesis (39). Overexpression of ERα upregulated hTNF-α gene expression and down-regulated β-conjugated protein signaling activity, which induced apoptosis and inhibited proliferation of LoVo colon cancer cells (40). Hai-ping Jiang et al. reported that an variant of ERα, ERα46, mediated growth inhibition and apoptosis of human HT-29 colon adenocarcinoma cells when estradiol present (41).

The ERβ gene exceeds the ERα gene in the etiology of colorectal cancer (42). ERβ is also the dominant estrogen receptor in the histologically intact colon. Véronique Giroux reported that ERβ deficiency promotes small intestinal tumorigenesis and suggested that regulation of the TGFβ signaling pathway may be a factor in he protective effect of estrogen on intestinal tumorigenesis (43). Francesco Caiazza et al. found that 17β-estradiol induced ERβ upregulation in colon cancer cells by activating p38/MAPK signal pathway (44). ERβ regulates p65 signaling in colon cells (45). Estradiol regulates miR-135b and mismatch repair gene MMR expression in colorectal cells via ERβ (46). Xian Xu et al. also reported that 17β-estradiol agonists inhibited the ability of human LoVo colorectal cancer cells to replicate and migrate via p53 signal pathway (47). The study conducted by Lu et al. shown that estrogen had a positive impact on mismatch repair and tumor suppression both *in vitro* and *in vivo*. This effect was achieved by the induction of MLH1 expression mediated by ERβ (48). A new ERβ agonist, OSU-ERb-12, has been reported to block tumor progression and limit cancer stem cell (CSC) subpopulations (49). The growth of the MC38 colon cancer line was found to be inhibited by diarylpropionitrile, a specific agonist of ERβ, as reported by Ewelina Motylewska (50).. In a study conducted by Nakayama et al., it was discovered that the combination of an ERβ ligand and TMX (tamoxifen) demonstrated a suppressive impact on colon cancer cells (51). Calycosin targets ER, upregulates PTEN, and

blocks the PI3K/Akt signaling pathway to slow the growth of colorectal cancer (52). The tumor suppressor protein known as WFDC3 plays a crucial role in inhibiting the spread of tumors in colorectal cancer. This inhibition is achieved through the promotion of ERβ-mediated transcriptional repression of TGFBR1 (53).

Liu Qiao et al. found epigenetic down-regulation of the GPER to act as a tumor suppressor in colorectal cancer (54). Lorna C Gilligan et al. reported that human colorectal cancers promote estradiol synthesis via GPER stimulation to enhance proliferation (55). Maria Abancens et al. identified a mechanistic role for the G protein-coupled membrane estrogen receptor GPER in preventing CRC progression by selectively reducing the tumorigenic effects of the overactive Wnt/β-linker signaling pathway in CRC (56).

The aforementioned findings demonstrate that estrogen and its associated receptors generally impede the progression of colorectal cancer by means of the Nrf2-related pathway, induction of apoptosis, suppression of c-myb protein, and attenuation of the transcription of the anti-apoptotic protein bcl-2. Additionally, estrogen promotes the up-regulation of hTNF-α gene expression and the down-regulation of β-catenin signaling activity, TGFβ-related signaling pathway, and Wnt/β-collagen signaling pathway. Furthermore, estrogen facilitates the up-regulation of p38/MAPK and p65 signaling while down-regulating the Wnt/β-collagen signaling pathway. Therefore, further studies are necessary to understand estrogen and its corresponding receptors in colorectal cancer cells.

3.3 progesterone and its receptors and colorectal cancer

Progesterone is an important naturally occurring sex hormone whose cellular effects are mediated by adsorption on the progesterone receptor and modulating hormone-responsive target genes in several cancer types (57). Zhang Y L et al. first analyzed the progesterone levels of 77 patients with CRC, and immunohistochemistry was conducted to identify the overexpression of progesterone receptor in colorectal cancer. S Singh et al. also discovered that the concentration of progesterone receptor in rectal cancer was significantly greater than that in the comparable normal tissues, demonstrating that the concentration of progesterone receptor mRNA has a strong link between cancer and normal tissues (58). The level of progesterone receptor (PGR) expression in CRC tissues correlates with sex, tumor size, degree of differentiation of the tumors, degree of infiltration of the tumor vasculature, and tumor clinical stage. The prognosis of CRC patients with low PGR expression is worse (59). Luteinizing hormone controls the proliferation, apoptosis, angiogenesis, and autophagy of cancer cells, among other cancer cell characteristics (60). Zhang Y L et al. further showed that progesterone increased the expression of growth arrest and DNA damage-inducible protein GADD45α and activated the JNK pathway. Progesterone exerts a stimulatory effect on the JNK pathway via GADD45α, leading to the inhibition of cell proliferation through the suppression of the cell cycle and the induction of apoptosis, thereby inhibiting the malignant advancement of colorectal cancer (59). ER and PR expression and p53 gene detection and DNA ploidy analysis in colorectal cancer can help in clinical classification and prognostic assessment of colorectal cancer patients (61, 62). The progestin drug medroxyprogesterone acetate (MPA), which causes cell cycle arrest by up-regulating cell surface Fas and FasL, has a significant inhibitory effect and causes human colon carcinoma to undergo apoptosis Live and *in vitro* LS174T cells (63). In women, folic acid helps to maintain endocrine function of the ovary. Wang H C et al. found showed that PGR activation in response to a requirement for folic acid (FA) regulated cell migration and proliferation is universal across all cell lines for cancer (64). Ting et al. employed Transwell invasion experiments to demonstrate that FA effectively decreased the invasive potential of colorectal cancer cell lines, namely COLO-205, LoVo, and HT-29 (65). The proliferation of colon cancer cells was found to be inhibited by the activation of PR with the administration of folic acid (FA) (66). In their study, Kuo et al. provided evidence that FA has the ability to suppress the growth of colorectal cancer cell lines by activating the folate receptorα (FRα)/cSrc/ERK1/2/NFκB/p53 pathway. Additionally, they demonstrated the inhibitory effects of FA on COLO-205 tumor growth in an *in vivo* setting (67). In colorectal adenocarcinoma, the presence of progesterone receptors is partially correlated with the presence of estradiol receptors (12).

17β-estradiol and progesterone monotherapies have the same anticancer effects and enhance the tumor-killing effects of CRC in men through the promotion of androgen deprivation mediated by ERβ and PGR, while also blocking oncogenic pathways regulated by ERα (68).

PAQR3, belonging to the progesterone and adipose Q receptor (PAQR) family, is a geographic regulator involved in the negative regulation of the Ras/Raf/MEK/ERK signaling cascade. Wang X et al. found that PAQR3 deletion significantly exacerbated small bowel survival time and tumor area in APC (Min/+) mice. Next, in SW-480 cells, PAQR3 overexpression was found to inhibit cell proliferation rate, anchorage-independent growth, epidermal growth factor-stimulated ERK phosphorylation, and epidermal growth factor-induced nuclear accumulation of β-connexin, and enhanced these colorectal cancers by PAQR3 knockdown. This series of experiments demonstrated the tumor suppressor activity of PAQR3 in the development of colorectal cancer (69).

In summary, progesterone and its receptor inhibit colorectal carcinogenesis and progression through upregulation of GADD45α to enhance the JNK pathway, inhibit cell cycle, induce apoptosis to inhibit cell proliferation, upregulation of cell-surface Fas and FasL to bring about a stop in the cell cycle, and upregulation of p27 to enhance the folate receptor (FR) α/cSrc/ERK1/2/NFκB/p53, etc., and its related drugs, receptor antagonists, have also demonstrated corresponding efficacy (70), but further understanding of more of the mechanisms of occurrence is needed (Table 1).

TABLE 1 Effect of sex steroid hormones secreted by the gonads and their receptors on colorectal cancer.

gonadotropin		Related Pathways	Acts with colorectal cancer cells	Related articles
Androgens and their receptors	mAR	Down-regulation of PI-3K and Akt activity induces p-Bad dephosphorylation/activation of p-Bad	inhibition	(26)
	mAR	Up-regulation of FAK / mTOR / p70S6K / PAK1 signalling pathway	Control of early testosterone-induced actin reorganisation in colon cancer cells	(27)
	mAR	Down-regulation of c-Src, GSK-3β and β-collagen signalling pathway inhibition	facilitation	(28)
Estrogen and its receptors	E2	Up-regulation of ERβ-related pathways in the absence of NRF2	facilitation	(34)
	E2	Induction of apoptosis, reduction of c-myb protein and reduction of transcription of the anti-apoptotic protein bcl-2	inhibition	(35)
	E2	p38/MAPK pathway induces ERβ upregulation	facilitation	(43)
	Estradiol agonists	P53 pathway	inhibition	(46)
	ERα	Up-regulation of hTNF-α gene expression down-regulates β-collagen signalling	facilitation	(39)
	GPER	Down-regulation of the Wnt/β-collagen signalling pathway	facilitation	(54)
Progesterone and its receptors	P	Up-regulation of GADD45α enhances JNK pathway, inhibits cell cycle, induces apoptosis and suppresses cell proliferation	facilitation	(59)
	MPA	Up-regulation of cell surface Fas and FasL causes cell cycle arrest	facilitation	(60)
	FA	Up-regulation of p27 enhances folate receptor (FR) α/cSrc/ERK1/2/ NFκB/p53 pathway	facilitation	(65)

mAR, Membrane Androgen Receptors; E2, Estrogen; ERα, Estrogen Receptors α; GPERG, protein estrogen-coupled receptor; MPA, Medroxyprogesterone acetate; FA, Folic acid;.

4 Androgens, estrogens, progesterones and their receptors in colorectal cancer TMEs

Androgens, estrogens, progesterone and their receptors have been much studied in some tumor microenvironments such as melanoma (71), breast cancer (72), prostate cancer (73), and recent studies have found their role in colorectal cancer. Estrogen stimulates melanoma growth in mouse models via ERα, biases macrophage polarization towards an immunosuppressive state, and thereby enhances CD8+ T-cell exhaustion function, exhaustion, and resistance to immune checkpoint blockade of ICB (74). Through the activation of stromal ER, which in turn normalizes tumor angiogenesis and adjusts the blood supply to the tumor, Estrogen encourages the proliferation of ER-negative cancer cells, preventing hypoxia and necrosis (72). In fibroblasts connected to breast cancer, the nuclear alternative estrogen receptor GPR30 mediates 17-estradiol-induced gene expression and migration (75).

The coregulator hydrogen peroxide-inducible gene 5 (Hic-5) is a metastable adaptor between focal adhesion and the nucleus of prostate myofibroblast cells, and it is a key mediator of AR signaling specificity and sensitivity (76). The induction of drug resistance in PC cells is facilitated by macrophages through the activation of a signaling cascade involving fibronectin (FN1), integrin α5 (ITGA5), and tyrosine kinase SRC (SRC). This cascade is triggered by the cytokine activin A (77). The prostate cancer tumor microenvironment's androgen-regulated SPARCL1 prevents metastatic spread (73).

The administration of progesterone has been found to facilitate immunomodulation and foster tumor formation within the mouse mammary gland (78). The involvement of membrane progesterone receptor alpha (mPRα) in the promotion of hypoxia-induced vascular endothelial growth factor production and angiogenesis in lung adenocarcinoma is mediated via the activation of STAT3 signaling pathway (79).

A few studies have been undertaken to reveal the function of three hormones in the tumor microenvironment of colorectal cancer. Simon Milette et al. experimentally found that MDSCs in liver metastases from colorectal cancer patients express TNFR2 and that in TNFR2-/- mice, the reduction of intrahepatic MDSCs coincided with the reduction of Treg accumulation at the metastatic site, further concluding that TNF receptor-2 promotes an immunosuppressive microenvironment in the liver that facilitates the colonization and growth of liver metastases. The study revealed that tamoxifen treatment led to an elevation in the accumulation of cytotoxic T cells in the liver of patients with colorectal cancer LM. Furthermore, the findings indicated that estrogen plays a role in regulating the immunological milieu in

the liver, which promotes metastasis (80). Postmenopausal women who undergo estrogen supplementation exhibit a decreased susceptibility to advanced colorectal cancer, Jiang L et al. found that inhibition of endogenous extracellular vesicle production reduced the size of MC38 tumors, increased the density of CD8T cells, and reduced the populations of CD4Foxp3Treg cells, PD-L1 macrophages, and MDSCs in MC38 tumors by immunofluorescence assay, flow cytometry, and other experiments. Transforming growth factor β1 (TGFβ) induces Treg cells, MC38-EVs significantly promote Treg cell induction *in vitro*, E2 reduces the level of TGF-β1 in MC38-EVs and impairs Treg induction in MC38-EVs *in vitro*, which in turn inhibits the growth of mouse colon cancer (81). In a study conducted by Vassiliki Tzelepi and colleagues, the authors observed an upregulation of estrogen signaling components in the microenvironment of colorectal cancer. Specifically, the expression levels of ERβ1, AIB1 (nuclear hormone receptor transcriptional co-activator 1), and TIF2 (transcriptional intermediate factor 2) were found to be increased in cancer-associated myofibroblasts. Furthermore, these elevated expression levels were found to be positively correlated with the progression of the disease (82). The programmed death receptor PD-1 holds significant immunological significance. In their study, Song C H et al. documented that estrogen effectively hinders the growth of MC38 tumors by suppressing the expression of PD-L1 and influencing the populations of cells associated with the tumor (83). Mifepristone, a compound that acts as an antagonist to progesterone receptors, has demonstrated positive effects on lifespan and overall well-being in different mouse models of cancer. These models encompass tumors that lack progesterone receptors. The mechanism behind this improvement involves the inhibition of immunomodulatory proteins that serve as natural killer cells within the tumor microenvironment. The utilization of antagonists targeting the luteinizing hormone receptor represents a potentially innovative approach in the field of immunotherapy, with the aim of combating cancer (70).

In summary, estrogen inhibits colorectal cancer liver metastasis via TNF receptor-2, reverses extracellular vesicle-mediated immunosuppression of the tumor microenvironment on colorectal cancer growth in mice, inhibits colorectal cancer tumor growth via down-regulation of PD-L1 expression and M1 macrophages, and progesterone receptor antagonists inhibit colorectal cancer liver metastasis by modulating NK cells. The current information about the three hormones and myeloid-derived cells, macrophages, T cells, and tumor-associated fibroblasts in colorectal TME is relevant, but the specific roles are not well understood. There have also been few studies related to these three hormones and other tumor microenvironment molecules. Therefore, further studies are needed.

5 Summary and prospects

This paper summarizes the relationship between androgens, estrogens and progesterone and colorectal cancer and its microenvironment. On the one hand, there is a new understanding of the mechanism of colorectal cancer development, progression and metastasis, androgen plays a promotional role in colorectal cancer development, while mAR promotes apoptosis of tumor cells; on the other hand, estrogen and progesterone-associated receptors are inhibitory to the progression of colorectal cancer. Although the association between these three elements and colorectal cancer is evident, the specific mechanisms involved are still unclear, particularly concerning the diverse cellular constituents and associated elements inside the tumor microenvironment of colorectal cancer. It is known that the accumulation of MDSCs and Treg cells in colorectal cancer liver metastases is TNFR2-dependent in females; estrogen, by reversing extracellular vesicle-mediated immunity, leads to a significant decrease in the PD-L1+M2-like macrophage, Treg cell, and MDSC populations, and an increase in the cytotoxic CD8+ T cell population increased, thereby suppressing the tumor microenvironment inhibiting the growth of mouse colon cancer; the present study investigates the role of estrogen signaling within the microenvironment of rectal cancer. Specifically, it examines the upregulation of ERβ1, AIB1, and TIF2 expression in cancer-associated myofibroblasts, and its correlation with disease progression. Furthermore, the study explores the inhibitory effect of estrogen on the growth of MC38 tumors, elucidating its mechanism of action through the downregulation of PD-L1 expression and modulation of tumor-associated cell populations; The efficacy of mifepristone, a progesterone receptor antagonist, has been demonstrated in enhancing lifespan and enhancing overall well-being in different spontaneous murine cancer models. This includes tumors that lack progesterone receptors. Mifepristone achieves this by inhibiting immunomodulatory proteins that act as natural killer cells within the tumor microenvironment. Mifepristone treatment for colorectal cancer has been less studied and large-scale controlled studies are needed to confirm its ability to inhibit colorectal cancer development. In particular, mifepristone modulates immune cells such as NK cells in the tumor microenvironment. Tamoxifen is more widely used in the treatment of colorectal cancer compared to mifepristone, but the mechanisms involved also need to be further elucidated.

Current studies have shown that the incidence of colorectal cancer is higher in men than in women, but the molecular mechanism of the gender difference is still unclear, so more in-depth studies are needed. The present review elucidates the relationship between these three hormones and the colorectal microenvironment, but the mechanisms related to other immune cells in the tumor microenvironment have not been elucidated yet, and the clinical application of these three hormones in colorectal cancer is not widespread enough, and the use of the hormones alone, hormone replacement therapy, or hormones in combination with other anti-tumor therapies is yet to be developed with the aim of preventing or restricting the growth of *in-situ* colorectal cancers or preventing their distant metastasis. metastasis. Therefore, the study of these three hormones and their receptors and colorectal cancer is very necessary. It is believed that the role of estrogen, androgens, progesterone, and their receptors in the tumor microenvironment of colorectal cancer and its treatment of CRC has potential.

Author contributions

WD: Writing – review & editing. WL: Writing – original draft. LL: Writing – original draft. LZ: Writing – original draft. ZQ: Writing – original draft. ZW: Writing – original draft.

Funding

The author(s) declare financial support was received for the research, authorship, and/or publication of this article. This work was supported by grants from National Natural Science Foundation of China (No. 82172855). The funding bodies played no role in the design of the study and collection, analysis, and interpretation of data and in writing the manuscript.

Conflict of interest

The authors declare that the research was conducted in the absence of any commercial or financial relationships that could be construed as a potential conflict of interest.

Publisher's note

References

1. Bray F, Ferlay J, Soerjomataram I, Siegel RL, Torre LA, Jemal A. Global cancer statistics 2018: GLOBOCAN estimates of incidence and mortality worldwide for 36 cancers in 185 countries. *CA Cancer J Clin* (2018) 68(6):394–424. doi: 10.3322/caac.21492

2. Stebbings WS, Vinson GP, Farthing MJ, Balkwill F, Wood RF. Effect of steroid hormones on human colorectal adenocarcinoma xenografts, of known steroid-receptor status, in nude mice. *J Cancer Res Clin Oncol* (1989) 115(5):439–44. doi: 10.1007/BF00393333

3. Moon JY, Choi MH, Kim J. Metabolic profiling of cholesterol and sex steroid hormones to monitor urological diseases. *Endocr Relat Cancer* (2016) 23(10):R455–67. doi: 10.1530/ERC-16-0285

4. Smith JP, Solomon TE. Effects of gastrin, proglumide, and somatostatin on growth of human colon cancer. *Gastroenterology* (1988) 95(6):1541–8. doi: 10.1016/S0016-5085(88)80075-1

5. Anderson NM, Simon MC. The tumor microenvironment. *Curr Biol* (2020) 30 (16):R921–r925. doi: 10.1016/j.cub.2020.06.081

6. Reisch N, Taylor AE, Nogueira EF, Asby DJ, Dhir V, Berry A, et al. Alternative pathway androgen biosynthesis and human fetal female virilization. *Proc Natl Acad Sci U.S.A.* (2019) 116(44):22294–9. doi: 10.1073/pnas.1906623116

7. Shaffer PL, Jivan A, Dollins DE, Claessens F, Gewirth DT. Structural basis of androgen receptor binding to selective androgen response elements. *Proc Natl Acad Sci U.S.A.* (2004) 101(14):4758–63. doi: 10.1073/pnas.0401123101

8. Campbell-Thompson M, Lynch IJ, Bhardwaj B. Expression of estrogen receptor (ER) subtypes and ERbeta isoforms in colon cancer. *Cancer Res* (2001) 61(2):632–40.

9. Pettersson K, Gustafsson JA. Role of estrogen receptor beta in estrogen action. *Annu Rev Physiol* (2001) 63:165–92. doi: 10.1146/annurev.physiol.63.1.165

10. Jacenik D, Beswick EJ, Krajewska WM, Prossnitz ER. G protein-coupled estrogen receptor in colon function, immune regulation and carcinogenesis. *World J Gastroenterol* (2019) 25(30):4092–104. doi: 10.3748/wjg.v25.i30.4092

11. Kolatorova L, Vitku J, Suchopar J, Hill M, Parizek A. Progesterone: A steroid with wide range of effects in physiology as well as human medicine. *Int J Mol Sci* (2022) 23(14). doi: 10.3390/ijms23147989

12. Sica V, Nola E, Contieri E, Bova R, Masucci MT, Medici N, et al. Estradiol and progesterone receptors in Malignant gastrointestinal tumors. *Cancer Res* (1984) 44 (10):4670–4.

13. Tutton PJ, Barkla DH. The influence of androgens, anti-androgens, and castration on cell proliferation in the jejunal and colonic crypt epithelia, and in dimethylhydrazine-induced adenocarcinoma of rat colon. *Virchows Arch B Cell Pathol Incl Mol Pathol* (1982) 38(3):351–5. doi: 10.1007/BF02892830

14. Izbicki JR, Hamilton SR, Wambach G, Harnisch E, Wilker DK, Dornschneider G, et al. Effects of androgen manipulations on chemically induced colonic tumours and on macroscopically normal colonic mucosa in male Sprague-Dawley rats. *Br J Cancer* (1990) 61(2):235–40. doi: 10.1038/bjc.1990.44

15. Anagnostopoulou V, Pediaditakis I, Alkahtani S, Alarifi SA, Schmidt EM, Lang F, et al. Differential effects of dehydroepiandrosterone and testosterone in prostate and colon cancer cell apoptosis: the role of nerve growth factor (NGF) receptors. *Endocrinology* (2013) 154(7):2446–56. doi: 10.1210/en.2012-2249

16. Dueland S, Guren MG, Olsen DR, Poulsen JP, Magne Tveit K. Radiation therapy induced changes in male sex hormone levels in rectal cancer patients. *Radiother Oncol* (2003) 68(3):249–53. doi: 10.1016/S0167-8140(03)00120-8

17. Mariani M, Zannoni GF, Sioletic S, Sieber S, Martino C, Martinelli E, et al. Gender influences the class III and V β-tubulin ability to predict poor outcome in colorectal cancer. *Clin Cancer Res* (2012) 18(10):2964–75. doi: 10.1158/1078-0432.CCR-11-2318

18. Yu X, Li S, Xu Y, Zhang Y, Ma W, Liang C, et al. Androgen maintains intestinal homeostasis by inhibiting BMP signaling via intestinal stromal cells. *Stem Cell Rep* (2023) 18(1):410. doi: 10.1016/j.stemcr.2022.11.022

19. Refaat B, Aslam A, Idris S, Almalki AH, Alkhaldi MY, Asiri HA, et al. Profiling estrogen, progesterone, and androgen receptors in colorectal cancer in relation to gender, menopausal status, clinical stage, and tumour sidedness. *Front Endocrinol (Lausanne)* (2023) 14:1187259. doi: 10.3389/fendo.2023.1187259

20. Catalano MG, Pfeffer U, Raineri M, Ferro P, Curto A, Capuzzi P, et al. Altered expression of androgen-receptor isoforms in human colon-cancer tissues. *Int J Cancer* (2000) 86(3):325–30. doi: 10.1002/(SICI)1097-0215(20000501)86:3<325::AID-IJC4>3.0.CO;2-G

21. Albasri AM, Elkablawy MA. Clinicopathological and prognostic significance of androgen receptor overexpression in colorectal cancer. Experience from Al-Madinah Al-Munawarah, Saudi Arabia. *Saudi Med J* (2019) 40(9):893–900. doi: 10.15537/smj.2019.9.24204

22. Kikuchi H, Uchida C, Hattori T, Isobe T, Hiramatsu Y, Kitagawa K, et al. ARA54 is involved in transcriptional regulation of the cyclin D1 gene in human cancer cells. *Carcinogenesis* (2007) 28(8):1752–8. doi: 10.1093/carcin/bgm120

23. Ferro P, Catalano MG, Raineri M, Reato G, dell'Eva R, Risio M, et al. Somatic alterations of the androgen receptor CAG repeat in human colon cancer delineate a novel mutation pathway independent of microsatellite instability. *Cancer Genet Cytogenet* (2000) 123(1):35–40. doi: 10.1016/S0165-4608(00)00296-X

24. Huang R, Wang G, Song Y, Wang F, Zhu B, Tang Q, et al. Polymorphic CAG repeat and protein expression of androgen receptor gene in colorectal cancer. *Mol Cancer Ther* (2015) 14(4):1066–74. doi: 10.1158/1535-7163.MCT-14-0620

25. Di Fabio F, Alvarado C, Gologan A, Youssef E, Voda L, Mitmaker E, et al. Somatic mosaicism of androgen receptor CAG repeats in colorectal carcinoma epithelial cells from men. *J Surg Res* (2009) 154(1):38–44. doi: 10.1016/j.jss.2008.05.013

26. Kim YR, Lee BK, Park RY, Nguyen NT, Bae JA, Kwon DD, et al. Differential CARM1 expression in prostate and colorectal cancers. *BMC Cancer* (2010) 10:197. doi: 10.1186/1471-2407-10-197

27. Gu S, Papadopoulou N, Gehring EM, Nasir O, Dimas K, Bhavsar SK, et al. Functional membrane androgen receptors in colon tumors trigger pro-apoptotic responses in *vitro* and reduce drastically tumor incidence in *vivo*. *Mol Cancer* (2009) 8:114. doi: 10.1186/1476-4598-8-114

28. Gu S, Papadopoulou N, Nasir O, Föller M, Alevizopoulos K, Lang F, et al. Activation of membrane androgen receptors in colon cancer inhibits the prosurvival signals Akt/bad in vitro and in *vivo* and blocks migration via vinculin/actin signaling. *Mol Med* (2011) 17(1-2):48–58. doi: 10.2119/molmed.2010.00120

29. Gu S, Kounenidakis M, Schmidt EM, Deshpande D, Alkahtani S, Alarifi S, et al. Rapid activation of FAK/mTOR/p70S6K/PAK1-signaling controls the early testosterone-induced actin reorganization in colon cancer cells. *Cell Signal* (2013) 25 (1):66–73. doi: 10.1016/j.cellsig.2012.08.005

30. Gu S, Honisch S, Kounenidakis M, Alkahtani S, Alarifi S, Alevizopoulos K, et al. Membrane androgen receptor down-regulates c-src-activity and beta-catenin

transcription and triggers GSK-3beta-phosphorylation in colon tumor cells. *Cell Physiol Biochem* (2014) 34(4):1402–12. doi: 10.1159/000366346

31. Sato R, Suzuki T, Katayose Y, Miura K, Shiiba K, Tateno H, et al. Steroid sulfatase and estrogen sulfotransferase in colon carcinoma: regulators of intratumoral estrogen concentrations and potent prognostic factors. *Cancer Res* (2009) 69(3):914–22. doi: 10.1158/0008-5472.CAN-08-0906

32. Zamani ARN, Avci ÇB, Ahmadi M, Pouyafar A, Bagheri HS, Fathi F, et al. Estradiol modulated colorectal cancer stem cells bioactivity and interaction with endothelial cells. *Life Sci* (2020) 257:118078. doi: 10.1016/j.lfs.2020.118078

33. Heijmans J, Wielenga MC, Rosekrans SL, van Lidth de Jeude JF, Roelofs J, Groothuis P, et al. Oestrogens promote tumorigenesis in a mouse model for colitis-associated cancer. *Gut* (2014) 63(2):310–6. doi: 10.1136/gutjnl-2012-304216

34. Kobayashi EH, Suzuki T, Funayama R, Nagashima T, Hayashi M, Sekine H, et al. Nrf2 suppresses macrophage inflammatory response by blocking proinflammatory cytokine transcription. *Nat Commun* (2016) 7:11624. doi: 10.1038/ncomms11624

35. Son HJ, Sohn SH, Kim N, Lee HN, Lee SM, Nam RH, et al. Effect of estradiol in an azoxymethane/dextran sulfate sodium-treated mouse model of colorectal cancer: implication for sex difference in colorectal cancer development. *Cancer Res Treat* (2019) 51(2):632–48. doi: 10.4143/crt.2018.060

36. Song CH, Kim N, Hee Nam R, In Choi S, Hee Son J, Eun Yu J, et al. 17β-Estradiol strongly inhibits azoxymethane/dextran sulfate sodium-induced colorectal cancer development in Nrf2 knockout male mice. *Biochem Pharmacol* (2020) 182:114279. doi: 10.1016/j.bcp.2020.114279

37. Wilkins HR, Doucet K, Duke V, Morra A, Johnson N. Estrogen prevents sustained COLO-205 human colon cancer cell growth by inducing apoptosis, decreasing c-myb protein, and decreasing transcription of the anti-apoptotic protein bcl-2. *Tumour Biol* (2010) 31(1):16–22. doi: 10.1007/s13277-009-0003-2

38. Abd Ellateef A, Mohamed AES, Elhakeem AA, Ahmed SF. Estrogen and progesterone expression in colorectal carcinoma: A clinicopathological study. *Asian Pac J Cancer Prev* (2020) 21(4):1155–62. doi: 10.31557/APJCP.2020.21.4.1155

39. Cho NL, Javid SH, Carothers AM, Redston M, Bertagnolli MM. Estrogen receptors alpha and beta are inhibitory modifiers of Apc-dependent tumorigenesis in the proximal colon of Min/+ mice. *Cancer Res* (2007) 67(5):2366–72. doi: 10.1158/0008-5472.CAN-06-3026

40. Hsu HH, Cheng SF, Chen LM, Liu JY, Chu CH, Weng YJ, et al. Over-expressed estrogen receptor-alpha up-regulates hTNF-alpha gene expression and down-regulates beta-catenin signaling activity to induce the apoptosis and inhibit proliferation of LoVo colon cancer cells. *Mol Cell Biochem* (2006) 289(1-2):101–9. doi: 10.1007/s11010-006-9153-3

41. Jiang HP, Teng RY, Wang Q, Zhang X, Wang HH, Cao J, et al. Estrogen receptor alpha variant ERalpha46 mediates growth inhibition and apoptosis of human HT-29 colon adenocarcinoma cells in the presence of 17beta-oestradiol. *Chin Med J (Engl)* (2008) 121(11):1025–31. doi: 10.1097/00029330-200806010-00012

42. Slattery ML, Sweeney C, Murtaugh M, Ma KN, Wolff RK, Potter JD, et al. Associations between ERalpha, ERbeta, and AR genotypes and colon and rectal cancer. *Cancer Epidemiol Biomarkers Prev* (2005) 14(12):2936–42. doi: 10.1158/1055-9965.EPI-05-0514

43. Giroux V, Lemay F, Bernatchez G, Robitaille Y, Carrier JC. Estrogen receptor beta deficiency enhances small intestinal tumorigenesis in ApcMin/+ mice. *Int J Cancer* (2008) 123(2):303–11. doi: 10.1002/ijc.23532

44. Caiazza F, Galluzzo P, Lorenzetti S, Marino M. 17Beta-estradiol induces ERbeta up-regulation via p38/MAPK activation in colon cancer cells. *Biochem Biophys Res Commun* (2007) 359(1):102–7. doi: 10.1016/j.bbrc.2007.05.059

45. Indukuri R, Hases L, Archer A, Williams C. Estrogen receptor beta influences the inflammatory p65 cistrome in colon cancer cells. *Front Endocrinol (Lausanne)* (2021) 12:650625. doi: 10.3389/fendo.2021.650625

46. He YQ, Sheng JQ, Ling XL, Fu L, Jin P, Yen L, et al. Estradiol regulates miR-135b and mismatch repair gene expressions via estrogen receptor-β in colorectal cells. *Exp Mol Med* (2012) 44(12):723–32. doi: 10.3858/emm.2012.44.12.079

47. Hsu HH, Kuo WW, Ju DT, Yeh YL, Tu CC, Tsai YLb, et al. Estradiol agonists inhibit human LoVo colorectal-cancer cell proliferation and migration through p53. *World J Gastroenterol* (2014) 20(44):16665–73. doi: 10.3748/wjg.v20.i44.16665

48. Lu JY, Jin P, Gao W, Wang DZ, Sheng JQ. Estrogen enhances mismatch repair by induction of MLH1 expression via estrogen receptor-β. *Oncotarget* (2017) 8 (24):38767–79. doi: 10.18632/oncotarget.16351

49. Banerjee A, Cai S, Xie G, Li N, Bai X, Lavudi K, et al. A novel estrogen receptor β Agonist diminishes ovarian cancer stem cells via suppressing the epithelial-to-mesenchymal transition. *Cancers (Basel)* (2022) 14(9). doi: 10.3390/cancers14092311

50. Motylewska E, Stasikowska O, Mełeń-Mucha G. The inhibitory effect of diarylpropionitrile, a selective agonist of estrogen receptor beta, on the growth of MC38 colon cancer line. *Cancer Lett* (2009) 276(1):68–73. doi: 10.1016/j.canlet.2008.10.050

51. Nakayama Y, Sakamoto H, Satoh K, Yamamoto T. Tamoxifen and gonadal steroids inhibit colon cancer growth in association with inhibition of thymidylate synthase, survivin and telomerase expression through estrogen receptor beta mediated system. *Cancer Lett* (2000) 161(1):63–71. doi: 10.1016/S0304-3835(00)00600-5

52. Zhu L, Liu S, Liao YF, Sheng YM, He JC, Cai ZX, et al. Calycosin suppresses colorectal cancer progression by targeting ERβ, upregulating PTEN, and inhibiting PI3K/Akt signal pathway. *Cell Biol Int* (2022) 46(9):1367–77. doi: 10.1002/cbin.11840

53. Liu T, Zhao M, Peng L, Chen J, Xing P, Gao P, et al. WFDC3 inhibits tumor metastasis by promoting the ERβ-mediated transcriptional repression of TGFBR1 in colorectal cancer. *Cell Death Dis* (2023) 14(7):425. doi: 10.1038/s41419-023-05956-0

54. Liu Q, Chen Z, Jiang G, Zhou Y, Yang X, Huang H, et al. Epigenetic down regulation of G protein-coupled estrogen receptor (GPER) functions as a tumor suppressor in colorectal cancer. *Mol Cancer* (2017) 16(1):87. doi: 10.1186/s12943-017-0654-3

55. Gilligan LC, Rahman HP, Hewitt AM, Sitch AJ, Gondal A, Arvaniti A, et al. Estrogen activation by steroid sulfatase increases colorectal cancer proliferation via GPER. *J Clin Endocrinol Metab* (2017) 102(12):4435–47. doi: 10.1210/jc.2016-3716

56. Abancens M, Harvey BJ, Mcbryan J. GPER agonist G1 prevents wnt-induced JUN upregulation in HT29 colorectal cancer cells. *Int J Mol Sci* (2022) 23(20). doi: 10.3390/ijms232012581

57. Tsai HW, Ho CL, Cheng SW, Lin YJ, Chen CC, Cheng PN, et al. Progesterone receptor membrane component 1 as a potential prognostic biomarker for hepatocellular carcinoma. *World J Gastroenterol* (2018) 24(10):1152–66. doi: 10.3748/wjg.v24.i10.1152

58. Singh S, Sheppard MC, Langman MJ. Sex differences in the incidence of colorectal cancer: an exploration of oestrogen and progesterone receptors. *Gut* (1993) 34(5):611–5. doi: 10.1136/gut.34.5.611

59. Zhang YL, Wen XD, Guo X, Huang SQ, Wang TT, Zhou PT, et al. Progesterone suppresses the progression of colonic carcinoma by increasing the activity of the GADD45α/JNK/c–Jun signalling pathway. *Oncol Rep* (2021) 45(6). doi: 10.3892/or.2021.8046

60. Dabizzi S, Noci I, Borri P, Borrani E, Giachi M, Balzi M, et al. Luteinizing hormone increases human endometrial cancer cells invasiveness through activation of protein kinase A. *Cancer Res* (2003) 63(14):4281–6.

61. Zhang Z, Gao W, Zhou L, Chen Y, Qin S, Zhang L, et al. Repurposing brigatinib for the treatment of colorectal cancer based on inhibition of ER-phagy. *Theranostics* (2019) 9(17):4878–92. doi: 10.7150/thno.36254

62. Liu D. Gene signatures of estrogen and progesterone receptor pathways predict the prognosis of colorectal cancer. *FEBS J* (2016) 283(16):3115–33. doi: 10.1111/febs.13798

63. Tanaka Y, Kato K, Mibu R, Uchida S, Asanoma K, Hashimoto K, et al. Medroxyprogesterone acetate inhibits proliferation of colon cancer cell lines by modulating cell cycle-related protein expression. *Menopause* (2008) 15(3):442–53. doi: 10.1097/gme.0b013e318156fb77

64. Wang HC, Huo YN, Lee WS. Activation of progesterone receptor is essential for folic acid-regulated cancer cell proliferation and migration. *J Nutr Biochem* (2023) 112:109205. doi: 10.1016/j.jnutbio.2022.109205

65. Ting PC, Lee WR, Huo YN, Hsu SP, Lee WS. Folic acid inhibits colorectal cancer cell migration. *J Nutr Biochem* (2019) 63:157–64. doi: 10.1016/j.jnutbio.2018.09.020

66. Kuo CT, Lee WS. Progesterone receptor activation is required for folic acid-induced anti-proliferation in colorectal cancer cell lines. *Cancer Lett* (2016) 378(2):104–10. doi: 10.1016/j.canlet.2016.05.019

67. Kuo CT, Chang C, Lee WS. Folic acid inhibits COLO-205 colon cancer cell proliferation through activating the FRα/c-SRC/ERK1/2/NFκB/TP53 pathway: in *vitro* and in *vivo* studies. *Sci Rep* (2015) 5:11187. doi: 10.1038/srep11187

68. Mahbub AA, Aslam A, Elzubier ME, El-Boshy M, Abdelghany AH, Ahmad J, et al. Enhanced anti-cancer effects of oestrogen and progesterone co-therapy against colorectal cancer in males. *Front Endocrinol (Lausanne)* (2022) 13:941834. doi: 10.3389/fendo.2022.941834

69. Wang X, Li X, Fan F, Jiao S, Wang L, Zhu L, et al. PAQR3 plays a suppressive role in the tumorigenesis of colorectal cancers. *Carcinogenesis* (2012) 33(11):2228–35. doi: 10.1093/carcin/bgs245

70. Check JH, Dix E, Sansoucie L, Check D. Mifepristone may halt progression of extensively metastatic human adenocarcinoma of the colon - case report. *Anticancer Res* (2009) 29(5):1611–3.

71. Lin M, Du T, Tang X, Liao Y, Cao L, Zhang Y, et al. An estrogen response-related signature predicts response to immunotherapy in melanoma. *Front Immunol* (2023) 14:1109300. doi: 10.3389/fimmu.2023.1109300

72. Shee K, Yang W, Hinds JW, Hampsch RA, Varn FS, Traphagen NA, et al. Therapeutically targeting tumor microenvironment-mediated drug resistance in estrogen receptor-positive breast cancer. *J Exp Med* (2018) 215(3):895–910. doi: 10.1084/jem.20171818

73. Hurley PJ, Hughes RM, Simons BW, Huang J, Miller RM, Shinder B, et al. Androgen-regulated SPARCL1 in the tumor microenvironment inhibits metastatic progression. *Cancer Res* (2015) 75(20):4322–34. doi: 10.1158/0008-5472.CAN-15-0024

74. Chakraborty B, Byemerwa J, Shepherd J, Haines CN, Baldi R, Gong W, et al. Inhibition of estrogen signaling in myeloid cells increases tumor immunity in melanoma. *J Clin Invest* (2021) 131(23). doi: 10.1172/JCI151347

75. Madeo A, Maggiolini M. Nuclear alternate estrogen receptor GPR30 mediates 17beta-estradiol-induced gene expression and migration in breast cancer-associated fibroblasts. *Cancer Res* (2010) 70(14):6036–46. doi: 10.1158/0008-5472.CAN-10-0408

76. Leach DA, Need EF, Trotta AP, Grubisha MJ, DeFranco DB, Buchanan G. Hic-5 influences genomic and non-genomic actions of the androgen receptor in prostate myofibroblasts. *Mol Cell Endocrinol* (2014) 384(1-2):185–99. doi: 10.1016/j.mce.2014.01.004

77. Li XF, Selli C, Zhou HL, Cao J, Wu S, Ma RY, et al. Macrophages promote anti-androgen resistance in prostate cancer bone disease. *J Exp Med* (2023) 220(4). doi: 10.1084/jem.20221007

78. Werner LR, Gibson KA, Goodman ML, Helm DE, Walter KR, Holloran SM, et al. Progesterone promotes immunomodulation and tumor development in the murine mammary gland. *J Immunother Cancer* (2021) 9(5). doi: 10.1136/jitc-2020-001710

79. Xia Z, Xiao J, Dai Z, Chen Q. Membrane progesterone receptor α (mPRα) enhances hypoxia-induced vascular endothelial growth factor secretion and angiogenesis in lung adenocarcinoma through STAT3 signaling. *J Transl Med* (2022) 20(1):72. doi: 10.1186/s12967-022-03270-5

80. Milette S, Hashimoto M, Perrino S, Qi S, Chen M, Ham B, et al. Sexual dimorphism and the role of estrogen in the immune microenvironment of liver metastases. *Nat Commun* (2019) 10(1):5745. doi: 10.1038/s41467-019-13571-x

81. Jiang L, Fei H, Yang A, Zhu J, Sun J, Liu X, et al. Estrogen inhibits the growth of colon cancer in mice through reversing extracellular vesicle-mediated immunosuppressive tumor microenvironment. *Cancer Lett* (2021) 520:332–43. doi: 10.1016/j.canlet.2021.08.011

82. Tzelepi V, Grivas P, Kefalopoulou Z, Kalofonos H, Varakis JN, Melachrinou M, et al. Estrogen signaling in colorectal carcinoma microenvironment: expression of ERbeta1, AIB-1, and TIF-2 is upregulated in cancer-associated myofibroblasts and correlates with disease progression. *Virchows Arch* (2009) 454(4):389–99. doi: 10.1007/s00428-009-0740-z

83. Song CH, Kim N, Nam RH, Choi SI, Jang JY, Kim JW, et al. Combination treatment with 17β-estradiol and anti-PD-L1 suppresses MC38 tumor growth by reducing PD-L1 expression and enhancing M1 macrophage population in MC38 colon tumor model. *Cancer Lett* (2022) 543:215780. doi: 10.1016/j.canlet.2022.215780

frontiers | Frontiers in Immunology

TYPE Review
PUBLISHED 08 January 2024
DOI 10.3389/fimmu.2023.1307228

OPEN ACCESS

EDITED BY
Asif Raza,
Penn State Milton S. Hershey Medical Center,
United States

REVIEWED BY
Anna Fakhardo,
The Pennsylvania State University,
United States
Hamid Aria,
Isfahan University of Medical Sciences, Iran
Seyma Demirsoy,
The Pennsylvania State University,
United States

*CORRESPONDENCE
Xiaorong Qi
qixiaorong11@163.com

RECEIVED 04 October 2023
ACCEPTED 18 December 2023
PUBLISHED 08 January 2024

CITATION
Long Y, Shi H, He Y and Qi X (2024) Analyzing the impact of metabolism on immune cells in tumor microenvironment to promote the development of immunotherapy.
Front. Immunol. 14:1307228.
doi: 10.3389/fimmu.2023.1307228

Analyzing the impact of metabolism on immune cells in tumor microenvironment to promote the development of immunotherapy

Yanru Long, Houhui Shi, Yuedong He and Xiaorong Qi*

Department of Gynecology and Obstetrics, Key Laboratory of Birth Defects and Related Diseases of Women and Children (Sichuan University), Ministry of Education, West China Second Hospital, Sichuan University, Chengdu, China

Tumor metabolism and tumor immunity are inextricably linked. Targeting the metabolism of tumors is a point worth studying in tumor immunotherapy. Recently, the influence of the metabolism of tumors and immune cells on the occurrence, proliferation, metastasis, and prognosis of tumors has attracted more attention. Tumor tissue forms a specific tumor microenvironment (TME). In addition to tumor cells, there are also immune cells, stromal cells, and other cells in TME. To adapt to the environment, tumor cells go through the metabolism reprogramming of various substances. The metabolism reprogramming of tumor cells may further affect the formation of the tumor microenvironment and the function of a variety of cells, especially immune cells, eventually promoting tumor development. Therefore, it is necessary to study the metabolism of tumor cells and its effects on immune cells to guide tumor immunotherapy. Inhibiting tumor metabolism may restore immune balance and promote the immune response in tumors. This article will describe glucose metabolism, lipid metabolism, amino acid metabolism, and immune cells in tumors. Besides, the impact of metabolism on the immune cells in TME is also discussed for analyzing and exploring tumor immunotherapy.

KEYWORDS

metabolism reprogramming, tumor microenvironment, immunotherapy, glucose metabolism, lipid metabolism, amino acid metabolism

1 Introduction

Tumor metabolism has been universally studied by a lot of researchers all over the world, and the heterogeneity of cellular metabolism is one of its most worthy hallmarks to be explored (1). In normal cells, the glycolysis and tricarboxylic acid (TCA) cycle can provide energy for them, but different from normal cells, tumor cells produce lactic acid via

glycolysis even if in an environment with sufficient oxygen, which is termed as "Warburg effect" (2–5) (Figure 1). The "Warburg effect" reflects the features of tumor cells changing their metabolism patterns to be suited to the tumor microenvironment (TME), which is known as "metabolism reprogramming", and metabolic reprogramming is significant for the growth of tumor cells (6–8). The proliferation of tumor cells is accompanied by the collection of non-tumor cells, forming a specific environment good for tumor growth and metastasis (9). At the same time, it reshapes the TME (10). The TME affects the occurrence, progression, and metastasis of tumors greatly, and is mainly composed of cellular and noncellular portions (11). The cellular portions consist of immune cells, endothelial cells, cancer-related fibroblasts, and so on (12). The non-cellular portions contain largely the extracellular matrix, which includes glycoproteins and protein polysaccharides, to support the structure of tissue (12–14). Additionally, the portions in TME have a non-negligible impact on the immune response. Immune cells undergo metabolic changes to adapt to the TME, thus destroying the effectiveness of the immune response (15). One of the points is that the function of the immune system is affected by tumor cells, so the immune system cannot identify tumor cells normally, for example, tumor cells produce specific metabolites to inhibit the function of antitumor immune cells, and another point is that tumor cells promote immunosuppressive cells to secrete immunosuppressive molecules, thus affecting anti-tumor immunity, which is favorable to immune escape and tumor metastasis to a certain extent (8).

The mechanism of tumor metabolism affecting immune escape is being studied in depth (12). It is indicated that the inhibited immune response is in connection with a variety of factors such as the metabolic patterns of substances in the TME (16). It is gradually found that the reprogramming of metabolism in TME has a huge impact on immunotherapy for tumors, for instance, glucose metabolism, amino acid metabolism, and fatty acid metabolism can regulate immune checkpoint therapy (12). Therefore, targeting metabolism reprogramming is a tumor treatment method worth studying. It is worth mentioning that much attention has been paid to tumor cell metabolism, but little is recognized about the role of immune cells in the TME. However, the metabolism of immune cells does not only affect their function but also has an impact on the occurrence and progression of tumors.

It is indicated that the immune response in the tumor microenvironment possibly be affected when the metabolism of immune cells changes, and the metabolism of immune cells is crucial to the growth of tumors (17). Recently, immunotherapies have been regarded as a promising tumor treatment by activating immune cells or through transplantation of engineered cells for targeting and eliminating tumor cells (14). It makes sense to analyze the function of immune cells in the TME and the influence of TME on immune cells, to provide some clues for facilitating the tumor immunotherapy (17).

2 The metabolism of tumor cells in TME

The TME, a place for the metabolism of cells, includes extracellular matrix, tumor cells, immune cells, stromal cells, and so on (18, 19). Tumor cell metabolism and proliferation require oxygen, but slow angiogenesis can lead to hypoxia in tumor tissue (20). Most tumor tissues form an environment that lacks nutrients and oxygen, so tumor cells are necessary to alter their metabolic patterns to adapt to such an environment (21–24). For instance, it is found that hypoxia can facilitate glycolysis in tumor cells, and can

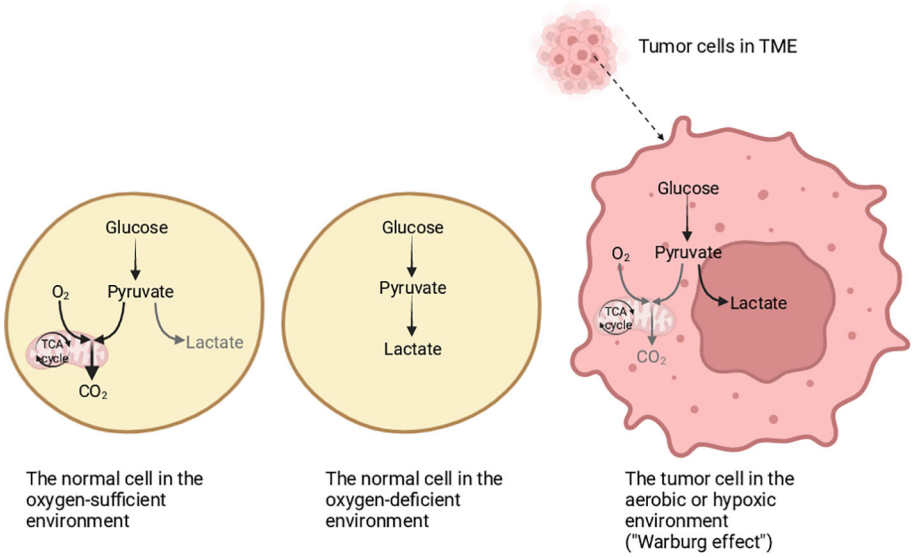

FIGURE 1
The differentiation of glucose metabolism in normal cells and tumor cells. In an oxygen-sufficient environment, the glucose metabolism in normal cells is mainly oxidative phosphorylation, and a small part is glycolysis. In an oxygen-deficient environment, the normal cells mainly obtain energy through glycolysis. In tumor cells, whether there is hypoxia or not, energy is mainly obtained through glycolysis, which is called the "Warburg effect". Created with "BioRender.com".

also promote lipid metabolism by activating the PI3K/AKT pathway (20). That is to say, tumor cells undergo metabolic reprogramming of several substances, including glucose, lipids, and amino acids, but the most famous one is the "Warburg effect" (25–27). Metabolism reprogramming is one of the ways for tumors to avoid the attack of the immune system and inhibit the immune response, which plays a crucial role in adapting to TME for tumor cells (28). Tumor cells can inhibit the function of immune cells by competitively ingesting nutrients such as amino acids, and can also affect the function of immune cells by producing complex and variable metabolites (29).

2.1 Glucose metabolism

In TME, whether oxygen is sufficient or not, tumor cells make use of plenty of glucose for glycolysis to generate lactic acid (30–32). As we all know, hypoxia-inducible factor-1 (HIF-1) induced by hypoxia can determine the modes of glucose metabolism, and a variety of substances in TME increase the amount of HIF-1 protein and also promote glycolysis (30). Also, it is found that the enhancement of glycolysis in tumor cells is regulated by many factors, such as HIF-1, p53, and PI3K/AKT pathways (33, 34). And the increase of aerobic glycolysis in tumor cells produces more lactic acid. If lactic acid continues increasing, it will lead to acidity or even acidosis in the cells (33). According to research, lactic acid can be excreted into the tumor matrix through monocarboxylate transporters 4 (MCT4), and it can not only promote the increase of HIF-1 and vascular endothelial growth factor (VEGF) but also be regarded as a source providing energy for tumor cells (20). What's more, lactic acid is dissociated into lactate and H+ in the body. The more lactic acid, the more H+ is produced. The increased H+ can reduce the pH of TME, causing tumor immunosuppression (35). Although the amount of ATP produced by monomolecular glucose through oxidative phosphorylation in mitochondria is higher than that of aerobic glycolysis, aerobic glycolysis produces ATP faster, which is beneficial for tumor cell growth (36, 37). In addition, aerobic glycolysis also reduces the demand of tumor cells for oxygen and mitochondria (20).

2.2 Lipid metabolism

When glucose is deficient in the TME, tumor cells and immune cells tend to perform lipid metabolism (38). In addition, immune cells can also make use of the ketone bodies produced by the fatty acids oxidation to obtain energy (20). Lipids include phospholipids, cholesterol, triglycerides, fatty acids, and many other types (39–42). Lipid metabolism includes anabolism and catabolism, and the catabolism is commonly known as β-oxidation (43).

Lipid metabolism is an important energy source, which can promote the proliferation of cells and enhance the function of cells (44). Apart from providing the energy needed for cell metabolism, lipids can also promote cell migration in other ways, for instance, lipids can form cell membranes, participate in signaling, and so on (45–48). In normal cells, lipids can be obtained by ingesting lipids outside the cell, or by synthesizing lipids in cells, and then metabolizing lipids (49, 50). The lipid metabolism in tumor cells is significantly different (51, 52). The activation of oncogenes induces lipid metabolism to provide energy for tumor cells, eventually promoting the proliferation and metastasis of tumors (53). The crazy proliferation of tumor cells needs the support of several lipids (54). Not only can tumor cells synthesize lipids by using some enzymes, including fatty acid synthase (FASN), sterol regulatory element-binding proteins (SREBPs), acetyl-coenzyme A (Ac CoA), stearoyl-CoA desaturase 1 (SCD1), acetylCoA carboxylase (ACC), but also they can absorb lipids directly from the external environment through different ways (45).

For example, low-density lipoprotein (LDL) can enter tumor cells with the help of LDL receptors. Besides, cholesterol can enter tumor cells mediated by fatty acid translocase, such as CD36 (20). In TME, because of the hypoxic environment, HIF promotes the intake and synthesis of fatty acids in tumor cells, which is beneficial for lipid accumulation (55). In addition to fatty acids, phospholipids and cholesterol are also two kinds of lipids that cannot be ignored, on the one side, cholesterol can not only form a cell membrane but also be converted into steroid hormones under certain conditions, on the other side, steroid hormones can spread freely from serum to cells (20). When steroid hormones bind to receptors in tumor tissue, tumor cells can proliferate, and this mechanism is probably related to the development of breast cancer (56). Cholesterol is a part of the cytomembrane, maintaining the structure of cells, and its metabolites can regulate the function of immune cells (57). Phospholipids are divided into glycerophospholipids and sphingolipids, which can not only form cell membranes but also participate in some signaling pathways, such as the PI3K signaling pathway, among them, phospholipids related to arachidonic acid (AA) have attracted widespread attention (58). In tumor cells, if lipids are abundant, they are probably stored in lipid droplets (LDs), and it is reported that the storage forms include triglycerides and cholesterol esters (45). Therefore, the obvious increase in the number of LDs has become one of the characteristics of tumors (20). Lipid metabolism is the basic metabolism and the energy source of tumor cells, eventually promoting the growth and development of tumors.

2.3 Amino acid metabolism

Apart from glucose metabolism and lipid metabolism, amino acid metabolism in TME has gradually attracted attention. Amino acids, organic compounds, are the basic units that make up proteins, and it has been shown that amino acids are related to tumor cell proliferation and metastasis (15). Although amino acids have a nonnegligible influence on the function of cells, they cannot directly enter into cells. It is demonstrated that the hydrophilic nature of amino acids determines that they cannot freely pass through the cell membrane, in fact, amino acids need to enter cells with the assistance of various transporters (17).

Besides, amino acid metabolism is reprogrammed in TME, and it has been confirmed that amino acid metabolism reprogramming includes changes in the intake rate of amino acids, changes in

pathways, and abnormality of key enzymes (17). Amino acids are of significance for tumor cells, such as arginine, methionine, glutamine, and so on (59). The rapid proliferation of tumor cells requires the intake of a large number of amino acids, and the uptake of amino acids requires the assistance of transport proteins, so amino acid transport proteins can regulate the uptake rate of amino acids and influence tumor development, for example, glutamine enters tumor cells with the assistance of alanine-serine-cysteine transporter 2 (ASCT2) (17). Compared with normal cells, tumor cells need more glutamine to proliferate, so the expression of ASCT2 in tumor cells increases. In addition, enzymes and signaling pathways related to amino acid metabolism can also affect tumor proliferation, for example, liver kinase B1 (LKB1), also known as serine-threonine kinase 11 (STK11), is inhibited when combined with asparagine (17). Therefore, asparagine metabolism can affect the proliferation and metastasis of tumor cells by affecting the LKB1-AMPK signaling pathway (15).

For tumor cells, plenty of amino acids can promote their growth and development. But, as mentioned above, amino acids need amino acid transport proteins to enter cells, so tumor cells cannot ingest amino acids indefinitely. Different tumor cells may ingest different types of amino acids. Nevertheless, amino acid metabolism is also vital for promoting tumor development, which is also worth studying.

3 Effect of metabolism on immune cells

As we all know, a tumor is a kind of disease characterized by immunodeficiency, and tumor cells can escape the recognition and removal of multiple immune cells in many pathways (60). The TME, characterized by nutrient deficiency, lactic acid, lipid accumulation, and hypoxia, influences the role of the immune system and hinders the immune response (Figure 2) (33, 44). Additionally, more and more studies have shown that some metabolites in TME can restrain immune activities (25). To cope with the pressure of the TME, immune cells regulate their metabolic patterns to inhibit tumor development (56). Therefore, we need to study the metabolic modes of immune cells in TME and the effects of immune cells on tumor growth.

The immune system is composed of many types of cells, including neutrophils, natural killer cells, macrophages, monocytes, eosinophils, and basophils, and the immune system mainly maintains the homeostasis of the internal environment through immune response (61). Usually, some pathological conditions, such as tumors and inflammation, may influence the immune cell metabolism (60). Tumor-infiltrated immune cells are dual, some of which has the effect of inhibiting tumor proliferation and metastasis, such as effector CD8+T (Teff) cells, memory CD8+T (Tmem) cells, natural killer cells (NK cells), B cells, M1 macrophages, dendritic cells (DCs), N1 neutrophils and so on, while others may be of benefit to the development of tumors, including Treg cells, M2 macrophages, myeloid-derived suppressor cells (MDSCs), and N2 neutrophils (62). Among them, cytotoxic T cells, T effector cells, dendritic cells, and B cells mainly remove cancer cells by recognizing specific antigens, while natural killer cells and macrophages block tumor development through non-specific immune responses (63). Although these cells can prevent tumor development to a certain extent, tumors gradually adapt and promote the role of cells suppressing the immune response, such as tumor-associated macrophages and regulatory T cells, and this feature of tumors forms an immunosuppressive microenvironment, which facilitates ultimately tumor proliferation and metastasis (64).

Generally speaking, immune cells can recognize and inhibit tumor cell proliferation, and even destroy tumor cells (20). However, in TME, the metabolism reprogramming of tumor cells can escape immune surveillance and influence the metabolism of immune cells to promote tumor development (52, 65).

The glucose metabolism reprogramming is beneficial for facilitating the proliferation and development of tumors, and it also has an influence on immune cells in TME (32). The proliferation of tumor cells and immune cells depends on glycolysis, tumor cells use glucose competitively, which makes immune cells lack nutrients and unable to perform their

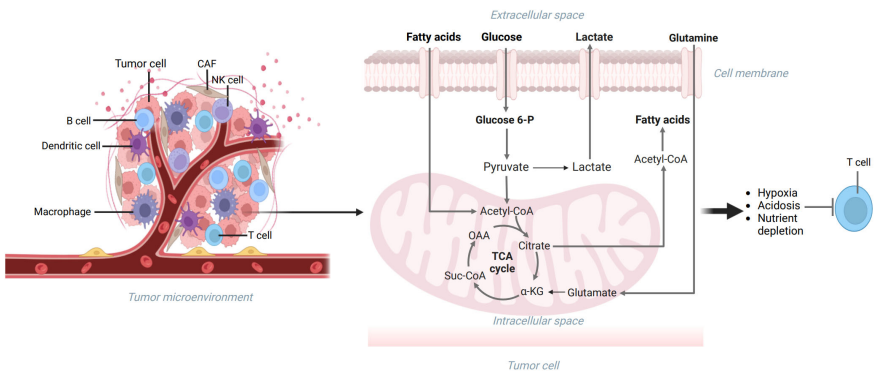

FIGURE 2
The TME includes extracellular matrix, tumor cells, and immune cells. The metabolism reprogramming of glucose, lipids, and amino acids can be seen in tumor cells, which can make the TME characterized by nutrient deficiency, lactic acid accumulation, hypoxia, and immunodeficiency. Created with "BioRender.com".

functions (66). In addition, metabolites produced by tumor cells, such as lactic acid, can also inhibit the role of immune cells, eventually weakening anti-tumor immunity and promoting tumor immune escape (67). It is understood that enzymes in the process of glycolysis may also affect the function of immune cells, among them, hexokinase 2 (HK2) and phosphofructokinase 1 (PFK1) respectively participate in the transformation of glucose into glucose 6phosphate and glucose 6-phosphate into fructose 6-phosphate (68). Besides, lactate dehydrogenase A (LDHA) and pyruvate kinase M2 (PKM2) participate in the process from phosphoenolpyruvate to pyruvate and then to lactic acid (32). Interestingly, HK2 is inseparable from the degree of infiltration of immune cells. PFK1 affects the differentiation of macrophages. PKM2 can promote oxidative phosphorylation and the "Warburg effect", in addition, LDHA can facilitate the production of lactic acid and affect immune cells, eventually leading to immunosuppression (32).

In TME, the variation of metabolic modes of tumor cells inhibits the immune response and promotes tumor development by influencing the composition and function of infiltrated immune cells (69). When glucose is deficient in TME, tumor-infiltrated immune cells may change their metabolic patterns, that is, to maintain their functions by ingesting and metabolizing fatty acids (22). It is found that immune cells that promote the development of tumors generally obtain energy through lipid metabolism to maintain their functions (20). However, it has been proved that excessive lipids may inhibit immune cells and impair the anti-tumor immune response (70). Accordingly, lipid metabolism in TME may impact the survival, progression, and function of immune cells (39). And now, the influence of lipid metabolism on the function of immune cells has been widely discussed.

Amino acid metabolism in TME can also have an effect on immune cells, which is characterized by complexity and diversity (5). For immune cells, amino acids can promote the synthesis of proteins, which are beneficial for immune cells. Not only can amino acid metabolism provide energy for immune cells, but the crucial enzymes in amino acid metabolism can influence immune cells (59). Nevertheless, as mentioned above, amino acids need transport proteins to enter into cells, so immune cells cannot ingest amino acids indefinitely. And different immune cells ingest different types of amino acids (15). Disappointingly, amino acid metabolism reprogramming in TME is harmful to immune cells, on the one hand, the increase of amino acid transporters on tumor cells can promote the entry of amino acids into tumor cells, while the number of amino acids entering immune cells decreases, on the other hand, once the amino acids metabolism products in tumor cells are released, they can damage immune cells in TME (17). Therefore, more and more attention has been paid to analyzing the impact of amino acid metabolism on immune cells.

3.1 Tumor-infiltrating T cells

T cells originate from the thymus and enter the cycle after completing differentiation, the survival and proliferation of these T cells primarily depend on oxidative phosphorylation and the oxidation of fatty acids (71). T cells have various types, including CD4+ cell groups and CD8+ cell groups. CD4+ cell groups include regulatory T cells (Treg), follicular helper T cells (Tfh), T helper cells 1 (Th1), T helper cells 2 (Th2), T helper cells 17 (Th17), while CD8+ cell groups include naive T cells, memory T cells (Tmem), effector T cells (Teff), activated cells, chronic activated T cells (56). Generally speaking, T cells trigger a variety of immune responses by recognizing antigens to maintain the balance of the immune system. In different TME, T cells influence tumor proliferation and tumor development by modulating the anti-tumor immune response (56). There are also differences in the effects of different T cells on tumors. Teff cells can damage tumor cells by producing cytokines, and this activity needs to increase the uptake of glucose and speed up glucose metabolism, while Tmem cells can exist in tumor tissue for a relatively long time, so they can help control tumor growth (20). Although Th17 cells inhibit anti-tumor immune response and promotes tumor proliferation, it also aggregates immune cells (56). Although Th2 cells may promote tumor development through immunosuppression, the subtype closest to immunosuppression in CD4+T cells is Treg (22). It is shown that Treg cells not only secrete inhibitory factors such as interleukin-4 (IL-4) and interleukin-10 (IL-10) but also express inhibitory molecules such as cytotoxic T-lymphocyte-associated protein 4 (CTLA-4) and programmed cell death protein 1 (PD-1) (20). Therefore, in TME, Treg cells inhibit the function of anti-tumor immune cells and ultimately inhibit the anti-tumor immune response, which is beneficial for the progress of tumors (71).

In TME, different types of T cells probably obtain energy in different metabolic pathways. CD8+ T cells are one of the essential immune cells in anti-tumor immunity(48). After being activated, CD8+ T cells are mainly transformed into effector T cells and memory T cells, and their metabolic pathways are completely different. The metabolic pathways in Teff mainly include glycolysis and glutamine metabolism, while in Tmem include oxidative phosphorylation and fatty acid oxidation (71). Apparently, effector T cells increase the uptake of glucose and speed up glucose metabolism (33).

Besides, it is confirmed that T helper cells (Th cells) mainly depend on glycolysis, while Treg cells primarily depend on fatty acid oxidation (56). However, it is guessed that the glucose metabolism of tumor cells affects the metabolism and role of many T cells. Because of the competitive use of glucose by tumor cells, the amount of glucose that the glycolysis-dependent cells can use is significantly reduced (34). Hence, the TME that lacks oxygen and glucose may inhibit the development and function of the glycolysis-dependent cells (71). Nevertheless, the function of some cells that mainly rely on lipid metabolism like Treg cells is not inhibited by the TME that lacks glucose and is full of lactic acid. These cells may also inhibit the immune response and facilitate immune escape (2). Besides, increased lactic acid has been proven to hinder immunity and facilitate tumor development. The lactic acid generated by glycolysis in tumor cells is transported outside the tumor cells through monocarboxylate transporter 1 (MCT1)/monocarboxylate transporter 1 (MCT4), thus forming an acidic TME, which may eventually inhibit the metabolism of cytotoxic T

lymphocytes (72) (Figure 3). Furthermore, as a key factor in promoting Th1 differentiation, interferon-γ (IFN-γ) changes its property in an acidic microenvironment, inducing Th1 to differentiate into Th2 and ultimately promoting tumor development (73). For example, glycolysis-induced infiltration of Th2 cells affects the treatment and prognosis of lung adenocarcinoma (73). Additionally, the increase of lactic acid in the TME can facilitate the intake of more lactic acid by Treg cells. And it is favorable for the immunosuppressive function of Treg cells. Hence, reducing the content of lactic acid in the TME or limiting the intake of lactic acid by Treg cells may do good for immunotherapy (72).

In addition to glucose metabolism, lipid metabolism can also influence the survival and function of T cells. In a nutrient-deficient TME, lipid metabolism provides T cells with the energy they need to survive. The oxidation of fatty acids affects the differentiation of Tmem cells (56). Tmem cells store lipids mainly by synthesizing fatty acids rather than ingesting fatty acids, and Treg cells seem to be similar to Tmem cells at this point. Besides, Teff cells also maintain their functions through lipid catabolization. Additionally, the content of fatty acids also affects the differentiation of Th17 and Treg cells. It is confirmed that when the content of fatty acids in TME is low, exogenous fatty acids impact the function of Th17 and Treg cells. Apart from fatty acids, other lipids, such as cholesterol and phospholipids, can impact the survival and role of T cells (56). If the intake and synthesis of cholesterol are insufficient or the discharge of cholesterol is increased, the proliferation of T cells is suppressed (56). Additionally, the cholesterol in TME hinders the immune response, causing the depletion of CD8+T cells and eventually promoting the growth of tumor cells (74). In fact, the increase of cholesterol in TME facilitates the expression of inhibitory molecules, such as PD-1, affecting the function of CD8 +T cells. However, when the content of cholesterol on the cell membrane increases, such as by inhibiting recombinant acetyl coenzyme acetyltransferase 1 (ACAT1), the function of CD8+T cells is promoted (56).

One of the necessary conditions for the proliferation of T cells is to ingest amino acids, so amino acid metabolism can influence the proliferation and role of T cells (15). In TME, the metabolic rate of tumor cells is many times higher than that of normal cells. Tumor cells competitively inhibit immune cells from ingesting amino acids, for example, the increased intake of glutamate by tumor cells reduces the intake of glutamate by T cells. So the proliferation and activation of T cells are hindered, especially effector T cells. Besides, the lack of tryptophan or cysteine inhibits the proliferation of T cells and affects the role of T cells (75). Moreover, CD8+T cells lose the expression of the mechanistic target of rapamycin (mTOR) due to the deficiency of RagD-dependent amino acids in TME. It has been proven to reduce the growth of T cells and inhibit the anti-tumor immune response (16). Some studies have proved that supplementing amino acids can restore the function of T cells to a certain extent (17).

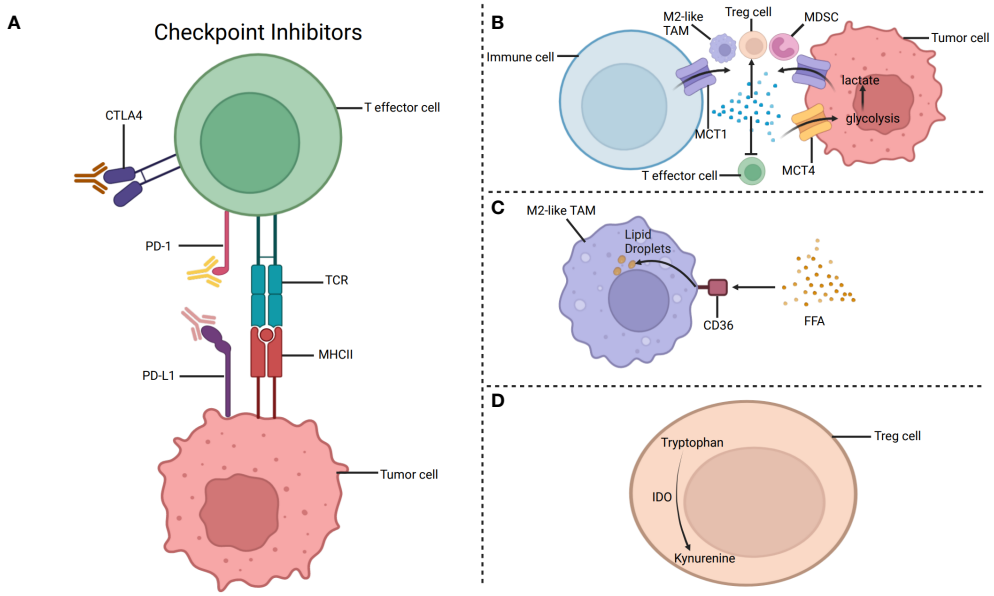

FIGURE 3
The metabolism targets for immunotherapy. **(A)** Targeting PD-1 and CTLA-4 to restore the immune function of T cells. **(B)** The lactic acid generated by glycolysis in tumor cells is transported outside the tumor cells through monocarboxylate transporter 1 (MCT1). Besides, lactic acid accumulation may inhibit the function of T effector cells and promote the function of M2-like TAMs, Treg cells, and MDSC. **(C)** CD36 is a glycoprotein that can help fatty acids pass through the cell membrane. Increased expression of CD36 enhances the fatty acid oxidation in M2like TAMs, eventually leading to immunosuppression. Therefore, CD36 inhibitors can hinder the intake of fatty acids by M2-like TAMs and ultimately achieve the purpose of inhibiting tumor progression. **(D)** IDO, produced by Tregs, decomposes tryptophan to specific metabolites, inhibiting the function of immune cells, such as effector T cells. Targeting IDO can inhibit tumor development by restoring tumor immunity. Created with "BioRender.com".

3.2 Tumor-associated macrophages

Macrophages, differentiated from monocytes, are widely found in organisms. It is known that macrophages can not only kill pathogens and maintain tissue homeostasis but also participate in immune regulation (45). Macrophages differentiate into M1 macrophages and M2 macrophages in the face of environmental changes (76). Macrophages can be aggregated by some cytokines and chemokines in the TME, including C-C motif chemokine ligand 2 (CCL2), vascular endothelial growth factor (VEGF), and macrophage colony-stimulating factor (M-CSF) (77). Macrophages in tumor tissue are referred to as tumor-associated macrophages (TAMs) (45). It is understood that TAMs are a class of immune cells that account for a large proportion of TME, and they are connected with tumor growth and tumor development (22). TAMs, as antigen-presenting cells, are heterogeneous cell groups in TME, which can transform from a static state to an activated state through the process of activation (78, 79). In TME, TAMs gather in hypoxic areas and quickly undergo glycolysis. In addition, TAMs can also secrete immunosuppressive cytokines, and vascular endothelial growth factors to promote tumor development (80). On the one hand, TAMs can promote tumor replication and invasion through colony-stimulating factor 1 and epidermal growth factor, on the other hand, they can express immunosuppressive factors like interleukin to facilitate the immune escape of tumor cells (81).

TAMs include M1-like macrophages and M2-like macrophages, and there are differences in their energy sources and metabolic patterns (45). Specifically, the energy source of M1-like macrophages is primarily glycolysis, while the energy of M2-like macrophages is mainly provided by fatty acid oxidation and oxidative phosphorylation (80). Interestingly, different types of macrophages have different metabolic patterns. In glucose metabolism, the expression of enzymes and factors connected with glycolysis in M1-like macrophages can be upregulated by HIF-1. Apart from this, IFN-γ can accelerate the consumption of glucose in M1-like macrophages and increase glycolysis. On the contrary, the glucose metabolism mode in M2-like macrophages is no longer glycolysis but is good for mitochondrial respiration and oxidative phosphorylation (45). In lipid metabolism, while the fatty acids oxidation is adjusted downward in M1-like macrophages, it can be upregulated in M2-like macrophages induced by IL-4. Besides, the metabolic characteristics of arachidonic acid are different in these two types of macrophages (80). In M2-like macrophages, the content of cyclooxygenase 2 (COX2) is higher, and the content of cyclooxygenase 1 (COX1) is lower. And it is in sharp contrast to M1-like macrophages. In amino acid metabolism, L-arginine is converted into nitric oxide (NO) and L-citrulline to promote urea circulation in M1-like macrophages, while it is converted into L-ornithine in M2-like macrophages (61).

Additionally, glutamine is related to the function of TAMs. Of course, the pathways associated with glutamine also participate in the polarization of TAMs (61). Furthermore, different types of TAMs play different functions in affecting the development of tumors (45). M1-like macrophages can produce tumor necrosis factors, inflammatory cytokines, and reactive oxygen species, which can promote inflammatory reactions and eliminate tumor cells, while M2-like macrophages produce different cytokines from M1-like macrophages, such as tumor-stimulating cytokines, which can promote tumor angiogenesis and tumor proliferation, leading to immunosuppression (82). In addition, M2-like macrophages can also produce a variety of chemokines to affect other immune cells (83).

Although TAMs can be found at all periods of tumor development, some studies have reported that M1-like macrophages are activated earlier than M2-like macrophages (Y. 45). Besides, the stimulation in TME can change TAMs from the type of pro-inflammatory to the type of anti-inflammatory, that is, from M1-like macrophages to M2-like macrophages (78, 79). More and more studies show that TAMs mostly express M2 phenotypes in TME. This feature can create an immunosuppressive microenvironment to affect tumor proliferation and metastasis (84).

Glucose metabolism, lipid metabolism, and amino acid metabolism in TME affect many aspects of TAMs. Lactic acid is a product of glycolysis in TME. Tumor cells can activate TAMs by producing lactic acid to stimulate immune escape (29). Lactic acid can also promote the glycolysis mode in M2-like macrophages, that is, oxidative phosphorylation (61). It indicates that key enzymes in glycolysis affect the polarization of TAMs. And it is suggested that targeting the activity of hexokinase (HK) can affect tumor development by affecting the polarization of macrophages (37). Besides, the reprogramming of glucose metabolism in macrophages also has an undesirable impact on their polarization. For instance, in TME, the glucose metabolism of TAMs has changed from oxidative phosphorylation to aerobic glycolysis, thus promoting the activation of M1-like TAM (61). Furthermore, lactic acid can facilitate the polarization of M2-like macrophages through many kinds of signaling pathways, including MCT1 and HIF-1, eventually promoting tumor development (80). In lipid metabolism, the metabolic mode of TAMs depends on the stage of the tumors and the requirements in the special environment (61). It is confirmed that some metabolites produced by the lipid metabolism of tumors affect the polarisation of TAMs (85). When the content of lipids in TAMs increases, TAMs polarize to M2-like macrophages, which eventually inhibit anti-tumor immune response and promote tumor development (76). M2-like macrophages increase the expression of arginase 1 (Arg1) and promote arginine metabolism, finally inhibiting immunity and promoting tumor development (45). Moreover, glutamine (Gln) metabolism is also vital for keeping the M2 phenotype of TAMs. Accordingly, it is demonstrated that Gln metabolism is a promising target (5). It can be seen that the function of TAMs and the influence of TME on TAMs are diverse and complex. In addition to the above, there are many aspects of TAMs and the impacts of TME on TAMs that deserve more attention and further research.

3.3 Natural killer cells

Natural killer cells (NK), a subgroup of inherent lymphocytes, have strong anti-infection and anti-tumor ability, and can directly

remove tumor cells by exerting cytotoxic activity (86). NK cells are elements of the innate immune response, which can aggregate other kinds of immune cells after being activated in TME (22). The function of NK cells is mainly regulated by inhibitory receptors, which hinder NK cells from exerting cytotoxic activity and help tumor cells escape from immunity (86). Apart from typical inhibitory receptors, checkpoint inhibitor receptors can also be expressed on NK cells (86). Additionally, interleukin-like cytokine stimulation can modulate the metabolism of NK cells through the mTOR signaling pathway (60). By upregulating the mTOR complex 1 (mTORC1) signaling, NK cells ingest a large amount of glucose and carry out aerobic glycolysis, which promotes the function of NK cells (22). It has shown that sterol regulatory element binding proteins (SREBPs) affect lipid metabolism through the regulation of mTORC1, but further research is needed to analyze the influence of SREBPs on lipid metabolism in NK cells (60).

The metabolism of various substances in TME affects the survival, proliferation, and role of NK cells. When the content of glucose in TME is low because of the increased glucose metabolism in tumor cells, the glycolysis induced by the mTORC1 signal is inhibited, thus inhibiting the anti-tumor function of NK cells (20). Besides, lactic acid can limit the function of NK cells by inhibiting the nuclear factor of activating T cells (NFAT) in NK cells, thus promoting immune escape (72). It is confirmed that if the content of lipids in NK cells increases, the function of NK cells will be inhibited, eventually leading to immune escape (39). For example, in the TME with a large number of fatty acids, NK cells absorb exogenous fatty acids, causing the suppression of glycolysis and weakening the function of NK cells (22). Apart from fatty acids, other lipids or regulatory factors may also affect NK cells. Prostaglandin E2 (PGE2) can affect the survival and growth of NK cells, and can inhibit the function of NK cells. In addition, adiponectin secreted by adipose tissue may also hinder NK cells by affecting fatty acid metabolism (60). What's more, the signaling pathways cannot be ignored. Signaling pathways connected with lipid metabolism in NK cells include mTOR and SREBPs (85). Some studies found that when NK cells are constantly exposed to IL-15, IL-15 may restrain the metabolism and function of NK cells through the mTOR signaling pathway (60). Therefore, it is speculated that the inhibitor of mTOR, rapamycin, may restore the function of NK cells under certain conditions (60). At present, although some studies have explored the relationship between NK cells and substance metabolism, there are not enough pieces of evidence. Apparently, it is necessary to carefully analyze the influence of substance metabolism on NK cells in TME to obtain more useful information.

3.4 Dendritic cells

Dendritic cells include the classical DC1 (cDC1), the heterogeneous group the classical DC1 (cDC2), the plasmacytoid DC (pDC), and other subgroups, which are indispensable in TME (87). Dendritic cells, responsible for presenting antigens, strengthen the anti-tumor effect by activating T cells. The classical DC1 can ingest and submit antigens to T cells, for instance, submitting antigens to MHC class I molecules on CD8+ T cells. The classical DC2 is believed to come from monocytes, which are divided into DC2 and DC3. They can submit the tumor antigen to CD4+ T cells. The plasmacytoid DC can be found frequently in tumors, which is connected with adverse outcomes and low survival rates (88). Some findings suggest that pDCs can promote Treg cells to secrete IL-10 to inhibit the immune response (86). The TME has a certain influence on dendritic cells. In addition to reducing the number of cDC1, tumor immune escape can also be achieved by directly inhibiting the function of cDC1 (86). Surprisingly, when the content of lipids in DC increases, the function of DC to present tumor-related antigens is weakened, causing the suppression of anti-tumor immunity (39). However, because the theory of how lipids inhibit the function of DCs has not been thoroughly studied, the way to restore the ability of DCs to present antigens may be found after in-depth research to restore anti-tumor immunity (22). At this stage, there is not much research on DCs. The function of DCs in TME and the mechanism of TME affecting DCs are not comprehensive. As a consequence, more research is needed to provide more information.

3.5 Other types of immune cells

Neutrophils, the main components of immune cells in the body, mainly obtain energy through glycolysis (22). They seem to promote the development of tumors in some cases. For example, when the content of glucose in TME is low, neutrophils obtain energy through fatty acid oxidation, thus inhibiting the immune response and promoting tumor growth (22). Neutrophils include N1 neutrophils and N2 neutrophils. N1 neutrophils mainly obtain energy through glycolysis to achieve anti-tumor function, while N2 neutrophils continue to ingest lipids, allowing lipids to accumulate in them and eventually prolonging their survival time (22). Besides, N2 neutrophils also inhibit the proliferation of some immune cells, such as NK cells, by secreting many kinds of enzymes, and ultimately facilitating the growth of tumors (22). MDSCs are also an important class of immune cells, which primarily depend on fatty acid oxidation to obtain energy to perform their immunosuppressive function (20). It is shown that TME has a large amount of lipids, which can promote MDSCs to ingest lipids. Therefore, MDSCs can play an antitumor function in TME, but when there is too much lipid, the function of MDSCs may be inhibited (89). There are also a variety of immune cells or other kinds of cells, playing various roles in the TME, which are affected by different factors in TME, too. For example, cancerassociated fibroblasts (CAFs) are vital stromal cells in TME, which are believed to induce epithelial-mesenchymal transition (EMT) and secrete immunosuppressive factors (40). CAFs can produce lactic acid through aerobic glycolysis, and then tumor cells ingest and use lactic acid, this is defined as the reverse "Warburg effect" (20). It is proved that CAFs may help lipids be transported to tumor cells to facilitate tumor proliferation and metastasis (22). The current research has a limited understanding of cells in TME, and some cells have not even been found. Therefore, more time is needed to understand and analyze the cells in the TME.

4 Targeting metabolism to explore and promote tumor immunotherapy

The methods for treating tumors include radiotherapy, chemotherapy, and targeted treatment. Regarding exploring how to treat tumors, people are committed to developing effective strategies without significantly damaging surrounding tissues and cells (22). In recent years, immunotherapy has been gradually studied and has become one of the most promising treatment methods today, and it is possible to obtain better therapeutic effects and lead to fewer side effects (20).

4.1 Some well-known immunotherapies related to immune cells

With the discovery that the immune system inhibits tumor proliferation, the immunotherapy of tumors has been gradually paid attention to and studied deeply (34). It is confirmed that tumors can inhibit anti-tumor immunity by establishing immune checkpoints, which is in favor of tumor immune escape (89). Immune checkpoint molecule CD28, cytotoxic T lymphocyte-associated protein-4 can lead to the depletion of immune cells, eventually promoting immunosuppression (34). At present, Immune checkpoint blockers (ICB) and adoptive-cell transfer (ACT) are important ways for immunotherapy that are related to immune cells (57). It has proved that targeting PD-1 and CTLA-4 may restore the immune function of T cells (Figure 3) (34). Notably, NK cells can also express PD-1, while the expression of PD-1 ligand (PD-L1) limits the delivery of antigens to CD8+T cells by DCs, so the anti-tumor immune response can be promoted by hindering the PD-1/PDL1 axis (34). Besides, blocking CTLA-4 can increase the infiltration of NK cells in the TME and indirectly enhance the antitumor effect of NK cells by depleting Treg cells. Moreover, it is found that lymphocyte activation gene 3 (LAG-3) is a promising method to treat tumors by blocking checkpoints (86). Strategies for T cell immune receptor with immunoglobulin and ITIIM domain (TIGIT) pathways and its associated receptors and ligands can provide new ideas for tumor treatment (86). Hopefully, it may be a promising strategy to combine metabolic regulators and ICB to promote the function of immune cells and augment immunotherapy (32). Additionally, ACT, such as using T cells amplified *in vitro*, enhances the ability of anti-tumor immunity by modifying immune cells, and one of the advantages of ACT is that the process of modifying immune cells does not affect other surrounding cells (34). However, ICB activates immune cells in tumors by modifying inhibitory signals, so it is limited by the TME (34).

4.2 Therapies worthy of further research

The influence of tumor cell metabolism on immune cells is gradually regarded as a crucial mechanism for tumor immune escape. It includes the competition between tumor cells and immune cells for substances in the TME, and the accumulation of metabolites produced by tumor cells in the microenvironment (2). Therefore, the characteristics of tumor cell metabolism provide a basis for finding therapeutic targets (34). Besides, the regulation of cell metabolism may be an important idea for tumor immunotherapy (2). Furthermore, it is confirmed that metabolism reprogramming of tumor cells forms an immunosuppressive TME, resulting in less effective tumor immunotherapy than expected (34). Therefore, analyzing the metabolism of tumor cells and the factors that inhibit the function of immune cells may enhance immunotherapy (20, 34). Since the 20th century, it has begun to study the connection between tumor cells and immune cells to discover more treatments and improve the effect of immunotherapy (39).

4.2.1 Therapies related to glucose metabolism

It has shown that the transporters, enzymes, and metabolites associated with glycolysis are not negligible to the drug resistance of tumors (72). Targeting the transport proteins and enzymes needed in the process of glycolysis in tumor cells may be a new idea for immunotherapy (80). The glycolysis inhibitors can prevent the growth of tumor cells and augment the therapeutic effect, which is a promising treatment method (30). Glucose transporters (GLUTs), with increased expression in a variety of tumors, are a crucial part of metabolism in tumor cells (90). The combination of glucose transporters inhibitors and other tumor treatment methods can promote tumor treatment and improve prognosis (34).

Key enzymes in glycolysis can be used as targets for tumor immunotherapy, for example, the inhibitor of PKM2, Shikonin, can inhibit glycolysis and block tumor cells from obtaining energy through glycolysis (32). The combination of PD-1 and PD-L1 on tumor cells inhibits the function of T cells in TME and promotes immune escape. It is demonstrated that both HK2 and PKM2 are connected with the expression of PD-L1, and the treatment targeting PKM2 combined with anti-PD-1 antibodies may be a hopeful treatment for tumors (32). Phosphoglycerate kinase 1 (PGK1), one of the enzymes in the glycolysis process, can promote the progress of breast cancer and have an impact on the prognosis of breast cancer patients (62). Therefore, PGK1 may also be worth an in-depth study of the therapeutic target.

The mammalian target of rapamycin (mTOR) is a serine/threonine protein kinase that turns into complexes with other molecules in tumor cells, including mTOR complex 1 (mTORC1) and mTOR complex 2 (mTORC2), and both of them can affect the function of immune cells and promote the growth of tumor cells (17). The activation of mTORC1 can promote the expression of some glucose transporters and glycolytic enzymes, ultimately promoting tumor cells to ingest glucose and stimulating the proliferation of tumors (72). Therefore, inhibiting the mTORC1 may be regarded as one of the targets of tumor treatment (56). However, it has been confirmed that mTOR inhibitors affect the metabolism of T cells, such as Teff cells, leading to inhibit immune response (34). It is necessary to explore how to better inhibit the PI3K/AKT/mTOR signaling pathway to maximize the efficacy of immunotherapy.

CD147 is highly expressed on the surface of tumor cells. It is proved that CD147 can promote the release of vascular endothelial growth factor and extracellular matrix metalloproteinase, which is closely related to the poor prognosis of tumors (2). Besides, it is shown that CD147 can promote glycolysis in tumor cells by assisting the transport of monocarboxylates (2). What's more, its monoclonal antibody (Licartin) can prevent the recrudesce and metastasis of liver cancer to a certain extent. Moreover, compared with the use of antiCD147 antibodies alone, the combination of multiple immunotherapy methods may achieve better anti-tumor effect (2). It is said that long noncoding RNA (lncRNA) can promote glycolysis in tumor cells and regulate some oncogenic signaling pathways, for example, TAMs enhance glycolysis of tumor cells by producing extracellular vesicles (EVs) to transfer lncRNA (91). It has been proved that targeting lncRNA in TAMs can inhibit glycolysis of tumor cells (30). Therefore, lncRNA can be used as one of the targets of tumor treatment providing a new idea (30).

4.2.2 Therapies related to lipid metabolism

The lipids in TME affect the proliferation and metastasis of tumors, targeting lipid production and ingestion in tumor cells can be regarded as an anti-tumor strategy (85). Lipids are related to the metabolism of tumor cells and the function of various immune cells. Therefore, studying the characteristics of lipids metabolism in the TME and various cells helps explore new ways to treat tumors.

The increase of free fatty acids in tumor cells promotes tumor metastasis (92). However, the metastasis of tumor cells is limited by saturated fatty acids and unsaturated fatty acids, if the content of unsaturated fatty acids in cell membrane phospholipids is low, the fluidity of the cell membrane will be reduced, eventually leading to a slowdown in the invasion of tumor cells (22). Therefore, maintaining the balance of saturated fatty acids and unsaturated fatty acids is of great importance for tumor metastasis. In cholesterol metabolism, low-density lipoprotein receptor (LDLR) is connected with tumor immune response, and inhibiting LDLR can promote anti-tumor immunity. Moreover, statins can inhibit tumor metastasis by reducing the cholesterol content in the tumor cell membrane, but its curative effect needs to be further confirmed (20). Apolipoprotein E (Apo E) can mediate cholesterol metabolism and may enhance or inhibit the immune response under different circumstances, so targeting Apo E can be regarded as a direction of tumor immunotherapy (39). Besides, the metastasis of some types of tumors can be blocked by inhibiting cholesterol esterification. Extracellular fatty acids (FAs) can promote the polarization of tumor TAMs, so targeting FAs affects the development of tumors. What's more, it is pointed out that inhibiting cholesterol efflux in TAMs can also be used as a way to treat tumors (39). However, the metabolism mechanism of cholesterol in TAMs is very complex and needs to be further explored (45).

In addition, phospholipids, a class of lipids containing phosphoric acid, have a certain influence on the TME and ultimately affect tumor proliferation and metastasis (19, 39). AA produces prostaglandin E2 (PGE2) with the help of cyclooxygenase-2 (COX2) (47). PGE2 is a tumor-related medium that can hinder the immune response and promote tumor proliferation in various ways (Y 60). TAMs can promote angiogenesis by secreting PGE2, promoting tumor development (93). Besides, PGE2 can facilitate the expression of PD-L1 in TAMs, contributing to immune escape (45). Therefore, targeting PGE2 and COX2 can hinder the expression of PD-L1 in TAMs, ultimately inhibiting immune escape. However, it is reported that the lipid metabolism regulated by different COXs in TAMs may have the opposite effects on the progression of tumors (43). It is said that cDC1 cells can enter the TME through the chemokine CCL5 secreted by NK cells, but prostaglandin E2 inhibits this process (Y. 45). Therefore, inhibiting the production of PGE2 can augment the number of cDC1 cells in TME and can cooperate with anti-PD-L1 to complete anti-tumor treatment. Suppressing the expression of COX1 or COX2 can inhibit the generation of PGE2 (86). As can be seen from the above, the COX2/PGE2 axis can be studied as a hopeful treatment (45).

CD36 is a glycoprotein that can help lipids pass through the cell membrane (19, 22). Increased expression of CD36 enhances the fatty acids oxidation in TAMs and Tregs, leading to immunosuppression (94) (Figure 3). Therefore, preventing these immunosuppressive cells from ingesting and metabolizing fatty acids may be a strategy worth studying to treat tumors (39). Moreover, increased expression of CD36 can also promote TAMs to ingest fatty acids and promote tumor development, so CD36 inhibitors can hinder the intake of fatty acids by TAMs and inhibit the negative impact of TAMs on immune response, ultimately achieving the purpose of inhibiting tumor progression (43). Furthermore, the high expression of CD36 can promote tumor growth and tumor metastasis by regulating the Src/PI3K/AKT signal pathway or activating the Wnt/TGF-β signal pathway (20). In addition, CD36 inhibitors can promote the submission of tumor-related antigens by DCs, decrease the amount of Treg cells, and promote the development of CD8+T cells. Using both CD36 inhibitors and anti-PD-1 could enhance the anti-tumor effects (20).

Fatty acid binding proteins (FABPs) are adipokines found in the cell membrane or cytoplasm, which can participate in the transportation of fatty acids and regulate fatty acid metabolism (95). Some studies have shown that fatty acid binding protein 4 (FABP4) can promote tumor growth, so inhibiting FABP4 can be used as a way to treat tumors (20). However, the impact of different phenotypes of FABP on tumor proliferation and development may be opposite, so it is necessary to specifically study the role of FABP to provide a basis for tumor treatment (43).

The activity of enzymes in TME connected with lipid metabolism also changes (39). ATP citric acid lyase (ACLY), fatty acid synthase (FASN), acetyl-CoA carboxylase (ACC), and acetyl-CoA (Ac CoA) are indispensable enzymes in lipid metabolism, which influence the metabolism of immune cells and tumor cells (85). ACLY decomposes cytosolic citrate in the cytoplasm into Ac CoA and oxaloacetic acid (56). ACLY inhibitors are still in their infancy, and further research is needed to provide a basis for tumor treatment (70). Ac CoA can be generated not only through ACLY but also through acetyl-CoA synthesis enzymes (ACSS). Therefore, ACSS2 inhibitors can be used to hinder the proliferation of tumors and seem to help ACLY inhibitors play a better anti-tumor role (56). ACC inhibitors combined with other treatment methods can inhibit tumor proliferation. What's more, AMPK has been proven

to be an inhibitor of ACC, and metformin can activate AMPK, so metformin is clinically used to promote anti-tumor immune response and inhibit tumor development (85). FASN is a key enzyme that regulates the *de novo* synthesis of fatty acids (20). And it catalyzes Ac CoA and malonyl-CoA to produce fatty acids (56). Inhibiting FASN can reduce the energy source of tumor cells and inhibit the role of M2 macrophages and Treg cells, eventually hindering the growth of tumors (20). But we also need to explore more deeply to obtain FASN inhibitors with better efficacy and fewer side effects to guide the clinical treatment of tumors. In addition to enzymes involved in fatty acid synthesis, enzymes related to fatty acid decomposition are also worth paying attention to (20). Carnitine palmitoyl transferase 1 (CPT1) is an enzyme involved in the beta-oxidation of fatty acids (89). It is found that inhibiting CPT1 can inhibit the role of immunosuppressive cells, such as TAMs and MDSCs, so inhibiting CPT1 can restore the immune response (20).

In addition, analyzing the signaling pathways connected with lipid metabolism reprogramming can also be used as a starting point for finding treatment methods (45). It is well-known that the AMPK/mTOR signaling pathway is related to lipid metabolism. The mTORC1 can promote the synthesis of fatty acids by regulating the activity of SREBPs, which are a class of transcription factors related to enzymes and other related molecules needed for lipid metabolism (96). As mentioned above, activating AMPK can achieve the purpose of inhibiting tumors, but it shows that AMPK may also promote the development of tumors. Therefore, AMPK agonists need to be further explored to inhibit tumor proliferation as much as possible (20). The mTOR signaling pathway is crucial for the growth of tumors, so inhibiting mTOR can play an anti-tumor role. However, it has been found that the influence of mTOR on the survival and development of immune cells is also worth paying attention to. Inhibiting mTOR may affect the role of immunosuppressive cells, such as Treg cells, hindering anti-tumor immune response (20). What's more, it is demonstrated that the AMPK/mTOR signaling pathway influences the metabolism of CD4+T cells. Inhibiting mTOR leads to increased lipid metabolism, which is in favor of the formation and survival of Treg cells (56). Nevertheless, mTOR inhibitors also seem to inhibit the function of Treg cells, so more research is needed to find mTOR inhibitors that maximize the anti-tumor effect.

The peroxisome proliferator-activated receptor (PPAR) signaling pathway cannot be ignored (20, 97). The PPAR has been found to include peroxisome proliferator-activated receptor α (PPARα), peroxisome proliferator-activated receptor γ (PPARγ), and peroxisome proliferator-activated receptor β/δ (PPARβ/δ) (40). Among them, PPARα mainly regulates oxidative phosphorylation in glucose metabolism, while PPARγ mainly affects lipid metabolism (92). PPARγ-mediated lipid metabolism may hinder immune response and facilitate tumor growth (43). Increased expression of PPAR-γ may promote lipid synthesis and increase the activity of immune cells, ultimately enhancing immunotherapy (60). Besides, PPAR-γ agonists can inhibit tumor growth by hindering angiogenesis and facilitating the function of CD8+T cells. Furthermore, the combined use of PPAR-γ agonists and anti-PD-1 can enhance the efficacy of tumor treatment (20). Unexpectedly, PPAR-γ inhibitors can also be used to treat some tumors by inhibiting M2-like macrophages from secreting tumor-promoting cytokines (43). Therefore, it is necessary to analyze the effect of specific PPAR-γ inhibitors or agonists. Some signaling pathways also need to be studied, such as SREBP and liver X receptor (LXR) signaling pathways (20). The intake and discharge of cholesterol are regulated by SREBPs and LXRs respectively (56). It has been proved that SREBP inhibitors and LXR agonists can promote anti-tumor immune response by regulating the role of immune cells (56). Interestingly, using both LXR agonists and PPAR inhibitors seems to enhance the anti-tumor effect (20).

There are many points worth paying attention to in normal lipid metabolism and lipid metabolism reprogramming. Analyzing them as deeply as possible may provide some basis for tumor treatment. In tumor tissue, the anabolic and catabolism of lipids are unbalanced, leading to lipid accumulation, which eventually affects the therapeutic effect and prognosis (98). It is not difficult to find that targeting transport proteins connected with fatty acid transport can inhibit the growth of tumors, but there are many ways to transport fatty acids. The treatment methods to block these routes need to be further studied as much as possible (22). It is worth noting that specific studies should be carried out on different stages of lipid metabolism to obtain treatment methods that can help improve the effect of immunotherapy (20). What's more, in different TMEs, the mechanism of lipid metabolism may be different, so different tumors may require specific treatments (45).

Obesity is one of the manifestations of lipid metabolism disorders. It has been found that excessive lipids may hinder the role of NK cells (60). And if the role of NK cells is impaired, the risk of tumors in obese people may increase. Besides, diverse degrees of obesity may have disparate effects on lipid metabolism (60). As the number of obese people increases year by year, it is particularly vital to analyze the features of lipid metabolism in immune cells and tumor cells. Whether obesity can lead to a bad prognosis of tumors is also worth an in-depth study (58).

4.2.3 Therapies related to amino acid metabolism

Of Note, tumor cells need more amino acids than normal cells and have stronger amino acid metabolism. Therefore, targeting amino acid metabolism can hinder the function of tumor cells without excessive damage to normal cells (17). Amino acid metabolism can affect the role of immune cells and the production of immune factors, which has a significant effect on tumor immunity (17). Targeting amino acid metabolism can restore tumor immune response, so it is worth studying deeply as a tumor treatment strategy. Immune checkpoint receptors, including PD-1 and CTLA4, limit the role of T cells by hindering T cells from ingesting and catabolizing amino acids (17). Hence, blocking immune checkpoints can promote amino acid metabolism in T cells (17).

Amino acid transporters are of significance in tumor proliferation and metastasis. It is reported that one of the ways that amino acid transporters affect tumor growth is to regulate the activity of mTORC1, for example, recombinant large neutral amino acid transporter 1 (LAT1) can increase the activity of mTORC1 to facilitate tumor growth and metastasis (17). It has shown that LAT1

can activate mTORC1 through the Ragulator-Rag complex and help to transmit VEGF-A signals through mTORC1 and promote angiogenesis (17). When the amount of LAT1 becomes less, the activity of mTORC1 decreases, and this is not good for tumor development (17). Hence, amino acid transporters can be used as targets for tumor treatment. However, there is a great deal of amino acid transport proteins in TME, thus inhibiting one amino acid transport protein may have an impact on other amino acid transport proteins (17).

Indoleamine 2,3-dioxygenase 1 (IDO1), indoleamine 2,3-dioxygenase 2 (IDO2) and Tryptophan-2,3-dioxygenase (TDO) are three enzymes in the tryptophan metabolism, and IDO1 is highly expressed (15). IDO1 promotes tumor development through immunosuppression, while TDO is connected with tumor proliferation and metastasis (98). Therefore, it is necessary to deeply analyze the role of IDO and its relevance to TDO. IDO, produced by tumor cells, TAMs and Tregs in the TME, decomposes tryptophan and generates specific metabolites (5) (Figure 3). IDO can inhibit the role of immune cells, such as effector T cells, and promote the formation of an immunosuppressive microenvironment (5). It has proved that dendritic cells expressing IDO can facilitate the production and proliferation of Treg cells, ultimately hindering tumor immunity (Xiao-han 99). And it can be seen that targeting IDO1, which is considered one of the meaningful strategies for treating tumors, can inhibit tumor development by restoring tumor immunity (83). There are also difficulties in the study of IDO/TDO inhibitors. Tumor cells may produce kynurenine (KYN), one of the metabolites of tryptophan, by using IDO or TDO alone, or by using IDO and TDO at the same time. Therefore, it is very important to identify the enzymes that produce KYN and select specific inhibitors for tumor treatment. For example, Epacadostat can inhibit the secretion of KYN by tumor cells that mainly express IDO1, but it hardly affects the tumor cells that mainly express TDO (83). Of course, the dose of inhibitors is also a factor that cannot be ignored (99). However, in addition to using IDO1 inhibitors alone, using both IDO1 inhibitors and ICB is also worth studying carefully. Furthermore, whether the use of both IDO inhibitors and PD-1/PD-L1 inhibitors is better than that of a certain inhibitor alone is worth further study (99). For instance, the IDO1 inhibitor, LY3381916, combined with the PD-L1 inhibitor, can minimize the activity of IDO1, eventually increasing the number of T cells and promoting anti-tumor immunity (15).

Glutamine can activate mTORC1 to promote tumor cell proliferation (5). Glutamine antagonists, such as JHU083, can inhibit glutamine metabolism in tumor cells and promote the formation of the TME beneficial for the survival of immune cells, ultimately achieving the purpose of treating tumors (5). Moreover, the simultaneous use of glutamine antagonists and anti-PD-1 antibodies can enhance the function of T cells, and its therapeutic effect is better than the use of antiPD-1 antibodies alone (5). Glutaminase (GLS), highly expressed in tumor cells, is an enzyme that breaks down glutamine into glutamate. Therefore, inhibiting glutamine enzymes may be used as a way to treat tumors (17). Besides, it is found that GLS antagonists, such as CB-839, can increase the content of Gln in TME by inhibiting the utilization of Gln by tumor cells. When Gln in TME increases, some signaling pathways can be activated to strengthen the anti-tumor activity of NK cells (17).

The growth of multiple T cells is connected with the amount of amino acids. Promoting the inflow of amino acids is conducive to the growth of T cells and eventually affects the anti-tumor immune response (75). Besides, it is indicated that the function of effector T cells can be improved by supplementing amino acids, and anti-tumor immunity can be enhanced when anti-PD-L1 antibody therapy is performed at the same time (5). Supplementing arginine or targeting enzymes related to the arginine metabolism probably enhances the role of T cells and reduces immunosuppression (15). Inhibiting the catabolism pathways of tryptophan and arginine hinders the function of Tregs in anti-tumor immunity, so these pathways could be taken as targets for tumor immunotherapy (89).

To sum up, targeting the amino acid transporters and metabolic enzymes related to amino acid metabolism reprogramming in TME is a hopeful strategy for tumor treatment, which can enhance anti-tumor immunity and inhibit the proliferation and metastasis of tumors with immune checkpoint inhibitors (17). Apparently, amino acid metabolism is important for tumor proliferation and metastasis. Of course, the connection between amino acid metabolism and other cells, such as vascular endothelial cells, in TME, is also worth continuing to study to have a deeper understanding of tumors and develop new promising treatment strategies (5). Although the current understanding of amino acid metabolism reprogramming in TME is limited, targeting amino acid metabolism is still a strategy worth studying to enhance anti-tumor immunity. Hence, more efforts are needed to study the significance of amino acid metabolism for tumor immunotherapy (15).

5 Discussion

Tumor cells and immune cells are two types of cells that cannot be ignored in TME, and their metabolism can affect the progression of tumors. Tumor cells change their metabolic patterns, namely metabolism reprogramming, to adapt to the TME and escape immune surveillance, ultimately facilitating the rapid proliferation and metastasis of tumors. The immune system includes anti-tumor immune cells, such as effector T (Teff) cells and M1 macrophages, as well as immunosuppressive cells that promote tumor development, such as Treg cells and M2 macrophages. In theory, anti-tumor immune cells can inhibit the proliferation of tumors by recognizing and destroying tumor cells to maintain the homeostasis of the body. However, tumor cells in TME can hinder the function of anti-tumor immune cells and promote the function of immunosuppressive cells through metabolism reprogramming, eventually forming an immunosuppressive microenvironment and promoting tumor development. Therefore, analyzing the metabolism reprogramming

in TME and the impact of metabolism reprogramming on immune cells may be an important approach for immunotherapy.

Tumor cells in different TMEs have diverse metabolic characteristics. The metabolism of tumor cells could be compensated, so the effect of antitumor treatment through a single target may be short-lived. For enhancing the efficacy of anti-tumor treatment, implementing multiple therapies at the same time may be a more comprehensive treatment. Future research should distinguish more clearly the same and different points between the metabolism of tumor cells and immune cells to analyze targeted treatment strategies so that targeting metabolism can better play an anti-tumor role together with immunotherapy.

Immunotherapy mainly includes specific immunotherapy and nonspecific immunotherapy (17). Tumor immunotherapy, such as blocking immune checkpoints, has been widely used in clinics. However, there are still some diseases that cannot be solved with existing immunotherapy (100). Furthermore, at diverse stages, the metabolic modes of tumor cells and immune cells may be disparate (60). However, the types and quantities of immune cells contained in different TME are different. Immunotherapy is more effective in tumors with more immune cells. It is demonstrated that autophagy, as the self-protection mechanism of cells, has a non-negligible effect on tumor cells and immune cells. Inhibiting autophagy probably be beneficial for anti-tumor immune response, so it may be a new immunotherapy method (20). Genes connected with metabolism possibly become targets for immunotherapy (101).

Although TME and tumor immunotherapy are still being explored, we can predict that immunotherapy can continue being expanded and developed with the development of science and technology to promote the treatment and prognosis of tumors.

Author contributions

YL: Writing – original draft. HS: Writing – original draft. YH: Supervision, Writing – review & editing. XQ: Supervision, Writing – review & editing.

Funding

The author(s) declare financial support was received for the research, authorship, and/or publication of this article. Sichuan Province Tianfu Qingcheng Program Foundation, Grant/Award (No. KZ258) and Sichuan Science and Technology Program (No. 22ZDYF2119).

Conflict of interest

The authors declare that the research was conducted in the absence of any commercial or financial relationships that could be construed as a potential conflict of interest.

Publisher's note

References

1. Fukushi A, Kim HD, Chang YC, Kim CH. Revisited metabolic control and reprogramming cancers by means of the warburg effect in tumor cells. *Int J Mol Sci* (2022) 23(17):10037. doi: 10.3390/ijms231710037

2. Li X, Xu W. CD147–mediated reprogrammed glycolytic metabolism potentially induces immune escape in the tumor microenvironment (Review). *Oncol Rep* (2019) 41 (5):2945–56. doi: 10.3892/or.2019.7041

3. Kooshki L, Mahdavi P, Fakhri S, Akkol EK, Khan H. Targeting lactate metabolism and glycolytic pathways in the tumor microenvironment by natural products: A promising strategy in combating cancer. *BioFactors* (2022) 48(2):359–83. doi: 10.1002/biof.1799

4. Wu S, Zhang H, Gao C, Chen J, Li H, Meng Z, et al. Hyperglycemia enhances immunosuppression and aerobic glycolysis of pancreatic cancer through upregulating bmi1-UPF1-HK2 pathway. *Cell Mol Gastroenterol Hepatol* (2022) 14(5):1146–65. doi: 10.1016/j.jcmgh.2022.07.008

5. Qiu H, Shao N, Liu J, Zhao J, Chen C, Li Q, et al. Amino acid metabolism in tumor: new shine in the fog? *Clin Nutr* (2023) 42(8):1521–305. doi: 10.1016/j.clnu.2023.06.011

6. Kong J, Yu G, Si W, Li G, Chai J, Liu Y, et al. Identification of a glycolysis-related gene signature for predicting prognosis in patients with hepatocellular carcinoma. *BMC Cancer* (2022) 22(1):142. doi: 10.1186/s12885-022-09209-9

7. Yang J, Liu DJ, Zheng JH, He RZ, Xu DP, Yang MW, et al. IRAK2-NF-κB signaling promotes glycolysisDependent tumor growth in pancreatic cancer. *Cell Oncol (Dordr)* (2022) 45(3):367–79. doi: 10.1007/s13402-022-00670-z

8. Xiang H, Yang R, Tu J, Xi Y, Yang S, Lv L, et al. Metabolic reprogramming of immune cells in pancreatic cancer progression. *Biomed Pharmacother* (2023) 157 (January):113992. doi: 10.1016/j.biopha.2022.113992

9. Li Y, Zhao L, Li XF. Hypoxia and the tumor microenvironment. *Technol Cancer Res Treat* (2021) 20(December):15330338211036304. doi: 10.1177/15330338211036304

10. Sun L, Suo C, Li S-t, Zhang H, Gao P. Metabolic reprogramming for cancer cells and their microenvironment: Beyond the Warburg Effect. *Biochim Biophys Acta (BBA) - Rev Cancer Cancer Metab* (2018) 1870 (1):51–66. doi: 10.1016/j.bbcan.2018.06.005

11. Lin Y, Xiao Y, Liu S, Hong L, Shao L, Wu J. Role of a lipid metabolism-related lncRNA signature in risk stratification and immune microenvironment for colon cancer. *BMC Med Genomics* (2022) 15(1):221. doi: 10.1186/s12920-022-01369-8

12. Zhu L, Zhu X, Wu Y. Effects of glucose metabolism, lipid metabolism, and glutamine metabolism on tumor microenvironment and clinical implications. *Biomolecules* (2022) 12(4):580. doi: 10.3390/biom12040580

13. Reina-Campos M, Moscat J, Diaz-Meco M. Metabolism shapes the tumor microenvironment. *Curr Opin Cell Biol* (2017) 48(October):47–53. doi: 10.1016/j.ceb.2017.05.006

14. Aung A, Kumar V, Theprungsirikul J, Davey SK, Varghese S. An engineered tumor-on-a-chip device with breast cancer-immune cell interactions for assessing T-cell recruitment. *Cancer Res* (2020) 80(2):263–75. doi: 10.1158/00085472.Can-19-0342

15. Yu M, Zhang S. Influenced tumor microenvironment and tumor immunity by amino acids. *Front Immunol* (2023) 14:1118448. doi: 10.3389/fimmu.2023.1118448

16. Zhang Y, Hu H, Liu W, Yan SM, Li Y, Tan L, et al. Amino acids and ragD potentiate mTORC1 activation in CD8(+) T cells to confer antitumor immunity. *J Immunother Cancer* (2021) 9(4):e002137. doi: 10.1136/jitc-2020-002137

17. Wang D, Wan X. Progress in research on the role of amino acid metabolic reprogramming in tumour therapy: A review. *Biomed Pharmacother* (2022) 156 (December):113923. doi: 10.1016/j.biopha.2022.113923

18. Li S, Fang Y. MS4A1 as a potential independent prognostic factor of breast cancer related to lipid metabolism and immune microenvironment based on TCGA database analysis. *Med Sci Monit* (2022) 28(January):e934597. doi: 10.12659/msm.934597

19. An D, Zhai D, Wan C, Yang K. The role of lipid metabolism in cancer radioresistance. *Clin Transl Oncol* (2023) 25(8):2332–49. doi: 10.1007/s12094-023-03134-4

20. Yang K, Wang X, Song C, He Z, Wang R, Xu Y, et al. The role of lipid metabolic reprogramming in tumor microenvironment. *Theranostics* (2023) 13(6):1774–808. doi: 10.7150/thno.82920

21. Kolb D, Kolishetti N, Surnar B, Sarkar S, Guin S, Shah AS, et al. Metabolic modulation of the tumor microenvironment leads to multiple checkpoint inhibition and immune cell infiltration. *ACS Nano* (2020) 14(9):11055–66. doi: 10.1021/acsnano.9b10037

22. Corn KC, Windham MA, Rafat M. Lipids in the tumor microenvironment: from cancer progression to treatment. *Prog Lipid Res* (2020) 80(November):101055. doi: 10.1016/j.plipres.2020.101055

23. Hao Y, Li D, Xu Y, Ouyang J, Wang Y, Zhang Y, et al. Investigation of lipid metabolism dysregulation and the effects on immune microenvironments in pan-cancer using multiple omics data. *BMC Bioinf* (2019) 20(Suppl 7):195. doi: 10.1186/s12859-019-2734-4

24. Gu X, Wei S, Li Z, Xu H. Machine learning reveals two heterogeneous subtypes to assist immune therapy based on lipid metabolism in lung adenocarcinoma. *Front Immunol* (2022) 13:1022149. doi: 10.3389/fimmu.2022.1022149

25. Yang Y, Li Y, Qi R, Zhang L. Development and validation of a combined glycolysis and immune prognostic model for melanoma. *Front Immunol* (2021) 12:711145. doi: 10.3389/fimmu.2021.711145

26. Ossoli A, Wolska A, Remaley AT, Gomaraschi M. High-density lipoproteins: A promising tool against cancer. *Biochim Biophys Acta (BBA) - Mol Cell Biol Lipids* (2022) 1867(1):159068. doi: 10.1016/j.bbalip.2021.159068

27. Xu K, Xia P, Liu P, Zhang X. A six lipid metabolism related gene signature for predicting the prognosis of hepatocellular carcinoma. *Sci Rep* (2022) 12(1):20781. doi: 10.1038/s41598-022-25356-2

28. Chen YJ, Guo X, Liu ML, Yu YY, Cui YH, Shen XZ, et al. Interaction between glycolysis–cholesterol synthesis axis and tumor microenvironment reveal that gamma-glutamyl hydrolase suppresses glycolysis in colon cancer. *Front Immunol* (2022) 13:979521. doi: 10.3389/fimmu.2022.979521

29. Yuan Y, Song J, Wu Q. Aberrant gene expression pattern in the glycolysis-cholesterol synthesis axis is linked with immune infiltration and prognosis in prostate cancer: A bioinformatics analysis. *Med (Baltimore)* (2022) 101(43):e31416. doi: 10.1097/md.0000000000031416

30. Chen F, Chen J, Yang L, Liu J, Zhang X, Zhang Y, et al. Extracellular vesicle-packaged HIF-1α-stabilizing lncRNA from tumour-associated macrophages regulates aerobic glycolysis of breast cancer cells. *Nat Cell Biol* (2019) 21(4):498–510. doi: 10.1038/s41556-019-0299-0

31. Cohen IJ, Pareja F, Socci ND, Shen R, Doane AS, Schwartz J, et al. Increased tumor glycolysis is associated with decreased immune infiltration across human solid tumors. *Front Immunol* (2022) 13:880959. doi: 10.3389/fimmu.2022.880959

32. Xu W, Weng J, Xu M, Zhou Q, Liu S, Hu Z, et al. Functions of key enzymes of glycolytic metabolism in tumor microenvironment. *Cell Reprogram* (2023) 25(3):91–8. doi: 10.1089/cell.2023.0010

33. Xia KG, Wang CM, Shen DY, Song XY, Mu XY, Zhou JW, et al. LncRNA NEAT1Associated aerobic glycolysis blunts tumor immunosurveillance by T cells in prostate cancer. *Neoplasma* (2022) 69(3):594–602. doi: 10.4149/neo_2022_211021N1497

34. Chelakkot C, Chelakkot VS, Shin Y, Song K. Modulating glycolysis to improve cancer therapy. *Int J Mol Sci* (2023) 24(3):2606. doi: 10.3390/ijms24032606

35. Webb BA, Chimenti M, Jacobson MP, Barber DL. Dysregulated pH: a perfect storm for cancer progression. *Nat Rev Cancer* (2011) 11(9):671–7. doi: 10.1038/nrc3110

36. Bi J, Bi F, Pan X, Yang Q. Establishment of a novel glycolysis-related prognostic gene signature for ovarian cancer and its relationships with immune infiltration of the tumor microenvironment. *J Transl Med* (2021) 19(1):382. doi: 10.1186/s12967021-03057-0

37. Da Q, Huang L, Huang C, Chen Z, Jiang Z, Huang F, et al. Glycolytic regulatory enzyme PFKFB3 as a prognostic and tumor microenvironment biomarker in human cancers. *Aging (Albany NY)* (2023) 15(10):4533–59. doi: 10.18632/aging.204758

38. Ma Y, Zhang S, Jin Z, Shi M. LipidMediated regulation of the cancer-immune crosstalk. *Pharmacol Res* (2020) 161(November):105131. doi: 10.1016/j.phrs.2020.105131

39. Ma K, Zhang L. Overview: lipid metabolism in the tumor microenvironment. *Adv Exp Med Biol* (2021) 1316:41–7. doi: 10.1007/978-981-33-6785-2_3

40. Zhong J, Guo J, Zhang X, Feng S, Di W, Wang Y, et al. The remodeling roles of lipid metabolism in colorectal cancer cells and immune microenvironment. *Oncol Res* (2022) 30(5):231–42. doi: 10.32604/or.2022.027900

41. Li J, Zhang S, Chen S, Yuan Y, Zuo M, Li T, et al. Lipid metabolism-related gene signature predicts prognosis and depicts tumor microenvironment immune landscape in gliomas. *Front Immunol* (2023) 14:1021678. doi: 10.3389/fimmu.2023.1021678

42. Shen L, Huang H, Li J, Chen W, Yao Y, Hu J, et al. Exploration of prognosis and immunometabolism landscapes in ER+ Breast cancer based on a novel lipid metabolism-related signature. *Front Immunol* (2023) 14:1199465. doi: 10.3389/fimmu.2023.1199465

43. Qiao X, Hu Z, Xiong F, Yang Y, Peng C, Wang D, et al. Lipid metabolism reprogramming in tumor-associated macrophages and implications for therapy. *Lipids Health Dis* (2023) 22(1):45. doi: 10.1186/s12944-023-01807-1

44. Liu L, Mo M, Chen X, Chao D, Zhang Y, Chen X, et al. Targeting inhibition of prognosis-related lipid metabolism genes including CYP19A1 enhances immunotherapeutic response in colon cancer. *J Exp Clin Cancer Res* (2023) 42(1):85. doi: 10.1186/s13046-023-02647-8

45. Xiang Y, Miao H. Lipid metabolism in tumor-associated macrophages. *Adv Exp Med Biol* (2021) 1316:87–101. doi: 10.1007/978981-33-6785-2_6

46. Jiang A, Chen X, Zheng H, Liu N, Ding Q, Li Y, et al. Lipid metabolism-related gene prognostic index (LMRGPI) reveals distinct prognosis and treatment patterns for patients with early-stage pulmonary adenocarcinoma. *Int J Med Sci* (2022) 19(4):711–28. doi: 10.7150/ijms.71267

47. Dai J, Li Q, Quan J, Webb G, Liu J, Gao K. Construction of a lipid metabolism-related and immune-associated prognostic score for gastric cancer. *BMC Med Genomics* (2023) 16(1):93. doi: 10.1186/s12920-023-01515-w

48. Wang R, Liu Z, Fan Z, Zhan H. Lipid metabolism reprogramming of CD8(+) T cell and therapeutic implications in cancer. *Cancer Lett* (2023) 567(July):216267. doi: 10.1016/j.canlet.2023.216267

49. Offer S, Menard JA, Pérez JE, de Oliveira KG, Indira Chandran V, Johansson MC, et al. Extracellular lipid loading augments hypoxic paracrine signaling and promotes glioma angiogenesis and macrophage infiltration. *J Exp Clin Cancer Res* (2019) 38(1):241. doi: 10.1186/s13046-019-1228-6

50. Yu Z, Zhou Y, Li Y, Dong Z. Integration of clinical and spatial data to explore lipid metabolism-related genes for predicting prognosis and immune microenvironment in gliomas. *Funct Integr Genomics* (2023) 23(2):82. doi: 10.1007/s10142-02301010-6

51. Xiong Y, Si Y, Feng Y, Zhuo S, Cui B, Zhang Z. Prognostic value of lipid metabolism-related genes in head and neck squamous cell carcinoma. *Immun Inflammation Dis* (2021) 9(1):196–209. doi: 10.1002/iid3.379

52. Li Z, Jin C, Lu X, Zhang Y, Zhang Y, Wen J, et al. Studying the mechanism underlying lipid metabolism in osteosarcoma based on transcriptomic RNA sequencing and single-cell data. *J Gene Med* (2023) 25(6):e3491. doi: 10.1002/jgm.3491

53. Chen J, Ye J, Lai R. A lipid metabolism-related gene signature reveals dynamic immune infiltration of the colorectal adenoma-carcinoma sequence. *Lipids Health Dis* (2023) 22(1):92. doi: 10.1186/s12944-023-01866-4

54. Chen Y, Yuan H, Yu Q, Pang J, Sheng M, Tang W. Bioinformatics analysis and structure of gastric cancer prognosis model based on lipid metabolism and immune microenvironment. *Genes (Basel)* (2022) 13(9):1581. doi: 10.3390/genes13091581

55. Mylonis I, Simos G, Paraskeva E. Hypoxia-inducible factors and the regulation of lipid metabolism. *Cells* (2019) 8(3):214. doi: 10.3390/cells8030214

56. He S, Cai T, Yuan J, Zheng X, Yang W. Lipid metabolism in tumor-infiltrating T cells. *Adv Exp Med Biol* (2021) 1316:149–67. doi: 10.1007/978-981-33-6785-2_10

57. Liu X, Hartman CL, Li L, Albert CJ, Si F, Gao A, et al. Reprogramming lipid metabolism prevents effector T cell senescence and enhances tumor immunotherapy. *Sci Transl Med* (2021) 13(587):eaaz6314. doi: 10.1126/scitranslmed.aaz6314

58. Prendeville H, Lynch L. Diet, lipids, and antitumor immunity. *Cell Mol Immunol* (2022) 19(3):432–44. doi: 10.1038/s41423021-00781-x

59. Fultang L, Gamble LD, Gneo L, Berry AM, Egan SA, De Bie F, et al. Macrophage-derived IL1β and TNFα Regulate arginine metabolism in neuroblastoma. *Cancer Res* (2019) 79(3):611–24. doi: 10.1158/0008-5472.Can-18-2139

60. Chen Y, Sui M. Lipid metabolism in tumor-associated natural killer cells. *Adv Exp Med Biol* (2021) 1316:71–85. doi: 10.1007/978-981-33-6785-2_5

61. Wang S, Liu R, Yu Q, Dong L, Bi Y, Liu G. Metabolic reprogramming of macrophages during infections and cancer. *Cancer Lett* (2019) 452(June):14–22. doi: 10.1016/j.canlet.2019.03.015

62. Li W, Xu M, Li Y, Huang Z, Zhou J, Zhao Q, et al. Comprehensive analysis of the association between tumor glycolysis and immune/inflammation function in breast cancer. *J Transl Med* (2020) 18(1):92. doi: 10.1186/s12967-02002267-2

63. Yang F, Wan F. Lipid metabolism in tumor-associated B cells. *Adv Exp Med Biol* (2021) 1316:133–47. doi: 10.1007/978-981-336785-2_9

64. Jung JG, Le A. Metabolism of immune cells in the tumor microenvironment. *Adv Exp Med Biol* (2021) 1311:173–85. doi: 10.1007/978-3-030-65768-0_13

65. Arabzadeh A, Quail DF. Myosin II in cancer cells shapes the immune microenvironment. *Trends Mol Med* (2019) 25(4):257–59. doi: 10.1016/j.molmed.2019.02.011

66. Zheng J, Xu W, Liu W, Tang H, Lu J, Yu K, et al. Traditional chinese medicine bu-shen-jian-pi-fang attenuates glycolysis and immune escape in clear cell renal cell carcinoma: results based on network pharmacology. *Biosci Rep* (2021) 41(6):BSR20204421. doi: 10.1042/bsr20204421

67. Li X, Zhang Y, Ma W, Fu Q, Liu J, Yin G, et al. Enhanced glucose metabolism mediated by CD147 contributes to immunosuppression in hepatocellular carcinoma. *Cancer Immunol Immunother* (2020) 69(4):535–48. doi: 10.1007/s00262-01902457-y

68. Li Y, Song Z, Han Q, Zhao H, Pan Z, Lei Z, et al. Targeted inhibition of STAT3 induces immunogenic cell death of hepatocellular carcinoma cells *via* glycolysis. *Mol Oncol* (2022) 16(15):2861–80. doi: 10.1002/1878-0261.13263

69. Yu W, Lei Q, Yang L, Qin G, Liu S, Wang D, et al. Contradictory roles of lipid metabolism in immune response within the tumor microenvironment. *J Hematol Oncol* (2021) 14(1):187. doi: 10.1186/s13045-021-01200-4

70. Zipinotti Dos Santos D, de Souza JC, Pimenta TM, da Silva Martins B, Junior RSR, Butzene SMS, et al. The impact of lipid metabolism on breast cancer: A review about its role in tumorigenesis and immune escape. *Cell Commun Signal* (2023) 21(1):161. doi: 10.1186/s12964-023-01178-1

71. Flerin NC, Pinioti S, Menga A, Castegna A, Mazzone M. Impact of immunometabolism on cancer metastasis: A focus on T cells and macrophages. *Cold Spring Harb Perspect Med* (2020) 10(9):a037044. doi: 10.1101/cshperspect.a037044

72. Huang Y. Targeting glycolysis for cancer therapy using drug delivery systems. *J Controlled Release* (2023) 353(January):650–62. doi: 10.1016/j.jconrel.2022.12.003

73. Zeng L, Liang L, Fang X, Xiang S, Dai C, Zheng T, et al. Glycolysis induces th2 cell infiltration and significantly affects prognosis and immunotherapy response to lung adenocarcinoma. *Funct Integr Genomics* (2023) 23(3):221. doi: 10.1007/s10142-023-01155-4

74. Zhao X, Lian X, Xie J, Liu G. Accumulated cholesterol protects tumours from elevated lipid peroxidation in the microenvironment. *Redox Biol* (2023) 62 (June):102678. doi: 10.1016/j.redox.2023.102678

75. Panetti S, McJannett N, Fultang L, Booth S, Gneo L, Scarpa U, et al. Engineering amino acid uptake or catabolism promotes CAR T-cell adaption to the tumor environment. *Blood Adv* (2023) 7(9):1754–61. doi: 10.1182/bloodadvances.2022008272

76. Luo Q, Zheng N, Jiang L, Wang T, Zhang P, Liu Y, et al. Lipid accumulation in macrophages confers protumorigenic polarization and immunity in gastric cancer. *Cancer Sci* (2020) 111(11):4000–11. doi: 10.1111/cas.14616

77. Bao D, Zhao J, Zhou X, Yang Q, Chen Y, Zhu J, et al. Mitochondrial fission-induced mtDNA stress promotes tumor-associated macrophage infiltration and HCC progression. *Oncogene* (2019) 38(25):5007–20. doi: 10.1038/s41388-019-0772-z

78. Bohn T, Rapp S, Luther N, Klein M, Bruehl TJ, Kojima N, et al. Tumor immunoevasion *via* acidosisDependent induction of regulatory tumor-associated macrophages. *Nat Immunol* (2018) 19(12):1319–29. doi: 10.1038/s41590-018-0226-8

79. Li M, Yang Y, Xiong L, Jiang P, Wang J, Li C. Metabolism, metabolites, and macrophages in cancer. *J Hematol Oncol* (2023) 16(1):80. doi: 10.1186/s13045-023-01478-6

80. Cao J, Zeng F, Liao S, Cao L, Zhou Y. Effects of glycolysis on the polarization and function of tumor–associated macrophages (Review). *Int J Oncol* (2023) 62(6):70. doi: 10.3892/ijo.2023.5518

81. Zang X, Zhang X, Hu H, Qiao M, Zhao X, Deng Y, et al. Targeted delivery of zoledronate to tumor-associated macrophages for cancer immunotherapy. *Mol Pharm* (2019) 16(5):2249–58. doi: 10.1021/acs.molpharmaceut.9b00261

82. Weigert A, Strack E, Snodgrass RG, Brüne B. mPGES-1 and ALOX5/-15 in tumor-associated macrophages. *Cancer Metastasis Rev* (2018) 37(2–3):317–34. doi: 10.1007/s10555-018-9731-3

83. Zhan Y, Qiao W, Yi B, Yang X, Li M, Sun L, et al. Dual role of pseudogene TMEM198B in promoting lipid metabolism and immune escape of glioma cells. *Oncogene* (2022) 41(40):4512–23. doi: 10.1038/s41388-022-02445-0

84. Ye J, Yang Y, Dong W, Gao Y, Meng Y, Wang H, et al. Drug-free mannosylated liposomes inhibit tumor growth by promoting the polarization of tumor-associated macrophages. *Int J Nanomed* (2019) 14:3203–20. doi: 10.2147/ijn.S207589

85. Kobayashi T, Lam PY, Jiang H, Bednarska K, Gloury R, Murigneux V, et al. Increased lipid metabolism impairs NK cell function and mediates adaptation to the lymphoma environment. *Blood* (2020) 136(26):3004–17. doi: 10.1182/blood.2020005602

86. Yenyuwadee S, Aliazis K, Wang Qi, Christofides A, Shah R, Patsoukis N, et al. Immune cellular components and signaling pathways in the tumor microenvironment. *Semin Cancer Biol* (2022) 86(November):187–201. doi: 10.1016/j.semcancer.2022.08.004

87. Hicks KC, Tyurina YY, Kagan VE, Gabrilovich DI. Myeloid cell-derived oxidized lipids and regulation of the tumor microenvironment. *Cancer Res* (2022) 82(2):187–94. doi: 10.1158/0008-5472.Can-21-3054

88. Qin H, Chen Y. Lipid metabolism and tumor antigen presentation. *Adv Exp Med Biol* (2021) 1316:169–89. doi: 10.1007/978981-33-6785-2_11

89. Lemos H, Huang L, Prendergast GC, Mellor AL. Immune control by amino acid catabolism during tumorigenesis and therapy. *Nat Rev Cancer* (2019) 19(3):162–75. doi: 10.1038/s41568019-0106-z

90. Takahashi H, Kawabata-Iwakawa R, Ida S, Mito I, Tada H, Chikamatsu K. Upregulated glycolysis correlates with tumor progression and immune evasion in head and neck squamous cell carcinoma. *Sci Rep* (2021) 11(1):17789. doi: 10.1038/s41598-02197292-6

91. Ho KH, Huang TW, Shih CM, Lee YT, Liu AJ, Chen PH, et al. Glycolysis-associated lncRNAs identify a subgroup of cancer patients with poor prognoses and a highInfiltration immune microenvironment. *BMC Med* (2021) 19(1):59. doi: 10.1186/s12916-021-01925-6

92. Çolakoğlu M, Tunçer S, Banerjee S. Emerging cellular functions of the lipid metabolizing enzyme 15-lipoxygenase-1. *Cell Prolif* (2018) 51(5):e12472. doi: 10.1111/cpr.12472

93. Chang X, Xing P. Identification of a novel lipid metabolism-related gene signature within the tumour immune microenvironment for breast cancer. *Lipids Health Dis* (2022) 21(1):43. doi: 10.1186/s12944-022-01651-9

94. Yan D, Adeshakin AO, Xu M, Afolabi LO, Zhang G, Chen YH, et al. Lipid metabolic pathways confer the immunosuppressive function of myeloid-derived suppressor cells in tumor. *Front Immunol* (2019) 10:1399. doi: 10.3389/fimmu.2019.01399

95. Hu BO, Lin J-Z, Yang X-B, Sang X-T. Aberrant lipid metabolism in hepatocellular carcinoma cells as well as immune microenvironment: A review. *Cell Proliferation* (2020) 53(3):e127725. doi: 10.1111/cpr.12772

96. Di Conza G, Tsai CH, Gallart-Ayala H, Yu YR, Franco F, Zaffalon L, et al. Tumor-induced reshuffling of lipid composition on the endoplasmic reticulum membrane sustains macrophage survival and pro-tumorigenic activity. *Nat Immunol* (2021) 22(11):1403–15. doi: 10.1038/s41590-021-01047-4

97. Zeng W, Yin X, Jiang Y, Jin L, Liang W. PPARα at the crossroad of metabolic-immune regulation in cancer. *FEBS J* (2022) 289(24):7726–39. doi: 10.1111/febs.16181

98. Trézéguet V, Fatrouni H, Merched AJ. Immuno-metabolic modulation of liver oncogenesis by the tryptophan metabolism. *Cells* (2021) 10(12):3469. doi: 10.3390/cells10123469

99. Liu X-h, Zhai X-y. Role of tryptophan metabolism in cancers and therapeutic implications. *Biochimie* (2021) 182(March):131–39. doi: 10.1016/j.biochi.2021.01.005

100. Jiang Z, Liu Z, Li M, Chen C, Wang X. Increased glycolysis correlates with elevated immune activity in tumor immune microenvironment. *EBioMedicine* (2019) 42(April):431–42. doi: 10.1016/j.ebiom.2019.03.068

101. Guo Z, Liang J. Characterization of a lipid droplet and endoplasmic reticulum stress related gene risk signature to evaluate the clinical and biological value in hepatocellular carcinoma. *Lipids Health Dis* (2022) 21(1):146. doi: 10.1186/s12944022-01759-y

frontiers | Frontiers in Immunology

TYPE Review
PUBLISHED 29 January 2024
DOI 10.3389/fimmu.2024.1331641

OPEN ACCESS

EDITED BY
Hao Chen,
Shandong University, China

REVIEWED BY
Ankit Tanwar,
Albert Einstein College of Medicine, United States
Chen Yang,
Tianjin Medical University Cancer Institute and Hospital, China

*CORRESPONDENCE
Xueyuan Cao
jd3d2ub@jlu.edu.cn

RECEIVED 01 November 2023
ACCEPTED 15 January 2024
PUBLISHED 29 January 2024

CITATION
Li D, Cao D, Sun Y, Cui Y, Zhang Y, Jiang J and Cao X (2024) The roles of epigallocatechin gallate in the tumor microenvironment, metabolic reprogramming, and immunotherapy. *Front. Immunol.* 15:1331641. doi: 10.3389/fimmu.2024.1331641

The roles of epigallocatechin gallate in the tumor microenvironment, metabolic reprogramming, and immunotherapy

Dongming Li[1], Donghui Cao[2], Yuanlin Sun[1], Yingnan Cui[1], Yangyu Zhang[2], Jing Jiang[2] and Xueyuan Cao[1]*

[1]Department of Gastric and Colorectal Surgery, General Surgery Center, The First Hospital of Jilin University, Changchun, China, [2]Division of Clinical Epidemiology, The First Hospital of Jilin University, Changchun, China

Cancer, a disease that modern medicine has not fully understood and conquered, with its high incidence and mortality, deprives countless patients of health and even life. According to global cancer statistics, there were an estimated 19.3 million new cancer cases and nearly 10 million cancer deaths in 2020, with the age-standardized incidence and mortality rates of 201.0 and 100.7 per 100,000, respectively. Although remarkable advancements have been made in therapeutic strategies recently, the overall prognosis of cancer patients remains not optimistic. Consequently, there are still many severe challenges to be faced and difficult problems to be solved in cancer therapy today. Epigallocatechin gallate (EGCG), a natural polyphenol extracted from tea leaves, has received much attention for its antitumor effects. Accumulating investigations have confirmed that EGCG can inhibit tumorigenesis and progression by triggering apoptosis, suppressing proliferation, invasion, and migration, altering tumor epigenetic modification, and overcoming chemotherapy resistance. Nevertheless, its regulatory roles and biomolecular mechanisms in the immune microenvironment, metabolic microenvironment, and immunotherapy remain obscure. In this article, we summarized the most recent updates about the effects of EGCG on tumor microenvironment (TME), metabolic reprogramming, and anti-cancer immunotherapy. The results demonstrated EGCG can promote the anti-cancer immune response of cytotoxic lymphocytes and dendritic cells (DCs), attenuate the immunosuppression of myeloid-derived suppressor cells (MDSCs) and regulatory T cells (Tregs), and inhibit the tumor-promoting functions of tumor-associated macrophages (TAMs), tumor-associated neutrophils (TANs), and various stromal cells including cancer-associated fibroblasts (CAFs), endothelial cells (ECs), stellate cells, and mesenchymal stem/stromal cells (MSCs). Additionally, EGCG can suppress multiple metabolic reprogramming pathways, including glucose uptake, aerobic glycolysis, glutamine metabolism, fatty acid anabolism, and nucleotide synthesis. Finally, EGCG, as an immunomodulator and immune checkpoint blockade, can enhance immunotherapeutic efficacy and

may be a promising candidate for antitumor immunotherapy. In conclusion, EGCG plays versatile regulatory roles in TME and metabolic reprogramming, which provides novel insights and combined therapeutic strategies for cancer immunotherapy.

KEYWORDS

epigallocatechin gallate, tumor microenvironment, antitumor immunity, metabolic reprogramming, immunotherapy

1 Introduction

Globally, there were approximately 10 million cancer-related deaths and 19.3 million new cases of cancer in 2020, according to cancer statistics (1–3). With cancer incidence gradually increasing yearly, the worldwide cancer burden is estimated to be close to 28.4 million cases in 2040, up 47% compared to 2020, and this rise is likely to further worsen as the risk factors caused by globalization and economic growth, resulting in even greater healthcare and economic burdens (3).

The tumor microenvironment (TME) and metabolic reprogramming, two notorious pathologic alterations, play pivotal roles in carcinogenesis and progression. It's commonly known that in addition to malignant tumor cells, TME contains various immune cells, such as lymphocytes and monocytes, as well as various stromal cells, such as fibroblasts and endotheliocytes, all of which have their own unique immunological or immunomodulatory capacity to determine whether a tumor will survive and form complex crosstalk with nearby cells (4). As a shelter for tumor survival, the TME continuously interacts with tumor cells to encourage tumor initiation, invasion, intravasation, metastasis, and treatment resistance (5, 6). Additionally, tumor cells have to spontaneously alter their metabolic flux in TME to maintain the bioenergy and biosynthesis required for their uncontrolled proliferation (7). Thus, the tumor cells rewire their metabolic program known as metabolic reprogramming, driven by the carcinogenic alterations in the tumor cells and the various host cytokines acting on tumor cells in TME (8). These metabolic changes in turn reshape the TME to restrict the immune response and create further obstacles to antitumor treatment (9). Consequently, targeting TME and metabolic reprogramming have been gradually recognized as crucial strategies to remove obstruction to antitumor therapy and immune response in recent years (5, 9, 10).

In fact, novel immunotherapeutic strategies targeting TME, including immune checkpoint blockade have been clinically applied in antitumor therapy (11). Although the rapid rise of immunotherapy has revolutionized the anti-cancer therapeutic landscape in the last decade, clinical outcomes show just a limited proportion of patients receive benefits from immunotherapy (12). This implies that how to regulate the communication between immune cells and tumor cells based on the complex TME to enhance the antitumor immune response and how to adopt better immunotherapy strategies to ameliorate the clinical survival of cancer patients still need to be explored at present.

Recently, the anti-cancer and immunomodulatory effects of many natural compounds have attracted increasing attention. Tea, as one of the oldest and most prevalent beverages globally, provides many bioactive ingredients, such as theanine, caffeine, vitamins, and various types of catechins that are proven to benefit human health (13, 14). In addition, the scientific community currently generally agrees drinking tea is fairly appropriate for humans, as there are few reports of serious adverse events from drinking tea (15). Generally, according to the difference in the degree of fermentation, tea can be classified into 6 categories: green, white, yellow, oolong, black, and dark teas, among which, green tea is made from the fresh leaves of tea bushes through the process of blanching, rolling, and drying, without specific fermentation, so a large number of catechins are retained (15, 16). Catechins are the foremost polyphenolic substances in green tea, mainly including epigallocatechin gallate (EGCG), epigallocatechin, epicatechin gallate, gallocatechin gallate, epicatechin, and gallocatechin, among which EGCG is the most abundant catechin in green tea (13, 16).

Accumulating evidence supports the antitumor activity of EGCG and reveals its various molecular targets and mechanisms in inhibiting tumorigenesis and progression, involving the modulation of multiple biological behaviors, including tumor proliferation, invasion, migration, apoptosis, autophagy, epigenetic modification, and therapeutic resistance (17–21). For example, in solid tumors, EGCG has been found to prevent tumor growth and proliferation by reducing the activation of molecules such as mitogen-activated protein kinases (MAPK), extracellular signal-regulated kinase (ERK), and protein kinase B (Akt), to induce cell cycle arrest by upregulating p21 transcription, to trigger mitochondrial cytochrome C-mediated apoptosis by diminishing Bcl-2 and Bcl-xL expression, and to attenuate malignant migration and invasion by reducing the levels of matrix metalloproteinases (MMPs) (16, 17, 19). Additionally, EGCG can regulate DNA methylation and histone acetylation levels through interacting with DNA methyltransferases and histone deacetylases to epigenetically control tumor genome expression (22).

Furthermore, evidence has revealed that EGCG remarkably overcomes chemotherapy resistance and re-sensitizes tumor cells to multiple chemotherapy drugs, such as cisplatin, 5-fluorouracil, doxorubicin, and daunorubicin (16, 23). Nevertheless, its regulatory roles and relevant mechanisms in TME, metabolic reprogramming, and cancer immunotherapy remain obscure and need to be further elucidated and discussed.

In this review, we summarized the most recent updates about the effects of EGCG on the immune microenvironment, metabolic reprogramming, and immunotherapy. Specifically, we elaborated on the roles of EGCG in the functions of immune cells and stromal cells, and the suppression of EGCG in glucose uptake, aerobic glycolysis, glutamine catabolism, fatty acid anabolism, and nucleotide synthesis in TME, as well as the potential value of EGCG-involved immunotherapy strategies, to provide important references to its clinical application.

2 Immunomodulatory roles in immune cells in TME

Recently, EGCG has gained a reputation for its immunomodulatory effects in the TME (24). To elucidate how EGCG acts on the immune microenvironment, we reviewed its immunoregulatory roles and relevant molecular targets in various immune cells in TME, including $CD8^+/CD4^+$ T cells, natural killer (NK) cells, dendritic cells (DCs), myeloid-derived suppressor cells (MDSCs), regulatory T cells (Tregs), tumor-associated macrophages (TAMs), and tumor-associated neutrophils (TANs) (Figure 1).

2.1 $CD8^+/CD4^+$ T lymphocytes

$CD8^+$ T cells, commonly known as cytotoxic T lymphocytes (CTLs), are the pivotal effector cells mediating anti-cancer immunity in the tumor immune microenvironment (TIME) (25). When the CTLs recognize the tumor antigens and are activated, they will release perforin and granzyme and initiate Fas ligand-mediated apoptosis to eradicate tumor cells (26). In addition, activated $CD4^+$ T cells can not only play an auxiliary role in enhancing the clonal expansion and antitumor activity of CTLs but kill tumor cells through direct cytotoxic effects (27, 28). However, these tumor clearance processes are not so smooth, hampered by various complicated factors in TIME. Thus, how to effectively stimulate or enhance the antitumor immune response of T lymphocytes has always been an important challenge in tumor immunotherapy.

Numerous biological experiments have provided convincing arguments in favor of EGCG as an immunological regulator of T lymphocytes. In the EGCG-treated murine metastatic melanoma cells, upregulated expression of granzyme B in $CD8^+$ T lymphocytes was detected in TME (29). In the E7-expressing murine xenograft

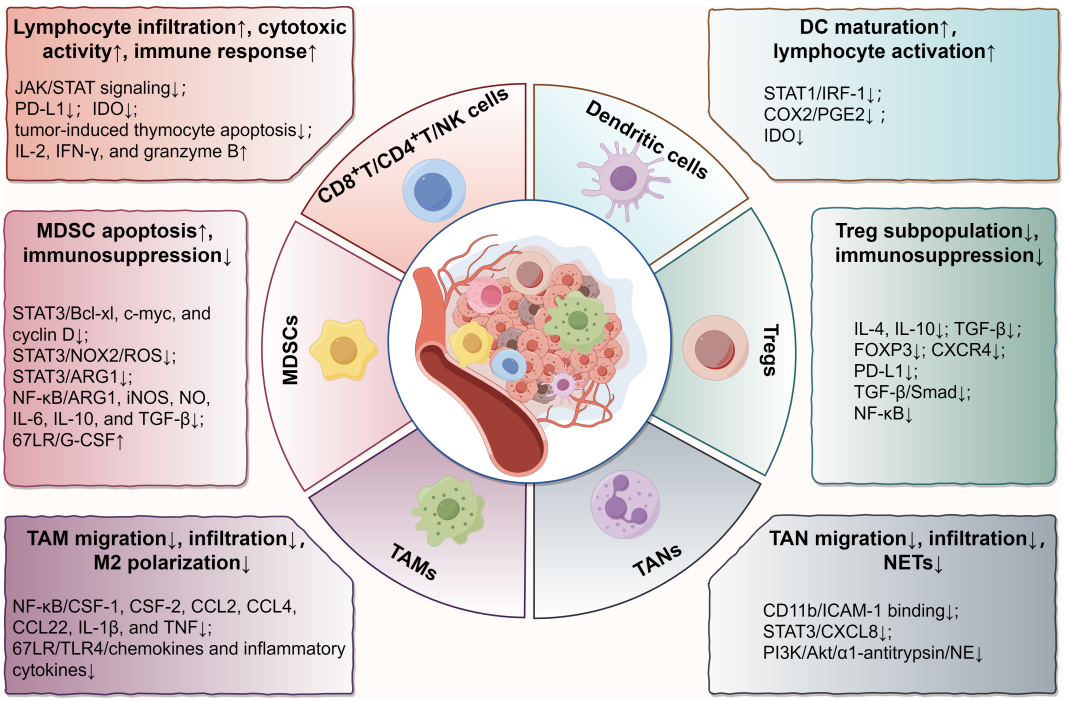

FIGURE 1
Main effects and molecular mechanisms of EGCG on immune cells, including T lymphocytes, NK cells, DCs, MDSCs, Tregs, TAMs, and TANs in tumor microenvironment. EGCG enhances the infiltration and antitumor immune response of cytotoxic lymphocytes, promotes the maturation and tumor antigen loading of DCs, attenuates the immunosuppressive effect of MDSCs and Tregs, and blocks the regulation of TAMs and TANs on tumor promotion, involving various biomolecular targets, such as STAT, NF-κB, TGF-β, TLR4, PI3K/Akt, PD-L1, IDO, and their relevant signaling pathways. The figure was drawn using Figdraw.

model, EGCG induced the generation of special $CD8^+$ T lymphocytes and enhanced the immune response of these cells (30). For the ultraviolet ray (UV)-exposed mice, EGCG prevented skin tumor development through enhancing the infiltration or recruitment of $CD8^+$ T lymphocytes into the TIME (31). Similarly, in a murine WEHI-3 leukemia model, EGCG exhibited an anti-cancer effect through boosting the proliferation of T cells and phagocytosis of macrophages (32). Furthermore, evidence suggested EGCG not only elevated the proportion of $CD8^+$ T lymphocytes *in vitro* but significantly increased the CD4 surface intensity on activated T lymphocytes and promoted the Th1 response when combined with resveratrol (33). Even 5-(3',5'-dihydroxyphenyl)-γ-valerolactone (EGC-M5), a primary metabolic product of EGCG metabolized by intestinal bacteria, was also found to dramatically boost the activity of $CD4^+$ T cells and the production of interferon-gamma (IFN-γ) (34). Collectively, cumulative evidence confirmed EGCG plays crucial immunomodulatory roles in the infiltration and activation of T lymphocytes *in vitro* and *in vivo*, which is beneficial for improving the anti-cancer immune response.

The mechanism behind the aforementioned immunomodulatory potential of EGCG for cytotoxic immune cells may be mainly attributed to the following points. Firstly, scientific studies demonstrated EGCG downregulates the expression of programmed cell death ligand 1 (PD-L1) through disrupting the Janus kinase (JAK)/signal transducer and activator of transcription (STAT) signaling pathway in melanoma (29). Due to the removal of PD-L1-mediated immunoinhibitory signals between tumor cells and CTLs in TME, these CTLs are reactivated to resume the antitumor immune response. Secondly, indoleamine 2,3-dioxygenase (IDO), a promoter of immune escape and immune tolerance in TME, can catalyze the catabolism of tryptophan to inhibit the proliferation of T lymphocytes, induce the apoptosis of T lymphocytes, and increase the infiltration of immunosuppressive cells, thus inhibiting the antitumor response of cytotoxic lymphocytes (35–37). With the JAK/STAT signal blocked by EGCG, its downstream IDO expression is subsequently suppressed (35, 38). Thirdly, substantial evidence confirmed EGCG activates the immune response of T lymphocytes by attenuating MDSC-mediated immunosuppression (39, 40). Finally, drawing from previous research, we hypothesized that EGCG might protect the thymus from tumor-induced thymocyte apoptosis and involution by reducing oxidative stress in thymocytes or modulating the JAK/STAT signaling pathway, thereby providing a prerequisite for T cell maturation, proliferation, and differentiation (41, 42). But further investigation is needed to confirm that.

2.2 Natural killer cells

NK cells, named for their capacity to automatically kill target cells, have been identified as the principal effector cells with cytotoxicity in the antitumor innate immunity (43). Interestingly, NK cells are equipped with various activating and inhibitory surface receptors that transmit either activating or suppressive signals to regulate their activation (44). For instance, as the most potent activating receptor, Fcγ receptor III also known as CD16, stimulates NK cells through the antibody-dependent cell-mediated cytotoxicity (ADCC) process, which is a crucial antitumor immune mechanism (45). Additionally, in normal cells, highly expressed major histocompatibility complex (MHC) class I (MHC-I) molecules interact with the inhibitory receptors of NK cells to protect themselves from attack by NK cells, while MHC-I molecules are often low expressed in tumor cells to evade $CD8^+$ T lymphocyte surveillance (46). Due to the absence of MHC-I-mediated inhibitory signals, NK cells identify this missing-self phenotype and respond to these tumor cells, eventually causing their lysis (44, 45).

In addition to increasing the antitumor immune response of T lymphocytes in the TIME, EGCG has been demonstrated to augment anti-cancer cytotoxicity of NK cells (47). Previous evidence revealed the NK cells extracted from the spleens of the EGCG-administered murine WEHI-3 leukemia model showed significantly enhanced cytotoxic activity against NK-sensitive target cells (murine lymphoma YAC-1 cells) compared to control (32). Soon after, another scientific study detected similar results and came to a consistent conclusion (48). Likewise, in the mouse models with bladder cancer, both EGCG and EGCG nanoparticles enhanced NK cell-mediated cytotoxicity, which appeared to be relevant to significantly upregulated levels of interleukin (IL)-2 and IFN-γ (49). Furthermore, evidence unveiled EGC-M5, a metabolic derivative of EGCG, also upregulated the cytotoxicity of NK cells, which was attributed to the increased levels of granzyme B in NK cells, while EGC-M5 did not affect the populations of NK cells with perforin (34). These findings fully demonstrated EGCG can effectively heighten the antitumor response of NK cells. Nevertheless, the detailed biomolecular mechanisms behind how EGCG regulates NK cell activity remain obscure, and require to be further investigated in the future.

2.3 Dendritic cells

As the strongest specialized antigen-presenting cells (APCs) in TIME to present cancer-associated antigens, DCs initiate the adaptive immune response of naive T lymphocytes by upregulating specific MHC and costimulatory molecules after maturation and activation (50). Since DCs regulate the critical immune response in the TME, DC vaccines used to activate antitumor CTLs may be a novel immunotherapy option (51, 52). Meanwhile, how to enhance the function of DCs in antitumor therapy has always been the fundamental area that researchers pay attention to.

Evidence suggested EGCG antagonized UV-induced inhibition of DC function though possibly protecting the levels of costimulatory molecules on the DC surface and regulating the release of certain cytokines, including IL-10 and IL-12 (53). EGCG was also discovered to avoid UV-induced loss of APC population in mouse models, which was possibly related to EGCG alleviating oxidative damage in the dermis as well as the epidermis at UV-exposed sites (54). These findings imply that EGCG may minimize UV-induced immunosuppression against cutaneous melanoma or basal cell carcinoma. Furthermore, some researchers detected more antigen-loaded DCs in the regional

lymph nodes of mice with oral EGCG, which were responsible for activating $CD8^+$ T cells (30). Notably, EGCG can significantly suppress STAT1 activation and binding to interferon regulatory factor 1 (IRF-1) promoter in IFN-γ-stimulated DCs, and prominently reduce cyclooxygenase-2 (COX-2) expression and prostaglandin E2 (PGE2) generation, thus attenuating the levels of IDO and reversing the IDO-mediated T lymphocyte suppression (38). The downregulation of IDO seems to explain the mechanism by which EGCG affects antitumor immunity through regulating DCs. In terms of studies involving tumor vaccines, evidence suggested that EGCG, as a DC maturation agent, effectively promoted DC maturation and enhanced the anti-cancer effects when administered in combination with mesothelin-specific DNA vaccine, implying this combination application may be a potent immunotherapy strategy against mesothelin-expressing ovarian cancer, pancreatic cancer, and malignant mesothelioma (55). Briefly, EGCG plays a significant regulatory role in DC maturation and immune function, which influences subsequent cytotoxic lymphocyte responses.

2.4 Myeloid-derived suppressor cells

MDSCs, a heterogeneous population of immature myeloid cells, belong to pathologically activated monocytes and granulocytes, including monocytic (M-MDSC) and granulocytic/polymorphonuclear (PMN-MDSC) subsets, and exhibit significant immunosuppressive activity in TME (56, 57). Ample evidence has confirmed the immunosuppressive mechanism of MDSCs on CTLs mainly involves the upregulated levels of arginase I (ARG1), inducible nitric oxide synthase (iNOS), and reactive oxygen species (ROS) (58–60). For instance, MDSCs can secrete ARG1 to cause local deprivation of L-arginine in the TME, which will impede CTL activation and inhibit T cell proliferation (60, 61). iNOS can compete with ARG1 for the identical substrate and metabolize L-arginine to produce nitric oxide (NO), which will block the IL-2 receptor signaling and nitrate the T cell receptor to result in immunosuppression (60, 62, 63). Moreover, in addition to mitochondria-generated and tumor-derived ROS, MDSCs produce a great deal of ROS in the TME through NADPH oxidase 2 (NOX2), which reduces CD3ζ expression in T lymphocytes, thereby limiting T lymphocyte activation and corresponding IFN-γ expression (59).

In a murine breast cancer model, several researchers found EGCG ameliorated MDSCs-mediated immunosuppression though reducing the frequencies of MDSCs in the peripheral blood, spleens, and tumor tissues, and *in vitro* experiments also confirmed EGCG prevented the growth and promoted the apoptosis of MDSCs (40). Another highly insightful investigation pointed the mice drinking EGCG-rich polyphenol E (PE) were manifested as a significant reduction in the tumor-infiltrating myeloid cells with the myeloid hallmarks CD11b or Gr-1 and an antagonism to the cancer-promoting effects of tumor-induced myeloid cells on neuroblastoma (39). Interestingly, when the researchers injected neuroblastoma cells into immunodeficient mice that drank PE-containing water, tumor growth was not affected, while the opposite was observed in immunocompetent mice inoculated with neuroblastoma cells (64). Subsequently, increased T-cell infiltration was detected in the murine tumors co-injected with PE-treated MDSCs, and increased tumor volumes were observed as the immune depletion of $CD8^+$ T cells (39). These results imply EGCG may directly target MDSCs to suppress their immunoinhibitory activities, thereby playing an antitumor role through functional cellular immunity dependent on $CD8^+$ T cells.

Further investigation revealed the inhibitory mechanisms of EGCG on MDSCs were attributed to the regulation of a repertoire of canonical and non-canonical pathways, the former mainly including the STAT3 and nuclear factor-kappaB (NF-κB) signaling pathways, and the latter mainly including the ECM-receptor interaction and focal adhesion (40). Among them, STAT3, the first identified transcription factor relevant to MDSCs expansion in tumors, can block the normal differentiation of myeloid cells and upregulate the expression of multiple antiapoptotic genes, such as Bcl-xL, c-myc, and cyclin D (60, 65). Relevant experiments confirmed activated STAT3 upregulated ARG1 expression in MDSCs through binding to ARG1 promoter, which explains why inhibiting STAT3 can significantly reduce ARG1 and abolish the inhibitory activity of MDSCs (66). Activated STAT3 was also found to induce ROS production in MDSCs through upregulating several subunits of NOX2 to increase ROS-mediated immunosuppression (67). Furthermore, STAT3 can regulate the levels of multiple immunosuppressive facilitators, such as IL-10, PD-L1, and S100 proteins, to promote the proportion and activation of MDSCs (68). Expectedly, evidence suggested EGCG dramatically attenuated STAT3 phosphorylation and downregulated the expression of the aforementioned downstream molecules, possibly due to a direct physical interaction between EGCG and the phosphopeptide binding domain formed by the STAT3 SH2 fold (40, 69). Of note, the phenolic hydroxyl groups of EGCG have strong antioxidant activity based on electron delocalization, which means EGCG can also directly quench the ROS generated by MDSCs in the TME (20). Similarly, EGCG can suppress NF-κB dose-dependently in MDSCs, thereby diminishing a range of downstream immunosuppressive mediators, such as ARG1, iNOS, NO, IL-6, IL-10, and transforming growth factor-beta (TGF-β) (40). Computational docking analysis also confirmed EGCG can directly inhibit NF-κB-mediated transcriptional activation due to the covalent connections between EGCG and p65 subunit (16, 70). Interestingly, EGCG appears to activate the 67 kDa laminin receptor (67LR) and granulocyte colony-stimulating factor (G-CSF) secretion to induce phenotypic differentiation of MDSCs from immature myeloid cells to more mature neutrophil-like cells that have hypersegmented nuclei and fail to inhibit IFN-γ release from CD3 splenocytes (39, 64, 71). In short, these results illuminate the underlying mechanisms by which EGCG targets MDSCs to rescue antitumor immunity.

2.5 Regulatory T cells

Tregs are immunosuppressive T cells with the characteristic forkhead box protein 3 (FOXP3) expression, mainly including

natural Tregs (nTregs) and induced Tregs (iTregs) (72). Normally, nTregs maintain autoimmune tolerance through attenuating T lymphocyte expansion and cytokine production to prevent an autoimmune response (73). However, in reaction to the stimulation of tumor antigens, TGF-β, and other soluble molecules in TME, peripheral naive T cells enter the TME and transform into iTregs, which together with nTregs recruited into tumor tissues constitute a tumor-associated Tregs pool (74). These Tregs overexpress inhibitory receptors, secrete suppressive cytokines, and disrupt metabolism to create obstacles for immune infiltration of effector cells into TME, which are linked to the poor prognosis of tumors notably (75). Therefore, depleting Tregs is a crucial strategy for enhancing antitumor immunity.

A previous clinical trial reported that in the vast majority of patients suffering from chronic lymphocytic leukemia, oral administration of green tea extracts significantly diminished the absolute number of circulatory Tregs, as well as the serum levels of inhibitory cytokines associated with Tregs (including IL-10 and TGF-β) (76). Another latest clinical trial revealed that in acute myeloid leukemia individuals who received oral green tea extracts (15% EGCG) alone or in combination with cytarabine for at least six months, not only a reduction in the frequencies of Tregs and CXC chemokine receptor (CXCR) 4 Treg subpopulation and the levels of IL-4 and TGF-β were observed, but the activated and cytotoxic phenotypes of $CD8^+$ T lymphocytes and NK cells were detected (77). In a co-culture environment involving cancer stem cells and peripheral blood cells from patients with renal clear cell carcinoma, EGCG combined with the first-line treatment sunitinib prominently also decreased the frequency of FOXP3 Tregs in comparison to monotherapy (78). In a murine melanoma model, changes in TME after treatment with EGCG or its nanoparticles were analyzed. The results demonstrated that EGCG or its nanoparticles could significantly inhibit PD-L1 expression and diminish the infiltration of immunosuppressive Tregs, which would ameliorate immune exhaustion and restore the tumor-killing ability of CTLs, thus enhancing the desired antitumor therapeutic effects (79). These suggest that in addition to MDSCs, EGCG may target Tregs to attenuate their immunosuppression in human tumors. Additionally, EGCG may be applied as an immunomodulatory adjuvant in combination with chemotherapy or targeted therapy for tumors. Unfortunately, the available evidence does not directly elucidate the mechanism by which EGCG regulates Tregs. Since TGF-β produced by tumor tissues facilitates the transformation of immature $CD4^+$ T lymphocytes into FOXP3 Tregs in TME and activates NF-κB and Smad signaling pathways to induce FOXP3 expression, we highly hypothesize EGCG reduces the number of Treg subpopulation through downregulating TGF-β/Smad expression and blocking NF-κB activity based on the previous relevant research (70, 80–82).

2.6 Tumor-associated macrophages

As the critical members of immune cells in TME, TAMs are mainly split up into two subpopulations of immune cells with diametrical functions, namely antitumor M1 macrophages that mediate cytotoxicity and ADCC to eradicate cancer cells and alternatively tumor-promoting M2 macrophages that demonstrably inhibit antitumor cellular immunity, promote neovascularization, and cause tumor progression (83). TAMs can induce the generation of a repertoire of mediators, including various growth factors, cytokines, and chemokines, multiple anti-apoptotic factors mediated by NF-κB, and abundant soluble immunosuppressive factors involved in IL−10, TGF-β, ARG1, IDO, and PD-L1, to reshape the TIME in favor of tumor progression and subvert local immune surveillance (84). Collectively, tumor-infiltrating TAMs in TME often act as both “tumor promoters” and “immunosuppressors”, suggesting that the macrophage-centric approaches are the key strategy for cancer prevention and therapy.

In TME, chemokines are essential for the recruitment and activation of macrophages. It was discovered that EGCG suppressed the migration and infiltration of TAMs through downregulating certain chemokines in TME. A scientific study in murine breast cancer model reported the suppressive effect of EGCG on tumor growth seemed to be closely correlated with the reduced infiltration of TAMs with the downregulation of monocyte chemokines, including macrophage-colony stimulating factor (CSF) -1 and C-C chemokine ligand (CCL) 2 (85). Investigation in endometrial cancer supported that EGCG inhibited the secretion of CXC chemokine ligand (CXCL) 12 from stromal cells, thereby limiting macrophage migration, infiltration, and differentiation toward TAMs (86). Likewise, the transcriptional crosstalk analysis in macrophage-like differentiated leukemia cells revealed EGCG significantly decreased the expression of CCL2, CCL4, CCL22, CSF-1, CSF-2, IL-1β, and tumor necrosis factor (87). Doubtlessly, the downregulation of these chemokines or cytokines is largely related to EGCG-mediated suppression of NF-κB signaling (88–90). Additional evidence unveiled EGCG attenuated activated macrophage migration dose-dependently through inducing the internalization of 67LR, a crucial molecule in cell activation and migration, on the membrane surface of macrophages (91). In fact, EGCG suppresses the toll-like receptor (TLR) 4 signaling via 67LR, thus attenuating the levels of macrophage chemokines and inflammatory cytokines (92, 93). These findings explain the non-negligible inhibitory roles of EGCG in TAMs, which may be closely related to its anti-inflammatory properties.

Besides macrophage recruitment and infiltration, the phenotype of TAMs in TME is also controlled by EGCG. M2 polarization is a common hallmark of TME, with downregulated IL-12 and upregulated IL-10, IL-4, and IL-13 as secretion profiles (94). Scientific evidence in breast cancer showed EGCG-induced upregulation of miR-16 that was transported to TAMs via exosomes and contributed to the inhibition of NF-κB through the downregulation of IKKα and the subsequent accumulation of Iκ-B, thereby resulting in a tilt of TAMs cytokine profiles from M2- into M1-like phenotype and inhibition of M2 polarization (85). This finding provides a novel mechanism for how EGCG exerts antitumor effects through manipulating TAMs in TME. Furthermore, a synergistic combination containing EGCG, curcumin, and resveratrol was reported to promote the phenotypic transformation of M2 macrophages into M1

macrophages through reducing the expression of IL-10 by 70% in the TAMs of murine xenograft tumors, while increasing the expression of IL-12 by 244%, which was considered to be related to suppressed STAT3 expression and inhibited STAT3 phosphorylation (95). Meanwhile, the liposome particles composed of the same formulation were demonstrated to cause M2 TAMs to repolarize into tumor-killing M1-like phenotypes and recruit tumoricidal NK cells in glioblastoma (96). These results provide credence that EGCG may evoke the switch of M2 macrophages to M1 macrophages.

2.7 Tumor-associated neutrophils

Recently, the complicated effects of neutrophils on carcinogenesis and progression have received considerable attention. Similar to TAMs, TANs can also be categorized into anti-cancer phenotype, which kills cancer cells by direct cytotoxic actions and indirect activation of adaptive immune responses, and alternatively cancer-promoting phenotype, which is involved in tumor proliferation, angiogenesis, and immunosuppression (97, 98). Evidence has demonstrated TANs not only promote invasion and angiogenesis by producing MMP-9, vascular endothelial growth factor (VEGF), and hepatocyte growth factor (HGF) but also promote distant migration and dissemination through ensnaring tumor cells via neutrophil extracellular traps (NETs) (99). Sufficient studies have also confirmed a high neutrophil-to-lymphocyte ratio is indeed linked to an unfavorable prognosis in multiple cancers (100–102). Hence, drugs targeting TANs offer a bright future for antitumor immunotherapy.

As early as the 1990s, researchers began to explore the roles of EGCG in neutrophil migration and infiltration. Wei et al. discovered EGCG attenuated the infiltration of neutrophils caused by phorbol ester-type skin tumor promoters in the skin tissue of SENCAR mice, and attributed this phenomenon to the inhibitory effect of EGCG on oxidative events (103). Hofbauer et al. mimicked neutrophil transmigration from the vascular lumen to tissue and found EGCG significantly suppressed the migration of neutrophils through monolayer endothelial cells after treating both of them with relevant plasma concentrations of EGCG (104). Such a finding suggests that EGCG may interfere with the entry of circulating neutrophils into TME. Subsequently, EGCG was found to inhibit neutrophil infiltration by acting directly on neutrophils, independent of both the cytotoxicity of EGCG and the influence of chemical inducers (105). However, the possible mechanisms behind this were not revealed, until one scholar explained this inhibitory effect of EGCG on neutrophils depends on the strong interactions between EGCG and CD11b expressed on the neutrophil surface, which competitively suppresses the binding of specific molecules to the CD11b and particularly leads to a markedly reduced ability of neutrophils to bind intercellular adhesion molecule 1 (ICAM-1), an adhesion molecule mediating the passage of neutrophils through endothelial cells (106). Additionally, a recent report illuminated EGCG blocked NET formation as well as STAT3 and CXCL8 expression in the colon cancer-derived TANs, thereby inhibiting the invasion and migration of colon tumor (107). Briefly, the blocking of CD11b/ICAM-1 signal and inhibition of STAT3/CXCL8 pathway may be the key mechanisms by which EGCG suppresses neutrophil migration and infiltration into the TME.

Neutrophil elastase (NE), a major serine protease of neutrophils, is stored in the primary granules of neutrophils and released into the surrounding environment with neutrophil stimulation and activation (108). Recently, scientists have come to realize NE is likely to be a driver of tumorigenesis, as NE significantly promotes tumor growth by reshaping TME, and NE suppression observably diminishes tumor burden and metastasis (109, 110). EGCG directly binds to NE via multiple hydrogen bonds and subsequently suppresses these enzyme activities, and increases the levels of α1-antitrypsin, a natural inhibitor of NE, by weakening the phosphorylation of phosphatidylinositol 3-kinase (PI3K)/Akt pathway, thereby reversing NE-induced migration of tumor cells (111). Furthermore, the inhibitory functions of EGCG in NE activity were also confirmed by biochemical assays, with the 50% inhibitory concentration ranging from 10.9μM to 25.3μM (112–114). Therefore, there is substantial evidence that EGCG can inhibit the enzyme activity of NE released by activated TANs in TME to prevent tumor progression.

3 Regulatory effects on stroma cells in TME

It's commonly known that tumorigenesis is usually accompanied by the formation of the tumor bed as well as the remodeling of the surrounding extracellular matrix (ECM), in which tumor stromal cells play a pivotal role, thus forming a suitable TME for tumor cell survival, so targeting relevant stromal cells is critical to cancer treatment. Given that, we reviewed the regulatory effects and relevant biomolecular mechanisms of EGCG on stroma cells in TME, including cancer-associated fibroblasts (CAFs), endothelial cells (ECs), stellate cells, and mesenchymal stem/stromal cells (MSCs) (Figure 2).

3.1 Cancer-associated fibroblasts

CAFs, the highly heterogeneous stromal cells in TME, play versatile roles in ECM remodeling, inducing angiogenesis, modulating tumor metabolism, excluding immune response, and promoting tumor progression and therapeutic resistance based on intricate signaling crosstalk with tumor cells (115, 116). However, CAF-centered clinical trials have mostly ended in failure, which means the therapeutic strategies by modulating CAFs to achieve clinical benefits face many challenges (117, 118). Fortunately, EGCG offers promising prospects for improving the TME by targeting CAFs.

As the "bad neighbors" of tumor cells, the proliferation and migration of CAFs are considered necessary for tumor progression. According to one study, EGCG prevented fibroblast adhesion to various ECM proteins by possibly binding to fibronectin and fibrinogen, affecting the expression and affinity of integrin α2β1,

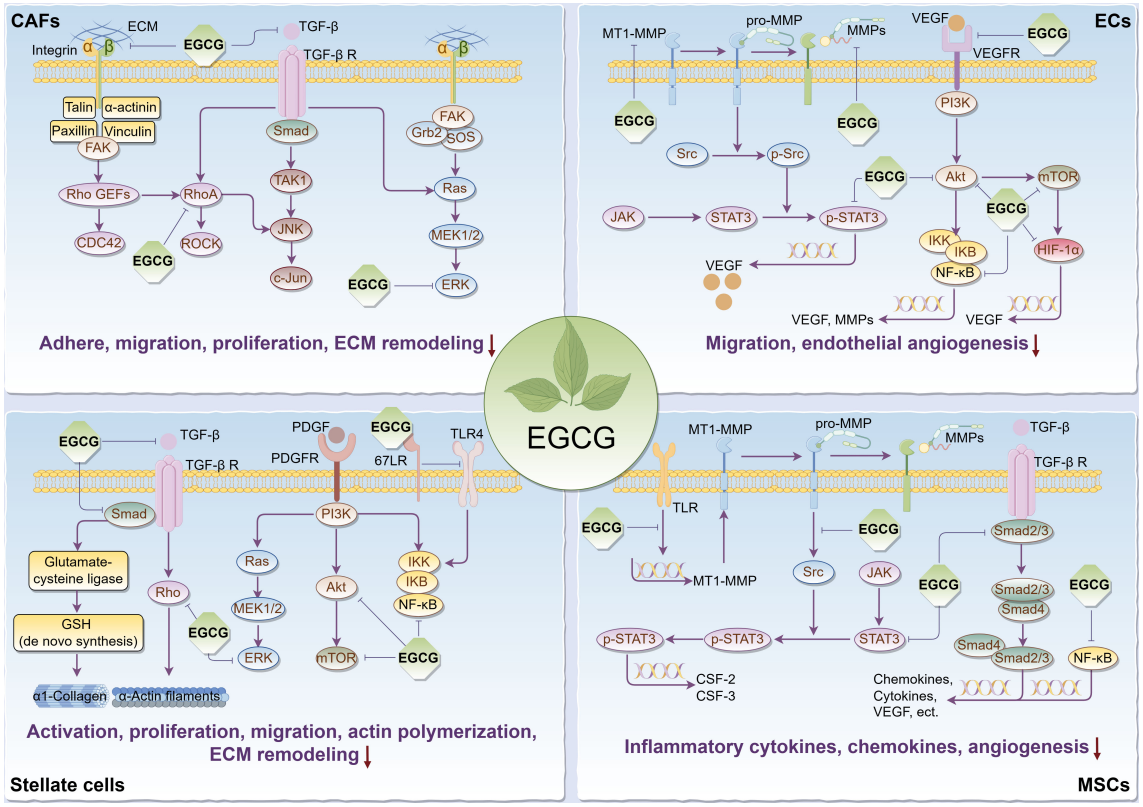

FIGURE 2
Main effects and molecular mechanisms of EGCG on tumor stromal cells, including CAFs, ECs, stellate cells, and MSCs in tumor microenvironment. EGCG inhibits tumor stromal cell activation, adhesion, proliferation, migration, inflammatory cytokine and chemokine secretion, actin polymerization, ECM remodeling, and angiogenesis. Main molecular mechanisms may be attributed to the inhibitory effect of EGCG on Rho/ROCK, ECM/integrin, RTKs/PI3K/Akt/mTOR, TGF-β/Samd, MAPK/ERK, JAK/STAT3, NF-κB, 67LR/TLR4, and HIF-1α signaling pathways. The figure was drawn using Figdraw.

and reducing the phosphorylation of focal adhesion kinase (FAK) and the organization of actin cytoskeleton (119). Simultaneously, EGCG reduced fibroblast migration on matrix proteins, which appears to be attributable to its suppressive effects on the expression and activity of MMPs in the stromal fibroblasts (119, 120). Some scholars found that in keloid, a benign skin tumor, EGCG significantly suppressed the proliferation, migration, and collagen production of pathological fibroblasts through blocking the STAT3 signaling, and this inhibitory effect on proliferation and migration was stronger than that of normal fibroblasts (121). These observations largely demonstrate EGCG is a potent inhibitor of stromal fibroblast behaviors. Nevertheless, whether EGCG induces fibroblast apoptosis remains controversial. Hung et al. considered the inhibitory roles of EGCG in fibroblasts were independent of its cytotoxic or pro-apoptotic activity, as the same concentration of EGCG had a specific suppressive effect on fibroblast adhesion to different matrix proteins, and no increase in lactate dehydrogenase (LDH) release and decrease in cell viability were detected during fibroblast culture treated with EGCG (119). Conversely, in the abnormal fibroblasts from transgenic mice overexpressing tumor-associated NADH oxidase, low concentrations of EGCG inhibited their growth, and their apoptosis was observed 48 hours later (122). This difference may be related to different sources of fibroblasts or different experimental conditions. Thus, further *in vitro* and *in vivo* experiments are urgently needed to verify EGCG's roles in the apoptosis of CAFs.

Not only that, there is additional evidence to support EGCG can impede cancer progression by targeting CAFs. In thioacetamide-induced rat hepatoma assay, EGCG effectively diminished hepatic fibrosis and fibroblast growth factor that can stimulate angiogenesis and proliferation of fibroblasts (123). A phase II clinical trial explored the effect of EGCG supplementation on biological markers in patients with prostate carcinoma before surgery, with the results suggesting a substantial reduction in the tumor-promoting HGF and VEGF levels (124). Further *in vitro* investigations confirmed the potential of EGCG to suppress the production of these two biomarkers in prostate CAFs. Considering that these two notorious biomarkers are primarily secreted from tumor myofibroblasts in TME, that implies EGCG may inhibit the differentiation of CAFs into prostate cancer-associated myofibroblasts. Then the researchers unveiled EGCG combined with luteolin in prostate CAFs synergically inhibited TGF-β-mediated myofibroblast phenotypes with fibronectin expression and diminished TGF-β-mediated ECM contraction, a promoter of tumor invasion (125). Mechanistically, both EGCG and luteolin attenuated the signaling activation of Ras homolog family member A (RhoA) necessary for TGF-β-mediated fibronectin expression in CAFs and inhibited downstream TGF-β-induced signaling, such as

ERK (125, 126). Meanwhile, as a potential inhibitor of RhoA, EGCG may also inhibit the recruitment and persistent education of CAFs in breast cancer by blocking the RhoA/Rho-associated kinase (ROCK) signaling pathway, thus suppressing the invasion of tumor cells (127, 128). In addition, a recent study revealed EGCG obstructed aerobic glycolysis in CAFs to disrupt their tumor-promoting capabilities. Taken together, EGCG can target CAFs to reverse tumor progression.

3.2 Endothelial cells

Among the tumor stroma cells, ECs are the primary contributors to the formation of the tumor vascular system. Even more to the point, tumor-associated endothelial cells (TECs) evolve into mesenchymal phenotypic cells by endothelial-mesenchymal transition, which drives various cancerous biological characteristics of tumors, including aberrant angiogenesis, CAF formation, tumor metabolism, invasion, metastasis, and resistance to treatment (129, 130). Given this, ECs are one of the key targets of antitumor therapy.

The transformation of ECs into capillaries requires endothelial growth, migration, invasion, and matrix remodeling (131). Extensive evidence has confirmed EGCG can suppress these angiogenic features. A previous study reported EGCG could not only inhibit endothelial growth but reduce endothelial migration and capillary tube formation on Matrigel, which was considered to be related to its inhibitory roles in the activities of MMPs during endothelial morphogenesis (132). Soon, several researchers using the dorsal air sac model found EGCG attenuated the invasion and tumor angiogenesis of human ECs, which was attributed to the effective inhibition of membrane-type 1 MMP (MT1-MMP) involved in MMPs activation (133). Subsequent research revealed EGCG dose-dependently reduced the expression and transcriptional activity of MMP-9 in ECs, at least by suppressing ROS, NF-κB, and activating protein-1, thereby blocking the invasion of ECs (134). In addition to EGCG directly targeting TECs, EGCG was found to inhibit VEGF-mediated mobilization of endothelial progenitors into the circulating bloodstream through suppressing MMP-9 generation in marrow stromal cells (135). Notably, a study reported EGCG's inhibitory effects on the abovementioned angiogenic features of ECs may be related to the inhibition of angiopoietin-2 secretion, which promotes vascular remodeling and sprouting (136). Some scholars, meanwhile, supported EGCG inhibited VEGF-induced migration of TECs through suppressing Akt phosphorylation in the PI3K/Akt signaling pathway during endothelial angiogenesis (135). Contrarily, this anti-angiogenic effect was not observed in normal ECs. Similar evidence also demonstrated EGCG inhibited endothelial morphogenesis through the suppression of VEGF receptor (VEGFR) binding (137). Furthermore, a recent study co-cultured neuroblastoma cells with human ECs in a novel three-dimensional *in vitro* model and found EGCG might inhibit the tumor vascularization microenvironment of TECs (138). These findings imply EGCG can directly block the angiogenic capacity of TECs in TME.

In TME, tumor cells typically produce high levels of VEGF, which is essential to support tumor growth and survival. These proangiogenic VEGF molecules can decisively drive new angiogenesis within tumors through inducing endothelial sprouting, proliferation, and migration and regulating the recruitment of circulating endothelial progenitors (139). Additionally, autocrine VEGF by ECs can also promote endothelial elongation, network formation, and branch (140). Therefore, targeting VEGF/VEGFR signaling has become a major treatment option for many cancers. A compelling body of evidence revealed EGCG can downregulate the expression levels of VEGF by inhibiting multiple tumor-related signaling molecules, such as PI3K, Akt, mammalian target of rapamycin (mTOR), hypoxia-inducible factor-1alpha (HIF-1α), NF-κB, and STAT3, thus inhibiting endothelial angiogenesis and tumor progression (16, 86, 141–143). Furthermore, studies confirmed EGCG significantly reduced basic fibroblast growth factor (bFGF) levels in ECs and tumor cells, by increasing bFGF ubiquitination and 20S proteasome activity, which led to bFGF degradation (144, 145). This is another pathway by which EGCG inhibits endothelial angiogenesis.

Accumulating evidence suggests EGCG in combination with other flavonoids or angiogenesis inhibitors can effectively inhibit endothelial angiogenesis. EGCG combined with silibinin synergistically facilitated the downregulation of proangiogenic VEGF, VEGFR2, and miR-17-92 family and the upregulation of anti-angiogenic miR-19b, when ECs were cocultured with tumor cells (146). Analogously, in comparison to EGCG alone, combined administration of EGCG and curcumin better attenuated the evolution of normal ECs to TECs stimulated by tumor medium supernatant or tumor tissue homogenate through inhibiting the JAK/STAT3/IL-8 pathway, thereby reversing endothelial angiogenesis (147). Furthermore, EGCG markedly decreased endoglin levels in human ECs treated with semaxanib, a potent and selective inhibitor of VEGFR, thus exerting its anti-angiogenic function through targeting proangiogenic endoglin/Smad family member 1 (Smad1) signaling, which means combination therapies including EGCG will be promising to address the resistance of tumor cells to anti-VEGF therapies (148).

3.3 Stellate cells

Stellate cells, resident lipid storage cells in the liver and pancreas, can differentiate into a myofibroblast phenotype in response to tissue injury, participating in pathologically inflammatory processes that result in the fibrosis of tumor tissues and the construction of growth-permitting TME (149). In the liver microenvironment, on the one hand, perivenous hepatic stellate cells (HSCs) are identified as the primary source of cancer-promoting CAFs after chronic liver injury (150). On the other hand, HSCs can generate growth differentiation factor 15 to promote the cell growth of hepatocellular carcinoma (HCC) (151). Additionally, evidence supports stellate cells can communicate with immune cells to promote tumor progression. For instance, the crosstalk between HSCs and TAMs drives the premalignant and malignant hepatic microenvironment through

ECM remodeling, immunosuppression, and pro-inflammatory cytokines (152). Even, HSCs inhibit breast cancer dormancy maintained by NK cells, since CXCL12 secreted by activated HSCs can induce NK cell quiescence through its homologous receptor CXCR4, which is closely related to tumor liver metastasis (153).

A compelling body of studies have demonstrated EGCG can restrain stellate cell activation and reverse stellate cell-mediated ECM remodeling. EGCG was found to disrupt TGF-β signaling through downregulating TGF-β receptor and Smad4 expression, resulting in stimulating the expression of glutamate-cysteine ligase to enhance *de novo* glutathione synthesis in HSCs, thereby inhibiting HSC proliferation associated with oxidative stress (154). Additional experiments suggested *de novo* glutathione synthesis was necessary for EGCG to block TGF-β signaling and diminished the expression of α1(I) collagen in activated HSCs (155). Meanwhile, it has been reported that EGCG abolished stress-fiber formation and altered α-actin distribution by inhibiting the Rho signaling required for HSC activation and proliferation (156). Furthermore, previous scientific studies reported EGCG blocked the proliferation and migration of hepatic and pancreatic stellate cells induced by platelet-derived growth factor (PDGF), a potent mitogen for stellate cells and regulator of early proliferative response (157, 158). The mechanisms mainly involve its inhibitory roles in the binding between PDGF and its receptor (PDGFR), the phosphorylation of PDGFR, and the signal transduction of downstream PI3K/Akt, ERK, NF-κB, and transcription factors activator protein-1 (157–159). Moreover, evidence supported EGCG suppressed the activation of HSCs possibly through its inhibitory effect on osteopontin, and hindered collagen fiber deposition in the ECM of hepatocytes, thereby reducing fibrosis in the liver microenvironment (160, 161). A recent report also confirmed EGCG blocked HSC activation and attenuated ECM deposition and fibrosis by inhibiting glutamate dehydrogenase (GDH) in glutamine metabolism pathway (162). Collectively, EGCG effectively prevents stellate cell activation and the resulting ECM remodeling by the above multiple pathways, which provides crucial insights into its antitumor targets.

In HCC, it was previously believed that the recurrence and metastasis after radiotherapy were only attributed to the invasive effects of remaining hepatoma cells, whereas it is now realized that this is closely relevant to the enhanced metastasis potential of remaining hepatoma cells caused by radiation treatment (163). There is evidence to support that radiotherapy-induced activation of HSCs provides favorable conditions for promoting the metastasis potential of HCC (164). *In vitro* experiments confirmed that radiotherapy enhanced TLR4 signaling in HSCs and upregulated ICAM-1, 67LR, IL-6, and CX3C chemokine ligand 1, among which EGCG bound to 67LR to inhibit TLR4 signaling and radiation-induced HSC invasion (163). This means EGCG may be beneficial to ameliorate the radiotherapeutic efficacy of HCC and decrease the chance of recurrence and metastasis after radiotherapy. In addition to attenuating the activation of HSCs, EGCG was found to inhibit HCC development by inducing the senescence of HSCs. Both *in vivo* and *in vitro* experiments detected EGCG triggered a series of senescence phenotypes in activated HSCs (165). However, the mechanism of how EGCG regulates the senescence process of HSCs in HCC remains unclear up to now.

3.4 Mesenchymal stem/stromal cells

MSCs, which are found in almost all human tissues and are given the ability to transdifferentiate into various connective tissue lineages, such as adipocytes and chondrocytes, can migrate to the tumorigenic sites to participate in the formation of tumor stroma (166). Substantial experimental data indicate the overall net effect of MSCs is toward promoting tumor progression (167). As a vital component of TME, MSCs facilitate tumor cell survival, support angiogenesis, promote epithelial-mesenchymal transition, and increase immune escape from the immune system (168, 169). As a result, increasing scholars have realized targeting MSCs in the TME may be an underlying strategy to ameliorate tumor patient outcomes.

Relevant data illuminated the regulatory effect of EGCG on the signaling cascade of MSCs, that is, EGCG attenuated TLR signaling and subsequent MT1-MMP expression, causing the suppression of MT1-MMP-mediated sequential phosphorylation of Src, JAK, and STAT3, thereby inhibiting the expression of CSF-2 and CSF-3 responsible for endothelial angiogenesis in TME (170). In triple-negative breast cancer (TNBC), EGCG was found to inhibit the paracrine crosstalk between adipose-derived MSCs and TNBC cells. For instance, on the one hand, evidence suggested EGCG prevented a pro-inflammatory and tumor-associated adipocyte-like phenotype (with upregulated CCL2, CCL5, CXCL8, IL-1β, IL-6, COX2, HIF-1α, and VEGF) induced by TNBC secretome in adipose-derived MSCs, primarily through the inhibitory effects of EGCG on Smad2 and NF-κB signaling pathways (171). On the other hand, an investigation revealed EGCG suppressed the differentiation of MSCs into adipocytes and prevented STAT3-mediated paracrine carcinogenic control of TNBC invasion phenotypes in response to adipocytes secretome (172). Nevertheless, apart from paracrine connections to tumor cells, whether EGCG can reverse MSC-induced changes in the immune microenvironment remains unclear. A host of research needs to be performed before further elaboration.

4 Regulatory roles in tumor metabolic reprogramming

Tumor metabolic reprogramming provides a constant supplement to tumor energy consumption and biosynthesis to meet uncontrolled proliferation, which concurrently provides critical targets for tumor therapy. To further elucidate EGCG's suppressive effects on tumor cell metabolism, we summarized the regulatory roles of EGCG in multiple upregulated metabolic pathways, including glucose uptake, aerobic glycolysis, glutamine metabolism, fatty acid anabolism, and nucleotide synthesis (Figure 3).

10.3389/fimmu.2024.1331641

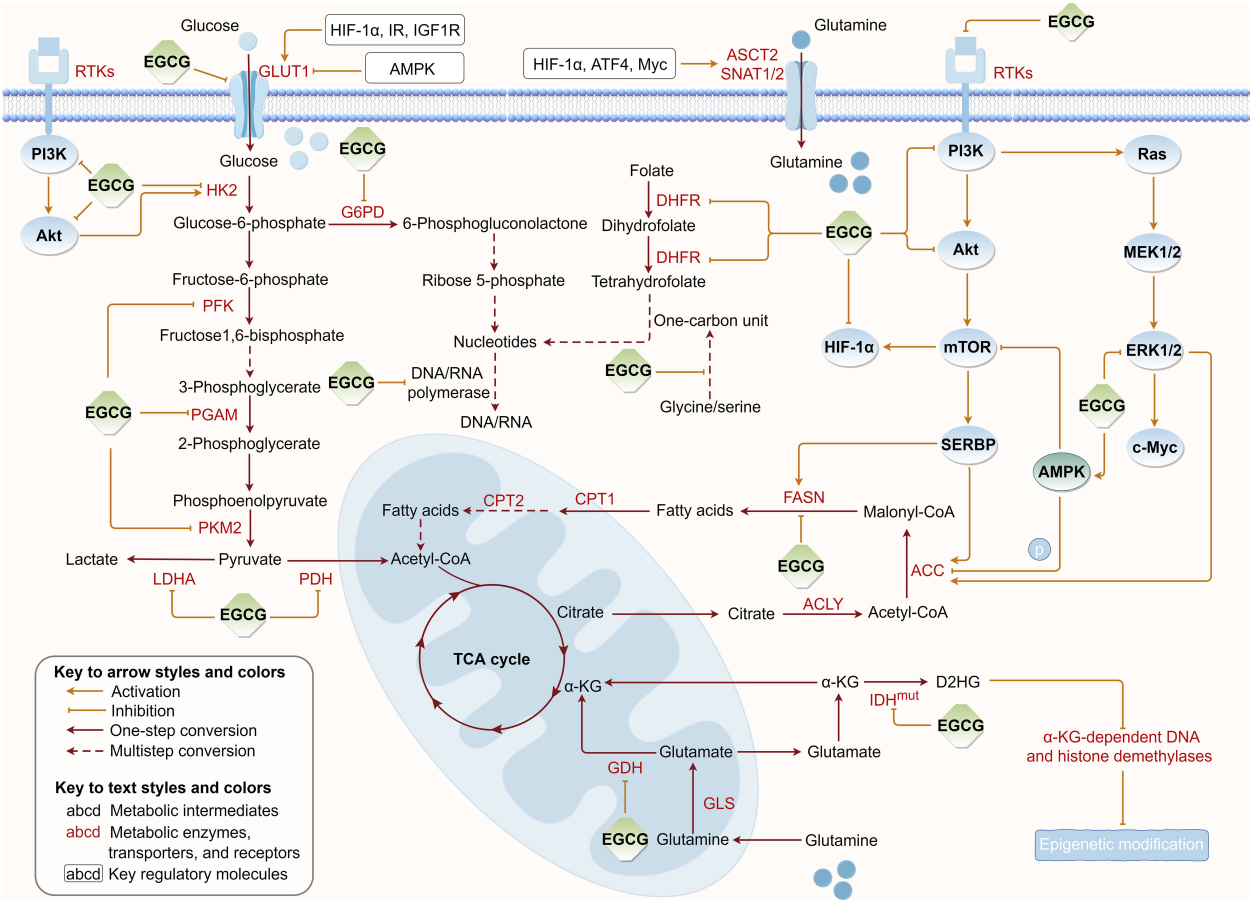

FIGURE 3
Regulation of EGCG on tumor metabolic reprogramming. EGCG downregulates the expression or/and directly inhibits the activity of various key metabolic enzymes and molecular proteins required for glucose uptake, aerobic glycolysis, glutamine metabolism, fatty acid anabolism, and nucleotide synthesis pathways. The figure was drawn using Figdraw.

4.1 Glucose uptake

The metabolic flux of glucose depends on glucose uptake by tumor cells, during which glucose enters tumor cells via active transport. On the cell membrane of tumor cells, glucose transporter (GLUT) proteins are often upregulated to promote glucose uptake and support tumor metabolism (173). Upregulated GLUT1 levels have been confirmed to be an important indicator of poor prognosis in multiple cancers, including lung, pancreatic, colorectal, ovarian, breast, bladder, esophageal, and oral cancers (174). Therefore, targeting GLUT offers excellent prospects for antitumor therapy.

A host of experimental findings shed light on the targeted inhibitory roles of EGCG in GLUT-dependent glucose uptake in tumors. Following exposure of colon cancer cells to different EGCG dosages, a sustained reduction in GLUT1 mRNA levels was detected (175). This inhibitory effect appears to be closely correlated with adenosine monophosphate (AMP)-activated protein kinase (AMPK) signaling after EGCG treatment. Similarly, EGCG was observed to reduce GLUT1 expression in breast cancer and pancreatic cancer, although the mechanism may be attributed to its inhibitory effect on HIF-1α, which is vital for regulating the genes encoding GLUT and ameliorating the activities of glycolytic enzymes (176, 177). As far as we know, EGCG's inhibitory effects on HIF-1α may partially result from the suppression of upstream insulin receptor (IR) and insulin-like growth factor-1 receptor (IGF1R) by EGCG (177). In addition, EGCG was discovered to limit GLUT-mediated glucose uptake through directly and competitively inhibiting GLUT1 in breast cancer cells (178). Relevant molecular docking also supported the direct interaction of EGCG with the glucose docking sites at the core of GLUT1 through hydrogen bonding and hydrophobic contacts (179). Briefly, EGCG can inhibit GLUT1 expression and target GLUT1 activity to interfere with glucose metabolism in tumor cells.

4.2 Aerobic glycolysis

Normal cells obtain energy by oxidative phosphorylation, while most solid tumor cells depend mainly on glycolysis to generate energy to adapt to their TME even when oxygen is abundant, a phenomenon named the "Warburg effect" (180). This pattern of energy supply seems uneconomical on the surface, but it is essential for tumor cells because it provides them with a survival advantage and makes their TME more favorable to tumor progression (181).

Hence, targeting the "Warburg effect" of tumor cells is an extremely promising treatment approach. This means that in the "Warburg effect", many crucial regulatory enzymes, including hexokinase (HK), phosphofructokinase (PFK), phosphoglycerate mutase-1 (PGAM1), pyruvate kinase (PK), and LDH can be considered as potential targets for antitumor drug development (182). It has been reported that a novel biological orthogonal probe was used to identify the direct target protein of EGCG based on *in situ* global proteomics profiling, and subsequent gene ontology analysis revealed these main targets belonged to enzymes regulating pivotal metabolic processes such as glycolysis and energy homeostasis (183). This investigation declared a unique EGCG interactome and provided an important reference for EGCG to regulate the metabolic process of glycolysis.

HK can catalyze the phosphorylation of hexose's sixth hydroxyl group to generate glucose-6-phosphate, the first rate-limiting stage in glycolysis. Preclinical experiments confirmed that EGCG dose-dependently suppressed the activity and mRNA levels of HK2, reduced glucose consumption, and impaired lactate and adenosine triphosphate (ATP) production, and thus the tumor growth was remarkably inhibited (176). Related evidence further pointed EGCG could significantly downregulate HK2 expression through strongly inhibiting epidermal growth factor receptor (EGFR) activation and downstream Akt phosphorylation, thus exerting its far-reaching antitumor effects through direct regulation of glycolysis (184). Molecular docking and dynamics simulation analysis also identified EGCG with obvious binding preference and selectivity for HK2 binding pocket, and could preferentially attach to the corresponding active site to form stable protein-ligand complexes (185). Taken together, these results imply EGCG, as a potential HK2 inhibitor, can potently inhibit the initiation process of glycolysis.

PFK is the second rate-limiting enzyme in glycolysis, responsible for catalyzing fructose-6-phosphate to fructose-1, 6-bisphosphate and mediating glycolytic flux in tumor progression (186). To date, an accumulating body of studies have confirmed the negative regulatory roles of EGCG in the activity and expression level of PFK. Previous investigators, while discovering the inhibitory effects of EGCG on GLUT1 and HK2, also noticed that PFK was an important antitumor target in breast and pancreatic cancer (176, 177). Additional researchers confirmed that EGCG mainly disrupted the glycolysis of pancreatic cancer cells through inhibiting the rate-limiting enzyme PFK, but this inhibitory effect was largely eliminated by catalase, suggesting its inhibitory effects on these enzymes depends on the amount of EGCG-induced hydroperoxide (187). Notably, when EGCG combined with gemcitabine was used to treat pancreatic cancer cells, the researchers detected the activity and protein expression of PKF were further inhibited, and the antitumor effect was further enhanced (187). This means EGCG as a strong combination partner for chemotherapy drugs can sensitize pancreatic cancer cells to gemcitabine. Furthermore, in HCC, to determine whether EGCG directly affects PFK, some researchers analyzed the activity of the purified enzyme. The results clearly indicated EGCG induced PFK transition from the fully active tetramers to the quite inactive dimers, implying its inhibitory role in glycolysis is primarily to reduce PFK activity by stabilizing it in an inactive oligomer conformation (188). Coincidentally, EGCG combined with sorafenib further inhibited PFK expression and tumor cell growth in HCC cells compared with EGCG or sorafenib alone, which provided another valuable reference for antitumor-targeted combination administration (188).

PK is the third crucial rate-limiting enzyme in glycolysis, catalyzing phosphoenolpyruvate to pyruvate. For pancreatic cancer, there has been sufficient evidence to demonstrate EGCG can effectively limit the expression and activity of PK (177, 187). For example, *in vitro* experiments showed 40μM EGCG reduced PKM2 levels in pancreatic cancer cells by 34% to 49%, and *in vivo* experiments demonstrated PKM2 levels were significantly decreased in murine pancreatic tumor xenografts (187). However, in breast cancer, EGCG suppressed the expression and activity of PK to a lesser extent, only reaching significance when treated with 80μM EGCG (176). Conversely, EGCG with the same concentration gradient was indicated to exert its inhibitory effects on HK and PFK to a greater extent. These findings imply that EGCG regulates PK in tumor glycolysis with certain differences, which may be the result of dependence on specific signaling pathways.

In addition to the aforementioned rate-limiting enzymes for glycolysis, evidence indicated EGCG could inhibit other metabolic enzymes associated with the "Warburg effect". For instance, EGCG significantly inhibits LDH in pancreatic cancer cells, an enzyme that catalyzes the conversion of pyruvate into lactate, and this suppression was observed to be comparable to that of oxamate, an inhibitor of LDH (177, 189). Additionally, screening analyses based on natural compounds identified the inhibitory effect of EGCG on PGAM1 tremendously exceeded that of known PGAM1 inhibitors (190). Further molecular interaction analysis also confirmed EGCG constituted eight hydrogen bonds with the residues of PGAM1, with the main hydrogen bonds from its phenol hydroxyl groups (190). Moreover, evidence revealed EGCG inhibited the expression of pyruvate dehydrogenase E1-α (PDHA1), a key regulator of pyruvate dehydrogenase (PDH), in primary effusion lymphoma, thereby controlling the metabolic flux between glycolysis and the tricarboxylic acid cycle (TCA) (191). Taken together, targeting these vital enzymes associated with glycolysis based on the versatile roles of EGCG is a viable approach for antitumor treatment. Nevertheless, though the growing number of evidence demonstrated a multi-pharmacological mode of action of EGCG on aerobic glycolysis of tumors, the underlying mechanism remains to be further investigated.

4.3 Glutamine metabolism

Besides glucose, glutamine is another vital nutrient supporting tumor cell survival, as well as a crucial carbon and nitrogen reservoir necessary for tumor growth and proliferation, supplying ribose, non-essential amino acids, citrate, and glycerol essential for tumor metabolism and supplementing the decreased oxidative phosphorylation caused by "Warburg effect" (192). Evidence has

demonstrated tumor cells often overexpress mitochondrial glutaminase (GLS) to catalyze the hydrolysis of glutamine to glutamate that is further converted to α-ketoglutarate (α-KG) by GDH or aminotransferase (162, 193). This means that with the glutamine metabolic pathway rewired in TME, glutamine continuously replenishes the intermediate α-KG for the TCA cycle to support the energy consumption caused by uncontrolled cell proliferation, leading to the consequences of cellular addiction to glutamine (194, 195). The reprogramming limits the glutamine utilization by immune cells and regulates PD-L1 levels of cancer cells, thus affecting the antitumor immune response and aiding tumor immune escape (196).

One study found EGCG effectively reduced total and sodium-dependent glutamine uptake in tumor cells (197). Unfortunately, it is unclear from current studies whether this suppression is related to the expression levels and transport activities of glutamine transporters including alanine/serine/cysteine transporter 2 (ASCT2), and sodium-coupled neutral amino acid transporter 1 and 2 (SNAT1, SNAT2), although these glutamine transporters are often upregulated in tumors. Relevant evidence has revealed the transcriptional programs of these transporters are largely regulated by HIF-1α, ATF4, and Myc (198, 199). Indeed, it has been observed that EGCG can markedly reduce the expression of these transcription factors in tumors (16, 200, 201). Given that, we speculate EGCG may downregulate the expression levels of the abovementioned glutamine receptors, but direct experimental results are still needed to confirm our hypothesis. In addition, to clarify the effect of EGCG on glutamine transporter activities, molecular docking simulations and dynamics analyses should be performed to explore the direct interaction of EGCG with them.

In tumor cells, GDH is the metabolic bridge between glutamate derived from glutamine metabolism and the TCA cycle. Similar to targeting rate-limiting enzymes in glycolysis, targeting GDH also can interfere with the energy generation of tumor cells. There have been an increasing number of studies, including tumor metabolomics analyses, shedding light on the inhibitory roles of EGCG in tumor glutamine metabolism by targeting GDH (202). Previous investigation demonstrated EGCG reduced GDH expression to disrupt glutaminolysis in primary effusion lymphoma cells, and EGCG-induced tumor cell death was attenuated if the deficient α-KG was supplemented (191). Meanwhile, a scientific study suggested EGCG could dose-dependently target GDH activity, which leads to increased oxidative stress and thus makes tumor cells sensitive to radiotherapy (203). Corresponding molecular dynamics simulations supported the abilities of EGCG to establish multiple non-bonding contacts at the adenosine diphosphate (ADP) activation site of GDH and to form multiple hydrogen bonds with a variety of amino acid residues of GDH (204). These results suggest that EGCG can block glutaminolysis for the energy supply of tumor cells.

Notably, isocitrate dehydrogenase (IDH) mutations are often found in multiple tumors, which induce the production of a new pro-oncogenic oncometabolite, D-2-hydroxyglutarate (D2HG), at the cost of α-KG, thus resulting in tumor metabolic alterations (203). Accumulation of D2HG can competitively block α-KG-dependent DNA and histone demethylases, to change epigenetic modifications, thereby indirectly regulating oncogene and anti-oncogene expression (191, 203). In response to IDH^{mut}-mediated metabolic stress, tumor cells activate a rescue mechanism composed of the glutamine metabolic pathway, which is accompanied by glutamine and glutamate becoming carbon donors to D2HG (203). Interestingly, there has been a growing body of evidence that EGCG significantly suppresses GDH and IDH activity to reduce D2HG production in tumor cells (191, 203). However, we have to recognize that EGCG is a pleiotropic compound that may have some undiscovered effects besides GDH and IDH inhibition, for instance, whether EGCG can inhibit glutamine metabolic pathway through targeting GLS is currently unknown.

4.4 Fatty acid anabolism

Fatty acids, the carboxylic acids with long hydrocarbon chains, are the main components of cellular phospholipids, sphingolipids, glycolipids, and triglycerides, which are mainly obtained from *de novo* lipogenesis (DNL) pathway or directly taken from the extracellular. In the DNL pathway, citrates produced by the TCA cycle are successively catalyzed by ATP citrate lyase (ACLY), acetyl-CoA carboxylase (ACC), and fatty acid synthase (FASN) to produce primary fatty acids (205). They can participate in various metabolic pathways to synthesize more complex lipids, such as diacylglycerols and triacylglycerols, or to convert to phosphatidylglycerols, such as phosphatidylethanolamine and phosphatidylserine (205). Although their biosynthesis in cancer has received relatively little attention compared to aerobic glycolysis and glutaminolysis, it has been recognized in recent years as a significant metabolic aberration necessary for tumorigenesis (206). There is considerable evidence of increased DNL in tumor cells, which may be due to a response to the reduced availability of serum-derived lipids in TME (207). Scientific research supports that the phenotypic reprogramming of fatty acid metabolism is strongly correlated with tumorigenesis, progression, and metastasis and worsens clinical outcomes of tumor patients (208, 209). In addition, this metabolic reprogramming in TME may lead to functional alterations of infiltrated immune cells, thus affecting the efficacy of antitumor immunotherapy (210). Therefore, targeting the DNL pathway in tumors has become an emerging strategy for antitumor therapy and a focus for researchers.

ACC, a rate-limiting enzyme in the reprogrammed DNL pathway, catalyzes the transformation of acetyl-CoA into malonyl-CoA (205). It has been reported that EGCG inhibited ACC protein expression to decrease the DNL pathway and ATP production, thereby inducing lipogenesis depletion-associated apoptosis in colorectal cancer cells (211). Further, *in vivo* experiments found this inhibitory effect on the DNL pathway was closely related to the inhibition of Akt and ERK phosphorylation (211). A similar investigation also revealed EGCG suppressed ACC protein expression in hepatoma cells and proposed the potential mechanism of anti-DNL should be attributed to EGCG's suppression on the receptor tyrosine kinases (RTKs), which mediate PI3K/Akt/mTOR complex 1 (mTORC1)/sterol regulatory element-binding protein 1 (SREBP1) axis (212). Additionally, it has been found that AMPK, a cellular energy level sensor that is activated when ATP decreases and ADP or AMP increases in

cancer, mediated the dysregulation of ACC phosphorylation to subsequently inhibit ACC activity, thus attenuating the lipogenesis of hepatoma cells (213). Based on such a mechanism, an important study unveiled EGCG suppressed ACC activity through enhancing AMPK-mediated ACC phosphorylation, ultimately arresting the cell cycle or inducing apoptosis in human hepatoma cells (214).

FASN, another vital enzyme that regulates lipogenesis, is extremely low in expression and activity in almost all normal adult tissues but is dramatically overexpressed or activated in many cancer types, catalyzing the synthesis of acetyl-CoA and malonyl-CoA into long-chain fatty acids (205, 215). Over the past two decades, there has been considerable evidence supporting EGCG as an effective natural FASN inhibitor whose inhibitory effect is synchronized with the reduced endogenous lipid synthesis and the increased apoptosis (216, 217). According to previous studies, the primary cause for the inactivation of FASN may be determined by the irreversible reaction of EGCG with the β-ketoacyl reductase domain of FASN (217). Meanwhile, several researchers revealed EGCG attenuated EGF-induced FASN expression at protein and mRNA levels, suppressed Akt activation, and blocked the contact of transcription factor Sp-1 with its target gene in breast cancer cells, thus exerting its anti-proliferative pharmacological effects (218). Subsequently, these researchers extended their findings that EGCG attenuated EGFR 2 (HER2) or/and EGFR 3 (HER3)-induced FASN overexpression in breast cancer cells through suppressing PI3K/Akt signaling (219). HER2 overexpression and PI3K/Akt overactivation also determine increased sensitivity to FASN suppression-induced tumor cell death (215). Furthermore, the suppression of RTKs/PI3K/Akt/mTORC1/SREBP1 axis was also identified as a pathway by which EGCG downregulates FASN expression in hepatoma cells (212). Moreover, EGCG was found to inhibit mTOR signaling and downregulate FASN expression by stimulating AMPK expression in hepatoma cells (214). Taken together, it is not difficult to conclude that these findings support EGCG suppresses FASN expression through downregulating RTKs/PI3K/Akt/mTOR/FASN cascade signaling, thus disrupting DNL pathway in tumors (218, 220). Interestingly, a small sample-size randomized controlled study that examined the levels of FANS expression in prostate tissues of male patients undergoing prostate biopsy following oral EGCG capsule treatment showed that EGCG supplementation did not reduce FANS expression in the prostate (221). This may be due to the fact that short-term EGCG supplementation is insufficient to cause biologically significant changes in FASN levels in prostate tissues. Hence, extending follow-up time and increasing the homogenous patient population should be considered in future clinical trials.

Of note, EGCG's inhibitory effects on fatty acid oxidation may not be as strong as it is on the DNL pathway. Numerous investigations have indicated EGCG has a slight to no inhibitory effect on the activity of carnitine palmitoyltransferase (CPT)-I, a vital rate-limiting enzyme in fatty acid catabolism, in comparison to the large inhibitory effect it had on FASN (222–224). Nevertheless, EGCG does cause the buildup of malonyl-CoA, which inhibits CPT action via acting as a regulator of CPT activity (212). Overall, the available evidence suggested that EGCG inhibited the DNL pathway without parallel stimulation of fatty acid oxidation.

Considering the pertinent studies from recent years, we have found targeting FASN with EGCG is advantageous to ameliorate the efficacy of anti-cancer therapy. Since EGCG can sensitize nasopharyngeal cancer to radiotherapy through inhibiting FANS, it may be developed as a radiosensitizer (225). Additionally, blocking FASN with EGCG has been found to significantly ameliorate the efficacy of cetuximab and pertuzumab in drug-resistant breast cancer, suggesting EGCG may synergize the antitumor effects of anti-EGFR and anti-HER2 therapies (226, 227). Even, inhibiting FANS expression using EGCG has been shown to significantly accelerate the differentiation of acute myeloid leukemia and re-sensitize all-trans retinoic acid-refractory tumor cells (228). Together, these findings have confirmed the feasibility of EGCG in combination treatment regimens.

4.5 Nucleotide metabolism

Nucleotides are critical substrates for a variety of anabolic pathways, particularly DNA and RNA biosynthesis processes (229). Due to the rapid growth and anabolism, tumor cells rely extensively on nucleotide synthesis pathways in addition to their large energy requirements (230). Recent research has demonstrated that enhanced nucleotide metabolism in tumors is strongly associated with many malignant behaviors, such as uncontrolled proliferation, chemotherapy resistance, immune evasion, and metastasis (231, 232). Intervention or modification of the dysregulation of nucleotide metabolism can promote tumor immunogenicity and increase antitumor immune response through disrupting purine and pyrimidine pools to increase mutagenicity and genomic instability (233).

With the development of metabolomics detection techniques, EGCG has been found to target tumor nucleotide anabolism. Metabolomic analysis of human colon cancer cells demonstrated EGCG affected nucleotide metabolic pathways and reduced the levels of uridine, uridine diphosphate (UDP), and ADP in tumor cells (234). Metabolomics results of lung cancer cells confirmed EGCG treatment significantly impaired the levels of adenine, cytosine, and 2-deoxycytidine in tumor cells (235). Similarly, our ongoing scientific investigation has also observed the regulatory effects of EGCG on purine and pyrimidine metabolic pathways in gastric cancer cells. Nevertheless, up to now, the mechanism by which EGCG interferes with *de novo* nucleotide biosynthesis in tumor cells has remained unclear. Based on the relevant findings, we are currently inclined to believe EGCG may block nucleotide biosynthesis through reducing the required feedstocks, including pentoses and one-carbon units. As previously mentioned, EGCG, as a PGAM1 inhibitor in glycolysis, was found to increase substrate 3-phosphoglycerate levels and decrease product 2-phosphoglycerate levels in tumor cells, thereby inhibiting 6-phosphogluconate dehydrogenase (G6PD) and leading to impaired pentose phosphate pathway (PPP) (190, 236). As a result, tumor cells may lack sufficient pentoses for nucleotide biosynthesis. In addition, glycine and serine are vital sources of one-carbon pool, where activated folate is the essential carrier. On the one hand, EGCG was

found to increase the levels of glycine and serine in tumor cells, which might mean decreased consumption in their use for one-carbon unit production (235). On the other hand, EGCG was shown to effectively attenuate the activity of dihydrofolate reductase (DHFR) and disrupt the folate cycle, thereby diminishing the cellular production of nucleotides by damaging the one-carbon pool (237, 238). Collectively, the available evidence supports the inhibitory role of EGCG in nucleotide anabolism, which lays the foundation for the subsequent blockage of cancerous DNA and RNA synthesis.

The uninterrupted synthesis of DNA and RNA utilizing nucleotides is the most prominent proliferative property of tumor cells. In the past two decades, there has been ample evidence to confirm the direct intervention of EGCG and catechin derivatives on DNA and RNA synthases (239–241). One study revealed EGCG selectively suppressed mammalian DNA polymerase activity but it did not significantly suppress the comparable enzymes in plants and prokaryotes (242). This inhibition was observed to be competitive for the DNA template but non-competitive for the deoxyribonucleoside triphosphate (dNTP) substrate (243). However, a recent study has unveiled EGCG severely disequilibrates dNTPs in tumor cells, thus inhibiting DNA *de novo* synthesis and cell proliferation, which makes it difficult to resist the suggestion that EGCG may act as a ribonucleotide reductase inhibitor in tumor cells (244). Additionally, EGCG was reported to suppress RNA polymerase transcription from both exterior and internal promoters of genes and inhibit the protein expression and promoter activity of TFIIIB required for accurate RNA polymerase initiation in cervical cancer cells (240). Even more incredibly, it's discovered that EGCG molecules bound to the double-stranded AG : CT oligomers of multiple nucleotide lengths, thus protecting the double-stranded DNA from being melted into single-stranded DNA, which subsequently leads to DNA replication disorders (245). These results fully confirmed EGCG can not only inhibit the anabolism of nucleotides but also prevent the synthetic transformation of nucleotides into nucleic acids.

Although we have concluded that EGCG regulates so many biological metabolic processes in tumors, whether there are other metabolic pathways controlled by EGCG remains unclear. Hence, abundant investigations are required to verify its regulatory effects and biological mechanisms on gluconeogenesis, mitochondria oxidative phosphorylation, glycogen metabolism, branched-chain amino acid metabolism, triglyceride metabolism, phospholipid metabolism, and cholesterol metabolism in tumors. In addition, its suppressive mechanism in PPP remains to be further revised and elaborated according to the results reported in the future literature. Corresponding *in vivo* animal experiments or organoid model experiments should also be implemented to systematically analyze EGCG's effects on tumor metabolites and metabolic pathways.

5 Potential in anti-cancer immunotherapy

Immunotherapy, a biomedical milestone in cancer, has epoch-making significance. Several immunotherapies, such as immune checkpoint blockers, tumor vaccines, adoptive immunotherapies, and nanomedicine immunotherapies, have achieved durable antitumor responses, but their overall efficacy has been unsatisfactory (246). We summarized the application status and therapeutic effects of EGCG in the above immunotherapies, aiming to arouse its attention in immunotherapy, so as to achieve better clinical outcomes for cancer patients who undergo immunotherapy.

5.1 Anti-immune checkpoints

It's well recognized that immune checkpoints including programmed death-1 (PD-1), PD-L1, and cytotoxic T lymphocyte antigen-4 (CTLA4) are mainly in charge of the immune escape of tumor cells under immune surveillance. The emergence of immune checkpoint inhibitors (ICIs) has revolutionized the treatment landscape for cancer, but only subset of patients can benefit from their immunotherapy (247). Therefore, innovative approaches are urgently needed to guide the development of novel immunotherapy combinations designed to maximize clinical benefits and survival outcomes.

Recent research has indicated that EGCG can play an antitumor immunological role by targeting PD-L1 molecule (248). Evidence suggested that unlike anti-immune checkpoint therapy, which simply obstructs PD-1/PD-L1 interactions, EGCG suppressed JAK/STAT signaling and downstream PD-L1 expression in melanoma cells, thereby reactivating CTLs to inhibit tumor cell growth (29). Further animal experiments revealed EGCG's tumor inhibition was comparable to anti-PD-1 treatment. Another study indicated EGCG downregulated IFN-γ and EGF-induced PD-L1 expression in non-small cell lung cancer cells through suppressing JAK2/STAT1 and EGFR/Akt signaling pathways and boosted IL-2 expression in cancer-specific T lymphocytes (249). Additionally, due to EGCG's "sealing effect" on multiple protein molecules, it may directly target the PD-L1 protein, thus disrupting the interaction between PD-1 and PD-L1. This possibility has been confirmed by molecular dynamics simulations in recent years. Relevant investigation revealed EGCG interacted directly and stably with the binding domain of PD-L1 dimer, in which non-polar interactions with pivotal residues played leading roles in their interactive binding (250). These findings suggest that EGCG may make ICIs more therapeutically effective and even may serve as an alternative approach to disrupt the PD-1/PD-L1 axis. Hence, EGCG in combination with ICIs seems viable as a novel therapeutic option. However, corresponding clinical studies are still needed to validate the abovementioned preclinical results. It is imperative to conduct large-sample and high-quality clinical trials to investigate the clinical benefits of EGCG in immunotherapy.

Of note, PD-1 and CTLA4 are mainly expressed on the T lymphocyte surface to put the brakes on the immune response. Based on the existing literature, it is unclear whether EGCG can inhibit the expressed levels of PD-1 and CTLA4 or interfere with their activities. However, other polyphenols may provide some reference for this role. For example, the natural polyphenol compound resveratrol was found to reduce the mRNA levels of PD-1 in pulmonary $CD8^+$ T and $CD4^+$ T cells, thus attenuating the lung metastasis of TNBC (251). Besides, the natural polyphenol

curcumin has been revealed to reduce CTLA4 expression in Tregs, thereby inhibiting the immunosuppressive capacity of these Tregs (252). Given this, we highly expect EGCG to be endowed with similar anti-PD-1 and anti-CTLA-4 activities, and we believe that future studies will bear witness.

5.2 Nanomedicine-based immunotherapy

Currently, nanomedicine-based immunotherapy, a subdiscipline of immunology, is undergoing rapid development as the medium for researching innovative therapeutic strategies (253). With the great advancements of nanomedicine in immunotherapy, EGCG-containing nanoassemblies to ameliorate the efficacy of tumor immunotherapy have attracted wide attention. It was reported that a phenolic-based tumor-permeated nano-framework composed of EGCG and phenylboronic acid-modified platinum nanoparticles could not only downregulate PD-L1 expression but effectively promote the maturation of DCs and facilitate the infiltration of CTLs, thus amplifying immunotherapy outcomes and generating a powerful antitumor immune response in terms of the suppression of primary tumor and metastasis (254). An EGCG-delivery responsive penetrating nanogels based on a nano-sized controlled releasing system of the soluble cyclodextrin-drug inclusion complex was also found to decrease the PD-L1 expression in tumor cells, promote DC maturation, stimulate CTL infiltration and activation, and attenuate the suppression effects from Tregs, thereby switching "cold" tumor to "hot" tumor (255). Interestingly, a new delivery nanosystem of fluorinated-coordinative-EGCG was measured not only to substantially suppress PD-L1 expression but also to achieve perfect siPD-L1 delivery and improve siPD-L1 accumulation in tumor cells, thus providing a versatile vehicle for antitumor immunotherapy (256). Meanwhile, an MMP-2 activated nanoparticle carrying EGCG dimer and immune checkpoint B7-H3 (CD276) bispecific antibodies was reported to induce the elimination of glioblastoma through increasing the ferroptosis and strengthening the immune checkpoint blockade treatment (257). In addition, based on EGCG and ursolic acid, several scholars constructed a novel "core-shell" co-assembly carrier-free nanosystem that synergized immunotherapy of liver cancer through activating innate and acquired immunity (258). In conclusion, these EGCG-based nanoassemblies play pivotal roles in anti-immune checkpoint immunotherapy and enhanced antitumor immunological response. Nevertheless, the potential toxicity and internal metabolic pathways of these nanosystems remain unclear. Hence, some caution should be maintained regarding the safety of these nanomedicines, even if their immunotherapeutic effects are undeniable. Also, comparative studies on the immunological efficacy of different EGCG nanoassemblies remain not available, suggesting that nanosystem-based cancer immunotherapy is still a long way off.

5.3 Tumor vaccines

In fact, ICIs are often only effective in limited populations due to poor immunogenicity and inadequate infiltration or accumulation of CTLs in TME (259). How to break through the limitations of cancer immunotherapy is an urgent problem and challenge that modern medicine is facing. Clinical practice has demonstrated tumor vaccines can enhance the activation and proliferation of immune effector cells, so tumor vaccines are recognized as the next immunotherapy frontier (260, 261). There was increasing evidence that combined treatment with immunomodulatory doses of EGCG could enhance the immune response of specific $CD8^+$ T lymphocytes and $CD4^+$ Th1 lymphocytes induced by DNA vaccine, and provide long-term anti-cancer protection for treated mice, causing a more excellent cure rate compared to monotherapy (30, 262). Additionally, EGCG was confirmed to enhance antigen-specific immunotherapy efficacy of mesothelin-specific chimeric DNA vaccine by boosting the maturation of DCs, which is promising to offer an effective approach for immunotherapy in malignant mesothelioma, ovarian cancer, and pancreatic cancer (55). Recently, some researchers have prepared coordination microparticle vaccines utilizing EGCG and aluminum ions as ligands to wrap single tumor cells, which can be effectively internalized by DCs through endocytosis, thus improving the efficiency of immunological uptake (263). Further investigation found these microparticles coated with tumor cells effectively activated DCs and significantly increased Th1-related cytokine production, with immunotherapeutic effects comparable to those of polyinosinic-polycytidylic acid (PolyI:C) (264). This encapsulation strategy holds promise for personalized immunotherapy customized to individual patient's cancer cells. Overall, EGCG, as an immunomodulator or an inhibitor of immune checkpoints, combined with tumor vaccines may be a valuable immunotherapy for tumor control.

5.4 Adoptive immunotherapy

Adoptive immunotherapy refers to the extraction, modification, and re-infusion of autologous or allogenic immune cells for therapeutic purposes (265). Antitumor immunotherapy with chimeric antigen receptor-modified T (CAR-T) cells has made tremendous progress and shown exhilarative clinical efficacy against hematological malignancies (266). Currently, the U.S. Food and Drug Administration has authorized five CAR-T immunotherapies for hematologic malignancies, however, the applicability of these immunotherapies in the field of solid tumors has lagged significantly (267, 268). Some of the major obstacles in solid tumors include inefficient CAR-T cell migration and infiltration, immunosuppressive TME, CAR-T cell manufacturing, lack of tumor-specific antigens, treatment-related toxicity, and antigen escape (267).

Since EGCG is able to improve the infiltration and CTL response and disrupt the inhibitory TME induced by immunosuppressive cells, it is ideally suited for adoptive immunotherapy in solid tumors. Several researchers prepared adoptive $CD8^+$ T cells conjugated with immunotherapeutic liposomal drugs, containing EGCG, poly lysine, and the TLR9 agonist CpG (269). The results of the study found that this adoptive immunotherapy reduced the frequencies of MDSCs, Tregs, and M2 macrophages and elevated the proportion of CTLs in tumor-infiltrating lymphocytes, thus significantly improving the

therapeutic efficacy in melanoma (269). Although the original intention of the investigators is that the inclusion of EGCG may facilitate the encapsulation efficiency and improve the stability of CpG, we consider its undeniable direct immunoregulatory roles in their CAR-T immunotherapy. Therefore, we recommend that immunotherapy studies combining CAR-T cells with EGCG be conducted as soon as possible to clarify its detailed effects in adoptive immunotherapy. In short, EGCG, as a potentially valuable companion to CAR-T immunotherapy, has a unique clinical application prospect that is expected to be translated into a treatment for solid tumors in the next few years.

6 Clinical application and limitation

Recently, ample preclinical observational studies have demonstrated green tea consumption is effective in reducing the risk of oral, prostate, breast, liver, gastric, and colorectal cancers to varying degrees (270–272). These results provide a theoretical basis for further clinical trials. A Phase II interventional clinical trial confirmed orally administered 800 mg or 1200 mg of EGCG once a day can dose-dependently downregulate the levels of oncology biomarkers, including proliferating cell nuclear antigen and clusterin, in patients' bladder cancer tissues (273). Similarly, a daily intake of 400 mg of EGCG was also effective in diminishing serum prostate-specific antigen levels in men with precancerous prostate lesions (274). In addition, randomized controlled trials have unveiled EGCG can alleviate the formation of colorectal adenoma to some extent and remarkably attenuate NF-κB levels in colorectal tumor tissues (275, 276). Moreover, a clinical trial has revealed EGCG can reduce the percentage of mammographic density, a well-recognized predictor of breast cancer risk, in young women (277). Relevant evidence from a presurgical clinical study also supports a notable positive correlation between EGCG's plasma levels and Ki-67 downregulation in breast tumor tissues (278). Overall, the above clinical studies have confirmed the biological potential of EGCG in antitumor therapy, which lays an important foundation for its further clinical application. Nevertheless, since these studies often lack further follow-up, it's unclear whether EGCG treatment can ameliorate the therapeutic prognosis and clinical survival of tumor patients. More regrettably, there are still no clinical studies reported on EGCG combined with chemoradiotherapy and immunotherapy based on existing literature and clinical trial database.

Although abundant preclinical and clinical studies have confirmed the therapeutic potential of EGCG on tumors, it is undeniable that the oral bioavailability of EGCG is relatively low, which is an important stumbling block limiting its further clinical application (23). The possible reasons are that EGCG is mainly absorbed by passive diffusion, is prone to instability in alkaline intestinal fluid, and may be subject to catabolism by intestinal microorganisms, which may significantly affect its bioavailability (16, 17). Therefore, the development of liposomal encapsulation or nanomodification is conducive to ameliorating its stability and biological availability and achieving clinical efficacy beyond expectations. Additionally, other non-oral administration routes, such as intravenous and intramuscular injections, should also be refined in subsequent animal experiments and clinical studies for safety assessment and optimal dose selection. Notably, under the premise of low bioavailability, clinicians and researchers should be fully vigilant about its hepatotoxicity caused by the use of large doses while pursuing the improvement of therapeutic efficacy (279).

7 Conclusion

In conclusion, EGCG can boost the anti-cancer potential of cytotoxic effector cells and disrupt the functions of immunosuppressive cells and tumor-promoting cells, thus reactivating the antitumor immune response in TME. In addition, EGCG can target multiple upregulated metabolic reprogramming pathways, including glucose uptake, aerobic glycolysis, glutamine metabolism, fatty acid anabolism, and nucleotide synthesis. Moreover, EGCG, as an immunomodulator and immune checkpoint blockade, can enhance the efficacy of antitumor immunotherapy and may be a viable option for immunotherapy. Briefly, EGCG plays versatile regulatory roles in TME and metabolic reprogramming, which provides novel insights and combined therapeutic strategies for anti-cancer immunotherapy.

Author contributions

DL: Conceptualization, Data curation, Visualization, Writing – original draft. DC: Conceptualization, Funding acquisition, Writing – review & editing. YS: Data curation, Visualization, Writing – review & editing. YC: Data curation, Visualization, Writing – review & editing. YZ: Writing – review & editing. JJ: Writing – review & editing. XC: Conceptualization, Funding acquisition, Writing – review & editing, Project administration.

Funding

The author(s) declare financial support was received for the research, authorship, and/or publication of this article. This work was supported by grants from National Natural Science Foundation of China (82002932), Jilin Province Department of Finance (JLSWSRCZX2021-073), and Scientific and Technological Development program of Jilin Province (20210101333JC).

Acknowledgments

All figures in this article were drawn utilizing the Figdraw tool. We appreciate the graphic technical support provided by Figdraw.

Conflict of interest

The authors declare that the research was conducted in the absence of any commercial or financial relationships that could be construed as a potential conflict of interest.

Publisher's note

References

1. Cao W, Chen HD, Yu YW, Li N, Chen WQ. Changing profiles of cancer burden worldwide and in China: a secondary analysis of the global cancer statistics 2020. *Chin Med J (Engl)* (2021) 134(7):783–91. doi: 10.1097/cm9.0000000000001474

2. Ferlay J, Colombet M, Soerjomataram I, Parkin DM, Piñeros M, Znaor A, et al. Cancer statistics for the year 2020: An overview. *Int J Cancer* (2021) 149:778–89. doi: 10.1002/ijc.33588

3. Sung H, Ferlay J, Siegel RL, Laversanne M, Soerjomataram I, Jemal A, et al. Global cancer statistics 2020: GLOBOCAN estimates of incidence and mortality worldwide for 36 cancers in 185 countries. *CA Cancer J Clin* (2021) 71(3):209–49. doi: 10.3322/caac.21660

4. Arneth B. Tumor microenvironment. *Medicina (Kaunas)* (2019) 56(1):15. doi: 10.3390/medicina56010015

5. Xiao Y, Yu D. Tumor microenvironment as a therapeutic target in cancer. *Pharmacol Ther* (2021) 221:107753. doi: 10.1016/j.pharmthera.2020.107753

6. de Visser KE, Joyce JA. The evolving tumor microenvironment: From cancer initiation to metastatic outgrowth. *Cancer Cell* (2023) 41(3):374–403. doi: 10.1016/j.ccell.2023.02.016

7. Raggi C, Taddei ML, Rae C, Braconi C, Marra F. Metabolic reprogramming in cholangiocarcinoma. *J Hepatol* (2022) 77(3):849–64. doi: 10.1016/j.jhep.2022.04.038

8. Dey P, Kimmelman AC, DePinho RA. Metabolic codependencies in the tumor microenvironment. *Cancer Discovery* (2021) 11(5):1067–81. doi: 10.1158/2159-8290.Cd-20-1211

9. Bader JE, Voss K, Rathmell JC. Targeting metabolism to improve the tumor microenvironment for cancer immunotherapy. *Mol Cell* (2020) 78(6):1019–33. doi: 10.1016/j.molcel.2020.05.034

10. Pitt JM, Marabelle A, Eggermont A, Soria JC, Kroemer G, Zitvogel L. Targeting the tumor microenvironment: removing obstruction to anticancer immune responses and immunotherapy. *Ann Oncol* (2016) 27(8):1482–92. doi: 10.1093/annonc/mdw168

11. Zhao L, Liu Y, Zhang S, Wei L, Cheng H, Wang J, et al. Impacts and mechanisms of metabolic reprogramming of tumor microenvironment for immunotherapy in gastric cancer. *Cell Death Dis* (2022) 13(4):378. doi: 10.1038/s41419-022-04821-w

12. Catalano M, Iannone LF, Nesi G, Nobili S, Mini E, Roviello G. Immunotherapy-related biomarkers: Confirmations and uncertainties. *Crit Rev Oncol Hematol* (2023) 192:104135. doi: 10.1016/j.critrevonc.2023.104135

13. Khan N, Mukhtar H. Tea polyphenols in promotion of human health. *Nutrients* (2018) 11(1):39. doi: 10.3390/nu11010039

14. Kochman J, Jakubczyk K, Antoniewicz J, Mruk H, Janda K. Health benefits and chemical composition of matcha green tea: a review. *Molecules* (2020) 26(1):85. doi: 10.3390/molecules26010085

15. Tang GY, Meng X, Gan RY, Zhao CN, Liu Q, Feng YB, et al. Health functions and related molecular mechanisms of tea components: an update review. *Int J Mol Sci* (2019) 20(24):6196. doi: 10.3390/ijms20246196

16. Li D, Cao D, Cui Y, Sun Y, Jiang J, Cao X. The potential of epigallocatechin gallate in the chemoprevention and therapy of hepatocellular carcinoma. *Front Pharmacol* (2023) 14:1201085. doi: 10.3389/fphar.2023.1201085

17. Gan RY, Li HB, Sui ZQ, Corke H. Absorption, metabolism, anti-cancer effect and molecular targets of epigallocatechin gallate (EGCG): An updated review. *Crit Rev Food Sci Nutr* (2018) 58(6):924–41. doi: 10.1080/10408398.2016.1231168

18. Negri A, Naponelli V, Rizzi F, Bettuzzi S. Molecular targets of epigallocatechin-gallate (EGCG): a special focus on signal transduction and cancer. *Nutrients* (2018) 10 (12):1936. doi: 10.3390/nu10121936

19. Romano A, Martel F. The role of EGCG in breast cancer prevention and therapy. *Mini Rev Med Chem* (2021) 21(7):883–98. doi: 10.2174/1389557520999201211194445

20. Alam M, Ali S, Ashraf GM, Bilgrami AL, Yadav DK, Hassan MI. Epigallocatechin 3-gallate: From green tea to cancer therapeutics. *Food Chem* (2022) 379:132135. doi: 10.1016/j.foodchem.2022.132135

21. Ferrari E, Bettuzzi S, Naponelli V. The potential of epigallocatechin gallate (EGCG) in targeting autophagy for cancer treatment: a narrative review. *Int J Mol Sci* (2022) 23(11):6075. doi: 10.3390/ijms23116075

22. Li F, Qasim S, Li D, Dou QP. Updated review on green tea polyphenol epigallocatechin-3-gallate as a cancer epigenetic regulator. *Semin Cancer Biol* (2022) 83:335–52. doi: 10.1016/j.semcancer.2020.11.018

23. Wang L, Li P, Feng K. EGCG adjuvant chemotherapy: Current status and future perspectives. *Eur J Med Chem* (2023) 250:115197. doi: 10.1016/j.ejmech.2023.115197

24. Moody R, Wilson K, Jaworowski A, Plebanski M. Natural compounds with potential to modulate cancer therapies and self-reactive immune cells. *Cancers (Basel)* (2020) 12(3):673. doi: 10.3390/cancers12030673

25. Raskov H, Orhan A, Christensen JP, Gögenur I. Cytotoxic CD8(+) T cells in cancer and cancer immunotherapy. *Br J Cancer* (2021) 124(2):359–67. doi: 10.1038/s41416-020-01048-4

26. Farhood B, Najafi M, Mortezaee K. CD8(+) cytotoxic T lymphocytes in cancer immunotherapy: a review. *J Cell Physiol* (2019) 234(6):8509–21. doi: 10.1002/jcp.27782

27. Borst J, Ahrends T, Bąbała N, Melief CJM, Kastenmüller W. CD4(+) T cell help in cancer immunology and immunotherapy. *Nat Rev Immunol* (2018) 18(10):635–47. doi: 10.1038/s41577-018-0044-0

28. Oh DY, Fong L. Cytotoxic CD4(+) T cells in cancer: Expanding the immune effector toolbox. *Immunity* (2021) 54(12):2701–11. doi: 10.1016/j.immuni.2021.11.015

29. Ravindran Menon D, Li Y, Yamauchi T, Osborne DG, Vaddi PK, Wempe MF, et al. EGCG inhibits tumor growth in melanoma by targeting JAK-STAT signaling and its downstream PD-L1/PD-L2-PD1 axis in tumors and enhancing cytotoxic T-cell responses. *Pharm (Basel)* (2021) 14(11):1081. doi: 10.3390/ph14111081

30. Kang TH, Lee JH, Song CK, Han HD, Shin BC, Pai SI, et al. Epigallocatechin-3-gallate enhances CD8+ T cell-mediated antitumor immunity induced by DNA vaccination. *Cancer Res* (2007) 67(2):802–11. doi: 10.1158/0008-5472.Can-06-2638

31. Katiyar S, Elmets CA, Katiyar SK. Green tea and skin cancer: photoimmunology, angiogenesis and DNA repair. *J Nutr Biochem* (2007) 18(5):287–96. doi: 10.1016/j.jnutbio.2006.08.004

32. Huang AC, Cheng HY, Lin TS, Chen WH, Lin JH, Lin JJ, et al. Epigallocatechin gallate (EGCG), influences a murine WEHI-3 leukemia model *in vivo* through enhancing phagocytosis of macrophages and populations of T- and B-cells. *In Vivo* (2013) 27(5):627–34.

33. Schwager J, Seifert N, Bompard A, Raederstorff D, Bendik I. Resveratrol, EGCG and vitamins modulate activated T lymphocytes. *Molecules* (2021) 26(18):5600. doi: 10.3390/molecules26185600

34. Kim YH, Won YS, Yang X, Kumazoe M, Yamashita S, Hara A, et al. Green tea catechin metabolites exert immunoregulatory effects on CD4(+) T cell and natural killer cell activities. *J Agric Food Chem* (2016) 64(18):3591–7. doi: 10.1021/acs.jafc.6b01115

35. Cheng CW, Shieh PC, Lin YC, Chen YJ, Lin YH, Kuo DH, et al. Indoleamine 2,3-dioxygenase, an immunomodulatory protein, is suppressed by (-)-epigallocatechin-3-gallate via blocking of gamma-interferon-induced JAK-PKC-delta-STAT1 signaling in human oral cancer cells. *J Agric Food Chem* (2010) 58(2):887–94. doi: 10.1021/jf903377e

36. Zhai L, Bell A, Ladomersky E, Lauing KL, Bollu L, Sosman JA, et al. Immunosuppressive IDO in cancer: mechanisms of action, animal models, and targeting strategies. *Front Immunol* (2020) 11:1185. doi: 10.3389/fimmu.2020.01185

37. Peng X, Zhao Z, Liu L, Bai L, Tong R, Yang H, et al. Targeting indoleamine dioxygenase and tryptophan dioxygenase in cancer immunotherapy: clinical progress and challenges. *Drug Des Devel Ther* (2022) 16:2639–57. doi: 10.2147/dddt.S373780

38. Jeong YI, Jung ID, Lee JS, Lee CM, Lee JD, Park YM. (-)-Epigallocatechin gallate suppresses indoleamine 2,3-dioxygenase expression in murine dendritic cells: evidences for the COX-2 and STAT1 as potential targets. *Biochem Biophys Res Commun* (2007) 354(4):1004–9. doi: 10.1016/j.bbrc.2007.01.076

39. Santilli G, Piotrowska I, Cantilena S, Chayka O, D'Alicarnasso M, Morgenstern DA, et al. Polyphenon [corrected] E enhances the antitumor immune response in neuroblastoma by inactivating myeloid suppressor cells. *Clin Cancer Res* (2013) 19 (5):1116–25. doi: 10.1158/1078-0432.Ccr-12-2528

40. Xu P, Yan F, Zhao Y, Chen X, Sun S, Wang Y, et al. Green tea polyphenol EGCG attenuates MDSCs-mediated immunosuppression through canonical and non-canonical pathways in a 4T1 murine breast cancer model. *Nutrients* (2020) 12 (4):1042. doi: 10.3390/nu12041042

41. Mandal D, Lahiry L, Bhattacharyya A, Chattopadhyay S, Siddiqi M, Sa G, et al. Black tea protects thymocytes in tumor-bearing animals by differential regulation of intracellular ROS in tumor cells and thymocytes. *J Environ Pathol Toxicol Oncol* (2005) 24(2):91–104. doi: 10.1615/jenvpathtoxoncol.v24.i2.30

42. Mandal D, Lahiry L, Bhattacharyya A, Bhattacharyya S, Sa G, Das T. Tumor-induced thymic involution via inhibition of IL-7R alpha and its JAK-STAT signaling pathway: protection by black tea. *Int Immunopharmacol* (2006) 6(3):433–44. doi: 10.1016/j.intimp.2005.09.005

43. Wu SY, Fu T, Jiang YZ, Shao ZM. Natural killer cells in cancer biology and therapy. *Mol Cancer* (2020) 19(1):120. doi: 10.1186/s12943-020-01238-x

44. Liu S, Galat V, Galat Y, Lee YKA, Wainwright D, Wu J. NK cell-based cancer immunotherapy: from basic biology to clinical development. *J Hematol Oncol* (2021) 14 (1):7. doi: 10.1186/s13045-020-01014-w

45. Myers JA, Miller JS. Exploring the NK cell platform for cancer immunotherapy. *Nat Rev Clin Oncol* (2021) 18(2):85–100. doi: 10.1038/s41571-020-0426-7

46. Handgretinger R, Lang P, André MC. Exploitation of natural killer cells for the treatment of acute leukemia. *Blood* (2016) 127(26):3341–9. doi: 10.1182/blood-2015-12-629055

47. Pan P, Huang YW, Oshima K, Yearsley M, Zhang J, Arnold M, et al. The immunomodulatory potential of natural compounds in tumor-bearing mice and humans. *Crit Rev Food Sci Nutr* (2019) 59(6):992–1007. doi: 10.1080/10408398.2018.1537237

48. Kuo CL, Chen TS, Liou SY, Hsieh CC. Immunomodulatory effects of EGCG fraction of green tea extract in innate and adaptive immunity via T regulatory cells in murine model. *Immunopharmacol Immunotoxicol* (2014) 36(5):364–70. doi: 10.3109/08923973.2014.953637

49. Hsieh DS, Wang H, Tan SW, Huang YH, Tsai CY, Yeh MK, et al. The treatment of bladder cancer in a mouse model by epigallocatechin-3-gallate-gold nanoparticles. *Biomaterials* (2011) 32(30):7633–40. doi: 10.1016/j.biomaterials.2011.06.073

50. Gardner A, de Mingo Pulido Á, Ruffell B. Dendritic cells and their role in immunotherapy. *Front Immunol* (2020) 11:924. doi: 10.3389/fimmu.2020.00924

51. Santos PM, Butterfield LH. Dendritic cell-based cancer vaccines. *J Immunol* (2018) 200(2):443–9. doi: 10.4049/jimmunol.1701024

52. Perez CR, De Palma M. Engineering dendritic cell vaccines to improve cancer immunotherapy. *Nat Commun* (2019) 10(1):5408. doi: 10.1038/s41467-019-13368-y

53. Jin SL, Zhou BR, Luo D. Protective effect of epigallocatechin gallate on the immune function of dendritic cells after ultraviolet B irradiation. *J Cosmet Dermatol* (2009) 8(3):174–80. doi: 10.1111/j.1473-2165.2009.00443.x

54. Katiyar SK, Mukhtar H. Green tea polyphenol (-)-epigallocatechin-3-gallate treatment to mouse skin prevents UVB-induced infiltration of leukocytes, depletion of antigen-presenting cells, and oxidative stress. *J Leukoc Biol* (2001) 69(5):719–26.

55. Chen YL, Chang MC, Chiang YC, Lin HW, Sun NY, Chen CA, et al. Immunomodulators enhance antigen-specific immunity and anti-tumor effects of mesothelin-specific chimeric DNA vaccine through promoting DC maturation. *Cancer Lett* (2018) 425:152–63. doi: 10.1016/j.canlet.2018.03.032

56. Tcyganov E, Mastio J, Chen E, Gabrilovich DI. Plasticity of myeloid-derived suppressor cells in cancer. *Curr Opin Immunol* (2018) 51:76–82. doi: 10.1016/j.coi.2018.03.009

57. Veglia F, Sanseviero E, Gabrilovich DI. Myeloid-derived suppressor cells in the era of increasing myeloid cell diversity. *Nat Rev Immunol* (2021) 21(8):485–98. doi: 10.1038/s41577-020-00490-y

58. Bronte V, Zanovello P. Regulation of immune responses by L-arginine metabolism. *Nat Rev Immunol* (2005) 5(8):641–54. doi: 10.1038/nri1668

59. Ohl K, Tenbrock K. Reactive oxygen species as regulators of MDSC-mediated immune suppression. *Front Immunol* (2018) 9:2499. doi: 10.3389/fimmu.2018.02499

60. Wu Y, Yi M, Niu M, Mei Q, Wu K. Myeloid-derived suppressor cells: an emerging target for anticancer immunotherapy. *Mol Cancer* (2022) 21(1):184. doi: 10.1186/s12943-022-01657-y

61. Grzywa TM, Sosnowska A, Matryba P, Rydzynska Z, Jasinski M, Nowis D, et al. Myeloid cell-derived arginase in cancer immune response. *Front Immunol* (2020) 11:938. doi: 10.3389/fimmu.2020.00938

62. Xue Q, Yan Y, Zhang R, Xiong H. Regulation of iNOS on immune cells and its role in diseases. *Int J Mol Sci* (2018) 19(12):3805. doi: 10.3390/ijms19123805

63. Szefel J, Danielak A, Kruszewski WJ. Metabolic pathways of L-arginine and therapeutic consequences in tumors. *Adv Med Sci* (2019) 64(1):104–10. doi: 10.1016/j.advms.2018.08.018

64. Santilli G, Anderson J, Thrasher AJ, Sala A. Catechins and antitumor immunity: Not MDSC's cup of tea. *Oncoimmunology* (2013) 2(6):e24443. doi: 10.4161/onci.24443

65. Lee JK, Won C, Yi EH, Seok SH, Kim MH, Kim SJ, et al. Signal transducer and activator of transcription 3 (Stat3) contributes to T-cell homeostasis by regulating pro-survival Bcl-2 family genes. *Immunology* (2013) 140(3):288–300. doi: 10.1111/imm.12133

66. Vasquez-Dunddel D, Pan F, Zeng Q, Gorbounov M, Albesiano E, Fu J, et al. STAT3 regulates arginase-I in myeloid-derived suppressor cells from cancer patients. *J Clin Invest* (2013) 123(4):1580–9. doi: 10.1172/jci60083

67. Corzo CA, Cotter MJ, Cheng P, Cheng F, Kusmartsev S, Sotomayor E, et al. Mechanism regulating reactive oxygen species in tumor-induced myeloid-derived suppressor cells. *J Immunol* (2009) 182(9):5693–701. doi: 10.4049/jimmunol.0900092

68. Sanchez-Pino MD, Dean MJ, Ochoa AC. Myeloid-derived suppressor cells (MDSC): When good intentions go awry. *Cell Immunol* (2021) 362:104302. doi: 10.1016/j.cellimm.2021.104302

69. Wang Y, Ren X, Deng C, Yang L, Yan E, Guo T, et al. Mechanism of the inhibition of the STAT3 signaling pathway by EGCG. *Oncol Rep* (2013) 30(6):2691–6. doi: 10.3892/or.2013.2743

70. Suhail M, Rehan M, Tarique M, Tabrez S, Husain A, Zughaibi TA. Targeting a transcription factor NF-κB by green tea catechins using *in silico* and *in vitro* studies in pancreatic cancer. *Front Nutr* (2022) 9:1078642. doi: 10.3389/fnut.2022.1078642

71. Orentas RJ. Reading the tea leaves of tumor-mediated immunosuppression. *Clin Cancer Res* (2013) 19(5):955–7. doi: 10.1158/1078-0432.Ccr-12-3792

72. Tie Y, Tang F, Wei YQ, Wei XW. Immunosuppressive cells in cancer: mechanisms and potential therapeutic targets. *J Hematol Oncol* (2022) 15(1):61. doi: 10.1186/s13045-022-01282-8

73. Malla RR, Vasudevaraju P, Vempati RK, Rakshmitha M, Merchant N, Nagaraju GP. Regulatory T cells: Their role in triple-negative breast cancer progression and metastasis. *Cancer* (2022) 128(6):1171–83. doi: 10.1002/cncr.34084

74. Wang J, Gong R, Zhao C, Lei K, Sun X, Ren H. Human FOXP3 and tumour microenvironment. *Immunology* (2023) 168(2):248–55. doi: 10.1111/imm.13520

75. Scott EN, Gocher AM, Workman CJ, Vignali DAA. Regulatory T cells: barriers of immune infiltration into the tumor microenvironment. *Front Immunol* (2021) 12:702726. doi: 10.3389/fimmu.2021.702726

76. D'Arena G, Simeon V, De Martino L, Statuto T, D'Auria F, Volpe S, et al. Regulatory T-cell modulation by green tea in chronic lymphocytic leukemia. *Int J Immunopathol Pharmacol* (2013) 26(1):117–25. doi: 10.1177/039463201302600111

77. Calgarotto AK, Longhini AL, Pericole de Souza FV, Duarte ASS, Ferro KP, Santos I, et al. Immunomodulatory effect of green tea treatment in combination with low-dose chemotherapy in elderly acute myeloid leukemia patients with myelodysplasia-related changes. *Integr Cancer Ther* (2021) 20:15347354211002647. doi: 10.1177/15347354211002647

78. Lyu C, Wang L, Stadlbauer B, Noessner E, Buchner A, Pohla H. Identification of EZH2 as cancer stem cell marker in clear cell renal cell carcinoma and the anti-tumor effect of epigallocatechin-3-gallate (EGCG). *Cancers (Basel)* (2022) 14(17):4200. doi: 10.3390/cancers14174200

79. Jannatun N, Zhang YQ, Wu B, Song QL, Cao GL, Luo WH, et al. Tea polyphenol coordinated with nanoparticles of ZIF-8 and coated with polydopamine and PEG for immuno-oncotherapy. *ACS Appl Nano Materials* (2023) 6(6):4379–89. doi: 10.1021/acsanm.2c05472

80. Farooqi AA, Pinheiro M, Granja A, Farabegoli F, Reis S, Attar R, et al. EGCG mediated targeting of deregulated signaling pathways and non-coding RNAs in different cancers: focus on JAK/STAT, wnt/β-catenin, TGF/SMAD, NOTCH, SHH/GLI, and TRAIL mediated signaling pathways. *Cancers (Basel)* (2020) 12(4):951. doi: 10.3390/cancers12040951

81. MaruYama T, Kobayashi S, Nakatsukasa H, Moritoki Y, Taguchi D, Sunagawa Y, et al. The curcumin analog GO-Y030 controls the generation and stability of regulatory T cells. *Front Immunol* (2021) 12:687669. doi: 10.3389/fimmu.2021.687669

82. Wang J, Wu Q, Ding L, Song S, Li Y, Shi L, et al. Therapeutic effects and molecular mechanisms of bioactive compounds against respiratory diseases: traditional chinese medicine theory and high-frequency use. *Front Pharmacol* (2021) 12:734450. doi: 10.3389/fphar.2021.734450

83. Pan Y, Yu Y, Wang X, Zhang T. Tumor-associated macrophages in tumor immunity. *Front Immunol* (2020) 11:583084. doi: 10.3389/fimmu.2020.583084

84. Xiang X, Wang J, Lu D, Xu X. Targeting tumor-associated macrophages to synergize tumor immunotherapy. *Signal Transduct Target Ther* (2021) 6(1):75. doi: 10.1038/s41392-021-00484-9

85. Jang JY, Lee JK, Jeon YK, Kim CW. Exosome derived from epigallocatechin gallate treated breast cancer cells suppresses tumor growth by inhibiting tumor-associated macrophage infiltration and M2 polarization. *BMC Cancer* (2013) 13:421. doi: 10.1186/1471-2407-13-421

86. Wang J, Man GCW, Chan TH, Kwong J, Wang CC. A prodrug of green tea polyphenol (-)-epigallocatechin-3-gallate (Pro-EGCG) serves as a novel angiogenesis inhibitor in endometrial cancer. *Cancer Lett* (2018) 412:10–20. doi: 10.1016/j.canlet.2017.09.054

87. Kassouri C, Rodriguez Torres S, Gonzalez Suarez N, Duhamel S, Annabi B. EGCG prevents the transcriptional reprogramming of an inflammatory and immune-suppressive molecular signature in macrophage-like differentiated human HL60 promyelocytic leukemia cells. *Cancers (Basel)* (2022) 14(20):5065. doi: 10.3390/cancers14205065

88. Lin JK. Cancer chemoprevention by tea polyphenols through modulating signal transduction pathways. *Arch Pharm Res* (2002) 25(5):561–71. doi: 10.1007/bf02976924

89. Korbecki J, Kojder K, Barczak K, Simińska D, Gutowska I, Chlubek D, et al. Hypoxia alters the expression of CC chemokines and CC chemokine receptors in a tumor-A literature review. *Int J Mol Sci* (2020) 21(16):5647. doi: 10.3390/ijms21165647

90. Korbecki J, Kojder K, Kapczuk P, Kupnicka P, Gawrońska-Szklarz B, Gutowska I, et al. The effect of hypoxia on the expression of CXC chemokines and CXC chemokine receptors-A review of literature. *Int J Mol Sci* (2021) 22(2):843. doi: 10.3390/ijms22020843

91. Ren X, Guo X, Chen L, Guo M, Peng N, Li R. Attenuated migration by green tea extract (-)-epigallocatechin gallate (EGCG): involvement of 67 kDa laminin receptor internalization in macrophagic cells. *Food Funct* (2014) 5(8):1915–9. doi: 10.1039/c4fo00143e

92. Bao S, Cao Y, Zhou H, Sun X, Shan Z, Teng W. Epigallocatechin gallate (EGCG) suppresses lipopolysaccharide-induced Toll-like receptor 4 (TLR4) activity via 67 kDa

laminin receptor (67LR) in 3T3-L1 adipocytes. *J Agric Food Chem* (2015) 63(10):2811–9. doi: 10.1021/jf505531w

93. Li YF, Wang H, Fan Y, Shi HJ, Wang QM, Chen BR, et al. Epigallocatechin-3-gallate inhibits matrix metalloproteinase-9 and monocyte chemotactic protein-1 expression through the 67-κDa laminin receptor and the TLR4/MAPK/NF-κB signalling pathway in lipopolysaccharide-induced macrophages. *Cell Physiol Biochem* (2017) 43(3):926–36. doi: 10.1159/000481643

94. Boutilier AJ, Elsawa SF. Macrophage polarization states in the tumor microenvironment. *Int J Mol Sci* (2021) 22(13):6995. doi: 10.3390/ijms22136995

95. Mukherjee S, Hussaini R, White R, Atwi D, Fried A, Sampat S, et al. TriCurin, a synergistic formulation of curcumin, resveratrol, and epicatechin gallate, repolarizes tumor-associated macrophages and triggers an immune response to cause suppression of HPV+ tumors. *Cancer Immunol Immunother* (2018) 67(5):761–74. doi: 10.1007/s00262-018-2130-3

96. Mukherjee S, Baidoo JNE, Sampat S, Mancuso A, David L, Cohen LS, et al. Liposomal triCurin, A synergistic combination of curcumin, epicatechin gallate and resveratrol, repolarizes tumor-associated microglia/macrophages, and eliminates glioblastoma (GBM) and GBM stem cells. *Molecules* (2018) 23(1):201. doi: 10.3390/molecules23010201

97. Masucci MT, Minopoli M, Carriero MV. Tumor associated neutrophils. Their role in tumorigenesis, metastasis, prognosis and therapy. *Front Oncol* (2019) 9:1146. doi: 10.3389/fonc.2019.01146

98. Que H, Fu Q, Lan T, Tian X, Wei X. Tumor-associated neutrophils and neutrophil-targeted cancer therapies. *Biochim Biophys Acta Rev Cancer* (2022) 1877 (5):188762. doi: 10.1016/j.bbcan.2022.188762

99. Mizuno R, Kawada K, Itatani Y, Ogawa R, Kiyasu Y, Sakai Y. The role of tumor-associated neutrophils in colorectal cancer. *Int J Mol Sci* (2019) 20(3):529. doi: 10.3390/ijms20030529

100. Templeton AJ, McNamara MG, Šeruga B, Vera-Badillo FE, Aneja P, Ocaña A, et al. Prognostic role of neutrophil-to-lymphocyte ratio in solid tumors: a systematic review and meta-analysis. *J Natl Cancer Inst* (2014) 106(6):dju124. doi: 10.1093/jnci/dju124

101. Capone M, Giannarelli D, Mallardo D, Madonna G, Festino L, Grimaldi AM, et al. Baseline neutrophil-to-lymphocyte ratio (NLR) and derived NLR could predict overall survival in patients with advanced melanoma treated with nivolumab. *J Immunother Cancer* (2018) 6(1):74. doi: 10.1186/s40425-018-0383-1

102. Cupp MA, Cariolou M, Tzoulaki I, Aune D, Evangelou E, Berlanga-Taylor AJ. Neutrophil to lymphocyte ratio and cancer prognosis: an umbrella review of systematic reviews and meta-analyses of observational studies. *BMC Med* (2020) 18(1):360. doi: 10.1186/s12916-020-01817-1

103. Wei H, Frenkel K. Relationship of oxidative events and DNA oxidation in SENCAR mice to *in vivo* promoting activity of phorbol ester-type tumor promoters. *Carcinogenesis* (1993) 14(6):1195–201. doi: 10.1093/carcin/14.6.1195

104. Hofbauer R, Frass M, Gmeiner B, Handler S, Speiser W, Kapiotis S. The green tea extract epigallocatechin gallate is able to reduce neutrophil transmigration through monolayers of endothelial cells. *Wien Klin Wochenschr* (1999) 111(7):278–82.

105. Takano K, Nakaima K, Nitta M, Shibata F, Nakagawa H. Inhibitory effect of (-)-epigallocatechin 3-gallate, a polyphenol of green tea, on neutrophil chemotaxis *in vitro* and *in vivo*. *J Agric Food Chem* (2004) 52(14):4571–6. doi: 10.1021/jf0355194

106. Kawai K. Comment on inhibitory effect of (-)-epigallocatechin 3-gallate, a polyphenol of green tea, on neutrophil chemotaxis *in vitro* and *in vivo*. *J Agric Food Chem* (2005) 53(4):1306. doi: 10.1021/jf040409y. author reply 1307-1308.

107. Zhang Z, Zhu Q, Wang S, Shi C. Epigallocatechin-3-gallate inhibits the formation of neutrophil extracellular traps and suppresses the migration and invasion of colon cancer cells by regulating STAT3/CXCL8 pathway. *Mol Cell Biochem* (2023) 478(4):887–98. doi: 10.1007/s11010-022-04550-w

108. Okeke EB, Louttit C, Fry C, Najafabadi AH, Han K, Nemzek J, et al. Inhibition of neutrophil elastase prevents neutrophil extracellular trap formation and rescues mice from endotoxic shock. *Biomaterials* (2020) 238:119836. doi: 10.1016/j.biomaterials.2020.119836

109. Lerman I, Hammes SR. Neutrophil elastase in the tumor microenvironment. *Steroids* (2018) 133:96–101. doi: 10.1016/j.steroids.2017.11.006

110. Zeng W, Song Y, Wang R, He R, Wang T. Neutrophil elastase: From mechanisms to therapeutic potential. *J Pharm Anal* (2023) 13(4):355–66. doi: 10.1016/j.jpha.2022.12.003

111. Xiaokaiti Y, Wu H, Chen Y, Yang H, Duan J, Li X, et al. EGCG reverses human neutrophil elastase-induced migration in A549 cells by directly binding to HNE and by regulating α1-AT. *Sci Rep* (2015) 5:11494. doi: 10.1038/srep11494

112. Hrenn A, Steinbrecher T, Labahn A, Schwager J, Schempp CM, Merfort I. Plant phenolics inhibit neutrophil elastase. *Planta Med* (2006) 72(12):1127–31. doi: 10.1055/s-2006-946700

113. Kim KC, Lee IS, Yoo ID, Ha BJ. Sesquiterpenes from the fruiting bodies of Ramaria formosa and their human neutrophil elastase inhibitory activity. *Chem Pharm Bull (Tokyo)* (2015) 63(7):554–7. doi: 10.1248/cpb.c15-00051

114. Kim KC, Kim DJ, Lee MS, Seo JY, Yoo ID, Lee IS. Inhibition of human neutrophil elastase by sesquiterpene lactone dimers from the flowers of inula britannica. *J Microbiol Biotechnol* (2018) 28(11):1806–13. doi: 10.4014/jmb.1807.07039

115. Biffi G, Tuveson DA. Diversity and biology of cancer-associated fibroblasts. *Physiol Rev* (2021) 101(1):147–76. doi: 10.1152/physrev.00048.2019

116. Wu F, Yang J, Liu J, Wang Y, Mu J, Zeng Q, et al. Signaling pathways in cancer-associated fibroblasts and targeted therapy for cancer. *Signal Transduct Target Ther* (2021) 6(1):218. doi: 10.1038/s41392-021-00641-0

117. Sahai E, Astsaturov I, Cukierman E, DeNardo DG, Egeblad M, Evans RM, et al. A framework for advancing our understanding of cancer-associated fibroblasts. *Nat Rev Cancer* (2020) 20(3):174–86. doi: 10.1038/s41568-019-0238-1

118. Chen Y, McAndrews KM, Kalluri R. Clinical and therapeutic relevance of cancer-associated fibroblasts. *Nat Rev Clin Oncol* (2021) 18(12):792–804. doi: 10.1038/s41571-021-00546-5

119. Hung CF, Huang TF, Chiang HS, Wu WB. (-)-Epigallocatechin-3-gallate, a polyphenolic compound from green tea, inhibits fibroblast adhesion and migration through multiple mechanisms. *J Cell Biochem* (2005) 96(1):183–97. doi: 10.1002/jcb.20509

120. Roomi MW, Kalinovsky T, Rath M, Niedzwiecki A. Cytokines, inducers and inhibitors modulate MMP-2 and MMP–9 secretion by human Fanconi anemia immortalized fibroblasts. *Oncol Rep* (2017) 37(3):1842–8. doi: 10.3892/or.2017.5368

121. Park G, Yoon BS, Moon JH, Kim B, Jun EK, Oh S, et al. Green tea polyphenol epigallocatechin-3-gallate suppresses collagen production and proliferation in keloid fibroblasts via inhibition of the STAT3-signaling pathway. *J Invest Dermatol* (2008) 128 (10):2429–41. doi: 10.1038/jid.2008.103

122. Yagiz K, Wu LY, Kuntz CP, James Morré D, Morré DM. Mouse embryonic fibroblast cells from transgenic mice overexpressing tNOX exhibit an altered growth and drug response phenotype. *J Cell Biochem* (2007) 101(2):295–306. doi: 10.1002/jcb.21184

123. Darweish MM, Abbas A, Ebrahim MA, Al-Gayyar MM. Chemopreventive and hepatoprotective effects of Epigallocatechin-gallate against hepatocellular carcinoma: role of heparan sulfate proteoglycans pathway. *J Pharm Pharmacol* (2014) 66(7):1032–45. doi: 10.1111/jphp.12229

124. McLarty J, Bigelow RL, Smith M, Elmajian D, Ankem M, Cardelli JA. Tea polyphenols decrease serum levels of prostate-specific antigen, hepatocyte growth factor, and vascular endothelial growth factor in prostate cancer patients and inhibit production of hepatocyte growth factor and vascular endothelial growth factor *in vitro*. *Cancer Prev Res (Phila)* (2009) 2(7):673–82. doi: 10.1158/1940-6207.Capr-08-0167

125. Gray AL, Stephens CA, Bigelow RL, Coleman DT, Cardelli JA. The polyphenols (-)-epigallocatechin-3-gallate and luteolin synergistically inhibit TGF-β-induced myofibroblast phenotypes through RhoA and ERK inhibition. *PloS One* (2014) 9 (10):e109208. doi: 10.1371/journal.pone.0109208

126. Chen R, Huang L, Hu K. Natural products remodel cancer-associated fibroblasts in desmoplastic tumors. *Acta Pharm Sin B* (2020) 10(11):2140–55. doi: 10.1016/j.apsb.2020.04.005

127. Daubriac J, Han S, Grahovac J, Smith E, Hosein A, Buchanan M, et al. The crosstalk between breast carcinoma-associated fibroblasts and cancer cells promotes RhoA-dependent invasion via IGF-1 and PAI-1. *Oncotarget* (2018) 9(12):10375–87. doi: 10.18632/oncotarget.23735

128. Boyle ST, Poltavets V, Kular J, Pyne NT, Sandow JJ, Lewis AC, et al. ROCK-mediated selective activation of PERK signalling causes fibroblast reprogramming and tumour progression through a CRELD2-dependent mechanism. *Nat Cell Biol* (2020) 22 (7):882–95. doi: 10.1038/s41556-020-0523-y

129. Watabe T, Takahashi K, Pietras K, Yoshimatsu Y. Roles of TGF-β signals in tumor microenvironment via regulation of the formation and plasticity of vascular system. *Semin Cancer Biol* (2023) 92:130–8. doi: 10.1016/j.semcancer.2023.04.007

130. Yin Z, Wang L. Endothelial-to-mesenchymal transition in tumour progression and its potential roles in tumour therapy. *Ann Med* (2023) 55(1):1058–69. doi: 10.1080/07853890.2023.2180155

131. Fassina G, Venè R, Morini M, Minghelli S, Benelli R, Noonan DM, et al. Mechanisms of inhibition of tumor angiogenesis and vascular tumor growth by epigallocatechin-3-gallate. *Clin Cancer Res* (2004) 10(14):4865–73. doi: 10.1158/1078-0432.Ccr-03-0672

132. Singh AK, Seth P, Anthony P, Husain MM, Madhavan S, Mukhtar H, et al. Green tea constituent epigallocatechin-3-gallate inhibits angiogenic differentiation of human endothelial cells. *Arch Biochem Biophys* (2002) 401(1):29–37. doi: 10.1016/s0003-9861(02)00013-9

133. Yamakawa S, Asai T, Uchida T, Matsukawa M, Akizawa T, Oku N. (-)-Epigallocatechin gallate inhibits membrane-type 1 matrix metalloproteinase, MT1-MMP, and tumor angiogenesis. *Cancer Lett* (2004) 210(1):47–55. doi: 10.1016/j.canlet.2004.03.008

134. Khoi PN, Park JS, Kim JH, Xia Y, Kim NH, Kim KK, et al. (-)-Epigallocatechin-3-gallate blocks nicotine-induced matrix metalloproteinase-9 expression and invasiveness via suppression of NF-κB and AP-1 in endothelial cells. *Int J Oncol* (2013) 43(3):868–76. doi: 10.3892/ijo.2013.2006

135. Ohga N, Hida K, Hida Y, Muraki C, Tsuchiya K, Matsuda K, et al. Inhibitory effects of epigallocatechin-3 gallate, a polyphenol in green tea, on tumor-associated endothelial cells and endothelial progenitor cells. *Cancer Sci* (2009) 100(10):1963–70. doi: 10.1111/j.1349-7006.2009.01255.x

136. Gallemit PEM, Yoodee S, Malaitad T, Thongboonkerd V. Epigallocatechin-3-gallate plays more predominant roles than caffeine for inducing actin-crosslinking, ubiquitin/proteasome activity and glycolysis, and suppressing angiogenesis features of human endothelial cells. *BioMed Pharmacother* (2021) 141:111837. doi: 10.1016/j.biopha.2021.111837

137. Kondo T, Ohta T, Igura K, Hara Y, Kaji K. Tea catechins inhibit angiogenesis *in vitro*, measured by human endothelial cell growth, migration and tube formation, through inhibition of VEGF receptor binding. *Cancer Lett* (2002) 180(2):139–44. doi: 10.1016/s0304-3835(02)00007-1

138. Wan X, Wang W, Liang Z. Epigallocatechin-3-gallate inhibits the growth of three-dimensional *in vitro* models of neuroblastoma cell SH-SY5Y. *Mol Cell Biochem* (2021) 476(8):3141–8. doi: 10.1007/s11010-021-04154-w

139. Patel SA, Nilsson MB, Le X, Cascone T, Jain RK, Heymach JV. Molecular mechanisms and future implications of VEGF/VEGFR in cancer therapy. *Clin Cancer Res* (2023) 29(1):30–9. doi: 10.1158/1078-0432.Ccr-22-1366

140. Helmlinger G, Endo M, Ferrara N, Hlatky L, Jain RK. Formation of endothelial cell networks. *Nature* (2000) 405(6783):139–41. doi: 10.1038/35012132

141. Zhu BH, Chen HY, Zhan WH, Wang CY, Cai SR, Wang Z, et al. (-)-Epigallocatechin-3-gallate inhibits VEGF expression induced by IL-6 via Stat3 in gastric cancer. *World J Gastroenterol* (2011) 17(18):2315–25. doi: 10.3748/wjg.v17.i18.2315

142. Gu JW, Makey KL, Tucker KB, Chinchar E, Mao X, Pei I, et al. EGCG, a major green tea catechin suppresses breast tumor angiogenesis and growth via inhibiting the activation of HIF-1α and NFκB, and VEGF expression. *Vasc Cell* (2013) 5(1):9. doi: 10.1186/2045-824x-5-9

143. Fu JD, Yao JJ, Wang H, Cui WG, Leng J, Ding LY, et al. Effects of EGCG on proliferation and apoptosis of gastric cancer SGC7901 cells via down-regulation of HIF-1α and VEGF under a hypoxic state. *Eur Rev Med Pharmacol Sci* (2019) 23 (1):155–61. doi: 10.26355/eurrev_201901_16759

144. Sartippour MR, Heber D, Zhang L, Beatty P, Elashoff D, Elashoff R, et al. Inhibition of fibroblast growth factors by green tea. *Int J Oncol* (2002) 21(3):487–91.

145. Sukhthankar M, Yamaguchi K, Lee SH, McEntee MF, Eling TE, Hara Y, et al. A green tea component suppresses posttranslational expression of basic fibroblast growth factor in colorectal cancer. *Gastroenterology* (2008) 134(7):1972–80. doi: 10.1053/j.gastro.2008.02.095

146. Mirzaaghaei S, Foroughmand AM, Saki G, Shafiei M. Combination of epigallocatechin-3-gallate and silibinin: a novel approach for targeting both tumor and endothelial cells. *ACS Omega* (2019) 4(5):8421–30. doi: 10.1021/acsomega.9b00224

147. Jin G, Yang Y, Liu K, Zhao J, Chen X, Liu H, et al. Combination curcumin and (-)-epigallocatechin-3-gallate inhibits colorectal carcinoma microenvironment-induced angiogenesis by JAK/STAT3/IL-8 pathway. *Oncogenesis* (2017) 6(10):e384. doi: 10.1038/oncsis.2017.84

148. Chen CY, Lin YJ, Wang CCN, Lan YH, Lan SJ, Sheu MJ. Epigallocatechin-3-gallate inhibits tumor angiogenesis: involvement of endoglin/Smad1 signaling in human umbilical vein endothelium cells. *BioMed Pharmacother* (2019) 120:109491. doi: 10.1016/j.biopha.2019.109491

149. Sherman MH. Stellate cells in tissue repair, inflammation, and cancer. *Annu Rev Cell Dev Biol* (2018) 34:333–55. doi: 10.1146/annurev-cellbio-100617-062855

150. Wang SS, Tang XT, Lin M, Yuan J, Peng YJ, Yin X, et al. Perivenous stellate cells are the main source of myofibroblasts and cancer-associated fibroblasts formed after chronic liver injuries. *Hepatology* (2021) 74(3):1578–94. doi: 10.1002/hep.31848

151. Myojin Y, Hikita H, Sugiyama M, Sasaki Y, Fukumoto K, Sakane S, et al. Hepatic stellate cells in hepatocellular carcinoma promote tumor growth via growth differentiation factor 15 production. *Gastroenterology* (2021) 160(5):1741–1754.e1716. doi: 10.1053/j.gastro.2020.12.015

152. Matsuda M, Seki E. Hepatic stellate cell-macrophage crosstalk in liver fibrosis and carcinogenesis. *Semin Liver Dis* (2020) 40(3):307–20. doi: 10.1055/s-0040-1708876

153. Correia AL, Guimaraes JC, Auf der Maur P, De Silva D, Trefny MP, Okamoto R, et al. Hepatic stellate cells suppress NK cell-sustained breast cancer dormancy. *Nature* (2021) 594(7864):566–71. doi: 10.1038/s41586-021-03614-z

154. Fu Y, Zheng S, Lu SC, Chen A. Epigallocatechin-3-gallate inhibits growth of activated hepatic stellate cells by enhancing the capacity of glutathione synthesis. *Mol Pharmacol* (2008) 73(5):1465–73. doi: 10.1124/mol.107.040634

155. Yumei F, Zhou Y, Zheng S, Chen A. The antifibrogenic effect of (-)-epigallocatechin gallate results from the induction of *de novo* synthesis of glutathione in passaged rat hepatic stellate cells. *Lab Invest* (2006) 86(7):697–709. doi: 10.1038/labinvest.3700425

156. Higashi N, Kohjima M, Fukushima M, Ohta S, Kotoh K, Enjoji M, et al. Epigallocatechin-3-gallate, a green-tea polyphenol, suppresses Rho signaling in TWNT-4 human hepatic stellate cells. *J Lab Clin Med* (2005) 145(6):316–22. doi: 10.1016/j.lab.2005.03.017

157. Sakata R, Ueno T, Nakamura T, Sakamoto M, Torimura T, Sata M. Green tea polyphenol epigallocatechin-3-gallate inhibits platelet-derived growth factor-induced proliferation of human hepatic stellate cell line LI90. *J Hepatol* (2004) 40(1):52–9. doi: 10.1016/s0168-8278(03)00477-x

158. Masamune A, Kikuta K, Satoh M, Suzuki N, Shimosegawa T. Green tea polyphenol epigallocatechin-3-gallate blocks PDGF-induced proliferation and migration of rat pancreatic stellate cells. *World J Gastroenterol* (2005) 11(22):3368–74. doi: 10.3748/wjg.v11.i22.3368

159. Chen A, Zhang L. The antioxidant (-)-epigallocatechin-3-gallate inhibits rat hepatic stellate cell proliferation *in vitro* by blocking the tyrosine phosphorylation and reducing the gene expression of platelet-derived growth factor-beta receptor. *J Biol Chem* (2003) 278(26):23381–9. doi: 10.1074/jbc.M212042200

160. Arffa ML, Zapf MA, Kothari AN, Chang V, Gupta GN, Ding X, et al. Epigallocatechin-3-gallate upregulates miR-221 to inhibit osteopontin-dependent hepatic fibrosis. *PloS One* (2016) 11(12):e0167435. doi: 10.1371/journal.pone.0167435

161. George J, Tsuchishima M, Tsutsumi M. Epigallocatechin-3-gallate inhibits osteopontin expression and prevents experimentally induced hepatic fibrosis. *BioMed Pharmacother* (2022) 151:113111. doi: 10.1016/j.biopha.2022.113111

162. Yin X, Peng J, Gu L, Liu Y, Li X, Wu J, et al. Targeting glutamine metabolism in hepatic stellate cells alleviates liver fibrosis. *Cell Death Dis* (2022) 13(11):955. doi: 10.1038/s41419-022-05409-0

163. Shen X, Zhao J, Wang Q, Chen P, Hong Y, He X, et al. The invasive potential of hepatoma cells induced by radiotherapy is related to the activation of hepatic stellate cells and could be inhibited by EGCG through the TLR4 signaling pathway. *Radiat Res* (2022) 197(4):365–75. doi: 10.1667/rade-21-00129.1

164. Ruan Q, Wang H, Burke LJ, Bridle KR, Li X, Zhao CX, et al. Therapeutic modulators of hepatic stellate cells for hepatocellular carcinoma. *Int J Cancer* (2020) 147(6):1519–27. doi: 10.1002/ijc.32899

165. Sojoodi M, Wei L, Erstad DJ, Yamada S, Fujii T, Hirschfield H, et al. Epigallocatechin gallate induces hepatic stellate cell senescence and attenuates development of hepatocellular carcinoma. *Cancer Prev Res (Phila)* (2020) 13(6):497–508. doi: 10.1158/1940-6207.Capr-19-0383

166. Tu Z, Karnoub AE. Mesenchymal stem/stromal cells in breast cancer development and management. *Semin Cancer Biol* (2022) 86(Pt 2):81–92. doi: 10.1016/j.semcancer.2022.09.002

167. Galland S, Stamenkovic I. Mesenchymal stromal cells in cancer: a review of their immunomodulatory functions and dual effects on tumor progression. *J Pathol* (2020) 250(5):555–72. doi: 10.1002/path.5357

168. Poggi A, Musso A, Dapino I, Zocchi MR. Mechanisms of tumor escape from immune system: role of mesenchymal stromal cells. *Immunol Lett* (2014) 159(1-2):55–72. doi: 10.1016/j.imlet.2014.03.001

169. Lan T, Luo M, Wei X. Mesenchymal stem/stromal cells in cancer therapy. *J Hematol Oncol* (2021) 14(1):195. doi: 10.1186/s13045-021-01208-w

170. Zgheib A, Lamy S, Annabi B. Epigallocatechin gallate targeting of membrane type 1 matrix metalloproteinase-mediated Src and Janus kinase/signal transducers and activators of transcription 3 signaling inhibits transcription of colony-stimulating factors 2 and 3 in mesenchymal stromal cells. *J Biol Chem* (2013) 288(19):13378–86. doi: 10.1074/jbc.M113.456533

171. Gonzalez Suarez N, Fernandez-Marrero Y, Torabidastgerdooei S, Annabi B. EGCG prevents the onset of an inflammatory and cancer-associated adipocyte-like phenotype in adipose-derived mesenchymal stem/stromal cells in response to the triple-negative breast cancer secretome. *Nutrients* (2022) 14(5):1099. doi: 10.3390/nu14051099

172. Gonzalez Suarez N, Rodriguez Torres S, Ouanouki A, El Cheikh-Hussein L, Annabi B. EGCG inhibits adipose-derived mesenchymal stem cells differentiation into adipocytes and prevents a STAT3-mediated paracrine oncogenic control of triple-negative breast cancer cell invasive phenotype. *Molecules* (2021) 26(6):1506. doi: 10.3390/molecules26061506

173. Zambrano A, Molt M, Uribe E, Salas M. Glut 1 in cancer cells and the inhibitory action of resveratrol as A potential therapeutic strategy. *Int J Mol Sci* (2019) 20 (13):3374. doi: 10.3390/ijms20133374

174. Barron CC, Bilan PJ, Tsakiridis T, Tsiani E. Facilitative glucose transporters: Implications for cancer detection, prognosis and treatment. *Metabolism* (2016) 65 (2):124–39. doi: 10.1016/j.metabol.2015.10.007

175. Hwang JT, Ha J, Park IJ, Lee SK, Baik HW, Kim YM, et al. Apoptotic effect of EGCG in HT-29 colon cancer cells via AMPK signal pathway. *Cancer Lett* (2007) 247 (1):115–21. doi: 10.1016/j.canlet.2006.03.030

176. Wei R, Mao L, Xu P, Zheng X, Hackman RM, Mackenzie GG, et al. Suppressing glucose metabolism with epigallocatechin-3-gallate (EGCG) reduces breast cancer cell growth in preclinical models. *Food Funct* (2018) 9(11):5682–96. doi: 10.1039/c8fo01397g

177. Hu L, Xu X, Chen X, Qiu S, Li Q, Zhang D, et al. Epigallocatechin-3-gallate decreases hypoxia-inducible factor-1 in pancreatic cancer cells. *Am J Chin Med* (2023) 51(3):761–77. doi: 10.1142/s0192415x23500362

178. Moreira L, Araújo I, Costa T, Correia-Branco A, Faria A, Martel F, et al. Quercetin and epigallocatechin gallate inhibit glucose uptake and metabolism by breast cancer cells by an estrogen receptor-independent mechanism. *Exp Cell Res* (2013) 319 (12):1784–95. doi: 10.1016/j.yexcr.2013.05.001

179. Ojelabi OA, Lloyd KP, De Zutter JK, Carruthers A. Red wine and green tea flavonoids are cis-allosteric activators and competitive inhibitors of glucose transporter 1 (GLUT1)-mediated sugar uptake. *J Biol Chem* (2018) 293(51):19823–34. doi: 10.1074/jbc.RA118.002326

180. Abdel-Wahab AF, Mahmoud W, Al-Harizy RM. Targeting glucose metabolism to suppress cancer progression: prospective of anti-glycolytic cancer therapy. *Pharmacol Res* (2019) 150:104511. doi: 10.1016/j.phrs.2019.104511

181. Chelakkot C, Chelakkot VS, Shin Y, Song K. Modulating glycolysis to improve cancer therapy. *Int J Mol Sci* (2023) 24(3):2606. doi: 10.3390/ijms24032606

182. Fukushi A, Kim HD, Chang YC, Kim CH. Revisited metabolic control and reprogramming cancers by means of the warburg effect in tumor cells. *Int J Mol Sci* (2022) 23(17):10037. doi: 10.3390/ijms231710037

183. Sahadevan R, Binoy A, Vechalapu SK, Nanjan P, Sadhukhan S. *In situ* global proteomics profiling of EGCG targets using a cell-permeable and Click-able bioorthogonal probe. *Int J Biol Macromol* (2023) 237:123991. doi: 10.1016/j.ijbiomac.2023.123991

184. Gao F, Li M, Liu WB, Zhou ZS, Zhang R, Li JL, et al. Epigallocatechin gallate inhibits human tongue carcinoma cells via HK2–mediated glycolysis. *Oncol Rep* (2015) 33(3):1533–9. doi: 10.3892/or.2015.3727

185. Khan A, Mohammad T, Shamsi A, Hussain A, Alajmi MF, Husain SA, et al. Identification of plant-based hexokinase 2 inhibitors: combined molecular docking and dynamics simulation studies. *J Biomol Struct Dyn* (2022) 40(20):10319–31. doi: 10.1080/07391102.2021.1942217

186. Al Hasawi N, Alkandari MF, Luqmani YA. Phosphofructokinase: a mediator of glycolytic flux in cancer progression. *Crit Rev Oncol Hematol* (2014) 92(3):312–21. doi: 10.1016/j.critrevonc.2014.05.007

187. Wei R, Hackman RM, Wang Y, Mackenzie GG. Targeting glycolysis with epigallocatechin-3-gallate enhances the efficacy of chemotherapeutics in pancreatic cancer cells and xenografts. *Cancers (Basel)* (2019) 11(10):1496. doi: 10.3390/cancers11101496

188. Li S, Wu L, Feng J, Li J, Liu T, Zhang R, et al. *In vitro* and *in vivo* study of epigallocatechin-3-gallate-induced apoptosis in aerobic glycolytic hepatocellular carcinoma cells involving inhibition of phosphofructokinase activity. *Sci Rep* (2016) 6:28479. doi: 10.1038/srep28479

189. Lu QY, Zhang L, Yee JK, Go VW, Lee WN. Metabolic consequences of LDHA inhibition by epigallocatechin gallate and oxamate in MIA paCa-2 pancreatic cancer cells. *Metabolomics* (2015) 11(1):71–80. doi: 10.1007/s11306-014-0672-8

190. Li X, Tang S, Wang QQ, Leung EL, Jin H, Huang Y, et al. Identification of epigallocatechin-3- gallate as an inhibitor of phosphoglycerate mutase 1. *Front Pharmacol* (2017) 8:325. doi: 10.3389/fphar.2017.00325

191. Yeh LC, Shyu HW, Jin YR, Chiou YH, Lin KH, Chou MC, et al. Epigallocatechin-3-gallate downregulates PDHA1 interfering the metabolic pathways in human herpesvirus 8 harboring primary effusion lymphoma cells. *Toxicol In Vitro* (2020) 65:104753. doi: 10.1016/j.tiv.2019.104753

192. Li S, Zeng H, Fan J, Wang F, Xu C, Li Y, et al. Glutamine metabolism in breast cancer and possible therapeutic targets. *Biochem Pharmacol* (2023) 210:115464. doi: 10.1016/j.bcp.2023.115464

193. Cluntun AA, Lukey MJ, Cerione RA, Locasale JW. Glutamine metabolism in cancer: understanding the heterogeneity. *Trends Cancer* (2017) 3(3):169–80. doi: 10.1016/j.trecan.2017.01.005

194. Katt WP, Cerione RA. Glutaminase regulation in cancer cells: a druggable chain of events. *Drug Discovery Today* (2014) 19(4):450–7. doi: 10.1016/j.drudis.2013.10.008

195. Xu L, Yin Y, Li Y, Chen X, Chang Y, Zhang H, et al. A glutaminase isoform switch drives therapeutic resistance and disease progression of prostate cancer. *Proc Natl Acad Sci USA* (2021) 118(13):e2012748118. doi: 10.1073/pnas.2012748118

196. Ma G, Zhang Z, Li P, Zhang Z, Zeng M, Liang Z, et al. Reprogramming of glutamine metabolism and its impact on immune response in the tumor microenvironment. *Cell Commun Signal* (2022) 20(1):114. doi: 10.1186/s12964-022-00909-0

197. Carmo F, Silva C, Martel F. Inhibition of glutamine cellular uptake contributes to the cytotoxic effect of xanthohumol in triple-negative breast cancer cells. *Nutr Cancer* (2022) 74(9):3413–30. doi: 10.1080/01635581.2022.2076889

198. van Geldermalsen M, Wang Q, Nagarajah R, Marshall AD, Thoeng A, Gao D, et al. ASCT2/SLC1A5 controls glutamine uptake and tumour growth in triple-negative basal-like breast cancer. *Oncogene* (2016) 35(24):3201–8. doi: 10.1038/onc.2015.381

199. Morotti M, Bridges E, Valli A, Choudhry H, Sheldon H, Wigfield S, et al. Hypoxia-induced switch in SNAT2/SLC38A2 regulation generates endocrine resistance in breast cancer. *Proc Natl Acad Sci USA* (2019) 116(25):12452–61. doi: 10.1073/pnas.1818521116

200. Boonyong C, Vardhanabhuti N, Jianmongkol S. Modulation of non-steroidal anti-inflammatory drug-induced, ER stress-mediated apoptosis in Caco-2 cells by different polyphenolic antioxidants: a mechanistic study. *J Pharm Pharmacol* (2020) 72 (11):1574–84. doi: 10.1111/jphp.13343

201. Xie L, Yi J, Song Y, Zhao M, Fan L, Zhao L. Suppression of GOLM1 by EGCG through HGF/HGFR/AKT/GSK-3β/β-catenin/c-Myc signaling pathway inhibits cell migration of MDA-MB-231. *Food Chem Toxicol* (2021) 157:112574. doi: 10.1016/j.fct.2021.112574

202. Sbirkov Y, Vergov B, Dzharov V, Schenk T, Petrie K, Sarafian V. Targeting glutaminolysis shows efficacy in both prednisolone-sensitive and in metabolically rewired prednisolone-resistant B-cell childhood acute lymphoblastic leukaemia cells. *Int J Mol Sci* (2023) 24(4):3378. doi: 10.3390/ijms24043378

203. Peeters TH, Lenting K, Breukels V, van Lith SAM, van den Heuvel C, Molenaar R, et al. Isocitrate dehydrogenase 1-mutated cancers are sensitive to the green tea polyphenol epigallocatechin-3-gallate. *Cancer Metab* (2019) 7:4. doi: 10.1186/s40170-019-0198-7

204. Chang SN, Keretsu S, Kang SC. Evaluation of decursin and its isomer decursinol angelate as potential inhibitors of human glutamate dehydrogenase activity through in silico and enzymatic assay screening. *Comput Biol Med* (2022) 151(Pt B):106287. doi: 10.1016/j.compbiomed.2022.106287

205. Koundouros N, Poulogiannis G. Reprogramming of fatty acid metabolism in cancer. *Br J Cancer* (2020) 122(1):4–22. doi: 10.1038/s41416-019-0650-z

206. Li Z, Zhang H. Reprogramming of glucose, fatty acid and amino acid metabolism for cancer progression. *Cell Mol Life Sci* (2016) 73(2):377–92. doi: 10.1007/s00018-015-2070-4

207. Röhrig F, Schulze A. The multifaceted roles of fatty acid synthesis in cancer. *Nat Rev Cancer* (2016) 16(11):732–49. doi: 10.1038/nrc.2016.89

208. Li C, Zhang L, Qiu Z, Deng W, Wang W. Key molecules of fatty acid metabolism in gastric cancer. *Biomolecules* (2022) 12(5):706. doi: 10.3390/biom12050706

209. Tan SK, Hougen HY, Merchan JR, Gonzalgo ML, Welford SM. Fatty acid metabolism reprogramming in ccRCC: mechanisms and potential targets. *Nat Rev Urol* (2023) 20(1):48–60. doi: 10.1038/s41585-022-00654-6

210. Luo Y, Wang H, Liu B, Wei J. Fatty acid metabolism and cancer immunotherapy. *Curr Oncol Rep* (2022) 24(5):659–70. doi: 10.1007/s11912-022-01223-1

211. Khiewkamrop P, Surangkul D, Srikummool M, Richert L, Pekthong D, Parhira S, et al. Epigallocatechin gallate triggers apoptosis by suppressing *de novo* lipogenesis in colorectal carcinoma cells. *FEBS Open Bio* (2022) 12(5):937–58. doi: 10.1002/2211-5463.13391

212. Khiewkamrop P, Phunsomboon P, Richert L, Pekthong D, Srisawang P. Epistructured catechins, EGCG and EC facilitate apoptosis induction through targeting *de novo* lipogenesis pathway in HepG2 cells. *Cancer Cell Int* (2018) 18:46. doi: 10.1186/s12935-018-0539-6

213. Lally JSV, Ghoshal S, DePeralta DK, Moaven O, Wei L, Masia R, et al. Inhibition of acetyl-CoA carboxylase by phosphorylation or the inhibitor ND-654 suppresses lipogenesis and hepatocellular carcinoma. *Cell Metab* (2019) 29(1):174–182.e175. doi: 10.1016/j.cmet.2018.08.020

214. Huang CH, Tsai SJ, Wang YJ, Pan MH, Kao JY, Way TD. EGCG inhibits protein synthesis, lipogenesis, and cell cycle progression through activation of AMPK in p53 positive and negative human hepatoma cells. *Mol Nutr Food Res* (2009) 53 (9):1156–65. doi: 10.1002/mnfr.200800592

215. Lupu R, Menendez JA. Pharmacological inhibitors of Fatty Acid Synthase (FASN)–catalyzed endogenous fatty acid biogenesis: a new family of anti-cancer agents? *Curr Pharm Biotechnol* (2006) 7(6):483–93. doi: 10.2174/138920106779116928

216. Brusselmans K, De Schrijver E, Heyns W, Verhoeven G, Swinnen JV. Epigallocatechin-3-gallate is a potent natural inhibitor of fatty acid synthase in intact cells and selectively induces apoptosis in prostate cancer cells. *Int J Cancer* (2003) 106 (6):856–62. doi: 10.1002/ijc.11317

217. Tian WX. Inhibition of fatty acid synthase by polyphenols. *Curr Med Chem* (2006) 13(8):967–77. doi: 10.2174/092986706776361012

218. Yeh CW, Chen WJ, Chiang CT, Lin-Shiau SY, Lin JK. Suppression of fatty acid synthase in MCF-7 breast cancer cells by tea and tea polyphenols: a possible mechanism for their hypolipidemic effects. *Pharmacogenomics J* (2003) 3(5):267–76. doi: 10.1038/sj.tpj.6500192

219. Pan MH, Lin CC, Lin JK, Chen WJ. Tea polyphenol (-)-epigallocatechin 3-gallate suppresses heregulin-beta1-induced fatty acid synthase expression in human breast cancer cells by inhibiting phosphatidylinositol 3-kinase/Akt and mitogen-activated protein kinase cascade signaling. *J Agric Food Chem* (2007) 55(13):5030–7. doi: 10.1021/jf070316r

220. Lin JK, Lin-Shiau SY. Mechanisms of hypolipidemic and anti-obesity effects of tea and tea polyphenols. *Mol Nutr Food Res* (2006) 50(2):211–7. doi: 10.1002/mnfr.200500138

221. Zhang Z, Garzotto M, Beer TM, Thuillier P, Lieberman S, Mori M, et al. Effects of ω-3 fatty acids and catechins on fatty acid synthase in the prostate: a randomized controlled trial. *Nutr Cancer* (2016) 68(8):1309–19. doi: 10.1080/01635581.2016.1224365

222. Puig T, Relat J, Marrero PF, Haro D, Brunet J, Colomer R. Green tea catechin inhibits fatty acid synthase without stimulating carnitine palmitoyltransferase-1 or inducing weight loss in experimental animals. *Anticancer Res* (2008) 28(6a):3671–6.

223. Puig T, Vázquez-Martín A, Relat J, Pétriz J, Menéndez JA, Porta R, et al. Fatty acid metabolism in breast cancer cells: differential inhibitory effects of epigallocatechin gallate (EGCG) and C75. *Breast Cancer Res Treat* (2008) 109(3):471–9. doi: 10.1007/s10549-007-9678-5

224. Relat J, Blancafort A, Oliveras G, Cufí S, Haro D, Marrero PF, et al. Different fatty acid metabolism effects of (-)-epigallocatechin-3-gallate and C75 in adenocarcinoma lung cancer. *BMC Cancer* (2012) 12:280. doi: 10.1186/1471-2407-12-280

225. Chen J, Zhang F, Ren X, Wang Y, Huang W, Zhang J, et al. Targeting fatty acid synthase sensitizes human nasopharyngeal carcinoma cells to radiation via downregulating frizzled class receptor 10. *Cancer Biol Med* (2020) 17(3):740–52. doi: 10.20892/j.issn.2095-3941.2020.0219

226. Blancafort A, Giró-Perafita A, Oliveras G, Palomeras S, Turrado C, Campuzano Ò, et al. Dual fatty acid synthase and HER2 signaling blockade shows marked antitumor activity against breast cancer models resistant to anti-HER2 drugs. *PloS One* (2015) 10(6):e0131241. doi: 10.1371/journal.pone.0131241

227. Giró-Perafita A, Palomeras S, Lum DH, Blancafort A, Viñas G, Oliveras G, et al. Preclinical evaluation of fatty acid synthase and EGFR inhibition in triple-negative breast cancer. *Clin Cancer Res* (2016) 22(18):4687–97. doi: 10.1158/1078-0432.Ccr-15-3133

228. Humbert M, Seiler K, Mosimann S, Rentsch V, Sharma K, Pandey AV, et al. Reducing FASN expression sensitizes acute myeloid leukemia cells to differentiation therapy. *Cell Death Differ* (2021) 28(8):2465–81. doi: 10.1038/s41418-021-00768-1

229. Shi DD, Savani MR, Abdullah KG, McBrayer SK. Emerging roles of nucleotide metabolism in cancer. *Trends Cancer* (2023) 9(8):624–35. doi: 10.1016/j.trecan.2023.04.008

230. Robinson AD, Eich ML, Varambally S. Dysregulation of *de novo* nucleotide biosynthetic pathway enzymes in cancer and targeting opportunities. *Cancer Lett* (2020) 470:134–40. doi: 10.1016/j.canlet.2019.11.013

231. Ma J, Zhong M, Xiong Y, Gao Z, Wu Z, Liu Y, et al. Emerging roles of nucleotide metabolism in cancer development: progress and prospect. *Aging (Albany NY)* (2021) 13(9):13349–58. doi: 10.18632/aging.202962

232. Mullen NJ, Singh PK. Nucleotide metabolism: a pan-cancer metabolic dependency. *Nat Rev Cancer* (2023) 23(5):275–94. doi: 10.1038/s41568-023-00557-7

233. Wu HL, Gong Y, Ji P, Xie YF, Jiang YZ, Liu GY. Targeting nucleotide metabolism: a promising approach to enhance cancer immunotherapy. *J Hematol Oncol* (2022) 15(1):45. doi: 10.1186/s13045-022-01263-x

234. Zhang Z, Zhang S, Yang J, Yi P, Xu P, Yi M, et al. Integrated transcriptomic and metabolomic analyses to characterize the anti-cancer effects of (-)-epigallocatechin-3-gallate in human colon cancer cells. *Toxicol Appl Pharmacol* (2020) 401:115100. doi: 10.1016/j.taap.2020.115100

235. Pan T, Han D, Xu Y, Peng W, Bai L, Zhou X, et al. LC-MS based metabolomics study of the effects of EGCG on A549 cells. *Front Pharmacol* (2021) 12:732716. doi: 10.3389/fphar.2021.732716

236. Hitosugi T, Zhou L, Elf S, Fan J, Kang HB, Seo JH, et al. Phosphoglycerate mutase 1 coordinates glycolysis and biosynthesis to promote tumor growth. *Cancer Cell* (2012) 22(5):585–600. doi: 10.1016/j.ccr.2012.09.020

237. Navarro-Perán E, Cabezas-Herrera J, Campo LS, Rodríguez-López JN. Effects of folate cycle disruption by the green tea polyphenol epigallocatechin-3-gallate. *Int J Biochem Cell Biol* (2007) 39(12):2215–25. doi: 10.1016/j.biocel.2007.06.005

238. Sánchez-Del-Campo L, Sáez-Ayala M, Chazarra S, Cabezas-Herrera J, Rodríguez-López JN. Binding of natural and synthetic polyphenols to human dihydrofolate reductase. *Int J Mol Sci* (2009) 10(12):5398–410. doi: 10.3390/ijms10125398

239. Matsubara K, Saito A, Tanaka A, Nakajima N, Akagi R, Mori M, et al. Catechin conjugated with fatty acid inhibits DNA polymerase and angiogenesis. *DNA Cell Biol* (2006) 25(2):95–103. doi: 10.1089/dna.2006.25.95

240. Jacob J, Cabarcas S, Veras I, Zaveri N, Schramm L. The green tea component EGCG inhibits RNA polymerase III transcription. *Biochem Biophys Res Commun* (2007) 360(4):778–83. doi: 10.1016/j.bbrc.2007.06.114

241. Mizushina Y, Saito A, Horikawa K, Nakajima N, Tanaka A, Yoshida H, et al. Acylated catechin derivatives: inhibitors of DNA polymerase and angiogenesis. *Front Biosci (Elite Ed)* (2011) 3(4):1337–48. doi: 10.2741/e337

242. Yoshida N, Kuriyama I, Yoshida H, Mizushina Y. Inhibitory effects of catechin derivatives on mammalian DNA polymerase and topoisomerase activities and mouse one-cell zygote development. *J Biosci Bioeng* (2013) 115(3):303–9. doi: 10.1016/j.jbiosc.2012.10.001

243. Mizushina Y, Saito A, Tanaka A, Nakajima N, Kuriyama I, Takemura M, et al. Structural analysis of catechin derivatives as mammalian DNA polymerase inhibitors. *Biochem Biophys Res Commun* (2005) 333(1):101–9. doi: 10.1016/j.bbrc.2005.05.093

244. Saiko P, Steinmann MT, Schuster H, Graser G, Bressler S, Giessrigl B, et al. Epigallocatechin gallate, ellagic acid, and rosmarinic acid perturb dNTP pools and inhibit *de novo* DNA synthesis and proliferation of human HL-60 promyelocytic leukemia cells: Synergism with arabinofuranosylcytosine. *Phytomedicine* (2015) 22(1):213–22. doi: 10.1016/j.phymed.2014.11.017

245. Kuzuhara T, Tanabe A, Sei Y, Yamaguchi K, Suganuma M, Fujiki H. Synergistic effects of multiple treatments, and both DNA and RNA direct bindings on, green tea catechins. *Mol Carcinog* (2007) 46(8):640–5. doi: 10.1002/mc.20332

246. Zhang Y, Zhang Z. The history and advances in cancer immunotherapy: understanding the characteristics of tumor-infiltrating immune cells and their therapeutic implications. *Cell Mol Immunol* (2020) 17(8):807–21. doi: 10.1038/s41423-020-0488-6

247. Yap TA, Parkes EE, Peng W, Moyers JT, Curran MA, Tawbi HA. Development of immunotherapy combination strategies in cancer. *Cancer Discovery* (2021) 11(6):1368–97. doi: 10.1158/2159-8290.Cd-20-1209

248. Liu K, Sun Q, Liu Q, Li H, Zhang W, Sun C. Focus on immune checkpoint PD-1/PD-L1 pathway: New advances of polyphenol phytochemicals in tumor immunotherapy. *BioMed Pharmacother* (2022) 154:113618. doi: 10.1016/j.biopha.2022.113618

249. Rawangkan A, Wongsirisin P, Namiki K, Iida K, Kobayashi Y, Shimizu Y, et al. Green tea catechin is an alternative immune checkpoint inhibitor that inhibits PD-L1 expression and lung tumor growth. *Molecules* (2018) 23(8):2071. doi: 10.3390/molecules23082071

250. Guo Y, Liang J, Liu B, Jin Y. Molecular mechanism of food-derived polyphenols on PD-L1 dimerization: a molecular dynamics simulation study. *Int J Mol Sci* (2021) 22(20):10924. doi: 10.3390/ijms222010924

251. Han X, Zhao N, Zhu W, Wang J, Liu B, Teng Y. Resveratrol attenuates TNBC lung metastasis by down-regulating PD-1 expression on pulmonary T cells and converting macrophages to M1 phenotype in a murine tumor model. *Cell Immunol* (2021) 368:104423. doi: 10.1016/j.cellimm.2021.104423

252. Zhao GJ, Lu ZQ, Tang LM, Wu ZS, Wang DW, Zheng JY, et al. Curcumin inhibits suppressive capacity of naturally occurring CD4+CD25+ regulatory T cells in mice *in vitro*. *Int Immunopharmacol* (2012) 14(1):99–106. doi: 10.1016/j.intimp.2012.06.016

253. Lakshmanan VK, Jindal S, Packirisamy G, Ojha S, Lian S, Kaushik A, et al. Nanomedicine-based cancer immunotherapy: recent trends and future perspectives. *Cancer Gene Ther* (2021) 28(9):911–23. doi: 10.1038/s41417-021-00299-4

254. Sun X, Zhang J, Xiu J, Zhao X, Yang C, Li D, et al. A phenolic based tumor-permeated nano-framework for immunogenic cell death induction combined with PD-L1 immune checkpoint blockade. *Biomater Sci* (2022) 10(14):3808–22. doi: 10.1039/d2bm00455k

255. Song Q, Zhang G, Wang B, Cao G, Li D, Wang Y, et al. Reinforcing the combinational immuno-oncotherapy of switching "Cold" Tumor to "Hot" by responsive penetrating nanogels. *ACS Appl Mater Interfaces* (2021) 13(31):36824–38. doi: 10.1021/acsami.1c08201

256. Wu P, Zhang H, Yin Y, Sun M, Mao S, Chen H, et al. Engineered EGCG-containing biomimetic nanoassemblies as effective delivery platform for enhanced cancer therapy. *Adv Sci (Weinh)* (2022) 9(15):e2105894. doi: 10.1002/advs.202105894

257. Fan R, Chen C, Mu M, Chuan D, Liu H, Hou H, et al. Engineering MMP-2 activated nanoparticles carrying B7-H3 bispecific antibodies for ferroptosis-enhanced glioblastoma immunotherapy. *ACS Nano* (2023) 17(10):9126–39. doi: 10.1021/acsnano.2c12217

258. Zhang B, Jiang J, Wu P, Zou J, Le J, Lin J, et al. A smart dual-drug nanosystem based on co-assembly of plant and food-derived natural products for synergistic HCC immunotherapy. *Acta Pharm Sin B* (2021) 11(1):246–57. doi: 10.1016/j.apsb.2020.07.026

259. Igarashi Y, Sasada T. Cancer vaccines: toward the next breakthrough in cancer immunotherapy. *J Immunol Res* (2020) 2020:5825401. doi: 10.1155/2020/5825401

260. Adamik J, Butterfield LH. What's next for cancer vaccines. *Sci Transl Med* (2022) 14(670):eabo4632. doi: 10.1126/scitranslmed.abo4632

261. Lin MJ, Svensson-Arvelund J, Lubitz GS, Marabelle A, Melero I, Brown BD, et al. Cancer vaccines: the next immunotherapy frontier. *Nat Cancer* (2022) 3(8):911–26. doi: 10.1038/s43018-022-00418-6

262. Song CK, Han HD, Noh KH, Kang TH, Park YS, Kim JH, et al. Chemotherapy enhances CD8(+) T cell-mediated antitumor immunity induced by vaccination with vaccinia virus. *Mol Ther* (2007) 15(8):1558–63. doi: 10.1038/sj.mt.6300221

263. Wang X, Liang J, Zhang C, Ma G, Wang C, Kong D. Coordination microparticle vaccines engineered from tumor cell templates. *Chem Commun (Camb)* (2019) 55(11):1568–71. doi: 10.1039/c8cc10004g

264. Wang X, Chen Z, Zhang C, Zhang C, Ma G, Yang J, et al. A generic coordination assembly-enabled nanocoating of individual tumor cells for personalized immunotherapy. *Adv Healthc Mater* (2019) 8(17):e1900474. doi: 10.1002/adhm.201900474

265. Mandriani B, Pelle E, Pezzicoli G, Strosberg J, Abate-Daga D, Guarini A, et al. Adoptive T-cell immunotherapy in digestive tract Malignancies: Current challenges and future perspectives. *Cancer Treat Rev* (2021) 100:102288. doi: 10.1016/j.ctrv.2021.102288

266. Ma S, Li X, Wang X, Cheng L, Li Z, Zhang C, et al. Current progress in CAR-T cell therapy for solid tumors. *Int J Biol Sci* (2019) 15(12):2548–60. doi: 10.7150/ijbs.34213

267. Pan K, Farrukh H, Chittepu V, Xu H, Pan CX, Zhu Z. CAR race to cancer immunotherapy: from CAR T, CAR NK to CAR macrophage therapy. *J Exp Clin Cancer Res* (2022) 41(1):119. doi: 10.1186/s13046-022-02327-z

268. Labanieh L, Mackall CL. CAR immune cells: design principles, resistance and the next generation. *Nature* (2023) 614(7949):635–48. doi: 10.1038/s41586-023-05707-3

269. Liu S, Liu H, Song X, Jiang A, Deng Y, Yang C, et al. Adoptive CD8(+)T-cell grafted with liposomal immunotherapy drugs to counteract the immune suppressive tumor microenvironment and enhance therapy for melanoma. *Nanoscale* (2021) 13(37):15789–803. doi: 10.1039/d1nr04036g

270. Guo Y, Zhi F, Chen P, Zhao K, Xiang H, Mao Q, et al. Green tea and the risk of prostate cancer: A systematic review and meta-analysis. *Med (Baltimore)* (2017) 96(13):e6426. doi: 10.1097/md.0000000000006426

271. Huang Y, Chen H, Zhou L, Li G, Yi D, Zhang Y, et al. Association between green tea intake and risk of gastric cancer: a systematic review and dose-response meta-analysis of observational studies. *Public Health Nutr* (2017) 20(17):3183–92. doi: 10.1017/s1368980017002208

272. Kim TL, Jeong GH, Yang JW, Lee KH, Kronbichler A, van der Vliet HJ, et al. Tea consumption and risk of cancer: an umbrella review and meta-analysis of observational studies. *Adv Nutr* (2020) 11(6):1437–52. doi: 10.1093/advances/nmaa077

273. Gee JR, Saltzstein DR, Kim K, Kolesar J, Huang W, Havighurst TC, et al. A phase II randomized, double-blind, presurgical trial of polyphenon E in bladder cancer patients to evaluate pharmacodynamics and bladder tissue biomarkers. *Cancer Prev Res (Phila)* (2017) 10(5):298–307. doi: 10.1158/1940-6207.Capr-16-0167

274. Kumar NB, Pow-Sang J, Egan KM, Spiess PE, Dickinson S, Salup R, et al. Randomized, placebo-controlled trial of green tea catechins for prostate cancer prevention. *Cancer Prev Res (Phila)* (2015) 8(10):879–87. doi: 10.1158/1940-6207.Capr-14-0324

275. Hu Y, McIntosh GH, Le Leu RK, Somashekar R, Meng XQ, Gopalsamy G, et al. Supplementation with Brazil nuts and green tea extract regulates targeted biomarkers related to colorectal cancer risk in humans. *Br J Nutr* (2016) 116(11):1901–11. doi: 10.1017/s0007114516003937

276. Seufferlein T, Ettrich TJ, Menzler S, Messmann H, Kleber G, Zipprich A, et al. Green tea extract to prevent colorectal adenomas, results of a randomized, placebo-controlled clinical trial. *Am J Gastroenterol* (2022) 117(6):884–94. doi: 10.14309/ajg.0000000000001706

277. Samavat H, Ursin G, Emory TH, Lee E, Wang R, Torkelson CJ, et al. A randomized controlled trial of green tea extract supplementation and mammographic density in postmenopausal women at increased risk of breast cancer. *Cancer Prev Res (Phila)* (2017) 10(12):710–8. doi: 10.1158/1940-6207.Capr-17-0187

278. Lazzeroni M, Guerrieri-Gonzaga A, Gandini S, Johansson H, Serrano D, Cazzaniga M, et al. A presurgical study of lecithin formulation of green tea extract in women with early breast cancer. *Cancer Prev Res (Phila)* (2017) 10(6):363–70. doi: 10.1158/1940-6207.Capr-16-0298

279. Hu J, Webster D, Cao J, Shao A. The safety of green tea and green tea extract consumption in adults - Results of a systematic review. *Regul Toxicol Pharmacol* (2018) 95:412–33. doi: 10.1016/j.yrtph.2018.03.019

10.3389/fimmu.2024.1331641

Appendix

67LR	67 kDa laminin receptor
α-KG	α-ketoglutarate
ACC	acetyl-CoA carboxylase
ACLY	ATP citrate lyase
ADCC	antibody-dependent cell-mediated cytotoxicity
ADP	adenosine diphosphate
Akt	protein kinase B
AMPK	adenosine monophosphate (AMP)-activated protein kinase
APCs	antigen-presenting cells
ARG1	arginase I
ASCT2	alanine/serine/cysteine transporter 2
ATP	adenosine triphosphate
bFGF	basic fibroblast growth factor
CAFs	cancer-associated fibroblasts
CAR-T	chimeric antigen receptor-modified T
CCL	C-C chemokine ligand
CTLs	cytotoxic T lymphocytes
COX-2	cyclooxygenase-2
CPT	carnitine palmitoyltransferase
CSF	colony stimulating factor
CTLA4	cytotoxic T lymphocyte antigen-4
CXCL	CXC chemokine ligand
CXCR	CXC chemokine receptor
D2HG	D-2-hydroxyglutarate
DCs	dendritic cells
DHFR	dihydrofolate reductase
DNL	*de novo* lipogenesis
dNTP	deoxyribonucleoside triphosphate
ECM	extracellular matrix
ECs	endothelial cells
EGCG	epigallocatechin gallate
EGC-M5	5-(3',5'-dihydroxyphenyl)-γ-valerolactone
EGFR	epidermal growth factor receptor
ERK	extracellular signal-regulated kinase
FAK	focal adhesion kinase
FASN	fatty acid synthase
FOXP3	forkhead box protein 3
G6PD	6-phosphogluconate dehydrogenase
G-CSF	granulocyte colony-stimulating factor
GDH	glutamate dehydrogenase
GLS	glutaminase
GLUT	glucose transporter
HCC	hepatocellular carcinoma
HER2	EGFR 2
HER3	EGFR 3
HGF	hepatocyte growth factor
HIF-1α	hypoxia-inducible factor-1alpha
HK	hexokinase
HSCs	hepatic stellate cells
ICAM-1	intercellular adhesion molecule 1
ICIs	immune checkpoint inhibitors
IDH	isocitrate dehydrogenase
IDO	indoleamine 2,3-dioxygenase
IFN-γ	interferon-gamma
IGF1R	insulin-like growth factor-1 receptor
IL	interleukin
iNOS	nitric oxide synthase
IR	insulin receptor
iTregs	induced Tregs
IRF-1	interferon regulatory factor 1
JAK	Janus kinase
LDH	lactate dehydrogenase
MAPK	mitogen-activated protein kinases
MDSCs	myeloid-derived suppressor cells
MHC	major histocompatibility complex
MHC-I	major histocompatibility complex class I
MMP	matrix metalloproteinase
MSCs	mesenchymal stem/stromal cells
mTOR	mammalian target of rapamycin
mTORC1	mTOR complex 1
MT1-MMP	membrane-type 1 MMP
NE	neutrophil elastase
NETs	neutrophil extracellular traps
NF-κB	nuclear factor-kappa B
NK cells	natural killer cells
nTregs	natural Tregs
NO	nitric oxide

Continued

NOX2	NADPH oxidase 2
PD-1	programmed death-1
PDGF	platelet-derived growth factor
PDGFR	PDGF receptor
PDH	pyruvate dehydrogenase
PDHA1	pyruvate dehydrogenase E1-α
PD-L1	programmed cell death ligand 1
PE	polyphenol E
PFK	phosphofructokinase
PGAM1	phosphoglycerate mutase-1
PGE2	prostaglandin E2
PI3K	phosphatidylinositol 3-kinase
PK	pyruvate kinase
PolyI:C	polyinosinic-polycytidylic acid
PPP	pentose phosphate pathway
RhoA	Ras homolog family member A
ROCK	Rho-associated kinase
ROS	reactive oxygen species
RTKs	receptor tyrosine kinases
Smad1	Smad family member 1
SNAT	sodium-coupled neutral amino acid transporter
SREBP1	sterol regulatory element-binding protein 1
STAT	signal transducer and activator of transcription
TAMs	tumor-associated macrophages
TANs	tumor-associated neutrophils
TCA	tricarboxylic acid cycle
TCR	T cell receptor
TECs	tumor-associated endothelial cells
TGF-β	transforming growth factor-beta
TIME	tumor immune microenvironment
TLR	toll-like receptor
TME	tumor microenvironment
TNBC	triple-negative breast cancer
Tregs	regulatory T cells
UDP	uridine diphosphate
UV	ultraviolet ray
VEGF	vascular endothelial growth factor
VEGFR	VEGF receptor

frontiers | Frontiers in Immunology

TYPE Original Research
PUBLISHED 12 April 2024
DOI 10.3389/fimmu.2024.1330228

OPEN ACCESS

EDITED BY
Wei Chong,
Shandong Provincial Hospital, China

REVIEWED BY
Shivam Priya,
The Ohio State University, United States
Amir Shadboorestan,
Tarbiat Modares University, Iran
Christoph F. A. Vogel,
University of California, Davis, United States

*CORRESPONDENCE
Jae Hwan Kim
kimjw7@yuhs.ac
Byoung Chul Cho
CBC1971@yuhs.ac
Kyoung-Ho Pyo
pkhpsh@gmail.com

†These authors have contributed equally to this work and share first authorship

RECEIVED 13 November 2023
ACCEPTED 09 January 2024
PUBLISHED 12 April 2024

CITATION
Kim DK, Lee CY, Han YJ, Park SY, Han H, Na K, Kim MH, Yang SM, Baek S, Kim Y, Hwang JY, Lee S, Kang S-s, Hong MH, Lim SM, Lee JB, Kim JH, Cho BC and Pyo K-H (2024) Exploring aryl hydrocarbon receptor expression and distribution in the tumor microenvironment, with a focus on immune cells, in various solid cancer types. *Front. Immunol.* 15:1330228. doi: 10.3389/fimmu.2024.1330228

Exploring aryl hydrocarbon receptor expression and distribution in the tumor microenvironment, with a focus on immune cells, in various solid cancer types

Dong Kwon Kim[1,2†], Chai Young Lee[2†], Yu Jin Han[2†], So Young Park[2], Heekyung Han[2], Kwangmin Na[2], Mi Hyun Kim[2], Seung Min Yang[2], Sujeong Baek[2], Youngtaek Kim[2], Joon Yeon Hwang[2], Seul Lee[1,2], Seong-san Kang[3], Min Hee Hong[4], Sun Min Lim[4], Jii Bum Lee[4], Jae Hwan Kim[2*], Byoung Chul Cho[4,5*] and Kyoung-Ho Pyo[2,4,5,6*]

[1]Brain Korea 21 PLUS Project for Medical Science, Yonsei University College of Medicine, Seoul, Republic of Korea, [2]Severance Biomedical Science Institute, Yonsei University College of Medicine, Seoul, Republic of Korea, [3]Jeuk Institute for Cancer Research, Jeuk Co. Ltd., Gumi, Republic of Korea, [4]Division of Medical Oncology, Department of Internal Medicine and Yonsei Cancer Center, Severance Hospital, Yonsei University College of Medicine, Seoul, Republic of Korea, [5]Yonsei New Il Han Institute for Integrative Lung Cancer Research, Yonsei University College of Medicine, Seoul, Republic of Korea, [6]Department of Research Support, Yonsei Biomedical Research Institute, Yonsei University College of Medicine, Seoul, Republic of Korea

Introduction: Aryl hydrocarbon receptor (AhR) is a transcription factor that performs various functions upon ligand activation. Several studies have explored the role of AhR expression in tumor progression and immune surveillance. Nevertheless, investigations on the distribution of AhR expression, specifically in cancer or immune cells in the tumor microenvironment (TME), remain limited. Examining the AhR expression and distribution in the TME is crucial for gaining insights into the mechanism of action of AhR-targeting anticancer agents and their potential as biomarkers.

Methods: Here, we used multiplexed immunohistochemistry (mIHC) and image cytometry to investigate the AhR expression and distribution in 513 patient samples, of which 292 are patients with one of five solid cancer types. Additionally, we analyzed the nuclear and cytosolic distribution of AhR expression.

Results: Our findings reveal that AhR expression was primarily localized in cancer cells, followed by stromal T cells and macrophages. Furthermore, we observed a positive correlation between the nuclear and cytosolic expression of AhR, indicating that the expression of AhR as a biomarker is independent of its localization. Interestingly, the expression patterns of AhR were categorized into three clusters based on the cancer type, with high AhR expression levels being found in regulatory T cells (Tregs) in non-small cell lung cancer (NSCLC).

Discussion: These findings are anticipated to serve as pivotal evidence for the design of clinical trials and the analysis of the anticancer mechanisms of AhR-targeting therapies.

KEYWORDS

aryl hydrocarbon receptor, tumor microenvironment, T-lymphocyte, macrophage, regulatory T cell

1 Introduction

Aryl hydrocarbon receptor (AhR) is a cytosolic ligand-activated transcription factor that is activated by various exogenous and endogenous molecules. Once activated, AhR translocates to the nucleus and forms a heterodimer with AhR nuclear translocator (ARNT). The AhR-ARNT complex then binds to specific DNA sequences known as xenobiotic response elements, which are located in the promoter region of a target gene, initiating the transcription of the downstream target genes (1, 2). AhR is widely expressed in the body and regulates the expression of various genes, thereby governing various cellular processes, including detoxification and metabolism (3–5). AhR can have different biological effects depending on its context, the cell type, and the activating ligand.

AhR plays an important role in carcinogenesis and tumor immunity (6–8). However, whether AhR positively or negatively regulates carcinogenesis remains inconclusive. DiNatale et al. demonstrated that AhR expression was higher in head and neck squamous cell carcinoma (HNSCC) tissues than in normal tissues, and AhR antagonists significantly decreased HNSCC cell migration (9). AhR has both tumor-promoting and suppressive effects in bladder cancer (10). AhR expression is higher in lung cancer tissues than in normal tissues, indicating that AhR has a tumor-suppressive role in carcinogenesis (11). In contrast, Breitenbucher et al. suggested that the knockdown of endogenous AhR in mice induced epithelial-mesenchymal transition signatures and metastasis (12).

Since AhR has been shown to be involved in carcinogenesis and tumor immunity, extensive studies have been conducted to elucidate the role of AhR in the tumor microenvironment (TME). Despite these efforts, the role of AhR in different cancer types at different stages remains unclear. The controversy surrounding the effect of AhR on carcinogenesis and tumor immunity may be attributed to the type, stage, and degree of cancer malignancy. Since AhR is an emerging potential target for anticancer therapy, clarifying its role in specific cancer types is crucial to facilitate patient stratification. Investigating the expression and localization of AhR may be a logical starting point since it may help unveil the molecular mechanisms involved in carcinogenesis.

Here, we evaluated the AhR expression and distribution in five solid cancer types: HNSCC, bladder cancer, colorectal cancer, esophageal cancer, and non-small cell lung cancer (NSCLC). Additionally, since AhR translocates from the cytosol to the nucleus upon activation, the comparison of the nuclear and cytosolic expression of AhR may provide valuable insights into the differential roles of AhR in each cancer type (13). To date, the number of AhR studies done on large cohorts is limited. By investigating a large cohort of patients with different clinical parameters, we aimed to address the knowledge gap regarding the expression of AhR in various cancers. Our findings may elucidate the mechanisms underlying AhR-mediated pathways in cancer and immune cells in the TME across different cancer types. We hope that our findings will pave the way for the development of anticancer therapies targeting AhR and for patient stratification to optimize the treatment approaches.

2 Methods

2.1 Sample preparation

Five tissue microarray (TMA) slides were purchased from Tissue Array. These slides were used to analyze the tissue samples from patients with different cancers: bladder cancer (Tissue ID: BL481d, 48 cores), colorectal cancer (Tissue ID: CO1002d, 100 cores), HNSCC (Tissue ID: HN802d, 80 cores), NSCLC (Tissue ID: LC10012b, 100 cores), and esophageal cancer (Tissue ID: ES1922a, 192 cores). Each TMA core had a specific size (2.0 mm for bladder cancer, 1.0 mm for colorectal cancer, 1.5 mm for HNSCC, 1.0 mm for NSCLC, and 1.0 mm for esophageal cancer). The clinical and demographic parameters of the patients are presented in Table 1. Out of a total of 520 cores, three cores from colorectal cancer, two cores from NSCLC, and two cores from esophageal cancer were excluded from the analysis due to their absence on the slides during the experimental evaluation.

2.2 Multiplexed immunohistochemistry (mIHC)

For the multiplexed immunohistochemical staining of the sections, we used BOND RX Fully Automated Research Stainer (cat: 21.2821; Leica Biosystems) and an Opal Polaris 7Color IHC Detection Kit (cat: P-000003, Akoya Biosciences). All procedures

TABLE 1 Demographic and clinical information of the patient samples from TMA slides of five solid cancer types, including age, sex, cancer grade, cancer stage, and metastasis.

Bladder			Colon			Esophagus			Head and neck			Lung		
Age	Total Number (n)	Percentage (%)	Age	Total Number (n)	Percentage (%)	Age	Total Number (n)	Percentage (%)	Age	Total Number (n)	Percentage (%)	Age	Total Number (n)	Percentage (%)
11-20	1	2.1	11-20	–	–	11-20	–	–	11-20	2	2.5	11-20	2	2
21-30	2	4.2	21-30	8	7.9	21-30	–	–	21-30	7	8.8	21-30	4	4
31-40	5	10.4	31-40	15	14.9	31-40	–	–	31-40	5	6.3	31-40	8	8
41-50	11	22.9	41-50	22	21.8	41-50	23	11.9	41-50	24	30	41-50	8	8
51-60	13	27.1	51-60	32	31.7	51-60	62	32.1	51-60	19	23.8	51-60	34	34
61-70	9	18.8	61-70	14	13.9	61-70	92	47.7	61-70	17	21.3	61-70	38	38
71-80	5	10.4	71-80	10	9.9	71-80	16	8.3	71-80	6	7.5	71-80	6	6
81-90	2	4.2	81-90	–	–	81-90	–	–	81-90	–	–	81-90	–	–
Sex	Total Number (n)	Percentage (%)	Sex	Total Number (n)	Percentage (%)	Sex	Total Number (n)	Percentage (%)	Sex	Total Number (n)	Percentage (%)	Sex	Total Number (n)	Percentage (%)
Female	13	27.1	Female	23	22.8	Female	40	20.7	Female	12	15	Female	18	18
Male	35	72.9	Male	78	77.2	Male	153	79.3	Male	68	85	Male	82	82
Grade	Total Number (n)	Percentage (%)	Grade	Total Number (n)	Percentage (%)	Grade	Total Number (n)	Percentage (%)	Grade	Total Number (n)	Percentage (%)	Grade	Total Number (n)	Percentage (%)
Unknown	–	–	Unknown	57	56.4	Unknown	97	50.3	Unknown	20	25	Unknown	58	58
1	–	–	1	12	11.9	1	30	15.5	1	16	20	1	3	3
1-2	–	–	1-2	–	–	1-2	–	–	1-2	1	1.3	1-2	–	–
2	–	–	2	25	24.8	2	34	17.6	2	33	41.3	2	18	18
2-3	–	–	2-3	–	–	2-3	–	–	2-3	–	–	2-3	2	2
3	–	–	3	7	6.9	3	32	16.6	3	10	12.5	3	19	19
Stage	Total Number (n)	Percentage (%)	Stage	Total Number (n)	Percentage (%)	Stage	Total Number (n)	Percentage (%)	Stage	Total Number (n)	Percentage (%)	Stage	Total Number (n)	Percentage (%)
Unknown	8	16.7	Unknown	64	63.4	Unknown	–	–	Unknown	10	12.5	Unknown	55	55
I	9	18.8	I	–	–	I	–	–	I	3	3.8	I	–	–
IA	–	–	IA	–	–	IA	–	–	IA	–	–	IA	1	1

(Continued)

10.3389/fimmu.2024.1330228

TABLE 1 Continued

Bladder			Colon			Esophagus			Head and neck			Lung		
IB	–	–	IB	–	–	IB	–	–	IB	–	–	IB	27	27
II	15	31.3	II	–	–	II	–	–	II	21	26.3	II	–	–
IIA			IIA	24	23.8	IIA	–	–	IIA	–	–	IIA	12	12
III	15	31.3	III	–	–	III	–	–	III	21	26.3	III	3	3
IIIB	–	–	IIIB	10	9.9	IIIB	–	–	IIIB	–	–	IIIB	2	2
IIIC	–	–	IIIC	2	2.0	IIIC	–	–	IIIC	–	–	IIIC	–	–
IV	1	2.1	IV	–	–	IV	–	–	IV	–	–	IV	–	–
IVA	–	–	IVA	–	–	IVA	–	–	IVA	25	31.3	IVA	–	–
Type	Total Number (n)	Percentage (%)	Type	Total Number (n)	Percentage (%)	Type	Total Number (n)	Percentage (%)	Type	Total Number (n)	Percentage (%)	Type	Total Number (n)	Percentage (%)
AT	–	–	AT	14	13.9	AT	71	36.8	AT	–	–	AT	45	45
Malignant	40	83.3	Malignant	37	36.6	Malignant	97	50.3	Malignant	70	87.5	Malignant	45	45
Metastasis	–	–	Metastasis	9	8.9	Metastasis	–	–	Metastasis	–	–	Metastasis	–	–
NAT	–	–	NAT	22	21.8	NAT	25	13.0	NAT	–	–	NAT	–	–
Normal	8	16.7	Normal	19	18.8	Normal	–	–	Normal	10	12.5	Normal	10	10

10.3389/fimmu.2024.1330228

were performed according to the manufacturer's instructions. In summary, deparaffinized sections were incubated with citrate- or Tris-based antigen unmasking solutions (for heat-induced epitope retrieval) at 98°C for 20 min. They were then treated with hydrogen peroxide and a protein-blocking reagent to prevent the nonspecific binding of antibodies to the sections. Sections were sequentially treated with the primary antibodies, horseradish peroxidase (HRP)-conjugated antibodies, and specific fluorophores to detect the proteins of interest. Multiple staining rounds were performed using the following anti-human antibodies: anti-AhR (cat: LS-C783005-100; LS Biosciences), anti-CD68 (cat: 76437; Cell Signaling Technology), anti-CD4 (cat: ab181724; Abcam), anti-CD8 (cat: CD8-4B11-L-CE; Leica Biosystems), anti-FoxP3 (cat: 98377; Cell Signaling Technology, anti-PanCK (cat: AE1/AE3-601-L-CE; Leica Biosystems). Tissue sections were counterstained with Spectral DAPI (4′,6-diamidino-2-phenylindole, cat: SKU FP1490; Akoya Biosciences).

2.3 Whole-slide scanning and matrix data generation

Images (200× magnification) of the whole tissue contents were generated using whole-slide scanning by using Vectra Polaris Automated Quantitative Pathology Imaging System (cat: CLS143455; Akoya Biosciences). Multispectral images for analysis were defined and selected within the whole tissue using Phenochart whole slide contextual viewer software (version 1.12 for Windows; Akoya Biosciences). The inForm® software (version 2.6 for Windows; Akoya Biosciences), equipped with an integrated algorithm for tissue analysis, was employed to transform the multispectral image data into numerical data. These data encompassed both numerical and spatial information regarding the tumor nest and stromal region, defining the cell components (nuclear, cytosolic, and membrane margins), classifying the cell populations and the intensities of each marker. Cell populations were discerned based on the distinctive patterns of CD marker expression, each exhibiting unique cellular properties, such as nuclear, cytosolic, and membranal sizes and shapes (CD4/8 = T cells; CD68 = macrophages; Pan-CK = epithelial cells or cancer cells; FoxP3 = Treg). The differentiation between the tumor nest and stroma, as well as the area calculations, were done based on the pan-cytokeratin staining patterns by utilizing an algorithm integrated into the inForm® software. The integrated matrix files were derived from the segmentation of cells and tissues from the TMA data.

2.4 Image cytometry and analysis

The required fluorescence values and labels were extracted from a previously obtained matrix file obtained using inForm®. These data included the fluorescence intensity in the nucleus and cytosol. The extracted CSV file was converted into an FCS file using the R program and the packages BioBase (R/Bioconductor, 3.17), FlowCore (R/Bioconductor, 2.10), and FlowViz (R/Bioconductor, 3.17). The FCS file was subsequently converted into a raw file for cytometric image analysis using FlowJo (version 10.9.0 for Windows). Through this process, we analyzed the cancer and immune cells within the TME and quantified the AhR expression levels (Supplementary Figure 1). The image cytometry data obtained were processed via gating to determine the proportion of cells expressing AhR by distinguishing them based on the T-cell markers CD4/8, the macrophage marker CD68, the cancer marker Pan-CK, and the Treg marker FoxP3 (Supplementary Figure 2). The image cytometry results obtained, which were distinguished based on the nuclear and cytosolic AhR expression, were used for analysis. A complex heatmap was generated using pheatmap (R/CRAN, 1.0.12), and the bar plots were visualized using ggplot2 (R/CRAN, 3.4.3) to generate the outcomes.

2.5 Statistical analysis

Data are reported as the mean ± SEM. Statistical analysis was performed using analysis of variance (ANOVA) with the Mantel-Cox log-rank test to assess the significant differences using GraphPad Prism (version 7.00 for Windows; GraphPad Software). Statistical analysis of the flow cytometry data was performed using the t-test in GraphPad Prism. The correlations between the nuclear and cytosolic AhR expression values between normal and malignant tissues were analyzed using the chi-square test with $\chi 2$ correction or Fisher's exact test for the categorical variables.

3 Results

3.1 Multiplexed immunohistochemistry (mIHC) analysis reveals differential AhR expression in the tumor microenvironment of five cancer types

To investigate AhR expression in the TME of the five cancer types (HNSCC, bladder cancer, colorectal cancer, esophageal cancer, and NSCLC), which contains cancer and immune cells, five TMA slides were subjected to mIHC analysis. The tissue samples from 520 healthy and malignant patients were successfully stained for cell phenotyping and analysis of the heterogeneity of AhR expression. Figure 1A illustrates the process flow used for image cytometry of the slides used for TMA. After performing mIHC staining, the TMA slides underwent whole-slide imaging to analyze the various fluorescence signals and quantify the relevant information from the discrete tumor nests and stromal regions identified, as well as to determine the expression of individual fluorescent markers in each cell within the TME. The acquired data were converted into a CSV matrix file and further processed into input files compatible with the image cytometry analysis ones, FCS files, for the subsequent analysis. The overall workflow of this analytical method is described in Supplementary Figure 1, and the gating method used for the image cytometry data is detailed in Supplementary Figure 2. Figure 1B shows a representative mIHC image of the cancer-adjacent colon tissue

10.3389/fimmu.2024.1330228

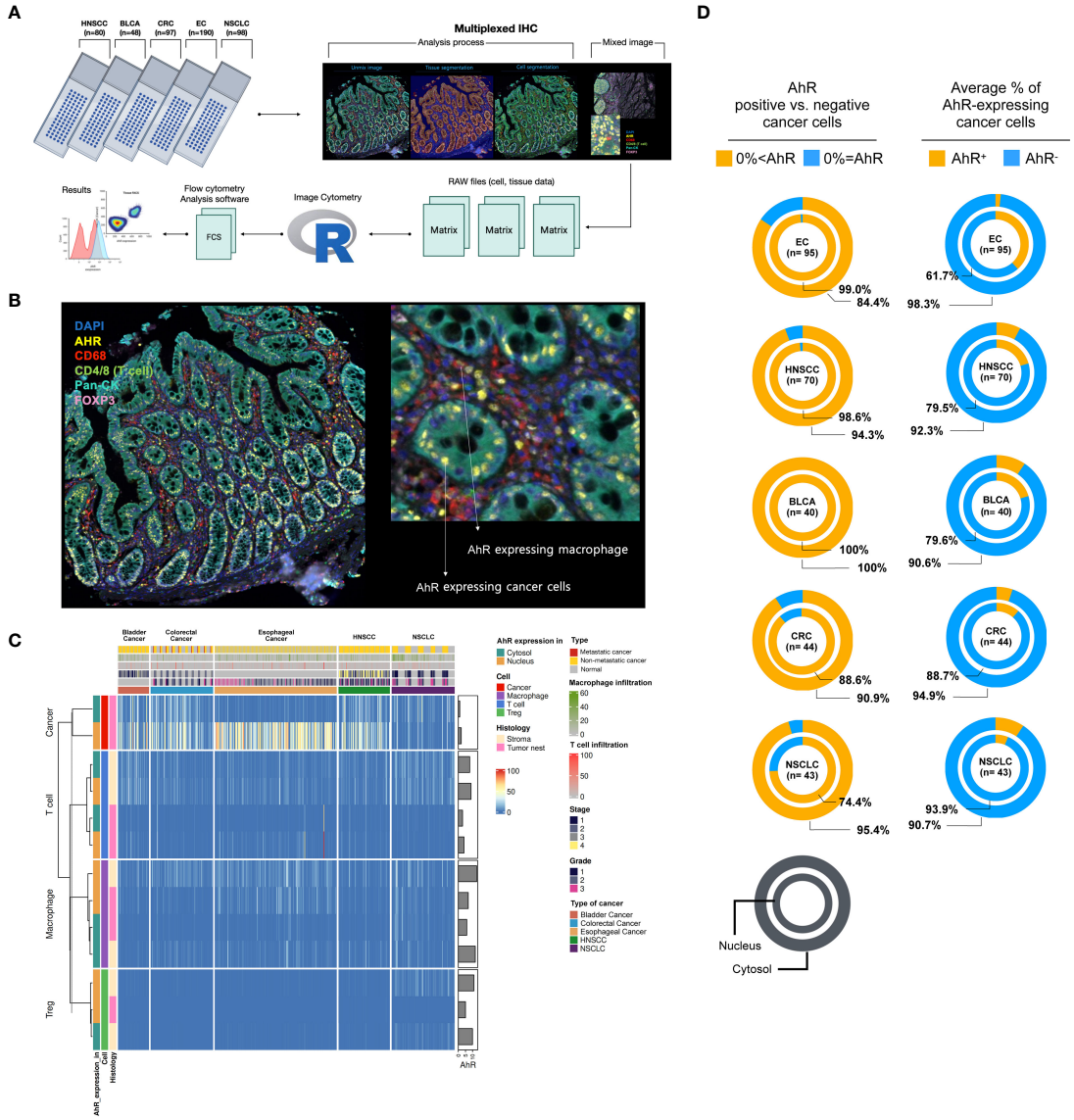

FIGURE 1
AhR expression and localization in the TME of bladder, colorectal, esophageal, head and neck, and non-small cell lung cancers. **(A)** Scheme of the workflow used for generating AhR expression data from five FFPE TMA slides: NSCLC (non-small cell lung cancer, N = 98), HNSCC (head and neck squamous cell carcinoma, N = 80), CRC (colorectal cancer, N = 97), EC (esophageal cancer, N = 190), and BLCA (bladder cancer, N = 48). Prior to cell segmentation and tissue segmentation using the deep-learning inForm algorithm, five TMA slides were stained with six antibodies, DAPI, and anti-AhR, -CD68, -CD4, -CD8, -Pan-CK, and -FoxP3, using Vectra Polaris for mIHC image generation. The resulting data were manipulated to perform image cytometry for phenotyping and AhR expression analysis. **(B)** Representative mIHC image of the region of interest stained with six antibodies: DAPI for nucleus, Pan-CK for cancer/epithelial cells, CD4 and CD8 for T cells, CD68 for macrophages, and FoxP3 for Tregs. **(C)** Heatmap summarizing the AhR expression in five different tissue samples: NSCLC, HNSCC, colorectal cancer, esophageal cancer, and bladder cancer. The resulting data were clustered based on the AhR expression in the cytosol or nucleus of cancer/epithelial cells, T cells, macrophages, and Tregs. **(D)** Pie charts depicting the AhR-positive (AhR^+) and -negative (AhR^-) cancer cells (left) and average percentage of AhR-expressing cancer cells (right) in the cytosol and nucleus of NSCLC, HNSCC, CRC (colorectal cancer), EC (esophageal cancer), and BLCA (bladder cancer) cells.

stained with six markers: DAPI for the nucleus, Pan-CK for cancer or epithelial cells, CD4 and CD8 for T cells, CD68 for macrophages, and FoxP3 for Tregs. AhR-expressing epithelial cells and macrophages are represented in yellow and are surrounded by cyan blue Pan-CK+ epithelial cells and red CD68+ macrophages, respectively, as indicated by the arrows (Figure 1B, image on the right). The columns in the heatmap in Figure 1C include clinical metadata such as the stage, grade, and metastasis, as well as information regarding T-cell and tumor-associated macrophage (TAM) infiltration. In the rows, the AhR expression levels in the nucleus and cytosol of each immune cell are presented as percentages. Additionally, the positional information of the cells, whether in the tumor nest or stroma, is provided in the rows. The key color in the heatmap indicates the proportion of cells expressing AhR among all cells constituting the tissue core. For example, 100% of nucleus AhR+ Pan-CK means that 100% of the cancer cells express AhR in the nucleus. Based on the dendrogram of each marker obtained through hierarchical clustering (H-clustering), the

AhR expression pattern was distinct between cancer and immune cells, with clear AhR expression patterns being observed within T cells, Tregs, and macrophages. In most cases, the highest AhR expression level was observed in the nucleus, and immune cells tended to have a higher AhR expression in the stroma than in the tumor nest. The clinical metadata and expression patterns for each core are shown in Supplementary Tables 1–5. AhR expression was the most pronounced in tumors. AhR expression was predominantly observed across the five cancer types, even when distinguishing between the nucleus and cytosol. In particular, for esophageal cancer, a 99% and 84.4% AhR expression was observed in the nucleus and cytosol, respectively, with the highest proportion of AhR non-expression being found in the cytosol (n = 95). Interestingly, bladder cancer exhibited a 100% AhR expression in both the nucleus and cytosol (n = 40). In colorectal cancer, AhR expression in the nucleus and cytosol was found in 88.6% and 90.9% of samples (n = 40), respectively. In NSCLC, nuclear and cytosolic AhR expression was observed in 74.4% and 95.4% of the samples (n = 43), with the highest proportion of non-expression being found in the nucleus (Figure 1D, left image). To further investigate this trend, we assessed the average AhR expression in malignant samples across five different cancer types. Notably, the average AhR expression does not indicate the percentage of individual cancer tissues expressing AhR. Instead, it signifies the average proportion of cells expressing AhR in the TME. The highest nuclear AhR expression (38.3%, n = 95) was found in esophageal cancer samples. Interestingly, in contrast with the nuclear expression proportion, the cytosolic expression was the lowest (1.7%) among all the cancer samples. In HNSCC, the nuclear and cytosolic AhR expression was 20.5% and 7.7%, respectively (n = 70). Similarly, bladder cancer demonstrated a comparable AhR expression pattern, with expression rates of 20.4% and 9.4%, respectively. In colorectal cancer, the nuclear and cytosolic AhR expression levels were 11.3% and 5.1% (n = 44), whereas in NSCLC, they were 6.1% and 9.3% (n = 43), respectively. Notably, NSCLC cells exhibited a higher AhR expression in the cytosol than in the nucleus, distinguishing it from other cancer types (Figure 1D, image on the right). Chi-square analysis was conducted to compare the nuclear and cytosolic AhR expression between normal and malignant tissues. Overall, no significant difference in AhR expression was observed between normal and malignant tissues across the three cancer types analyzed (colorectal cancer, esophageal cancer, and NSCLC). Bladder cancer and HNSCC were excluded from the chi-square analysis because samples lacking AhR characteristics (AhR expression = 0%) were absent in both cancer types (Supplementary Table 6).

3.2 AhR expression patterns in head and neck squamous cell carcinoma (HNSCC)

To comprehensively analyze the AhR expression patterns in individual cancer types, heat maps were created for each specific cancer type and analyzed. The clusters in the heatmap shown in Figure 2A were divided based on the nuclear or cytosolic AhR expression in cancer and immune cells in the head and neck tissue samples. Upon examination of both normal and malignant head and neck tissue samples, H-clustering based on AhR expression revealed that the highest AhR expression was found in these cancer cells, particularly in the nucleus, as opposed to the cytosol. Although AhR was not detected in immune cells within the tumor nest region, AhR was expressed in T cells and macrophages in the stromal regions (Figure 2A). The influence of the different cancer stages on AhR expression in HNSCC cells was further investigated, and a diminishing trend in AhR expression with an advancing cancer grade was observed (Figure 2B). Representative mIHC images of AhR-expressing cancer cells and immune cells (macrophages, T cells, and Tregs) in malignant head and neck tissues are found in Figure 2C (left side). AhR expression in cancer cells, localized to the nucleus, was characterized by distinct yellow staining in the DAPI regions of each cancer cell line, as identified via cyan blue Pan-CK staining. A diffuse expression, with a lower yellow staining intensity surrounding the nucleus, illustrates the cytosolic AhR expression. Macrophages were identified by the red CD68 staining of the cell body. Overlapping blue DAPI and yellow AhR staining indicated AhR expression. T-cell AhR expression is represented by yellow staining in the nucleus and cell body region and phenotyped by green CD4/8 staining. To identify the Tregs, FoxP3, which stains the nucleus of T cells, was used. Tregs were identified by a magenta FoxP3 stained nucleus surrounded by a green CD4/8 stained cell body region. AhR expression in Tregs is illustrated by the overlap of magenta FoxP3 and yellow AhR staining. On the right side of Figure 2C, the five images demonstrate the absence of AhR expression in both cancer and immune cells. These cells lack yellow staining in both the nucleus and cytosol (Figure 2C). To investigate the correlation between AhR expression in the nucleus and cytosol, the percentage of cells expressing AhR in each compartment in individual head and neck samples was examined. The analysis revealed a statistically significant positive correlation between the parameters, indicating a positive relationship between AhR expression in the nucleus and cytosol ($P < 0.0001$) (Figure 2D). Figure 2E reveals a strong positive relationship between AhR expression in individual immune cell types in the tumor nest and that in the stroma (Figure 2E). The potential effect of immune cell infiltration into the tumor nest on AhR expression in malignant tissues was investigated. Although not statistically significant, a positive correlation was observed between the TAM infiltration degree and AhR expression in HNSCC cells ($P = 0.0514$) (Figure 2F). In contrast, no discernible correlation was observed between the T-cell infiltration degree in the tumor nest and AhR expression in malignant tissues (Figure 2G).

3.3 AhR expression patterns in bladder cancer

AhR expression was high in bladder cancer cells, similar to the results obtained in HNSCC cells. Similar to HNSCC, the AhR expression was higher in the nucleus than in the cytosol. Additionally, AhR was detected in T cells and macrophages in the stromal regions (Figure 3A). In contrast with HNSCC, which shows a AhR expression decrease with an increasing cancer grade, AhR

10.3389/fimmu.2024.1330228

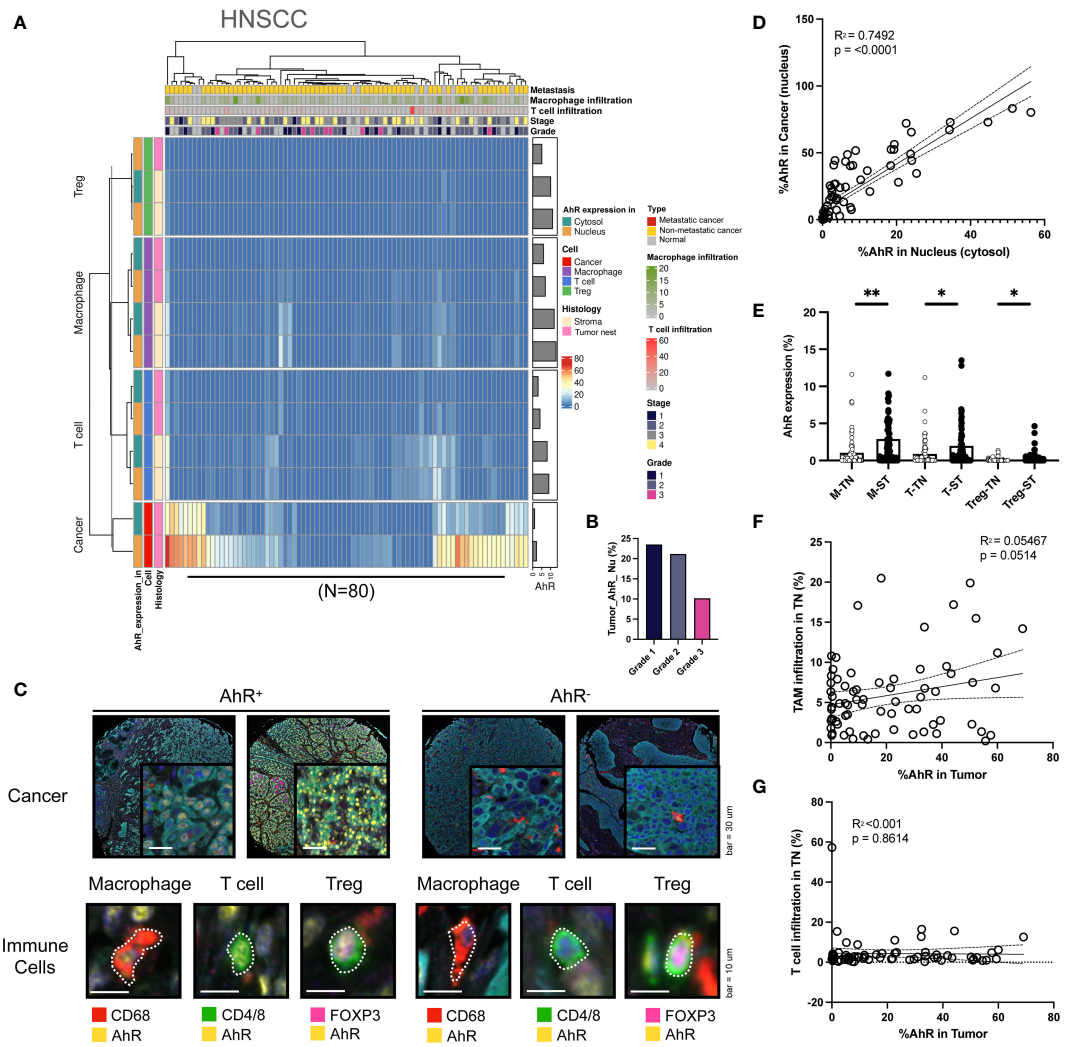

FIGURE 2
AhR expression patterns in head and neck squamous cell carcinoma (HNSCC). **(A)** Heatmap summarizing the AhR expression and localization in cancer/epithelial cells, T cells, macrophages, and Tregs in normal and malignant head and neck tissues (N = 80). **(B)** AhR expression in cancer cells in malignant head and neck tissues with varying cancer grades. **(C)** Representative images of AhR-expressing (AhR^+) and non-AhR-expressing (AhR^-) head and neck cancer cells, along with AhR-expressing immune cells, including macrophages, T cells, and Tregs. **(D)** AhR expression in the cytosol was positively correlated with that in the nucleus ($P < 0.0001$). **(E)** AhR expression in T cells (T), macrophages (M), and Tregs in the stroma (ST) and tumor nest (TN). **(F)** Correlation plot showing no significant correlation between AhR expression in the cancer cell nucleus and the TAM infiltration degree in the tumor nest (TN)($P = 0.0514$). **(G)** Correlation plot showing no significant correlation between AhR expression in the cancer cell nucleus and the T-cell infiltration degree in the TN. *$P < 0.05$; **$P < 0.01$.

expression was consistent across grade 1–3 cancers, whereas it increased in the stage 4 bladder cancer samples (Figure 3B). The images on the left in Figure 3C illustrate representative mIHC images of AhR-expressing cancer and immune cells (macrophages, T cells, and Tregs), which can be distinguished by the yellow AhR stained areas in the bladder cancer tissues. In contrast, the cancer and immune cells in the right images exhibit no AhR expression, as indicated by the absence of yellow regions. Similar to what was found for HNSCC, the nuclear AhR expression was significantly positively correlated with the cytosolic one ($P < 0.0001$) (Figure 3D). Similar to those in HNSCC, the AhR expression levels in specific immune cell types (macrophages, T cells, and Tregs) in the tumor nest were positively correlated with the stromal ones (Figure 3E). No clear relationship between the tumor-associated macrophages (TAM) infiltration level in the tumor nest and AhR expression was observed in cancer cells (Figure 3F). Nevertheless, the T-cell infiltration level in the tumor nest was positively correlated with AhR expression in cancer cells (Figure 3G).

3.4 AhR expression patterns in colorectal cancer

In colorectal cancer cells, the nuclear AhR expression was higher than the cytosolic one. AhR was also detected T cells and macrophages in the stroma (Figure 4A). The AhR expression in cancer cells increased with an increasing colorectal cancer grade, similar to the results obtained for HNSCC (Figure 4B). In Figure 4C,

10.3389/fimmu.2024.1330228

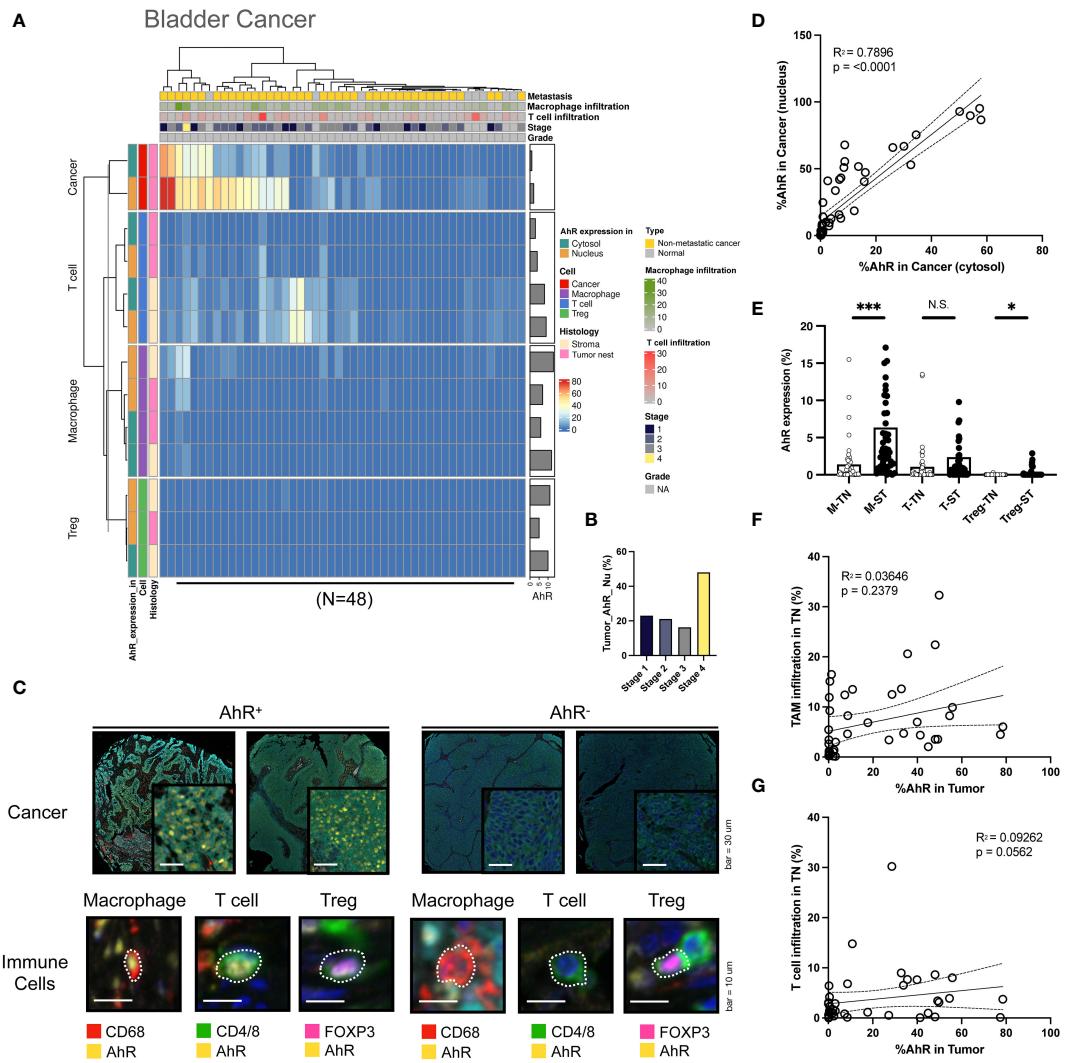

FIGURE 3
AhR expression patterns in bladder cancer. **(A)** Heatmap summarizing the AhR expression and localization in cancer/epithelial cells, T cells, macrophages, and Tregs in normal and malignant bladder tissues (N = 48). **(B)** AhR expression in malignant bladder tissues of varying cancer stages. **(C)** Representative images of AhR-expressing (AhR^+) and non-AhR^-expressing (AhR^-) bladder cancer cells, along with AhR-expressing immune cells, including macrophages, T cells, and Tregs. **(D)** AhR expression in the cytosol is positively correlated with the nuclear AhR expression ($P < 0.0001$). **(E)** AhR expression in T cells (T), macrophages (M), and Tregs in the stroma (ST) and tumor nest (TN). **(F)** Correlation plot showing no significant correlation between AhR expression in cancer cell nucleus and the TAM infiltration degree in the TN($P = 0.0562$). **(G)** Correlation plot showing no significant correlation between the AhR expression in cancer cell nucleus and the T-cell infiltration degree in the TN. N.S., no significant difference, $*P < 0.05$, $***P < 0.001$.

the images on the left show mIHC images of AhR-expressing cancer cells and immune cells (macrophages, T cells, and Tregs) in colorectal tissues, which are stained in yellow. In contrast, the images on the right depict cancer and immune cells lacking AhR expression, as evidenced by the absence of yellow staining (Figure 4C). Similar to the results obtained for the other cancer types, the nuclear and cytosolic AhR expression were significantly positively correlated in colorectal cancer (Figure 4D). The AhR expression levels in each immune cell type (macrophages, T cells, and Tregs) within the tumor nest were positively correlated with the stromal AhR expression in the corresponding cell type, which was comparable to that found in bladder cancer and HNSCC (Figure 4E). The immune cell infiltration degree in the tumor nest was not correlated with AhR expression in the tumor region for either TAMs or T cells (Figures 4F, G).

3.5 AhR expression patterns in esophageal cancer

Similar to the aforementioned cancer types, AhR is abundantly expressed in esophageal cancer cells. AhR expression was higher in the nucleus than in the cytosol. Compared with that in bladder cancer and HNSCC, the nuclear AhR expression in cancer cells was significantly higher than the cytosolic one. Moreover, AhR-expressing T cells and macrophages were not only observed in the stromal regions, but also

10.3389/fimmu.2024.1330228

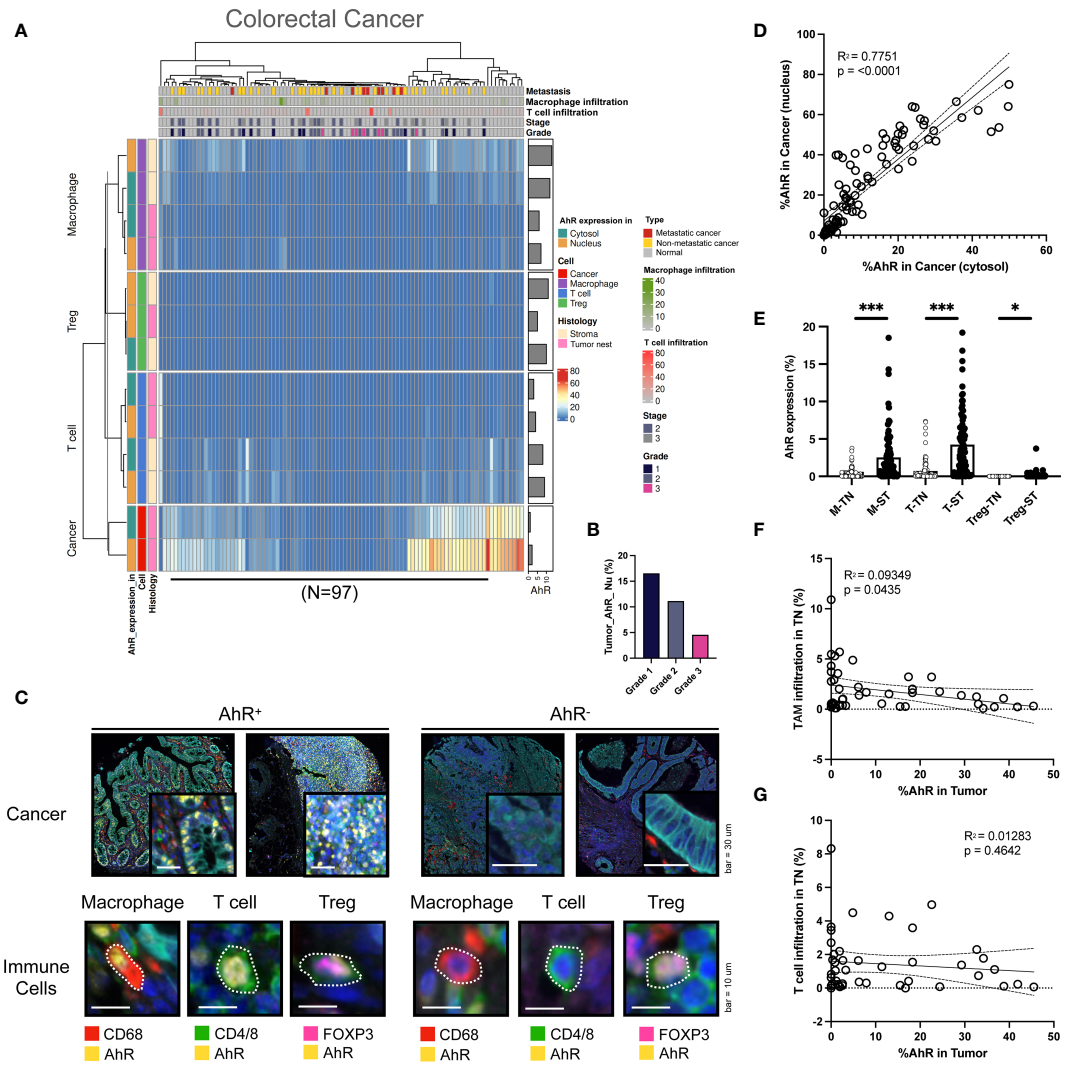

FIGURE 4
AhR expression patterns in colorectal cancer. **(A)** Heatmap summarizing the AhR expression and localization in cancer/epithelial cells, T cells, macrophages, and Tregs in normal and malignant colorectal tissues (N = 97). **(B)** AhR expression in malignant colorectal tissues of varying cancer grades. **(C)** Representative images of AhR-expressing (AhR^+) and non-AhR-expressing (AhR^-) colorectal cancer cells, along with AhR-expressing immune cells, including macrophages, T cells, and Tregs. **(D)** AhR expression in the cytosol is positively correlated with the nuclear AhR expression ($P < 0.0001$). **(E)** AhR expression in T cells (T), macrophages (M), and Tregs in the stroma (ST) and tumor nest (TN). **(F)** Correlation plot showing an increase in AhR expression in cancer cell nucleus as the degree of TAM infiltration in the TN decreased. **(G)** Correlation plot showing no significant correlation between AhR expression in cancer cell nucleus and the T-cell infiltration degree in the TN. *P < 0.05, ***P < 0.001.

within the tumor nest, indicating that AhR is expressed in the immune cells that infiltrated the tumor nest. This pattern was not observed in other cancer types (Figure 5A). In contrast with that obtained for the aforementioned cancer types, the nuclear AhR expression in cancer cells increased with an advancing cancer grade (Figure 5B). The images on the left in Figure 5C show mIHC images of AhR-expressing cancer and immune cells (macrophages, T cells, and Tregs) in esophageal tissues, stained yellow. Conversely, the images on the right depict cancer and immune cells that do not express AhR, as evidenced by the absence of yellow staining. Compared with the other cancer types, the nuclear and cytosolic AhR expressions were significantly positively correlated in esophageal cancer (Figure 5D). The AhR expression levels in each immune cell type (macrophages, T cells, and Tregs) within the tumor nest were positively correlated with the stromal AhR expression in the corresponding cell type, a pattern consistent with those found for the other cancer types (Figure 5E). No clear pattern was found between the immune cell infiltration degree in the tumor nest and AhR expression in the tumor region for either TAMs or T cells (Figures 5F, G).

3.6 AhR expression patterns in non-small cell lung cancer (NSCLC)

Although AhR expression was elevated in NSCLC cells, similar to what was found in other cancer types, it was significantly higher in the cytosol than in the nucleus. Furthermore, T cells and macrophages in the stromal environment expressed AhR, consistent with the results

10.3389/fimmu.2024.1330228

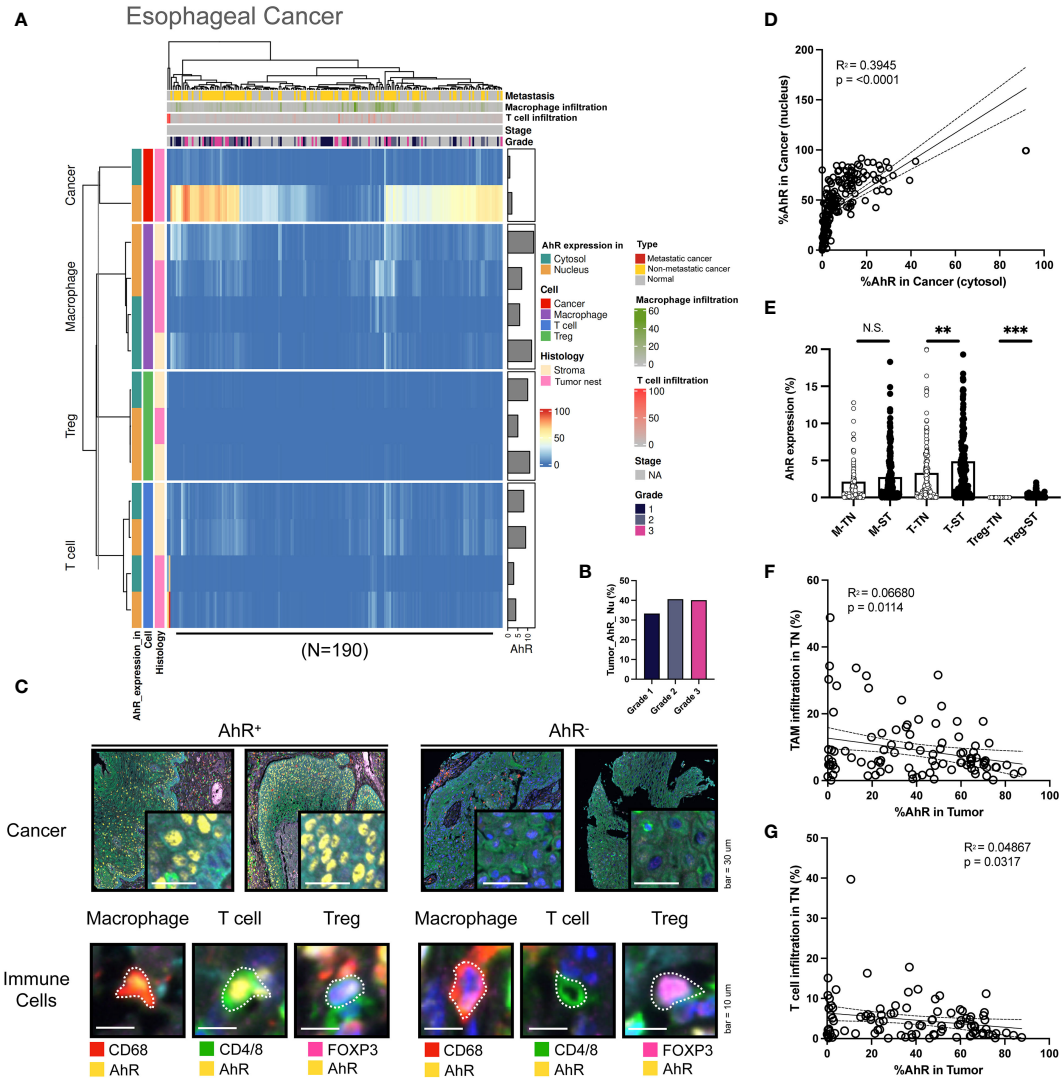

FIGURE 5
AhR expression patterns in esophageal cancer. **(A)** Heatmap summarizing the AhR expression and localization in cancer/epithelial cells, T cells, macrophages, and Tregs in normal and malignant esophageal tissues (N = 190). **(B)** AhR expression in malignant esophageal tissues of varying cancer grades. **(C)** Representative images of AhR-expressing (AhR^+) and non-AhR-expressing (AhR^-) esophageal cancer cells, along with AhR-expressing immune cells, including macrophages, T cells, and Tregs. **(D)** AhR expression in the cytosol is positively correlated with the nuclear AhR expression ($P < 0.0001$). **(E)** AhR expression in T cells (T), macrophages (M), and Tregs in the stroma (ST) and tumor nest (TN). **(F)** Correlation plot showing no significant correlation between AhR expression in cancer cell nucleus and the TAM infiltration degree in the TN. **(G)** Correlation plot showing no significant correlation between AhR expression in cancer cell nucleus and the T-cell infiltration degree in the TN. N.S., no significant difference, $^{**}P < 0.01$, $^{***}P < 0.001$.

obtained for other cancer types. AhR-expressing macrophages were not solely confined to the stroma, but were also identified within the tumor nest, representing a distinct AhR expression pattern in TAMs. Notably, AhR expression was found in Tregs within the stromal regions in both normal and malignant samples, a pattern that was not observed in the remaining four cancer types examined here (Figure 6A). No clear relationship between AhR expression and the NSCLC grade was found (Figure 6B). The images on the left in Figure 5C show representative mIHC images of AhR-expressing cancer and immune cells (macrophages, T cells, and Tregs), which are distinguished by the yellow AhR staining in lung tissues. In contrast, the cancer and immune cells in the images on the right exhibit no AhR expression, as indicated by the absence of yellow (Figure 6C). To investigate the correlation between the nuclear and cytosolic AhR expression, the percentage of cells expressing AhR in the nucleus and cytosol in individual bladder samples was examined. The analysis revealed a significantly positive correlation between these parameters, indicating a positive correlation between the nuclear and cytosolic AhR expression (Figure 6D). The AhR expression levels in each immune cell type (macrophages, T cells, and Tregs) within the tumor nest were positively correlated with the stromal AhR expression in the corresponding cell type, consistent with the findings observed in similar cancer types (Figure 6E). Again, no discernible correlation was observed between the extent of immune cell infiltration in the tumor nest and AhR expression in the tumor region for either TAMs or T cells (Figures 6F, G).

10.3389/fimmu.2024.1330228

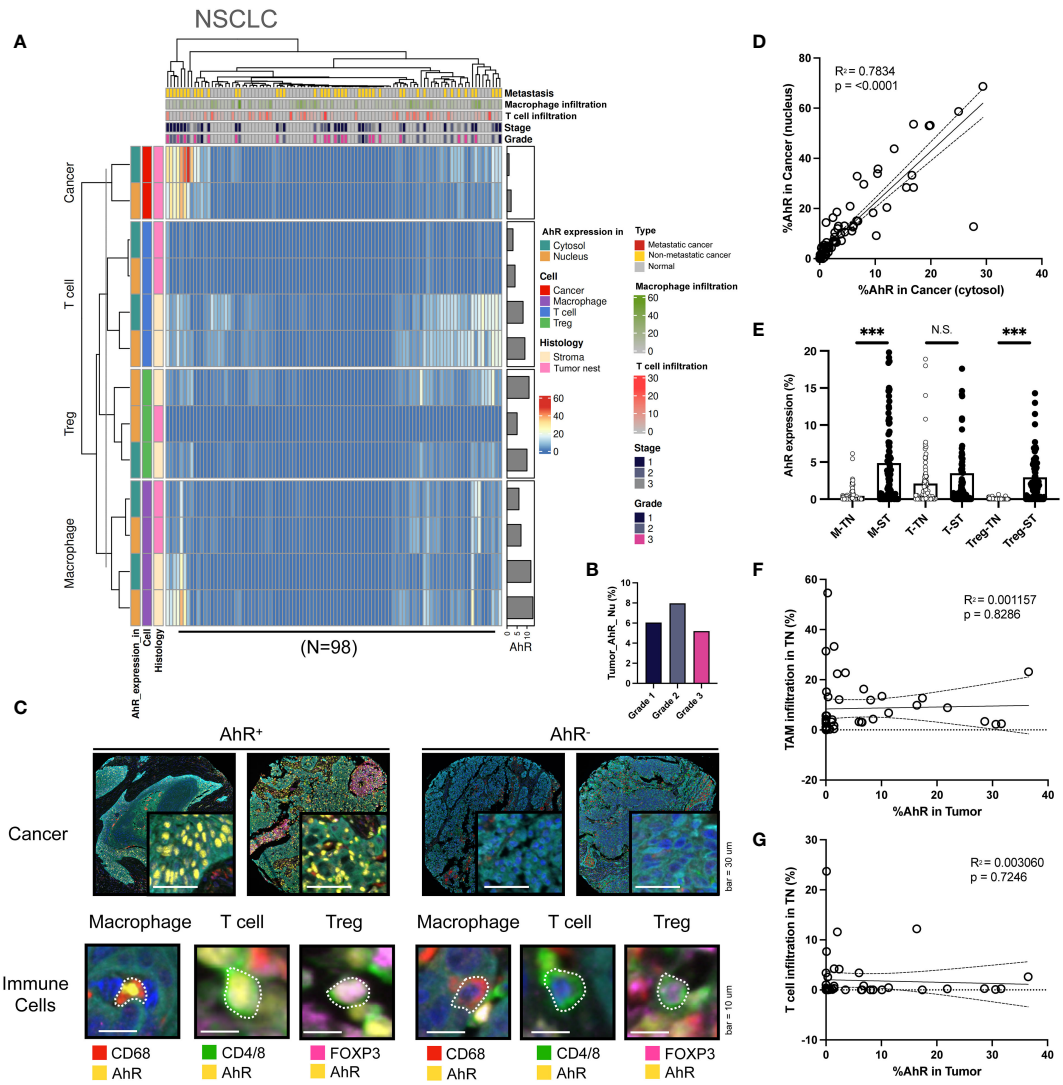

FIGURE 6
AhR expression patterns in non-small cell lung cancer (NSCLC). **(A)** Heatmap summarizing the AhR expression and localization in cancer/epithelial cells, T cells, macrophages, and Tregs in normal and malignant lung tissues (N = 98). **(B)** AhR expression in malignant NSCLC tissues of varying cancer grades. **(C)** Representative images of AhR-expressing (AhR^+) and non-AhR-expressing (AhR^-) lung cancer cells, along with AhR-expressing immune cells, including macrophages, T cells, and Tregs. **(D)** The AhR expression in the cytosol is positively correlated with the nuclear AhR expression ($P < 0.0001$). **(E)** AhR expression in T cells (T), macrophages (M), and Tregs in the stroma (ST) and tumor nest (TN). **(F)** Correlation plot showing no significant correlation between AhR expression in cancer cell nucleus and the TAM infiltration degree in the TN. **(G)** Correlation plot showing no significant correlation between AhR expression in cancer cell nucleus and the T-cell infiltration degree in the TN. N.S., no significant difference, ***$P < 0.001$.

3.7 Differential AhR expression based on the cell type and location affects cancer characteristics

To thoroughly compare the five cancer types based on AhR expression, we applied a k-means clustering algorithm. K-means clustering and PCA were applied to individual tumor cores, each containing 13 features representing the AhR expression patterns, to identify meaningful clusters with significant components ($P < 0.05$; silhouette width = 0.45; Supplementary Figure 3). These clusters were distinguished along PC1 in the PCA plot, indicating a clear separation within each group (Figures 7A, B). Specifically, we focused on the analysis of cancer cells and macrophages situated at the extremes of PC1 and Tregs located at opposite ends (Figure 7C). Cluster 1 displayed the highest AhR expression in the cancer nucleus, whereas cluster 3 exhibited the lowest AhR expression in the cancer nucleus. AhR expression in the stromal macrophage nuclei was the most pronounced in cluster 2 (Figure 7D). This suggests that each cluster possesses distinct characteristics depending on the AhR expression and location. Consequently, we generated pie charts to explore the distribution of the five cancer types within each cluster (Figure 7E). In cluster 1, NSCLC was entirely absent, with esophageal cancer representing the largest proportion. The distinct features of cluster 1 were primarily attributed to esophageal cancer. In contrast, cluster 2 was notably different from cluster 1, with a 5% prevalence of

10.3389/fimmu.2024.1330228

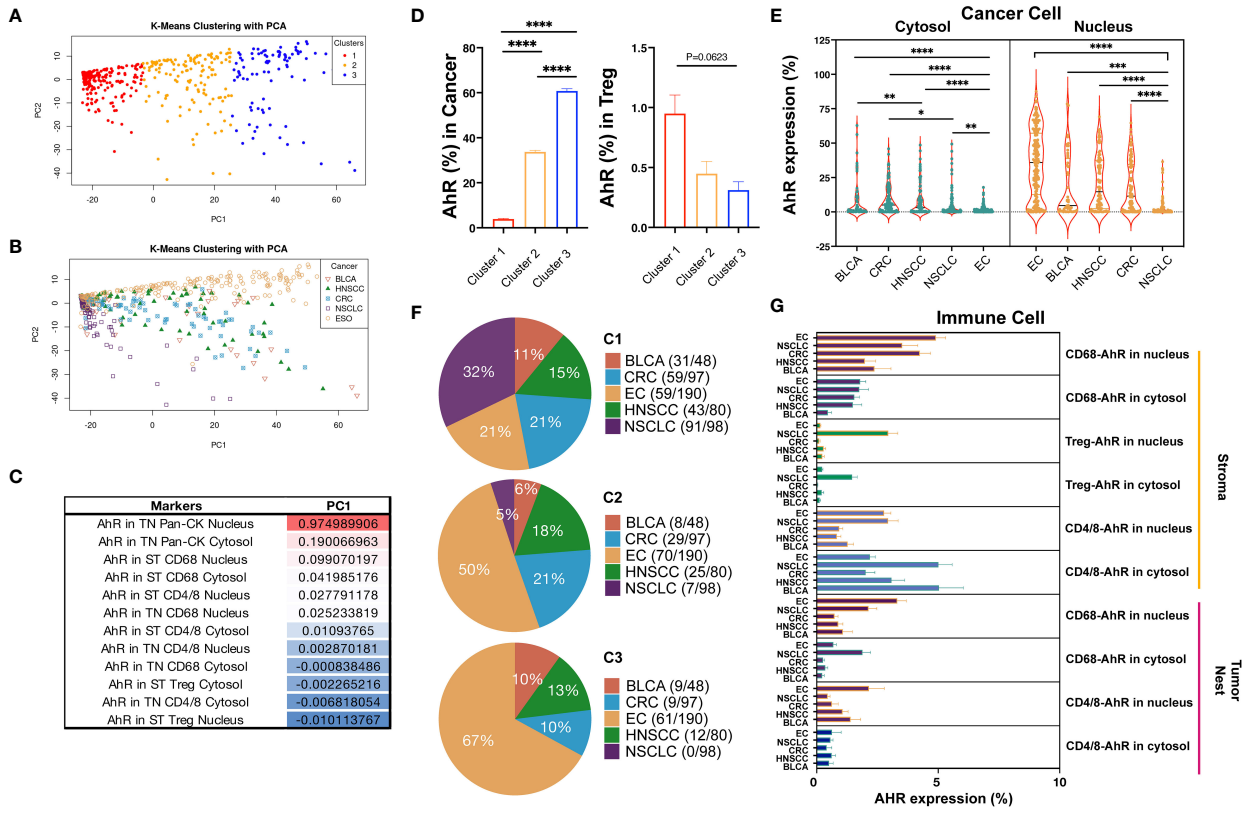

FIGURE 7
Differential AhR expression based on different cell types and locations. **(A)** PCA plot distinguishing the three clusters from each group. **(B)** PCA plot distinguishing the five cancer types from each group. **(C)** PC1 table displaying the AhR expression in different locations, including the cytosol vs. nucleus, tumor nest (TN) vs. stroma (ST), and different markers (Pan-CK, CD68, CD4/8, and Treg). **(D)** Bar graph showing the AhR expression in cancer cell nucleus and stromal Treg nucleus in three different clusters. **(E)** Pie chart representing the distribution of the five cancer types within the three different clusters. **(F)** Violin plot portraying the AhR expression in the cytosol vs. nucleus in the five cancer types. **(G)** Bar graph depicting the AhR expression in the tumor and immune cell types in the five cancer types. *P < 0.05, **P < 0.01, ***P < 0.001, ****P < 0.0001.

NSCLC and a relatively higher proportion of HNSCC and colorectal cancer. The AhR expression in macrophages within cluster 2 was noticeable higher than in cluster 1. Cluster 3, which had the highest NSCLC proportion, generally displayed a lower AhR expression than the other clusters. To precisely assess AhR expression in cancer and immune cells, we conducted quantitative statistical comparisons (Figures 7F, G). Although AhR was expressed in both the cytosol and nucleus of the tumor cells, its nuclear expression was generally higher. However, a similar expression pattern was observed in immune cells.

4 Discussion

We conducted analyses using hundreds of cores across five cancer types by employing mIHC, machine learning, and quantification methods. In contrast with conventional approaches, we utilized a high-throughput (HT) approach, yielding objective and quantitative results (Supplementary Figure 1). Additionally, using unbiased clustering, we analyzed the AhR expression patterns, identified the characteristics of three common clusters across cancer types, and examined their distribution in five solid tumors (Figure 7). One of the HT analysis advantages is its ability to quantitatively analyze AhR-expressing cells in the TME. Simultaneously, it allows the analysis of the cell nucleus and cytosol within and outside the tumor, enabling the statistical analysis of patterns. This yielded intriguing results summarizing the proteomic and cellular pathology-based outcomes that could not be achieved using methods such as single-cell RNA-seq. AhR expression is prominent in the TME, particularly in the nucleus. The AhR expression in tumors was notably higher than in immune cells in the TME. These findings are consistent with previous ones (14–17). The mIHC results for NSCLC showed that AhR was predominantly expressed in the nucleus in cancer cells, in accordance with our findings (18, 19). AhR is involved in detoxifying the environmental toxin polycyclic aromatic hydrocarbon, a tobacco smoke component. Thus, the smoking habits may influence AhR expression. No significant AhR expression differences between smokers and non-smokers have been found. Here, we did not investigate the potential impact of the smoking status on AhR expression because of the lack of information on the patient smoking status (11). Particularly, we observed that AhR was predominantly expressed in the nucleus in the five cancer types. AhR is expressed in the nucleus and performs various functions in the TME after interacting with ARNT. The increased presence of AhR is associated with drug resistance mechanisms due to an enhanced drug metabolism. Additionally,

approximately 5,000 genes (20) regulated by AhR are highly relevant to epigenetic alterations (20, 21) and the differentiation associated with tumor heterogeneity (22–24). Although the analysis of 43 tumor cores done here may not be sufficient to draw definitive conclusions, the elevated cytosolic AhR expression found in NSCLC compared to that found in the other four cancer types is intriguing. AhR activates non-canonical signaling pathways in the cytosol (25). Furthermore, through signaling pathways involving protein kinase A (PKA), nuclear factor κB (NF-kB), and steroid receptor-coactivator-1 (Src1) in the cytosol, AhR might influence aspects such as cancer cell survival and resistance (26–29). Investigating how the AhR expression pattern in NSCLC differs from that in other cancer types is crucial.

AhR expression was not directly correlated with the tumor stage, grade, or metastasis, presenting a different pattern from those found previously (15, 30). Previously, a higher correlation with factors such as the stage and grade was reported in 25 patients with oral squamous cell carcinoma (30). These results indicate a different direction from that of our research findings. Such discrepancies may stem from the differences in patient tissues. For more reliable results, exploring the association between AhR activity and specific drug treatments, especially in patients with stage 3 or 4 cancer, would be valuable. In particular, patients with stage 3 or 4 cancer receiving anticancer drugs constitute an important population which was only studied to a low extent here, since we predominantly included stage 1 and 2 patients (90.06%). This result disparity is closely linked to the differences observed in previous studies.

Although AhR expression was predominantly high in cancer cells, it was only found in 2.12% and 0.44% of T cells and macrophages, respectively. Although AhR expression was also observed in Tregs, Treg infiltration varied depending on the tumor type, thereby influencing the results. AhR expression in immune cells is influenced by an increased kynurenine (Kyn) level induced by indoleamine 2,3-dioxygenase 1 (IDO1), which is the mechanism of action of anticancer agents targeting AhR. AhR expression in immune cells leads to a decreased immune activity due to Kyn, showing inhibitory effects on T-cell differentiation and anticancer functions, along with cytokine modulation (31). Additionally, AhR-high macrophages play a crucial role in increasing the levels of immunosuppressive cytokines, such as TGF-beta and IL-10, which are anti-inflammatory cytokines, in the TME (32). This implies a potential possibility for the polarization of M2 macrophages by these cytokines. Furthermore, AhR influences Treg differentiation and activation (33).

Although AhR expression differs among cancer types, AhR is generally expressed in most tumors. Interestingly, the expression pattern can be categorized into three clusters: Cluster 1, in which tumors exhibit a high AhR expression; cluster 3, characterized by relatively low AhR expression levels in tumors but a high expression in Tregs; and cluster 2, which represents a mixed pattern. This AhR expression pattern was observed across all five solid tumors analyzed here. The distinct AhR expression patterns observed across clusters suggest the potential application of AhR inhibitors in anticancer drug development and as predictive and prognostic biomarkers.

AhR expression has not been analyzed across various cancer types using mIHC. Although some studies have obtained pathological results from certain IHC analyses (34), large-scale results obtained using quantification methods are lacking. In particular, with the recent development of machine-learning techniques for analyzing pathological tissues, such analyses have become feasible. The nuclear or cytosolic AhR expression has been described (35–37). However, since these results were not obtained using multiplex analysis, ensuring the accuracy of the results obtained is challenging because the cells with a similar size and morphology to those of tumor cells may also be stained. Previous analyses of AhR expression in immune cells have often focused on specific immune cell types and have not been conducted using large clinical samples. Consequently, the results generated conceptual outcomes excluding the overall AhR expression distribution. In contrast, we comprehensively analyzed the heterogeneous AhR expression patterns in the TME. This approach allowed us to estimate the functional implications of AhR and identify the potential mechanisms of action for AhR-targeting drugs.

The limitations of this study are the inability to establish a correlation between AhR expression and immune checkpoint inhibitors, such as IDO and programmed death-ligand 1 (PD-L1). While we mainly focused on analyzing AhR expression and distribution, we failed to demonstrate their interaction with clinically significant mechanisms mediated by molecules such as IDO1, indoleamine 2,3-dioxygenase 2 (IDO2), tryptophan 2,3-dioxygenase (TDO), and PD-L1. Nevertheless, our data suggest a positive correlation between the increase in the amount of tumor-infiltrating lymphocytes (TILs) and TAMs and PD-L1 expression. Second, most tumors were obtained from surgical samples. Considering the tendency of AhR to react with chemical substances, a response to specific drugs is possible, especially since recent studies have reported an increase in AhR activity due to drugs such as chemotherapeutics or TKIs. Therefore, the frequency and increasing trend of AhR expression observed here may be more pronounced in patients treated with specific medications. Third, the limited clinical information available for the TMA prevents the direct validation of the patient outcomes. However, leveraging public databases, such as TCGA, could offer an opportunity to more comprehensively evaluate the impact of AhR on tumors. These issues should be addressed in future studies. Careful analysis is required to interpret AhR expression changes before and after anticancer treatment, especially if the transition from cluster 1 to clusters 2 or 3 is possible. Additionally, our observation of AhR expression in immune cells, particularly the significant increase observed in the stroma, led to hypotheses regarding the accessibility of various AhR ligands due to stromal vascular characteristics. Moreover, the high Kyn expression in macrophages may influence the stromal immune cell concentration. Experimental validation of these hypotheses is expected to contribute to a better understanding and interpretation of our findings.

AhR-targeting anticancer therapies are being actively developed. Particularly, small-molecule inhibitors such as BAY-241696 and IK-175 are currently being investigated in various solid tumors and have shown promising results (NCT05472506,

NCT04200963, and NCT04999202). Recently developed AhR inhibitors, such as DA-4505, BAY-241696, and IK-175, have been presented at international scientific conferences during preclinical research. These drugs play a crucial role in immune cell activation in the TME. Notably, they are correlated with IDO, making biomarker and clinical-based mechanism of action analyses essential for novel drug development. The analysis of the AhR expression patterns conducted here is a significant milestone in this research field.

5 Conclusion

Our HT method employing mIHC and image cytometry based on AhR expression identified three distinct clusters. Cluster 1 exhibited high AhR expression in cancer cell nucleus, while cluster 3 showed the lowest. In cluster 2, stromal macrophage nucleus had the highest AhR expression. Cluster 1 was dominated by esophageal cancer, while cluster 2 had a higher proportion of HNSCC and colorectal cancer, with a small NSCLC presence. Cluster 3 had the highest NSCLC representation but lower AhR expression overall. By demonstrating different expression patterns of AhR in cancer cells and immune cells, our findings are anticipated to provide a fundamental basis for both biological and immunological research on drugs targeting AhR.

Data availability statement

The original contributions presented in the study are included in the article/Supplementary Material. Further inquiries can be directed to the corresponding authors. The datasets generated for this study can be found in the Code Ocean: https://doi.org/10.24433/CO.1505908.v1.

Ethics statement

All tissues were collected under the highest ethical standards with the donor being informed completely and with their consents. We followed standard medical care and protected the donors' privacy. All human tissues were collected under HIPPA approved protocols. The studies were conducted in accordance with the local legislation and institutional requirements. The participants provided their written informed consent to participate in this study.

Author contributions

DK: Conceptualization, Data curation, Formal analysis, Investigation, Methodology, Resources, Software, Validation, Visualization, Writing – original draft, Writing – review & editing. CL: Conceptualization, Data curation, Investigation, Methodology, Resources, Validation, Visualization, Writing – original draft, Writing – review & editing. YH: Conceptualization, Data curation, Investigation, Methodology, Resources, Validation, Visualization, Writing – original draft, Writing – review & editing. SP: Formal analysis, Resources, Writing – review & editing. HH: Writing – review & editing, Data curation, Resources, Software. KN: Resources, Validation, Writing – review & editing. MK: Methodology, Resources, Writing – review & editing. SY: Resources, Visualization, Writing – review & editing. SB: Investigation, Resources, Writing – review & editing, Validation. YK: Resources, Validation, Writing – review & editing. JH: Data curation, Resources, Writing – review & editing. SL: Investigation, Resources, Writing – review & editing. S-SK: Methodology, Resources, Writing – review & editing. MH: Resources, Validation, Writing – review & editing. SML: Resources, Validation, Writing – review & editing. JL: Resources, Validation, Writing – review & editing. JK: Formal analysis, Methodology, Project administration, Software, Writing – review & editing. BC: Funding acquisition, Resources, Writing – review & editing. K-HP: Conceptualization, Data curation, Formal analysis, Investigation, Methodology, Project administration, Resources, Software, Supervision, Validation, Visualization, Writing – original draft, Writing – review & editing.

Funding

The author(s) declare financial support was received for the research, authorship, and/or publication of this article. This research was supported by the Bio & Medical Technology Development Program of the National Research Foundation (NRF) and funded by the Korean government (MSIT) (No. 2022M3E5F3081138). This work was also supported by the National Research Foundation of Korea (NRF) grant funded by the Korea government (MSIT) (No. 2022R1A2C3005817).

Conflict of interest

Author SS-K was employed by the company JEUK Co., Ltd.

The remaining authors declare that the research was conducted in the absence of any commercial or financial relationships that could be construed as a potential conflict of interest.

Publisher's note

Supplementary material

The Supplementary Material for this article can be found online at: https://www.frontiersin.org/articles/10.3389/fimmu.2024.1330228/full#supplementary-material

References

1. Larigot L, Juricek L, Dairou J, Coumoul X. Ahr signaling pathways and regulatory functions. *Biochim Open* (2018) 7:1–9. doi: 10.1016/j.biopen.2018.05.001

2. Nebert DW. Aryl hydrocarbon receptor (Ahr): "Pioneer member" of the basic-helix/loop/helix per-arnt-sim (Bhlh/pas) family of "Sensors" of foreign and endogenous signals. *Prog Lipid Res* (2017) 67:38–57. doi: 10.1016/j.plipres.2017.06.001

3. Girer NG, Tomlinson CR, Elferink CJ. The aryl hydrocarbon receptor in energy balance: the road from dioxin-induced wasting syndrome to combating obesity with ahr ligands. *Int J Mol Sci* (2020) 22(1). doi: 10.3390/ijms22010049

4. Hahn ME. Aryl hydrocarbon receptors: diversity and evolution. *Chem Biol Interact* (2002) 141(1–2):131–60. doi: 10.1016/s0009-2797(02)00070-4

5. Veldhoen M, Hirota K, Westendorf AM, Buer J, Dumoutier L, Renauld JC, et al. The aryl hydrocarbon receptor links th17-cell-mediated autoimmunity to environmental toxins. *Nature* (2008) 453(7191):106–9. doi: 10.1038/nature06881

6. Leclerc D, Staats Pires AC, Guillemin GJ, Gilot D. Detrimental activation of ahr pathway in cancer: an overview of therapeutic strategies. *Curr Opin Immunol* (2021) 70:15–26. doi: 10.1016/j.coi.2020.12.003

7. Murray IA, Patterson AD, Perdew GH. Aryl hydrocarbon receptor ligands in cancer: friend and foe. *Nat Rev Cancer* (2014) 14(12):801–14. doi: 10.1038/nrc3846

8. Safe S, Zhang L. The role of the aryl hydrocarbon receptor (Ahr) and its ligands in breast cancer. *Cancers (Basel)* (2022) 14(22). doi: 10.3390/cancers14225574

9. DiNatale BC, Smith K, John K, Krishnegowda G, Amin SG, Perdew GH. Ah receptor antagonism represses head and neck tumor cell aggressive phenotype. *Mol Cancer Res* (2012) 10:1369–79. doi: 10.1158/1541-7786.MCR-12-0216

10. Yu J, Lu Y, Muto S, Ide H, Horie S. The dual function of aryl hydrocarbon receptor in bladder carcinogenesis. *Anticancer Res* (2020) 40(3):1345–57. doi: 10.21873/anticanres.14076

11. Lin P, Chang H, Tsai WT, Wu MH, Liao YS, Chen JT, et al. Overexpression of aryl hydrocarbon receptor in human lung carcinomas. *Toxicol Pathol* (2003) 31(1):22–30. doi: 10.1080/01926230390173824

12. Nothdurft S, Thumser-Henner C, Breitenbucher F, Okimoto RA, Dorsch M, Opitz CA, et al. Functional screening identifies aryl hydrocarbon receptor as suppressor of lung cancer metastasis. *Oncogenesis* (2020) 9(11):102. doi: 10.1038/s41389-020-00286-8

13. Chang CY, Puga A. Constitutive activation of the aromatic hydrocarbon receptor. *Mol Cell Biol* (1998) 18(1):525–35. doi: 10.1128/MCB.18.1.525

14. Yin XF, Chen J, Mao W, Wang YH, Chen MH. Downregulation of aryl hydrocarbon receptor expression decreases gastric cancer cell growth and invasion. *Oncol Rep* (2013) 30(1):364–70. doi: 10.3892/or.2013.2410

15. Xue P, Fu J, Zhou Y. The aryl hydrocarbon receptor and tumor immunity. *Front Immunol* (2018) 9:286. doi: 10.3389/fimmu.2018.00286

16. Wang Z, Snyder M, Kenison JE, Yang K, Lara B, Lydell E, et al. How the ahr became important in cancer: the role of chronically active ahr in cancer aggression. *Int J Mol Sci* (2020) 22(1). doi: 10.3390/ijms22010387

17. Mo Z, Li P, Cao Z, Zhang S. A comprehensive pan-cancer analysis of 33 human cancers reveals the immunotherapeutic value of aryl hydrocarbon receptor. *Front Immunol* (2021) 12:564948. doi: 10.3389/fimmu.2021.564948

18. Han SC, Wang GZ, Yang YN, Fang WF, Sun BB, Zhang JD, et al. Nuclear ahr and membranous pd-L1 in predicting response of non-small cell lung cancer to pd-1 blockade. *Signal Transduct Target Ther* (2023) 8(1):191. doi: 10.1038/s41392-023-01416-5

19. Peng Y, Ouyang L, Zhou Y, Lai W, Chen Y, Wang Z, et al. Ahr promotes the development of non-small cell lung cancer by inducing slc7a11-dependent antioxidant function. *J Cancer* (2023) 14(5):821–34. doi: 10.7150/jca.82066

20. Lo R, Matthews J. High-resolution genome-wide mapping of ahr and arnt binding sites by chip-seq. *Toxicol Sci* (2012) 130(2):349–61. doi: 10.1093/toxsci/kfs253

21. Wajda A, Lapczuk-Romanska J, Paradowska-Gorycka A. Epigenetic regulations of ahr in the aspect of immunomodulation. *Int J Mol Sci* (2020) 21(17). doi: 10.3390/ijms21176404

22. Stanford EA, Wang Z, Novikov O, Mulas F, Landesman-Bollag E, Monti S, et al. The role of the aryl hydrocarbon receptor in the development of cells with the molecular and functional characteristics of cancer stem-like cells. *BMC Biol* (2016) 14:20. doi: 10.1186/s12915-016-0240-y

23. Sweeney C, Lazennec G, Vogel CFA. Environmental exposure and the role of ahr in the tumor microenvironment of breast cancer. *Front Pharmacol* (2022) 13:1095289. doi: 10.3389/fphar.2022.1095289

24. Elson DJ, Kolluri SK. Tumor-suppressive functions of the aryl hydrocarbon receptor (Ahr) and ahr as a therapeutic target in cancer. *Biol (Basel)* (2023) 12(4). doi: 10.3390/biology12040526

25. Wright EJ, De Castro KP, Joshi AD, Elferink CJ. Canonical and non-canonical aryl hydrocarbon receptor signaling pathways. *Curr Opin Toxicol* (2017) 2:87–92. doi: 10.1016/j.cotox.2017.01.001

26. Beischlag TV, Wang S, Rose DW, Torchia J, Reisz-Porszasz S, Muhammad K, et al. Recruitment of the ncoa/src-1/P160 family of transcriptional coactivators by the aryl hydrocarbon receptor/aryl hydrocarbon receptor nuclear translocator complex. *Mol Cell Biol* (2002) 22(12):4319–33. doi: 10.1128/MCB.22.12.4319-4333.2002

27. Vogel CF, Sciullo E, Li W, Wong P, Lazennec G, Matsumura F. Relb, a new partner of aryl hydrocarbon receptor-mediated transcription. *Mol Endocrinol* (2007) 2 (12):2941–55. doi: 10.1210/me.2007-0211

28. Taylor RT, Wang F, Hsu EL, Hankinson O. Roles of coactivator proteins in dioxin induction of cyp1a1 and cyp1b1 in human breast cancer cells. *Toxicol Sci* (2009) 107(1):1–8. doi: 10.1093/toxsci/kfn217

29. Vogel CFA, Haarmann-Stemmann T. The aryl hydrocarbon receptor repressor - more than a simple feedback inhibitor of ahr signaling: clues for its role in inflammation and cancer. *Curr Opin Toxicol* (2017) 2:109–19. doi: 10.1016/j.cotox.2017.02.004

30. Martano M, Stiuso P, Facchiano A, De Maria S, Vanacore D, Restucci B, et al. Aryl hydrocarbon receptor, a tumor grade–Associated marker of oral cancer, is directly downregulated by polydatin: A pilot study. *Oncol Rep* (2018) 40(3):1435–42. doi: 10.3892/or.2018.6555

31. Gutierrez-Vazquez C, Quintana FJ. Regulation of the immune response by the aryl hydrocarbon receptor. *Immunity* (2018) 48(1):19–33. doi: 10.1016/j.immuni.2017.12.012

32. Campesato LF, Budhu S, Tchaicha J, Weng CH, Gigoux M, Cohen IJ, et al. Blockade of the ahr restricts a treg-macrophage suppressive axis induced by L-kynurenine. *Nat Commun* (2020) 11(1):4011. doi: 10.1038/s41467-020-17750-z

33. Meyer BK, Pray-Grant MG, Vanden Heuvel JP, Perdew GH. Hepatitis B virus X-associated protein 2 is a subunit of the unliganded aryl hydrocarbon receptor core complex and exhibits transcriptional enhancer activity. *Mol Cell Biol* (1998) 18(2):978–88. doi: 10.1128/MCB.18.2.978

34. Wang GZ, Zhang L, Zhao XC, Gao SH, Qu LW, Yu H, et al. The aryl hydrocarbon receptor mediates tobacco-induced pd-L1 expression and is associated with response to immunotherapy. *Nat Commun* (2019) 10(1):1125. doi: 10.1038/s41467-019-08887-7

35. Davarinos NA, Pollenz RS. Aryl hydrocarbon receptor imported into the nucleus following ligand binding is rapidly degraded *via* the cytosplasmic proteasome following nuclear export. *J Biol Chem* (1999) 274(40):28708–15. doi: 10.1074/jbc.274.40.28708

36. Richter CA, Tillitt DE, Hannink M. Regulation of subcellular localization of the aryl hydrocarbon receptor (Ahr). *Arch Biochem Biophys* (2001) 389(2):207–17. doi: 10.1006/abbi.2001.2339

37. Dietrich C, Kaina B. The aryl hydrocarbon receptor (Ahr) in the regulation of cell-cell contact and tumor growth. *Carcinogenesis* (2010) 31(8):1319–28. doi: 10.1093/carcin/bgq028

frontiers | Frontiers in Immunology

TYPE Original Research
PUBLISHED 18 April 2024
DOI 10.3389/fimmu.2024.1364329

OPEN ACCESS

EDITED BY
Wei Chong,
Shandong Provincial Hospital, China

REVIEWED BY
Mulong Du,
Nanjing Medical University, China
Xuesi Dong,
Southeast University, China
Peng Song,
Nanjing Drum Tower Hospital, China
Giuseppe Schepisi,
Scientific Institute of Romagna for the Study and Treatment of Tumors (IRCCS), Italy
Kenichi Takayama,
Tokyo Metropolitan Institute of Gerontology, Japan

*CORRESPONDENCE
Gaoxiang Ma
gaoxiang_ma@163.com
Haixia Zhu
00zlingling@163.com
Lian-Wen Qi
Qilw@cpu.edu.cn

†These authors have contributed equally to this work

RECEIVED 02 January 2024
ACCEPTED 01 April 2024
PUBLISHED 18 April 2024

CITATION
Fan Y, Ge Y, Niu K, Li Y, Qi L-W, Zhu H and Ma G (2024) *MLXIPL* associated with tumor-infiltrating CD8+ T cells is involved in poor prostate cancer prognosis. *Front. Immunol.* 15:1364329. doi: 10.3389/fimmu.2024.1364329

MLXIPL associated with tumor-infiltrating CD8+ T cells is involved in poor prostate cancer prognosis

Yuanming Fan[1†], Yuqiu Ge[2†], Kaiming Niu[1†], Ying Li[1], Lian-Wen Qi[3*], Haixia Zhu[4*] and Gaoxiang Ma[1,5*]

[1]State Key Laboratory of Natural Medicines, School of Traditional Chinese Pharmacy, China Pharmaceutical University, Nanjing, China, [2]Department of Public Health and Preventive Medicine, Wuxi School of Medicine, Jiangnan University, Wuxi, China, [3]The Clinical Metabolomics Center, China Pharmaceutical University, Nanjing, China, [4]Clinical Laboratory, Tumor Hospital Affiliated to Nantong University, Nantong, China, [5]Department of Oncology, Pukou Hospital of Chinese Medicine affiliated to China Pharmaceutical University, Nanjing, China

Introduction: Within tumor microenvironment, the presence of preexisting antitumor CD8+ T Q7 cells have been shown to be associated with a favorable prognosis in most solid cancers. However, in the case of prostate cancer (PCa), they have been linked to a negative impact on prognosis.

Methods: To gain a deeper understanding of the contribution of infiltrating CD8 + T cells to poor prognosis in PCa, the infiltration levelsof CD8+ T cells were estimated using the TCGA PRAD (The Cancer Genome Atlas Prostate Adenocarcinoma dataset) and MSKCC (Memorial Sloan Kettering Cancer Center) cohorts.

Results: Bioinformatic analyses revealed that CD8+ T cells likely influence PCa prognosis through increased expression of immune checkpoint molecules and enhanced recruitment of regulatory T cells. The MLXIPL was identified as the gene expressed in response to CD8+ T cell infiltration and was found to be associated with PCa prognosis. The prognostic role of MLXIPL was examined in two cohorts: TCGA PRAD (p = 2.3E-02) and the MSKCC cohort (p = 1.6E-02). Subsequently, MLXIPL was confirmed to be associated with an unfavorable prognosis in PCa, as evidenced by an independent cohort study (hazard ratio [HR] = 2.57, 95% CI: 1.42- 4.65, p = 1.76E-03).

Discussion: In summary, the findings suggested that MLXIPL related to tumor-infiltrating CD8+ T cells facilitated a poor prognosis in PCa.

KEYWORDS

prostate cancer, prognosis, CD8+ T cell, MLXIPL, cohort study

Introduction

Prostate cancer (PCa) is the most common malignancy in the male urogenital system worldwide (1). As the most common contemporary intervention, radical prostatectomy, radiotherapy, and hormone therapy, have been used for many years. Over the last two decades, the landscape of treatments has changed significantly with the approval of several agents, including chemotherapeutics (docetaxel and cabazitaxel), androgen-receptor signaling inhibitors (abiraterone acetate, enzalutamide, apalutamide, and darolutamide), radioligand therapies (radium-223 and 177Lu-PSMA-617), and PARP-inhibitors (Olaparib). The introduction of them have significantly expanded our therapeutic armamentarium against PCa and contributed to an increased overall survival rate among patients with PCa (37716332) (2, 3). However, advanced PCa, such as metastatic PCa and castration-resistant PCa, continues to pose significant challenges in terms of cure, as suitable therapies are currently lacking (4).

The tumor represents an organ-like structure that emerges from the co-evolution of malignant cells and their immediate environment. The tumor microenvironment (TME) is composed of many different cellular and acellular components. The progression of the tumor, its resistance to therapeutic interventions, as well as invasion and metastasis, are all properties arising from the bidirectional interactions occurring between cancer cells and the TME. Increasing realization of the significance of the TME in cancer biology has shifted cancer research from a cancer-centric model to one that considers the TME as a whole (5, 6). Specially, the TME plays a key role in the procession from primary towards metastatic PCa, in particular bone metastases. Moreover, the interplay between TME and PCa cells is important for AR signaling regulation and response to hormone therapy (7).

Within TME, the presence of preexisting antitumor CD8+ T cells has consistently shown associations with longer disease-free survival and/or overall survival across various cancers with different histological features and anatomical locations. These findings have been observed in both primary tumor settings and metastatic settings (8, 9). Altogether, tumor-infiltrating CD8+ T cells have been consistently associated with a favorable prognosis in the majority of solid cancer types (10). However, in the cases of PCa and clear cell renal cell carcinoma, infiltrating CD8+ T cells have been found to correlate with shorter progression-free survival and overall survival (11, 12). In the case of clear cell renal cell carcinoma, previous studies have confirmed a negative association between the presence of an exhausted phenotype in infiltrating CD8+ T cells and prognosis (13, 14). However, it remains to be established whether a similar pattern exists in PCa.

To comprehend the mechanisms by which infiltrating CD8+ T cells contribute to an unfavorable prognosis in PCa, a comprehensive analysis was conducted. Initially, a comparison was made regarding mutations, immune checkpoint gene expression, and the composition of infiltrating immunoregulatory cells among high and low CD8+ T cells groups. Importantly, potential genes responsive to CD8+ T cells were identified and validated using the independent cohorts. This study may offer novel insights for researchers in understanding the characteristics of CD8 + T cells associated with an unfavorable prognosis in PCa.

Materials and methods

Study population

For our independent cohort (NanTong cohort), a total of 94 prostate cancer patients were recruited. All of patients underwent prostate biopsy for diagnosis of prostate cancer. The follow-up protocol involved conducting telephone calls subsequent to the initial diagnosis. Prostate cancer tissues were obtained during tumorectomy procedures and were immediately frozen at -80°C for subsequent analyses. The extraction of tissue RNA was performed in accordance with the manufacturer's instructions. Clinicopathological findings were assessed based on the tumor–node–metastasis (TNM) classification system. Informed consent was obtained from all patients.

RNA sequencing and clinical data acquisition

In this study, two publicly available databases were utilized: The Cancer Genome Atlas Prostate Adenocarcinoma (TCGA PRAD) (https://portal.gdc.cancer.gov/) and the Memorial Sloan Kettering Cancer Center (MSKCC) (http://cbio.mskcc.org/cancergenomics/prostate/data/). The TCGA PRAD and MSKCC cohorts were acquired for subsequent analyses. Within the TCGA database, data included transcripts per million (TPM) of RNA sequencing and matched somatic mutation datasets of PCa, were obtained using the TCGA biolinks package in the R software. Additionally, matched tumor purity estimated by immunohistochemistry (IHC) data was downloaded (15), and matched batch information was obtained from https://bioinformatics.mdanderson.org/MQA/. For cases where a gene symbol had multiple expression measurements, the measurement with higher expression was retained. Due to significant RNA degradation in a portion of TCGA PRAD samples, 333 cases were utilized. Ultimately, 282 samples with survival information related to biochemical recurrence were included in our analysis. For the MSKCC cohort sequenced by microarray, normalized log2 mRNA expression data was downloaded.

Batch effects analysis

Referring to the previous study (16), we selected principal component analysis to analyzed and visualize batch effects of TCGA PRAD.

Tumor immune microenvironment analysis

The CIBERSORT algorithm, a computational method used to estimate the composition of different immune cell types in a tissue sample from bulk gene expression profiles, was applied to the TCGA PRAD and MSKCC dataset (17). Analyses were performed using 1,000 permutations and default statistical parameters in

reference to LM22 matrix. The threshold for categorizing CD8+ T cell infiltration into high and low groups was established by comparing the differences in biochemical recurrence. According to different sequencing methods in this study, the cutoff value was calculated for each data, respectively. The cutoff value selected was the one that yielded the lowest *p*-value. The cytolytic score, which serves as an indicator of local immune cytolytic activity, was calculated as the geometric mean of gene expression values for granzyme A and perforin (18). To estimate T-cell exhaustion level, the murine T-cell exhaustion signature was obtained (19, 20). The murine genes were manually converted to their corresponding human gene equivalents. The degree of T-cell exhaustion was assessed by calculating the mean expression of up-regulated genes minus the mean expression of down-regulated genes.

Somatic mutation frequency analysis

The somatic mutations were analyzed using the "maftools" R package. The tumor mutation burden (TMB) score was calculated for each patient in accordance with established methods. Oncoplots were utilized to visually present the somatic mutation signatures. The identification of cancer driver genes was achieved through the implementation of the oncodrive CLUST algorithm. Differentially mutated genes were identified by Fisher's exact test.

Differentially expressed gene analysis

Before differential expressed gene analysis, the genes with TPM equal to 0 among more than 10% samples were filtered in TCGA PRAD. Differential gene analysis was performed using multiple statistical approaches, including the Wilcoxon rank sum test and signed rank test, DESeq2 and edgeR (21). The genes with an adjusted *p*-value less than 0.05 and an absolute log2 scaled fold change more than 0.5849625 were further analyzed. The false discovery rate (FDR) method was employed for adjusting *p*-values.

Survival and receiver operating characteristic analyses

The Least Absolute Shrinkage and Selection Operator (LASSO) method was employed to identify stable prognostic candidate genes using biochemical recurrence as the endpoint. The prognostic candidate genes were subsequently validated using the log-rank test, as well as univariate and multivariate Cox proportional hazards regression analysis, with biochemical recurrence as the endpoint. To compute the risk score for each patient, the following formula was utilized:

$$\text{risk score} = \sum_{i=1}^{n} [coef(mRNAi) * Expression(mRNAi)]$$

Risk scores were computed by Cox regression coefficients of the adjusted covariates in both the TCGA and MSKCC cohorts. Additionally, the predictive value of the risk score was evaluated using the area under the receiver operating characteristic curve.

Functional enrichment analysis

Gene annotation enrichment analyses were conducted on the DEGs between the low and high CD8+ T cell groups using the R package clusterProfiler (22). The analysis included identification of Kyoto Encyclopedia of Genes and Genomes (KEGG) and Gene Ontology (GO) terms. Statistical significance was determined using an adjusted *p*-value cutoff of< 0.05. Additionally, gene set enrichment analysis (GSEA) was performed to identify consistent biological differences between the high and low CD8+ T cell groups, with an adjusted *p*-value cutoff of< 0.05 indicating statistical significance.

Quantitative real-time polymerase chain reaction

The *MLXIPL* expression in NanTong cohort was measured by qRT-PCR. The relative expression of *MLXIPL* mRNA was calculated by $2^{-\Delta Ct}$ method with the normalization to *GAPDH*. Primer sequences of *MLXIPL* were F: AAGATCC GCCTGAACAACG and R: CACTTGTGGTATTCCCGCATC. Primer sequences of *GAPDH* were F: CTGGGCTACA CTGAGCACC and R: AAGTGGTCGTTGAGGGCAATG.

Immunohistochemistry

The immunohistochemistry (IHC) analysis was conducted using rabbit anti-ChREBP (1:200, ab101500, Abcam, Cambridgeshire, England) following the manufacturer's instructions. Immunostaining intensity was categorized into four grades: 0 (no expression), 1 (mildly positive), 2 (moderately positive), and 3 (markedly positive). The proportion of positive-staining cells was assessed and categorized into five grades: 0 (0%), 1 (1–25%), 2 (26–50%), 3 (51–75%), and 4 (>75%). To generate the IHC score, the percentage of tumor cells showing positivity and the staining intensities were multiplied.

Statistical analysis

For comparisons between two subtypes, the Wilcoxon rank sum and signed rank tests were employed. Discrete data comparisons were conducted using Fisher's exact test. Spearman's correlation analysis was utilized to explore the relationships. All statistical tests were two-sided, and $p< 0.05$ was considered statistically significant unless otherwise stated. The thresholds for *p*-values were set at 0.05, 0.01, and 0.001 (*, ** and ***, respectively). All statistical analyses were performed using R software, version 4.3.1.

Results

CD8+ T cell negatively associated with prognosis of PCa

We investigated the batch effect of TCGA PRAD dataset (Supplementary Figure S1). Principal component analysis indicated no batch effects. The baseline characteristics of these two cohorts are present in Supplementary Table S1. In line with previous studies (11, 12), patients with higher levels of infiltrated CD8+ T cells exhibited poorer prognosis trend (Figure 1A). MSKCC cohort supported this result (Figure 1B).

The presence of higher densities of CD8+ T cells has been suggested to be associated with more advanced tumors (10). We examined clinicopathological characteristics, namely age, tumor purity, histopathological subtype, T and N stages, and Gleason score, in relation to the level of CD8+ T cells in TCGA PRAD (Supplementary Figures S2A–F) and clinicopathological characteristics, namely age, prostate specific antigen (PSA) level, T and N stages, and Gleason score and *ERG*-fusion status, in relation to the level of CD8+ T cells in MSKCC (Supplementary Figures S2I–O). The results indicated that compared with other histopathological type, less CD8+ T cells infiltrated in acinar PCa and age, tumor purity, PSA level, T, N stages, Gleason grade and *ERG*-fusion are not correlated to CD8+ T cell infiltration level.

Given the negative association of exhausted T cells with ccRCC prognosis (13, 14), cytolytic score and T cell exhaustion levels were calculated. Greater immune cytolytic activity was evident in the high CD8+ T cell group (Supplementary Figures S2G, P). Comparable levels of exhausted T cells were observed in the TCGA PRAD cohort. In the MSKCC cohort, levels of exhausted T cells were elevated in the high CD8+ T cell group (Supplementary Figures S2H, Q). This suggests that T cell exhaustion may partially elucidate the poor prognosis associated with CD8+ T cells.

In summary, our study reaffirmed the observation that CD8+ T cells are linked to an unfavorable prognosis based on available data. Our findings suggest that CD8+ T cells are associated with a poorer prognosis, rather than a higher degree of malignancy resulting in increased infiltration of these T cells.

CD8+ T cell related poor prognosis is mediated by increased immune checkpoint genes expression and Tregs

To gain further insights into how CD8+ T cells contribute to the poor prognosis of PCa, we explored whether this involvement is mediated through the TME. Within the TME, immunosuppression can be generated through two possible mechanisms: (1) the presence of differential mutations, which may modulate the

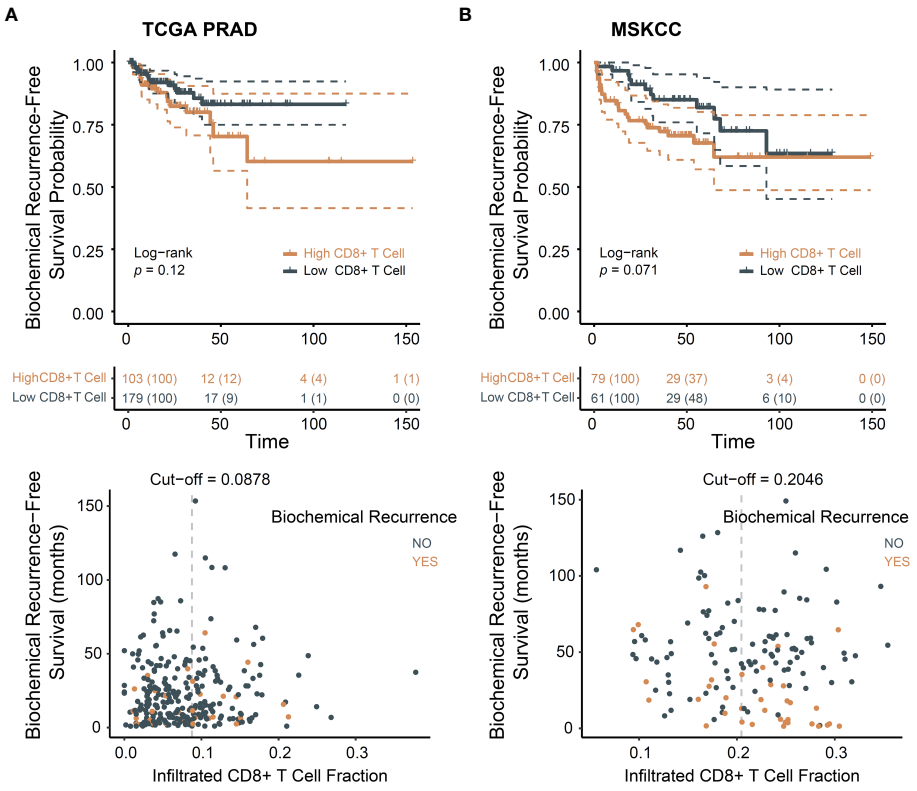

FIGURE 1
CD8+ T cells infiltration associated with poor prognosis in PCa. **(A)** Biochemical recurrence-free survival for CD8+ T cells in TCGA dataset; **(B)** Biochemical recurrence-free survival for CD8+ T cells in MSKCC dataset.

immune response in distinct ways; and (2) the presence of tumor-infiltrating T cells that can be suppressed through feedback-induced expression of checkpoint molecules and recruitment of immunoregulatory cells (18).

To investigate the potential role of mutations in mediating the association between CD8+ T cells and poor prognosis in PCa, we conducted somatic mutation frequency analysis. Both the low and high CD8+ T cell groups exhibited low TMB status and similar mutational patterns (Figure 2A). High rate of *SPOP*, *TP53*, *TTN* and *FOXA1* mutations were found. Missense mutations were found to be the most prevalent variant classification. Notably, *SPOP* were identified as driver genes despite CD8+ T cell infiltration level (Supplementary Figure S3A). SNPs emerged as the most frequent variant type (Supplementary Figure S3B). The results showed comparable frequencies of transitions and transversion between the low and high CD8+ T cell groups (Figure 2B). Results of Fisher's exact test confirmed that CD8+ T cell infiltration level was not implicated in gene mutations (Supplementary Table S2). Collectively, these results indicate that the association between CD8+ T cells and poor prognosis in PCa is not driven by somatic mutations.

Subsequently, we explored the correlation between immune checkpoint genes and the level of CD8+ T cell infiltration. After filtering the genes utilized in the LM22 matrix, six genes—specifically, *ITGAL*, *CD74*, *HAVCR2*, *CD274*, *SIGLEC15*, and *TIGIT*—were selected based on a review of the literature (23, 24). Increased *ITGAL*, *CD74* and *TIGIT* were observed in the high-density CD8+ T cell subgroup (Figure 2C). The relative abundances of 22 infiltrating immune cells were investigated. Notably, elevated immunosuppressive regulatory T cells (Tregs) were observed (Figure 2D). These findings suggested that CD8+ T cells may facilitate an unfavorable prognosis through a feedback mechanism involving the abnormality of immune checkpoint gene expression and recruitment or differentiation of immune cells specialized in immune suppression.

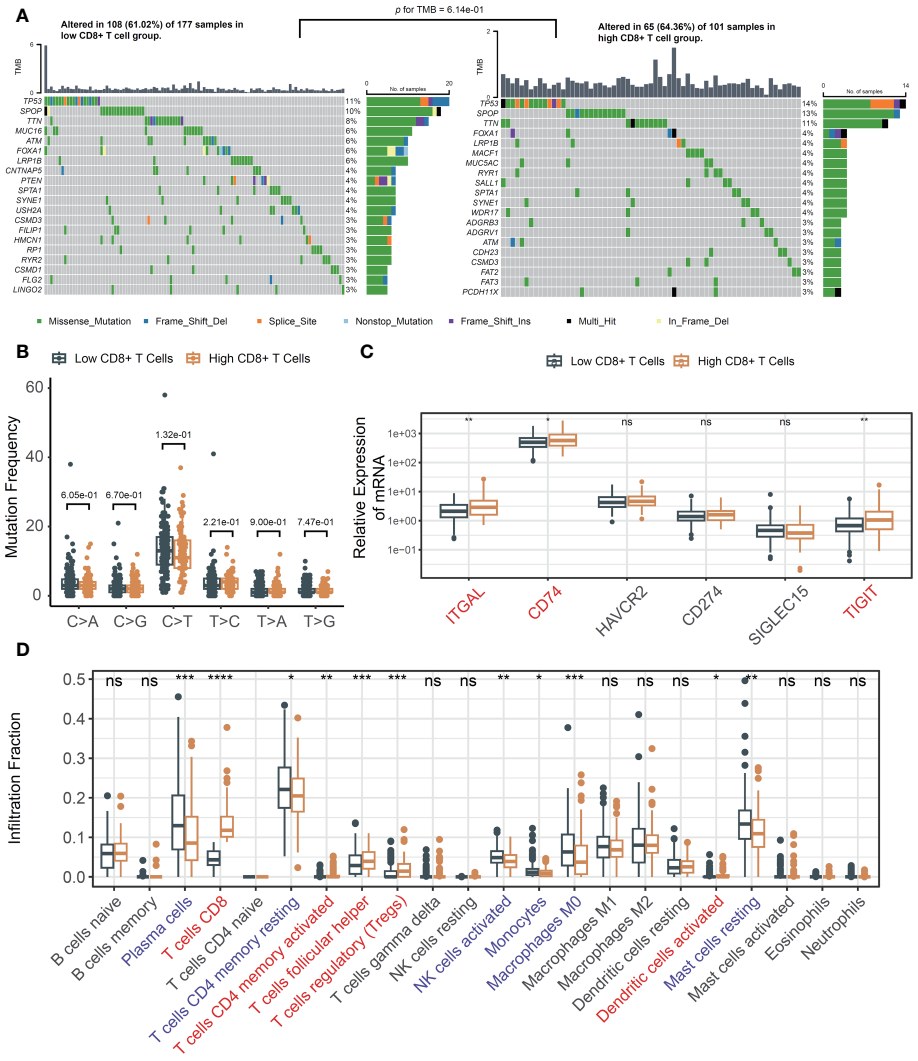

FIGURE 2
The changes of TME in response to infiltrated CD8+ T cells. **(A)** Oncoplots across tumor-infiltrating CD8+ T cells and comparison of TMBs; **(B)** The mutation frequency analysis of SNPs in TCGA; **(C)** Immune checkpoint genes in low and high infiltrated CD8+ T cell groups; **(D)** The fraction of tumor-infiltrating immune cells across the density of CD8+ T cells. ns, not significant, *p< 0.05, **p< 0.01, ***p< 0.001, ****p< 0.0001.

10.3389/fimmu.2024.1364329

Identification *MLXIPL* mediated by CD8+ T cells

We hypothesized that protein-coding genes influenced by CD8+ T cells should (1) alter in response to CD8+ T cell infiltration and (2) play a significant role in PCa prognosis. Initially, a differential expression analysis was conducted to compare the low and high CD8+ T cell groups. Three distinct methods, Wilcoxon rank sum test, DESeq2, and edgeR, were utilized. Genes with an adjusted p-value below 0.05 and an absolute log2-scaled fold change exceeding 0.5849625 were identified as DEGs. In total, 74, 233 and 356 DEGs were identified using each respective method. In total, 55 genes exhibited an increase, while 2 genes showed a decrease in the high CD8+ T cell group (Figures 3A, B). Among them, 34 genes were involved in the LM22 matrix. Furthermore, we conducted a screening of genes associated with the prognosis of PCa. Among 55 DEGs, *MLXIPL* was identified using LASSO Cox analysis with the TCGA dataset (Figure 3C). Specifically, *MLXIPL* showed elevated expression in the high CD8+ T cell group (p = 2.06E-4, Supplementary Figure S4A) and exhibited a significant correlation with the level of CD8+ T cells (*rho* = 0.25, p = 2.92E-5, Supplementary Figure S4B). These findings were confirmed using the MSKCC dataset (p = 3.81e-10, Supplementary Figure S4C; *rho* = 0.67, p = 9.54E-20, Supplementary Figure S4D).

We conducted a functional enrichment analysis to explore the biological pathways that exhibit alterations in response to CD8+ T cell infiltration. Based on KEGG database, we identified a total of 23 significantly enriched pathways majorly related to such as cell communication, immune responses, and immune checkpoint pathways (Figure 3D). The most of significant altered pathways were linked to functions cell communication, antigen presentation, and immune responses. Based on KEGG, GSEA revealed 31 upregulated and 11 downregulated pathways. Consistent with the results of the enrichment analysis, these altered pathways were associated with upregulated cell communication, antigen presentation, and immune responses (Supplementary Figure S5). Collectively, these findings suggested that changes in cell communication occur in response to CD8+ T cell infiltration, which may contribute to an unfavorable prognosis of PCa.

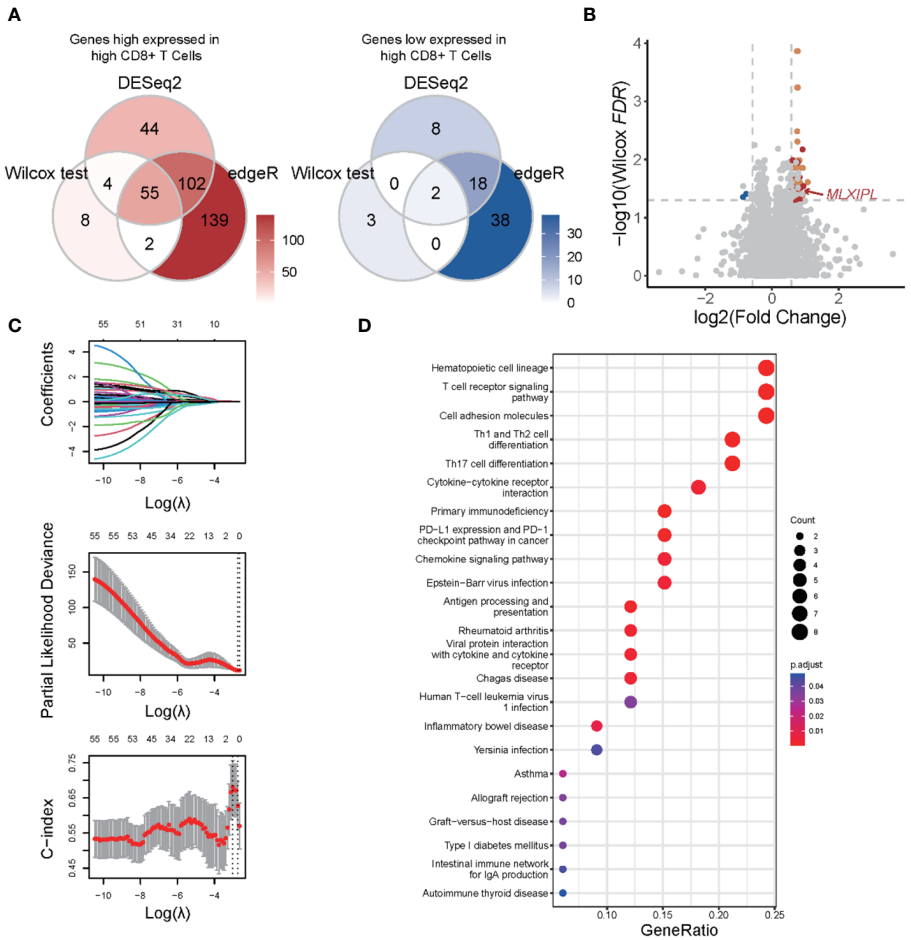

FIGURE 3
Functional enrichment analysis of differentially expressed genes in response to CD8+ T cells. **(A)** Venn plots of differentially expressed genes identified by Wilcoxon rank sum and signed rank test, DESeq2 and edgeR; **(B)** Volcano plot of differential expression genes; **(C)** LASSO with biochemical recurrence as the endpoint; **(D)** Functional enrichment analysis based on KEGG database.

10.3389/fimmu.2024.1364329

MLXIPL mediated by CD8+ T cells facilitated unfavorable prognosis

Elevated expression of *MLXIPL* mediated by CD8+ T cells was correlated with an increased rate of biochemical recurrence (log-rank p = 2.30E-02, Figure 4A). Univariate and multivariate Cox proportional hazards regression models validated that *MLXIPL* significantly contributed to a poor prognosis (crude p = 4.20E-03, adjusted p = 6.70E-02, Supplementary Figure S6). Moreover, the risk score, computed using *MLXIPL*, age, T stage and Gleason score, exhibited strong predictive capabilities for PCa prognosis (1-year AUC = 0.70; 3-year AUC = 0.72; 5-year AUC = 0.82, Figure 4B). The C-index value of the model was 0.72 (95% CI: 0.64-0.80).

Consistently, *MLXIPL* remained an independent predictor, unaffected by variables such as age, PSA levels, tumor purity, T and N stages, and Gleason score. In the high *MLXIPL* group, we observed a decreased acinar adenocarcinoma ratio and an increased number of nodes (Supplementary Figures S7A–F). Additionally, reduced mutation frequency and TMB were observed in high *MLXIPL* group (Supplementary Figure S7G). All TMBs were less than 10 mutations

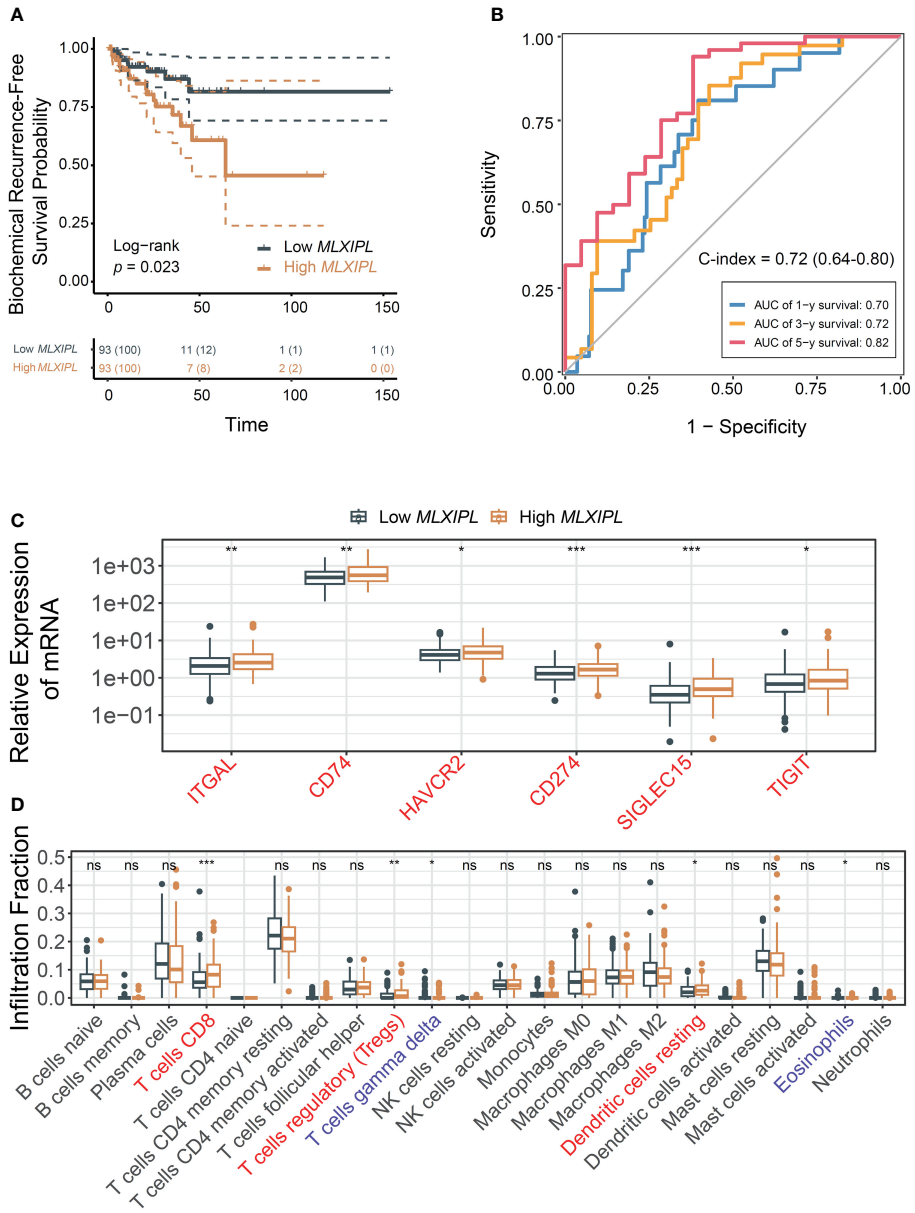

FIGURE 4
MLXIPL induced poor PCa prognosis in TCGA PRAD. **(A)** Survival analysis of biochemical recurrence for *MLXIPL* expression (top tertile *vs* bottom tertile) in TCGA PRAD; **(B)** ROC curves of biochemical recurrence in 1, 3 and 5 year(s); **(C)** Immune checkpoint genes out of LM22 matrix expressed in response to *MLXIPL* expression (top binary *vs* bottom binary); **(D)** The fraction of tumor-infiltrating immune cells across *MLXIPL* expression (top binary *vs* bottom binary). ns, not significant, *p< 0.05, **p< 0.01, ***p< 0.001.

per megabase (MB), indicating a low TMB level. Moreover, somatic mutation frequency analysis revealed no mutation was associated with *MLXIPL* expression (Supplementary Table S3). Consistent with the results above, *ITGAL*, *CD74*, and *TIGIT* showed elevated expression in response to *MLXIPL* (Figure 4C). Furthermore, *MLXIPL* was associated with the infiltration fraction of several immune cells (Figure 4D). Specifically, the high *MLXIPL* group demonstrated an increased infiltration of regulatory T cells.

Validation the prognostic role of *MLXIPL*

To validate the findings, we investigated the role of MSKCC in PCa prognosis using the MSKCC cohort. High *MLXIPL* was associated with poor prognosis (log-rank p = 1.6E-02, Figure 5A). Univariate and multivariate Cox proportional hazards regression models confirmed that *MLXIPL* was associated with poor prognosis (crude p = 1.46E-02, adjusted p = 4.23E-01, Supplementary Figure S8). The AUC values of

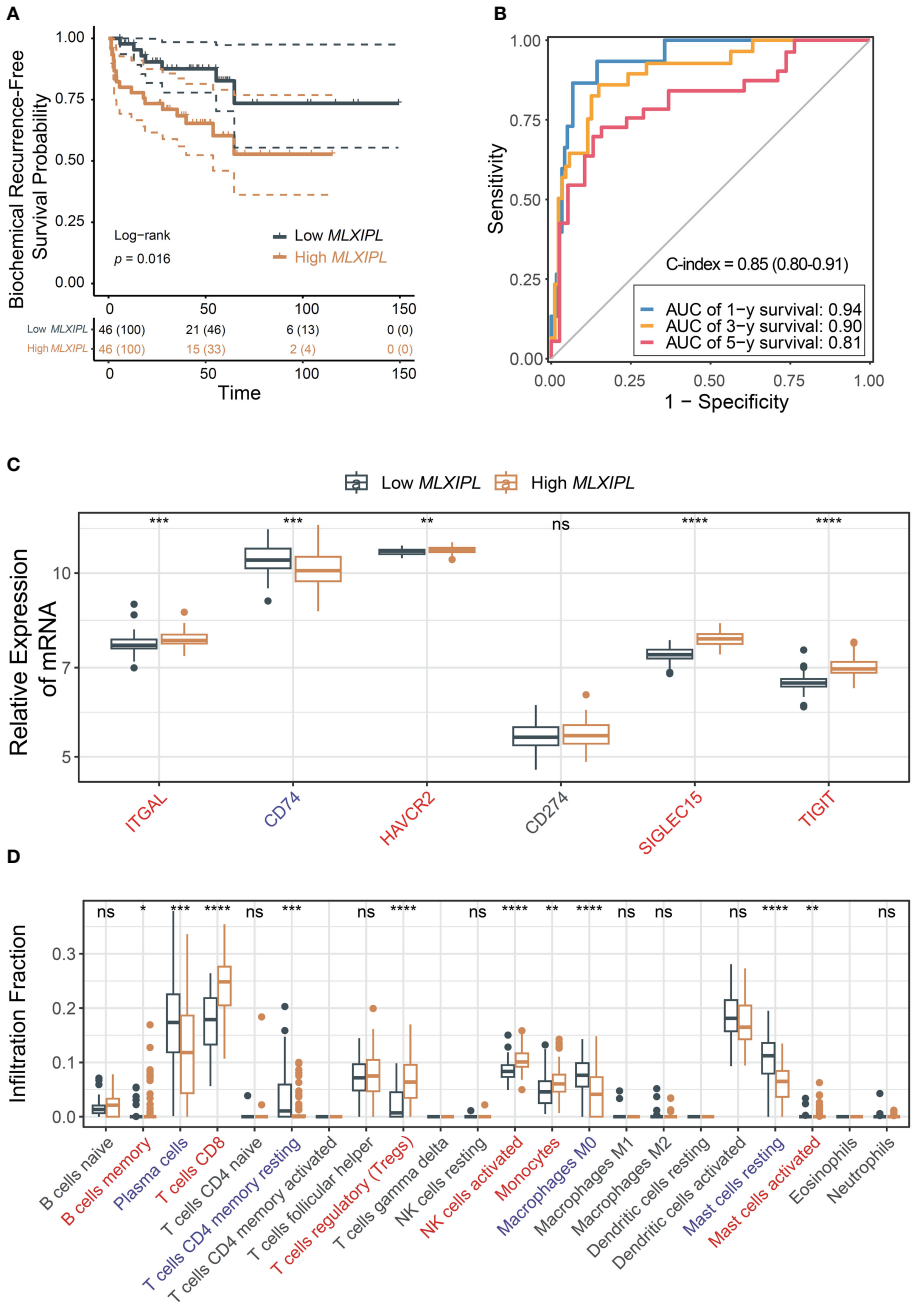

FIGURE 5
Validation of the role *MLXIPL* in MSKCC cohort. **(A)** Biochemical recurrence-free survival for *MLXIPL* (top tertile *vs* bottom tertile); **(B)** ROC curves of biochemical recurrence in 1, 3 and 5 year(s); **(C)** Immune checkpoint relevant genes out of LM22 matrix expressed in low and high *MLXIPL* groups (top binary *vs* bottom binary); **(D)** The fraction of tumor-infiltrating immune cells across *MLXIPL* expression (top binary *vs* bottom binary). ns, not significant, *p< 0.05, **p< 0.01, ***p< 0.001, ****p< 0.0001.

the risk score, calculated based on *MLXIPL*, T stage, and Gleason score, for predicting 1-, 3-, and 5-year biochemical recurrence were 0.94, 0.90, and 0.81, respectively (Figure 5B). The C-index value of the model was 0.85 (95% CI: 0.80-0.91). *MLXIPL* was implicated in N stage, while not correlated to age, PSA level, T stage, Gleason score, metastasis and *ERG*-fusion status (Supplementary Figure S9). Four immune checkpoint genes, namely *ITGAL*, *HAVCR2*, *SIGLEC15* and *TIGIT*, increased and *CD74* decreased (Figure 5C). Among them, *ITGAL* and *TIGIT* also elevated in TCGA. Additionally, *MLXIPL* were related to infiltration fraction of several immune cells (Figure 5D). As anticipated, Tregs infiltration increased in the high *MLXIPL* group.

In summary, these results suggest that CD8+ T cells may modulate *MLXIPL*, thereby affecting PCa prognosis by upregulating *ITGAL* and *TIGIT* and recruiting immunosuppressive Tregs.

Establishment of the nomogram survival model

Finally, we examined the role of *MLXIPL* in our own cohort, comprising 94 PCa patients with follow-up information (Supplementary Table S4). Briefly, the mean ages were 60.02 ± 7.08 and 61.04 ± 7.37 in the low and high *MLXIPL* groups, respectively. The results showed that *MLXIPL* expression was not correlated to age, T stage, N stage and Gleason score (Supplementary Figure S10).

Consistent with previous findings, *MLXIPL* promoted to poor prognosis (log-rank p = 7.2E-04, Figure 6A; crude HR = 2.22, 95% CI: 1.33-3.72, p = 2.42E-03; adjusted HR = 2.57, 95% CI: 1.42-4.65, p = 1.76E-03, Supplementary Figure S11). Moreover, when combined with clinicopathologic characteristics, *MLXIPL* demonstrated high predictive performance. The AUC values of the risk score, calculated based on *MLXIPL*, age, T stage, and Gleason score, for predicting 1-, 2-, and 3-year overall survival were 0.77, 0.75, and 0.80, respectively (Figure 6B). The C-index value of the model was 0.76 (95% CI: 0.65-0.86). To further improve prognostic prediction, a nomogram model was established using multivariable Cox regression in the NanTong cohort to estimate the 1-, 2-, and 3-year biochemical recurrence, incorporating *MLXIPL* expression, age, T stage, and Gleason grade as variables (Figure 6C).

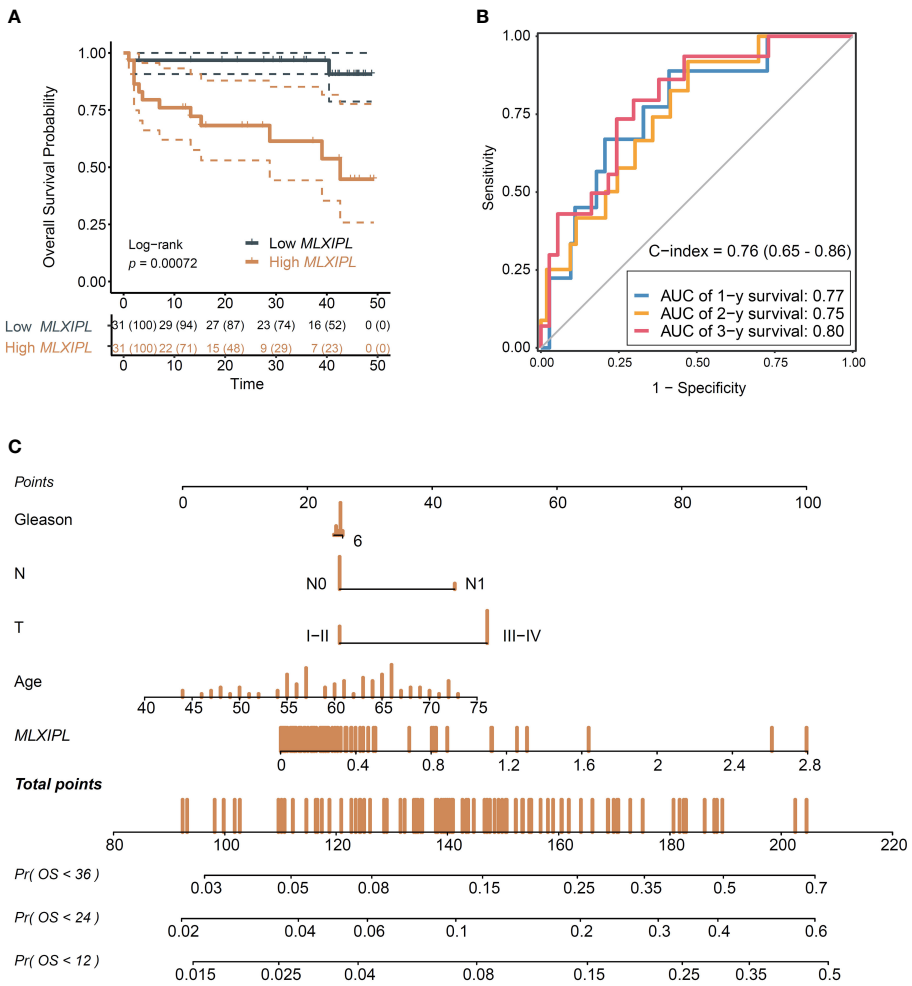

FIGURE 6
Validation of the role *MLXIPL* in NanTong cohort. **(A)** Overall survival for *MLXIPL* (top tertile *vs* bottom tertile); **(B)** ROC curves of overall survival in 1-, 3- and 5-year(s); **(C)** Nomogram for overall survival of PCa. ROC, receiver operating characteristic.

Furthermore, we investigated the protein levels of *MLXIPL* in human prostate tissue microarray to understand its role in PCa tumorigenesis. The baseline characteristics of 59 PCa patients, including 55 pairs of normal adjacent tissue and tumor samples, are presented in Supplementary Table S5. In summary, the mean age of the 59 men was 66.83 ± 5.50. IHC results revealed an elevation in MLXIPL protein levels in the tumor tissue (unpaired p = 1.03E-2, paired p = 3.27E-2, Supplementary Figure S12).

Discussion

This study aimed to comprehend the mechanisms by which infiltrating CD8+ T cells contribute to an unfavorable prognosis in PCa. The findings suggest that the poor prognosis of PCa observed may be attributed to increased expression of immune checkpoint molecules and recruitment of Tregs. Importantly, *MLXIPL* associated with CD8+ T cells was identified and validated. In summary, this study provides new insights into the potential mechanisms by which CD8+ T cells contribute to poor prognosis in PCa.

In this study, we identified *MLXIPL* as a potential downstream target of CD8+ T cells associated with poor prognosis. *MLXIPL* (max-like protein X interacting protein like, also known as Carbohydrate-Responsive Element-Binding Protein, ChREBP) initially identified in 2001, has a key role in regulating metabolic switch (25). The activity of ChREBP is regulated by several mechanisms, including post-translational modifications and interactions with other proteins. For example, phosphorylation of ChREBP by AMP-activated protein kinase (AMPK) under low glucose conditions inhibits its transactivation activity, preventing the induction of lipogenic genes (26). Additionally, ChREBP forms a complex with its partner MLX (Max-like protein X), which is necessary for its DNA-binding activity (27). Understanding these regulatory mechanisms is crucial for elucidating the role of *MLXIPL* in metabolic switches. ChREBP predominantly localizes in the nucleus in response to high glucose levels, which is essential for its function as a transcription factor (28). Under low glucose conditions, ChREBP is primarily found in the cytoplasm, where it remains inactive. This glucose-dependent nuclear-cytoplasmic shuttling is critical for its ability to regulate metabolic pathways adaptively.

Accumulating evidence suggests that *MLXIPL* has a crucial role in cancer pathology and tumorigenesis. Tong et al. observed suppression of *MLXIPL* in hepatoma and colorectal cancer switched aerobic glycolysis to mitochondrial respiration, reduced lipogenesis and nucleotide synthesis and decreased proliferative and tumorigenic potential (28). Through triggering the expression of the PI3K regulatory subunit p85α, *MLXIPL* sustains the activity of the pro-oncogenic PI3K/AKT signaling pathway in hepatocellular cancer. In parallel, increased *MLXIPL* activity reprograms glucose and glutamine metabolic fluxes into fatty acid and nucleic acid synthesis by increasing the expression of genes involved in lipogenesis, glutamine metabolism and *de novo* pyrimidine synthesis to support tumor growth (29). Furthermore, increased MLXIPL staining has been observed in breast cancer, exhibiting a clear positive correlation with malignant progression (30). However, in gastric tumor, *MLXIPL* inhibits proliferation and promotes apoptosis via targeting the cyclin D1-Rb-E2F1 pathway (31). As for PCa, Kaushik et al. reported that *MLXIPL* contribute to CRPC progress in AR-V7-positive 22RV1 cells (32). Given multifaceted role of MLXIPL, the pro-tumorigenic mechanism of *MLXIPL* in PCa may be different from the ones that *MLXIPL* exerts in other tumors. Therefore, the role of *MLXIPL* in PCa remains to be investigated.

The potential mechanisms by which *MLXIPL* is induced in cancer cells by T cell infiltration may be as follows: (1) CD8+ T cells release various cytokines and chemokines upon activation and infiltration into the tumor microenvironment (33). It is possible that one or more of these immune mediators directly or indirectly upregulate *MLXIPL* expression in cancer cells. For example, IFN-γ, a cytokine commonly produced by activated T cells, has been shown to influence the expression of various genes within tumor cells and could potentially modulate *MLXIPL* expression (34). (2) Direct interactions between CD8+ T cells and cancer cells through cell surface receptors and their ligands might play a role in inducing MLXIPL. The engagement of specific immune checkpoints or adhesion molecules could trigger signaling pathways within cancer cells that lead to increased expression of *MLXIPL*. (3) The infiltration of CD8+ T cells and their interaction with other components of the TME, such as fibroblasts, endothelial cells, and other immune cells, could lead to changes in the TME that indirectly promote *MLXIPL* expression in cancer cells. For instance, alterations in hypoxia levels, nutrient availability, or extracellular matrix composition could affect the metabolic state of cancer cells, potentially inducing *MLXIPL* as part of a broader metabolic reprogramming.

To avoid confounding factors, we compared clinicopathological characteristics, TMB, cytolytic scores and exhaustion levels of CD8 + T cells. Most of them were comparative. The density of CD8+ T cells and expression of *MLXIPL* was lower in prostate acinar adenocarcinoma compared to other histopathological subtypes of PCa. Thus, *MLXIPL* may serve as a potential biomarker for the malignant histopathological subtypes of PCa. Moreover, we observed a correlation between *MLXIPL* expression and the number of nodes (N stage) in commonly available data, however, this result cannot be confirmed in the validation cohort. The different results may be account for the difference of race and country. To clarify the role of *MLXIPL* in PCa, further validation across multicenter cohorts is essential.

In the last decade, immunotherapeutic agents have emerged as highly effective therapies for many cancers (35, 36). In patients with advanced PCa, immunotherapy treatments have largely failed (37–39). The disappointing outcomes of immunotherapy treatments in prostate cancer, including immune checkpoint inhibitors and CAR-T cell therapies, can be attributed to several key factors. (1) Low Mutational Burden: PCa typically exhibits a low mutational burden, which may contribute to its poor immunogenicity (40). A low

number of neoantigens presented by the tumor cells results in decreased recognition and activation of the immune system against the tumor (41). (2) Immunologically "Cold" Tumor Microenvironment: Prostate cancer often presents an immunologically "cold" microenvironment characterized by limited infiltration and activity of T cells. This environment is less responsive to immunotherapies that rely on the presence and activity of T cells to exert their anti-tumor effects (42). (3) Role of Androgens: Androgens and the AR signaling play a significant role in modulating immune responses. Research indicates that androgens can suppress T cell function and the production of IFNγ, directly affecting the effectiveness of T cell-targeted cancer immunotherapies (43). (4) AR Activity in T Cells: In castration-resistant prostate cancer, AR activity within T cells has been shown to limit the efficacy of checkpoint blockade therapies. Blocking AR signaling can sensitize the tumor-bearing host to effective checkpoint blockade by directly enhancing CD8 T cell function, preventing T cell exhaustion, and improving responsiveness to PD-1 targeted therapy via increased IFNγ expression (43). Given these challenges, strategies combining AR blockade with PD-1/PD-L1 inhibitors have been proposed and shown potential therapeutic effects in some studies (44). Schepisi et al. suggests that the development of CAR-T cell therapies targeting specific prostate cancer antigens could offer a new avenue for treatment (45). These findings underscore the need for a more nuanced understanding of prostate cancer's unique immune evasion mechanisms and suggest that optimizing treatment may require approaches tailored to these specific challenges. In our study, we postulated that *MLXIPL* expression is associated with the immune responses in PCa. In addition, as a central metabolic coordinator, *MLXIPL* responses to environmental and hormonal signals (25). Thus, inhibiting *MLXIPL* may improve responses of immunotherapy treatments in PCa.

A significant limitation of our study is the absence of direct experimental validation for our findings. While we utilized bioinformatics analyses to explore the role of CD8+ T cells and *MLXIPL* in PCa and validated our findings within our own cohort, experimental validation was not conducted. To replicate the TME, it is essential to use spontaneous tumor models (e.g., $Pten^{Pc-/-}$), rather than xenograft or allograft models, or to isolate CD8+ T cells. However, these approaches are time- and cost-intensive. Future research should prioritize incorporating functional assays and mechanistic investigations to strengthen the validity of our results.

Conclusions

This study unveiled a potential mechanism through which infiltrated CD8+ T cells contribute to a poorer prognosis in PCa. We identified *MLXIPL* as a potential downstream target of CD8+ T cells. *MLXIPL* holds promise as a target to enhance immunotherapy response, and a combination approach involving *MLXIPL* inhibition and immunotherapy may enhance the treatment efficacy for PCa.

Data availability statement

The original contributions presented in the study are included in the article/Supplementary Materials, further inquiries can be directed to the corresponding authors.

Ethics statement

The studies involving humans were approved by China Pharmaceutical University. The studies were conducted in accordance with the local legislation and institutional requirements. Written informed consent for participation in this study was provided by the participants' legal guardians/next of kin.

Author contributions

YF:. YG:. KN: Data curation, Visualization, Writing – review & editing. YL:. LQ:. HZ: Data curation, Visualization, Writing – review & editing. GM: Writing – original draft, Writing – review & editing.

Funding

The author(s) declare financial support was received for the research, authorship, and/or publication of this article. This work was supported by the National Natural Science Foundation of China (No. 82003979) and the China Postdoctoral Science Foundation (No. 2020M671660).

Conflict of interest

The authors declare that the research was conducted in the absence of any commercial or financial relationships that could be construed as a potential conflict of interest.

Publisher's note

Supplementary material

The Supplementary Material for this article can be found online at: https://www.frontiersin.org/articles/10.3389/fimmu.2024.1364329/full#supplementary-material

References

1. Rawla P. Epidemiology of prostate cancer. *World J Oncol*. (2019) 10:63–89. doi: 10.14740/wjon1191

2. Hamdy FC, Donovan JL, Lane JA, Mason M, Metcalfe C, Holding P, et al. 10-year outcomes after monitoring, surgery, or radiotherapy for localized prostate cancer. *N Engl J Med*. (2016) 375:1415–24. doi: 10.1056/NEJMoa1606220

3. Miszczyk M, Rajwa P, Yanagisawa T, Nowicka Z, Shim SR, Laukhtina E, et al. The efficacy and safety of metastasis-directed therapy in patients with prostate cancer: A systematic review and meta-analysis of prospective studies. *Eur Urol*. (2024) 85:125–38. doi: 10.1016/j.eururo.2023.10.012

4. Komura K, Sweeney CJ, Inamoto T, Ibuki N, Azuma H, Kantoff PW. Current treatment strategies for advanced prostate cancer. *Int J Urol*. (2018) 25:220–31. doi: 10.1111/iju.13512

5. Hanahan D, Coussens LM. Accessories to the crime: functions of cells recruited to the tumor microenvironment. *Cancer Cell*. (2012) 21:309–22. doi: 10.1016/j.ccr.2012.02.022

6. Elhanani O, Ben-Uri R, Keren L. Spatial profiling technologies illuminate the tumor microenvironment. *Cancer Cell*. (2023) 41:404–20. doi: 10.1016/j.ccell.2023.01.010

7. Kang J, La Manna F, Bonollo F, Sampson N, Alberts IL, Mingels C, et al. Tumor microenvironment mechanisms and bone metastatic disease progression of prostate cancer. *Cancer Lett*. (2022) 530:156–69. doi: 10.1016/j.canlet.2022.01.015

8. Fridman WH, Pages F, Sautes-Fridman C, Galon J. The immune contexture in human tumours: impact on clinical outcome. *Nat Rev Cancer*. (2012) 12:298–306. doi: 10.1038/nrc3245

9. Fridman WH, Zitvogel L, Sautes-Fridman C, Kroemer G. The immune contexture in cancer prognosis and treatment. *Nat Rev Clin Oncol*. (2017) 14:717–34. doi: 10.1038/nrclinonc.2017.101

10. Bruni D, Angell HK, Galon J. The immune contexture and Immunoscore in cancer prognosis and therapeutic efficacy. *Nat Rev Cancer*. (2020) 20:662–80. doi: 10.1038/s41568-020-0285-7

11. Kaur HB, Guedes LB, Lu J, Maldonado L, Reitz L, Barber JR, et al. Association of tumor-infiltrating T-cell density with molecular subtype, racial ancestry and clinical outcomes in prostate cancer. *Mod Pathol*. (2018) 31:1539–52. doi: 10.1038/s41379-018-0083-x

12. Petitprez F, Fossati N, Vano Y, Freschi M, Becht E, Luciano R, et al. PD-L1 expression and CD8(+) T-cell infiltrate are associated with clinical progression in patients with node-positive prostate cancer. *Eur Urol Focus*. (2019) 5:192–6. doi: 10.1016/j.euf.2017.05.013

13. Giraldo NA, Becht E, Pagès F, Skliris G, Verkarre V, Vano Y, et al. Orchestration and prognostic significance of immune checkpoints in the microenvironment of primary and metastatic renal cell cancer. *Clin Cancer Res*. (2015) 21:3031–40. doi: 10.1158/1078-0432.CCR-14-2926

14. Granier C, Dariane C, Combe P, Verkarre V, Urien S, Badoual C, et al. Tim-3 expression on tumor-infiltrating PD-1(+)CD8(+) T cells correlates with poor clinical outcome in renal cell carcinoma. *Cancer Res*. (2017) 77:1075–82. doi: 10.1158/0008-5472.CAN-16-0274

15. Aran D, Sirota M, Butte AJ. Systematic pan-cancer analysis of tumour purity. *Nat Commun*. (2015) 6:8971. doi: 10.1038/ncomms9971

16. Zhou L, Chi-Hau Sue A, Bin Goh WW. Examining the practical limits of batch effect-correction algorithms: When should you care about batch effects? *J Genet Genomics*. (2019) 46:433–43. doi: 10.1016/j.jgg.2019.08.002

17. Newman AM, Liu CL, Green MR, Gentles AJ, Feng W, Xu Y, et al. Robust enumeration of cell subsets from tissue expression profiles. *Nat Methods*. (2015) 12:453–7. doi: 10.1038/nmeth.3337

18. Rooney MS, Shukla SA, Wu CJ, Getz G, Hacohen N. Molecular and genetic properties of tumors associated with local immune cytolytic activity. *Cell*. (2015) 160:48–61. doi: 10.1016/j.cell.2014.12.033

19. Wherry EJ, Ha SJ, Kaech SM, Haining WN, Sarkar S, Kalia V, et al. Molecular signature of CD8+ T cell exhaustion during chronic viral infection. *Immunity*. (2007) 27:670–84. doi: 10.1016/j.immuni.2007.09.006

20. McKinney EF, Lee JC, Jayne DR, Lyons PA, Smith KG. T-cell exhaustion, co-stimulation and clinical outcome in autoimmunity and infection. *Nature*. (2015) 523:612–6. doi: 10.1038/nature14468

21. Li Y, Ge X, Peng F, Li W, Li JJ. Exaggerated false positives by popular differential expression methods when analyzing human population samples. *Genome Biol*. (2022) 23:79. doi: 10.1186/s13059-022-02648-4

22. Wu T, Hu E, Xu S, Chen M, Guo P, Dai Z, et al. clusterProfiler 4.0: A universal enrichment tool for interpreting omics data. *Innovation (Camb)*. (2021) 2:100141. doi: 10.1016/j.xinn.2021.100141

23. Zhuo Z, Lin H, Liang J, Ma P, Li J, Huang L, et al. Mitophagy-related gene signature for prediction prognosis, immune scenery, mutation, and chemotherapy response in pancreatic cancer. *Front Cell Dev Biol*. (2021) 9:802528. doi: 10.3389/fcell.2021.802528

24. Wu Y, Hao X, Wei H, Sun R, Chen Y, Tian Z. Blockade of T-cell receptor with Ig and ITIM domains elicits potent antitumor immunity in naturally occurring HBV-related HCC in mice. *Hepatol*. (2023) 77:965–81. doi: 10.1002/hep.32715

25. Abdul-Wahed A, Guilmeau S, Postic C. Sweet sixteenth for chREBP: established roles and future goals. *Cell Metab*. (2017) 26:324–41. doi: 10.1016/j.cmet.2017.07.004

26. Kim MH, Kang KS. Isoflavones as a smart curer for non-alcoholic fatty liver disease and pathological adiposity via ChREBP and Wnt signaling. *Prev Med*. (2012) 54:S57-63. doi: 10.1016/j.ypmed.2011.12.018

27. Ma L, Tsatsos NG, Towle HC. Direct role of ChREBP.Mlx in regulating hepatic glucose-responsive genes. *J Biol Chem*. (2005) 280:12019–27. doi: 10.1074/jbc.M413063200

28. Tong X, Zhao F, Mancuso A, Gruber JJ, Thompson CB. The glucose-responsive transcription factor ChREBP contributes to glucose-dependent anabolic synthesis and cell proliferation. *Proc Natl Acad Sci U S A*. (2009) 106:21660–5. doi: 10.1073/pnas.0911316106

29. Benichou E, Seffou B, Topçu S, Renoult O, Lenoir V, Planchais J, et al. The transcription factor ChREBP Orchestrates liver carcinogenesis by coordinating the PI3K/AKT signaling and cancer metabolism. *Nat Commun*. (2024) 15:1879. doi: 10.1038/s41467-024-45548-w

30. Airley RE, McHugh P, Evans AR, Harris B, Winchester L, Buffa FM, et al. Role of carbohydrate response element-binding protein (ChREBP) in generating an aerobic metabolic phenotype and in breast cancer progression. *Br J Cancer*. (2014) 110:715–23. doi: 10.1038/bjc.2013.765

31. Zhang J, Zhang J, Fu Z, Zhang Y, Luo Z, Zhang P, et al. CHREBP suppresses gastric cancer progression via the cyclin D1-Rb-E2F1 pathway. *Cell Death Discovery*. (2022) 8:300. doi: 10.1038/s41420-022-01079-1

32. Kaushik AK, Shojaie A, Panzitt K, Sonavane R, Venghatakrishnan H, Manikkam M, et al. Inhibition of the hexosamine biosynthetic pathway promotes castration-resistant prostate cancer. *Nat Commun*. (2016) 7:11612. doi: 10.1038/ncomms11612

33. Aichele P, Neumann-Haefelin C, Ehl S, Thimme R, Cathomen T, Boerries M, et al. Immunopathology caused by impaired CD8+ T-cell responses. *Eur J Immunol*. (2022) 52:1390–5. doi: 10.1002/eji.202149528

34. Kang H, Seo MK, Park B, Yoon SO, Koh YW, Kim D, et al. Characterizing intrinsic molecular features of the immune subtypes of salivary mucoepidermoid carcinoma. *Transl Oncol*. (2022) 24:101496. doi: 10.1016/j.tranon.2022.101496

35. Wei SC, Duffy CR, Allison JP. Fundamental mechanisms of immune checkpoint blockade therapy. *Cancer Discovery*. (2018) 8:1069–86. doi: 10.1158/2159-8290.CD-18-0367

36. Sharma P, Allison JP. Dissecting the mechanisms of immune checkpoint therapy. *Nat Rev Immunol*. (2020) 20:75–6. doi: 10.1038/s41577-020-0275-8

37. Beer TM, Kwon ED, Drake CG, Fizazi K, Logothetis C, Gravis G, et al. Randomized, double-blind, phase III trial of ipilimumab versus placebo in asymptomatic or minimally symptomatic patients with metastatic chemotherapy-naive castration-resistant prostate cancer. *J Clin Oncol*. (2017) 35:40–7. doi: 10.1200/JCO.2016.69.1584

38. Antonarakis ES, Piulats JM, Gross-Goupil M, Goh J, Ojamaa K, Hoimes CJ, et al. Pembrolizumab for treatment-refractory metastatic castration-resistant prostate cancer: multicohort, open-label phase II KEYNOTE-199 study. *J Clin Oncol*. (2020) 38:395–405. doi: 10.1200/JCO.19.01638

39. Sharma P, Pachynski RK, Narayan V, Fléchon A, Gravis G, Galsky MD, et al. Nivolumab plus ipilimumab for metastatic castration-resistant prostate cancer: preliminary analysis of patients in the checkMate 650 trial. *Cancer Cell*. (2020) 38:489–499.e3. doi: 10.1016/j.ccell.2020.08.007

40. Lawrence MS, Stojanov P, Polak P, Kryukov GV, Cibulskis K, Sivachenko A, et al. Mutational heterogeneity in cancer and the search for new cancer-associated genes. *Nature*. (2013) 499:214–8. doi: 10.1038/nature12213

41. Sridaran D, Bradshaw E, DeSelm C, Pachynski R, Mahajan K, Mahajan NP. Prostate cancer immunotherapy: Improving clinical outcomes with a multi-pronged approach. *Cell Rep Med*. (2023) 4:101199. doi: 10.1016/j.xcrm.2023.101199

42. Bilusic M, Madan RA, Gulley JL. Immunotherapy of prostate cancer: facts and hopes. *Clin Cancer Res*. (2017) 23:6764–70. doi: 10.1158/1078-0432.CCR-17-0019

43. Guan X, Polesso F, Wang C, Sehrawat A, Hawkins RM, Murray SE, et al. Androgen receptor activity in T cells limits checkpoint blockade efficacy. *Nature*. (2022) 606:791–6. doi: 10.1038/s41586-022-04522-6

44. Kissick HT, Sanda MG, Dunn LK, Pellegrini KL, On ST, Noel JK, et al. Androgens alter T-cell immunity by inhibiting T-helper 1 differentiation. *Proc Natl Acad Sci U S A*. (2014) 111:9887–92. doi: 10.1073/pnas.1402468111

45. Schepisi G, Cursano MC, Casadei C, Menna C, Altavilla A, Lolli C, et al. CAR-T cell therapy: a potential new strategy against prostate cancer. *J Immunother Cancer*. (2019) 7:258. doi: 10.1186/s40425-019-0741-7

frontiers | Frontiers in Immunology

TYPE Review
PUBLISHED 25 April 2024
DOI 10.3389/fimmu.2024.1388574

OPEN ACCESS

EDITED BY
Hao Chen,
Shandong University, China

REVIEWED BY
Fei Zhou,
Northwestern University, United States
Wenqing Zhang,
The Ohio State University, United States

*CORRESPONDENCE
Hui Zhu
drzhuh@126.com

RECEIVED 20 February 2024
ACCEPTED 16 April 2024
PUBLISHED 25 April 2024

CITATION
Li J, Lu S, Chen F and Zhu H (2024) Unveiling the hidden role of extracellular vesicles in brain metastases: a comprehensive review. *Front. Immunol.* 15:1388574. doi: 10.3389/fimmu.2024.1388574

Unveiling the hidden role of extracellular vesicles in brain metastases: a comprehensive review

Ji Li, Shuangqing Lu, Feihu Chen and Hui Zhu*

Department of Radiation Oncology, Shandong Cancer Hospital and Institute, Shandong First Medical University and Shandong Academy of Medical Sciences, Jinan, Shandong, China

Background: Extracellular vesicles (EVs) are small, transparent vesicles that can be found in various biological fluids and are derived from the amplification of cell membranes. Recent studies have increasingly demonstrated that EVs play a crucial regulatory role in tumorigenesis and development, including the progression of metastatic tumors in distant organs. Brain metastases (BMs) are highly prevalent in patients with lung cancer, breast cancer, and melanoma, and patients often experience serious complications and are often associated with a poor prognosis. The immune microenvironment of brain metastases was different from that of the primary tumor. Nevertheless, the existing review on the role and therapeutic potential of EVs in immune microenvironment of BMs is relatively limited.

Main body: This review provides a comprehensive analysis of the published research literature, summarizing the vital role of EVs in BMs. Studies have demonstrated that EVs participate in the regulation of the BMs immune microenvironment, exemplified by their ability to modify the permeability of the blood-brain barrier, change immune cell infiltration, and activate associated cells for promoting tumor cell survival and proliferation. Furthermore, EVs have the potential to serve as biomarkers for disease surveillance and prediction of BMs.

Conclusion: Overall, EVs play a key role in the regulation of the immune microenvironment of brain metastasis and are expected to make advances in immunotherapy and disease diagnosis. Future studies will help reveal the specific mechanisms of EVs in brain metastases and use them as new therapeutic strategies.

KEYWORDS

brain metastasis, extracellular vesicles, immune microenvironment, molecular mechanism, immunotherapy

Introduction

Metastases are typically associated with unfavorable prognoses and represent the primary cause of mortality in cancer patients (1). Brain metastasis (BMs) is a common clinical occurrence, particularly in patients with advanced non-small-cell lung cancer (NSCLC), with BMs developing in up to 40% of cases (2). The majority of patients with brain metastases experience significant changes in nervous system function, adversely impacting their quality of life. However, due to the limited treatment options, the prognosis remains unfavorable. As a result, brain metastases significantly impact the survival time and quality of life for patients. Early-stage patients with BMs often face challenges in receiving optimal treatment due to a lack of symptoms. However, there is still a lack of noninvasive and highly accurate tumor biomarkers in the early stages, which could play a significant role in BMs screening. Despite substantial progress in chemotherapy, radiotherapy, and targeted therapy, patients with advanced BMs continue to have a poor prognosis, imposing a substantial burden on families and society. Therefore, there is an urgent need for additional prognostic and risk indicators.

In the current phase of scientific exploration and implementation, researchers are investigating the structure, related technologies, and mechanisms of exosomes. A significant milestone was reached at the end of 2018 when the International Society for EVs issued guidelines to establish standardized nomenclature for EVs. Presently, the majority of techniques used for isolating exosomes result in the isolation of heterogeneous populations of EVs derived from various biogenic sources. For the sake of precision and clarity, we will henceforth refer to these vesicles as "EVs," which are commonly referred to as "exosomes" in scientific literature. The Minimal Information for Studies of Extracellular Vesicles 2018 (MISEV2018) guidelines specify the use of membrane vesicles derived from small cells (3).

EVs, composed of nanoscale vesicle structures secreted by the majority of cells, comprise three distinct types of vesicles, exosomes (30-150 nm), microvesicles (100-1000 nm), and apoptotic bodies (1000-5000 nm). Cells can secrete exosomes in various states, apoptotic bodies are secreted during apoptosis, and microparticles are released when cells receive external stimuli such as radiation. EVs play a pivotal role in intercellular communication and participate in various physiological functions (4). As an illustration, the cargo of fatty acids carried by tumor EVs and particles (EVPs), specifically palmitic acid, induces the secretion of tumor necrosis factor (TNF) by Kupffer cells. This process creates a pro-inflammatory microenvironment, inhibits fatty acid metabolism and oxidative phosphorylation, and contributes to the formation of fatty liver (5). Moreover, studies have indicated that tumor type-specific proteins present in EVPs can aid in the classification of unknown primary tumors. The protein content of EVPs can serve as a dependable biomarker for the detection and identification of different types of cancer (6). The aforementioned studies demonstrate the significant impact of EVs on the onset and progression of tumors; however, the influence on brain metastases remains uncertain. The presence of the blood-brain barrier represents a fundamental distinction between the brain and other bodily tissues and organs. Owing to the distinctive structure of EVs, they possess the ability to traverse the blood-brain barrier and influence the onset and progression of brain metastases. In recent times, there has been a growing number of articles that elucidate the role of EVs or exosomes in the context of brain metastases. This surge in research output has fueled the expansion of exosome-related investigations in this field.

The objective of this review is to present a comprehensive overview of the recent major advancements in the field, focusing on the role and application of EVs in brain metastases. A comprehensive literature search was conducted using Embase, PubMed, Web of Science, and Clinicaltrials.gov databases to identify relevant publications until November 1, 2023. The screening process for literature pertaining to "Brain metastasis" [Mesh], "Exosomes" [Mesh], and "Extracellular vesicles" adhered to the guidelines established in MISEV 2018.

Abbreviations: sEVs, small extracellular vesicles; miRNAs, microRNA; circRNA, circular RNA; lncRNA, long noncoding RNA; CAF, Cancer-associated fibroblast; TAM, Tumour-associated macrophage; IL, Interleukin; 5-FU, 5-Fluorouracil; MDSC, Myeloid-derived suppressor cell; PD-1, Programmed death receptor protein 1; PD-L1, Programmed death-ligand 1; BMs, Brain metastasis; NSCLC, non-small-cell lung cancer; MVBs, Multivesicular bodies; APCs(MVBs), Antigen presenting cells; TNBC, Triple-negative breast cancer; TLR2, Toll-like receptor 2; BBB, Blood-brain barrier; BCP, B cell precursor; CNS, Central nervous system; VEGF, Vascular endothelial growth factor; HDL, High-density lipoproteins; LDL, Low-density lipoproteins.

Characteristics of extracellular vesicles

Structure and Biological Origin of Extracellular Vesicles

In their study, researchers observed the transformation of sheep reticulocytes into mature red blood cells, during which they release small vesicles containing transferrin metabolites. Initially dismissed as cell debris, further research recognized these vesicles as distinct structures (7). The process begins with the plasma membrane forming early endosomes, which evolve into multivesicular bodies (MVBs) through vesicle formation (8). MVBs are crucial for various cellular functions, including endocytosis, protein sorting, storage, transport, and the release into the extracellular space, either by degradation or fusion with the cell membrane (9). Although the endosomal sorting complex required for transport (ESCRT) has been implicated in exosome formation, evidence suggests ESCRT-independent pathways also play significant roles (10–12). Novel mechanisms, such as one controlled by RAB31, further expand our understanding of exosome biogenesis (Figure 1).

Extracellular vesicles (EVs) are categorized into exosomes (30-150 nm), microvesicles (100-1000 nm), and apoptotic bodies (1000-5000 nm) (13, 14), each carrying vital biological materials like proteins, DNA, RNA, enzymes, and lipids (15, 16). Initially mistaken for waste, these vesicles are now recognized for their

10.3389/fimmu.2024.1388574

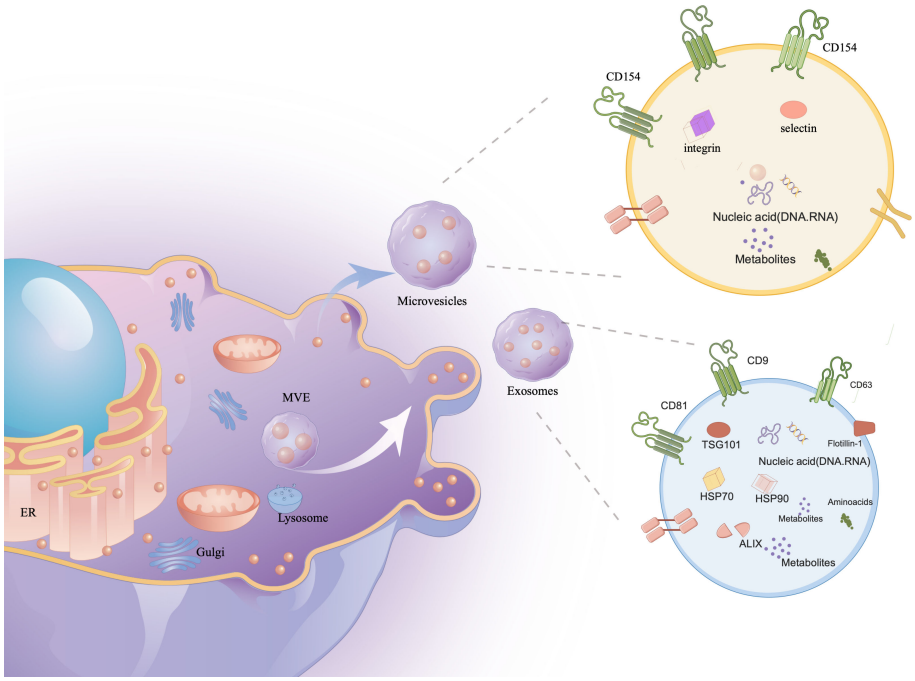

FIGURE 1
The contents of exosomes. The cell membrane invagination will form endosome, which will then form multivesicular bodies (MVB), which will be secreted to the exocytosomes as exosomes. Exosomes contain a variety of proteins, lipids, DNA, RNA and other important information of the mother cell.

critical roles in human development and regulation. They influence biomarker levels and act as therapeutic agents and drug delivery systems, especially in autoimmune diseases (17–19).

Exosomes are considered the most applicable vesicles due to their nanometric size and ease of isolation. These single-cell exosomes have a membrane structure composed of bilayers of lipids, measuring 30-150 nm in size and having a density of approximately 1.13-1.21 g/ml (20). Exosomes are produced in most human cells and are widely distributed in various bodily fluids, including blood, urine, cerebrospinal fluid, tears, saliva, milk, ascites, lymph, and amniotic fluid (21). Ectosomes (difference with exosomes), also known as microparticles or microvesicles, derived from plasma membranes, exhibit similar functions to exosomes (22). Apoptotic bodies, observed during apoptosis, are also referred to as apoptotic vesicles. They can be mistakenly identified as other EVs (23). The functionality of EVs largely relies on their complex and diverse cargo. Approximately 76% of this cargo consists of proteins, while 15% comprises mRNA. The remaining components include DNAs, microRNAs (miRNAs), circular RNAs (circRNAs), and long noncoding RNAs (lncRNAs). These components have the potential to significantly alter recipient cells that interact with exosomes (24–38).

In the current state, there is a lack of optimal separation strategies or markers for distinguishing between different sources of EVs. Therefore, it is challenging to propose specific and universally applicable markers for MVB-derived "exosomes" compared to other small EVs. The term "exosomes" refers to EV preparations that have been isolated from larger vesicles, but these preparations are actually mixtures of exosomal and non-exosomal EV particles (29). Following the guidelines of MISEV2018, we have used the term "small extracellular vesicles (sEVs)" to refer to vesicles with diameters of either 200 nm or 100 nm, instead of using the term "exosomes" (4).

Characterization, storage, and separation of sEVs

Various protocols have been employed for the separation of sEVs (30, 31).Currently, ultracentrifugation is widely used for the isolation of sEVs (32). Classic techniques, including density gradients (33), immunoisolation (34), precipitation (35), and filtration (36), are also utilized. Each method has advantages and disadvantages in terms of recovery, specificity, time, and cost (37, 38). Despite the development of several novel techniques in recent years (39–42), complete isolation of sEVs remains challenging. Therefore, a combination of methods will remain recommended in the future. Identifying sEVs is also challenging. MISEV2018 guidelines recommend providing quantitative descriptions of both the EV source and EV preparation. EV characteristics are routinely assessed by detecting and analyzing protein content. For positive identification, EVs must contain at least one transmembrane/lipid-bound protein (typically CD9, CD63, CD81, and integrin) and one cytosolic protein (typically ALIX, TSG101, syntenin, and HSP70). Additionally, the levels of at least one negative protein, such as albumin, lipoproteins, or ribosomal proteins, must be determined. Furthermore, analysis of functional proteins, including histones, cytochrome C, calnexin, and Grp94 (7), is required for sEVs.

Western blotting is the most commonly used method for detecting proteins on the surface and within a cell. Fluorescent microscopy enables the detection of structures that have been labeled with fluorescent dyes (43). Flow cytometry has limitations in detecting SEVs due to their small size and low amount of surface antigens (44). In recent years, there has been a significant improvement in the affordability and accessibility of mass spectrometry techniques (45). However, when it comes to protein extraction, a large quantity of small extracellular vesicles (sEVs) is required, which can often reduce the overall efficiency of the process (9). To fully characterize the heterogeneity of individual vesicles, it is recommended to employ two complementary techniques, such as transmission electron microscopy or atomic force microscopy (46). These imaging techniques provide valuable insights into the structural characteristics of sEVs, allowing for a better understanding of their composition and behavior. In addition to extracting and characterizing sEVs, proper storage conditions are essential for maintaining the integrity and preserving the characteristics of these vesicles. Currently, there is no general consensus regarding the storage conditions for the original samples from which sEVs are extracted, specifically whether they should be stored at -80°C and used promptly when conducting experiments (47, 48).

EVs regulate the microenvironment of brain metastases

EVs affect the pre-metastatic immune microenvironment

Recent studies have demonstrated the crucial role of exosomes in establishing a pre-metastatic immune microenvironment for brain metastasis. Hoshino et al. conducted an analysis on the biodistribution of tumor-secreted exosomes and discovered that integrins (ITGs) fuse with T cells in a tissue-specific manner, thereby facilitating organ-specific colonization and creating a pre-metastatic microenvironment for brain metastasis (49). Moreover, tumor-secreted CEMIP$^+$ exosomes are taken up by brain endothelial and microglial cells, resulting in the upregulation of pro-inflammatory cytokines encoded by Ptgs2, Tnf, and Ccl/Cxcl, which promotes brain vascular remodeling and metastasis (50). This suggests that exosomes have the ability to modify the premetastatic immune microenvironment, facilitating tumor metastasis to target organs. Additionally, researchers have discovered that cancer-derived extracellular miR-122 modifies glucose utilization in recipient premetastatic niche cells, leading to the reprogramming of systemic energy metabolism to aid disease progression. Consequently, glucose becomes more readily available to metastatic tumor cells in the brain, allowing for their initial expansion (51). Moreover, miR-19a transferred from astrocyte EVs to metastatic breast cancer cells downregulates PTEN and increases proliferation of the recipient tumor cells (52). It has also been observed that the expression of serum exo-AnxA2 is elevated in African-American (AA) women with triple-negative breast cancer (TNBC), promoting angiogenesis (53). EVs derived from breast tumors can interact with Toll-like receptor 2 (TLR2) on macrophages, stimulating the nuclear factor kappa-light-chain-enhancer of activated B cells (NF-κB) signaling pathway and increasing the production of pro-inflammatory cytokines such as IL-6 and tumor necrosis factor alpha (TNF-α) (54). Additionally, these EVs released from drug-resistant MCF7 breast cancer cells stimulate IL-6 expression and decrease macrophage chemotaxis (55). Tumor-derived EVs containing tumor necrosis factor-related apoptosis inducing ligand (TRAIL) induce apoptosis *in vitro* (using the oligodendroglioma G26/24 cell line) (56). Furthermore, in breast cancer, loss of XIST activates MSN-c-Met and reprograms microglia through exosomal miR-503, thus promoting brain metastasis (57). miR-210 has been reported as a pro-angiogenic miRNA in normal adult mouse brain (58) and is overexpressed in cells that specifically metastasized to the brain (59). The possibility of EV miR-210 participating in brain metastasis and angiogenesis of breast cancer needs further study.

Researchers have demonstrated that EVs derived from melanoma, particularly exosomes, activate pro-inflammatory signaling in both lung fibroblasts and astrocytes (60). This exosome-mediated pro-inflammatory reprogramming plays a crucial functional role in the recruitment of immune cells by activated fibroblasts and astrocytes (61). Additionally, blasts from B cell precursor (BCP)-acute lymphoblastic leukemia (ALL) release multiple cytokines and exosomes containing IL-15. These exosomes bind to and are internalized by astrocytes and brain vessel endothelial cells. Consequently, astrocytes produce VEGF-AA, which disrupts the integrity of the blood-brain barrier (BBB) (62).

Exosomes derived from human brain microvascular endothelial cells (HBMECs) induce an increase in S100A16 levels in SCLC brain metastasis. The protective effect mediated by S100A16 is related to the up-regulation of prohibitin (PHB)-1, a protein found in the mitochondria's inner membrane. PHB-1 helps preserve mitochondrial membrane potential (DCm) and supports the survival of SCLC cells in the brain (63). Zhang and colleagues have recently shown that miR-19a from astrocytes downregulates PTEN expression in cancer cells. This downregulation leads to increased secretion of CCL2 and recruitment of myeloid cells, ultimately promoting brain metastasis (52). Furthermore, the transfer of exosomal cargo induces transcriptomic changes that enhance the inflammatory phenotype of stromal cells, similar to that of cancer-associated fibroblasts (CAFs) (64). Overall, extracellular vesicle-derived miRNA, proteins, and genes contribute to the creation of a pre-metastatic microenvironment and promote tumor metastasis by influencing the phenotype of intracranial immune cells while improving the metastatic ability of tumor cells (Figure 2).

EVs affect blood-brain barrier permeability

The central nervous system (CNS) is tightly regulated by the blood-brain barrier (BBB) and the neurovascular unit (NVU), composed of endothelial cells (ECs), pericytes, and astrocytic endfeet, to ensure normal brain function (65). The primary event in brain metastasis is the infiltration of cancer cells through the blood-brain barrier (BBB). Researchers have demonstrated that

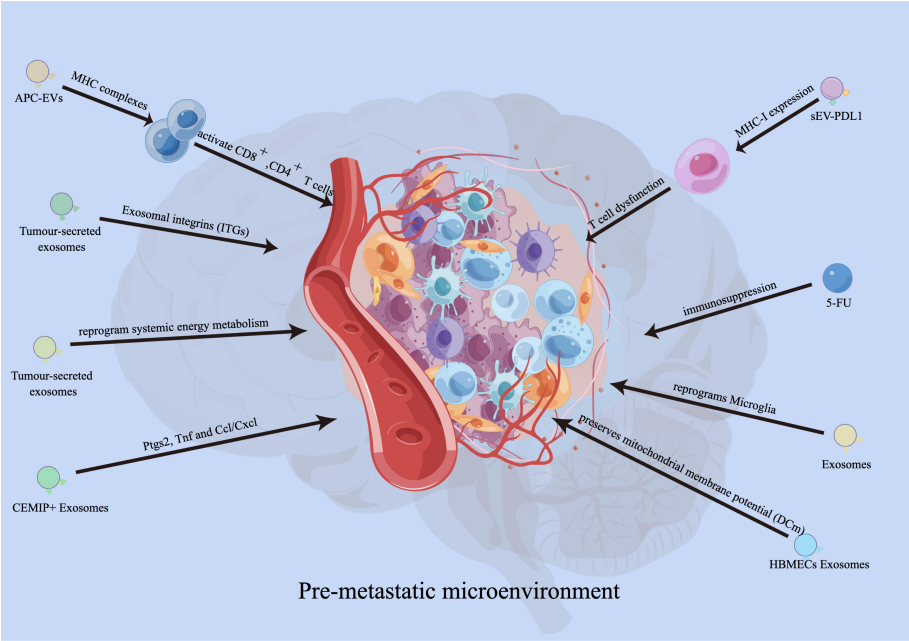

FIGURE 2
Functions of EVs in developing pre-metastatic microenvironment. EVs derived from antigen presenting cells (APCs) can also activate $CD8^+$and $CD4^+$ T cells. Exosomes carrying PD-L1 promoted tumor growth and reduced the number of T cells in the spleen and lymph nodes in mouse experiments. Integrins (ITGs) fuse with target cells in a tissue-specific manner to direct organ-specific colonization. Tumour-secreted $CEMIP^+$ exosomes uptaked by brain endothelial and microglial cells, upregulating the pro-inflammatory cytokines encoded by Ptgs2, Tnf and Ccl/Cxcl, promote brain vascular remodelling and metastasis. Human brain microvascular endothelial cells (HBMECs)-derived exosomes induce the elevated S100A16 in SCLC brain metastasis, and the S100A16-mediated protective effect is related to the up-regulation of prohibitin (PHB)-1.

exosomes can cross the BBB and transport cargo, bypassing the mononuclear phagocyte system (MPS) (66). Tumor-derived EVs can breach the intact BBB *in vivo* by utilizing transcytosis as the underlying mechanism. Researchers have also identified and characterized the mechanism by which tumor-derived EVs overcome the low physiological rate of transcytosis in the BBB. This is achieved by reducing brain endothelial expression of rab7 and enhancing transport efficiency (67). A study demonstrated that TGF-β1-mediated exosomal lnc-MMP2-2 derived from non-small cell lung cancer (NSCLC) increases BBB permeability and facilitates brain metastasis of NSCLC (68). In addition, lncRNA GS1-600G8.5 was found to be significantly upregulated in breast cancer cells with a high propensity for brain metastasis, in contrast to exosomes derived from poorly metastatic breast cancer cells. Disruption of the BBB by exosomal lncRNA GS1-600G8.5 promoted the passage of breast cancer cells, potentially through the targeting of tight junction proteins. These studies have provided a novel understanding of the role of exosomal lncRNAs in cancer brain metastasis (69) (Table 1). Evs derived from MDA-MB-231 breast cancer cells reduce the expression of the tightly connected molecule ZO-1 by loading miR-105 (70). Another study on BMS breast cancer cells also confirmed the effect of EV miR-181c on the localization of actin filaments, resulting in increased brain endothelial permeability (71). These may be the potential mechanisms by which tumor-derived EVs affects the integrity of the blood-brain barrier. The findings indicate that EVs can compromise the integrity of the blood-brain barrier and facilitate the formation of brain metastases.

EVs affect the survival and proliferation of tumor cells

Tumor suppressor genes, such as PTEN, encode the phosphatase PTEN. Expression of PTEN in metastatic tumor cells is hindered by the presence of EV-miR-19 released from astrocytes. Moreover, tumor cells lacking PTEN engage in the recruitment of $IBA1^+$ myeloid cells to enhance proliferation. Consequently, the recruited myeloid cells secrete NF-kb and CCL2, thereby inhibiting their own apoptosis and promoting the occurrence of brain metastasis (72). The underlying phenomenon can be illustrated as follows. The miRNA derived from stromal cells within the tumor microenvironment stimulates cell proliferation while concurrently inhibiting cell apoptosis, thus promoting tumor growth.

Tumor-derived exosomes have the potential to enhance tumor cell proliferation. A recent study observed an increase in the expression of miR-503, a negative regulator of the X-inactive specific transcript, in breast cancer patients with brain metastasis. Subsequently, the upregulation of miR-503 in microglia promotes the transformation from an M1 to an M2 phenotype (73). The acquisition of an M2 phenotype by microglia facilitates an immunosuppressive tumor environment by impeding T cell proliferation. These findings confirm that tumor-derived exosomes have the ability to modulate immune cell function, promoting immune evasion mechanisms and creating a conducive environment for tumor cell proliferation (74). Exosomes derived from antigen presenting cells (APCs), in addition to containing MHC complexes, have the ability to directly or indirectly activate $CD8^+$ T cells and $CD4^+$ T cells (75). Dendritic cell-derived

TABLE 1 Role of sEVs in brain metastasis.

Type	Contents	Donor cells	Recipient cells	Function	Ref.
Protein	ITGs	Cancer cells	T cells	establish pre-metastatic microenvironment	(49)
Protein	CEMIP	Cancer cells	brain endothelial and microglial cells	promote brain vascular remodelling and metastasis	(50)
Protein	TRAIL	G26/24 cell line	Astrocyte	induce astrocyte apoptosis *in vitro*	(56)
Protein	IL-15	BCP-ALL	astrocytes, brain vessel endothelial cells	disrupts the integrity of the blood-brain barrier (BBB)	(58)
Protein	S100A16	HBMECs	Cancer cells	supports the survival of SCLC cells in brain	(59)
miRNA	miR-19a	Astrocyte	Cancer cells	enhanced the proliferation of the recipient tumour cells	(60)
miRNA	miR-122	Cancer cells	niche cells	reprogram systemic energy metabolism to facilitate disease progression	(51)
miRNA	miR-503	Cancer cells	Microglia	promote Brain Metastasis	(53)
lncRNA	lnc-MMP2-2	Cancer cells	brain vessel endothelial cells	increases BBB permeability	(66)
lncRNA	lncRNA GS1-600G8.5	Cancer cells	brain vessel endothelial cells	disrupted the BBB	(67)
miRNA	miR-210	Cancer cells	brain vessel endothelial cells	promote brain vascular remodelling and metastasis	(58)
miRNA	miR-105	Cancer cells	brain vessel endothelial cells	disrupted the BBB	(70)
miRNA	miR-181c	Cancer cells	brain vessel endothelial cells	disrupted the BBB	(71)
Protein	IL-6	Cancer cells	Macrophage	promote Brain Metastasis	(55)

exosomes are capable of inducing a pro-inflammatory cytokine profile, while exosomes derived from tumor cells typically induce a pro-tumorigenic immune profile. Remarkably, exosomes carrying PD-L1, identical in structure to the surface of tumor cells, are capable of binding to T cells (76). An experiment conducted with $CD8^+$ T cells demonstrated that PD-L1-incorporated exosomes inhibit their proliferation. In mouse experiments, exosomes carrying PD-L1 were found to promote tumor growth and decrease the number of T cells in the spleen and lymph nodes (76). During the early stages of apoptosis, decline in mitochondrial membrane potential and increase in radical production can be observed. Exosomes play a significant role in preventing the decline in mitochondrial membrane potential during the early stages of apoptosis through the actions of PHB, a protein found in the mitochondrial inner membrane (77). These findings suggest that exosomes have the ability to regulate tumor cell stability and promote their proliferation by modulating mitochondrial membrane potential. Overall, EVs, particularly exosomes, can significantly impact the survival and proliferation of tumor cells through their influence on mitochondrial function.

Application potential of extracellular vesicles in disease monitoring and prediction of BMs

EVs as potential tumor markers for brain metastasis

Pathologists commonly perform tissue biopsies for cancer diagnosis and treatment monitoring purposes. In contrast, liquid biopsies offer minimal invasiveness, the potential for serial testing, and the ability to detect cancer at an earlier, more treatable stage. With rising expectations for liquid biopsy technologies, exosomes are emerging as a valuable resource for early cancer detection.

It has been demonstrated in previous studies that cells release exosomes, abundant in blood, cerebrospinal fluid (CSF), and urine. Currently, the detection method is becoming more specialized and sensitive. *In vitro* experiments showed higher expression levels of these exosome miRNAs in CRC cell lines compared to non-tumor cells (78). Patients with gastric cancer (GC) exhibited a significant increase in plasma LINC00152 levels compared to healthy controls (79). Exo-miRNAs can serve as biomarkers for early-stage prognosis of brain metastases. Skog et al. (80) previously reported the isolation of serum-derived EVs from patients with brain tumors and the detection of specific genetic alterations in the EGFR gene. Cerebrospinal fluid (CSF) has been found to be a suitable biofluid for analyzing the macromolecular contents of EVs in previous EV studies. Chen et al. demonstrated that mutant IDH1 G395A can be detected in CSF EVs with a sensitivity of 63% and a specificity of 100% (81). Figueroa et al. (2019) reported that, in comparison to the gold standard qPCR method used for detecting the EGFRvIII transcript in brain tumor tissue, extracellular vesicular RNA analysis allows for the detection of the oncogene EGFRvIII with a sensitivity of 60% and a specificity exceeding 98% (82). Manda et al. conducted similar studies on plasma, which yielded an 80% sensitivity and a 79% specificity (83). Akers et al. demonstrated that miR-21 (84) and miRNA signature (85) from CSF EVs can differentiate between tumor and non-tumor disease states.

EVs as new targets for brain metastasis therapy

Exosomes are believed to play a role in the development, metastasis, and cell proliferation of brain metastasis. Directly targeting the proteins and nucleic acids within exosomes has the potential to suppress cancer development. This research is expected to generate novel insights for the diagnosis and treatment of brain metastasis. Cell surface molecules, such as ANXA2 (86) and miRMA (87), are considered potential targets for brain metastasis therapy. PD-L1 (Programmed Cell Death-Ligand 1) is expressed in EVs secreted by tumors and can metastasize to other cells. Binding of PD-L1 with PD-1 activates the PD-1/PD-L1 pathway, resulting in diminished anti-tumor activity of T cells and induction of T-cell apoptosis. This pathway ultimately facilitates immune escape by tumor cells (76, 88). Reducing the expression of Rab27a and using an exosome inhibitor (GW4869) not only impacted exosome production but also inhibited the release of PD-L1 from exosomes (89). Therefore, these findings have the potential to unleash powerful anticancer effects. This represents a significant stride towards precision medicine and personalized treatment for brain metastasis.

EVs as new drug delivery systems for brain metastasis therapy

In patients with central nervous system (CNS) metastases, the efficacy of standard chemotherapies or targeted agents is constrained by the limited penetration of antineoplastic agents across the blood-brain barrier (90). Exosomes serve as a promising drug delivery system to overcome the challenge of chemotherapeutic drugs crossing the blood-brain barrier. Using exosomes as drug delivery systems offers several advantages, such as low toxicity, membrane-like structure, flexibility, high drug carrying capacity, passive targeting, good biocompatibility, as well as improved drug bioavailability and sustained release (91, 92). The loading methods of drugs into exosomes can be categorized into two types: endogenous and exogenous approaches (93). In endogenous loading, parent cells undergo genetic modification to express specific proteins or nucleic acids to be packaged in the released vesicles. Alternatively, drugs can be loaded exogenously by incorporating them into exosomes derived from cell culture media or body fluids, such as urine, blood, saliva, or breast milk. Various vesicular systems, including niosomes, proniosomes, ethosomes, ufasomes, pharmacosomes, transferosomes, and phytosomes, have been extensively investigated due to their capability to deliver drugs to the target site while minimizing toxicity to healthy tissues (94).

The study examined zebrafish embryos to assess the effectiveness of exosomes in delivering anticancer drugs to the brain *in vivo* (95). Additionally, experiments with mice demonstrated the ability of exosomes to transport siRNA across the blood-brain barrier and into the brain (96). In an initial study, the researchers investigated whether naturally brain-targeted exosomes, derived from brain endothelial cells, could transport siRNA specific to the tumor marker vascular endothelial growth factor (VEGF) across the blood-brain barrier (BBB) in both *in vitro* and *in vivo* settings. The researchers successfully suppressed zebrafish tumors that were xenografted with VEGF through the delivery of VEGF using exosomes, and subsequently achieved tumor knockdown in zebrafish utilizing the delivered VEGF. These findings provide support for the potential use of natural exosome vesicles in targeted delivery of siRNA to the brain for the treatment of brain diseases (97). In another study, it was demonstrated that exosomes, namely Exo-cur which encapsulated curcumin, and Exo-JSI124 which inhibited signal transducer and activator of transcription 3 (Stat3), could be noninvasively delivered to microglia cells through intranasal administration. The study further revealed the preventive effect of intranasally administered Exo-cur or Exo-JSI124 on LPS-induced brain inflammation in mice (98). A similar study reported that niosomes incorporating folic acid were taken up by rat brain models with an uptake rate of approximately 48.15% (99). This suggests that exosome is a novel treatment strategy for brain tumors and metastases.

The practical application of EVs in the treatment of brain metastases

sEVs hold immense potential in the field of cancer immunotherapy (49). Immunotherapy-related clinical trials have gradually emerged as a result of the development of PD-1/PD-L1 research for MSI-H and dMMR patients. Recent research in tumor immunotherapy has primarily focused on inhibitors of the programmed death receptor protein 1 (PD-1) and programmed death-ligand 1 (PD-L1) to enhance immunity and overcome immune suppression by activating and promoting immune cells (80). Previous studies have predominantly explored the role of soluble PD-L1, with limited research on sEV-PD-L1. sEVs, with their secretory properties, can harbor inhibitors and killers of T cells within the local tumor microenvironment. Moreover, they possess the ability to migrate to distant sites, potentially facilitating tumor immune evasion (100). According to Fan et al. (101), the stability of sEV-PDL1 and its impact on T cell function can serve as indicators of a patient's immune status and long-term prognosis. Furthermore, a 2020 study by Zhang et al. (102) revealed that after two or more cycles of chemotherapy, 5-FU can upregulate the expression of sEV-PD-L1, leading to immunosuppression.

Potential advantages and challenges of EVs as a treatment strategy for BMs

Since the beginning of this decade, EVs have attracted considerable attention. A new perspective on brain metastasis prevention and treatment is presented by this research that expands our understanding of the functions of small extracellular vesicles (sEVs) and the mechanism of development of tumors. In general, BM metastasis-related sEVs are characterized by complex cargo as the primary mechanisms of action. Furthermore, many

unknown mechanisms and molecules, as well as communication between BM cells and the tumor microenvironment, contribute to the overall complexity and uncertainty. With the deeper investigation of exosomes, exosomes are expected to become a new target for cancer treatment and potential tool for early diagnosis of brain metastases.

According to these results, exosome-carried molecules can serve as biomarkers for the detection of diseases in its early stages. On the other hand, exosomes show a relatively high stability. Tissue-specific protein in exosome is found to be stable when stored at -80°C or colder, probably for a extended periods of time. Moreover, EVs can be obtained from autologous dissected primary tumor cells in clinical applications, making them biocompatible and safe options for personalized cancer therapy.

Opportunities and challenges coexist, of course. It is unknown which molecules play a dominant role in the comprehensive effect as well as the mechanisms that underlie the complex cargo. Several large-scale and multicenter studies have not been conducted due to immaturity of technology, diversity of detection methods and results, and high detection costs. A further challenge to the universality in existing research may be the genetic differences between East and West, between countries, and even between regions. Thus, scientific findings must be validated before being applied to clinical practice, a collaborative effort between clinicians, pharmacists, and other professional scientists is urgently needed to evaluate the safety, effectiveness, and stability of sEVs. Regardless, it is foreseeable that in the near future, sEVs will be an important tool for accurate early diagnosis and personalized and efficient treatment of cancers due to their unique biological characteristics, offering infinite power to overcome cancers.

Application potential of nanoscale biomembrane vesicles for brain metastasis therapy

Nanoparticles in nano drugs are commonly categorized as vesicular, lipid-based, or polymeric. Several vesicular systems, such as niosomes, proniosomes, ethosomes, ufasomes, pharmacosomes, transferosomes, and phytosomes, have been extensively studied for their potential to deliver drugs to target sites while minimizing damage to healthy tissues. Consequently, nanoscale biomembrane vesicles show promising potential for treating brain metastases.

Liposomes

Liposomes are vesicles composed of a lipid bilayer that encapsulates an aqueous core, offer a promising mechanism for drug delivery due to their biocompatibility as nanovesicles and their ability to protect encapsulated drug molecules from degradation (103, 104). Additionally, liposomal preparations have advantages over other nanocarriers and are considered the gold standard in nanomedicine, with numerous clinically approved liposomal products available for various diseases (105). However, their application in the treatment of brain metastases is rarely reported. Conventional liposomes have limitations such as their inability to interact with high-density lipoproteins (HDL) and low-density lipoproteins (LDL) (106). These problems can be overcome by using stealth liposomes, which are modified with biocompatible, inert, and hydrophilic polymers such as polyethylene glycol (PEG), poly(2-ethyl-2-oxazoline) (PEOZ), polyacrylamide (PAA), polyvinyl pyrrolidone (PVP), and poly-2-methyl-2-oxazoline (PMOZ) (107). These liposomal modifications have been extensively studied for the treatment of autoimmune diseases like rheumatoid arthritis (RA) and psoriasis. Recently, liposomal-based vesicular drug delivery systems that can cross the blood-brain barrier (BBB) and target injured vasculature sites in inflammatory tissues have emerged as potential candidates for treating multiple sclerosis (MS) (108). This provides a strong theoretical basis for exploring the application of this drug delivery system in the treatment of brain metastases.

Niosomes

Niosomes are a type of vesicular nanocarrier that has revolutionized drug delivery in recent years due to their numerous advantages (109). Niosomes can have different sizes and structures, small unilamellar vesicles (SUVs) are niosomes ranging from 10 to 100 nm in size, while large unilamellar vesicles (LUVs) are niosomes ranging from 100 to 3000 nm in size (110). Studies have demonstrated that the unique surface chemistry of niosomes enables them to cross the blood-brain barrier (BBB) and offers the potential for active targeting through surface modification with ligands (111). Numerous studies have shown that niosomes can cross the blood-brain barrier, offering relief from the symptoms of various autoimmune diseases that impact brain function (112). A similar study reported that niosome-incorporated folic acid was taken up by rat models' brains at an uptake rate of approximately 48.15% (113) (Figure 3). Inflamed areas contain a higher concentration of macrophages, which are immune-related cells responsible for triggering inflammation, making them a primary target for drug development (114). Researchers have shown that targeting macrophages with biocompatible nanovesicular systems can greatly enhance the treatment of autoimmune diseases such as rheumatoid arthritis (RA) (115). Niosomes also hold promise for the treatment of brain metastases.

Conclusions

EVs serve as crucial intercellular communication mediators with potential benefits and obstacles in managing brain metastases (BMs). EVs transport metastatic factors, miRNA, and proteins, facilitating the migration, colonization, and regulation of cancer cells in brain tissue. Moreover, EVs hold promise as biomarkers for monitoring and predicting the progression and prognosis of brain metastases. However, there are ongoing challenges in addressing the preparation, purification, stability, persistence, safety, and biodistribution of EVs as a therapeutic strategy. Hence, future research should prioritize optimizing EVs' preparation techniques, developing drug delivery systems, and

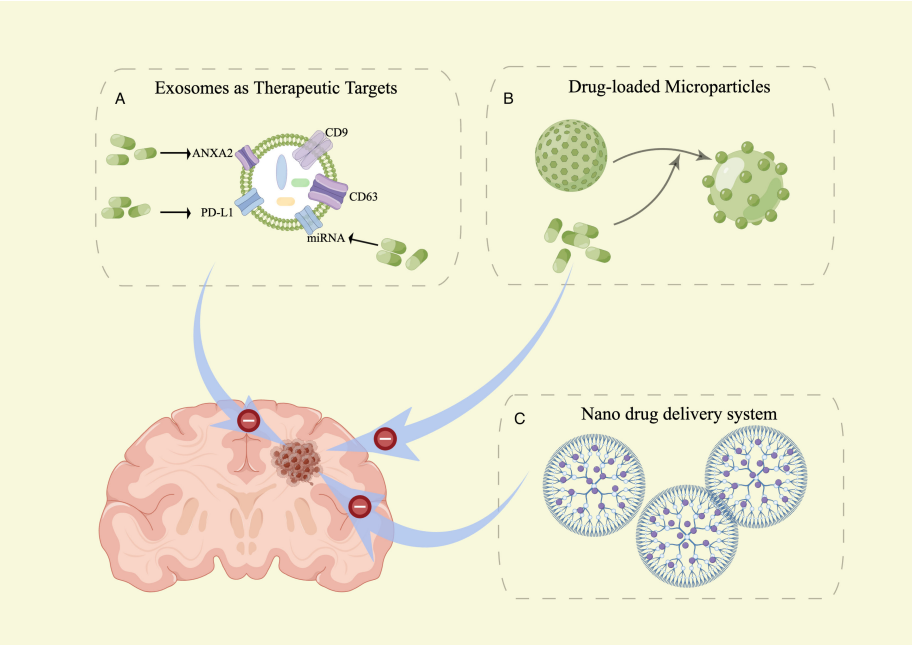

FIGURE 3
sEVs as tools and targets in brain metastasis therapy. **(A)** sEVs as a new target for brain metastasis therapy. **(B)** sEVs as a new drug delivery system for brain metastasis therapy. **(C)** Article-meta Nanoscale biomembrane vesicles Applications.

conducting clinical experiments to enhance their therapeutic potential for brain metastases. Meanwhile, there are more clinical studies targeting primary brain tumors, and there is a lack of the application of EVs as diagnostic and therapeutic drugs for metastatic brain tumors, indicating a limited amount of research on the mechanisms of EVs in metastatic brain tumors. Understanding the mechanism of action of EVs is crucial in guiding the development of effective clinical applications based on EVs.

In conclusion, extracellular vesicles play a significant regulatory role in managing lung cancer brain metastases and have potential value in therapeutic and diagnostic applications. Future studies should prioritize enhancing mechanistic research and conducting clinical trials to promote the practical utilization of extracellular vesicles as a treatment strategy and overcome associated challenges. These efforts will offer brain metastases patients personalized and innovative treatment alternatives, ultimately enhancing their quality of life and prognosis.

Author contributions

JL: Software, Writing – original draft. SL: Supervision, Writing – review & editing. FC: Formal analysis, Writing – review & editing. HZ: Funding acquisition, Writing – review & editing.

Funding

The author(s) declare financial support was received for the research, authorship, and/or publication of this article. This work was supported by the Shandong Province Natural Science Foundation innovation and development joint fund project [grant number: ZR2022LZL008] and the foundation of Natural Science Foundation of Shandong (ZR2023QH378).

Conflict of interest

The authors declare that the research was conducted in the absence of any commercial or financial relationships that could be construed as a potential conflict of interest.

Publisher's note

References

1. Hanahan D, Weinberg RA. Hallmarks of cancer: the next generation. *Cell*. (2011) 144:646–74. doi: 10.1016/j.cell.2011.02.013

2. Cagney DN, Martin AM, Catalano PJ, Redig AJ, Lin NU, Lee EQ, et al. Incidence and prognosis of patients with brain metastases at diagnosis of systemic Malignancy: a population-based study. *Neuro Oncol*. (2017) 19:1511–21. doi: 10.1093/neuonc/nox077

3. Théry C, Witwer KW, Aikawa E, et al. Minimal information for studies of extracellular vesicles 2018 (MISEV2018): a position statement of the International Society for Extracellular Vesicles and update of the MISEV2014 guidelines. *J Extracell Vesicles*. (2018) 7:1535750. doi: 10.1080/20013078.2018.1535750

4. Möller A, Lobb RJ. The evolving translational potential of small extracellular vesicles in cancer. *Nat Rev Cancer*. (2020) 20:697–709. doi: 10.1038/s41568-020-00299-w

5. Wang G, Li J, Bojmar L, et al. Tumour extracellular vesicles and particles induce liver metabolic dysfunction. *Nature*. (2023) 618:374–82. doi: 10.1038/s41586-023-06114-4

6. Hoshino A, Kim HS, Bojmar L, et al. Extracellular vesicle and particle biomarkers define multiple human cancers. *Cell*. (2020) 182:1044–1061.e18. doi: 10.1016/j.cell.2020.07.009

7. Pan BT, Johnstone RM. Fate of the transferrin receptor during maturation of sheep reticulocytes *in vitro*: selective externalization of the receptor. *Cell*. (1983) 33:967–78. doi: 10.1016/0092-8674(83)90040-5

8. Doyle LM, Wang MZ. Overview of extracellular vesicles, their origin, composition, purpose, and methods for exosome isolation and analysis. *Cells*. (2019) 8:727. doi: 10.3390/cells8070727

9. Borges FT, Reis LA, Schor N. Extracellular vesicles: structure, function, and potential clinical uses in renal diseases. *Braz J Med Biol Res*. (2013) 46:824–30. doi: 10.1590/1414-431X20132964

10. Li XH, Zhang J, Li DF, Wu W, Xie ZW, Liu Q. Physiological and pathological insights into exosomes in the brain. *Zool Res*. (2020) 41:365–72. doi: 10.24272/j.issn.2095-8137.2020.043

11. Wei D, Zhan W, Gao Y, et al. RAB31 marks and controls an ESCRT-independent exosome pathway. *Cell Res*. (2021) 31:157–77. doi: 10.1038/s41422-020-00409-1

12. Tian X, Shen H, Li Z, Wang T, Wang S. Tumor-derived exosomes, myeloidderived suppressor cells, and tumor microenvironment. *J Hematol Oncol*. (2019) 12:84. doi: 10.1186/s13045-019-0772-z

13. Yenuganti VR, Afroz S, Khan RA, Bharadwaj C, Nabariya DK, Nayak N, et al. Milk exosomes elicit a potent anti-viral activity against dengue virus. *J Nanobiotechnology*. (2022) 20:317. doi: 10.1186/s12951-022-01496-5

14. Frydrychowicz M, Kolecka-Bednarczyk A, Madejczyk M, Yasar S, Dworacki G. Exosomes - structure, biogenesis and biological role in non-small-cell lung cancer. *Scand J Immunol*. (2015) 81:2–10. doi: 10.1111/sji.12247

15. Pegtel DM, Gould SJ. Exosomes. *Annu Rev Biochem*. (2019) 88:487–514. doi: 10.1146/annurev-biochem-013118-111902

16. Harding CV, Heuser JE, Stahl PD. Exosomes: looking back three decades and into the future. *J Cell Biol*. (2013) 200:367–71. doi: 10.1083/jcb.201212113

17. Barile L, Vassalli G. Exosomes: Therapy delivery tools and biomarkers of diseases. *Pharmacol Ther*. (2017) 174:63–78. doi: 10.1016/j.pharmthera.2017.02.020

18. Boulanger CM, Loyer X, Rautou PE, Amabile N. Extracellular vesicles in coronary artery disease. *Nat Rev Cardiol*. (2017) 14:259–72. doi: 10.1038/nrcardio.2017.7

19. Tan L, Wu H, Liu Y, Zhao M, Li D, Lu Q. Recent advances of exosomes in immune modulation and autoimmune diseases. *Autoimmunity*. (2016) 49:357–65. doi: 10.1080/08916934.2016.1191477

20. Perez-Hernandez J, Cortes R. Extracellular vesicles as biomarkers of systemic lupus erythematosus. *Dis Markers*. (2015) 2015:613536. doi: 10.1155/2015/613536

21. Zöller M. Janus-faced myeloid-derived suppressor cell exosomes for the good and the bad in cancer and autoimmune disease. *Front Immunol*. (2018) 9:137 PMID: 29456536. doi: 10.3389/fimmu.2018.00137

22. Cocucci E, Meldolesi J. Ectosomes and exosomes: shedding the confusion between extracellular vesicles. *Trends Cell Biol*. (2015) 25:364–72. doi: 10.1016/j.tcb.2015.01.004

23. Atkin-Smith GK, Tixeira R, Paone S, Mathivanan S, Collins C, Liem M, et al. A novel mechanism of generating extracellular vesicles during apoptosis via a beads-on-a-string membrane structure. *Nat Commun*. (2015) 6:7439. doi: 10.1038/ncomms8439

24. Li Y, Zhao J, Yu S, Wang Z, He X, Su Y, et al. Extracellular vesicles Long RNA sequencing reveals abundant mRNA, circRNA, and lncRNA in human blood as potential biomarkers for Cancer diagnosis. *Clin Chem*. (2019) 65:798–808. doi: 10.1373/clinchem.2018.301291

25. Makarova J, Turchinovich A, Shkurnikov M, Tonevitsky A. Extracellular miRNAs and cell-cell communication: problems and prospects. *Trends Biochem Sci*. (2021) 46:640–51. doi: 10.1016/j.tibs.2021.01.007

26. Wang S, Zhang K, Tan S, Xin J, Yuan Q, Xu H, et al. Circular RNAs in body fluids as cancer biomarkers: the new frontier of liquid biopsies. *Mol Cancer*. (2021) 20:13. doi: 10.1186/s12943-020-01298-z

27. Sun Z, Yang S, Zhou Q, Wang G, Song J, Li Z, et al. Emerging role of exosome-derived long non-coding RNAs in tumor microenvironment. *Mol Cancer*. (2018) 17:82. doi: 10.1186/s12943-018-0831-z

28. Campos-Carrillo A, Weitzel JN, Sahoo P, Rockne R, Mokhnatkin JV, Murtaza M, et al. Circulating tumor DNA as an early cancer detection tool. *Pharmacol Ther*. (2020) 207:107458. doi: 10.1016/j.pharmthera.2019.107458

29. Mathieu M, Martin-Jaular L, Lavieu G, Thery C. Specificities of secretion and uptake of exosomes and other extracellular vesicles for cell-to-cell communication. *Nat Cell Biol*. (2019) 21:9–17. doi: 10.1038/s41556-018-0250-9

30. Monguio-Tortajada M, Galvez-Monton C, Bayes-Genis A, Roura S, Borras FE. Extracellular vesicle isolation methods: rising impact of size-exclusion chromatography. *Cell Mol Life Sci*. (2019) 76:2369–82. doi: 10.1007/s00018-019-03071-y

31. Patel GK, Khan MA, Zubair H, Srivastava SK, Khushman M, Singh S, et al. Comparative analysis of exosome isolation methods using culture supernatant for optimum yield, purity and downstream applications. *Sci Rep*. (2019) 9:5335. doi: 10.1038/s41598-019-41800-2

32. Gardiner C, Di Vizio D, Sahoo S, Thery C, Witwer KW, Wauben M, et al. Techniques used for the isolation and characterization of extracellular vesicles: results of a worldwide survey. *J Extracell Vesicles*. (2016) 5:32945. doi: 10.3402/jev.v5.32945

33. Lazaro-Ibanez E, Lasser C, Shelke GV, Crescitelli R, Jang SC, Cvjetkovic A, et al. DNA analysis of low- and high-density fractions defines heterogeneous subpopulations of small extracellular vesicles based on their DNA cargo and topology. *J Extracell Vesicles*. (2019) 8:1656993.

34. He M, Crow J, Roth M, Zeng Y, Godwin AK. Integrated immunoisolation and protein analysis of circulating exosomes using microfluidic technology. *Lab Chip*. (2014) 14:3773–80. doi: 10.1039/C4LC00662C

35. Li P, Kaslan M, Lee SH, Yao J, Gao Z. Progress in exosome isolation techniques. *Theranostics*. (2017) 7:789–804. doi: 10.7150/thno.18133

36. Kornilov R, Puhka M, Mannerstrom B, Hiidenmaa H, Peltoniemi H, Siljander P, et al. Efficient ultrafiltration-based protocol to deplete extracellular vesicles from fetal bovine serum. *J Extracell Vesicles*. (2018) 7:1422674. doi: 10.1080/20013078.2017.1422674

37. Dong L, Zieren RC, Horie K, Kim CJ, Mallick E, Jing Y, et al. Comprehensive evaluation of methods for small extracellular vesicles separation from human plasma, urine and cell culture medium. *J Extracell Vesicles*. (2020) 10:e12044. doi: 10.1002/jev2.12044

38. Yang D, Zhang W, Zhang H, Zhang F, Chen L, Ma L, et al. Progress, opportunity, and perspective on exosome isolation - efforts for efficient exosome-based theranostics. *Theranostics*. (2020) 10:3684–707. doi: 10.7150/thno.41580

39. Crescitelli R, Lasser C, Lotvall J. Isolation and characterization of extracellular vesicle subpopulations from tissues. *Nat Protoc*. (2021) 16:1548–80. doi: 10.1038/s41596-020-00466-1

40. Wu Y, Zhang N, Wu H, Sun N, Deng C. Magnetic porous carbon-dependent platform for the determination of N-glycans from urine exosomes. *Mikrochim Acta*. (2021) 188:66. doi: 10.1007/s00604-021-04728-x

41. Lin Q, Huang Z, Ye X, Yang B, Fang X, Liu B, et al. Lab in a tube: isolation, extraction, and isothermal amplification detection of exosomal long noncoding RNA of gastric cancer. *Talanta*. (2021) 225:122090. doi: 10.1016/j.talanta.2021.122090

42. Yang HC, Ham YM, Kim JA, Rhee WJ. Single-step equipment-free extracellular vesicle concentration using super absorbent polymer beads. *J Extracell Vesicles*. (2021) 10:e12074. doi: 10.1002/jev2.12074

43. Wu M, Chen Z, Xie Q, et al. One-step quantification of salivary exosomes based on combined aptamer recognition and quantum dot signal amplification. *Biosens Bioelectron*. (2021) 171:112733. doi: 10.1016/j.bios.2020.112733

44. Tian Y, Xue C, Zhang W, et al. Refractive index determination of individual viruses and small extracellular vesicles in aqueous media using nano-flow cytometry. *Anal Chem*. (2022). doi: 10.1021/acs.analchem.2c02833

45. Shao H, Im H, Castro CM, Breakefield X, Weissleder R, Lee H. New Technologies for Analysis of extracellular vesicles. *Chem Rev*. (2018) 118:1917–50. doi: 10.1021/acs.chemrev.7b00534

46. Witwer KW, Soekmadji C, Hill AF, Wauben MH, Buzas EI, Di Vizio D, et al. Updating the MISEV minimal requirements for extracellular vesicle studies: building bridges to reproducibility. *J Extracell Vesicles*. (2017) 6:1396823. doi: 10.1080/20013078.2017.1396823

47. Mendt M, Kamerkar S, Sugimoto H, McAndrews KM, Wu CC, Gagea M, et al. Generation and testing of clinical-grade exosomes for pancreatic cancer. *JCI Insight*. (2018) 3:e99263. doi: 10.1172/jci.insight.99263

48. Maroto R, Zhao Y, Jamaluddin M, Popov VL, Wang H, Kalubowilage M, et al. Effects of storage temperature on airway exosome integrity for diagnostic and functional analyses. *J Extracell Vesicles*. (2017) 6:1359478. doi: 10.1080/20013078.2017.1359478

49. Xu Z, Zeng S, Gong Z, Yan Y. Exosome-based immunotherapy: a promising approach for cancer treatment. *Mol Cancer*. (2020) 19:160. doi: 10.1186/s12943-020-01278-3

50. Rodrigues G, Hoshino A, Kenific CM, Matei IR, Steiner L, Freitas D, et al. Tumour exosomal CEMIP protein promotes cancer cell colonization in brain metastasis. *Nat Cell Biol*. (2019) 21:1403–12. doi: 10.1038/s41556-019-0404-4

51. Fong MY, Zhou W, Liu L, et al. Breast-cancer-secreted miR-122 reprograms glucose metabolism in premetastatic niche to promote metastasis. *Nat Cell Biol*. (2015) 17:183–94. doi: 10.1038/ncb3094

52. Zhang L, Zhang S, Yao J, et al. Microenvironment-induced PTEN loss by exosomal microRNA primes brain metastasis outgrowth. *Nature*. (2015) 527:100–4. doi: 10.1038/nature15376

53. Chaudhary P, Gibbs LD, Maji S, Lewis CM, Suzuki S, Vishwanatha JK. Serum exosomal-annexin A2 is associated with African-American triple-negative breast cancer and promotes angiogenesis. *Breast Cancer Res*. (2020) 22:11. doi: 10.1186/s13058-020-1251-8

54. Chow A, Zhou W, Liu L, et al. Macrophage immuno- modulation by breast cancer-derived exosomes requires Toll-like receptor 2-mediated activation of NF-kappaB. *Sci Rep*. (2014) 4:5750. doi: 10.1038/srep05750

55. Jaiswal R, Johnson MS, Pokharel D, et al. Microparticles shed from multidrug resistant breast cancer cells provide a parallel survival pathway through immune evasion. *BMC Cancer*. (2017) 17:104. doi: 10.1186/s12885-017-3102-2

56. Lo Cicero A, Schiera G, Proia P, et al. Oligodendroglioma cells shed microvesicles which contain TRAIL as well as molecular chaperones and induce cell death in astrocytes. *Int J Oncol*. (2011) 39:1353–7.

57. Li X, Nie S, Lv Z, et al. Overexpression of Annexin A2 promotes proliferation by forming a Glypican 1/c-Myc positive feedback loop: prognostic significance in human glioma. *Cell Death Dis*. (2021) 12:261. doi: 10.1038/s41419-021-03547-5

58. Zeng L, He X, Wang Y, et al. MicroRNA-210 overexpression induces angiogenesis and neurogenesis in the normal adult mouse brain. *Gene Ther*. (2014) 21:37–43. doi: 10.1038/gt.2013.55

59. Camacho L, Guerrero P, Marchetti D. MicroRNA and protein profiling of brain metastasis competent cell-derived exosomes. *PloS One*. (2013) 8:e73790. doi: 10.1371/journal.pone.0073790

60. Alečković M, Kang Y. Welcoming treat: astrocyte-derived exosomes induce PTEN suppression to foster brain metastasis. *Cancer Cell*. (2015) 28:554–6. doi: 10.1016/j.ccell.2015.10.010

61. Paggetti J, Haderk F, Seiffert M, Janji B, Distler U, Ammerlaan W, et al. Exosomes released by chronic lymphocytic leukemia cells induce the transition of stromal cells into cancer-associated fibroblasts. *Blood*. (2015) 126:1106–17. doi: 10.1182/blood-2014-12-618025

62. O'Brown NM, Pfau SJ, Gu C. Bridging barriers: a comparative look at the blood–brain barrier across organisms. *Genes Dev*. (2018) 32:466–78.

63. Xu ZH, Miao ZW, Jiang QZ, et al. Brain microvascular endothelial cell exosome-mediated S100A16 up-regulation confers small-cell lung cancer cell survival in brain. *FASEB J*. (2019) 33:1742–57. doi: 10.1096/fj.201800428R

64. Hodge AL, Baxter AA, Poon IKH. Gift bags from the sentinel cells of the immune system: The diverse role of dendritic cell-derived extracellular vesicles. *J Leukoc Biol*. (2022) 111:903–20. doi: 10.1002/JLB.3RU1220-801R

65. Pandit R, Chen L, Götz J. The blood-brain barrier: Physiology and strategies for drug delivery. *Adv Drug Delivery Rev*. (2020) 165-166:1–14. doi: 10.1016/j.addr.2019.11.009

66. Lark DS, LaRocca TJ. Expression of exosome biogenesis genes is differentially altered by aging in the mouse and in the human brain during alzheimer's disease. *J Gerontol A Biol Sci Med Sci*. (2022) 77:659–63. doi: 10.1093/gerona/glab322

67. Morad G, Carman CV, Hagedorn EJ, et al. Tumor-derived extracellular vesicles breach the intact blood-brain barrier via transcytosis. *ACS Nano*. (2019) 13:13853–65. doi: 10.1021/acsnano.9b04397

68. Wu D, Deng S, Li L, et al. TGF-β1-mediated exosomal lnc-MMP2-2 increases blood-brain barrier permeability via the miRNA-1207-5p/EPB41L5 axis to promote non-small cell lung cancer brain metastasis. *Cell Death Dis*. (2021) 12:721. doi: 10.1038/s41419-021-04072-1

69. Lu Y, Chen L, Li L, Cao Y. Exosomes derived from brain metastatic breast cancer cells destroy the blood-brain barrier by carrying lncRNA GS1-600G8.5. *BioMed Res Int*. (2020) 2020:7461727. doi: 10.1155/2020/7461727

70. Zhou W, Fong MY, Min Y, et al. Cancer-secreted miR-105 destroys vascular endothelial barriers to promote metastasis. *Cancer Cell*. (2014) 25:501–15. doi: 10.1016/j.ccr.2014.03.007

71. Tominaga N, Kosaka N, Ono M, et al. Brain metastatic cancer cells release microRNA-181c-containing extracellular vesicles capable of destructing blood-brain barrier. *Nat Commun*. (2015) 6:6716. doi: 10.1038/ncomms7716

72. Fazakas C, Kozma M, Molnár K, et al. Breast adenocarcinoma-derived exosomes lower first-contact de-adhesion strength of adenocarcinoma cells to brain endothelial layer. *Colloids Surf B Biointerfaces*. (2021) 204:111810. doi: 10.1016/j.colsurfb.2021.111810

73. Hu W, Liu C, Bi Z-Y. Comprehensive landscape of extracellular vesicle-derived RNAs in cancer initiation, progression, metastasis and cancer immunology. *Mol Cancer*. (2020) 19:102. doi: 10.1186/s12943-020-01199-1

74. Kinjyo I, Bragin D, Grattan R, Winter SS, Wilson BS. Leukemia-derived exosomes and cytokines pave the way for entry into the brain. *J Leukoc Biol*. (2019) 105:741–53. doi: 10.1002/JLB.3A0218-054R

75. Skog J, Wurdinger T, van Rijn S, et al. Glioblastoma microvesicles transport RNA and proteins that promote tumour growth and provide diagnostic biomarkers. *Nat Cell Biol*. (2008) 10:1470–6. doi: 10.1038/ncb1800

76. Chen G, Huang AC, Zhang W, et al. Exosomal PD-L1 contributes to immunosuppression and is associated with anti-PD-1 response. *Nature*. (2018) 560:382–6. doi: 10.1038/s41586-018-0392-8

77. Picca A, Guerra F, Calvani R, et al. Mitochondrial dysfunction and aging: insights from the analysis of extracellular vesicles. *Int J Mol Sci*. (2019) 20:805. doi: 10.3390/ijms20040805

78. Song Q, Yu H, Han J, Lv J, Lv Q, Yang H. Exosomes in urological diseases - Biological functions and clinical applications. *Cancer Lett*. (2022) 544:215809. doi: 10.1016/j.canlet.2022.215809

79. Guo X, Lv X, Ru Y, et al. Circulating exosomal gastric cancer-associated long noncoding RNA1 as a biomarker for early detection and monitoring progression of gastric cancer: A multiphase study. *JAMA Surg*. (2020) 155:572–9. doi: 10.1001/jamasurg.2020.1133

80. Li X, Shao C, Shi Y, Han W. Lessons learned from the blockade of immune checkpoints in cancer immunotherapy. *J Hematol Oncol*. (2018) 11:31. doi: 10.1186/s13045-018-0578-4

81. Chen WW, Balaj L, Liau LM, et al. BEAMing and droplet digital PCR analysis of mutant IDH1 mRNA in glioma patient serum and cere-brospinal fluid extracellular vesicles. *Mol Ther Nucleic Acids*. (2013) 2:109. doi: 10.1038/mtna.2013.28

82. Figueroa JM, Skog J, Akers J, et al. Detection of wtEGFR amplifica- tion and EGFRvIII mutation in CSF-derived extracellular vesicles of glioblastoma patients. *Neuro Oncol*. (2017). doi: 10.1093/neuonc/nox085

83. Manda SV, Kataria Y, Tatireddy BR, et al. Exosomes as a biomarker platform for detecting epidermal growth factor receptor-positive high-grade gliomas. *J Neurosurg*. (2017), 1–11. doi: 10.3171/2016.11.JNS161187

84. Akers JC, Ramakrishnan V, Kim R, et al. MiR-21 in the extracellular vesicles (EVs) of cerebrospinal fluid (CSF): a platform for glioblastoma biomarker development. *PloS One*. (2013) 8:78115. doi: 10.1371/journal.pone.0078115

85. Akers JC, Hua W, Li H, et al. A cerebrospinal fluid microRNA signature as biomarker for glioblastoma. *Oncotarget*. (2015) 6:20829–20839.

86. Zhang M, Fan Y, Che X, Hou K, Zhang C, Li C, et al. 5-FU-induced upregulation of Exosomal PD-L1 causes immunosuppression in advanced gastric Cancer patients. *Front Oncol*. (2020) 10:492. doi: 10.3389/fonc.2020.00492

87. Kanchan RK, Siddiqui JA, Mahapatra S, Batra SK, Nasser MW. microRNAs orchestrate pathophysiology of breast cancer brain metastasis: advances in therapy. *Mol Cancer*. (2020) 19:29. doi: 10.1186/s12943-020-1140-x

88. Poggio M, Hu T, Pai CC, et al. Suppression of exosomal PD-L1 induces systemic anti-tumor immunity and memory. *Cell*. (2019) 177:414–427.e13. doi: 10.1016/j.cell.2019.02.016

89. Wang J, Zhang H, Sun X, et al. Exosomal PD-L1 and N-cadherin predict pulmonary metastasis progression for osteosarcoma patients. *J Nanobiotechnology*. (2020) 18:151. doi: 10.1186/s12951-020-00710-6

90. Chang L, Ruiz P, Ito T, Sellers WR. Targeting pan-essential genes in cancer: Challenges and opportunities. *Cancer Cell*. (2021) 39:466–79. doi: 10.1016/j.ccell.2020.12.008

91. Liang Y, Duan L, Lu J, Xia J. Engineering exosomes for targeted drug delivery. *Theranostics*. (2021) 11:3183–95. doi: 10.7150/thno.52570

92. Zhong J, Xia B, Shan S, et al. High-quality milk exosomes as oral drug delivery system. *Biomaterials*. (2021) 277:121126. doi: 10.1016/j.biomaterials.2021.121126

93. Zhang YF, Shi JB, Li C. Small extracellular vesicle loading systems in cancer therapy: Current status and the way forward. *Cytotherapy*. (2019) 21:1122–36. doi: 10.1016/j.jcyt.2019.10.002

94. Neupane YR, Mahtab A, Siddiqui L, et al. Biocompatible nanovesicular drug delivery systems with targeting potential for autoimmune diseases. *Curr Pharm Des*. (2020) 26:5488–502. doi: 10.2174/1381612826666200523174108

95. Terstappen GC, Meyer AH, Bell RD, Zhang W. Strategies for delivering therapeutics across the blood-brain barrier. *Nat Rev Drug Discovery*. (2021) 20:362–83. doi: 10.1038/s41573-021-00139-y

96. Alvarez-Erviti L, Seow Y, Yin H, Betts C, Lakhal S, Wood MJ. Delivery of siRNA to the mouse brain by systemic injection of targeted exosomes. *Nat Biotechnol*. (2011) 29:341–5. doi: 10.1038/nbt.1807

97. Yang T, Fogarty B, LaForge B, et al. Delivery of small interfering RNA to inhibit vascular endothelial growth factor in zebrafish using natural brain endothelia cell-secreted exosome nanovesicles for the treatment of brain cancer. *AAPS J*. (2017) 19:475–86. doi: 10.1208/s12248-016-0015-y

98. Zhuang X, Xiang X, Grizzle W, et al. Treatment of brain inflammatory diseases by delivering exosome encapsulated anti-inflammatory drugs from the nasal region to the brain. *Mol Ther*. (2011) 19:1769–79. doi: 10.1038/mt.2011.164

99. Ravouru N, Kondreddy P, Korakanchi D, Haritha M. Formulation and evaluation of niosomal nasal drug delivery system of folic acid for brain targeting. *Curr Drug Discovery Technol*. (2013) 10:270–82. doi: 10.2174/15701638113109990031

100. Fan Y, Liu Y, Qu X. ASO author reflections: the prognostic role of Exosomal PD-L1 in patients with gastric Cancer. *Ann Surg Oncol*. (2019) 26:851–2. doi: 10.1245/s10434-019-07864-0

101. Fan Y, Che X, Qu J, Hou K, Wen T, Li Z, et al. Exosomal PD-L1 retains immunosuppressive activity and is associated with gastric Cancer prognosis. *Ann Surg Oncol*. (2019) 26:3745–55. doi: 10.1245/s10434-019-07431-7

102. Zhang M, Fan Y, Che X, Hou K, Zhang C, Li C, et al. 5-FU-induced Upregulation of Exosomal PD-L1 causes immunosuppression in advanced gastric Cancer patients. *Front Oncol*. (2020) 10:492. doi: 10.3389/fonc.2020.00492

103. Suri R, Neupane YR, Mehra N, Jain GK, Kohli K. Sirolimus loaded polyol modified liposomes for the treatment of Posterior Segment Eye Diseases. *Med Hypotheses*. (2020) 136109518. doi: 10.1016/j.mehy.2019.109518

104. Cvjetinović Đ, Prijović Ž, Janković D, et al. Bioevaluation of glucose-modified liposomes as a potential drug delivery system for cancer treatment using 177-Lu radiotracking. *J Control Release*. (2021) 332:301–11. doi: 10.1016/j.jconrel.2021.03.006

105. Di J, Xie F, Xu Y. When liposomes met antibodies: Drug delivery and beyond. *Adv Drug Delivery Rev*. (2020) 154-155:151–62. doi: 10.1016/j.addr.2020.09.003

106. Song X, Luo Y, Ma L, et al. Recent trends and advances in the epidemiology, synergism, and delivery system of lycopene as an anti-cancer agent. *Semin Cancer Biol*. (2021) 73:331–46. doi: 10.1016/j.semcancer.2021.03.028

107. Immordino ML, Dosio F, Cattel L. Stealth liposomes: review of the basic science, rationale, and clinical applications, existing and potential. *Int J Nanomedicine*. (2006) 1:297–315.

108. Cressey P, Amrahli M, So PW, Gedroyc W, Wright M, Thanou M. Image-guided thermosensitive liposomes for focused ultrasound enhanced co-delivery of carboplatin and SN-38 against triple negative breast cancer in mice. *Biomaterials*. (2021) 271:120758. doi: 10.1016/j.biomaterials.2021.120758

109. Ag Seleci D, Seleci M, Walter J-G, Stahl F, Scheper T. Niosomes as nanoparticular drug carriers: fundamentals and recent applications. *J Nanomater*. (2016) 2016. doi: 10.1155/2016/737230

110. Gharbavi M, Amani J, Kheiri-Manjili H, Danafar H, Sharafi A. Niosome: A promising nanocarrier for natural drug delivery through blood-brain barrier. *Adv Pharmacol Sci*. (2018) 2018:6847971. doi: 10.1155/2018/6847971

111. Bartelds R, Nematollahi MH, Pols T, et al. Niosomes, an alternative for liposomal delivery. *PloS One*. (2018) 13:e0194179. doi: 10.1371/journal.pone.0194179

112. Mor S, Battula SN, Swarnalatha G, et al. Preparation of casein biopeptide-loaded niosomes by high shear homogenization and their characterization. *J Agric Food Chem*. (2021) 69:4371–80. doi: 10.1021/acs.jafc.0c05982

113. A P, Agrawal M, Dethe MR, et al. Nose-to-brain drug delivery for the treatment of Alzheimer's disease: current advancements and challenges. *Expert Opin Drug Deliv*. (2022) 19:87–102. doi: 10.1080/17425247.2022.2029845

114. D'Atri D, Zerrillo L, Garcia J, et al. Nanoghosts: Mesenchymal Stem cells derived nanoparticles as a unique approach for cartilage regeneration. *J Control Release*. (2021) 337:472–81. doi: 10.1016/j.jconrel.2021.05.015

115. Zhang Q, Yuan R, Li C, et al. Macrophage depletion with clodronate-containing liposomes affects the incidence and development of rheumatoid arthritis. *Z Rheumatol*. (2019) 78:996–1003. doi: 10.1007/s00393-018-0563-x

frontiers | Frontiers in Immunology

TYPE Original Research
PUBLISHED 01 May 2024
DOI 10.3389/fimmu.2024.1369289

OPEN ACCESS

EDITED BY
Asif Raza,
Penn State Milton S. Hershey Medical Center, United States

REVIEWED BY
Deanna Edwards,
Vanderbilt University Medical Center, United States
Prathyusha Bagam,
National Center for Toxicological Research (FDA), United States

*CORRESPONDENCE
Fuxun Yu
yufuxun@gzu.edu.cn
Tao Wang
wangtaoGPPH@gzu.edu.cn

RECEIVED 12 January 2024
ACCEPTED 22 April 2024
PUBLISHED 01 May 2024

CITATION
Li X, Li X, Yang B, Sun S, Wang S, Yu F and Wang T (2024) Enhancing breast cancer outcomes with machine learning-driven glutamine metabolic reprogramming signature.
Front. Immunol. 15:1369289.
doi: 10.3389/fimmu.2024.1369289

Enhancing breast cancer outcomes with machine learning-driven glutamine metabolic reprogramming signature

Xukui Li[1,2], Xue Li[1,2], Bin Yang[1,2], Songyang Sun[1,2], Shu Wang[3], Fuxun Yu[1,2]* and Tao Wang[1,2]*

[1]Research Laboratory Center, Guizhou Provincial People's Hospital, Guiyang, Guizhou, China, [2]NHC Key Laboratory of Pulmonary Immune-related Diseases, Guizhou Provincial People's Hospital, Guizhou University, Guiyang, Guizhou, China, [3]Department of Breast Surgery, Guizhou Provincial People's Hospital, Guiyang, Guizhou, China

Background: This study aims to identify precise biomarkers for breast cancer to improve patient outcomes, addressing the limitations of traditional staging in predicting treatment responses.

Methods: Our analysis encompassed data from over 7,000 breast cancer patients across 14 datasets, which included in-house clinical data and single-cell data from 8 patients (totaling 43,766 cells). We utilized an integrative approach, applying 10 machine learning algorithms in 54 unique combinations to analyze 100 existing breast cancer signatures. Immunohistochemistry assays were performed for empirical validation. The study also investigated potential immunotherapies and chemotherapies.

Results: Our research identified five consistent glutamine metabolic reprogramming (GMR)-related genes from multi-center cohorts, forming the foundation of a novel GMR-model. This model demonstrated superior accuracy in predicting recurrence and mortality risks compared to existing clinical and molecular features. Patients classified as high-risk by the model exhibited poorer outcomes. IHC validation in 30 patients reinforced these findings, suggesting the model's broad applicability. Intriguingly, the model indicates a differential therapeutic response: low-risk patients may benefit more from immunotherapy, whereas high-risk patients showed sensitivity to specific chemotherapies like BI-2536 and ispinesib.

Conclusions: The GMR-model marks a significant leap forward in breast cancer prognosis and the personalization of treatment strategies, offering vital insights for the effective management of diverse breast cancer patient populations.

KEYWORDS

breast cancer, glutamine metabolism programming, prognosis, immunotherapy, BI-2536

Introduction

Breast cancer (BC) remains the most prevalent malignant tumor among women worldwide, leading to the highest number of cancer-related deaths in this population (1). In 2022, the estimated incidence of BC reached approximately 2.26 million cases globally, underscoring its significant impact on women's health (2). Given its rising prevalence, particularly in developing countries like China, there is a pressing need for improved diagnostic, treatment, and prognostic strategies for BC. BC is categorized into non-invasive and invasive types, with the latter's ability to metastasize to distant organs such as the bones, liver, lungs, and brain, often rendering it incurable (3). Despite advancements in treatment technologies, the prognosis for late-stage BC patients remains dismal (4). Thus, developing an effective predictive model is crucial for enhancing treatment outcomes for BC patients.

Metabolic reprogramming is pivotal in tumor development, exemplified by the Warburg effect, which highlights the crucial role of cancer cell metabolism in supporting cancer survival and proliferation (5). This metabolic reprogramming is characterized by the preferential conversion of glucose to lactate under aerobic conditions (6). Beyond glucose, glutamine is also a significant contributor to redox balance, essential for the metabolic reconfiguration of tumor cells (7). As a versatile amino acid abundant in the human bloodstream, glutamine supports various metabolic processes. It contributes to the synthesis of purines and pyrimidines, participates in the tricarboxylic acid cycle, and supports the biosynthesis of hexosamines, nucleotides, and asparagine, besides being a critical respiratory fuel for tumor cells (8). The aberrant metabolism of glutamine is increasingly recognized as a vital component of BC cell survival and growth (9). Research suggests that glutamine metabolism reprogramming (GMR) within the tumor microenvironment (TME) may significantly affect the anti-tumor immune response (7). Given glutamine's essential role in supporting oxidative metabolism in certain cancer cell lines, investigating glutamine metabolism abnormalities in BC is of paramount importance for improving treatment and prognosis (10). This study aims to develop a novel prognostic model centered on GMR to enhance BC patients outcomes.

Methods and materials

Data acquisition

The dataset for training was meticulously assembled from the TCGA database, encompassing gene profiles, mutational data, and clinical information pertinent to breast cancer cases. We ensured the inclusion of samples with available survival data, guaranteeing dataset completeness and accuracy.

To strengthen and validate our findings, we sourced additional datasets from the GEO database, specifically from studies GSE93601, GSE76250, GSE70947, GSE202203, GSE96058, GSE58812, GSE21653, GSE86166, GSE20685, GSE20711, GSE88770, GSE6532. This approach allowed for cross-validation of our results across diverse datasets, enhancing the reliability of our findings.

Single-cell sequencing technique

Our study utilized single-cell data from the GEO database (GSE161529) (11). The initial step involved discarding genes with zero expression levels, retaining those with non-zero expression. We normalized the expression matrix using the "SC Transform" function from the Seurat R package. Dimensionality reduction was achieved through PCA and UMAP methods, followed by cell cluster identification using the "FindNeighbors" and "Find Clusters" functions. The DoubletFinder R package helped in eliminating doublets, ensuring data accuracy (12). Cells with either 15% mitochondrial gene content or fewer than 500 genes were excluded, refining the dataset further.

Post-quality control, approximately 43,766 cells were preserved for in-depth analyses. Celltypist facilitated the categorization of cell types, laying a robust foundation for our research (13). Tumor cells were identified using the copyKAT algorithm (14).

Cell-cell communication analysis

We generated CellChat objects for each group using the "CellChat" R package, with "CellChatDB.human" as our reference database (15). All analyses utilized default parameters. To compare interaction counts and intensities across groups, we amalgamated CellChat objects via the "mergeCellChat" function. Differences in cell interactions and signaling pathways were visualized and analyzed using specific functions.

Functional analysis

We utilized the GO and KEGG databases for a comprehensive evaluation of differential GMR-related gene expression between tumor and normal tissues (16, 17). The Enrichplot package and clusterProfiler algorithm facilitated this analysis, with a focus on Gene Set Enrichment Analysis between distinct risk subgroups (18). A False Discovery Rate below 0.05 was considered significant.

Calculating the GMR-score

We utilized the TCGA-BRCA dataset to conduct a differential gene expression analysis between tumor and normal breast tissues. This analysis allowed us to identify a set of 67 genes with differential expression associated with glutamine metabolism. Our development of the GMR-score integrated these gene expressions, drawing from a selection of genes determined through the GeneCards database with a relevance score exceeding the threshold of 8. The heatmap and network generated as a result visualized not only the expression but also the interconnections

among these GMR genes. We applied the ssGSEA and Ucell algorithms to bulk and single-cell data to compute the GMR-score, which provided an indirect estimation of glutamine metabolism-related gene activity within the breast cancer tissues (19, 20). It is crucial to emphasize that the GMR-score, while designed to estimate glutamine metabolic activity and provide insights into the metabolic adaptations within the tumor microenvironment, does not directly measure metabolic flux. Instead, it functions as an estimator, based on gene expression data indicative of glutamine metabolic pathways, enabling us to distinguish between the gene expression profiles of tumor versus normal tissue, and offering a potential link to the metabolic state of the tumor. Spearman analysis elucidated the association between GMR-score and immune cell infiltrations, providing a comprehensive evaluation of the GMR-score in breast cancer.

Construction of the GMR model and nomogram

To establish a GMR-based prognostic model specifically tailored for BC patients, we employed a comprehensive workflow initially proposed by Liu et al. (21). This approach integrated a diverse set of ten computational algorithms, including Random Forest (RSF), LASSO (Least Absolute Shrinkage and Selection Operator), Gradient Boosting Machine (GBM), Survival-SVM (Support Vector Machine), SuperPC (Supervised Principal Components), Ridge Regression, plsRcox (Partial Least Squares Regression for Cox's model), CoxBoost, Stepwise Cox, and Elastic Net (Enet). Notably, RSF, LASSO, CoxBoost, and Stepwise Cox play critical roles in reducing dimensionality and selecting relevant variables.

Utilizing the TCGA-BRCA dataset as our training cohort, we applied these algorithms to generate a prognostic signature. Subsequently, we evaluated the performance of the model across all available cohorts, which included TCGA and five external datasets, by calculating the average concordance index (C-index). This metric served as a measure of the model's discriminative ability, and through this process, we were able to identify the most consistent and reliable prognostic model for BC.

The formulation of the GMR-model stands as a pivotal outcome of this research, offering a valuable tool for assessing BC outcomes. The model's robustness and accuracy were thoroughly validated through various methods, including calibration curves, decision curve analysis (DCA), and multivariate Cox regression analyses. These validation steps were instrumental in confirming the relevance and association of the identified prognostic GMR genes with BC. The risk scores for individual patients were calculated using the following formula:

$$riskscore = \sum_{i=1}^{n}(\beta_i \times Exp_i)$$

In this equation, 'n' represents the total number of GMR genes included in the model, 'Exp' denotes the expression levels of the GMR genes, and 'β' signifies the coefficients derived from the multivariate Cox regression model. Based on the calculated risk scores, patients were stratified into high-risk and low-risk groups.

To validate the generalizability and reliability of our GMR-model, we utilized several external datasets, ensuring that our findings were consistent beyond the initial TCGA training set. The survival disparities between the high-risk and low-risk groups were assessed using Kaplan-Meier (KM) survival analysis, with a p-value less than 0.05 considered statistically significant. This step was crucial to confirm the prognostic value of the GMR-model in different patient cohorts and settings.

Genomic alteration analysis

To delineate genetic disparities between high- and low-risk BC subgroups, we conducted a comprehensive analysis of genetic mutation frequencies and copy number alterations (CNA) utilizing data from the TCGA-BRCA database.

We calculated the tumor mutation burden (TMB) for each subgroup, extracting the relevant data from raw mutation files. Utilizing maftools, we subsequently mapped the mutation landscape, focusing on the 28 genes (mutation rate > 5%) that exhibited the highest mutation frequencies. Following procedures outlined in a previously published study (22), we utilized the deconstructSigs package to identify patient-specific mutational signatures. This analysis brought to light four prominent mutational signatures (SBS1, SBS3, SB11, SBS12) within the BC dataset, all of which demonstrated elevated mutation frequencies.

In addition to these mutational signatures, our investigation extended to chromosomal aberrations. We pinpointed the five regions most frequently subjected to amplification and deletion events, giving special attention to four predominant genes located in chromosomal regions 8q24.21 and 9p23. This meticulous analysis aims to uncover the genetic underpinnings that may contribute to the variance in risk and prognosis between the two BC patient subgroups.

Identifying TME disparities

To assess immune cell infiltration levels precisely and exhaustively, we analyzed the prevalence of adversely infiltrated immune cells in patients categorized by the GMR-model. IOBR package employs a comprehensive suite of algorithms, including MCPcounter, EPIC, xCell, CIBERSORT, quanTIseq, and TIMER, ensuring a robust and multifaceted examination (23–29).

In addition, we evaluated the ESTIMATE and TIDE indices to glean insights into the immune microenvironment's state and structure within the TME (30, 31). This evaluation is crucial, as it provides valuable information for immunotherapy strategies and enhances our understanding of the potential outcomes for BC patients.

To augment our analysis, we also quantified immune checkpoints, thereby offering an additional layer of insight into the immune state. This quantification serves as a preliminary tool for predicting patient responsiveness to immune checkpoint inhibitors (ICIs) therapy, a vital component in personalized cancer treatment strategies.

Determining therapeutic targets and drugs

After removing duplicates, we gathered a comprehensive collection of 6,125 compounds from the Drug Repurposing Hub (https://clue.io/repurposing). Our objective was to predict chemotherapeutic responses and identify potential therapeutic targets. The selection of these targets, associated with BC outcomes, was based on Spearman correlation analysis. Specifically, we looked at the relationship between risk scores and gene expression levels, focusing on cases where the correlation coefficient exceeded 0.15 and the P-value was less than 0.05. To pinpoint genes associated with adverse prognosis (correlation coefficient < -0.15, P < 0.05), we examined the relationship between CERES scores and risk scores for brain cells using data from the Cancer Cell Line Encyclopedia (CCLE) (32).

To refine our drug response predictions, we employed the CTRP and PRISM datasets, both of which provide extensive drug screening and molecular information across various cancer cell lines. Our analysis included differential expression assessments between bulk samples and cell lines. Utilizing the pRRophetic package, we applied a ridge regression model for predicting drug responses. This model, trained using expression data and drug response information from solid cancer cell lines, exhibited robust performance, as validated through standard 10-fold cross-validation (33).

Furthermore, we conducted a Connectivity Map (CMap) analysis to identify the most promising therapeutic drugs for BC. This involved comparing gene expression profiles between different risk subgroups and submitting the top 300 genes (comprising 150 up-regulated and 150 down-regulated genes) to the CMap platform (https://clue.io/query). Interestingly, the CMap scores showed a negative correlation with the potential therapeutic efficacy in BC, providing valuable insights for drug selection.

Immunohistochemistry experiment

In our study, we collected tissue samples from 30 BC patients undergoing surgery at the Guizhou Provincial People's Hospital. These samples were then processed through Hematoxylin and Eosin (HE) staining, adhering to standard protocols. The diagnostic evaluations of these stained specimens were carried out by two independent pathologists, ensuring an unbiased and thorough analysis. Detailed demographic and clinical information of the patient cohort is provided in Supplementary Table S1.

Furthermore, we conducted immunohistochemistry (IHC) on the paraffin-embedded tissue specimens, employing methodologies that have been outlined in previous publications (34, 35). The antibodies utilized in this process are comprehensively listed in Supplementary Table S2. The evaluation of the protein expression levels was conducted following well-established protocols and scoring criteria. Consistent with the practices established in our prior research (35), the assessment was independently carried out by two pathologists, ensuring a reliable and accurate interpretation of the protein expression levels.

Results

Deciphering the impact of GMR-related genes in BC

The overall design of this study is displayed in Figure 1. In this study, we used TCGA-BRCA database to screen differentially expressed genes (DEGs) of GMR between tumor and normal samples. Significant DEGs were shown in the heatmap (Figure 2A). To systematically clarify the relationship between prognostic DEGs, we categorized them into three groups and constructed a regulatory network illustrating their interactions, with most showing significant associations (Supplementary Figure S1A). Further exploring the link between GMR genes and BC, we developed a GMR-score, based on the prognostic DEGs associated with glutamine metabolism. The GMR score was computed using the ssGSEA and Ucell algorithms for bulk and single-cell data, respectively. These algorithms allowed us to quantitatively estimate the activity level of glutamine metabolism-related genes in individual samples, providing an indirect measure of glutamine metabolism activity within the tumor microenvironment. This analysis revealed that the GMR-scores were markedly lower compared to control cohorts (Figure 2B), a finding corroborated by three additional datasets (GSE93601, GSE76250, and GSE70947) (Figures 2C–E). These results underscore the critical role of GMR-related gene expression differences in BC development. Subsequently, we delved deeper into the functions and pathways of these DEGs. The KEGG results showed that pathways related to biosynthesis of amino acids, carbon metabolism, and HIF-1 signaling pathway show a higher gene ratio, suggesting these pathways are upregulated in the tumor environment and may contribute to tumorigenesis (Figure 2F). However, pathways such as AMPK signaling pathway, and Valine, leucine and isoleucine

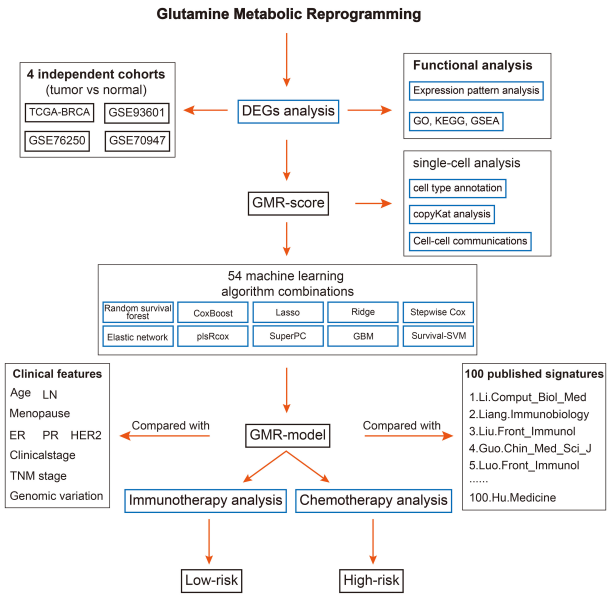

FIGURE 1
The overall flow of this study.

10.3389/fimmu.2024.1369289

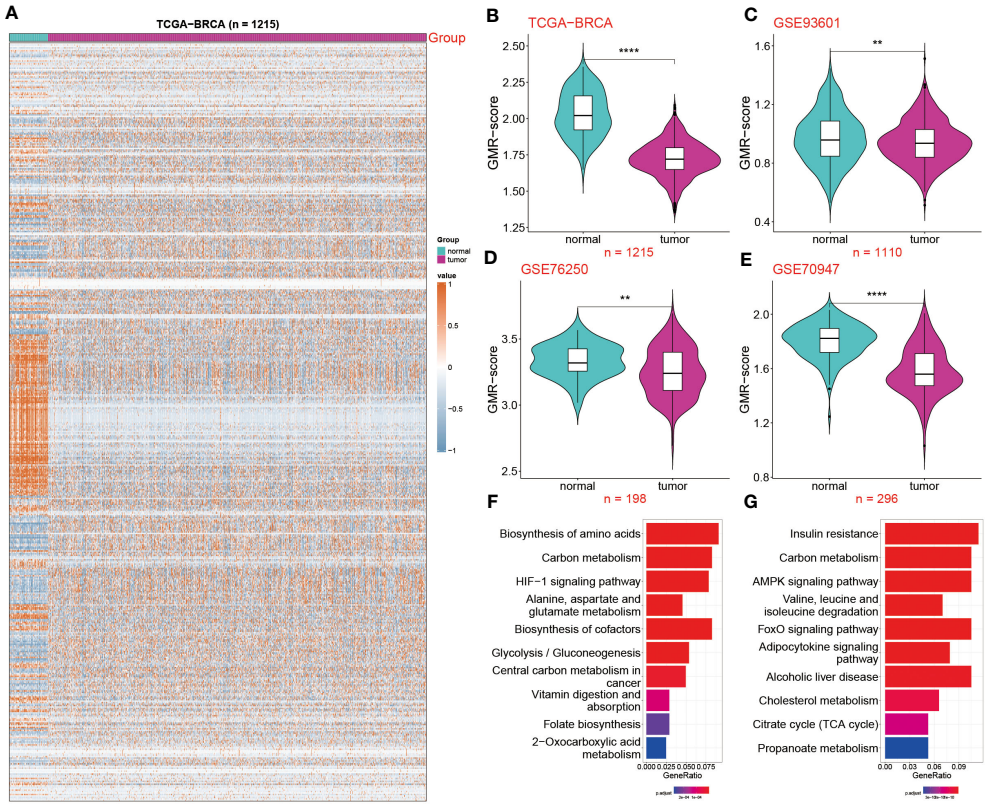

FIGURE 2
Deciphering the impact of GMR-related genes in BC. **(A)** Expression profile of GMR related regulators in breast cancer and normal tissues. **(B–E)** The GMR-score was compared among two groups in the four datasets: TCGA-BRCA, GSE93601 GSE76250 and GSE70947. **(F, G)** KEGG enrichment analysis of the up and down-regulated GMR genes. **P < 0.01, ****P < 0.0001.

degradation were most inhibited. The downregulation of these pathways could reflect a suppression of normal metabolic processes in tumor tissues (Figure 2G).

Extensive research by scholars on tumors consistently suggests that the TME directly influences tumor onset and progression. Building on this, we delved into the correlation patterns between the GMR-score and 25 types of infiltrating immune cells (Supplementary Figure S1B). Notably, multiple cells, including Th1 cells, resting dendritic cells, resting CD4 memory T cells, and Th17 cells, exhibit a positive correlation with the GMR-score, while T cells follicular helper, memory B cells, plasma cells are negatively correlated. In addition, we also demonstrated the strongest positive and negative correlation (Supplementary Figures S1C, D). Through these analyses, we concluded that lower GMR-score and less immune cell infiltration are the key reasons for the development of BC.

Unraveling GMR complexities at single-cell level

To explore the GMR activity among different immune infiltrating cells, we enrolled 8 BC patients including tumor and normal tissues and conducted in-depth exploration of the single-cell data (Figures 3A, B). We then divided the 43,766 cells into 15 clusters and ultimately annotated 9 cell types (Figures 3C, D). The representative markers and top 3 DEGs for each cell type were demonstrated (Figures 3E, F). Among the annotated cell types, we observed the decrease in the Plasma cell, Macrophage, Fibroblast, Endothelial cell and B cell in tumor tissue compared to the normal group, the percentage of T cell, Mast cell, Epithelial cell and DC were significantly increased in tumor tissues (Figure 3G). The Ucell algorithm was used to calculate the GMR-scores for each cell (Figure 3H). Subsequently, based on the Kruskal-Wallis method, the correlation between GMR-score and nine cell types was estimated (Figure 3I). To explore the GMR-score in cancer cell, we performed copyKAT analysis of Epithelial cells (Figure 3J). We observed continuous reduction of GMR-score in normal tissue, tumor-diploid and tumor-aneuploid, which were in keeping with the bulk sequence results (Figure 3K).

Illuminating the dynamics of cell-cell interactions in BC

Subsequently, we utilized Cellchat analysis to identify alterations in the quantity and intensity of cellular communication between normal cells and tumor cells. We found that the number and intensity of interactions between BC cells are significantly lower than those of normal cells (Figure 4A). In particular, compared with

10.3389/fimmu.2024.1369289

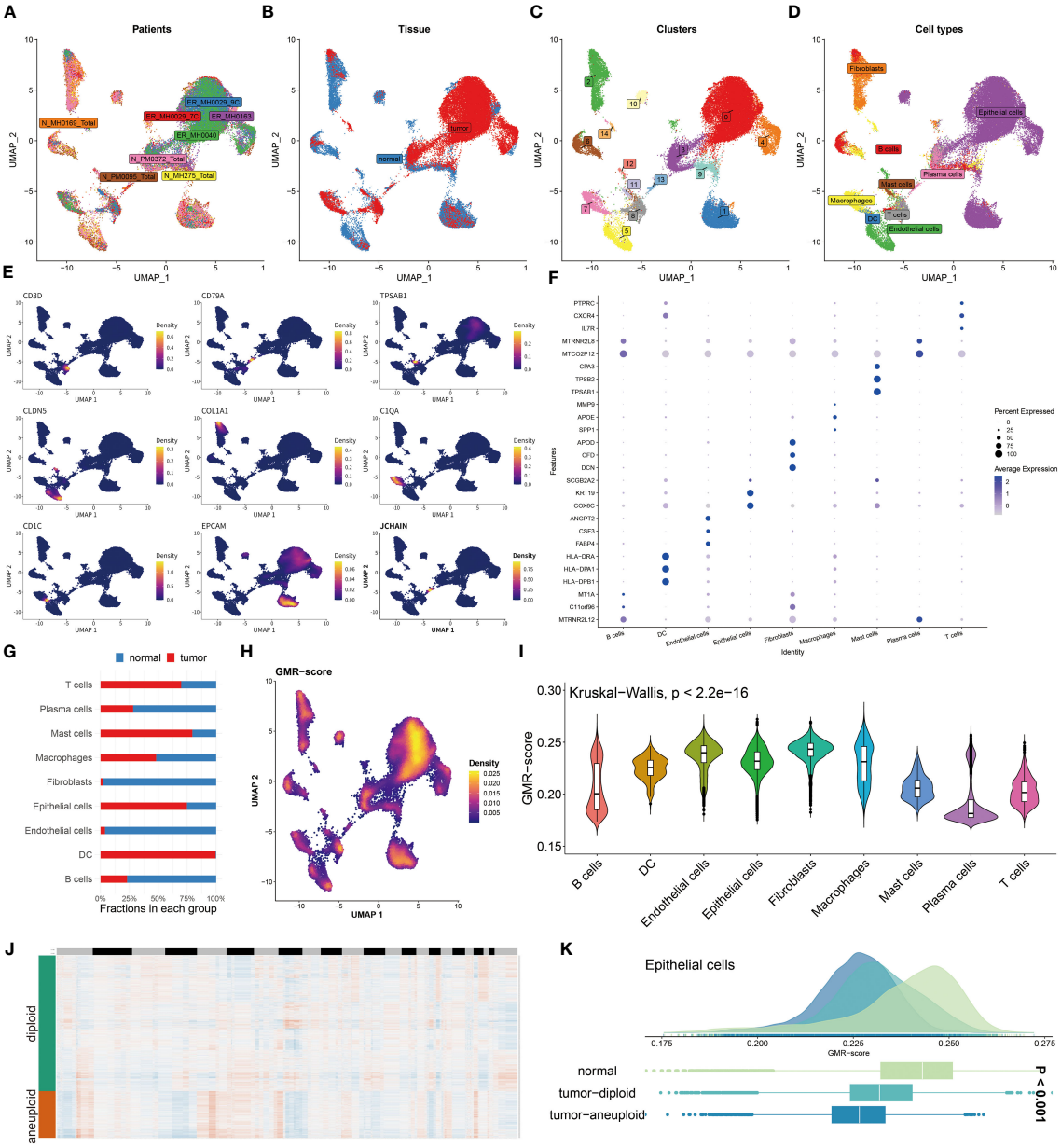

FIGURE 3
Unraveling GMR complexities at single-cell level. **(A, B)** Distribution of cells collected from tumor and normal tissues of eight patients. **(C, D)** Distribution of cell clusters and annotated cell types. **(E)** UMAP plots showing the expression levels of representative marker genes representing nine cell subtypes. **(F)** Top 3 differentially expressed genes in each cell type. **(G)** A stacked bar chart showing the fractions of each cell type in normal and tumor tissues. **(H)** UMAP plots showing the distribution of GMR-scores in each cell. **(I)** Violin plot demonstrating the difference of GMR-score in each cell type. **(J)** CopyKat algorithm evaluates the genomic variations. **(K)** Comparison of GMR-score among normal, tumor diploid and aneuploid epithelial cells.

the normal group, the communication of epithelial cells to endothelial cells, Fibroblasts, T cells has been reduced, while the communication between B Cells and epithelial is more frequent (Figure 4B). We further explored the specific pathways between the normal and tumor groups by comparing the differences in the interactions. Signal pathways such as SPP1, GALECTIN, CD99, MIF, APP, FN1, and MK are significantly active in BC patients, while LAMININ, MHC-1, and SELE exhibit greater activity in normal individuals (Figure 4C). In addition, to continuously detect changes in the submission or acquisition signals between different groups, a comparison based on the intensity of 2D spatial outgoing and incoming interactions is conducted. The scatter plot shows that epithelial cells and T cells serve as the main sources in the normal group, while DC and Mast cells are significant sources in BC patients (Figure 4D). Finally, the plot shows a stronger possibility of interaction among immune cells, including B cells, DC, Macrophages, Mast cells, and T cells in the BC group, while the communication between LGALS9 and CD44, MDK and LRP1, and MIF and CD74+CXCR4/CD44 is unique to the BC group (Figure 4E).

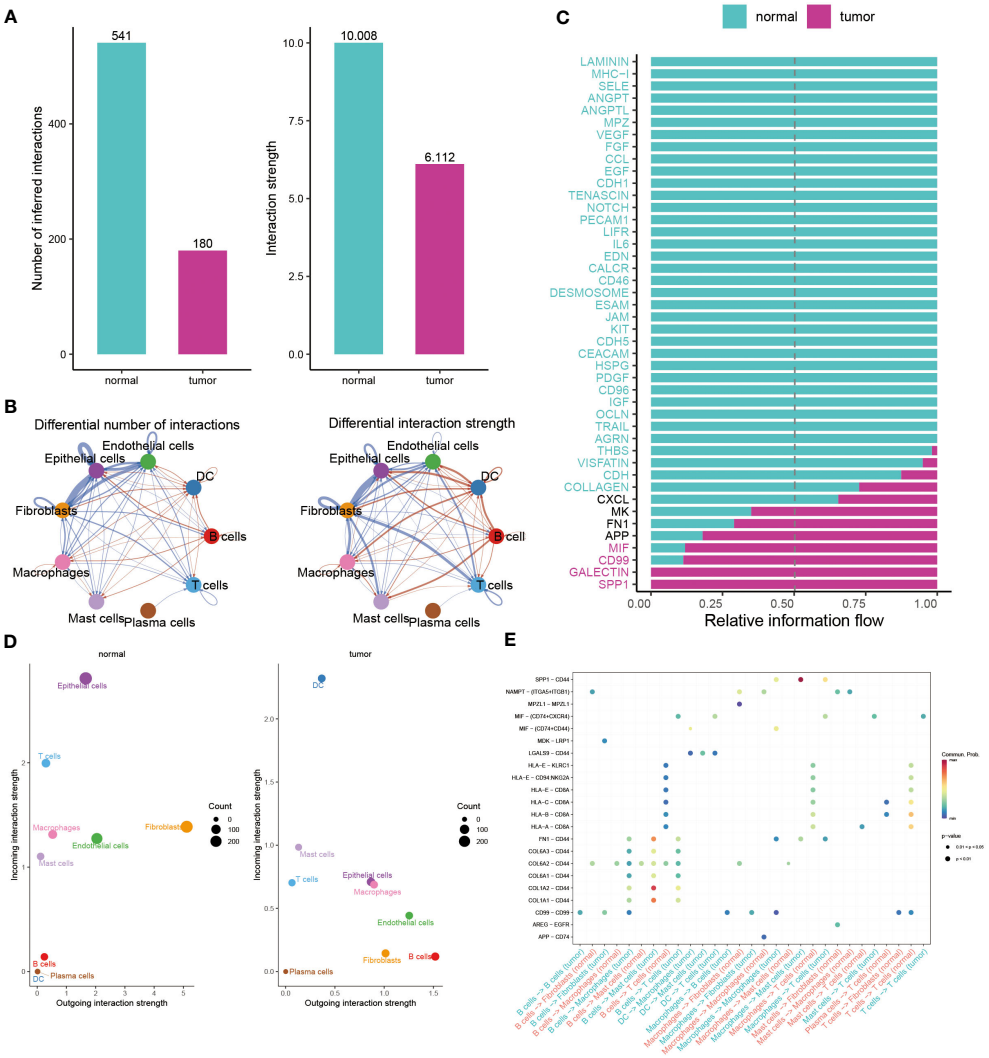

FIGURE 4
Illuminating the dynamics of cell-cell interactions in BC. **(A, B)** Bar and circle charts showing the differences in the number of interactions (left), strength of interactions (right) in the network of cell-cell communication between normal and tumor groups. **(C)** Stacked plots exhibiting the differences in intercellular signaling pathways between tumor and normal groups. Green and red colors denote up-regulated signaling pathways in normal and tumor samples. **(D)** Scatter plot illustrating the difference in incoming interaction strengths in normal groups (left) and tumor patients (right). Larger circles indicate stronger strengths. **(E)** Dot plot presenting the distribution of distinctive signaling molecules in T cells, B cells, and macrophages between the two groups.

Developing the GMR prognosis model through machine learning

The results clearly indicate a significant link between GMR related genes and BC. We then employed machine learning analyses on the TCGA training group and five external cohorts, using 54 combinations of 10 machine learning methods. This approach yielded an average C-index for the six groups (Figure 5A). Our analysis led to the selection of Random Survival Forest for constructing a GMR prognosis model, pinpointing five key genes (SLC19A1, SGTA, PGK1, ETFA, TH) linked to BC prognosis (Figures 5B, C). Patients were then stratified into high-risk and low-risk groups based on risk scores derived from these genes. The heatmap showed these genes were notably upregulated in the high-risk group (Figure 5D). Kaplan-Meier survival curves revealed significantly higher survival rates in the low-risk group (Figure 5E). Recurrence risk predictions indicated a considerably increased risk in the high-risk group (Figure 5F). The ROC curve, assessing the prognostic model's efficiency (Figure 5G), demonstrated AUC values above 0.5 across the first, third, and fifth years, affirming the model's predictive accuracy and reliability. Considering the dataset's correlation between risk scores and survival status, we concluded that the low-risk group has a better survival outlook, whereas the high-risk group faces a higher probability of mortality.

Assessment and validation of the GMR-model

In this study, univariate and multivariate Cox regression analyses were employed to assess the independence of our prognostic model relative to other clinical factors in BC patients.

10.3389/fimmu.2024.1369289

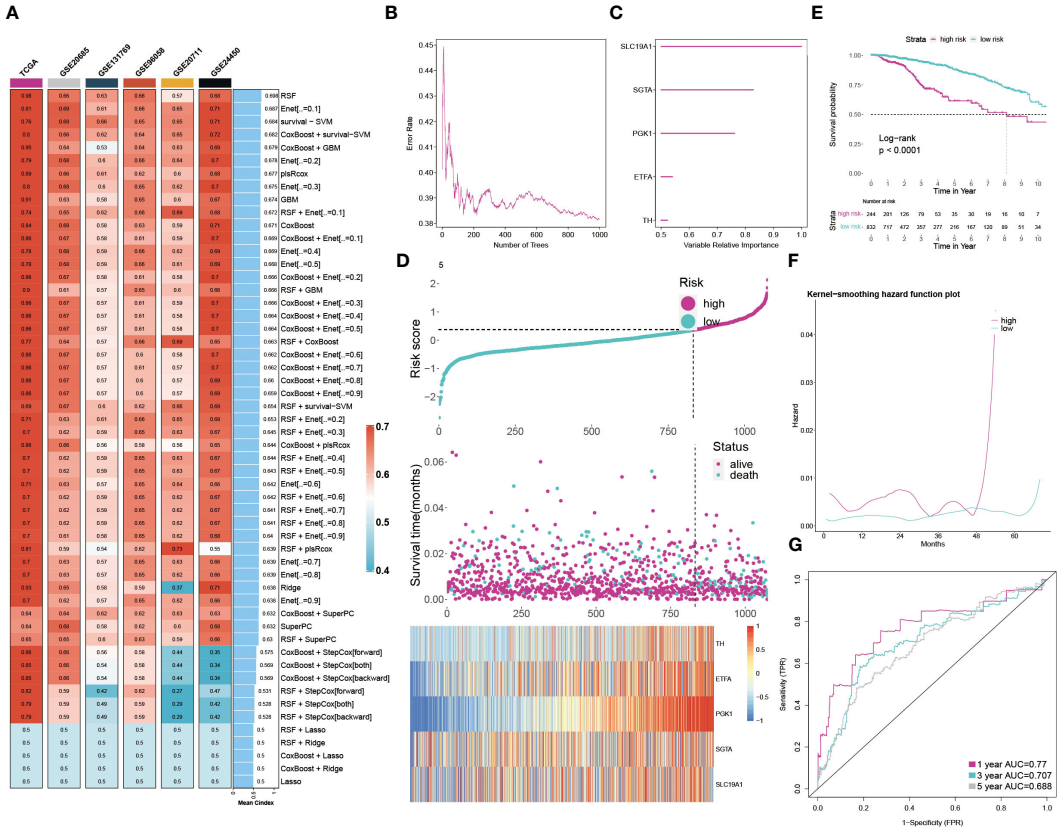

FIGURE 5
Developing the GMR prognosis model through machine learning. **(A)** The C-index of 54 machine learning algorithm combinations in six cohorts. **(B)** The error rate in several different trees. **(C)** The importance of each GMR gene. **(D)** Distribution between risk score and survival status and gene expression. **(E)** KM survival illustrates the survival probability in these two groups. **(F)** The kernel-smoothing hazard function plot demonstrates the correlation between relapse hazard and moths in two populations. **(G)** The ROC curves visualize the AUC values of the GMR-model at one-, three-, and five-year.

Univariate analysis revealed that several indicators, such as risk score, menopause status, stage, and TNM classification, significantly impacted survival rates. Notably, multivariate analysis showed that both risk score and age met the significance threshold ($P < 0.05$), affirming the predictive independence of our GMR-model for BC patient outcomes (Figure 6A). Recognizing the clinical importance of staging, we developed a GMR-nomogram that integrates risk score, stage, and age to accurately forecast one-, three-, and five-year survival probabilities for BC patients (Figure 6B). The calibration curve is used to calibrate the accuracy of the 1-year, 3-year, and 5-year nomograms, indicating a high degree of consistency with actual survival rates (Figure 6C). In addition, the GMR-model chart is higher than the two extreme curves (Treat All and Treat None), indicating that the GMR-column chart has reliable predictive ability (Figure 6D). Furthermore, there was no statistically significant difference ($p > 0.05$) between the predicted values of the GMR column chart and the ideal observed values, further demonstrating the predictive ability of the GMR model (Figure 6E). We also compared our model with clinical pathological factors and found that the GMR-model better reflects the prognostic correlation of BC with other pathological factors besides age (Figure 6F). Then, we compared the predictive ability of the GMR-model and these 100 signatures in the training group and 10 external cohorts using the C-index. Our GMR-model showed significantly better superior accuracy than other models in almost all queues (ranking first in five queues, second in five queues, and fourth in one queue), revealing the robustness of the GMR-model (Supplementary Figure S2).

Multi-omics analysis of genetic variations

To systematically evaluate genomic heterogeneity based on the GMR-model, we calculated gene mutations and CNV between high-risk and low-risk groups. We observed the significant mutation frequency changes of TP53, PIK3CA, TTN, CDH1 and APOB ($P < 0.05$). Further analysis revealed that amplification or deletion of copy numbers were also detected in high-risk BC patients, such as 3p26.32, 5p15.33, 6q21, 8q24.21, and 10p15.1 amplification and 8p23, 9p21.3, 9p23, 10q26.3, and 17q21.31 deletion. In addition, our findings were confirmed by the amplification of oncogenes TMEM75, MYC, CASC8, CCDC26 in the 8q24.21 fragment and the deletion of tumor suppressor genes PYPRD, NFIB, MPZD, and TYRP1 in the 9p23 fragment (Figure 7A).

TMB was notably higher in the high-risk group compared to the low-risk group (Figure 7B). Further examination of the key tumor

10.3389/fimmu.2024.1369289

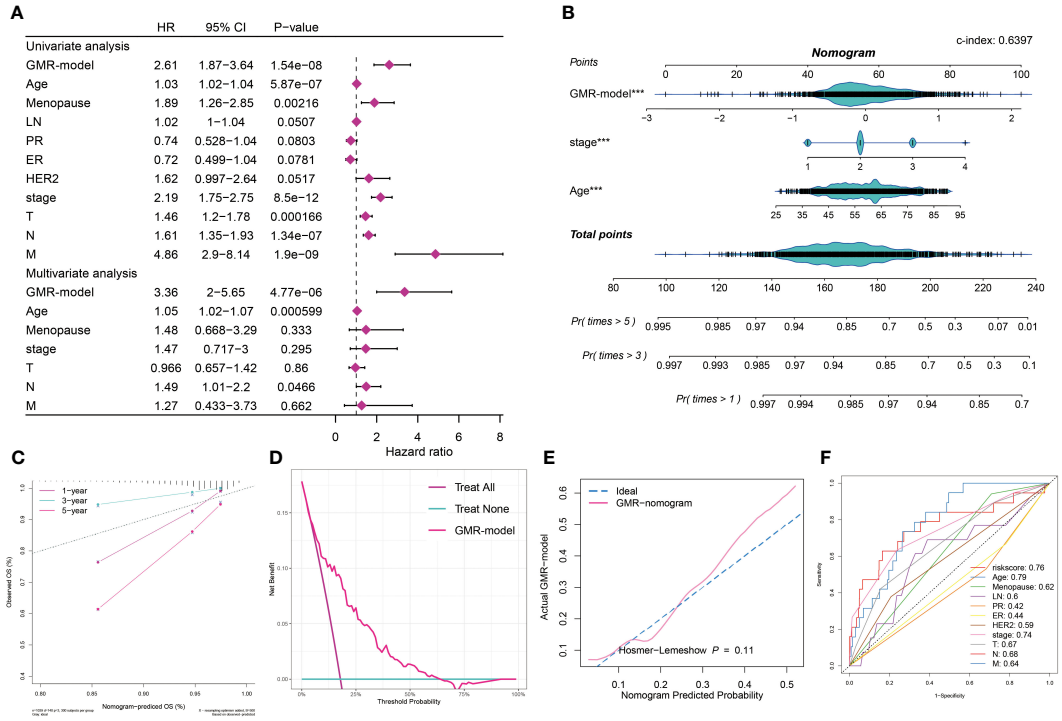

FIGURE 6
Assessment and validation of the GMR-model. **(A)** Univariate and multivariate Cox regression analysis of prognostic ability for GMR-model and other clinical pathological features. **(B)** GMR-nomogram was built consisting of risk score, age and stage index to predict 1-, 3-, and 5-year OS of BC. **(C)** Correction curve demonstrating the observed OS (%) and the predicted OS (%) of the nomogram. **(D)** DCA curves indicates two extreme lines drawn from treat all and treat none, respectively. **(E)** Evaluate the accuracy of GMR column charts and ideal curves using the Hosmer-Lemeshow method. **(F)** 11 ROC curves respectively unfolding the corresponding AUC values of the risk score and ten clinicopathological indexes. ***P < 0.001.

suppressor gene TP53 revealed a significantly elevated mutation rate in the high-risk group (Figure 7C). Additionally, a heatmap illustrated the expression profiles of eight GMR modulators, with ETFA, PGK1, TH, SLC19A1, and SGTA exhibiting higher expression in the high-risk group (Figure 7D). Risk assessment considering survival status and clinical staging in BC patients indicated that those with poorer survival outcomes and less favorable clinical stages had higher risk scores (Figures 7E, F). We further observed the GMR-score were markedly lower in the high-risk group compared to low-risk cohorts (Figure 7G). To understand potential BC mechanisms, functional annotation and gene enrichment analyses were performed. The results suggested that, in the high-risk group compared to the low-risk group, immune-related processes were suppressed while metabolic pathways were activated (Figures 7H, I). These findings provide insights into the mechanisms potentially driving BC progression.

Immune landscape diversity across GMR groups

We next explored the difference of tumor infiltrating lymphocytes (TILs) between the two subgroups. Six immune infiltrating algorithms were used to estimate different TIL. In low-risk patients, the tumor microenvironment is characterized by a substantial infiltration of immune cells, including CD4 T cells and CD8 T cells, which are classified as tumor-infiltrating lymphocytes (TILs), as well as a notable presence of M2 macrophages and DCs. In the high-risk group, the relative content of M1 macrophages, pro-B cells, Th1 cells, and Th2 cells were significantly increased (Figure 8A). We further showed that patients with low risk exhibited increased immune cell infiltration, marked by a greater prevalence of immune-checkpoint genes, correlating with better prognoses (Figure 8B). For a more in-depth examination of the TME and to confirm our findings, IHC staining, targeting key cellular markers and immune-checkpoint genes, was conducted. The representative IHC images and statistical outcomes are presented in Figures 8C, D.

Predicting immunotherapy response using the GMR-model

Our analysis of the TME suggested that those at low risk might respond better to immunotherapy. This hypothesis stemmed from their higher levels of immune cell infiltration and increased expression of ICI genes. To validate this, we utilized ESTIMATE analysis, which showed significantly higher ESTIMATE, immune, and stromal scores, alongside lower tumor purity, in the low-risk group (Figure 9A). TIDE analysis, a tool for predicting immunotherapy efficacy, generally correlates negatively with treatment response. Our findings indicated higher TIDE and

10.3389/fimmu.2024.1369289

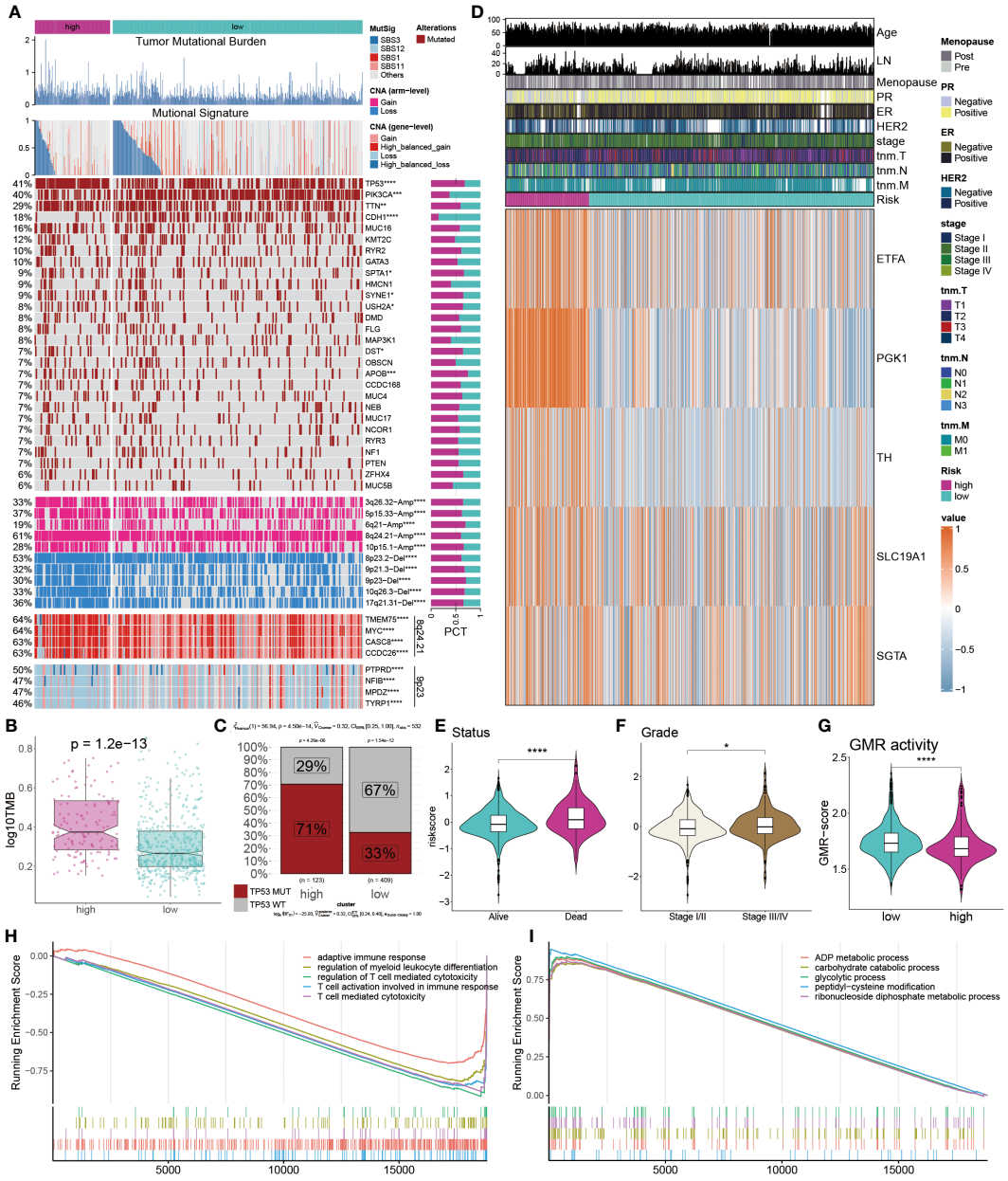

FIGURE 7
Multi-omics analysis of genetic variations. **(A)** Distribution of TMB, mutational signatures, gene mutation, CNVs and oncogenes. **(B)** Comparison of TMB between the two groups. **(C)** Proportions of TP53 mutation in the two groups. **(D)** Heatmap displays the distribution of GMR regulators and clinicopathological factors in the two groups. **(E, F)** Comparison of survival status and clinical grade between GMR groups. **(G, H)** Functional annotation and gene enrichment analysis for high-risk patients. *P < 0.05, ***P < 0.001, ****P < 0.0001.

Dysfunction values in low-risk patients, although differences in Exclusion scores between low- and high-risk groups were not statistically significant (P > 0.05) (Figure 9B). KM survival curves, representing four different risk and TIDE combinations, suggested that low-risk patients with high TIDE values had better outcomes, underscoring the pivotal role of risk score in prognosis (Figure 9C).

Furthermore, we assessed tumor immunogenicity based on proliferation, wound healing, homologous recombination deficiency, and chromosomal segments. Our results showed a positive correlation between these indices and risk score, indicating poorer prognoses in high-risk BC patients (Figure 9D). The suitability of different patient groups for ICI therapy remains unclear. However, immune profiling score (IPS) analysis using the TCGA dataset revealed exceptionally high scores in low-risk BC patients, suggesting a greater likelihood of benefiting from immunotherapy, whether standalone or in combination (Figure 9E). Finally, evaluating responses to PD1, PDL1, CTLA4, and MAGE-A3 treatments indicated that low-risk patients primarily respond to anti-PD-L1 therapy (Bonferroni corrected P < 0.05) (Figure 9F). In summary, our GMR-model effectively predicts ICI therapy responsiveness across different groups, with

10.3389/fimmu.2024.1369289

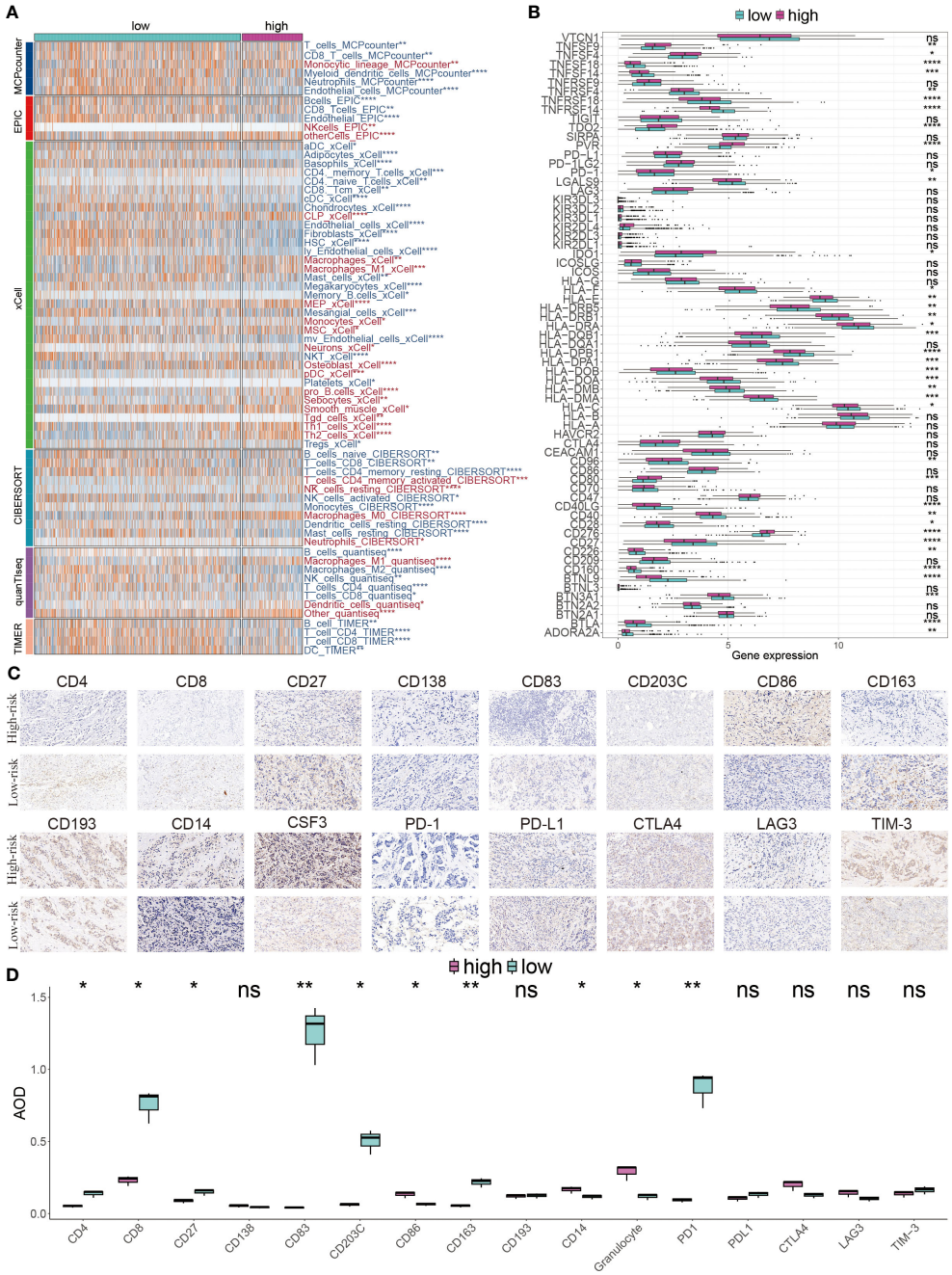

FIGURE 8
Immune landscape diversity across GMR groups. **(A)** The distribution of distinctive infiltrated immune cells between two risk subgroups calculated using multiple algorithms. **(B)** The differential expression profiles of immune-checkpoint genes between two GMR groups. **(C)** IHC image of infiltrated immune cells targeting the reproductive makers. **(D)** Statistical result of **(C)**. *P < 0.05, **P < 0.01, ***P < 0.001, ****P < 0.0001.

low-risk BC patients seemingly more favorable candidates for this treatment approach in a clinical setting.

Chemotherapy response and new treatment avenues for high-risk BC

In exploring new cancer treatments, targeted therapy has been considered, yet chemotherapy remains vital in clinical cancer management. Our model, aimed at predicting chemotherapy responses in BC patients, is particularly crucial for those at high risk. A key step is identifying therapeutic targets to tackle currently undruggable challenges. Using Spearman's correlation analysis, we discovered four proteins more abundant in high-risk patients, suggesting a greater susceptibility to chemotherapy in this group. The CERES scores corroborate these proteins as therapeutic targets for this demographic (Figure 10A). Additionally, these proteins associated anti-cancer drugs demonstrated increased drug

10.3389/fimmu.2024.1369289

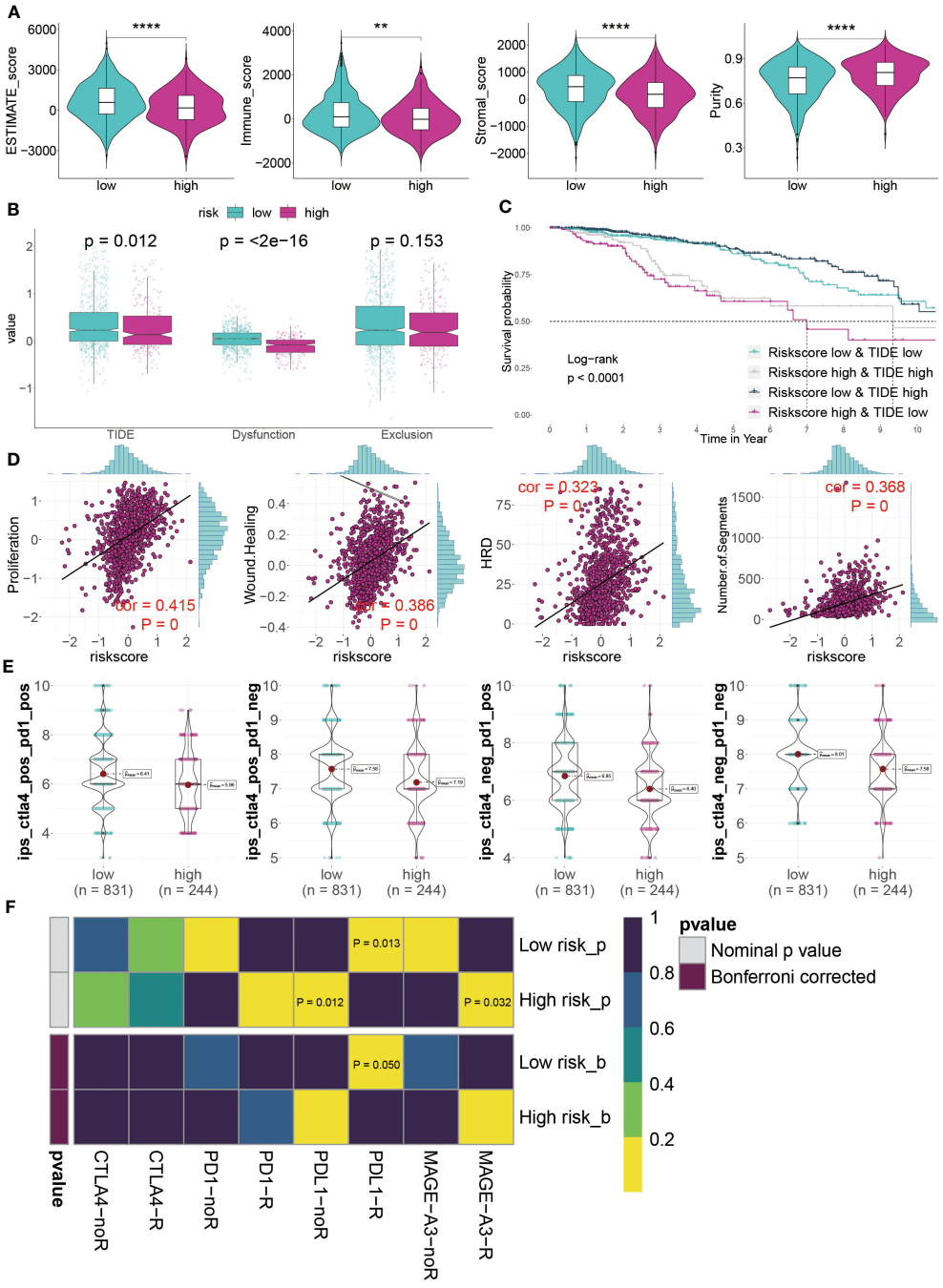

FIGURE 9
Predicting immunotherapy response using the GMR-model. **(A)** Distinctive scores of estimate algorithm, including estimate scores, immune scores, stromal scores, and tumor purity. **(B)** Comparison of TIDE algorithm between GMR groups. **(C)** KM survival curve analysis of patients with different combinations of risk scores and TIDE in TCGA cohort. **(D)** The relationship between proposition, wound healing, homologous recognition defect, and number of segments risk scores. **(E)** IPS (Immunophenoscore) value of each combination among two risk groups. **(F)** Putative ICIs therapy response in two risk BC patients. **P < 0.01, ****P < 0.0001.

sensitivity (Figure 10B). Consequently, CDK4, SLC25A13, and ACAT2 are proposed as potential therapeutic targets for high-risk BC.

Further, we sought potential drugs using PRISM and CTRP datasets. Seven candidate compounds were identified: paclitaxel, BI-2536, GSK461364, and SB-743921 from CTRP (Figure 10C), and LY2606368, ispinesib, and volasertib from PRISM (Figure 10D). Lower AUC values in high-risk patients indicated better chemotherapy response. However, to determine the most effective drugs, we conducted a multi-faceted analysis, incorporating clinical status, experimental evidence, mRNA expression levels, and CMap scores. Based on a CMap score criterion of < -35, BI-2536 and ispinesib emerged as the chosen therapeutic drugs for high-risk BC (Figure 10E, Supplementary Table S3).

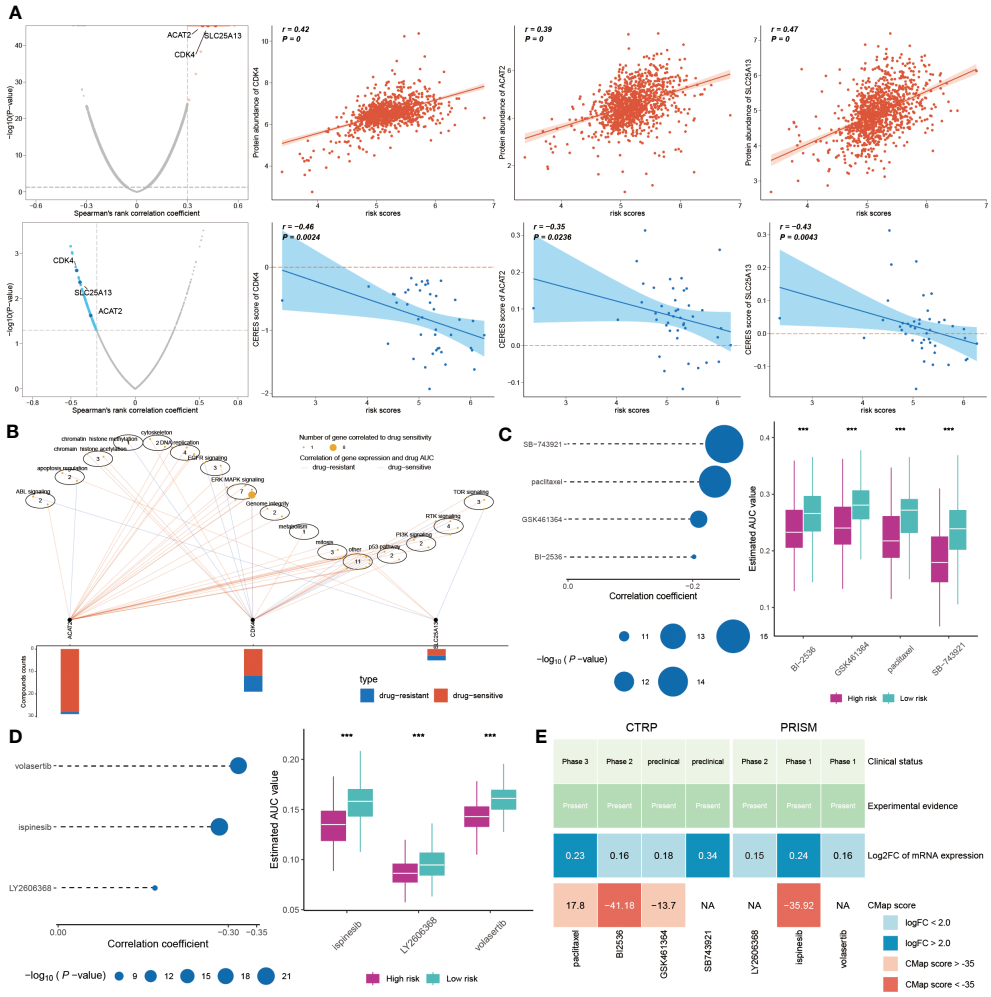

FIGURE 10
Chemotherapy response and new treatment avenues for high-risk BC. **(A)** Spearman correlations between risk score and gene abundance and CERES score of drug targets. **(B)** Spearman correlation between gene expression of potential targets and drug sensitivity across cancer cell line. **(C, D)** Four compounds obtained from CTRP and three compounds obtained from PRISM were subjected to Spearman correlation analysis. The block diagram correspondingly shows the difference in estimated AUC values of different compounds within the two groups. **(E)** This graph displays the clinical status, experimental evidence, mRNA expression levels, and CMap scores of four drugs for CTRP and three drugs for PRISM, respectively. ***P < 0.001.

Discussion

Glutamine metabolism is one of the key metabolic pathways in all cells, and normal glutamine metabolism is particularly important for the normal occurrence and development of cells. Thus, abnormal glutamine metabolism often brings irreversible damage to cells, which is considered as the key factor to promote the progress of solid tumors such as BC (9). Therefore, based on the particularity of glutamine metabolism and the status of treatment and prognosis of BC, we urgently need to identify reliable and accurate glutamine metabolism related markers to predict the survival and immune response of BC patients. In this project, we obtained regulatory factors related to GMR and analyzed the relationship between GMR and BC heterogeneity.

The relevance of scoring systems in evaluating the activities of metabolic pathways, including glutamine metabolism, in cancer has been well-documented in the literature. For instance, the study by Giunchi et al. reviews the metabolic landscape of prostate cancer, emphasizing metabolic alterations and their potential as diagnostic and therapeutic targets, underscoring the importance of metabolic pathways in cancer development and progression (36). Similarly, Sudarshan et al. discuss the metabolic effects of genes and signaling pathways implicated in renal cancer, highlighting the role of altered metabolism in the pathogenesis of this malignancy (37). This further validates the use of scoring systems like our GMR-score to quantitatively assess metabolic alterations in cancer. These studies collectively support the premise that metabolic scoring systems can effectively represent the activity levels of specific metabolic pathways, including glutamine metabolism, and their association with cancer. By adopting a quantitative approach to assess these metabolic activities, our GMR-score provides a robust tool for understanding the metabolic reprogramming in cancer, reinforcing the validity of our approach in linking specific metabolic pathways with cancer-associated gene expression changes.

While highlighting the role of GMR in the prognosis of BC, we constructed a model of 5 GMR related genes based on one training

set and five external datasets and compared it with 100 existing models. The results indicate that the GMR prediction model is more robust, independent, and reliable. Subsequently, GMR-nomogram was established to predict the survival probability of BC patients at 1, 3, and 5 years, which has the best predictive ability compared to other clinical pathological features based on AUC values. Of note, five GMR genes (SLC19A1, SGTA, PGK1, ETFA, TH) were upregulated in the high-risk group.

Our discussion extended to the genetic differences between the two risk groups. The low-risk group was characterized by low TMB and fewer mutated genes, whereas the high-risk group exhibited higher TMB and more mutations in genes such as TP53 and PIK3CA. TP53, a quintessential tumor suppressor gene, has been implicated in BC progression and poor prognosis due to its mutations (38). CNV analysis revealed that high-risk patients also displayed notable aberrations in gene amplifications and deletions. The human genome locus 8q24.21, often referred to as a "gene desert" due to its sparse protein-coding genes, has been linked to various cancer phenotypes despite covering a 4.1MB region (39). This area houses the well-studied oncogene MYC, implicated in approximately 20% of human cancers (40). Also located in this region is the OCT4 pseudogene POU5F1B, which has been observed to amplify in cancers (41). Beyond oncogenic protein-coding genes, the 8q24.21 region is a hub for many lncRNAs associated with different cancers. These lncRNAs function independently of MYC, highlighting the complexity and significance of this genomic region in cancer biology and risk stratification (42). This indicates that due to the role of MYC in accelerating tumor progression, it further promotes tumor development. According to reports, 9p23 deficiency may lead to chronic myeloid leukemia (43). CDKN2A and CDKN2B are tumor suppressor genes located at 9p21, and their deletion inevitably increases tumor risk. These characteristics indicate poor prognosis in BC patients, but also lay the foundation for the response of low-risk patients to ICI treatment.

Our findings illustrate that the GMR-model effectively categorizes tumors into low-risk and high-risk groups, which correspond to distinct immune phenotypes within the TME. Specifically, the low-risk group demonstrated a high infiltration of $CD8^+$ T cells, aligning with an "immune-inflamed" phenotype, indicative of a robust antitumor immune response. Conversely, the high-risk group was characterized by an "immune desert" phenotype, with a notable presence of TP53 mutations, suggesting a reduced capacity for eliciting an effective immune response. The distinction between "immune-inflamed" and "immune desert" phenotypes is crucial for predicting the efficacy of immunotherapeutic interventions. Traditionally, the direct prediction of immunotherapy responses from genome-wide gene expression data has been challenging. However, our GMR-model provides a nuanced framework that not only encapsulates the interplay between genomic alterations and immune responses but also enhances the predictive capabilities for immunotherapy outcomes beyond the binary classification of risk levels. This underscores the importance of considering both genomic and immune contexts in designing personalized immunotherapeutic strategies.

BI 2536 is a highly selective and potent PLK 1 inhibitor that can regulate the malignant behavior of gastric cancer cells in combination with cisplatin (44). Schöffski P. et al. conducted parallel phase II experiments on the treatment of BC with BI 2536 over a decade ago (45). Ispinesib (also known as SB-715992, CK-0238273) was the first small molecule inhibitor of KSP, an effective, specific, and allosteric inhibitor. Inhibiting KSP activity by preventing the release of ADP without altering the release of KSP-ADP complex in microtubules. It is reported that ispinesib inhibits cell proliferation by inducing medium-term cell division dysfunction of pancreatic cancer cells (46). These results enhance the persuasiveness of these two drugs for treating high-risk BC patients.

Conclusion

Our study introduces a groundbreaking GMR prognostic model for breast cancer, offering precise prognosis and treatment response predictions. This model distinguishes high-risk patients, guiding targeted chemotherapy, and identifies low-risk patients likely to benefit from immunotherapies. Highlighting the pivotal role of glutamine metabolism-related genes in breast cancer, the GMR model marks a significant step in personalized cancer therapy, promising enhanced patient care and treatment outcomes.

Data availability statement

The datasets presented in this study can be found in online repositories. The names of the repository/repositories and accession number(s) can be found in the article/Supplementary Material.

Ethics statement

The studies involving humans were approved by Ethics Committee of Guizhou Provincial People's Hospital. The studies were conducted in accordance with the local legislation and institutional requirements. The participants provided their written informed consent to participate in this study.

Author contributions

XL (1^{st} author): Data curation, Formal analysis, Investigation, Validation, Writing – original draft. XL (2^{nd} author): Data curation, Formal analysis, Investigation, Methodology, Writing – original draft. BY: Investigation, Resources, Supervision, Validation, Writing – review & editing. SS: Methodology, Software, Supervision, Validation, Writing – review & editing. SW: Resources, Validation, Writing – review & editing. FY: Conceptualization, Funding acquisition, Resources, Supervision, Validation, Writing – review & editing. TW: Conceptualization, Data curation, Formal analysis, Funding acquisition, Investigation, Methodology, Validation, Visualization, Writing – original draft, Writing – review & editing.

Funding

The author(s) declare financial support was received for the research, authorship, and/or publication of this article. This work was supported by the Talent Fund of Guizhou Provincial People's Hospital ([2022]-33), Guiyang Bureau of Science and Technology major special program ([2022]-4-1), Doctor Fund of Guizhou Provincial People's Hospital (GSYSBS[2016]-1), and the Foundation of Health and Family Planning Commission of Guizhou Province (GZWKJ2022-255).

Conflict of interest

The authors declare that the research was conducted in the absence of any commercial or financial relationships that could be construed as a potential conflict of interest.

Publisher's note

Supplementary material

The Supplementary Material for this article can be found online at: https://www.frontiersin.org/articles/10.3389/fimmu.2024.1369289/full#supplementary-material

References

1. Britt KL, Cuzick J, Phillips. KA. Key steps for effective breast cancer prevention. *Nat Rev Cancer*. (2020) 20:417–36. doi: 10.1038/s41568-020-0266-x

2. Wilkinson L, Gathani T. Understanding breast cancer as a global health concern. *Br J Radiol*. (2022) 95:20211033. doi: 10.1259/bjr.20211033

3. Sun YS, Zhao Z, Yang ZN, Xu F, Lu HJ, Zhu ZY, et al. Risk factors and preventions of breast cancer. *Int J Biol Sci*. (2017) 13:1387–97. doi: 10.7150/ijbs.21635

4. Wang S, Xiong Y, Zhang Q, Su D, Yu C, Cao Y, et al. Clinical significance and immunogenomic landscape analyses of the immune cell signature based prognostic model for patients with breast cancer. *Brief Bioinform*. (2021) 22:bbaa311. doi: 10.1093/bib/bbaa311

5. DeBerardinis RJ, Lum JJ, Hatzivassiliou G, Thompson. CB. The biology of cancer: metabolic reprogramming fuels cell growth and proliferation. *Cell Metab*. (2008) 7:11–20. doi: 10.1016/j.cmet.2007.10.002

6. Tao H, Zhong X, Zeng A, Song. L. Unveiling the veil of lactate in tumor-associated macrophages: a successful strategy for immunometabolic therapy. *Front Immunol*. (2023) 14:1208870. doi: 10.3389/fimmu.2023.1208870

7. Ma G, Zhang Z, Li P, Zhang Z, Zeng M, Liang Z, et al. Reprogramming of glutamine metabolism and its impact on immune response in the tumor microenvironment. *Cell Commun Signal*. (2022) 20:114. doi: 10.1186/s12964-022-00909-0

8. Carrascosa JM, Martínez P, Núñez de Castro. I. Nitrogen movement between host and tumor in mice inoculated with Ehrlich ascitic tumor cells. *Cancer Res*. (1984) 44:3831–5.

9. Wang L, Xu T, Yang X, Liang Z, Zhang J, Li D, et al. Immunosuppression induced by glutamine deprivation occurs *via* activating PD-L1 transcription in bladder cancer. *Front Mol Biosci*. (2021) 8:687305. doi: 10.3389/fmolb.2021.687305

10. Zhang J, Pavlova NN, Thompson. CB. Cancer cell metabolism: the essential role of the nonessential amino acid, glutamine. *EMBO J*. (2017) 36:1302–15. doi: 10.15252/embj.201696151

11. Pal B, Chen Y, Vaillant F, Capaldo BD, Joyce R, Song X, et al. A single-cell RNA expression atlas of normal, preneoplastic and tumorigenic states in the human breast. *EMBO J*. (2021) 40:e107333. doi: 10.15252/embj.2020107333

12. McGinnis CS, Murrow LM, Gartner. ZJ. DoubletFinder: doublet detection in single-cell RNA sequencing data using artificial nearest neighbors. *Cell Syst*. (2019) 8:329–337.e4. doi: 10.1016/j.cels.2019.03.003

13. Domínguez Conde C, Xu C, Jarvis LB, Rainbow DB, Wells SB, Gomes T, et al. Cross-tissue immune cell analysis reveals tissue-specific features in humans. *Science*. (2022) 376:eabl5197. doi: 10.1126/science.abl5197

14. Gao R, Bai S, Henderson YC, Lin Y, Schalck A, Yan Y, et al. Delineating copy number and clonal substructure in human tumors from single-cell transcriptomes. *Nat Biotechnol*. (2021) 39:599–608. doi: 10.1038/s41587-020-00795-2

15. Jin S, Guerrero-Juarez CF, Zhang L, Chang I, Ramos R, Kuan CH, et al. Inference and analysis of cell-cell communication using CellChat. *Nat Commun*. (2021) 12:1088. doi: 10.1038/s41467-021-21246-9

16. Ashburner M, Ball CA, Blake JA, Botstein D, Butler H, Cherry JM, et al. Gene ontology: tool for the unification of biology. *Gene Ontology Consortium Nat Genet*. (2000) 25:25–9. doi: 10.1038/75556

17. Kanehisa M, Sato Y, Kawashima M, Furumichi M, Tanabe. M. KEGG as a reference resource for gene and protein annotation. *Nucleic Acids Res*. (2016) 44:D457–62. doi: 10.1093/nar/gkv1070

18. Yu G, Wang LG, Han Y, He. QY. clusterProfiler: an R package for comparing biological themes among gene clusters. *OMICS*. (2012) 16:284–7. doi: 10.1089/omi.2011.0118

19. Hänzelmann S, Castelo R, Guinney. J. GSVA: gene set variation analysis for microarray and RNA-seq data. *BMC Bioinf*. (2013) 14:7. doi: 10.1186/1471-2105-14-7

20. Andreatta M, Carmona SJ. UCell: Robust and scalable single-cell gene signature scoring. *Comput Struct Biotechnol J*. (2021) 19:3796–8. doi: 10.1016/j.csbj.2021.06.043

21. Liu Z, Guo C, Dang Q, Wang L, Liu L, Weng S, et al. Integrative analysis from multi-center studies identities a consensus machine learning-derived lncRNA signature for stage II/III colorectal cancer. *EBioMedicine*. (2022) 75:103750. doi: 10.1016/j.ebiom.2021.103750

22. Wang L, Liu Z, Liang R, Wang W, Zhu R, Li J, et al. Comprehensive machine-learning survival framework develops a consensus model in large-scale multicenter cohorts for pancreatic cancer. *Elife*. (2022) 11:e80150. doi: 10.7554/eLife.80150

23. Becht E, Giraldo NA, Lacroix L, Buttard B, Elarouci N, Petitprez F, et al. Estimating the population abundance of tissue-infiltrating immune and stromal cell populations using gene expression. *Genome Biol*. (2016) 17:218. doi: 10.1186/s13059-016-1070-5

24. Racle J, Gfeller D. EPIC: A tool to estimate the proportions of different cell types from bulk gene expression data. *Methods Mol Biol*. (2020) 2120:233–48. doi: 10.1007/978-1-0716-0327-7_17

25. Aran D, Hu Z, Butte. AJ. xCell: digitally portraying the tissue cellular heterogeneity landscape. *Genome Biol*. (2017) 18:220. doi: 10.1186/s13059-017-1349-1

26. Newman AM, Liu CL, Green MR, Gentles AJ, Feng W, Xu Y, et al. Robust enumeration of cell subsets from tissue expression profiles. *Nat Methods*. (2015) 12:453–7. doi: 10.1038/nmeth.3337

27. Finotello F, Mayer C, Plattner C, Laschober G, Rieder D, Hackl H, et al. Molecular and pharmacological modulators of the tumor immune contexture revealed by deconvolution of RNA-seq data. *Genome Med*. (2019) 11:34. doi: 10.1186/s13073-019-0638-6

28. Li T, Fan J, Wang B, Traugh N, Chen Q, Liu JS, et al. TIMER: A web server for comprehensive analysis of tumor-infiltrating immune cells. *Cancer Res*. (2017) 77:e108–10. doi: 10.1158/0008-5472.Can-17-0307

29. Zeng D, Ye Z, Shen R, Yu G, Wu J, Xiong Y, et al. IOBR: multi-omics immuno-oncology biological research to decode tumor microenvironment and signatures. *Front Immunol*. (2021) 12:687975. doi: 10.3389/fimmu.2021.687975

30. Yoshihara K, Shahmoradgoli M, Martinez E, Vegesna R, Kim H, Torres-Garcia W, et al. Inferring tumour purity and stromal and immune cell admixture from expression data. *Nat Commun*. (2013) 4:2612. doi: 10.1038/ncomms3612

31. Jiang P, Gu S, Pan D, Fu J, Sahu A, Hu X, et al. Signatures of T cell dysfunction and exclusion predict cancer immunotherapy response. *Nat Med*. (2018) 24:1550–8. doi: 10.1038/s41591-018-0136-1

32. Meyers RM, Bryan JG, McFarland JM, Weir BA, Sizemore AE, Xu H, et al. Computational correction of copy number effect improves specificity of CRISPR-Cas9 essentiality screens in cancer cells. *Nat Genet*. (2017) 49:1779–84. doi: 10.1038/ng.3984

33. Yang C, Huang X, Li Y, Chen J, Lv Y, Dai. S. Prognosis and personalized treatment prediction in TP53-mutant hepatocellular carcinoma: an in silico strategy towards precision oncology. *Brief Bioinform*. (2021) 22:bbaa164. doi: 10.1093/bib/bbaa164

34. Wang T, Li T, Li B, Zhao J, Li Z, Sun M, et al. Immunogenomic landscape in breast cancer reveals immunotherapeutically relevant gene signatures. *Front Immunol.* (2022) 13:805184. doi: 10.3389/fimmu.2022.805184

35. Wang T, Ba X, Zhang X, Zhang N, Wang G, Bai B, et al. Nuclear import of PTPN18 inhibits breast cancer metastasis mediated by MVP and importin β2. *Cell Death Disease.* (2022) 13:720. doi: 10.1038/s41419-022-05167-z

36. Giunchi F, Fiorentino M, Loda. M. The metabolic landscape of prostate cancer. *Eur Urol Oncol.* (2019) 2:28–36. doi: 10.1016/j.euo.2018.06.010

37. Sudarshan S, Karam JA, Brugarolas J, Thompson RH, Uzzo R, Rini B, et al. Metabolism of kidney cancer: from the lab to clinical practice. *Eur Urol.* (2013) 63:244–51. doi: 10.1016/j.eururo.2012.09.054

38. Blondeaux E, Arecco L, Punie K, Graffeo R, Toss A, De Angelis C, et al. Germline TP53 pathogenic variants and breast cancer: A narrative review. *Cancer Treat Rev.* (2023) 114:102522. doi: 10.1016/j.ctrv.2023.102522

39. Huppi K, Pitt JJ, Wahlberg BM, Caplen. NJ. The 8q24 gene desert: an oasis of non-coding transcriptional activity. *Front Genet.* (2012) 3:69. doi: 10.3389/fgene.2012.00069

40. Dang CV, O'Donnell KA, Zeller KI, Nguyen T, Osthus RC, Li. F. The c-Myc target gene network. *Semin Cancer Biol.* (2006) 16:253–64. doi: 10.1016/j.semcancer.2006.07.014

41. Hayashi H, Arao T, Togashi Y, Kato H, Fujita Y, De Velasco MA, et al. The OCT4 pseudogene POU5F1B is amplified and promotes an aggressive phenotype in gastric cancer. *Oncogene.* (2015) 34:199–208. doi: 10.1038/onc.2013.547

42. Wilson C, Kanhere A. 8q24.21 locus: A paradigm to link non-coding RNAs, genome polymorphisms and cancer. *Int J Mol Sci.* (2021) 22:1094. doi: 10.3390/ijms22031094

43. Wafa A, Asa'ad M, Ikhtiar A, Liehr T, Al-Achkar. W. Deletion 9p23 to 9p11.1 as sole additional abnormality in a Philadelphia positive chronic myeloid leukemia in blast crisis: a rare event. *Mol Cytogenet.* (2015) 8:59. doi: 10.1186/s13039-015-0165-0

44. Lian G, Li L, Shi Y, Jing C, Liu J, Guo X, et al. BI2536, a potent and selective inhibitor of polo-like kinase 1, in combination with cisplatin exerts synergistic effects on gastric cancer cells. *Int J Oncol.* (2018) 52:804–14. doi: 10.3892/ijo.2018.4255

45. Schöffski P, Blay JY, De Greve J, Brain E, Machiels JP, Soria JC, et al. Multicentric parallel phase II trial of the polo-like kinase 1 inhibitor BI 2536 in patients with advanced head and neck cancer, breast cancer, ovarian cancer, soft tissue sarcoma and melanoma. The first protocol of the European Organization for Research and Treatment of Cancer (EORTC) Network Of Core Institutes (NOCI). *Eur J Cancer.* (2010) 46:2206–15. doi: 10.1016/j.ejca.2010.03.039

46. Murase Y, Ono H, Ogawa K, Yoshioka R, Ishikawa Y, Ueda H, et al. Inhibitor library screening identifies ispinesib as a new potential chemotherapeutic agent for pancreatic cancers. *Cancer Sci.* (2021) 112:4641–54. doi: 10.1111/cas.15134

frontiers | Frontiers in Immunology

TYPE Original Research
PUBLISHED 12 July 2024
DOI 10.3389/fimmu.2024.1384354

OPEN ACCESS

EDITED BY
Hao Chen,
Shandong University, China

REVIEWED BY
Slavko Mojsilovic,
University of Belgrade, Serbia
Marjan Rafat,
Vanderbilt University, United States

*CORRESPONDENCE
Ola Habanjar
ola.habanjar@uca.fr

RECEIVED 09 February 2024
ACCEPTED 20 June 2024
PUBLISHED 12 July 2024

CITATION
Habanjar O, Nehme R, Goncalves-Mendes N, Cueff G, Blavignac C, Aoun J, Decombat C, Auxenfans C, Diab-Assaf M, Caldefie-Chézet F and Delort L (2024) The obese inflammatory microenvironment may promote breast DCIS progression. *Front. Immunol.* 15:1384354. doi: 10.3389/fimmu.2024.1384354

The obese inflammatory microenvironment may promote breast DCIS progression

Ola Habanjar[1]*, Rawan Nehme[1], Nicolas Goncalves-Mendes[1], Gwendal Cueff[1], Christelle Blavignac[2], Jessy Aoun[1], Caroline Decombat[1], Céline Auxenfans[3], Mona Diab-Assaf[4], Florence Caldefie-Chézet[1] and Laetitia Delort[1]

[1]Université Clermont-Auvergne, INRAE, UNH, Clermont-Ferrand, France, [2]Université Clermont-Auvergne, Centre d'Imagerie Cellulaire Santé (CCIS), Clermont-Ferrand, France, [3]Banque de tissus et de cellules, Hôpital Edouard-Herriot, Lyon, France, [4]Equipe Tumorigénèse Moléculaire et Pharmacologie Anticancéreuse, Faculté des Sciences II, Université libanaise Fanar, Beirut, Lebanon

Introduction: Ductal carcinoma *in situ* (DCIS), characterized by a proliferation of neoplastic cells confined within the mammary ducts, is distinctly isolated from the surrounding stroma by an almost uninterrupted layer of myoepithelial cells (MECs) and by the basement membrane. Heightened interactions within the adipose microenvironment, particularly in obese patients, may play a key role in the transition from DCIS to invasive ductal carcinoma (IDC), which is attracting growing interest in scientific research. Adipose tissue undergoes metabolic changes in obesity, impacting adipokine secretion and promoting chronic inflammation. This study aimed to assess the interactions between DCIS, including *in situ* cancer cells and MECs, and the various components of its inflammatory adipose microenvironment (adipocytes and macrophages).

Methods: To this end, a 3D co-culture model was developed using bicellular bi-fluorescent DCIS-like tumoroids, adipose cells, and macrophages to investigate the influence of the inflammatory adipose microenvironment on DCIS progression.

Results: The 3D co-culture model demonstrated an inhibition of the expression of genes involved in apoptosis (*BAX, BAG1, BCL2, CASP3, CASP8*, and *CASP9*), and an increase in genes related to cell survival (*TP53*, *JUN*, and *TGFB1*), inflammation (*TNF-α, PTGS2, IL-6R*), invasion and metastasis (TIMP1 and MMP-9) in cancer cells of the tumoroids under inflammatory conditions versus a non-inflammatory microenvironment. On the contrary, it confirmed the compromised functionality of MECs, resulting in the loss of their protective effects against cancer cells. Adipocytes from obese women showed a significant increase in the expression of all studied myofibroblast-associated genes (myoCAFs), such as *FAP* and *α-SMA*. In contrast, adipocytes from normal-weight women expressed markers of inflammatory fibroblast phenotypes (iCAF) characterized by a significant increase in the expression of *LIF* and inflammatory cytokines such as *TNF-α, IL-1β, IL-8*, and *CXCL-10*. These changes also influenced macrophage polarization, leading to a pro-inflammatory M1 phenotype. In contrast, myoCAF-associated adipocytes, and the cancer-promoting microenvironment polarized macrophages towards an

M2 phenotype, characterized by high CD163 receptor expression and IL-10 and TGF-β secretion.

Discussion: Reciprocal interactions between the tumoroid and its microenvironment, particularly in obesity, led to transcriptomic changes in adipocytes and macrophages, may participate in breast cancer progression while disrupting the integrity of the MEC layer. These results underlined the importance of adipose tissue in cancer progression.

KEYWORDS

ductal carcinoma *in situ*, obesity, microenvironment, inflammation, tumoroid, myoepithelial cells, macrophages

Highlights

- Development of a 3D co-culture model reproducing the inflammatory adipose tumor microenvironment of DCIS in obese patients.
- Investigation of the bidirectional communication between DCIS-like tumoroid and its microenvironment (adipose cells, macrophages).
- Exploring the impact of obesity-related chronic low-grade inflammation on DCIS development and progression.
- Repression of the expression of genes involved in apoptosis and stimulation of those involved in cell survival and inflammation in obesity.
- Compromised functionality of myoepithelial cells, leading to loss of their protective effects against cancer cells.
- Suppression of adipocyte-differentiation-related genes by DCIS-like tumoroid.
- Importance of understanding these interactions for unraveling tumor progression mechanisms and identifying potential therapeutic targets.

1 Introduction

Ductal carcinoma *in situ* (DCIS) is an intraductal neoplastic proliferation of atypical epithelium separated from the surrounding stroma by an almost continuous layer of myoepithelium and basement membrane (1). The term "*in situ*" means that cancer cells are confined within the ductal system and have not disseminated into adjacent tissues. Typically identified through mammography screenings, DCIS, despite being non-invasive, has been substantiated by various clinical observational studies as a potential precursor to invasive ductal mammary cancer (IDC) (2). If left untreated or inadequately managed, an estimated 30% of DCIS cases may progress, invading the contiguous breast tissue and evolving into IDC (3, 4).

As per the American Cancer Society's 2021 estimates for the United States, around 49,290 new DCIS cases and 268,600 IDC cases were diagnosed in women, constituting approximately 20% to 25% of all breast cancers documented in the literature (5). Consequently, DCIS has emerged as a significant clinical challenge due to its escalating incidence and the potential for progression to IDC. The myoepithelial cell (MEC) layer, identifiable through specific markers such as p63 and α-smooth muscle actin (α-SMA) (6), plays a pivotal role in the normal breast structure. This layer acts as a "natural tumor suppressor," regulating both normal mammary epithelial development and preventing cancer invasion, distinguishing DCIS from IDC (7).

Cancer cells derived from luminal epithelial cells establish direct contact with the stroma and adipose tissue before becoming invasive (8). Barsky and coworkers were the first to use functional assays to show that MECs have numerous antitumorigenic properties, such as the ability to inhibit tumor cell invasion and angiogenesis (9, 10). Research studies have demonstrated significant gene expression changes in MECs within the tumor microenvironment (TME) between DCIS and IDC. These alterations involve alterations in the expression of genes related to cell adhesion, extracellular matrix remodeling, invasion, and metastasis, particularly influencing leptin and inflammation-related genes (11). Notably, MECs are deemed critical in both the maintenance of DCIS and the invasion process (12). The involvement of the adipose microenvironment, particularly in obese patients, and the degradation of the basement membrane, are important factors in this process as well as an area of active investigation (13).

Mammary epithelia are surrounded by mammary adipose tissue, constituting the major component of the TME. It is composed of several cell types, including adipose stem cells (ASCs), preadipocytes (PA), mature adipocytes (MA), fibroblasts, and endothelial and immune cells, which have a range of functions (14). Numerous investigations demonstrate that stromal cells within the breast adipose tissue adjacent to the tumor establish a distinct TME capable of intricately modulating cancer progression (15). This regulatory capacity derives from the intricate

bidirectional crosstalk among cancer cells, adipose cells, and immune cells (16). Adipocytes, originally considered as a simple energy storage depot, are now recognized as endocrine cells releasing a variety of hormones, growth factors, chemokines, and adipokines (17). The process of adipocyte differentiation begins with ASCs, which are multipotent cells found in various tissues that can differentiate into multiple cell types, including adipocytes. The committed ASCs undergo proliferation and differentiate into pre-adipocytes (PAs) which are considered intermediate cells possessing the potential to further differentiate into mature adipocytes (MAs) (18). PAs undergo growth arrest and begin to accumulate lipid droplets within the cytoplasm, which is accompanied by the upregulation of genes involved in lipid metabolism, such as adipocyte protein 2 (AP2) and the main adipogenic transcription factor, peroxisome proliferator-activated receptor gamma (PPAR-γ). The cells acquire the characteristic features of MAs, including a round shape, a large lipid-filled vacuole, and the ability to secrete adipokines such as adiponectin and leptin (19, 20).

The adipose tissue is an endocrine organ as well as an immune organ, as it is physiologically infiltrated by innate immune cells. Adipocytes and immune cells have a strong potential to influence tumor behavior and cancer aggressiveness through heterotypic signaling of soluble factors such as cytokines and growth factors (21). Adipose tissue can exert both paracrine and endocrine effects on breast tumor development. In the early stages of carcinogenesis and during breast cancer evasion, TME can be reorganized by cancer cells to generate a TME favorable for cancer cell proliferation and invasion into the surrounding tissue (22). In addition, recent work suggests that breast cancer cells may stimulate the dedifferentiation of MAs resulting in phenotypic changes and the generation of fibroblast-like cells *i.e.* adipocyte-derived fibroblasts (ADF) (23). In addition, TME plays an important role in macrophage polarization. Macrophages constitute a highly heterogeneous population of cells that undergo extensive changes in their intracellular metabolism in response to environmental and inflammatory stimuli. Unpolarized macrophages (M0) can differentiate into either classically activated pro-inflammatory macrophages (M1-like macrophages) or activated anti-inflammatory macrophages (M2-like macrophages M2a, M2b, M2c, M2d) or immunosuppressive tumor-associated macrophages (TAM) type M2, which play a central role as tumor-protecting cells, in breast cancer growth and progression (24). In lean animals, the adipose tissue microenvironment is predominantly composed of M2 macrophages, maintaining a ratio of approximately 4:1 compared to M1 macrophages. However, with the onset of obesity, this equilibrium is significantly disrupted, shifting to a ratio of roughly 1.2:1 in favor of M1 macrophages. This shift is attributed to the augmented recruitment and infiltration of pro-inflammatory M1 macrophages into the adipose tissue, which in turn exacerbates tissue inflammation (25–27).

Several studies have investigated the association between obesity and DCIS and have found a positive correlation. Obesity, classified according to a body mass index (BMI) ≥ 30 kg/m^2 (28), is associated with an increased risk of breast cancer, particularly in postmenopausal women (29). In addition, obesity increases the risk of death in pre-and post-menopausal breast cancer patients, but the risk is lower in premenopausal than in postmenopausal women (depending on estrogen receptor status) (30–32). In obese subjects, adipose tissue expansion leads to biological dysfunction and the creation of chronic low-grade inflammation. Thus, the secretory and metabolic profiles of adipocytes are affected by increased secretion of pro-inflammatory adipokines that could promote breast cancer development, growth, and progression (33). Furthermore, studies have shown that by stimulating inflammatory pathways, there is a correlation between the degree of adiposity/obesity and adipocyte size and number (34, 35), chronic low-level inflammation with less secretion of anti-inflammatory adipokines (adiponectin) and higher secretions of pro-inflammatory proteins (TNF-α, Leptin, IL-6, IFN-γ, and TGF-β1) which may lead to an increased risk of cancer (36). Overweight and obesity can also stimulate macrophage recruitment and the repolarization of macrophages from the M2-like to the M1-like phenotype. So, reciprocal interactions between adipocytes, macrophages, and breast cancer cells drive functional effects on the behavior of these cells. The adipose tissue can act on MECs and may potentially contribute to the loss of their tumor suppressor status. Understanding this interplay between the adipose tissue and MECs within the DCIS TME represents an important challenge to better recognize the DCIS to IDC progression. By secreting various adipokines, cytokines, and growth factors, the adipose tissue can modulate the surrounding microenvironment, alter the MEC phenotype and viability (11), and affect the surrounding stromal cells, immune cells, or cancer cells, as a result influencing tumor progression and invasion (16).

Therefore, our work aimed to develop and optimize a 3D co-culture model to evaluate the reciprocal interactions between the TME (adipose cells and macrophages) and the DCIS (MECs and cancer cells) and to better understand the impact of this crosstalk on the possible progression to IDC. A co-culture system between i) bicellular fluorescent DCIS-like tumoroids previously developed constituted by DCIS cells (MCF-10DCIS-mcherry) surrounded by MECs (Hs578bst-GFP), and ii) adipose cells (PAs or MAs) organized into spheroids and iii) macrophages (M0 or M1-type) was realized to study the crosstalk and cell interactions that can occur indirectly *via* soluble factors and secretions released by all cell types. In this article, an obese inflammatory microenvironment is reproduced and compared to the microenvironment of a normal-weighted patient by examining cytokine-activated/suppressed signaling pathways, changes in the microenvironment, and effects of inflammation. Mounting evidence suggests that the breast TME, composed of cancer cells, MECs, immune cells, and adipose cells, is a key factor in promoting DCIS to IDC transition, particularly in obese patients.

2 Materials and methods

2.1 Cell culture

2.1.1 Myoepithelial cells

Human Hs578Bst myoepithelial cells (RRID: CVCL_0807) (MECs) were obtained and certificated by the American Type Culture Collection (LGC standard, ATCC, HTB-125, Cheyenne, WY, Laramie County). They were transduced using EF1A-EGFP (Vector Builder ID: VB900083-7716 grp) (multiplicity of infection = 40) and

then sorted to select cells exhibiting similar size and fluorescent signals according to the previously detailed protocol (6). Hs578Bst-GFP were expanded in a growth medium consisting of Dulbecco's Modified Eagle Medium/Ham's F-12 (DMEM/F-12, Gibco, ThermoFisher Scientific, Waltham, MA, USA), supplemented with 50 $\mu g.mL^{-1}$ gentamycin (ThermoFisher Scientific), 10% fetal bovine serum (FBS; Eurobio Scientific, Saclay, France), 2 mM L-glutamine (L-Gln, Gibco), and 30 $ng.mL^{-1}$ epidermal growth factor (EGF, Merck Millipore, Burlington, Massachusetts, USA) at 37°C and 5% CO_2. The growth medium was changed 2–3 times per week. At 80–85% confluence, cells were passaged by using 0.25% w/v trypsin-EDTA 0.53 mM solution (ThermoFisher Scientific) and seeded with the recommended ratio 1:3. Cells were used for experiments before passage 22 to prevent the risk of senescence. All experiments were cultured in a 5% CO_2-humidified incubator at 37°C.

2.1.2 Cancer cells

The human breast cancer cell line MCF10DCIS (RRID: CVCL_5552) (DCIS) was obtained and certified by Wayne State University. They were transduced using EF1A-mCherry (Vector Builder ID: VB900084-0158zxv) (multiplicity of infection = 5) and then sorted to select cells exhibiting similar size and fluorescent signals according to the previously detailed protocol (6). MCF10-DCIS-mcherry was expanded in a growth medium consisting of DMEM/F-12 (Gibco), supplemented with 50 $\mu g.mL^{-1}$ gentamycin, 5% horse serum (Gibco), 2 mM L-Gln, 1.1 mM $CaCl_2$ (Merck Millipore) and 10 mM HEPES (Gibco) at 37°C and 5% CO_2. The growth medium was replaced every 2 days. At 80–85% confluence, cells were passaged using 0.25% w/v trypsin-EDTA 0.53 mM solution. All experiments were cultured in a 5% CO_2-humidified incubator at 37°C.

2.1.3 Adipose cells

Human adipose stem cells (hASCs) were provided by the Cell and Tissue Bank (Hôpital Edouard-Herriot, Lyon, France). They were obtained from patients undergoing surgery for cosmetic purposes without associated pathology in accordance with the Helsinki Declaration, from anonymous healthy donors. The surgical residue was harvested following French regulations including a declaration of Ministry of Higher Education and Research of France (DC no.2008162) and procurement of written informed consent from the patients. hASCs were extracted from postmenopausal normal weight (Nw) or obese (Ob) postmenopausal women. The characterization of hASCs was performed as previously described (37).

hASCs were differentiated into PAs by culturing them in a differentiation medium validated by our team, consisting of consisting of DMEM/F-12, supplemented with 50 $\mu g.mL^{-1}$ gentamycin, 10% FBS, 2 mM L-Gln, 5 $\mu g.mL^{-1}$ basic-fibroblast growth factor (bFGF) (Sigma-Aldrich, St. Louis, MO, USA) at 37°C and 5% CO_2 (37). The growth medium was replaced every 2 days. At 80-85% confluence, cells were passaged using 0.25% w/v trypsin-EDTA 0.53 mM solution. All experiments were cultured in a 5% CO_2-humidified incubator at 37°C.

For differentiation into MAs, hASCs were seeded at the confluence of 33,500 cells/c in a differentiation medium validated by our team consisting of DMEM/F12 supplemented with 10% FBS, 2 mM L-Gln, hydrocortisone (25 $mg.mL^{-1}$), insulin (3.5 $mg.mL^{-1}$), T3 (6.5 $mg.mL^{-1}$), dexamethasone (980 $mg.mL^{-1}$), rosiglitazone (1.78 $mg.mL^{-1}$), isobutyl-methylxanthine (IBMX) (100 $mg.mL^{-1}$, only for the first 3 days), and gentamycin (50 $mg.mL^{-1}$). The medium was replaced every two days (38). MAs of normal weight (Nw-MA) or obese (Ob-MA) women were obtained after 8 days of differentiation. All experiments were cultured in a 5% CO_2-humidified incubator at 37°C. The evaluation of MA differentiation efficiency was carried out as previously detailed (37, 38).

2.1.4 Macrophages

The human monocytic leukemia cell line (THP-1) (ATCC, TIB-202) was cultured in a growth medium consisting of RPMI-1640 medium supplemented with 50 $\mu g.\ mL^{-1}$ gentamycin, 10% FBS and 2 mM L-Gln at 37°C and 5% CO_2. The growth medium was replaced every 2-3 days. For the activation of THP-1 cells into M0 macrophages, THP-1 cells (4×10^5/mL) were incubated in 6-well plates in a complete growth medium containing 16.2 nM phorbol 12-myristate 13-acetate (PMA, Sigma-Aldrich) for 72h. Then, M0 macrophages were polarized into pro-inflammatory M1-like macrophages by incubation with 20 ng/mL of IFN-γ (Gibco) and 10 $pg.\ mL^{-1}$ of lipopolysaccharides (LPS, Sigma-Aldrich) for 24 h at 37°C and 5% CO_2. All experiments were cultured in a 5% CO_2-humidified incubator at 37°C. The validation of the efficacy of the M0/M1 polarization was checked by flow cytometry.

2.1.5 Flow cytometry

For adjustment, two macrophage subtypes were used: M0 and M1-like macrophages. Cells were collected and adjusted to a density of $1 \times 10^6 cells.mL^{-1}$ with DPBS (PBS; without Ca^{2+} and Mg^{2+}, pH 7.4). Then, 1 mL of cell suspension was dispensed into each of the polystyrene flow cytometry tubes for unstained controls, Fluorescence Minus One (FMO) control, and fully stained samples. Functional markers diluted to 1/25 in PBS were used to identify macrophages subtypes: M0 using CD14-PE-VIO 770-Human (130-110-521, Miltenyi Biotec) and M1 using CD80-PE-Human-REA661 (130-123-253, Miltenyi Biotec). To accurately gating cell populations, isotype controls were used diluted to 1/50 in PBS: REA-PE VIO770 (130-113-440, Miltenyi Biotec) and REA-PE REA293 (130-113-438, Miltenyi Biotec). To adjust viability staining, killed cells (with ethanol) were used and stained with Viobility dye (Miltenyi Biotec) at the same dilution as recommended by the manufacturer. All antibodies and isotypes were titrated to determine the optimal concentration considering separation (by staining index), reduction of overflow spread, and detection range of the compensation beads. Cells were first stained for viability using Viobility dye 405/520(130-130-404) for 10 min at 4°C. Then, cells were stained with 4 µL of CD14-PE-VIO-770-Human (130-110-521) and 4 µL of CD80-PE-Human-REA661 (130-123-253) in a total volume of ~100 µL for 15 min at 4°C and 15 min at room temperature. After staining, cells were washed once with PBS (without Ca^{2+} and Mg^{2+}), centrifuged at 300 g for 5 min at RT, resuspended in 500 µL of PBS, and then placed at 4°C for

acquisition. Samples were acquired within 1h of storage. Flow cytometry was performed, after optimization of the panel, using a BD-LSRII flow cytometer (minimum 30,000 live cells counted) to check macrophage activation (M0%) and polarization (M1%). Instrument setup and performance tracking were performed daily using instrument-specific Cytometer Setup and Tracking (CS&T) beads (BD) using the CS&T program. Results were analyzed with FACSDiva version 9.1 software (BD Biosciences, Becton, Dickinson, and Company headquarters). Macrophages undergo active development and exhibit distinct polarization states, characterized by their response to inflammation. They were categorized into two main phenotypes: non-inflammatory M0 (90% $CD14^+$&$CD80^-$) and inflammatory M1 macrophages(90%$CD80^+$). These macrophage subtypes can be effectively distinguished using specific antibodies that target unique markers on their cell surfaces (Supplementary Materials No 1).

2.2 Spheroid generation

The objective was to generate 3D spheroids using non-adherent agarose mold gel in which the cells cannot adhere to the support and thus can multiply in 3D and form multicellular micro-tissues. Agarose (ThermoFisher Scientific)was prepared with sterilized 0.9% w/v NaCl (Sigma-Aldrich), subsequently sterilized, and then put in MicroTissues® 3D Petri Dishes® (81 wells, Sigma-Aldrich) according to the manufacturer's instructions to obtain an agarose mold (6, 39).

2.2.1 Adipospheroid generation

Two types of spheroids have been developed: Pre-adipospheroids made up of PA and Adipospheroids made up of MAs.

For pre-adipospheroids, a total of 200,000 hASCs/agarose mold were seeded in the agarose mold and cultured in DMEM/F12 medium (supplemented with 10% FBS, 2 mM L-Gln, 50 $\mu g.mL^{-1}$ gentamycin, 5 $\mu g.mL^{-1}$ bFGF) for 3 days at 37°C in 5% CO_2, resulting in the assembly of 81 potential Nw-PA and Ob-PA pre-adipospheroids per agarose mold. Concerning the formation of adipospheroids, a total of 200,000 hASCs/agarose mold were seeded in agarose mold and cultured in DMEM/F12 medium (supplemented with 10% FBS, 2 mM L-Gln, 50 $\mu g.mL^{-1}$ gentamycin, 5 $\mu g.mL^{-1}$ bFGF) at 37°C in 5% CO_2. On day 2, the medium was replaced by the differentiation medium (as described previously) (38), resulting in the assembly of 81 potential Nw-MA and Ob-MA adipospheroids per agarose mold.

2.2.2 Bi-fluorescent DCIS-like tumoroid generation

A total of 100,000 MCF10DCIS-mcherry cells were seeded into each agarose mold and cultured in MCF10DCIS medium for 72 hours at 37°C in 5% CO_2, which led to the assembly of 81 potential MCF10DCIS tumoroids per agarose mold according to the previously detailed protocol (6). After 72 hours of incubation, a total of 30,000 Hs578Bst-GFP cells were added to each agarose mold containing the previously formed MCF10DCIS tumoroids, slowly shaken for 20 min at room temperature, then cultured in MECs medium for 12 hours at 37°C in 5% CO_2 (6). The cell culture medium penetrates the tumoroids by diffusion.

2.3 Effect of conditioned media

Conditioned media (CM) were collected from the culture of Nw-PA, Ob-PA, Nw-MA, and Ob-MA (same patient) after differentiation of Nw-PA and Ob-PA respectively. CM was also obtained from the culture of M0 and M1-type macrophages. To minimize oxidation of the CM and ensure better long-term preservation for subsequent analysis, the oxygen was removed from CM ampoules and replaced with nitrogen. All CM (n=3) were harvested and centrifuged at 12,000 g for 15 mins to remove debris. The samples were then frozen at -80°C until use.

The impact of the different CMs on bi-fluorescent DCIS–like tumoroid viability was monitored. For that, DCIS-like tumoroids previously formed in agarose molds were transferred to the wells of a 96-well ultra-low-binding U-shaped-bottom plate (Corning, Somerville, MA, USA) (one single tumoroid in one well) and cultured in 200 µL of undiluted CM for 72 hours at 37°C in 5% CO_2. Using IncuCyte® (Sartorius, Göttingen, Allemagne), green and red fluorescence intensity variation was measured to monitor the cell viability of each cell line and monitor the impact of obesity, adipose, and inflammatory microenvironments on cancer cells and MECs viability (n=3 for each CM).

2.4 3D co-culture model

A 3D co-culture system was set up to evaluate the reciprocal interactions between DCIS-like tumoroids and the adipose microenvironment (Figure 1) mimicking either an inflammatory adipose microenvironment found in obese people (Ob-TME), or a standard adipose microenvironment found in normal-weight individuals (Nw-TME).

2.4.1 Model implementation

For the 3D model mimicking a Nw-TME, THP-1 monocytes were first seeded at the bottom of the wells of a 6-well plate and activated in M0 according to the protocol detailed above. Then these macrophages were co-cultured for 72h with both agarose molds containing DCIS-like tumoroids and adipospheroids made up with either Nw-PA or Nw-MA (Conditions 1 and 2) (Figure 1B) and compared to their respective controls without tumoroids (Control 1: Nw-PA-M0; Control 2: Nw-MA-M0) (Supplementary Materials No 2).

For the 3D model mimicking an obese inflammatory adipose microenvironment, THP-1 monocytes were polarized into M1-like pro-inflammatory macrophages, representing the predominant phenotype within the inflammatory microenvironment associated with obesity. Subsequently, these macrophages were co-cultured with both DCIS-like tumoroids and adipospheroids constituted by Ob-PA or Ob-MA (Conditions 3 and 4) (Figure 1B) and compared

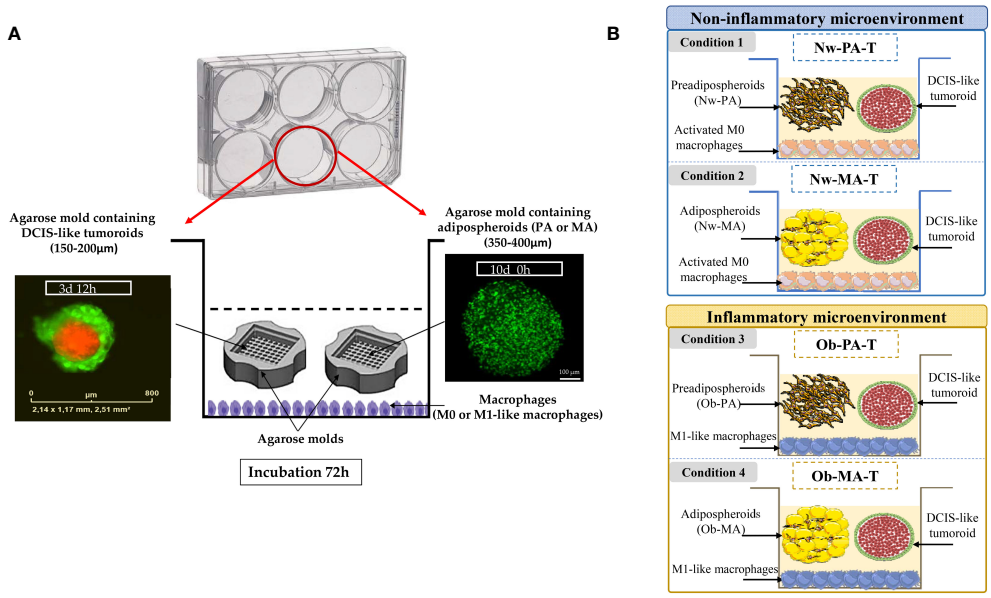

FIGURE 1
(A) Co-culture model mimicking a DCIS surrounding by its adipose inflammatory microenvironment. THP-1 cells (4 x 10^5/mL) were incubated in 6-well plates in a complete growth medium for three days, differentiated in macrophages (M0), and polarized into M1-like macrophages by incubation with IFN-γ and lipopolysaccharides for 24 h. M0 or M1-like macrophages were co-incubated with two-cell-type, DCIS-like tumoroids (IncuCyte® objective ×4) and adipospheroids (PA or MA) both formed in the agarose mold (confocal microscopy of adipospheroids stained with Bodipy, Micro Zeiss Cell Observer Spinning Disk, ×20 Plan Apochromat 20×/0.8 M27). **(B)** Description of the experimental design. A total of 4 conditions (3 independent experiments) mimicking a Nw- and Ob-TME were generated: Condition 1 *Nw-PA-T*: "Normal-weight tumor microenvironment with PA", co-culture of M0 + NwPA + DCIS-like tumoroids, Condition 2 *Nw-MA-T*: "Normal-weight tumor microenvironment with MA", co-culture of M0 + NwMA + DCIS-like tumoroids, Condition 3 *Ob-PA-T*: "Obese inflammatory adipose tissue with PA", co-culture of M1-like macrophages + Ob-PA + DCIS-like tumoroids, Condition 4 *Ob-MA-T*: "Obese inflammatory adipose tumor microenvironment with MA", co-culture of M1-like macrophages + Ob-MA + DCIS-like tumoroids.

to their respective controls (Control 3: Ob-PA-M1; Control 4: Ob-MA-M1) (Supplementary Materials No 2).

Cells were co-cultured in a medium containing 7 mL of DMEM/F-12 supplemented with 50 µg. mL^{-1} gentamicin, 10% fetal bovine serum (FBS), 2 mM L-glutamine (L-Gln), and 30 ng. mL^{-1} epidermal growth factor (EGF). This medium represents the joint co-culture-conditioned media facilitating paracrine communications among distinct cellular types.

After 72 hours of incubation, the co-culture-conditioned medium was utilized for the quantification and identification of various cytokines across all co-culture conditions. The total RNA from each cell type was extracted using TRIZOL (ThermoFisher Scientific), and RT-qPCRs were subsequently conducted. These experiments were conducted independently at least three times.

A total of 2 conditions (3 independent experiments) mimicking an Nw-TME were generated (Figure 1B):

- Condition 1 *Nw-PA-T*: "Normal-weight tumor microenvironment with PA", co-culture of M0 + NwPA + DCIS-like tumoroids *vs* Control 1 *Nw-PA-M0* "Normal-weight adipose tissue with PA", co-culture of M0 + Nw-PA.
- Condition 2 *Nw-MA-T*: "Normal-weight tumor microenvironment with MA", co-culture of M0 + NwMA + DCIS-like tumoroids *vs* Control 2 *Nw-MA-M0:* "Normal-weight adipose tissue with MA", co-culture of M0 + Nw-MA.

A total of 2 conditions (3 independent experiments) mimicking an Ob-TME were generated (Figure 1B):

- Condition 3 *Ob-PA-T*: "Obese inflammatory adipose tissue with PA", co-culture of M1-like macrophages + Ob-PA + DCIS-like tumoroids *vs* Control 3 *Ob-PA-M1*: "Obese inflammatory adipose tissue with PA", co-culture of M1-like macrophages + Ob-PA.
- Condition 4 *Ob-MA-T*: "Obese inflammatory adipose tumor microenvironment with MA", co-culture of M1-like macrophages + Ob-MA + DCIS-like tumoroids *vs* Control 4 *Ob-MA-M1*:" Obese inflammatory adipose tissue with MA", co-culture of M1-like macrophages + Ob-MA.

2.4.2 Selection and sorting

After co-culture, the bi-fluorescent DCIS-like tumoroids were trypsinized using 0.25% w/v trypsin-EDTA 0.53 mM solution (ThermoFisher Scientific) to obtain a cell suspension containing both cell types. A BD Cell Analyser FACSAria SORP Cell Analyzer/Sorter (BD Biosciences, Franklin Lakes, New Jersey, USA) was used to separate the two cell types according to fluorescent signal type and BD FACSDiva™ CS&T Research was used to monitor the performance of the cytometer each day and to generate reproducible data. The prerequisites necessary for this process

were to adjust the selection using untransformed and non-fluorescent cells of each cell line, to know cell diameters, to choose an appropriate pressure to avoid cell shock, to filter the cells before passing them, and to eliminate aggregates (if any). Finally, cancer cells were recovered separately from the myoepithelial cells and total RNA was extracted with TRIZOL to perform qRT-PCR.

2.4.3 Evaluation of gene expression by quantitative real-time PCR

Following the co-culture, total RNA was extracted with TRIZOL reagent (Invitrogen, ThermoFisher Scientific). After the evaluation of the quantity and purity of RNA (Tecan Spark®, Männedorf, Switzerland), DNase treatment was applied to remove any remaining genomic DNA (DNase I Amplification grade, Invitrogen) and cDNA reverse transcription (HighCap cDNA RT Kit RNAse inhib, Invitrogen) was performed according to the manufacturer's recommendations. Concerning pre- and adipospheroids, macrophages, and MECs, amplification reaction assays were carried out using SYBRGreen PCR Master Mix (Applied Biosystems, Waltham, Massachusetts, USA) and primers (Table 1) on a StepOne™ machine (Applied Biosystems). The thermal cycling conditions were 50°C for 2 min followed by an initial denaturation step at 95°C for 10 min, 40 cycles at 95°C for 30 s, 60°C for 30 s, and 72°C for 30 s. The experiments were carried out in duplicate for each data point. The analysis was conducted on 7 genes for macrophages (*TNF-α, IL-6, IL-1β, IL-8, TGF-β, IL-10, CD163*), 13 genes for adipocytes (*PPAR-γ, AP2, HSL, Leptin, Adiponectin, TNF-α, IL-6, IL-1β, IL-8, CXCL-10, FAP, LIF, α-SMA*) and 4 genes for MECs (*BAX, PCNA, α-SMA, CDH1*). The reference genes *GAPDH* and *β-actin* were used as an internal control for the normalization of RNA quantity and quality differences among the samples.

Concerning cancer cells, qPCRs were performed on plates designed by Applied Biosystems (TaqMan Array 96 well Fast Plate, Customformat 32, Applied Biosystems) using PowerUp SYBRgreen (Applied Biosystems) with TaqMAN on a Quantstudio 3 machine (Thermo Fisher). The thermal cycling conditions were 50°C for 2 min followed by an initial denaturation step at 95°C for 2 min, 40 cycles at 95°C for 1 s and 60°C for 20 s. The analysis was conducted on 20 genes (*ESR1, CYP19A1, ERBB2, PGR, TP53, JUN, TGFB1, BAX, BAG1, BCL2, CASP3, CASP8, CASP9, THBS1, TIMP1, VEGFa, MMP9, TNF-α, PTGS2, IL-6R*) and 3 references genes (*18S, GAPDH, HPRT1).* The reference genes *GAPDH* and *HPRT1* were used as an internal control for the normalization of RNA quantity and quality differences among the samples.

Genes were considered significantly expressed and their transcript was measurable if their corresponding Ct value was less than 35. The relative quantification method ($RQ = 2^{-\Delta\Delta CT}$) was used to calculate the relative gene expression of given samples with $\Delta\Delta CT = [\Delta CT\ (sample1) - \Delta CT\ (sample2)]$ and $\Delta CT = [CT\ (target\ gene) - CT\ (reference\ gene)$. Three independent experiments were performed. $p<0.05$ was considered significant.

Concerning the analysis of genes expressed in MECs, adipocytes, and macrophages, relative mRNA gene expression (RQ) was normalized to *GAPDH* and *β-actin* in the four conditions Nw-PA-T (M0+Nw-PA+Tumoroids), Nw-MA-T (M0 +Nw-MA+Tumoroids), Ob-PA-T (M1+Ob-PA+Tumoroids), and Ob-MA-T (M1+Ob-MA +Tumoroids) and compared to their respective control 1, 2, 3 and 4 to evaluate the impact of DCIS-like tumoroids on each group. *The P-value* corresponded to the comparison between the control and condition.

Concerning the analysis of genes expressed in cancer cells, relative mRNA expression (RQ) of genes was normalized to *GAPDH* and *HPRT1* in the four conditions. The *p-value* corresponded to the comparison between co-cultured tumoroids compared to "Tumoroids alone"; the *p2-value* corresponded to the comparison between Nw-PA-T and Ob-PA-T; the *p3-value* corresponded to the comparison between Nw-MA-T and Ob-MA-T.

2.4.4 Determination of cytokine concentrations

ProcartaPlex™ Immunoassays (ThermoFisher Scientific) was used for all assays. All samples were run in triplicate and were assayed for 12 human cytokines (IFN-γ, IL-12 p70, IL-1β, IL-2, IL-23, IL-6, IL-8, IL-17a, MIP-1α, leptin, adiponectin and TNF-α). Cytokine levels were measured using optimal concentrations of standards and antibodies in accordance with the manufacturer's instructions. After completion of all the steps in the assay, the plates were read in the Luminex Bio-Plex 200 System (Biorad, France) and the data were analyzed using Bio-Plex Manager™ 4.1 software with five-parameter logistic regression (5PL) curve fitting.

2.4.5 Statistical analyses

Most of the statistical analysis was done thanks to the R software with the RStudio IDE (R 4.2.2, RStudio 2022.07.2). All the plots created with R come from ggplot in its tidyverse implementation (1.3.2). At each step the data were prepared thanks to dplyr functions (1.0.10).

In qPCR analyses, the RQ (Relative Quantification) data have been analyzed. Firstly, heatmap was created through the pheatmap package (1.0.12) on the basis of group means of fully scaled values. In heatmap function, the "ward.D2" algorithm was chosen and an optimal number of clusters for both groups and genes was visually set. To better isolate clusters of genes, correlograms were drawn thanks to the corrplot package (0.92), based on parametric Pearson correlations coefficients run with the same ward.D2 agglomerative method. Finally, differential analysis on co-cultures has been performed on a series of genes. This was done with the tools of stats and lsmeans packages in the aforementioned versions. For cell viability statistical significance among several groups was assessed using one-way ANOVA followed by Tukey's multiple comparisons test in GraphPad Prism software version 8 (GraphPad Software, San Diego, USA).

For flow cytom*etry data, relevant tools have been applied for these frequencies data, i.e. mainly the rcompanion package (2.4.21) and its methods. To evaluate the variations in cell type frequencies between co-culture, the Cochran-Mantel-Haenszel method has been chosen in a global and in a pairwise approach. To represent these variations, a barplot where all the co-culture has been

TABLE 1 PCR primer sequences.

Gene	Species	Forward Primer sequence (5′-3′)	Reverse Primer sequence (5′-3′)
GAPDH	Human	CACATGGCCTCCAAGGAGTAA	TGAGGGTCTCTCTCTTCCTCTTGT
β-actin	Human	CCTGGCACCCAGCACAAT	GCCGATCCACACGGAGTACT
Il-8	Human	CTGGCCGTGGCTCTCTTG	CCTTGGCAAAACTGCACCTT
Il-1β	Human	CCTGTCCTGCGTGTTGAAAGA	GGGAACTGGGCAGACTCAAA
Il-6	Human	GCTGCAGGCACAGAACCA	ACTCCTTAAAGCTGCGCAGAA
TNF-α	Human	TCTTCTCGAACCCCGAGTGA	GGAGCTGCCCCTCAGCTT
CXCL-10	Human	GGAAATCGTGCGTGACATTA	AGGAAGGAAGGCTGGAAGAG
PPAR-γ	Human	GGATTCAGCTGGTCGATATCAC	GTTTCAGAAATGCCTTGCAGT
Ap2	Human	ATCACATCCCCATTCACACT	ACTTGTCTCCAGTGAAAACTTTG
HSL	Human	GCCTGGGCTTCCAGTTCAC	CCTGTCTCGTTGCGTTTGTAGT
Leptin	Human	CGGAGAGTACAGTGAGCCAAGA	CGGAATCTCGCTCTGTCATCA
Adiponectin	Human	CCCAAAGAGGAGAGGAA	TCAGAAACAGGACACAAC
BAX	Human	CCTGTGCACCAAGGTGCCGGAACT	CCACCCTGGTCTTGGATCCAGCCC
CD163	Human	CGGTCTCTGTGATTTGTAACCAG	TACTATGCTTTCCCCATCCATC
TGF-β	Human	GACATCAAAAGATAACCACTC	TCTATGACAAGTTCAAGCAGA
IL-10	Human	GGGGGTTGAGGTATCAGAGGTAA	GCTCCAAGAGAAAGGCATCTACA
LIF	Human	GAAAGCTTTGGTAGGTTCTTCGTT	TGCAGGTCCAGCCATCAGA
FAP	Human	TCCAGTCTCCAGCTGGGAAT	GTTGGGAGACCCATGAATCTCT
α-SMA	Human	TGCCTGATGGGCAAGTGAT	TCTCTGGGCAGCGGAAAC
PCNA	Human	AGGCACTCAAGGACCTCATCA	GAGTCCATGCTCTGCAGGTTT
CDH1	Human	ACAGCCCCGCCTTATGATT	TCGGAACCGCTTCCTTCA

normalized to a value of 1, helps compare the proportions of each labeling.

For cytokine concentration data, two-way ANOVA has been first performed to assess the variations of the twelve measured cytokines. This analysis considered the type of macrophage or adipocyte cells in the microenvironment as two predictors in linear models. Here the anova_test function from the rstatix package (0.7.1) was used in a type 2 setting to calculate *p-values* for main effects and interactions. In these linear models, contributions (effect size) were calculated thanks to the lsr package (0.5.2). To complete these results, a deeper analysis was conducted with the lsmeans package (2.30-0). With this tool, all pairwise comparisons are assessed for main and simple effects, giving the relevant *p-values* translated into CLD (Compact Letter Display) that help interpretations. For a one-way ANOVA style analysis, the replicates "group" factor has been treated with seventeen levels, each corresponding to an original combination of cell types. The basic stats package (4.2.2) was used with its a function to detect overall variations amongst these seventeen groups, with an fdr adjustment applied to *p-values*. On the same but standardized data, PCAs were produced to visualize each sample and group on a multivariate basis, the distributions being calculated from the twelve cytokines abundances. At this step, we used the FactoMineR (2.7) and factoextra (1.0.7) tools to generate PCAs.

3 Results

3.1 Impact of the adipose inflammatory microenvironment on DCIS-like tumoroids

3.1.1 Impact of the adipose inflammatory microenvironment on cancer cells from DCIS-like tumoroids

We first sought to identify the impact of the adipose inflammatory microenvironment on MCF-10DCIS-RFP cancer cells from the DCIS-like tumoroids by measuring the real-time viability by Incucyte® and we showed that CM of Ob-PA, Ob-MA, and M1 significantly increased the percentage of red intensity which is proportional to the viability of MCF-10DCIS-RFP cancer cells (Figure 2A).

Then, we wanted to identify the underlying mechanism by which adipose tissue might act on cancer cells of DCIS-like tumoroids by focusing on changes in gene expression. We studied the modification of the expression of genes involved in apoptosis (*BAX, BAG1, BCL2, CASP3, CASP8, CASP9*), angiogenesis (*THBS1, TIMP1, VEGFα*), inflammation (*MMP9, TNF-α, PTGS2, IL-6R*), cell cycle/pro-oncogenesis/transcription factors (*TP53, JUN, TGFB1*), and cytokines/hormonal pathways (*ESR1, CYP19A1, ERBB2, PGR*).

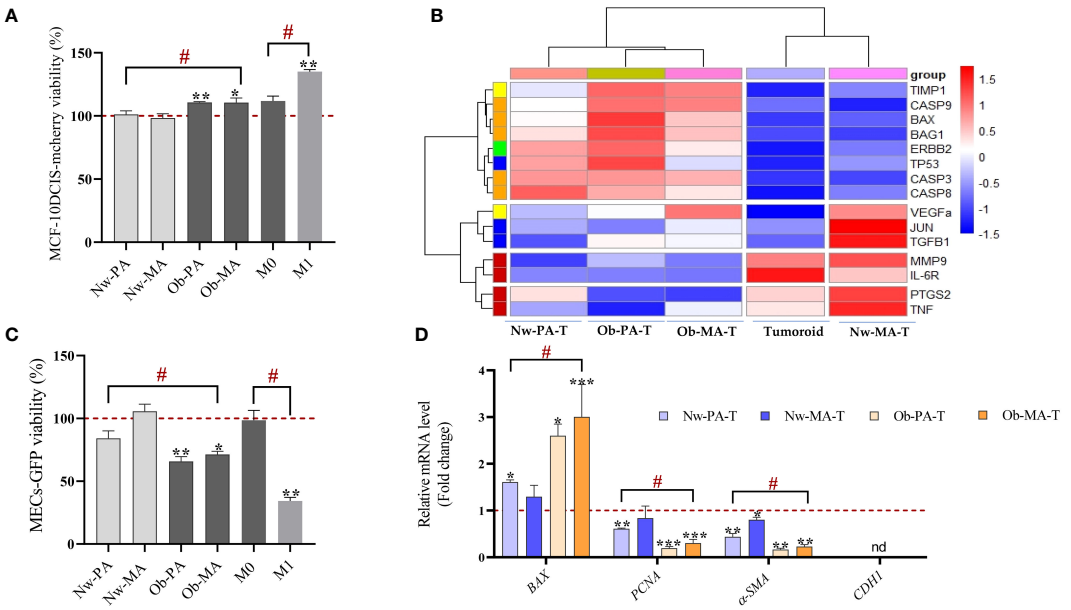

FIGURE 2
Impact of the adipose inflammatory microenvironment on cancer cells from DCIS-like tumoroids. **(A, B)** Impact of the adipose inflammatory microenvironment on cancer cells sorted from DCIS-like tumoroids. **(A)** Conditioned media from PA (Nw-PA, Ob-PA), MA (Nw-MA, Ob-MA) and macrophages (M0, M1) were obtained after 48h of culture and their impact on cell viability was assessed by measuring the fluorescence intensity using the IncuCyte® system to monitor the fluorescence intensity of MCF10-DCIS-mcherry breast cancer cells. **(B)** Hierarchical clustering (heatmap) illustrates the variations of ΔCt mRNA expression of 15 genes normalized to GAPDH expressed by MCF10-DCIS cancer cells sorted from DCIS-like tumoroids co-cultured in the Nw-TME or the Ob-TME and compared to control (DCIS cells sorted from DCIS-like tumoroids control). The heatmap color code is categorized by gene type as follows: green for hormone-related genes, yellow for angiogenesis, blue for cell cycle, pro-oncogenes/transcription factors, red for inflammation, orange for apoptosis, and purple for proliferation. **(C, D)** Impact of the adipose inflammatory microenvironment on MECs sorted from DCIS-like tumoroids. **(C)** Conditioned media from PA (Nw-PA, Ob-PA), MA (Nw-MA, Ob-MA) and macrophages (M0, M1) were obtained after 48h of culture and their impact on cell viability was assessed by measuring the fluorescence intensity using the IncuCyte® system to monitor the fluorescence intensity of Hs578Bst-GFP myoepithelial cells, M0: activated macrophages; M1: pro-inflammatory macrophages. **(D)** Relative mRNA expression (RQ) of 4 genes normalized to GAPDH expressed by MECs sorted from DCIS-like tumoroids co-cultured in the Nw-TME or the Ob-TME and compared to control (MECs sorted from DCIS-like tumoroids control). Results are expressed as percentage compared to each cultured media control (PA, MA, and macrophages cultured media). All data represent the means of 3-6 replicates ± SEM. * $p<0.05$, ** $p \leq 0.01$ *** $p \leq 0.001$ represent significant differences compared to control and # represents a significant difference between normal-weight and obese condition. Nw-PA, adipose stem cells from normal-weight women; Ob-PA, adipose stem cells from obese women; Nw-MA, mature adipocytes from normal-weight women; Ob-MA, mature adipocytes from obese women; M0, activated macrophages; M1, pro-inflammatory macrophages. PCNA, Proliferating cell nuclear antigen; SMA-α, smooth muscle actin; CDH1, E-cadherin.

Hierarchical clustering enabled clear discrimination between control tumoroids and tumoroids co-cultured with Nw-TME or Ob-TME with under-expressed genes (red font) and over-expressed genes (blue font) (Figure 2B). The heatmap revealed that the conditions Nw-PA-T, Ob-PA-T, and Ob-MA-T were particularly associated with an overexpression of genes related to inflammation and on the contrary with a down-regulation of genes related to apoptosis and angiogenesis. Nw-MA-T was associated with a lower expression of all genes related to cycle/pro-oncogene/transcription factor, VEGF, and TNF-α.

Apoptosis and cell cycle. All apoptosis-related genes (*BAX, BAG1, CASP3, CASP8*, and *CASP9* except *BCL2*), *TP53*, and *TGF-β* involved in cell growth were significantly expressed by cancer cells in all groups (Tables 2, 3). The Ob-PA-T mainly decreased the expression of *BAX* (RQ=0.084; $p \leq 0.001$, $p2 \leq 0.001$), *BAG1* (RQ=0.101; $p \leq 0.001$, $p2 \leq 0.05$), and *TP53* (RQ=0.019, $p \leq 0.001$, $p2 \leq 0.05$) to a greater extent than Nw-PA-T (Table 2). In addition, Ob-MA-T mainly decreased the expression of all apoptosis-related genes such as *BAX* (RQ=0.21; $p \leq 0.001$, $p3 \leq 0.001$), *BAG1* (RQ=0.208; $p \leq 0.001$, $p3 \leq 0.001$), *CASP3* (RQ=0.215; $p \leq 0.001$, $p3 \leq 0.001$), *CASP8* (RQ=0.262; $p \leq 0.001$, $p3 \leq 0.05$), and *CASP9* (RQ=0.169; $p \leq 0.001$, $p3 \leq 0.05$) (Table 3). On the contrary, the expressions of *CASP3*, *CASP8*, and *CASP9* were similarly reduced in Ob-PA-T and Nw-PA-T. Nw-MA-T only slightly decreased the expression of *BAX* (RQ=0.8; $p \leq 0.01$) and *CASP8* (RQ=0.551, $p \leq 0.05$). The expression of *TP53* and *TGF-β* was reduced in Nw-MA-T and mainly in Ob-MA-T (Table 3).

Inflammation. All the studied genes involved in inflammation (*MMP9, PTGS2, TNF-α*, and *IL-6R*) were expressed by cancer cells. Ob-PA-T increased the expression of *PTGS2* and *TNF-α* expression by a factor of nearly 4 (RQ=3.888, $p \leq 0.01$, $p2 \leq 0.05$) and 10 (RQ=9.96, $p \leq 0.001$, $p2 \leq 0.01$) respectively (Table 2). In addition, Ob-MA-T had the most potent effect on the upregulation of all inflammatory genes by a factor near 28 for *MMP9* (RQ=28.724, $p \leq 0.001$, $p3 \leq 0.001$), 4 for *PTGS2* (RQ=4.163, $p \leq 0.001$, $p3 \leq 0.001$), 2 for *TNF-α* (RQ=2, $p<0.05$, $p3<0.05$) and for *IL-6R* (RQ=2.24, $p \leq 0.05$) which may be due to obesity-associated inflammation (Table 3). *IL-6R* expression was increased by a factor of 2 similarly within the Nw and Ob-PA-T which can be due to high IL-6 level in supernatant. *MMP9* expression increased by a factor of 40 within

10.3389/fimmu.2024.1384354

TABLE 2 Relative mRNA expression (RQ) of 20 normalized genes expressed by tumor cells sorted from tumoroids co-cultured either with Nw—PA-T or Ob-PA-T and compared to Tumoroid control (*p-value*).

Category	Groups	Tumoroids	*Nw-PA-T*		*Ob-PA-T*		
	Genes	RQ	RQ	*p-value*	RQ	*p-value*	*p2-value*
Apoptosis	*BAX*	1	0.27	≤ 0.001	0.084	≤ 0.001	≤ 0.001
	BAG1	1	0.28	≤ 0.001	0.101	≤ 0.001	< 0.05
	BCL2	nd	nd	nd	nd	nd	nd
	CASP3	1	0.19	≤ 0.001	0.162	≤ 0.001	0.965
	CASP8	1	0.118	≤ 0.001	0.173	≤ 0.001	0.623
	CASP9	1	0.41	≤ 0.01	0.15	≤ 0.01	0.1723
Angiogenesis	*VEGFa*	1	0.522	≤ 0.01	0.43	≤ 0.01	0.391
	THBS2	nd	nd	nd	nd	nd	nd
	TIMP1	1	0.322	≤ 0.001	0.099	≤ 0.001	0.01
Inflammation	*MMP9*	1	40.861	≤ 0.001	10.456	≤ 0.001	≤ 0.001
	PTGS2	1	1.119	0.981	3.888	≤ 0.01	< 0.05
	IL-6R	1	2.54	< 0.05	2.132	< 0.05	0.998
	TNF-α	1	3	≤ 0.01	9.96	≤ 0.01	≤ 0.05
Cycle/ pro-oncogene/ Transcription factor	*TP53*	1	0.049	≤ 0.001	0.019	≤ 0.001	< 0.05
	JUN	1	0.899	0.587	1.067	0.7073	0.2340
	TGFB1	1	1.065	0.4677	0.466	≤ 0.001	≤ 0.001
Hormonal pathway	*ERBB2*	1	0.064	≤ 0.001	0.039	≤ 0.001	< 0.05
	ESR1	nd	nd	nd	nd	nd	nd
	CYP19A1	nd	nd	nd	nd	nd	nd
	PGR	nd	nd	nd	nd	nd	nd

p2-value corresponded to the comparison between Nw-PA-T and Ob-PA-T. nd, not determined.

Nw-PA-T (RQ=40.861, $p \leq 0.001$), which is much higher than in Ob-PA-T in which expression increased 10-fold (RQ=10.456, $p \leq 0.001$, $p2 \leq 0.001$) (Table 2) while Nw-MA-T had a non-significant effect on all the inflammation-related gene expression.

Angiogenesis. A significantly decreased *TIMP1* expression in cancer cells was observed within Nw-PA-T (RQ=0.322, $p \leq 0.001$), Ob-PA-T (RQ=0.099, $p \leq 0.001$, $p2 = 0.01$) (Table 2), Nw-MA-T (RQ=0.579, $p \leq 0.001$) and Ob-MA-T (RQ=0.121, $p \leq 0.001$, $p3 \leq 0.001$) (Table 3), which can contribute to tumor migration and progression. Surprisingly, the expression of *VEGF* was similarly decreased in cancer cells within all TME groups.

Hormonal pathway. The hormonal-related genes studied (*ESR1, CYP19A1*, and *PGR*) were not expressed by MCF10-DCIS cancer cells that are HER2-enriched (ER–, PR–, HER2+/ERBB2+) intrinsic molecular subtypes of breast cancer (33). *ERBB2* (HER2) expression decreased in cancer cells co-cultured with Nw-PA-T (RQ=0.064, $p \leq 0.001$) (Table 2) and Nw-MA-T (RQ=0.436, $p \leq 0.001$) (Table 3), this expression continued to decrease in Ob-PA-T (RQ=0.039, $p \leq 0.001$, $p2<0.05$) (Table 2) and Ob-MA-T (RQ=0.127, $p \leq 0.001$, $p3<0.01$) (Table 3).

3.1.2 Impact of the adipose inflammatory microenvironment on MECs sorted from DCIS-like tumoroids

As previously, we evaluated the impact of the adipose microenvironment on Hs578Bst-GFP MECs of the DCIS-like tumoroids, by measuring the real-time viability by Incucyte®. We found that only the CMs obtained from the inflammatory adipose microenvironment, *ie* Ob-PA, Ob-MA, and pro-inflammatory macrophages M1-like, significantly decreased the percentage of the green intensity that is proportional to the viability of the continuous layer of Hs578Bst-GFP MECs (Figure 2C). Then we studied the alteration of the expression of genes involved in apoptosis (*BAX*), DNA replication and repair processes (*PCNA*), and myoepithelial cell differentiation markers (*α-SMA*, *E-cadherin*) and all were significantly expressed by MECs in all conditions except *E-cadherin* (not expressed in the control and all experimental condition) (Figure 2D). We found that MECs co-cultured with the inflammatory adipose microenvironment presented the highest increase in *BAX* expression and the lowest decrease in *PCNA* and *α-SMA* expression. Indeed, the Ob-PA-T had a more potent effect than the Nw-PA-T on the

TABLE 3 Relative mRNA expression (RQ) of 20 normalized genes expressed by tumor cells sorted from tumoroids co-cultured with Nw-MA-T or Ob-MA-T (*p-value*).

Category	Groups	Tumoroids	*Nw-MA-T*		*Ob-MA-T*		
	Genes	RQ	RQ	*p-value*	RQ	*p-value*	*p3-value*
Apoptosis	*BAX*	1	0.82	≤ 0.01	0.21	≤ 0.001	≤ 0.001
	BAG1	1	1.096	0.473	0.208	≤ 0.001	≤ 0.001
	BCL2	nd	nd	nd	nd	nd	nd
	CASP3	1	0.905	0.579	0.215	≤ 0.001	≤ 0.001
	CASP8	1	0.551	≤ 0.01	0.262	≤ 0.001	< 0.05
	CASP9	1	1.815	0.21	0.169	≤ 0.001	< 0.05
Angiogenesis	*VEGF a*	1	0.272	≤ 0.001	0.286	≤ 0.001	0.985
	THBS2	nd	nd	nd	nd	nd	nd
	TIMP1	1	0.523	≤ 0.001	0.121	≤ 0.001	≤ 0.001
Inflammation	*MMP9*	1	0.587	0.999	28.724	≤ 0.001	≤ 0.001
	PTGS2	1	0.454	0.245	4.163	≤ 0.001	≤ 0.001
	IL-6R	1	1.437	0.536	2.24	< 0.05	0.179
	TNF-α	1	0.20	0.0823	2	< 0.05	< 0.05
Cycle/pro-oncogene/ Transcription factor	*TP53*	1	0.328	≤ 0.001	0.2	≤ 0.001	0.116
	JUN	1	0.211	< 0.05	0.784	0.555	0.0629
	TGFB1	1	0.173	≤ 0.001	0.546	< 0.05	≤ 0.001
Hormonal pathway	*ERBB2*	1	0.436	≤ 0.001	0.127	≤ 0.001	≤ 0.01
	ESR1	nd	nd	nd	nd	nd	nd
	CYP19A1	nd	nd	nd	nd	nd	nd
	PGR	nd	nd	nd	nd	nd	nd

p3-value corresponded to the comparison between Nw-MA-T and Ob-MA-T. nd, not determined.

downregulation of *PCNA* (RQ=0.192, $p \leq 0.001$) and *α-SMA* (RQ=0.165; $p \leq 0.001$) and the upregulation of *BAX* (RQ=2.5; $p \leq 0.001$). When we focused on the TME constituted with MA and M1-type macrophages, we observed that Ob-MA-T had a more potent effect than Nw-MA-T on *α-SMA* downregulation (RQ=0.22, $p \leq 0.01$). Ob-MA-T also increased *BAX* expression by a factor of 3 (RQ=3; $p \leq 0.001$) and decreased *PCNA* expression (RQ=0.3; $p \leq 0.05$) while Nw-MA-T did not affect the proliferation and pro-apoptotic activity of MECs of DCIS-like tumoroids but can affect its contractile properties.

3.2 Impact of DCIS-like tumoroids on its adipose inflammatory microenvironment

We investigated the underlying mechanisms by which DCIS-like tumoroids might act on adipose tissue by focusing on gene expression changes. We first measured the expression of genes involved in adipocyte differentiation (*PPAR-γ, AP2, HSL, Adiponectin, Leptin*), cancer-associated fibroblast (CAF) markers (*LIF, FAP, α-SMA*), and inflammation (*IL-6, IL-8, IL-1β, CXCL-10, TNF-α*). CAFs can exhibit diverse phenotypes and functions, influenced by various factors including tumor type, stage, and microenvironmental cues like cancer-associated myofibroblasts (myoCAF) characterized by the expression of α-SMA and FAP, and inflammatory cancer-associated fibroblast (iCAF) phenotypes characterized by expression of LIF and strong expression of inflammatory cytokines and chemokines. Then we evaluated the expression of genes involved in the inflammatory response and macrophage polarization (*IL-1β, IL-6, IL-8, TNF-α, TGF-β, IL-10, CD163*) in macrophages.

3.2.1 The reprogramming of adipose cells within the TME

3.2.1.1 DCIS-like tumoroids suppressed adipocyte-differentiation-related genes and affected adipokine secretions

DCIS-like tumoroids decreased the expression of genes involved in adipocytes (Figure 3A) through the downregulation of the expression of *PPAR-γ* and *AP2* (also known as FABP4), which are key regulators of adipogenesis and lipid metabolism.

In the presence of tumoroids, the expression of *AP2* was similarly downregulated by 50% in Nw-PA-T ($p \leq 0.01$), Ob-PA-T ($p \leq 0.01$), and Ob-MA-T ($p \leq 0.001$) while *PPAR-γ* was downregulated by 50% only within Nw-PA-T ($p \leq 0.01$) and Ob-PA-T ($p \leq 0.01$). This positive feedback loop between PPAR-γ and

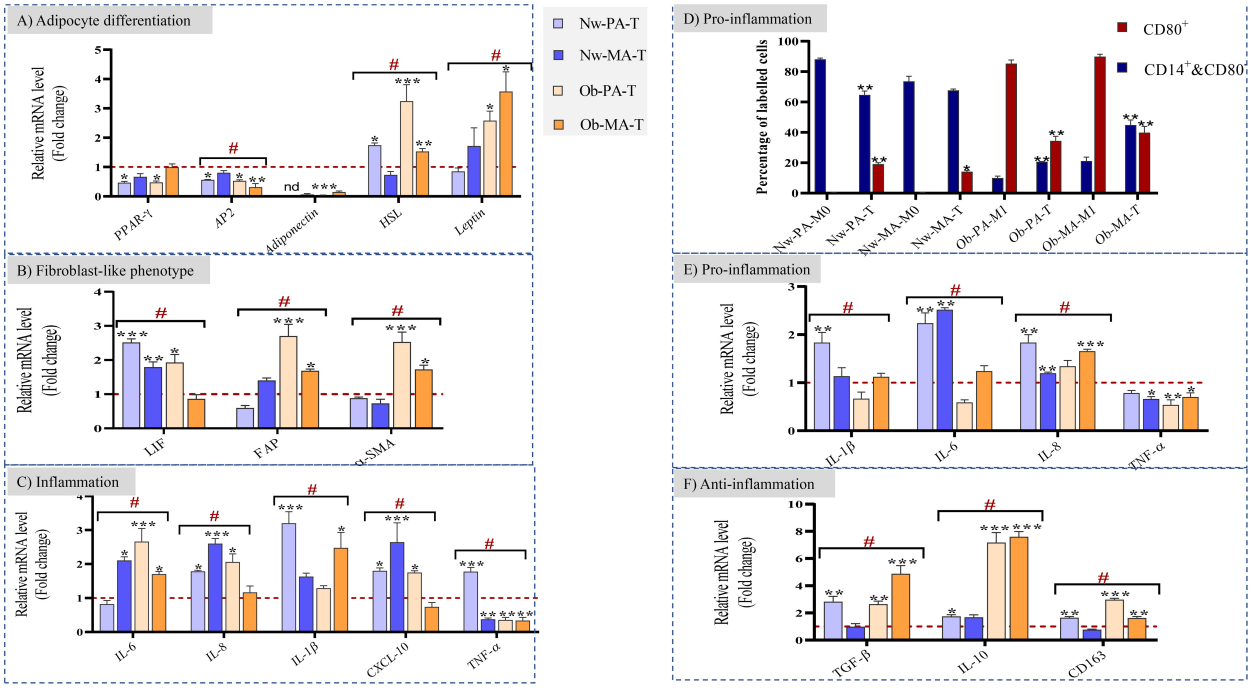

FIGURE 3
(A–C) Impact of the Nw-TME and Ob-TME on adipocyte differentiation, fibroblast-like phenotype and inflammation. Pre-adipospheroids (Nw-PA, Ob-PA) and adipospheroids (Nw-MA, Ob-MA) were co-cultured with macrophages (M0 or M1) and DCIS-like tumoroids. The mRNA relative expression of **(A)** adipocyte differentiation-related genes (*PPAR-γ, AP2, Adiponectin, HSL, Leptin*), **(B)** genes related to cancer-associated fibroblast phenotype (*LIF, FAP, α-SMA*) **(C)** genes related to inflammation (*IL-6, IL-8, IL-1β, CXCL-10, TNF-α*), and was measured by qRT-PCR. GAPDH was used as control. The four conditions Nw-PA-T (M0+Nw-PA+Tumoroids), ObPA-T (M1+Ob-PA+Tumoroids), Nw-MA-T (M0+Nw-MA+Tumoroids), and Ob-MA-T (M1+Ob-MA +Tumoroids) were normalized to their respective control (M0+Nw-PA, M1+Ob-PA, M0+Nw-MA, M1+Ob-MA) (red line) to follow the impact of DCIS-like tumoroids on each group. LIF, leukemia inhibitory factor; FAP, fibroblast activation protein; SMA-α, smooth muscle actin. **(D–F)** Impact of the Nw-TME and Ob-TME on macrophage polarization. THP-1 monocytes were activated into M0 and polarized into M1-like macrophages. **(D)** The quantification of each type of macrophages was measured by flow cytometry: Quantification of positive CD14+CD80- and CD80+ macrophage percentage is shown as bar graphs. Macrophages of adipose tissue co-cultured with adipocytes without cancer are used as control Nw-PA-M0 (M0 +Nw-PA), Ob-PA-M1 (M1+Ob-PA), Nw-MA-M0 (M0+Nw-MA), Ob-MA (M1+Ob-MA).The gene expression of **(E)** proinflammatory (*IL-1β, IL-6, IL-8, TNFα*) and **(F)** anti-inflammatory (*TGF-β, IL-10, CD163*) cytokines was measured by qRT-PCR. β-actin was used as control. The four conditions Nw-PA-T (M0 +Nw-PA+Tumoroids), Ob-PA-T (M1+Ob-PA+Tumoroids), Nw-MA-T (M0+Nw-MA+Tumoroids), and Ob-MA-T (M1+Ob-MA +Tumoroids) were normalized to their respective control (M0+Nw-PA, M1+Ob-PA, M0+Nw-MA, M1+Ob-MA) (red line) to follow the impact of DCIS-like tumoroids on each group. All data represent the means of 3-6 replicates ± SEM. *$p<0.05$, **$p \leq 0.01$ ***$p \leq 0.001$ represent significant differences compared with the control and # represents a significant difference between normal-weight and obese condition. nd, not determined.

AP2 reinforces and maintains the pre-adipocyte phenotype. As a result, the adipocytes may maintain a more undifferentiated or less specialized state associated with decreased adiponectin levels.

Next, considering the importance of adipokines in obesity and related metabolic syndromes, the gene expression of *Adiponectin, HSL* (hormone-sensitive lipase), and *Leptin* was evaluated. The *Adiponectin* gene expression was significantly downregulated in all tumor microenvironments (TME), including Nw-MA-T (RQ=0.06, $p \leq 0.001$), Ob-PA-T (RQ=0.03, $p \leq 0.001$), and Ob-MA-T (RQ=0.14, $p \leq 0.001$), and undetermined in Nw-PA-T. On the other hand, the gene expressions of *HSL* and *Leptin* were significantly increased, exhibiting the most potent effect within the two TMEs (Ob-PA-T and Ob-MA-T) associated with obesity.

3.2.1.2 DCIS-like tumoroids may enhance CAF-like phenotypes and affect inflammatory cytokine expression

Following exposure to DCIS-like tumoroids, Nw adipose cells (PAs and MAs) might exhibit an iCAF phenotype with highly increased levels of *LIF* (Nw-PA-T: RQ=2.5, $p \leq 0.001$; NwMA: RQ=1.8, $p \leq 0.05$) (Figure 3B) and inflammatory cytokines (Figure 3C). However, following exposure to DCIS-like tumoroids, Ob-PA and Ob-MA expressed higher levels of all studied myoCAF genes (Figure 3B): *FAP* (Ob-PA-T: RQ=2.69, $p \leq 0.001$; Ob-MA: RQ=1.7, $p \leq 0.05$) and *α-SMA* (Ob-PA: RQ=2.54, $p \leq 0.001$; Ob-MA: RQ=1.7, $p \leq 0.05$). These iCAF-like phenotypes were positively correlated with a high increase in expression of *TNF-α, IL-1β, IL-8*, and *CXCL-10* whereas myoCAF-like phenotypes were positively correlated with a high increase in gene levels of *IL-6*, and high decrease in *TNF-α*. These changes lead adipocytes to produce pro-inflammatory cytokines. So, adipose cells associated with tumors from Nw individuals could adopt a cancer-educated inflammatory phenotype, whereas obesity mainly leads to the development of a myofibroblastic cancer-associated phenotype.

3.2.2 DCIS-like tumoroids affected inflammatory cytokine expression and macrophage polarization

To determine the polarization state of macrophages (whether they were in an unpolarized M0 state or polarized into M1 or M2 phenotypes), we employed flow cytometry to analyze their specific

CD markers. Then, we were able to quantitatively measure the percentage of each macrophage subtype (M0 and M1) relative to the control employing specific surface antibody labeling. The $CD14^+CD80^-$cell population can include both M0 and M2 macrophage subtypes. CD14 is a surface marker that is expressed on monocytes and macrophages (THP1/M0/M1/M2) and CD80 is expressed on pro-inflammatory M1-like macrophages. Similar to previous results, within the Nw-TME, $CD14^+CD80^-$ cell percentage significantly decreased to 64% in Nw-PA-T ($p \leq 0.01$), while $CD80^+$ M1 percentage increased to 20% in Nw-PA-T ($p \leq 0.001$) and 13% in Nw-MA-T ($p \leq 0.05$) comparing to control (NwPA+M0 -and Nw-MA+M0) (Figure 3D). The inflammatory state activated by adipocytes resembling to iCAF-like phenotype led to the polarization of macrophages into pro-inflammatory M1-like macrophages with high expression of pro-inflammatory cytokines (Figure 3E). However, DCIS-like tumoroids reduced the $CD80^+$ M1 percentage within the obese TME: from 95% to 34.36% (Ob-PA-T, $p \leq 0.01$) and from 89.9% to 39.7% (Ob-MA-T, $p \leq 0.01$), while it increased the $CD14^+$&$CD80^-$ cell percentage from 9% to 20% (Ob-PA-T, $p \leq 0.001$) and from 21.16% to 45% (Ob-MA-T, $p \leq 0.001$), comparing to control (Ob-PA+M1, Ob-MA+M1) (Figure 3F). This increased percentage of $CD14^+CD80^-$ can be explained by the polarization of macrophages to the M2 phenotype that highly expressed the CD163 receptors may be due to the secretion of adipocytes having myoCAF-like phenotype and cancer promoter microenvironment.

3.3 Reciprocal interactions between adipose microenvironment and DCIS-like tumoroid through cytokine secretions

The reciprocal cell interactions in the co-culture 3D model were assessed on cytokine secretions by collecting conditioned media. As there was no contact between the different cell types in the experiment, the crosstalk was exclusively mediated by soluble factors. We used the conditions without tumoroids as controls and then we compared the variation between the normal weight and obese microenvironments (Figure 4).

3.3.1 Pre-adipospheroids altered their cytokine secretions upon co-culture with DCIS-like tumoroids

Within both Nw-TME and Ob-TME, DCIS-like tumoroids significantly upregulated the production of IL-8, a pro-tumorigenic cytokine that stimulates migration and invasion to promote invasion and metastasis but downregulated the production of IL-17A, MIP-1α, leptin, and adiponectin (Figure 4A). In Nw-PA-T, tumoroids significantly increased the secretion of proinflammatory cytokines such as IL-1β, TNF-α, and IL-2 contrary to the Ob-PA-T. Ob-PA-T increased the production of IL-6 and IL-23 and decreased the production of certain pro-inflammatory cytokines such as TNF-α and IFN-γ, followed by the decrease of IL-2, IL-12, and IL-1β. There was no significant variation between Nw-PA-T and Ob-PA-T concerning the secretion of adiponectin, IL-17A, leptin, IL-8, IL-12, and IL-23, but there were significant variations in the other remaining cytokines between these 2 microenvironments. Therefore, we need to monitor more specifically the global interactions of these 12 cytokines as a function of the different microenvironments using PCA analysis (Figure 4B). In this analysis, we performed a two-dimensional PCA using appropriate statistical techniques and tools. We explored the relationship between the cytokines (89.7% of the total variable) and evaluated the ensemble (Dim1:68.1%; Dim2: 21.6%). Consistent with the previous results in Figure 4A, we found that inflammatory cytokines such as MIP-1α, TNF-α, IFN-γ, and leptin are the most dominant cytokines associated with inflammatory microenvironment with PA (Ob-PA+M1). Once this microenvironment was co-cultured with cancer, we found that the overall profile of these cytokines varied in the opposite direction to dimension 1 and approached the variables of dimension 2. This can be explained by the decrease in concentrations of inflammatory cytokines (Dim1, MIP-1α, TNF-α, IFN-γ, and leptin) and the increase in concentrations of IL-8, IL-6, and IL-23 (Dim 2).

3.3.2 Adipospheroids altered their cytokine secretions upon co-culture with DCIS-like tumoroids

In both Nw-TME and Ob-TME, DCIS-like tumoroids significantly downregulated the production of adiponectin and MIP-1α, two anti-tumor cytokines, and decreased the secretion of pro-inflammatory cytokines such as TNF-α (Figure 4A). Within Nw-MA-T, tumoroids significantly decreased TNF-α production and increased the level of pro-inflammatory cytokines, notably IL-2, IL-23, IL-6, and IL-8. However, within Ob-MA-T, a strong reduction of pro-inflammatory cytokines such as TNF-α and IL-1β followed by decreases in IFN-γ, IL-2, IL-12, and IL-6 were noted. There was no significant variation between Nw-TME and Ob-TME regarding the levels of adiponectin, IL-17A, leptin, IL12, MIP-1α, and TNF-α, but there was significant variation in the rest of the cytokines between these 2 microenvironments. To link the global interactions of these 12 cytokines more specifically to the different microenvironments, a PCA analysis was carried out (Figure 4C) to explore the relationship between the cytokines (84.2% of total variable) and evaluate the whole (Dim1:62.1%; Dim2: 22.6%). Consistent with the previous results, we found that anti-inflammatory cytokines such as adiponectin were the most dominant cytokine in the Nw-TME (Nw-MA+M0). In addition, we noted that in the presence of cancer, the microenvironment (Nw-MA+M0+Tumoroids *vs* Nw-MA+M0) shifted in the opposite direction to dim 2 with significant decreases in adiponectin levels and increases in IL-8, IL-23, and leptin secretion.

4 Discussion

Using a 3D co-culture model between bi-fluorescent DCIS-like tumoroids (constituted by cancer and myoepithelial cells), adipose cells, and macrophages, the influence of the inflammatory adipose microenvironment found in the obese patient was investigated on DCIS progression. The reciprocal interactions between adipose

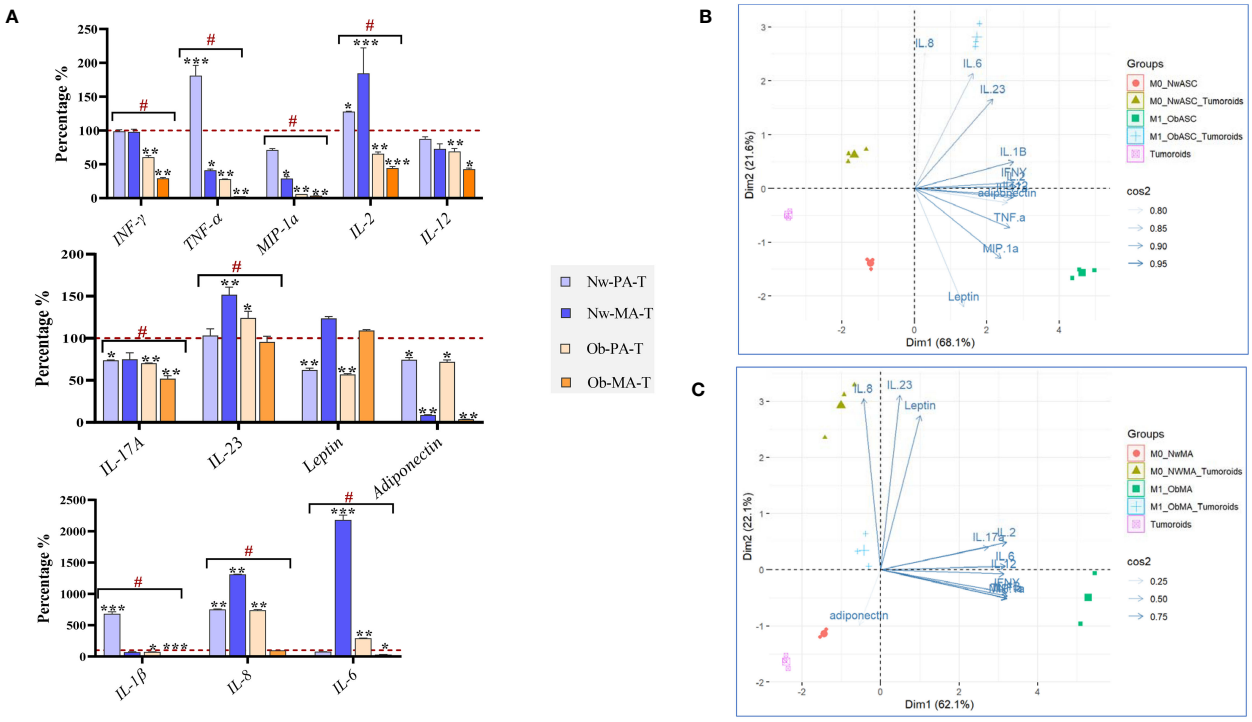

FIGURE 4
Evaluation of cytokine production in the 3D co-culture model. DCIS-like tumoroids were co-cultured with pre-adipospheroids (Nw-PA, Ob-PA) or adipospheroids (Nw-MA, Ob-MA) and with macrophages (M0 or M1). **(A)** Measurement of 12 pro-inflammatory cytokines levels (pg/µL) using Procarta-Plex™ Immunoassays was realized for each experimental condition. The percentages compared to the controls were calculated and presented as follows ± SEM. We used the Nw microenvironent (Nw-PA+M0) and the obese microenvironent (Ob-PA+M1) as controls for the normal weight and obese conditions respectively. Then we compared the variation between Nw and obese TME. All data represent the means of 3 replicates ± SEM *p < 0.05, **p ≤ 0.01, ***p ≤ 0.001 represent significant differences compared with the control and **#** represents a significant difference between normal-weight and obese condition. **(B, C)** Individual Principal Component Analysis (PCA) was realized to follow the 12 cytokine interactions within all Nw/Ob preadipose tissue **(B)** and Nw/Ob mature adipose tissue **(C)**. Cos2 (cosine squared) measures the quality of the representation of the variables on the principal components. **(B)** 75% of the variance of IL-8, IL-23, leptin, IL-17a, IL-2, IL-6, IL-12, IFN-γ, MIP-1α is explained by the selected principal component and 25% of the variance of adiponectin is explained by the selected principal component. **(C)** The selected principal component explains 95% of the variance of IL-23, IL-1, IFN-γ, adiponectin, TNF-α, and MIP-1α, 90% of the variance of IL-6, and 85% of the variance of leptin.

tissue and DCIS were explored, including signaling pathways, phenotypic changes, and the effects of inflammation.

Our model revealed that obese conditions repress the expression of genes involved in apoptosis and promote genes involved in cell survival and inflammation. Indeed, Ob-PA-T and Ob-MA-T exhibited notable downregulation of apoptosis-related genes such as *BAX*, *BAG1*, and *CASP3*, surpassing the level observed in Nw-PA-T, with Nw-MA-T also showing decreased expression. A similar decrease in caspase gene expression (*CASP3, 8, 9*) was observed in both TMEs. This reduction reflects the suppression of TP53's antitumor activity with an increase in the level of tumor propagation, which is followed by a reduction in the expression of the pro-apoptotic proteins BAX and BAG1, preventing apoptosis and promoting cell survival (40). This observation suggests an activation of the apoptotic signaling pathway, leading to caspase activation and the promotion of programmed cell death. Concurrently, it indicates the stimulation of tumor progression through the inhibition of MEC proliferation.

In addition, MMP-9 produced by tumor cells drives malignant progression and metastasis (41) and high levels of inflammatory cytokines such as TNF-α, IL-1β, Il-6, and IL-8 present in CM can also significantly increase MMP-9 expression (42, 43). TIMP1 (Tissue Inhibitor of Metalloproteinase 1) and MMPs are both involved in the regulation of extracellular matrix (ECM) remodeling, TIMP1 specifically inhibits the activity of several MMPs, including MMP-1 and MMP-9. The significant decrease in TIMP1 expression in Nw and Ob-TME cancer cells may contribute to tumor progression and elevated production of MMP9, an inducible enzyme that may also play an important role in angiogenesis (44).

In various glandular tissues, including mammary glands, ECMs act as a barrier and defense against cancer cell invasion (45). They play a role in inhibiting cancer cell invasion and migration, and in maintaining normal tissue architecture. In particular, α-SMA plays an important role in maintaining the structural integrity and contractile properties of various glandular tissues, including mammary glands. Loss of α-SMA expression in ECM from DCIS tumors has been associated with an increased risk of tumor progression and invasion (12). In addition, E-cadherin (CDH1), a cell adhesion molecule essential for epithelial cell integrity and tissue organization, is expressed in MECs and facilitates cell-cell adhesion via calcium-dependent interactions. The absence of E-cadherin expression in

MECs cultured with all tumor microenvironment (TME) groups suggests a potential evolution towards a more migratory and invasive phenotype, disrupting the integrity of glandular tissue and allowing cancer cells to escape (46). Furthermore, the inflammatory and cancer-associated microenvironments induced in all studied groups may compromise ECM functionality, diminish their protective effects against cancer cells, and contribute to decreased viability and increased apoptotic pathways. These findings are consistent with previous research demonstrating a decreased MEC viability in inflammatory adipose microenvironments (11). Overall, our results suggest that obesity may promote the progression and invasiveness of ductal carcinoma *in situ* in the tumor microenvironment. Understanding these mechanisms could help identify factors contributing to DCIS development and facilitate the development of strategies to inhibit its invasion.

We showed that adipocytes significantly reduced their differentiation capacity under our experimental conditions, except Nw-MA-T, in agreement with a previous study reporting a reduced adipogenic differentiation capacity of ASCs from breast cancer TME (47). DCIS-like tumoroid can reduce adipocyte differentiation (PPAR-γ, AP2), decrease tumor-suppressor adipokine (adiponectin), and increase both adipocyte lipolysis (HSL) and tumor-enhancer adipokine (leptin) gene expression. Our results are consistent with a previous study that reported a similar reduction in the adipocyte differentiation capacity of ASCs in the context of invasive breast cancer (47). Overexpression of HSL, an enzyme (lipase E) involved in the degradation of stored triglycerides (lipolysis) in adipose tissue, in adipose cells (PA and MA) can indeed lead to increased lipolysis, which refers to the breakdown of stored lipids (fatty acids) in adipocytes. It has been suggested that tumor-induced factors or signals released by cancer cells may induce lipolysis in adipocytes (48, 49). This finding is in agreement with a previous study carried out on invasive ductal carcinoma (48, 49). Indeed, previous studies utilizing co-culture and 3D models have provided valuable insights into the metabolic interactions between adipocytes and cancer cells, specifically focusing on the transfer of lipids, particularly fatty acids (FFAs), from adipocytes to breast cancer cells (49). These studies have shown that under lean and obese conditions, breast cancer cells can efficiently capture FFAs released by adipocyte lipolysis by breaking down stored triglycerides. But this FFA transfer is enhanced under obese conditions, as obesity is associated with adipose tissue dysfunction, characterized by adipocyte hypertrophy, impaired adipokine secretion, and dysregulated lipid metabolism, which can increase FFA release and promote their uptake by cancer cells to provide an energy source supporting their growth and survival (50). The altered transcriptomic profiles observed in PAs within TME may indicate a potential dedifferentiation or reprogramming process, eventually leading to the development of a distinct subtype known as cancer-associated adipocytes (51). Finally, these findings underscored the critical role of cell interactions within TME highlighting how obesity-induced adipose tissue dysfunction can facilitate cancer progression.

On the other hand, tumor cells actively interact with adipose cells and manipulate them to create a supportive environment for tumor growth that may enhance CAF-like phenotypes and affect inflammatory cytokine expression (52). They may reprogram adipocyte phenotypes to cancer-associated fibroblast (CAF)-like and mesenchymal phenotype with proliferative capacity. CAFs are a heterogeneous population of fibroblasts that reside within the tumor stroma and play critical roles in tumor development and progression (53). Our findings revealed a strong correlation between iCAF-like phenotypes and increased expression of TNF-α, IL-1β, IL-8, and CXCL-10, while myoCAF-like phenotypes were associated with increased IL-6 levels and decreased TNF-α, suggesting distinct cytokine-driven pathways in adipocyte behavior (54). Particularly in Nw-PA-T conditions, adipocytes may adopt an iCAF-resembling phenotype, indicative of greater pro-inflammatory cytokine secretion, potentially contributing to an inflammatory microenvironment supporting cancer progression (55–57). Conversely, obesity-associated chronic inflammation likely promotes myoCAF-like phenotypes, emphasizing the significant impact of obesity on adipocyte dedifferentiation and tumor microenvironment dynamics (58). These results align with previous studies indicating a propensity for ASCs from obese patients to adopt myoCAF-like phenotypes upon exposure to low-malignant cancer cells (58). In addition, an ex-vivo correlation has been established, showing that breast cancer tissue sections from patients exhibit differential expression of the iCAF marker (LIF) (59–61), and the myoCAF marker (αSMA), depending on their obesity status (59, 62, 63). In Nw-MA, there may be a less pronounced but present iCAF phenotype, potentially correlating with elevated levels of immunomodulatory and inflammatory cytokines (57). Notably, tumoroids within the Nw-TME upregulate pro-inflammatory cytokines, suggesting a pro-inflammatory medium in this context. In contrast, adipocytes, macrophages, and cancer cells from the obese TME may exhibit dysfunctional behavior, possibly linked to myoCAF-like phenotypes (58). These myoCAFs can modulate immune cell activation and cytokine secretion, resulting in reduced pro-inflammatory cytokine levels and increased anti-inflammatory molecules such as IL-10, ultimately promoting an immunosuppressive environment (64). This dynamic interplay between obesity, inflammation, and tumor microenvironment highlights the multifaceted nature of adipocyte-macrophage interactions in cancer progression.

In obesity, macrophages tend to switch from an M2- to an M1-like phenotype, whereas in tumor progression, there's often a switch from M1 to M2 macrophages (65), which creates an immunosuppressive microenvironment favoring tumor growth (66). CD163-positive macrophages, characteristic of the M2 alternatively activated macrophages, are associated with immunosuppression and tumor progression (67). Our findings corroborate existing literature, showing that TME conditions, particularly influenced by obesity, express high levels of immunosuppressive factors like TGF-β, IL-10, and CD163 (68) (69). Furthermore, our study highlighted the complex interplay between tumor cells and macrophages, as evidenced by the polarization of M0 macrophages towards an inflammatory M1-like phenotype in Nw-MA-T conditions, while Ob-TME promoted an anti-inflammatory response and polarization towards M2-like macrophages (70). This modulation of macrophage polarization within the TME reflects the dynamic nature of tumor-immune interactions and underscores the potential mechanisms driving tumor progression and immunosuppression.

Within both Nw-TME and Ob-TME, DCIS-like tumoroids upregulated IL-8 production, a pro-tumorigenic cytokine

promoting migration and invasion (57, 71) while downregulating IL-17A, MIP-1α, leptin, and adiponectin. In Nw-PA-T, tumoroids notably increased the secretion of proinflammatory cytokines (IL-1β, TNF-α, and IL-2), capable of activating signaling pathways like STAT3, PI3K, and MAPK (72), and inducing EMT (73), unlike Ob-PA-T. This elevated proinflammatory cytokine secretion in Nw-PA-T, influenced by adipocytes resembling an iCAF-like phenotype and M1-like phenotypes, suggests a role in driving inflammation-associated tumor progression. Inflammatory cytokines TNF-α, IL-6, and IL-1β (57) may directly activate adipocyte signaling pathways, downregulating adiponectin and leptin production (74). Additionally, immunosuppressive factors from macrophages, like TGF-β and IL-10, inhibit IL-17A and MIP-1α production (69). IL-6 has been shown to trigger cancer cell proliferation by activating the JAK/STAT3, ERK1/2, and STAT3/NFκB pathways in breast cancer cells and can lead to increased levels of IL-23, which is a link between tumor-associated inflammation and tumor immune evasion and can also activate NF-κB signaling (75). Our findings underscore the importance of considering the intricate balance between M1 and M2 macrophages in the TME and suggest potential therapeutic strategies targeting macrophage polarization to disrupt tumor-promoting immunosuppressive mechanisms.

In addition, various immunosuppressive factors produced by macrophages, such as TGF-β and IL-10, can inhibit IL-17A and MIP-1α production. Leptin, as an obesity-associated hormone present in co-cultured CMs, can reduce TNF-α levels through positive feedback (74).

Our findings strongly indicate that obesity significantly influences the tumor microenvironment, potentially impacting the trajectory of breast cancer development. These insights could hold great significance for guiding future targeted therapies aimed at addressing the complex interplay between obesity, inflammation, and tumor progression.

5 Conclusion

In our present investigation, we have elucidated a substantial and reciprocal interplay between diverse constituents of the TME and DCIS-like tumoroids. Notably, the influence of TMEs derived from obese individuals exhibited a more pronounced impact compared to those from individuals with normal weight. Among the various TME components, Ob-PA-T demonstrated the most potent and predominant effect on reprogramming the entire TME, suggesting an increase in tumor progression and invasiveness. This intercellular communication can induce transcriptomic changes, reflecting alterations in gene expression patterns in adipose cells and macrophages, subsequently fueling the invasiveness of breast cancer cells and potentially disrupting the integrity of the MEC layer (Figure 5). Crucially, both Nw and Ob adipocytes changed their

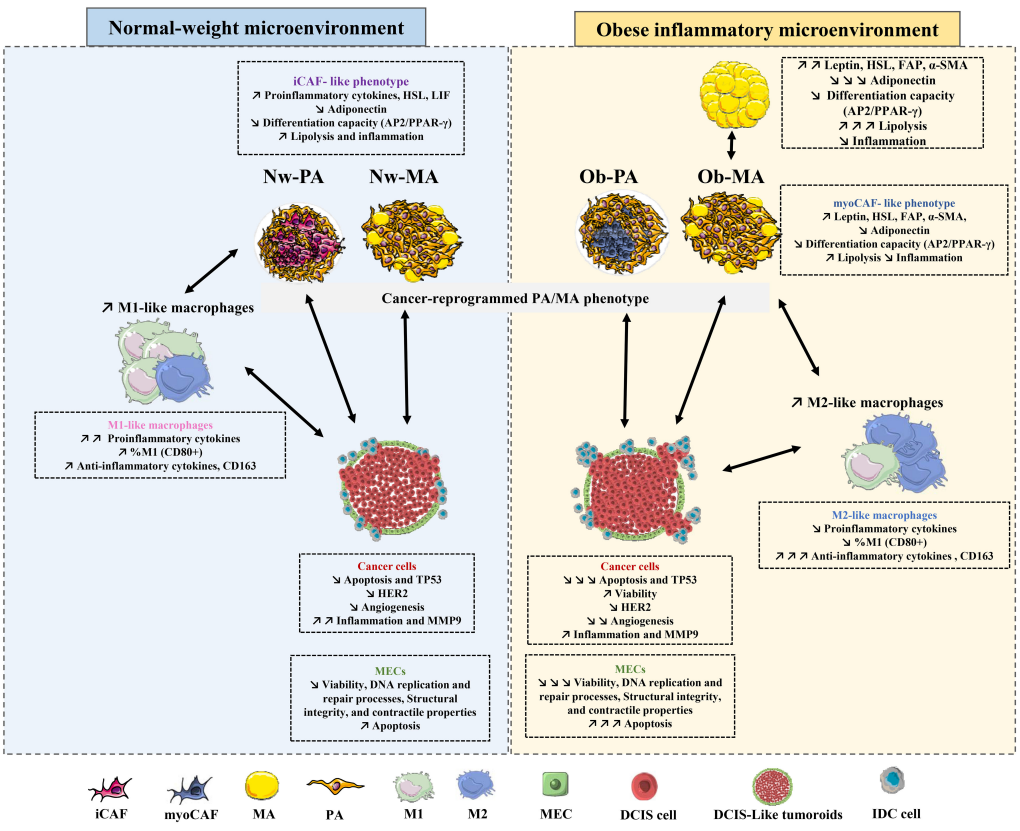

FIGURE 5
Graphical summary of the intercellular interactions between tumoroids, adipose cells, and macrophages.

transcriptome and may adopt distinct iCAF or myoCAF-like profiles, respectively, thereby influencing macrophage polarization and repolarization. These adipose-tissue-associated alterations released a variety of factors, including inflammatory cytokines, adipokines, and extracellular matrix components, capable of promoting cancer cell invasiveness and proliferation. These factors activated signaling pathways in cancer cells, which can lead to increased migratory and invasive capacities. Furthermore, they stimulated cell cycle progression and supported cell survival, contributing to increased proliferation and decreased apoptosis of cancer cells. Moreover, the factors derived from adipose tissue could disrupt the integrity of the MEC layer surrounding DCIS cells, altering cell adhesion, polarity, and signaling pathways. This disturbance in the MEC layer compromises its tumor suppressor function, as the intact MEC layer serves as a physical barrier inhibiting cancer cell invasion and dissemination.

Although existing evidence suggests a connection between adipose tissue and its impact on cancer progression and the MEC layer, further studies are warranted to validate these findings and provide a more comprehensive understanding of the underlying molecular mechanisms.

Data availability statement

The original contributions presented in the study are included in the article/Supplementary Material. Further inquiries can be directed to the corresponding author.

Ethics statement

The surgical residue was harvested following French regulations including a declaration to the Research Ministry (DC no.2008162) and procurement of written informed consent from the patients.

Author contributions

OH: Formal analysis, Investigation, Validation, Writing – original draft, Writing – review & editing. RN: Formal analysis, Investigation, Writing – review & editing. NG-M: Formal analysis, Methodology, Writing – review & editing. GC: Formal analysis, Methodology, Writing – review & editing. CB: Formal analysis, Methodology, Writing – review & editing. JA: Writing – review & editing, Formal analysis, Methodology. CD: Project administration, Writing – review & editing. CA: Project administration, Writing – review & editing. MD-A: Project administration, Writing – review & editing. FC-C: Conceptualization, Formal analysis, Funding acquisition, Investigation, Project administration, Validation, Writing – original draft, Writing – review & editing. LD: Conceptualization, Formal analysis, Funding acquisition, Investigation, Methodology, Project administration, Validation, Writing – original draft, Writing – review & editing.

Funding

The author(s) declare financial support was received for the research, authorship, and/or publication of this article. This work was supported by the National Research Institute for Agriculture, Food and the Environment and by the Ligue contre le cancer-Association de lutte contre le cancer. (Comités du Puy-de-Dôme et de l'Allier).

Acknowledgments

We would also like to thank the “Plate-forme CMF du service d’Hématologie biologique du CHU de Clermont-Ferrand” and the “Service de Biochimie et Génétique Moleculaire du CHU Clermont-Ferrand ».

Conflict of interest

The authors declare that the research was conducted in the absence of any commercial or financial relationships that could be construed as a potential conflict of interest.

Publisher’s note

Supplementary material

The Supplementary Material for this article can be found online at: https://www.frontiersin.org/articles/10.3389/fimmu.2024.1384354/full#supplementary-material

References

1. Sinn H-P, Kreipe H. A brief overview of the WHO classification of breast tumors, 4th edition, focusing on issues and updates from the 3rd edition. *Breast Care Basel Switz.* (2013) 8:149–54. doi: 10.1159/000350774

2. Casasent AK, Almekinders MM, Mulder C, Bhattacharjee P, Collyar D, Thompson AM, et al. Learning to distinguish progressive and non-progressive ductal carcinoma *in situ*. *Nat Rev Cancer.* (2022) 22:663–78. doi: 10.1038/s41568-022-00512-y

3. Cowell CF, Weigelt B, Sakr RA, Ng CK, Hicks J, King TA, et al. Progression from ductal carcinoma *in situ* to invasive breast cancer: revisited. *Mol Oncol*. (2013) 7:859–69. doi: 10.1016/j.molonc.2013.07.005

4. Sanders ME, Schuyler PA, Simpson JF, Page DL, Dupont WD. Continued observation of the natural history of low-grade ductal carcinoma *in situ* reaffirms proclivity for local recurrence even after more than 30 years of follow-up. *Mod Pathol*. (2015) 28:662–9. doi: 10.1038/modpathol.2014.141

5. Siegel RL, Miller KD, Fuchs HE, Jemal A. Cancer statistics, 2021. *CA Cancer J Clin*. (2021) 71:7–33. doi: 10.3322/caac.21654

6. Habanjar O, Maurin AC, Vituret C, Vachias C, Longechamp L, Garnier C, et al. A bicellular fluorescent ductal carcinoma *in situ*-like Tumoroid to study the progression of carcinoma: practical Approaches and Optimization. *Biomater Sci*. (2023) 3308–20. doi: 10.1039/D2BM01470J

7. Allred DC. Ductal carcinoma *in situ*: terminology, classification, and natural history. *J Natl Cancer Inst Monogr*. (2010) 2010:134–8. doi: 10.1093/jncimonographs/lgq035

8. Melchor L, Molyneux G, Mackay A, Magnay FA, Atienza M, Kendrick H, et al. Identification of cellular and genetic drivers of breast cancer heterogeneity in genetically engineered mouse tumour models. *J Pathol*. (2014) 233:124–37. doi: 10.1002/path.4345

9. Nguyen M, Lee MC, Wang JL, Tomlinson JS, Shao ZM, Alpaugh ML, et al. The human myoepithelial cell displays a multifaceted anti-angiogenic phenotype. *Oncogene*. (2000) 19:3449–59. doi: 10.1038/sj.onc.1203677

10. Sternlich MD, Safarians S, Rivera SP, Barsky SH. Characterizations of the extracellular matrix and proteinase inhibitor content of human myoepithelial tumors. *Lab Investig J Tech Methods Pathol*. (1996) 74:781–96.

11. Delort L, Cholet J, Decombat C, Vermerie M, Dumontet C, Castelli FA, et al. The adipose microenvironment dysregulates the mammary myoepithelial cells and could participate to the progression of breast cancer. *Front Cell Dev Biol*. (2021) 8:571948. doi: 10.3389/fcell.2020.571948

12. Sirka OK, Shamir ER, Ewald AJ. Myoepithelial cells are a dynamic barrier to epithelial dissemination. *J Cell Biol*. (2018) 217:3368–81. doi: 10.1083/jcb.201802144

13. Lo P-K, Zhang Y, Yao Y, Wolfson B, Yu J, Han SY, et al. Tumor-associated myoepithelial cells promote the invasive progression of ductal carcinoma *in situ* through activation of TGFβ signaling. *J Biol Chem*. (2017) 292:11466–84. doi: 10.1074/jbc.M117.775080

14. Hennighausen L, Robinson GW. Information networks in the mammary gland. *Nat Rev Mol Cell Biol*. (2005) 6:715–25. doi: 10.1038/nrm1714

15. Wang Y-Y, Lehuédé C, Laurent V, Dirat B, Dauvillier S, Bochet L, et al. Adipose tissue and breast epithelial cells: a dangerous dynamic duo in breast cancer. *Cancer Lett*. (2012) 324:142–51. doi: 10.1016/j.canlet.2012.05.019

16. Lengyel E, Makowski L, DiGiovanni J, Kolonin MG. Cancer as a matter of fat: the crosstalk between adipose tissue and tumors. *Trends Cancer*. (2018) 4:374–84. doi: 10.1016/j.trecan.2018.03.004

17. Rajala MW, Scherer PE. Minireview: the adipocyte—At the crossroads of energy homeostasis, inflammation, and atherosclerosis. *Endocrinology*. (2003) 144:3765–73. doi: 10.1210/en.2003-0580

18. Zhang K, Yang X, Zhao Q, Li Z, Fu F, Zhang H, et al. Molecular mechanism of stem cell differentiation into adipocytes and adipocyte differentiation of Malignant tumor. *Stem Cells Int*. (2020) 2020:1–16. doi: 10.1155/2020/8892300

19. Arimochi H, Sasaki Y, Kitamura A, Yasutomo K. Differentiation of preadipocytes and mature adipocytes requires PSMB8. *Sci Rep*. (2016) 6:26791. doi: 10.1038/srep26791

20. Rosen ED, MacDougald OA. Adipocyte differentiation from the inside out. *Nat Rev Mol Cell Biol*. (2006) 7:885–96. doi: 10.1038/nrm2066

21. Dirat B, Bochet L, Dabek M, Daviaud D, Dauvillier S, Majed B, et al. Cancer-associated adipocytes exhibit an activated phenotype and contribute to breast cancer invasion. *Cancer Res*. (2011) 71:2455–65. doi: 10.1158/0008-5472.CAN-10-3323

22. Schäfer M, Werner S. Cancer as an overhealing wound: an old hypothesis revisited. *Nat Rev Mol Cell Biol*. (2008) 9:628–38. doi: 10.1038/nrm2455

23. Bochet L, Lehuédé C, Dauvillier S, Wang YY, Dirat B, Laurent V, et al. Adipocyte-derived fibroblasts promote tumor progression and contribute to the desmoplastic reaction in breast cancer. *Cancer Res*. (2013) 73:5657–68. doi: 10.1158/0008-5472.CAN-13-0530

24. Habanjar O, Diab-Assaf M, Caldefie-Chezet F, Delort L. The impact of obesity, adipose tissue, and tumor microenvironment on macrophage polarization and metastasis. *Biology*. (2022) 11:339. doi: 10.3390/biology11020339

25. Lumeng CN, DelProposto JB, Westcott DJ, Saltiel AR. Phenotypic switching of adipose tissue macrophages with obesity is generated by spatiotemporal differences in macrophage subtypes. *Diabetes*. (2008) 57:3239–46. doi: 10.2337/db08-0872

26. Castoldi A, Naffah de Souza C, Câmara NOS, Moraes-Vieira PM. The macrophage switch in obesity development. *Front Immunol*. (2016) 6:637. doi: 10.3389/fimmu.2015.00637

27. Ruggiero AD, Key C-CC, Kavanagh K. Adipose tissue macrophage polarization in healthy and unhealthy obesity. *Front Nutr*. (2021) 8:625331. doi: 10.3389/fnut.2021.625331

28. Sung H, Siegel RL, Torre LA, Pearson-Stuttard J, Islami F, Fedewa SA, et al. Global patterns in excess body weight and the associated cancer burden. *CA Cancer J Clin*. (2019) 9(2):88–112. doi: 10.3322/caac.21499

29. Picon-Ruiz M, Morata-Tarifa C, Valle-Goffin JJ, Friedman ER, Slingerland JM. Obesity and adverse breast cancer risk and outcome: mechanistic insights and strategies for intervention: Breast Cancer, Inflammation, and Obesity. *CA Cancer J Clin*. (2017) 67:378–97. doi: 10.3322/caac.21405

30. Pettersson A, Graff RE, Ursin G, Santos Silva ID, McCormack V, Baglietto L, et al. Mammographic density phenotypes and risk of breast cancer: a meta-analysis. *J Natl Cancer Inst*. (2014) 106(5):dju078. doi: 10.1093/jnci/dju078

31. Olefsky JM, Glass CK. Macrophages, inflammation, and insulin resistance. *Annu Rev Physiol*. (2010) 72:219–46. doi: 10.1146/annurev-physiol-021909-135846

32. Boyd NF, Martin LJ, Sun L, Guo H, Chiarelli A, Hislop G, et al. Body size, mammographic density, and breast cancer risk. *Cancer Epidemiol biomark Prev Publ Am Assoc Cancer Res Cosponsored Am Soc Prev Oncol*. (2006) 15:2086–92. doi: 10.1158/1055-9965.bEPI-06-0345

33. Quail DF, Dannenberg AJ. The obese adipose tissue microenvironment in cancer development and progression. *Nat Rev Endocrinol*. (2019) 15:139–54. doi: 10.1038/s41574-018-0126-x

34. Laforest S, Ennour-Idrissi K, Ouellette G, Gauthier MF, Michaud A, Durocher F, et al. Associations between markers of mammary adipose tissue dysfunction and breast cancer prognostic factors. *Int J Obes*. (2021) 45:195–205. doi: 10.1038/s41366-020-00676-3

35. Spalding KL, Arner E, Westermark PO, Bernard S, Buchholz BA, Bergmann O, et al. Dynamics of fat cell turnover in humans. *Nature*. (2008) 453:783–7. doi: 10.1038/nature06902

36. Larsson SC, Mantzoros CS, Wolk A. Diabetes mellitus and risk of breast cancer: a meta-analysis. *Int J Cancer*. (2007) 121:856–62. doi: 10.1002/ijc.22717

37. Bougaret L, Delort L, Billard H, Lequeux C, Goncalves-Mendes N, Mojallal A, et al. Supernatants of adipocytes from obese versus normal weight women and breast cancer cells: *in vitro* impact on angiogenesis. *J Cell Physiol*. (2017) 232:1808–16. doi: 10.1002/jcp.25701

38. Nehme R, Chervet A, Decombat C, Longechamp L, Rossary A, Boutin R, et al. Aspalathus linearis (Rooibos) targets adipocytes and obesity-associated inflammation. *Nutrients*. (2023) 15:1751. doi: 10.3390/nu15071751

39. Habanjar O, Diab-Assaf M, Caldefie-Chezet F, Delort L. 3D cell culture systems: tumor application, advantages, and disadvantages. *Int J Mol Sci*. (2021) 22:12200. doi: 10.3390/ijms222212200

40. Goyal A, Wang Y, Graham MM, Doseff AI, Bhatt NY, Marsh CB. Monocyte survival factors induce akt activation and suppress caspase-3. *Am J Respir Cell Mol Biol*. (2002) 26:224–30. doi: 10.1165/ajrcmb.26.2.4640

41. Mehner C, Hockla A, Miller E, Ran S, Radisky DC, Radisky ES. Tumor cell-produced matrix metalloproteinase 9 (MMP-9) drives Malignant progression and metastasis of basal-like triple negative breast cancer. *Oncotarget*. (2014) 5:2736–49. doi: 10.18632/oncotarget.v5i9

42. Sun W, Liu DB, Li WW, Zhang LL, Long GX, Wang JF, et al. Interleukin-6 promotes the migration and invasion of nasopharyngeal carcinoma cell lines and upregulates the expression of MMP-2 and MMP-9. *Int J Oncol*. (2014) 44:1551–60. doi: 10.3892/ijo.2014.2323

43. Roomi MW, Kalinovsky T, Rath M, Niedzwiecki A. Modulation of MMP-2 and MMP-9 secretion by cytokines, inducers and inhibitors in human glioblastoma T-98G cells. *Oncol Rep*. (2017) 37:1907–13. doi: 10.3892/or.2017.5391

44. Arkell J, Jackson CJ. Constitutive secretion of MMP9 by early-passage cultured human endothelial cells. *Cell Biochem Funct*. (2003) 21:381–6. doi: 10.1002/cbf.1037

45. Pandey PR. Role of myoepithelial cells in breast tumor progression. *Front Biosci*. (2010) 15:226. doi: 10.2741/3617

46. Techasen A, Loilome W, Namwat N, Khuntikeo N, Puapairoj A, Jearanaikoon P, et al. Loss of E-cadherin promotes migration and invasion of cholangiocarcinoma cells and serves as a potential marker of metastasis. *Tumor Biol*. (2014) 35:8645–52. doi: 10.1007/s13277-014-2087-6

47. Rey F, Lesma E, Massihnia D, Ciusani E, Nava S, Vasco C, et al. Adipose-derived stem cells from fat tissue of breast cancer microenvironment present altered adipogenic differentiation capabilities. *Stem Cells Int*. (2019) 2019:1–15. doi: 10.1155/2019/1480314

48. Balaban S, Shearer RF, Lee LS, van Geldermalsen M, Schreuder M, Shtein HC, et al. Adipocyte lipolysis links obesity to breast cancer growth: adipocyte-derived fatty acids drive breast cancer cell proliferation and migration. *Cancer Metab*. (2017) 5:1. doi: 10.1186/s40170-016-0163-7

49. Rebeaud M, Bouche C, Dauvillier S, Attané C, Arellano C, Vaysse C, et al. A novel 3D culture model for human primary mammary adipocytes to study their metabolic crosstalk with breast cancer in lean and obese conditions. *Sci Rep*. (2023) 13:4707. doi: 10.1038/s41598-023-31673-x

50. Bezaire V, Mairal A, Ribet C, Lefort C, Girousse A, Jocken J, et al. Contribution of adipose triglyceride lipase and hormone-sensitive lipase to lipolysis in hMADS adipocytes. *J Biol Chem*. (2009) 284:18282–91. doi: 10.1074/jbc.M109.008631

51. Corrêa LH, Corrêa R, Farinasso CM, De Sant'Ana Dourado LP, Magalhães KG. Adipocytes and macrophages interplay in the orchestration of tumor microenvironment: new implications in cancer progression. *Front Immunol*. (2017) 8:1129. doi: 10.3389/fimmu.2017.01129

52. Anderson NM, Simon MC. The tumor microenvironment. *Curr Biol*. (2020) 30: R921–5. doi: 10.1016/j.cub.2020.06.081

53. Liu T, Han C, Wang S, Fang P, Ma Z, Xu L, et al. Cancer-associated fibroblasts: an emerging target of anti-cancer immunotherapy. *J Hematol Oncol.J Hematol Oncol*. (2019) 12:86. doi: 10.1186/s13045-019-0770-1

54. Howe LR, Subbaramaiah K, Hudis CA, Dannenberg AJ. Molecular pathways: adipose inflammation as a mediator of obesity-associated cancer. *Clin Cancer Res*. (2013) 19:6074–83. doi: 10.1158/1078-0432.CCR-12-2603

55. Monteran L, Erez N. The dark side of fibroblasts: cancer-associated fibroblasts as mediators of immunosuppression in the tumor microenvironment. *Front Immunol*. (2019) 10:1835. doi: 10.3389/fimmu.2019.01835

56. Nurmik M, Ullmann P, Rodriguez F, Haan S, Letellier E. In search of definitions: Cancer-associated fibroblasts and their markers. *Int J Cancer*. (2020) 146:895–905. doi: 10.1002/ijc.32193

57. Ritter A, Kreis NN, Roth S, Friemel A, Safdar BK, Hoock SC, et al. Cancer-educated mammary adipose tissue-derived stromal/stem cells in obesity and breast cancer: spatial regulation and function. *J Exp Clin Cancer Res*. (2023) 42:35. doi: 10.1186/s13046-022-02592-y

58. Strong AL, Pei DT, Hurst CG, Gimble JM, Burow ME, Bunnell BA. Obesity enhances the conversion of adipose-derived stromal/stem cells into carcinoma-associated fibroblast leading to cancer cell proliferation and progression to an invasive phenotype. *Stem Cells Int*. (2017) 2017:1–11. doi: 10.1155/2017/9216502

59. Muchlińska A, Nagel A, Popęda M, Szade J, Niemira M, Zieliński J, et al. Alpha-smooth muscle actin-positive cancer-associated fibroblasts secreting osteopontin promote growth of luminal breast cancer. *Cell Mol Biol Lett*. (2022) 27:45. doi: 10.1186/s11658-022-00351-7

60. Viswanadhapalli S, Dileep KV, Zhang KYJ, Nair HB, Vadlamudi RK. Targeting LIF/LIFR signaling in cancer. *Genes Dis*. (2022) 9:973–80. doi: 10.1016/j.gendis.2021.04.003

61. Ghanei Z, Mehri N, Jamshidizad A, Joupari MD, Shamsara M. Immunization against leukemia inhibitory factor and its receptor suppresses tumor formation of breast cancer initiating cells in BALB/c mouse. *Sci Rep*. (2020) 10:11465. doi: 10.1038/s41598-020-68158-0

62. Vathiotis IA, Moutafi MK, Divakar P, Aung TN, Qing T, Fernandez A, et al. Alpha-smooth muscle actin expression in the stroma predicts resistance to trastuzumab in patients with early-stage HER2-positive breast cancer. *Clin Cancer Res*. (2021) 27:6156–63. doi: 10.1158/1078-0432.CCR-21-2103

63. Kim S, You D, Jeong Y, Yu J, Kim SW, Nam SJ, et al. TP53 upregulates α–smooth muscle actin expression in tamoxifen–resistant breast cancer cells. *Oncol Rep*. (2019) 41:1075–82. doi: 10.3892/or.2018.6910

64. Kak G, Raza M, Tiwari BK. Interferon-gamma (IFN-γ): Exploring its implications in infectious diseases. *Biomol Concepts*. (2018) 9:64–79. doi: 10.1515/bmc-2018-0007

65. Galdiero MR, Garlanda C, Jaillon S, Marone G, Mantovani A. Tumor associated macrophages and neutrophils in tumor progression. *J Cell Physiol*. (2013) 228:1404–12. doi: 10.1002/jcp.24260

66. Suganami T, Ogawa Y. Adipose tissue macrophages: their role in adipose tissue remodeling. *J Leukoc Biol*. (2010), 33–9. doi: 10.1189/jlb.0210072

67. Skytthe MK, Graversen JH, Moestrup SK. Targeting of CD163+ Macrophages in inflammatory and Malignant diseases. *Int J Mol Sci*. (2020) 21:5497. doi: 10.3390/ijms21155497

68. Da Silva TA, Zorzetto-Fernandes ALV, Cecílio NT, Sardinha-Silva A, Fernandes FF, Roque-Barreira MC. CD14 is critical for TLR2-mediated M1 macrophage activation triggered by N-glycan recognition. *Sci Rep*. (2017) 7:7083. doi: 10.1038/s41598-017-07397-0

69. Komai T, Inoue M, Okamura T, Morita K, Iwasaki Y, Sumitomo S, et al. Transforming growth factor-β and interleukin-10 synergistically regulate humoral immunity via modulating metabolic signals. *Front Immunol*. (2018) 9:1364. doi: 10.3389/fimmu.2018.01364

70. Kwon H, Pessin JE. Adipokines mediate inflammation and insulin resistance. *Front Endocrinol*. (2013) 4:71. doi: 10.3389/fendo.2013.00071

71. Morein D, Erlichman N, Ben-Baruch A. Beyond cell motility: the expanding roles of chemokines and their receptors in Malignancy. *Front Immunol*. (2020), 952. doi: 10.3389/fimmu.2020.00952

72. Chen W, Qin Y, Liu S. Cytokines, breast cancer stem cells (BCSCs) and chemoresistance. *Clin Transl Med*. (2018) 7. doi: 10.1186/s40169-018-0205-6

73. Rogic A, Pant I, Grumolato L, Fernandez-Rodriguez R, Edwards A, Das S, et al. High endogenous CCL2 expression promotes the aggressive phenotype of human inflammatory breast cancer. *Nat Commun*. (2021) 12:6889. doi: 10.1038/s41467-021-27108-8

74. Ouchi N, Walsh K. Adiponectin as an anti-inflammatory factor. *Clin Chim Acta*. (2007) 380:24–30. doi: 10.1016/j.cca.2007.01.026

75. Habanjar O, Bingula R, Decombat C, Diab-Assaf M, Caldefie-Chezet F, Delort L. Crosstalk of inflammatory cytokines within the breast tumor microenvironment. *Int J Mol Sci*. (2023) 24:4002. doi: 10.3390/ijms24044002

10.3389/fimmu.2024.1384354

Glossary

ADF	adipocyte-derived fibroblast
AP2	adipocyte protein 2
ASC	adipose stem cell
BMI	body mass index
CAF	cancer-associated fibroblasts
CASP	caspase
CDH1	E-cadherin
CM	conditioned media
CXCL	C-X-C motif ligand
DCIS	ductal carcinoma *in situ*
EGFP	enhanced green fluorescent protein
EMT	epithelial-to-mesenchymal transition
ER	estrogen receptor
FAP	fibroblast activation protein
FFA	free fatty acid
HIF-1α	hypoxia-inducible factor-1α
GFP	green fluorescent protein
HR	hormone receptor
HSL	hormone-sensitive lipase
IDC	invasive ductal carcinoma
iCAF	inflammatory cancer-associated fibroblast
IFN-γ	interferon-γ
IL	interleukin
LIF	leukemia inhibitory factor
LPS	lipopolysaccharides
MA	mature adipocyte
MEC	myoepithelial cell
MMP	matrix metallopeptidase
MSC	mesenchymal stem cells
myoCAF	cancer-associated myofibroblasts
NF-κB	nuclear factor kappa-light-chain-enhancer of activated B cells
Nw-ASC	hASC from normal-weight women
PA	Pre-adipocyte
Nw-PA-T	normal-weight tumor microenvironment with Nw-PA
Nw-MA	MA from normal-weight women
Nw-MA-T	normal-weight tumor microenvironment with Nw-MA
Nw-TME	standard adipose tumor microenvironment found in normal-weight individuals
Ob-ASC	ASC from obese women
Ob-PA-T	obese inflammatory adipose tumor microenvironment with Ob-PA
Ob-MA	MA from obese women
Ob-MA-T	obese inflammatory adipose tumor microenvironment with Ob-MA
Ob-TME	inflammatory adipose tumor microenvironment found in obese people
PPAR-γ	peroxisome proliferator-activated receptor gamma
RFP	red fluorescent protein
SMA-α	smooth muscle actin
TAM	tumor-associated macrophage
TGF-β	transforming growth factor-β
TME	tumor microenvironment
TNFα	tumor necrosis factor-α
VEGF	vascular endothelial growth factor

frontiers | Frontiers in Immunology

TYPE Original Research
PUBLISHED 19 July 2024
DOI 10.3389/fimmu.2024.1344954

OPEN ACCESS

EDITED BY
Yiju Wei,
Shandong First Medical University, China

REVIEWED BY
Song Xu,
Tianjin Medical University General Hospital, China
Mehak Gupta,
Vertex Pharmaceuticals, United States
Jaime Villegas,
Andres Bello University, Chile

*CORRESPONDENCE
Bing Guan
g_bguan@163.com

RECEIVED 27 November 2023
ACCEPTED 02 July 2024
PUBLISHED 19 July 2024

CITATION
Peng D, Liang M, Li L, Yang H, Fang D, Chen L and Guan B (2024) Circ_BBS9 as an early diagnostic biomarker for lung adenocarcinoma: direct interaction with IFIT3 in the modulation of tumor immune microenvironment.
Front. Immunol. 15:1344954.
doi: 10.3389/fimmu.2024.1344954

Circ_BBS9 as an early diagnostic biomarker for lung adenocarcinoma: direct interaction with IFIT3 in the modulation of tumor immune microenvironment

Daijun Peng[1], Mingyu Liang[2], Lingyu Li[1], Haisheng Yang[1], Di Fang[1], Lingling Chen[1] and Bing Guan[1]*

[1]Department of Pathology, Jinshan Branch of Shanghai Sixth People's Hospital, Shanghai, China, [2]Department of Automation, Shanghai Jiao Tong University, Shanghai, China

Background: Introduction: Circular RNAs (circRNAs) have been identified as significant contributors to the development and advancement of cancer. The objective of this study was to examine the expression and clinical implications of circRNA circ_BBS9 in lung adenocarcinoma (LUAD), as well as its potential modes of action.

Methods: The expression of Circ_BBS9 was examined in tissues and cell lines of LUAD through the utilization of microarray profiling, quantitative real-time polymerase chain reaction (qRT-PCR), and western blot analysis. In this study, we assessed the impact of circ_BBS9 on the proliferation of LUAD cells, as well as its influence on ferroptosis and tumor formation. To analyze these effects, we employed CCK-8 assays and ferroptosis assays. The identification of proteins that interact with Circ_BBS9 was achieved through the utilization of RNA pull-down and mass spectrometry techniques. A putative regulatory network comprising circ_BBS9, miR-7150, and IFIT3 was established using bioinformatics study. The investigation also encompassed the examination of the correlation between the expression of IFIT3 and the invasion of immune cells.

Results: Circ_BBS9 was significantly downregulated in LUAD tissues and cell lines. Low circ_BBS9 expression correlated with poor prognosis. Functional experiments showed that circ_BBS9 overexpression inhibited LUAD cell

Abbreviations: LUAD, Lung adenocarcinoma; CCK-8, Cell counting kit-8; NSCLC, Non-small cell lung cancer; RBPs, RNA-binding proteins; ROS, Reactive oxygen species; GPX4, Glutathione peroxidase 4; FTH1, Ferritin heavy chain 1; TME, The tumor microenvironment; TAMs, Tumor-associated macrophages; DCs, Dendritic cells; NK cells, Natural killer cells; MDSCs, Myeloid-derived suppressor cells; TGF-β, Transforming growth factor-beta; ROC, Receiver Operating Characteristic; TCGA, The Cancer Genome Atlas; GEO, Gene Expression Omnibus; DEGs, Different Expressed Genes; GO, Gene Ontology; KEGG, Kyoto Encyclopedia of Genes and Genomes; GSEA, Gene Ser Enrichment Analysis; FDR, False Discovery Rate; RT-PCR, Real Time Polymerase Chain Reaction; BP, Biological Process; CC, Cellular Components; MF, Molecular Functions; HPA, Human Protein Atlas; AUC, Area Under the Curve; OE, Overexpression; NC, Negative Control; MDA, Malondialdehyde; NS, No Significance.

proliferation and promoted ferroptosis *in vitro* and suppressed tumor growth *in vivo*. Mechanistically, circ_BBS9 was found to directly interact with IFIT3 and regulate its expression by acting as a sponge for miR-7150. Additionally, IFIT3 expression correlated positively with immune infiltration in LUAD.

Conclusion: Circ_BBS9 has been identified as a tumor suppressor in lung adenocarcinoma (LUAD) and holds promise as a diagnostic biomarker. The potential mechanism of action involves the modulation of ferroptosis and the immunological microenvironment through direct interaction with IFIT3 and competitive binding to miR-7150. The aforementioned findings offer new perspectives on the pathophysiology of LUAD and highlight circ_BBS9 as a potentially valuable target for therapeutic interventions.

KEYWORDS

circular ribonucleic acids (circRNAs), lung adenocarcinoma (LUAD), circ_BBS9, ferroptosis, IFIT3, immune microenvironment

Introduction

Lung cancer, being a prominent contributor to deaths due to cancer on a global scale (1), poses substantial challenges. Non-small cell lung cancer (NSCLC) comprises the majority, approximately 85%, of reported cases among the various histological types of lung cancer. Lung adenocarcinoma (LUAD), which is a specific subtype of non-small cell lung cancer (NSCLC), accounts for approximately 40% of all cases of lung cancer. The majority of LUAD cases arise from the glandular epithelium located in the peripheral regions of the lung (2). Despite significant advancements in contemporary technologies in the field of lung cancer treatment during the previous decade, there are still persistent challenges that hinder progress, as evidenced by the relatively low 5-year survival rate of approximately 10%-20% (2). In recent years, there have been notable developments in the field of medical treatments, specifically in targeted therapies like erlotinib, immunotherapy options such as pembrolizumab or nivolumab, and the utilization of combined surgical procedures (3, 4). However, the current limitations of conventional tumor markers, including their relatively lower specificity and sensitivity, contribute to the persistently low overall 5-year survival rate (OS) observed in late-stage LUAD patients (5, 6). Therefore, it is imperative to conduct comprehensive research on the tumorigenesis and progression mechanisms of LUAD in order to identify novel and more efficient diagnostic and therapeutic biomarkers that can improve the prognosis of patients with LUAD.

Circular RNAs (circRNAs) are a subclass of non-coding RNAs that are produced via back-splicing, an atypical splicing process (7). The 5' and 3' ends of linear mRNA are joined in this manner to create a circular structure. Circular RNAs are complex molecules that perform multiple functions, including post-transcriptional regulation and gene transcription regulation. Furthermore, they display a wide range of expression patterns that are specific to different tissues and developmental stages. They are associated with various normal and pathological conditions, particularly implicated in cancer pathogenesis. With the advancements in high-throughput RNA sequencing (RNA-seq) and bioinformatics, numerous functional circular RNAs have been discovered (8). Some functionally characterized circRNAs play critical roles in gene regulation through various mechanisms, such as acting as "sponges" for miRNAs, interacting with proteins, and regulating transcription and splicing. Circular RNAs (circRNAs) have been observed to engage in interactions with various RNA-binding proteins (RBPs), leading to the regulation of associated protein activity and the manifestation of a wide range of biological functions (9, 10).

In recent years, circRNAs have drawn substantial attention due to their prospective applications in cancer diagnosis, prevention, targeted therapy, and their role as dependable diagnostic and prognostic biomarkers. Numerous circRNAs manifest tumor-specific functionalities within cancers, playing a contributory role in modulating cancer progression and metastasis. Research suggests that the aberrant expression of circRNAs is intricately linked to various critical aspects, such as the activation of the PI3K/AKT signaling pathway, facilitation of cell cycle progression, promotion of metastasis, and modulation of anti-tumor immunity across diverse cancers, encompassing lung adenocarcinoma and others (11–14). These circular RNAs also actively contribute to the advancement and immune evasion strategies of various malignant tumors, including colorectal cancer, breast cancer, gastric cancer, hepatocellular carcinoma, among others (15–18). The dysregulated expression of circRNAs plays a pivotal role in the progression of cancer. The distinctive expression patterns of these circRNAs exhibit promising diagnostic potential and could emerge as viable targets for therapeutic interventions. Hence, a comprehensive

comprehension of the biological functions and roles of circRNAs in distinct cancer types, along with their influence on signaling pathways, holds immense significance for early cancer detection and precision-based therapies.

Iron-dependent cell death, termed ferroptosis, represents a distinct form of programmed cell death that is iron-reliant and exhibits notable disparities from apoptosis and autophagy (19). It hinges on iron-mediated oxidative injury, heightened accumulation of iron, generation of free radicals, and the supply and buildup of lipid peroxides in fatty acids (20). Various studies have implicated connections between ferroptosis and diverse conditions, encompassing cancer, neurological disorders, and infections (19, 21, 22). Its defining features encompass the accrual of reactive oxygen species (ROS) and the depletion of glutathione. In contrast to apoptosis, necrosis, and autophagy, ferroptosis presents marked distinctions in cellular structure and function. Its mechanism relies on iron-facilitated lipid peroxidation and is intricately governed by numerous cellular metabolic and signaling pathways (23). The principal mechanisms underlying ferroptosis revolve around the catalytic action of ferrous iron or lipoxygenases, leading to the peroxidation of highly abundant unsaturated fatty acids situated on the cellular membrane, ultimately instigating cell demise. Distinctive features characterizing ferroptosis encompass escalated lipid ROS levels, intracellular accumulation of ferrous iron ions, buildup of lipid peroxides, and the decreased expression of factors that inhibit ferroptosis, such as glutathione peroxidase 4 (GPX4) and ferritin heavy chain 1 (FTH1) (23). Downregulation of GPX4 expression stands as a pivotal factor in impeding ferroptosis, functioning by scavenging lipid ROS and thwarting GPX4-mediated cell demise. This factor exhibits a close association with tumor progression (24, 25). FTH1, an integral constituent of ferritin crucial for preserving intracellular iron equilibrium, serves to prevent adverse consequences arising from iron overload (26, 27). Consequently, inhibiting FTH1 might potentially contribute to the induction of ferroptosis.

It's noteworthy that the regulation of circRNAs is also linked to ferroptosis in the context of cancer progression, potentially opening new avenues for future cancer therapies (28). Although circRNAs play a critical regulatory role in tumor cell metabolism, their specific involvement in the atypical metabolism associated with tumor-induced ferroptosis remains incompletely understood. Advancing research in this domain holds the promise of unveiling the potential contribution of circRNAs to cancer therapy.

For a long time, chemotherapy, radiation therapy, and surgery have been the mainstays of cancer treatment, achieving significant progress. However, these traditional treatment methods exhibit notable limitations in patients with advanced or metastatic malignancies and often come with severe side effects. To confront these challenges, immunotherapy stands out as an immensely promising approach that is gradually gaining traction. It works by reinvigorating immune surveillance and promoting the immune system's clearance of tumors (29). The tumor microenvironment (TME) is defined as a complex, diverse multicellular environment crucial for tumor development, typically composed of various immune cells, including T and B lymphocytes, tumor-associated macrophages (TAMs), dendritic cells (DCs), natural killer cells (NK cells), neutrophils, and myeloid-derived suppressor cells (MDSCs) (29). Tumor-infiltrating T cells play a crucial role in molding a favorable TME. Nevertheless, regulatory T cells (Tregs) exert immune-suppressive functions by releasing factors like IL-10 and transforming growth factor-beta (TGF-β). These actions assist cancer cells in evading immune defenses (30). Within lung cancer, tumor cells additionally express immune-inhibitory factors such as IL-10 and TGF-β, thereby fostering the recruitment of regulatory T cells (Tregs) and MDSCs (31, 32). The immune microenvironment significantly influences the initiation, infiltration, and metastasis of tumors, exerting a pivotal impact on cancer diagnosis, prevention, and prognosis (33, 34).

With the rapid development of nanomedicine, various functional dendritic macromolecules and dendritic macromolecule-based nanohybrids have been explored in the treatment and diagnosis of cancer. Recently, they have shown great promise in cancer immunotherapy, providing more opportunities for efficient cancer immunotherapy (35). Studies have investigated the intrinsic immune-modulating effects of tumor-targeted nano adjuvants and their ability to simultaneously trigger the release of tumor antigens, thereby reversing immune suppression and achieving potent antitumor immunity, with significant application potential in breast cancer treatment (36). The emergence of these novel approaches in cancer therapeutics, immunotherapy presents a beacon of hope for patients grappling with lung adenocarcinoma, potentially extending their survival rates. Despite these significant advancements, cancer still finds ways to counteract any treatment strategy through dynamic evolution and developing mechanisms of drug resistance. The intricacies inherent in lung adenocarcinoma have led to a constrained scope of research findings, resulting in a dearth of standardized tools capable of effectively guiding clinical decisions in this complex domain. It is essential to further study and develop prognostic biomarkers for lung adenocarcinoma. Therefore, gaining a deeper understanding of the interactions between tumor cells and host immune cells within the tumor microenvironment will help us better comprehend how tumors evade attacks from the immune system, thereby driving the development of precision medicine and individualized combined immunotherapy.

Bioinformatics methodologies have notably contributed to our research endeavors. Through the exploration of immune-related genes, we've achieved a more profound comprehension of the intricate relationship and interaction pathways linking LUAD with the immune microenvironment. This holds promise for inspiring early diagnosis, improving prognosis, and developing new therapeutic targets (37). We performed microarray analyses on expression profile datasets pertaining to lung adenocarcinoma and circular RNA expressions. Via meticulous experimental validation, we successfully identified differentially expressed circular RNAs and delineated their potential roles in the pathogenesis of LUAD. In this study, we amalgamated diverse lung adenocarcinoma sample datasets at multiple levels, incorporating clinical data and database analyses. Leveraging several well-established bioinformatics analysis tools, we investigated the correlation between the expressions of circ_BBS9

and IFIT3 and their implications on prognosis. We identified that overexpression of circ_BBS9 inhibits lung adenocarcinoma cell proliferation and promotes ferroptosis of lung adenocarcinoma cells. Additionally, the protein IFIT3, which directly interacts with circ_BBS9, is involved in immune infiltration and participates in the formation of the immune microenvironment. We also established a potential transcriptional network involving "circ_BBS9"-"hsa-miR-7150"-"IFIT3," which might be involved in the pathogenesis of LUAD. Ultimately, our research uncovered the promising potential of circ_BBS9 as a groundbreaking biomarker for early diagnosis and treatment strategies. Furthermore, our identification of the direct interaction between circ_BBS9 and IFIT3 sheds light on their collective role in shaping the immune microenvironment within LUAD. These discoveries unveil novel molecular mechanisms and offer potential therapeutic targets, presenting extensive opportunities in advancing the diagnosis and treatment of LUAD.

Materials and methods

Clinical tissue collection

All validation samples were collected with the consent of the patients and obtained ethical approval from the Jinshan Branch of the Shanghai Sixth People's Hospital, China. All patients were diagnosed with LUAD based on their histological and pathological characteristics. Clinical samples included tumor tissues and adjacent non-tumor lung tissues. None of the patients had received any preoperative chemotherapy or radiation therapy. Excised tissues were stored at -80°C for long-term preservation.

Expression analysis

The data were sourced from The Cancer Genome Atlas (TCGA: https://cancergenome.nih.gov) and the Gene Expression Omnibus (GEO: https://www.ncbi.nlm.nih.gov/geo/) datasets (GSE101684, GSE112214, GSE101586, GSE116959, and GSE72094). Protein expression analysis was conducted using the Human Protein Atlas (https://www.proteinatlas.org) to assess the expression of circ_BBS9 and IFIT3 proteins in lung adenocarcinoma patients.

A comprehensive analysis of circ_BBS9 and IFIT3 expression necessitated the utilization of various resources, including Tumor Immune Estimation Resource (TIMER: https://cistrome.shinyapps.io/timer/) (38), Gene Expression Profiling Interactive Analysis (GEPIA: http://gepia.cancer-pku.cn/) (39), and UALCAN (http://ualcan.path.uab.edu/home) (40). The gene expression profile interaction analysis of BBS9 and IFIT3 in lung adenocarcinoma was performed using GEPIA (http://gepia.cancer-pku.cn/).

Analysis of differentially expressed genes

Different Expressed Genes (DEGs) data from 3 GEO databases (GSE101684, GSE112214, GSE101586) of LUAD was extracted and processed using Python package "pandas","scipy" and some other essential packages. Statistical analyses were also calculated with python ($|\log_2(FC)| > 1$, adj.P<0.05). Finally, the results were visualized with the ChiPlot tools.

Survival and prognostic analysis

The survival package and survminer package were employed to assess the correlation between expression levels and the survival rate associated with circ_BBS9 across various clinical features within the GEO dataset (GSE72094). The ROC package was utilized to construct the Receiver Operating Characteristic (ROC) curve for diagnostic purposes.

Enrichment analyses

To uncover potential mechanisms, we conducted Gene Ontology (GO) and Kyoto Encyclopedia of Genes and Genomes (KEGG) analyses with OmicShare tools (https://www.omicshare.com/tools). Genes associated with IFIT3 were collected using STRING (https://cn.string-db.org/) and GeneMania (https://genemania.org/).

Gene set enrichment analysis

We conducted Gene Set Enrichment Analysis (GSEA) employing OmicShare tools (https://www.omicshare.com/tools). Enrichment map analysis was subsequently applied to interpret the GSEA results. Significance was determined by a nominal p-value < 0.05, and a false discovery rate (FDR) q-value<0.25.

RNA extraction and real-time PCR

Total RNA from the cells was extracted using TRIzol™ (ThermoFisher, USA), followed by reverse transcription using the first-strand cDNA synthesis kit (TaKaRa, Japan). Subsequently, real-time polymerase chain reaction (RT-PCR) was conducted.

The primers are as follows:

has_circ_0049271 forward: 5`-AACTTCGCTGAGCAGATTGG-3`,

reverse: 5`-TAAGCAACACCACCACCTCT-3`;

has_circ_0004789 forward: 5`-CCATCAACCGCCTCAAAGAC-3`,

reverse: 5`-TTGCCCAGATCCATCAACCA-3`;

has_circ_0003162 forward: 5`-CTGTCTCAGGAACCTTGGG-3`,

reverse: 5`-CCACCAATCACGGGCTTTAA-3`;

has_circ_0061817 forward: 5`-CCTGTCCTCCTAAACCTCCA-3`,

reverse: 5`-TCTCGCTGACCAAGAACTGA-3`;

has_circ_0015278 forward: 5`-TACAACCCCAGAACCAACCA-3`,

reverse: 5`-AGAACACTGACCCCAACTCC-3`.

GAPDH was used as an internal control.

Cell culture

Lung normal epithelial cells (BEAS-2B) and lung cancer cell lines (A549, H1299) were obtained from ATCC (Manassas, USA). These cell lines were cultured in RPMI-1640 medium (Gibco, USA) supplemented with 10% fetal bovine serum (FBS, Biological Industries, Israel) and 1% penicillin-streptomycin solution (Solarbio, China). The cells were maintained in a humidified incubator at 37°C with 5% CO2.

Cell transfection

H1299

In this experiment, we used Lipofectamine™ 2000 transfection reagent to transfect hsa-circ-0003162-1 and NC into H1299 cells, as shown in Table 1. One day prior to transfection, cells were seeded into a 6-well plate at a density of 5 x 10^5 cells per well. After 24 hours, the cell confluency was observed to reach 80% to 90%, at which point hsa-circ-0003162-1 was transfected.

Medium Replacement: The original medium in each well was discarded and replaced with fresh medium. Transfection reagent and RNA were diluted with OPTI-MEM and incubated at room temperature for 5 minutes. The amount of transfection reagent and OPTI-MEM added per well is shown in Table 2. The 50 µL diluted interference fragments and 50 µL diluted transfection reagent were mixed well and incubated at room temperature for 15 minutes. The 100 µL incubated mixture was then added to the cell samples. After 6 hours, the medium was replaced with fresh medium.

A549

Using Lipofectamine™ 2000 transfection reagent, the circ-0003162 overexpression plasmid and empty vector were transfected into A549 cells. One day prior to transfection, cells were seeded into a 6-well plate at a density of 3 x 10^5 cells per well. After 24 hours, the cell confluency was observed to reach 80% to 90%, at which point the circ-0003162 plasmid was transfected.

Medium Replacement: The original medium in each well was discarded and replaced with fresh medium. The transfection reagent and plasmid were diluted with OPTI-MEM and incubated at room temperature for 5 minutes. The amount of transfection reagent and OPTI-MEM added per well is shown in Table 3. The 50 µL diluted plasmid and 50 µL diluted transfection reagent were mixed well and incubated at room temperature for 20 minutes. The 100 µL incubated mixture was then added to the cell samples. After 6 hours, the medium was replaced with fresh medium.

TABLE 1 The sequences of hsa-circ-0003162 and negative control.

	Sequence (5'to 3')
hsa-circ-0003162-1	GGUGUAAAAGUGUGAAAGATT UCUUUCACACUUUUACACCTT
Negative control	UUCUCCGAACGUGUCACGUTT ACGUGACACGUUCGGAGAATT

TABLE 2 Transfection reagent and OPTI-MEM added per well in H1299 cells.

	Reagent Dosage	OPTI-MEM
Lipofectamine™ 2000	20 µl	180 µl
hsa-circ-0003162-1	5 µl	45 µl
NC	5 µl	45 ul

TABLE 3 Transfection reagent and OPTI-MEM added per well in A549 cells.

	Reagent Dosage	OPTI-MEM
Lipofectamine™ 2000	10µl	90µl
pD circ–0003162	2ug	Up to 50µl
pD circ	2ug	Up to 50ul

Cell counting kit 8 assay

To assess cell viability, a Cell Counting Kit-8 (CCK-8) assay kit was employed following the manufacturer's instructions. Briefly, cells were seeded in 96-well plates at a density of 1000 cells per well, in culture medium containing 10% fetal bovine serum and penicillin-streptomycin (5000 U/mL), and were maintained at 37°C in a humidified atmosphere with 5% CO2. After 24 hours of incubation, 10 µL of CCK-8 reagent was added to each well of the 96-well plates and incubated for 2 hours at 37°C in a humidified atmosphere with 5% CO2. The absorbance of each well was measured at 450 nm using a microplate reader.

Immunofluorescence assays

Cells were seeded onto 24-well plates. After fixation (4% paraformaldehyde, 15 minutes at room temperature) and blocking (3% BSA, 30 minutes at room temperature), the primary antibody (1:250, Abcam, derived from rabbit) was incubated at 4°C overnight. Subsequently, the corresponding fluorescent secondary antibody (1:500, Abcam, derived from goat) was incubated for 1 hour at room temperature. Anti-fade 4`,6-diamidino-2-phenylindole (DAPI) was employed for cell nuclei labeling. Images were captured using a fluorescence microscope.

Measurement of ROS

Dihydroethidium (Beyotime, #S0063) was employed as a molecular probe for detecting ROS in red fluorescence. FerroOrange (DOJINDO, #F374) was quantified using a flow cytometer or visualized under a fluorescence microscope.

Measurement of MDA levels

To measure MDA levels, a lipid peroxidation assay kit was employed according to the manufacturer's instructions. Briefly, 1 × 10^6 cells were collected in 300 µL of MDA lysis buffer containing 3 µL of butylated hydroxytoluene (BHT, 100×, to reduce interfering lipid oxidation), and the samples were homogenized on ice. After centrifugation at 13,000 g for 10 minutes, the insoluble material was removed. Subsequently, 600 µ L of thiobarbituric acid (TBA) solution, which reacts with other compounds in the samples to produce colored products, was added to each experimental sample or vial containing a standard sample. The MDA-TBA adducts were allowed to form by incubating for 60 minutes at 95°C. After cooling to 25°C in an ice bath, 200 µ L of each reaction mixture was pipetted into a 96-well plate for colorimetric assays, and the absorbance was measured at 532 nm.

Fe^{2+} content measurement

Following cell treatment based on the grouping, the cells were washed twice with FBS-free DMEM. Subsequently, a working solution of Ferro Orange (1 µmol/L; excitation wavelength: 540 nm, emission wavelength: 580 nm; Dojindo, Kumamoto, Japan) was prepared using FBS-free DMEM as per the manufacturer's instructions. The solution was then incubated at 37°C in a 5% CO2 incubator for 30 minutes and finally photographed using a multifunctional microplate detection system (CYTATION5, BIOTEK, USA).

Protein extraction and western blot

Cells were collected, washed with ice-cold phosphate-buffered saline (PBS), and lysed for 30 minutes in RIPA buffer containing 50mM Tris/HCl (pH 7.5), 150mM NaCl, 1% NP40, 1% Triton X-100, 2.5mM sodium pyrophosphate, 1mM β-glycerophosphate, 1mM EDTA, 1mM Na3VO4, and 1µg/mL leupeptin. Cell lysates were then centrifuged at 14,000g for 10 minutes at 4°C, and the protein concentration was measured using the BCA Protein Assay kit (Pierce, Rockford, IL). Aliquots of lysates (twenty micrograms of protein) were boiled with sample loading buffer (Beyotime; P0015) for 5 minutes and resolved by sodium dodecyl sulfate-polyacrylamide gel electrophoresis (SDS-PAGE). After electrophoresis, proteins were electrophoretically transferred onto a polyvinylidene difluoride (PVDF; Roche) membrane using a Semi-Dry Electroblotter (Bio-Rad). Following transfer, the membrane was blocked for 2 hours at room temperature in phosphate-buffered saline (PBS) containing 5% (w/v) nonfat milk and 0.1% (v/v) Tween-20. The membranes were then incubated with primary antibodies against human GPX4 (1:5000, Abcam, USA), GAPDH (1:500, Proteintech, China), FTH1 (1:1000, Abcam, USA)and IFIT3 (1:2000, CST, USA)at 4°C overnight, followed by a 1-hour incubation at room temperature with horseradish peroxidase (HRP)-linked anti-rabbit secondary antibody (Proteintech, SA00001–2; 1:50000) or anti-mouse secondary antibody (Proteintech, SA00001–1; 1:100000). After four washes with PBS containing 0.1% (v/v) Tween-20, immunoreactive bands were visualized using Chemistar™ High-sig ECL Western Blotting Substrate (Tanon; 180–501).

Pull-down assay

A biotin-labeled oligonucleotide probe specific to circ_BBS9 was synthesized commercially (RiboBio, China). In brief, the biotin-labeled oligonucleotide probes were incubated with BeyoMag™ streptavidin magnetic beads (Beyotime; P2151) for 60 minutes at room temperature. Once bound to the streptavidin magnetic beads, the probe-beads were incubated with whole cell lysates overnight at 4°C. Following three washes with ice-cold PBS, miRNAs or proteins that were pulled down by the probe-coated beads were collected.

RNA immunoprecipitation assay

To perform the RNA immunoprecipitation (RIP) assay, cells were harvested and resuspended in 1 mL of lysis buffer containing a protease inhibitor cocktail and RNase inhibitor. After centrifugation at 13,000 rpm for 10 minutes at 4°C, the supernatant was incubated with 30-40 µL of Protein A-Sepharose beads (Genescript) and 2 µg of primary antibodies (Proteintech, derived from rabbit) for 4 hours at 4°C. Subsequently, the beads were washed with ice-cold 1×PBS. Following this, the beads were incubated with Proteinase K (Sigma) using Trizol reagent (Invitrogen Life Technologies), and the purified RNA was subjected to qRT-PCR analysis.

TF-miRNA-mRNA regulatory network

Transcription factors (TFs) targeting IFIT3 were predicted based on CHEA (https://maayanlab.cloud/Harmonizome/) and GRNdb (http://www.grndb.com/). miRNAs targeting IFIT3 were predicted based on three different databases: miRWalk (http://mirwalk.umm.uni-heidelberg.de/), TargetScan (https://www.targetscan.org/vert_80/), and mirDIP (http://ophid.utoronto.ca/mirDIP/). StarBase V2.0 (https://starbase.sysu.edu.cn/index.php) was used to predict miRNA expression levels, prognostic value, and interaction sites. The final results were visualized by initially employing the venn3 function in in matplotlib_venn in python for creating a Venn diagram. Subsequently, based on the diagram results, graphical adjustments were made using the 'pyplot' module from Matplotlib to generate a comprehensive visualization."

Immune infiltration analysis

The relationship between immune infiltration and IFIT3 was assessed using TIMER 2.0 (38) and TISIDB (41). In brief, TIMER 2.0 was employed to elucidate the association between GPER and tumor-infiltrating immune cells (TIICs). TISIDB elucidated the relationship between tumor-infiltrating lymphocyte (TIL) abundance and IFIT3 expression.

Statistical analysis of data

In this study, different statistical tests were employed for data analysis, depending on the data characteristics and comparison requirements:

(1). For the comparison of expression levels between two groups, an unpaired t-test was employed.

(2). When dealing with more than two groups, an initial Analysis of Variance (ANOVA) test was conducted to assess whether significant differences existed among all groups. Subsequently, based on the inter-group variations obtained through Tukey's multiple comparisons test, a secondary unpaired t-test was performed to ascertain significant differences between two groups, yielding the final statistical conclusions depicted in the figures.

(3). For survival curve statistical analysis, the Log-Rank (Mantel-Cox) method was used to compare two curves and evaluate statistical differences.

In this paper, significance levels (*, **, ***) are used to indicate p-values of less than 0.05, 0.01, and 0.001, respectively. Smaller p-values signify greater statistical significance in the differences between the compared data.

Results

Characteristics of differentially expressed CircRNAs in LUAD

To investigate the role of circRNAs in the progression of lung adenocarcinoma, we conducted a merged analysis using lung adenocarcinoma expression microarray datasets from the GEO database (GSE101684, GSE11221, GSE101586) (Figure 1A). We employed a heatmap (Figure 1B) and a volcano plot (Figure 1C) to screen for differentially expressed circRNAs. In this process, a total of 31 differentially expressed circRNAs were identified, with the noteworthy observation that these circRNAs primarily exhibited a downregulation trend. Subsequently, we excluded two upregulated circRNAs and focused on the remaining 29 differentially expressed downregulated circRNAs for further investigation.

Through the study of these differentially expressed circRNAs, we conducted Kyoto Encyclopedia of Genes and Genomes (KEGG) analysis (Figure 1D). The results revealed that the downregulated circRNAs play important roles in ubiquitin-mediated proteolysis, cytokine-cytokine receptor interaction, metabolism, and the regulation of various signaling pathways. Furthermore, Gene Ontology (GO) term analysis (Figure 1E) also disclosed that these circRNAs are associated with biological processes (BP) related to cell metabolism, bioregulation, and stimulus response, cellular components (CC) involving cellular anatomical entities and protein-containing complexes, and molecular functions encompassing binding and catalytic activity.

Further research included Gene Set Enrichment Analysis (GSEA). This analysis (Figure 1F) demonstrated significant enrichment of these circRNAs in cellular metabolism, cell cycle, proliferation, invasion, antigen response, inflammation, and various signaling pathways. These findings underscore the crucial role of these downregulated circRNAs in the progression of lung adenocarcinoma, potentially affecting cell functions and disease mechanisms through multiple pathways.

Expression and survival of circ_BBS9 in LUAD tissues

For an in-depth investigation, we selected five circRNAs (has_circ_0049271, has_circ_0004789, has_circ_0003162, has_circ_0061817, has_circ_0015278) with the greatest downregulation and that had not been previously reported in the field of lung adenocarcinoma for further study. We employed qRT-PCR to assess the expression levels of these five downregulated circRNAs in two human lung adenocarcinoma cell lines (A549 and H1299) and one human normal lung epithelial cell line (BEAS-2B) (Figure 2A). The results indicated that three circRNAs (has_circ_0004789, has_circ_0061817, has_circ_0003162) exhibited low expression in lung adenocarcinoma cell lines.

To further validate these results, we collected clinical samples from 15 patients diagnosed with lung adenocarcinoma, comprising both cancer tissues and adjacent normal tissues. We used qRT-PCR to measure the mRNA levels of these three circRNAs (has_circ_0004789, has_circ_0061817, has_circ_0003162) in the cancer tissues and adjacent normal tissues of three patients (Figure 2B). The results indicated that has_circ_0003162 had significantly lower expression in cancer tissues compared to adjacent normal tissues. Therefore, we selected has_circ_0003162 as the subject for further investigation. These series of experimental findings underscore the potential importance of has_circ_0003162 in lung adenocarcinoma and provide a foundation for further mechanistic research.

Has_circ_0003162, derived from the BBS9 gene on chromosome 7, was unambiguously identified as our screened circ_BBS9 through divergent primer amplification and Sanger sequencing (Figure 2C). To validate our findings, we verified the expression of circ_BBS9 in cancer tissues and adjacent tissues of 12 additional lung adenocarcinoma patients (Figure 2D). The results showed a significant reduction in the expression level of circ_BBS9 in lung adenocarcinoma tissues.

To further explore the relationship between circ_BBS9 and LUAD, we used UALCAN to analyze the expression of BBS9 in various tumors (Figure 2E). We compared the expression levels of BBS9 in tumor tissues and adjacent normal tissues, revealing differential expression of circ_BBS9 in various tumor tissues. Using data from the GEO database (GSE116959), we assessed the mRNA expression of BBS9 in LUAD tissues and non-tumor tissues (Figure 2F) and validated the protein-level expression of BBS9 in LUAD through the Human Protein Atlas (HPA) (Figure 2G). We found a consistent trend of downregulated BBS9 expression in LUAD, regardless of the different databases or methods used for analysis. Furthermore, in different tumor grades, the expression of BBS9 was significantly lower in G2 and G3 compared to G1 (Figure 2H), suggesting a correlation between BBS9 and tumor grading.

Subsequently, we analyzed the prognosis of 398 lung adenocarcinoma patients from the GEO database who expressed the BBS9 gene (Figure 2I). The results indicated that patients with high circ_BBS9 expression had a better survival prognosis. Through receiver operating characteristic (ROC) curve analysis (Figure 2J), we confirmed the diagnostic value of circ_BBS9 in LUAD, with an area under the curve (AUC) of 0.5693, suggesting a strong correlation between circ_BBS9 and the diagnosis of LUAD. In summary, circ_BBS9 may serve as a potential biomarker with significant clinical implications for the diagnosis and prognosis of LUAD.

Impact of circ_BBS9 on the proliferation of A549 and H1299 LUAD cells

In order to assess the functional significance of circ_BBS9, we conducted *in vitro* experiments using A549 and H1299 LUAD cells. Employing siRNA interference techniques, we successfully reduced the expression levels of circ_BBS9 in H1299 cells (Figure 3A). Cellular viability was examined through CCK-8 assays (Figure 3B), revealing a significant increase in cell proliferation in the si_circ_BBS9 group. Furthermore, immunofluorescence analysis of H1299 cells was performed to detect Ki67-positive cell nuclei (displayed as green fluorescence) (Figure 3C), and the results indicated a noteworthy elevation in the percentage of Ki67-positive cell nuclei in the si_circ_BBS9 group. This suggests that circ_BBS9 promotes the proliferation of LUAD cells.

Simultaneously, we employed the overexpression technique (OE-RNA) to overexpress circ_BBS9 in A549 cells, successfully elevating the expression levels of circ_BBS9 (Figure 3D). In the CCK-8 assay, the OE_circ_BBS9 group exhibited a noticeable decrease in cell proliferation (Figure 3E). Immunofluorescence analysis revealed a significant reduction in the percentage of Ki67-positive cell nuclei in the OE_circ_BBS9 group compared to the control group (Figure 3F). These findings indicate that OE_circ_BBS9 inhibits the proliferation of LUAD cells.

These results underscore the crucial regulatory role of circ_BBS9 in LUAD cells. Its downregulation enhances cell proliferation, while its overexpression suppresses cell proliferation, emphasizing the potential involvement of circ_BBS9 in the pathophysiological processes of LUAD.

The effect of circ_BBS9 on ferroptosis in A549 and H1299 LUAD cells

To further assess the impact of circ_BBS9 on LUAD progression, a series of experiments were conducted. Initially, we investigated whether known cell death inhibitors would affect the mode of cell death in OE_circ_BBS9 LUAD cells. Various cell death inhibitors, including the Ferroptosis inhibitor ferrostatin-1, apoptosis inhibitor Z-VAD-fmk, necroptosis inhibitor necrostatin-1 (Nec-1), and autophagy inhibitor 3-MA, were employed to determine the mode of cell death in OE_circ_BBS9 LUAD cells through CCK-8 assays (Figure 4A). We transfected the circ_BBS9 overexpression plasmid into A549 cells and observed that DMSO, VAD, Nec, and 3-MA significantly inhibited cell proliferation. However, the Ferrostatin-1 group did not impact the proliferation of LUAD cells. Thus, we ruled out other known modes of cell death and proceeded with investigating ferroptosis.

The process of ferroptosis is often accompanied by an increase in ROS. Therefore, we employed fluorescence probe-based detection to assess ROS expression and observe the occurrence of ferroptosis. The addition of the ferroptosis inducer erastin in H1299 cells led to an elevation in ROS. However, the introduction of erastin in the si_circ_BBS9 group resulted in reduced ROS expression (Figure 4B), indicating that si_circ_BBS9 inhibits ferroptosis in LUAD cells. In A549 cells, OE_circ_BBS9 caused an increase in ROS levels. When we added the ferroptosis inhibitor Fer-1 to the OE_circ_BBS9 group, it lowered the ROS expression induced by overexpression, thereby suppressing ferroptosis (Figure 4C). These results demonstrate that OE_circ_BBS9 promotes ferroptosis in LUAD cells.

Malondialdehyde (MDA) is a natural product of lipid oxidation in biological organisms. The measurement of MDA is widely used as an indicator of the extent of lipid oxidation, and it can be employed to assess the degree of lipid peroxidation. We observed an increase in MDA concentration after introducing the erastin in H1299 cells, while adding the erastin inducer to the si_circ_BBS9 group led to a decrease in MDA concentration (Figure 4D). This indicates that si_circ_BBS9 inhibits ferroptosis in LUAD cells. In A549 cells overexpressing OE_circ_BBS9, MDA concentration increased, but when we added the Fer-1 to the OE_circ_BBS9 group, MDA concentration decreased (Figure 4E). These results demonstrate that OE_circ_BBS9 promotes ferroptosis in LUAD cells.

Iron ions form complexes with proteins, and in acidic environments, iron dissociates from the complexes and is then reduced to ferrous iron. It eventually forms a purple-red compound with ferrozine, which can be quantified through colorimetry in the wavelength range of 540-580 nm. This method is used to measure iron ion concentration. In H1299 cells, the introduction of the erastin resulted in an increase in ferrous iron ion concentration, whereas adding the erastin inducer to the si_circ_BBS9 group led to a decrease in ferrous iron ion concentration (Figure 4F). This indicates that si_circ_BBS9 inhibits ferroptosis in LUAD cells. In A549 cells overexpressing OE_circ_BBS9, ferrous iron ion concentration increased, but when we added the Fer-1 to the OE_circ_BBS9 group, ferrous iron ion concentration decreased (Figure 4G). These results demonstrate that OE_circ_BBS9 promotes ferroptosis in LUAD cells.

Glutathione peroxidase 4 (GPX4) mitigates the toxicity of lipid peroxides through its catalytic activity, maintaining the stability of the lipid bilayer membrane, thereby inhibiting the occurrence of ferroptosis. Ferritin heavy chain 1 (FTH1) can disrupt autophagosomes, thus inhibiting ferroptosis. The expression of GPX4 and FTH1 was assessed through Western blot analysis. In H1299 cells, the introduction of the erastin led to decreased expression of GPX4 and FTH1, while adding the erastin inducer to the si_circ_BBS9 group resulted in increased expression of GPX4 and FTH1 (Figure 4H). These findings indicate that si_circ_BBS9 inhibits ferroptosis in LUAD cells. In A549 cells overexpressing

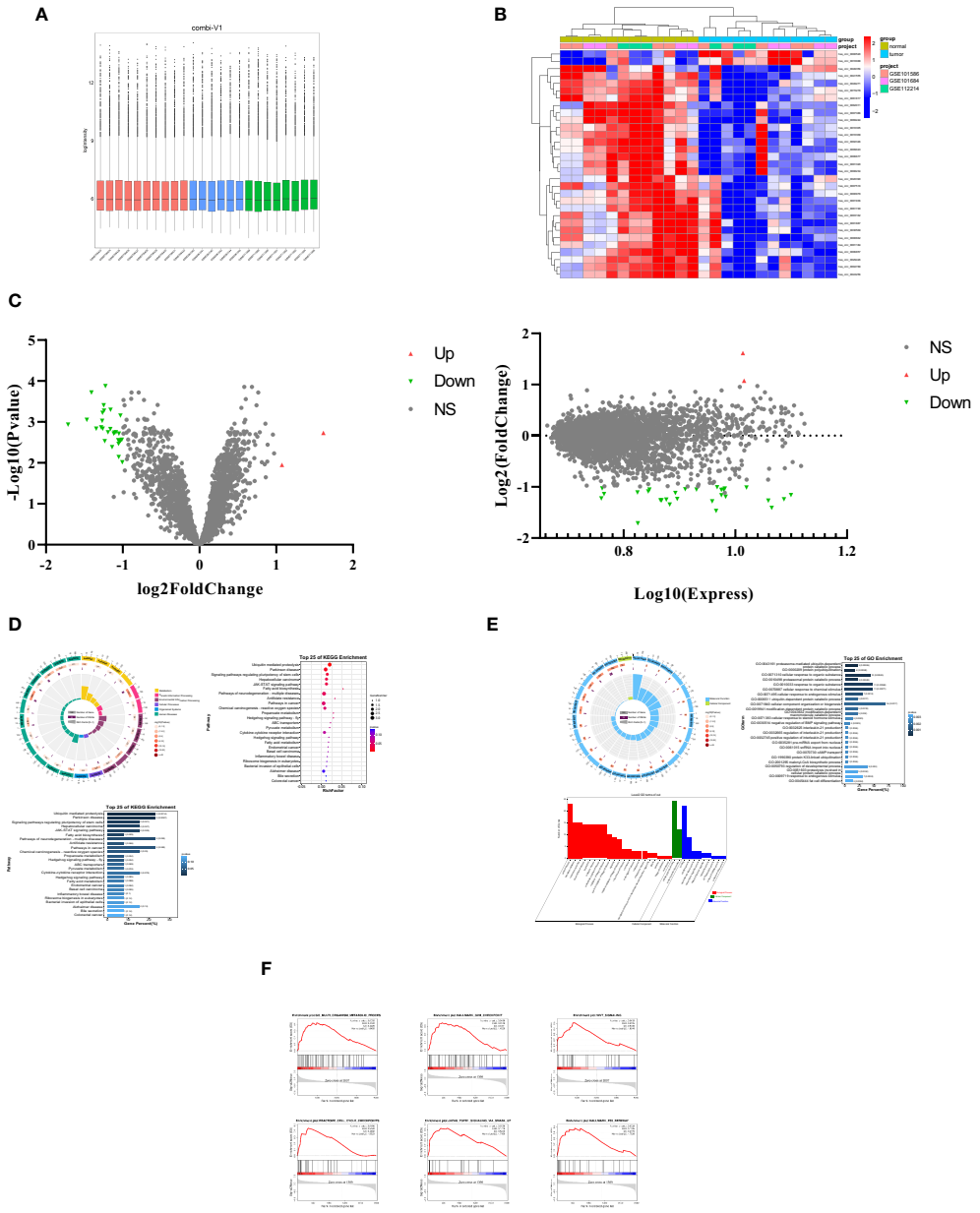

FIGURE 1
Characteristics of differentially expressed CircRNAs in LUAD. **(A)** The lung cancer expression microarray dataset from the GEO Database. **(B)** A cluster heap map presented the significantly dys regulated circRNAs in human LUAD tissues relative to adjacent normal tissues. The red and blue strips represent high and low expression, respectively. **(C)** Scatter plot and Volcano plot of differentially expressed circRNAs in LUAD and adjacent normal tissues. **(D)** Differential expression of circRNAs in KEGG pathway analysis results. **(E)** Differential expression of circRNAs in GO analysis results Results. **(F)** GSEA (Gene Set Enrichment Analysis) of differentially expressed circRNAs.

OE_circ_BBS9, the expression of GPX4 and FTH1 decreased, but when we added the Fer-1 to the OE_circ_BBS9 group, the expression of GPX4 and FTH1 increased (Figure 4I). These results demonstrate that OE_circ_BBS9 promotes ferroptosis in LUAD cells.

These experimental results underscore the role of circ_BBS9 in regulating the process of ferroptosis and its impact on lipid oxidation and iron ion homeostasis. This contributes to a deeper understanding of the biological mechanisms of circ_BBS9 in LUAD.

Circ_BBS9 interacts with IFIT3, mediating protein ubiquitination and subsequently affecting protein stability

To identify potential proteins that interact with circ_BBS9 in LUAD, we employed biotinylated circ_BBS9 probes for circ_RNA pull-down analysis, followed by silver staining SDS-PAGE analysis (Figure 5A). Bands of proteins that differed between the Control

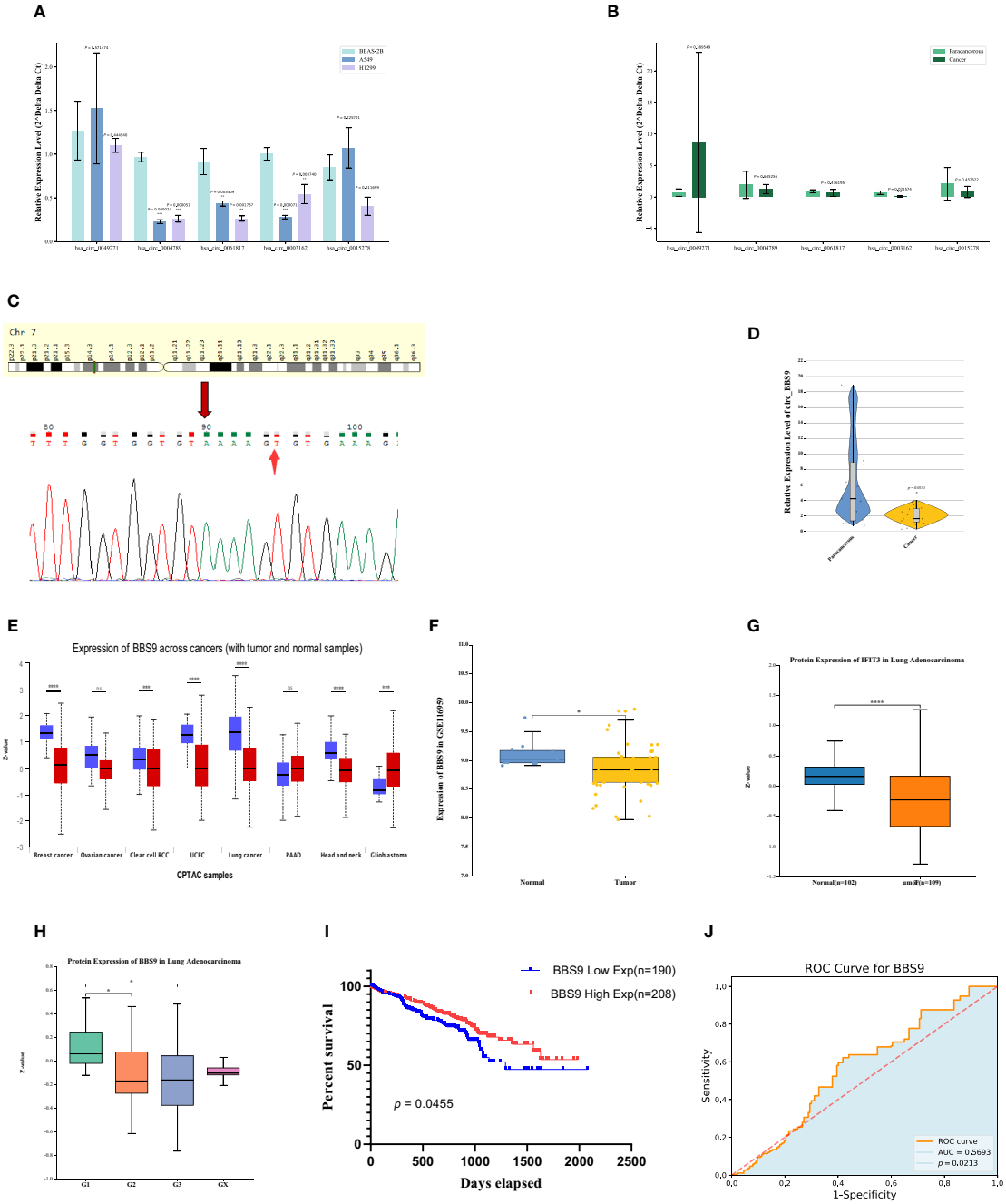

FIGURE 2
Expression and survival of Circ BBS9 in LUAD Tissues. **(A)** Expression of differentially downregulated circRNAs in A549, H1299, and (BEAS-2B) determined by qRT-PCR assays. **(B)** Expression of differentially downregulated circRNAs in clinical samples determined by qRT-PCR assays. **(C)** sequencing of PCR products revealing the circularization site of circRNA as indicated (Arrows) in the figure above. **(D)** Expression of circ BBS9 in 15 clinical samples as obtained by qRT PCR assays. **(E)** BBS9 expression in different cancer types analyzed by UALCAN. **(F)** In the GEO database, BBS9 exhibits lower mRNA expression levels in LUAD compared to normal tissues (p <0.05). **(G)** In the HAP database, the protein expression level of BBS9 is lower in LUAD compared to normal tissues (p < 0.001). **(H)** The expression of BBS9 in LUAD is correlated with Tumor Grade (p < 0.05). **(I)** Survival curves of overall survival in GSE72094 LUAD patients. **(J)** The predictive ability of variable BBS9 in LUAD.

and circ_BBS9 groups were excised and sent to the mass spectrometry platform for protein identification (Figure 5B).

Among the potential proteins interacting with circ_BBS9, circ_RNA pull-down and immunoprecipitation (IP) cell lysate silver staining experiments revealed a successful pull-down of circ_BBS9. Furthermore, these experiments demonstrated a robust binding between circ_BBS9 and IFIT3 protein within A549 cells (Figure 5A). Additionally, RNA immunoprecipitation (RIP-PCR) experiments showed the enrichment of circ_BBS9 within the IP-IFIT3 group, providing further support for the molecular interaction between circ_BBS9 and IFIT3 (Figure 5C). Moreover, Western blot (WB) analysis of the pulled-down proteins revealed a

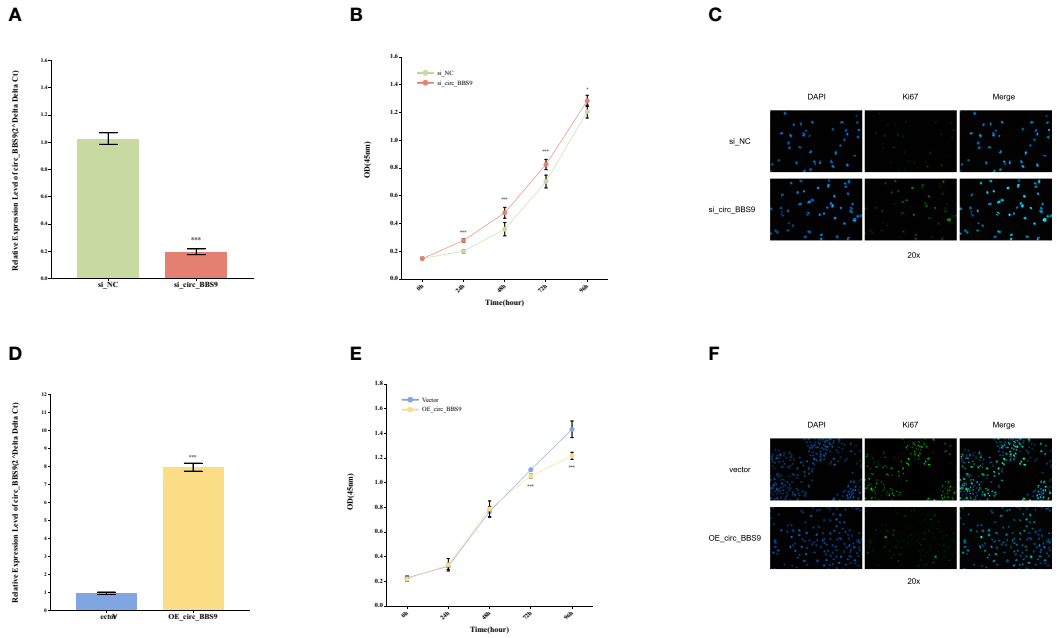

FIGURE 3
Impact of Circ_BBS9 on the Proliferation of A549 and H1299 LUAD Cells. **(A)** Comparison of circ_BBS9 expression levels between the negative control (NC) group and the si_circ_BBS9 group in H1299 cells using qRT-PCR. **(B)** Comparison of cell viability between the negative control (NC) group and si_circ_BBS9 group in H1299 cells using a CCK-8 assay. **(C)** Immunofluorescence detection of Ki67 cell proliferation in the negative control (NC) group and si_circ_BBS9 group in H1299 cells. **(D)** Comparison of circ_BBS9 expression levels between the Vector group and OE_circ_BBS9 group in A549 cells using qRT-PCR. **(E)** Comparison of cell viability between the Vector group and OE_circ_BBS9 group in A549 cells using CCK-8 assay. **(F)** Assessment of Ki67 cell proliferation in A549 cells for the Vector group and OE_circ_BBS9 group using immunofluorescence.

significant increase in IFIT3 protein levels in A549 cells with circ_BBS9 knockdown (Figure 5D).

In addition, we performed co-immunoprecipitation experiments with A549 cells using a ubiquitination antibody (Figure 5E) and assessed IFIT3 protein stability (Figure 5F). Consequently, we postulate that circ_BBS9 may stabilize the IFIT3 protein through direct interaction.

To further validate our findings, we utilized Gene Expression Profiling Interactive Analysis (GEPIA) to confirm this association. Our analysis revealed a positive correlation between BBS9 and IFIT3 in LUAD (Figure 5G). These results provide experimental evidence for the interaction between circ_BBS9 and IFIT3, emphasizing its potential significance in LUAD.

Construction of the upstream regulatory network of IFIT3

We utilized miRNA databases, mirDIP, and TargetScan resources to explore the upstream miRNA regulatory factors controlling IFIT3 (Figure 6A). Initially, through these databases, we obtained a set of predicted miRNAs, totaling 18. Subsequently, we conducted expression and survival analysis for these predicted miRNAs (Figures 6B, C) to further refine our selection. During the analysis, it became evident that only 9 of the miRNAs had available expression data. Therefore, we performed statistical analysis on the expression of these 9 miRNAs, with particular focus on hsa-miR-7150 and hsa-miR-487b-5p. We also conducted statistical analysis of their overall survival. The results indicated that hsa-miR-7150 was the most likely miRNA involved in the regulation of IFIT3.Furthermore, we provided the complementary sequences between IFIT3 and hsa-miR-7150 (Figure 6D), implying the potential existence of a miRNA-mRNA interaction between them.

Based on these findings, we constructed a molecular regulatory network in LUAD (Figure 6E), which includes circ_BBS9, hsa-miR-7150, and IFIT3. This network aids in gaining a better understanding of the regulatory mechanisms of IFIT3 and its role in LUAD.

The relationship between IFIT3 expression and the prognosis of LUAD

To establish the relationship between IFIT3 and LUAD, we conducted a series of data analyses. First, we used UALCAN to analyze the expression of IFIT3 in different tumors (Figure 7A). The results showed differential expression of IFIT3 in various tumor tissues. We analyzed data from the TCGA database (Figure 7B) and the GSE116959 GEO database (Figure 7C), assessing the mRNA expression levels of IFIT3 in LUAD tissue and non-tumor tissue, and validated the protein-level expression of IFIT3 in LUAD using the Human Protein Atlas (HPA) database (Figure 7D).

Through the analysis from these different databases and methods, we consistently observed significant downregulation of IFIT3 in LUAD tissues, indicating that IFIT3 expression in LUAD is negatively regulated. Furthermore, we found that the expression levels of IFIT3 increased with higher tumor grades (Figure 7E),

suggesting a correlation between IFIT3 and tumor grade, indicating its potential role in the development of LUAD.

These analytical results strengthen the association between the downregulation of IFIT3 expression and tumor progression in LUAD, providing important clues for further research into the function and potential role of IFIT3.

GO and KEGG analysis related to IFIT3

Through the Gene-Gene interaction network in GeneMania (Figure 8A) and the construction of a Protein-Protein Interaction (PPI) network using the STRING database (Figure 8B), we identified 20 genes associated with IFIT3. These 21 related genes

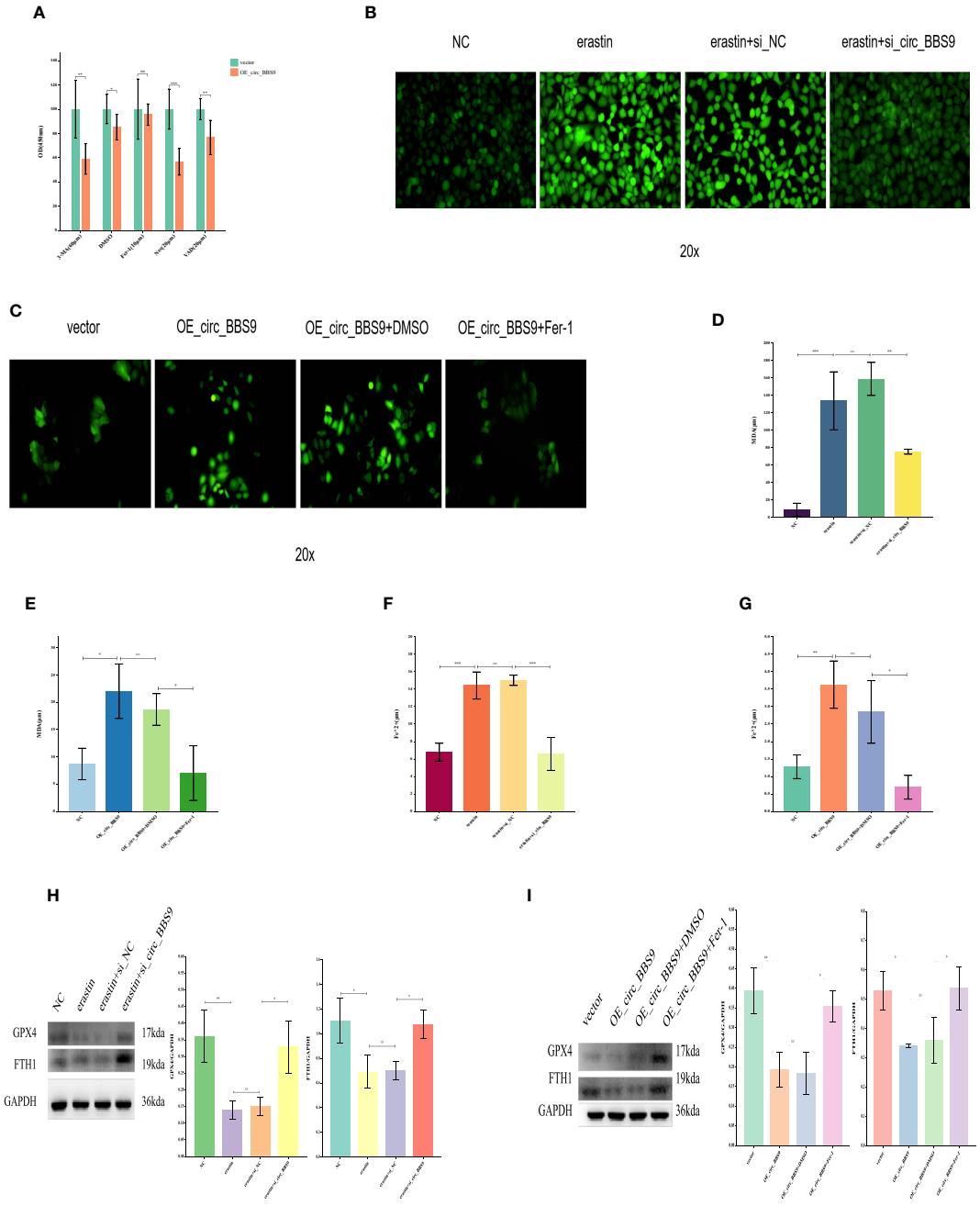

FIGURE 4
The Effect of Circ_BBS9 on Ferroptosis in A549 and H1299 LUAD Cells. **(A)** CCK-8 assay to determine the cell death mechanism in lung adenocarcinoma cells. **(B)** Detection of ROS in H1299 cells using a fluorescence probe. **(C)** Detection of ROS in A549 cells using a fluorescence probe. **(D)** Measurement of MDA content in H1299 cells using a colorimetric assay. **(E)** Measurement of MDA content in A549 cells using a colorimetric assay. **(F)** Measurement of iron ion concentration in H1299 cells using a colorimetric assay. **(G)** Measurement of iron ion concentration in A549 cells using a colorimetric assay. **(H)** Detection of ferroptosis inhibitor GPX4 and FTH1 expression in H1299 cells using Western Blot method. **(I)** Detection of ferroptosis inhibitor GPX4 and FTH1 expression in A549 cells using Western Blot method.

were utilized for performing GO and KEGG analysis (Figure 8C) to gain a deeper understanding of the biological functions and pathways associated with IFIT3.

In the analysis results, the top 25 KEGG pathways, cellular components (CC), biological processes (BP), and molecular functions (MF) were identified. These pathways include the JAK-STAT signaling pathway and cytokine signaling in the immune system. These findings provide valuable insights into the significant roles of IFIT3 and its related genes in cellular signal transduction and immune system functions. They contribute to a better understanding of their functions and regulatory mechanisms. These bioinformatics analyses offer a strong basis for further experimental research.

The research on the correlation between the expression of IFIT3 and immune infiltration

The preliminary investigation of IFIT3's involvement in immune infiltration was carried out using the TIMER database (Figure 9A). The results indicate that IFIT3 positively correlates with various immune cells, including neutrophils, CD8+ T cells, macrophages, dendritic cells, CD4+ T cells, suggesting that IFIT3 regulates the infiltration of different immune cells. Spearman correlation and p-values were used for this analysis. Further exploration of the correlation between IFIT3 expression and immune infiltration was conducted using the TISIDB (Figure 9B), showing positive correlations with various immune cells, including NKT cells, Th1 cells, Treg cells, CD56 cells, activated dendritic cells, macrophages, activated CD4 T cells, activated CD8 T cells, Th2 cells, and neutrophils. The expression of IFIT3 is associated with the regulation of immune infiltration-related immune factors, immune subtypes, and immune cells.

Additionally, the analysis was extended to investigate the correlation between IFIT3 expression and immune modulators (Figure 9C), immune stimulators (Figure 9E), chemokines (Figure 9G), and chemokine receptors (Figure 9I). The results revealed a positive correlation between IFIT3 expression and most immune modulators (Figure 9D). In LUAD, the top three positive correlations were observed with PDCD1LG2 (rho = 0.54, P < 2.2e-16), CD274 (rho = 0.523, P < 2.2e-16), and HAVCR2 (rho=0.519, P<2.2e-16). Similarly, a positive correlation was found between IFIT3 expression and most immune stimulators (Figure 9F), with the top three positive correlations in LUAD being CD80 (rho = 0.503, P < 2.2e-16), CD86 (rho = 0.498, P < 2.2e-16), and ICOS (rho=0.488, P<2.2e-16). Furthermore, a positive correlation was identified between IFIT3 expression and most chemokines (Figure 9H), with the top three positive correlations in LUAD being CXCL11 (rho=0.597, P<2.2-16), CXCL10 (rho=0.566, P<2.2-16), and CCL8 (rho=0.529, P<2.2-16). Finally, a positive correlation was observed between IFIT3 expression and most chemokine receptors (Figure 9J), with the top three positive correlations in LUAD being CCR5 (rho = 0.489, P < 2.2e-16), CCR1 (rho = 0.476, P < 2.2e-16), and CCR2 (rho=0.395, P<2.2e-16).

Discussion

Research on Circular RNA (circRNA) represents an emerging field that has garnered significant attention owing to rapid technological progress. CircRNAs exert pivotal roles in a diverse range of physiological and pathological processes. Their critical implications in cancer initiation, progression, and the development of drug resistance have been well-documented (42, 43). Furthermore, their prevalence in exosomes and bodily fluids enables them to modulate the tumor microenvironment via intercellular communication. As a result, strategies based on circRNA for diagnosis and therapeutics carry immense potential in cancer management and are poised to emerge as highly promising cancer biomarkers.

The dysregulated expression of circular RNAs (circRNAs) exerts a substantial impact on tumor development. In this study, we integrated data from GEO databases, conducted microarray analyses, and scrutinized clinical samples to identify the most significantly downregulated circRNA candidate genes. Following meticulous data screening, we recognized the importance of constructing a comprehensive framework to delineate the involvement of circ_BBS9 in the malignant progression and immune regulation of LUAD. Our research extensively delved into the role of circ_BBS9 in LUAD, examining aspects such as gene expression patterns, molecular functions, and immune infiltration within the context of the disease.

The results from bioinformatics analyses conducted across various databases and utilizing different methods consistently revealed a notable downregulation trend in circ_BBS9 expression within LUAD cells and tissues (Figures 1B, C, 2F, G). Subsequent validation using clinical samples substantiated these findings, demonstrating significantly lower circ_BBS9 expression levels in LUAD tissues in comparison to non-tumor tissues (Figures 2A, B, D). Furthermore, the observed decrease in circ_BBS9 expression corresponded with higher tumor grades (Figure 2H), implying a potential correlation between reduced circ_BBS9 expression levels and an unfavorable prognosis in LUAD (Figures 2I, J). Consequently, our findings suggest a plausible association between the loss of circ_BBS9 and the progression of LUAD. Annotation results from GO and KEGG analysis further indicate that circ_BBS9 is involved in the regulation of cellular metabolism, biological regulation, cytokine interactions, and various signaling pathways (Figures 1D, E). GSEA results also show a close association between circ_BBS9 and various pathways including cellular metabolism, the cell cycle, proliferation, infiltration, antigen response, inflammatory reactions, and multiple signaling pathways, such as the P53, WNT, NF-κB signaling pathways, and the G2M checkpoint (Figure 1F). Our study demonstrates that the expression of circ_BBS9 is correlated with patient prognosis and tumor grade. Additionally, our laboratory experiments confirm that the overexpression of circ_BBS9 can significantly inhibit the proliferation of LUAD cells (Figures 3E, F), suggesting its potential as a tumor suppressor in LUAD.

CircRNAs have been associated with drug resistance in hepatocellular carcinoma (HCC) cells and their regulatory roles in autophagy (44, 45). Previous research has suggested that

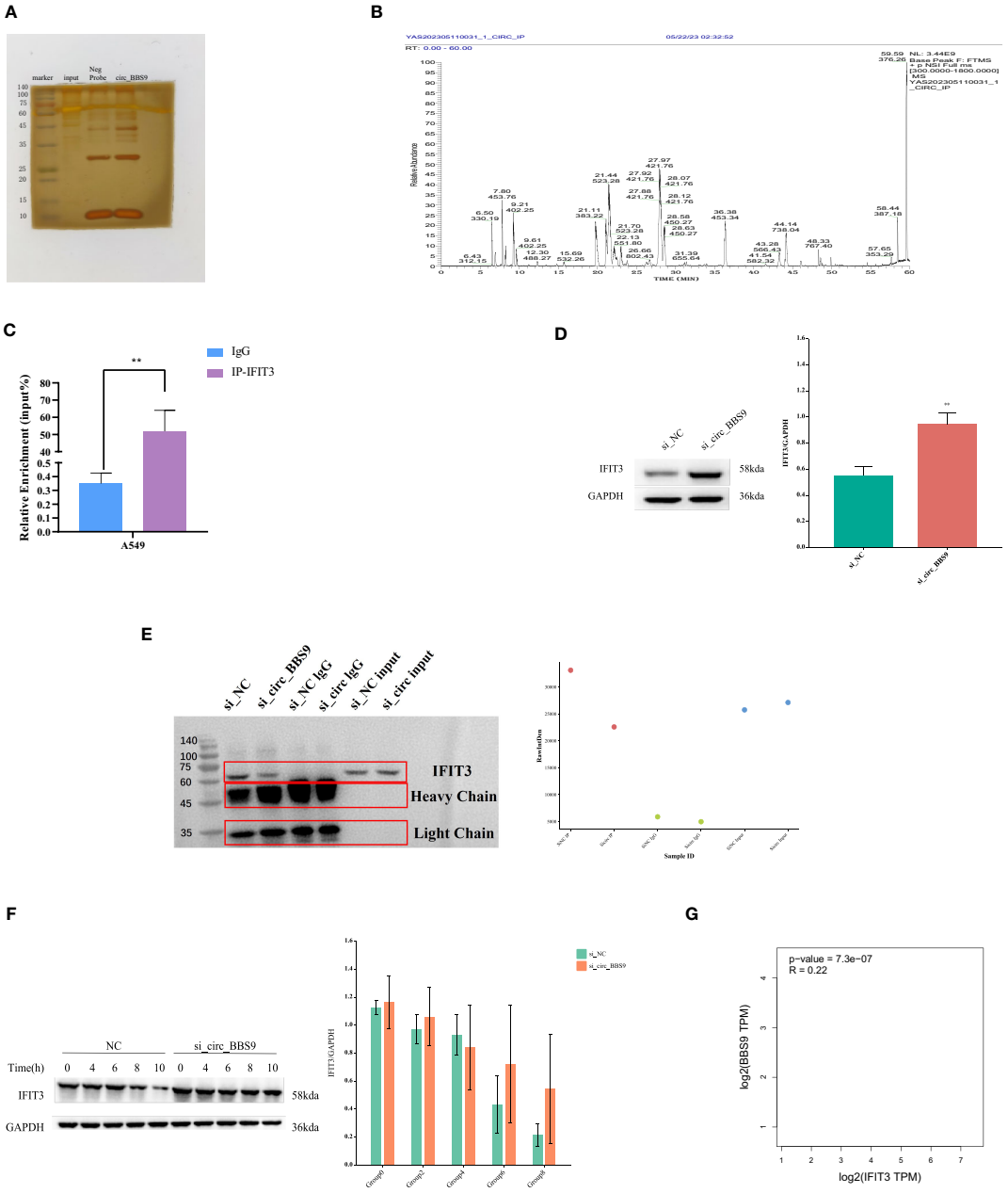

FIGURE 5
Circ_BBS9 interacts with IFIT3, mediating protein ubiquitination and subsequently affecting protein stability. **(A)** RNA pulldown was performed using biotin-labeled circ_BBS9 probe, followed by mass spectrometry analysis. **(B)** RNA pulldown assay was performed to verify the interaction between circ_BBS9 and IFIT3 in A549 cell. **(C)** RBP immunoprecipitation (RIP) assay was performed using IG-IFIT3 or IgG antibodies, followed by qRT-PCR assay for circ_BBS9 expression in A549 cell. **(D)** Western blot was performed to detect the expression of IFIT3 in GAPDH and si_circ_BBS9. **(E)** Co-immunoprecipitation (Co-IP) experiments were conducted on A549 cells using ubiquitination antibodies. **(F)** Experiments on the stability of IFIT3 protein. **(G)** Gene expression profiling interactive analysis (GEPIA: http://gepia.cancerpku.cn/).

circRNAs may play a vital role in autophagic regulation, prompting further exploration of their potential roles in ferroptosis. Recent studies have confirmed that circular RNAs can promote or inhibit ferroptosis by modulating the post-transcriptional levels of key ferroptosis-related proteins, through different molecular pathways, which contribute to the progression of various cancers. The molecular mechanism of ferroptosis primarily involves the loss or activation of GPX4, iron metabolism, and lipid peroxidation. One study discovered that in lung cancer, the overexpression of circ_SCN8A led to elevated levels of intracellular Fe2+, ROS, and MDA while decreasing the levels of glutathione (GSH). Additionally, circ_SCN8A enhances the expression of fatty acid-binding protein 4 (ACSL4) by binding to miR-1290, promoting lung cancer cell proliferation and migration, and inhibiting ferroptosis (46). Hence, we believe that ferroptosis regulated by circRNAs could become a novel cancer treatment strategy. However, our understanding of the mechanisms of circRNAs in ferroptosis regulation remains incomplete. In our study,

overexpression of circ_BBS9 experimentally validated significantly increased ROS levels (Figure 4C), elevated MDA and divalent iron ion concentrations (Figures 4E, G), and reduced the expression levels of GPX4 and FTH1 (Figure 4I), further confirming the role of circ_BBS9 in promoting ferroptosis in LUAD cells. These findings suggest that circ_BBS9 holds potential as a biomarker and therapeutic target for LUAD, offering a new avenue for research into ferroptosis-induced treatments for LUAD. Currently, some drugs and radiotherapy have been found to induce cell ferroptosis, making RNA molecules an area of significant interest in research. Our study provides a new research direction for exploring the potential of circ_BBS9 as a biomarker and molecular therapy for LUAD.

Ferroptosis has become a significant focus in contemporary cancer research. While directly manipulating ferroptosis pathways may not be the most effective overall strategy, revealing its regulatory pathways establishes a new theoretical foundation for precise and targeted cancer therapies. The revelation of ferroptosis has inaugurated novel research trajectories within the cancer domain, gradually unveiling its clinical significance in cancer progression. Hence, intervening in cancer progression by modulating cellular ferroptosis has become a pivotal area of

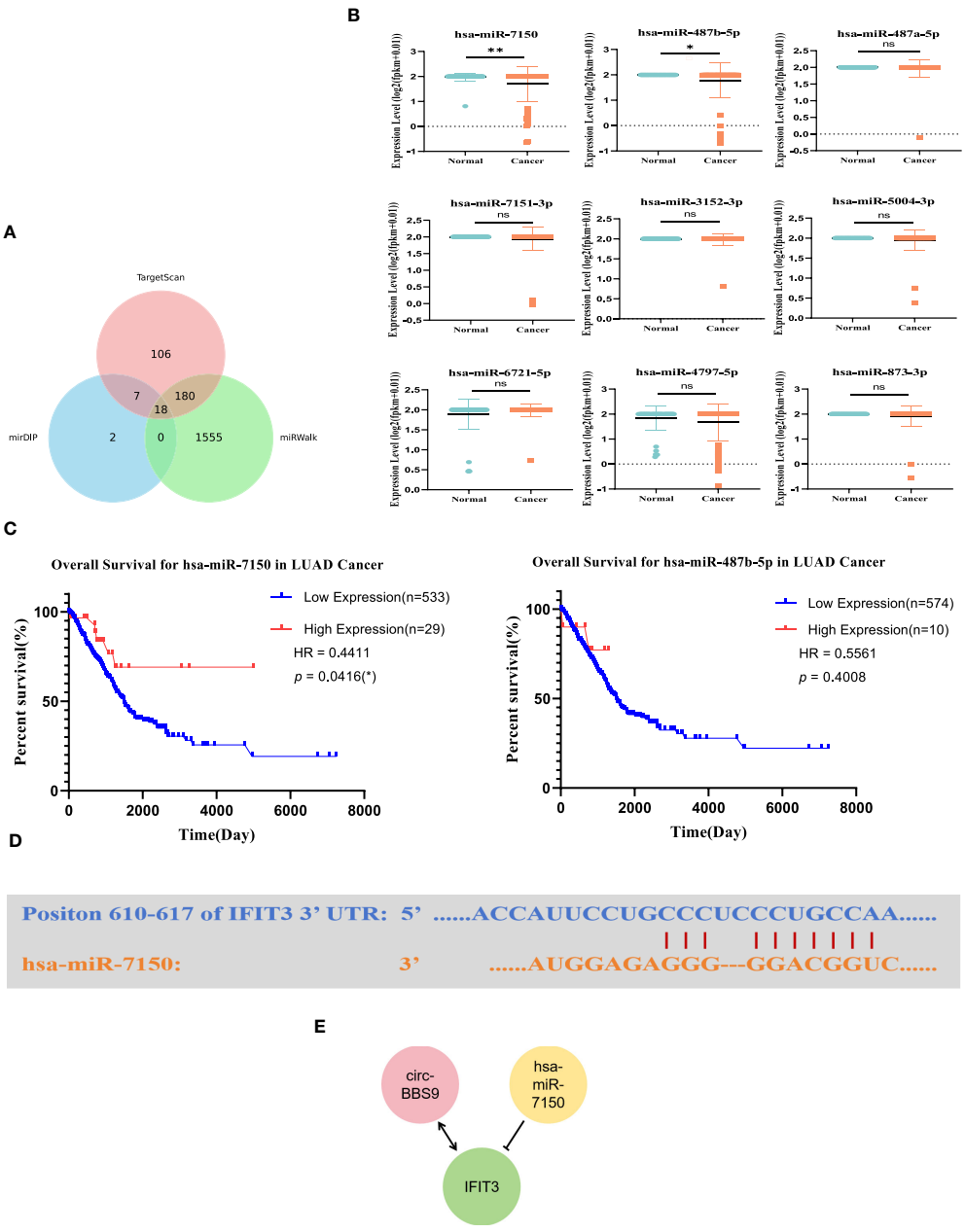

FIGURE 6
Construction of the Upstream Regulatory Network of IFIT3. **(A)** Venn diagram found that potential miRNAs of IFIT3. **(B)** Predicted miRNA expression levels. **(C)** Predicted miRNA survival levels. **(D)** Predicted interaction of IFIT3 and has-miR-7150. **(E)** Potential upstream TF-miRNA-mRNA regulatory network of IFIT3.

investigation in research. It is crucial to emphasize that our study remains in its nascent stages, particularly regarding the exploration of mechanisms through which circ_BBS9 regulates ferroptosis in LUAD. Consequently, further exploration, including validation in more extensive cohorts of lung cancer patients and diverse lung cancer tissue samples, alongside rectifying systematic biases inherent in various databases, constitutes an integral part of our future research endeavors.

In recent years, the advent and efficacy of targeted immunotherapies have begun to reshape the management of cancer (47, 48). Infiltrative immune cells are a crucial component of the TME (49). The interaction between the TME and the host immune system is complex, necessitating the identification of predictive biomarkers for personalized treatment. Infiltration of innate immune cells and the production and aggregation of inflammatory chemokines are often indicative of tumor-associated inflammation. Immune-inflammatory responses can activate a cascade of molecular signaling pathways associated with tumor cell generation, proliferation, and metastasis (50–52). Furthermore, distinct subtypes of the tumor microenvironment (TME) are significantly correlated with patient prognosis, predicting the immune response rate and sensitivity to chemotherapy drugs. This information can be utilized to screen patients for sensitivity to immunotherapy and chemotherapy drugs (53). It is widely recognized that an imbalance in T-cell subpopulations is common in cancer patients (54). The cytokines and chemokines secreted by TH1 cells play a major role as effector molecules in immune cell signaling. Some studies have found that

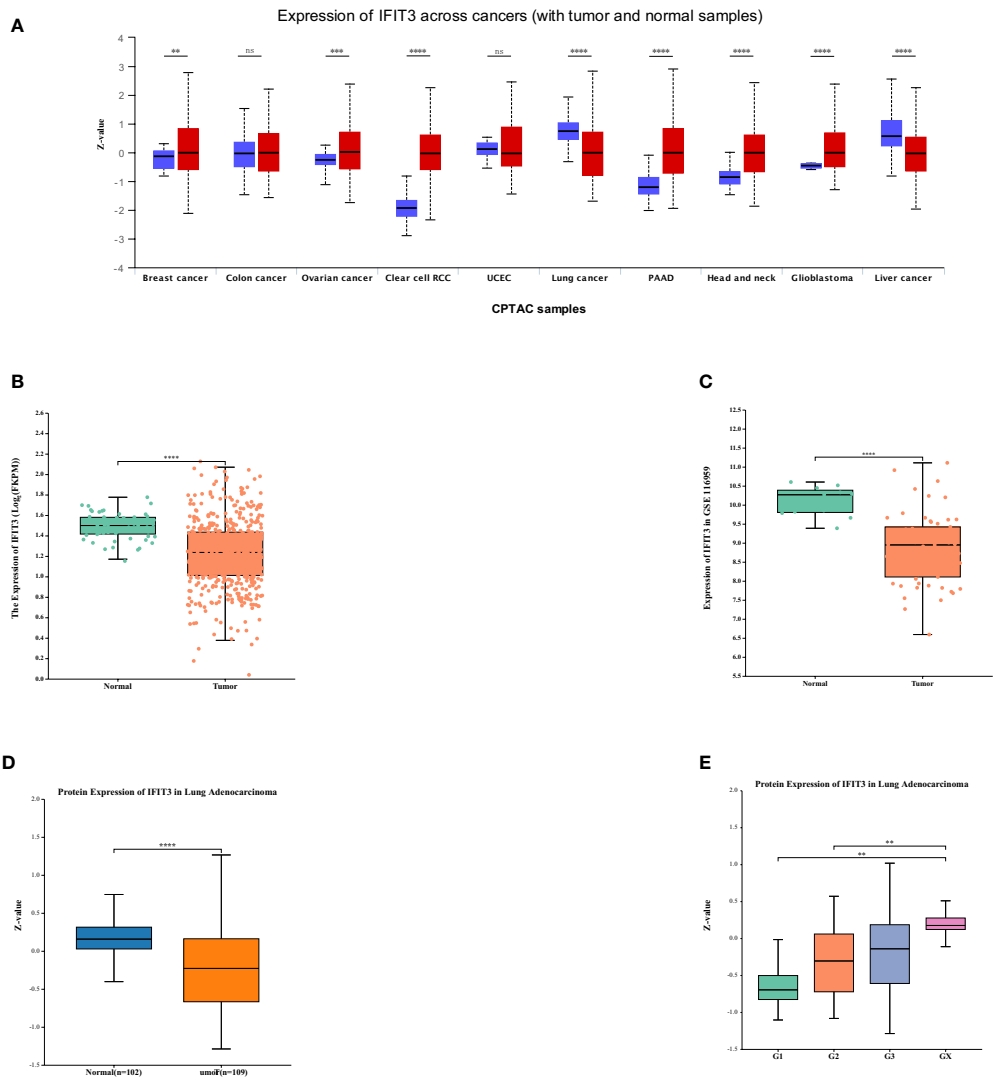

FIGURE 7
The Relationship Between IFIT3 Expression and the Prognosis of LUAD. **(A)** IFIT3 expression in different cancer types analyzed by UALCAN. **(B)** IFIT3 mRNA is expressed at a low level in TCGA. **(C)** IFIT3mRNA is expressed at a low level in GEO. **(D)** In the HAP database, the protein expression level of IFIT3 in LUAD is significantly lower than in normal tissues ($P < 0.001$). **(E)** The expression of IFIT3 in LUAD is significantly correlated with Tumor Grade ($p < 0.01$).

TH1 cells can promote anti-tumor immune responses, reduce cancer cell proliferation, and guide them into a dormant state by activating the STAT1 signaling pathway (55).

With the deepening investigation into circRNAs, an increasing body of research has shown that circRNAs can interact with RNA-binding proteins (RBPs) to modulate cancer progression. For instance, circ_NDUFB2 has been demonstrated to impact the occurrence and development of non-small cell lung cancer by regulating the ubiquitination and degradation of IGF2BP2 (14). In this study, we conducted microarray analysis of the expression profile of circRNAs using a LUAD expression chip dataset. Through circRNA pull-down and mass spectrometry detection, we successfully identified the protein IFIT3 (Figures 5A–C), which directly interacts with circ_BBS9. We observed that IFIT3 is under-expressed in LUAD (Figures 7B–D) and increases with tumor grade (Figure 7E). Additionally, IFIT3 exhibits differential expression across various tumor tissues (Figure 7A). Through GO and KEGG analysis of 21 genes related to IFIT3 (Figures 8A, B), it is shown (Figure 8C) that IFIT3 plays a crucial role in cytokine signaling pathway in the JAK-STAT signaling pathway and immune system. Moreover, we explored the upstream miRNA regulatory factors for IFIT3 using tools like miRNA databases, mirDIP, and TargetScan (Figures 6A–D). From these investigations and considering expression and survival data from databases, we have identified a potential transcriptional network involving "circ_BBS9," "hsa-miR-7150," and "IFIT3," suggesting its potential involvement in the pathogenesis of LUAD. It may exert its effects by modulating ferroptosis and immune microenvironment through direct interaction with IFIT3 and competitive binding to miR-7150. A study has revealed the upregulation of hsa-miR-7150 expression in tissue samples from advanced gastric cancer patients (56).

It's worth noting that this transcriptional network was selected through bioinformatics analysis and preliminary functional exploration, and further refinement of this network will be required in future studies. Establishing the functional transcriptional network of LUAD requires the utilization of new effective methods and bioinformatics tools, as well as more *in vitro*

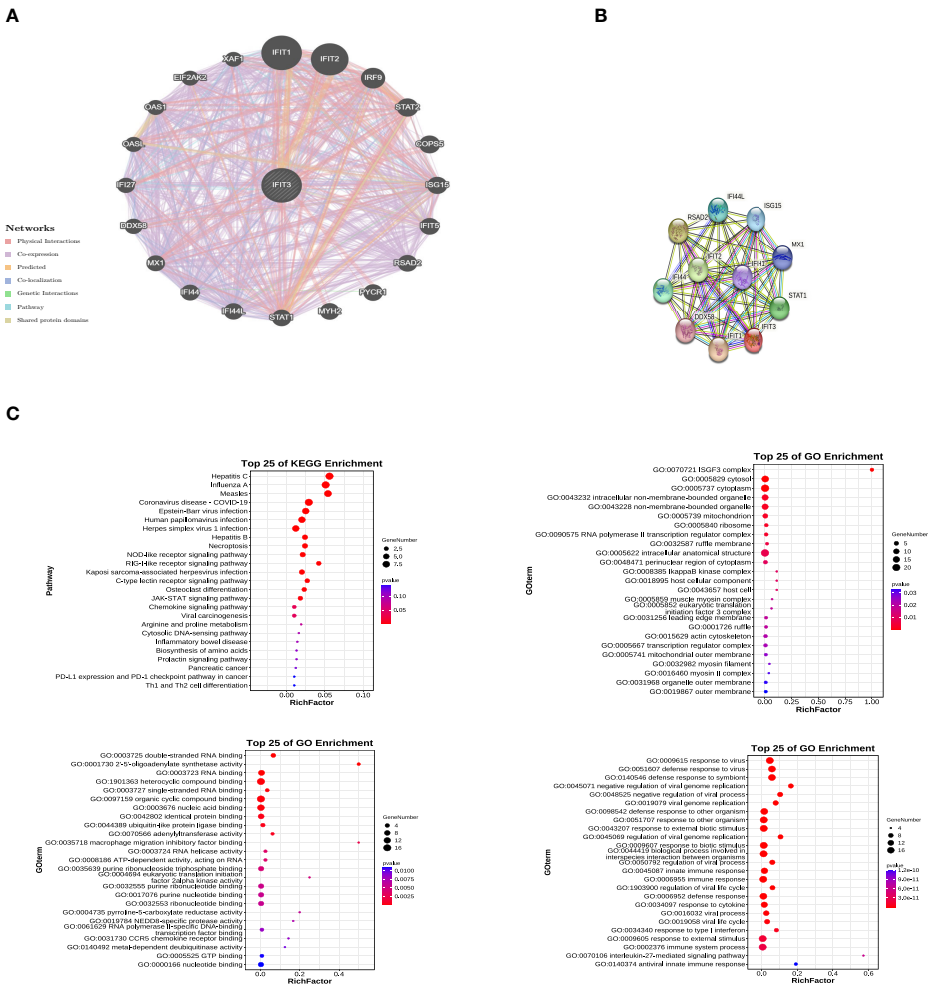

FIGURE 8
GO and KEGG Analysis Related to IFIT3. **(A)** The gene network of GPER and associated genes was analyzed using Gene Mania. **(B)** The protein network of GPER was constructed using STRING. **(C)** 21 related genes were used for conducting GO and KEGG analysis.

and *in vivo* experiments to reveal its potential pathogenic mechanisms and identify new diagnostic biomarkers. Therefore, future research may involve further experimental investigations to delve into the associated molecular mechanisms.

Following the construction of this network, we conducted further analysis with the aim of investigating the association between IFIT3 in LUAD and immune infiltration to explore the link between gene expression and immune cell infiltration. Although prior research has indicated the potential impact of immune infiltration on the behavior and prognosis of cancer patients, the mechanism of interaction between IFIT3 and the TME remains unclear. Our analysis reveals that the expression of

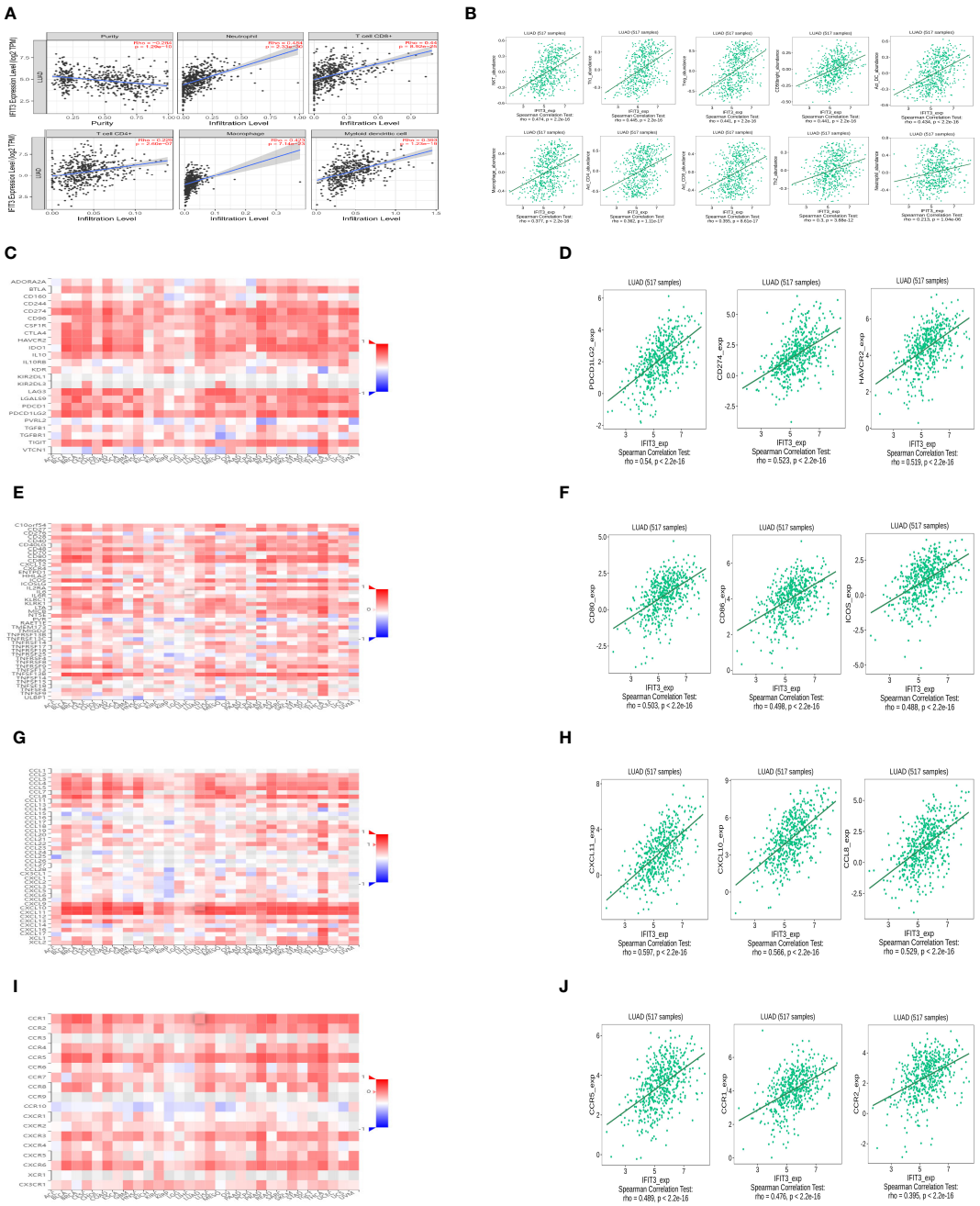

FIGURE 9
The research on the correlation between the expression of IFIT3 and immune infiltration. **(A)** Relationship between IFIT3 expression and immune infiltration level generated from TIMER. **(B)** Correlation of IFIT3 expression and immune infiltration from TISIDB. **(C)** Correlations between IFIT3 expression and immune inhibitors in all kinds of human cancers analyzed by TISIDB. **(D)** The IFIT3 expression was positively associated with most of the immuneinhibitors. **(E)** Correlations between IFIT3 expression and immuneostimulators in all types of human cancers analyzed by TISIDB. **(F)** The IFIT3 expression was positively associated with most of the immunostimulators. **(G)** Correlations between IFIT3 expression and chemokines in all types of human cancers analyzed by TISIDB. **(H)** The IFIT3 expression was positively associated with most of the chemokines. **(I)** Correlations between IFIT3 expression and chemokine receptors. in all types of human cancers analyzed by TISIDB. **(J)** The IFIT3 expression was positively associated with most of the chemokine receptors.

IFIT3, a protein that directly interacts with circ_BBS9, is positively correlated with the infiltration of T-helper cells and Th1 cells (Figure 9B). Furthermore, in the IFIT3-related PPI network, STAT1, recognized as a critical downstream factor of Th1 cells, is identified. IFIT3 also exhibits differential expression across various tumors. Previous studies have suggested that IFIT3 enhances the interferon (IFN) effector signaling pathway by promoting the formation and nuclear localization of the STAT1-STAT2 heterodimer in hepatocellular carcinoma (57). Our analysis also indicates a positive correlation between IFIT3 expression and immunosuppressive cells, like Treg cells (Figure 9B), and immunosuppressive molecule CD274 (Figure 9D). Meanwhile, immune-activated cells and markers, such as anti-tumor T cells, neutrophils, and Th1 cells, also exhibit a positive correlation with IFIT3 expression (Figure 9A). All of these findings support the potential of IFIT3 as a marker or target for distinguishing malignant tumors. Therefore, the regulation of IFIT3 expression at the genetic level may provide a new target for immunotherapy in LUAD.

Current research suggests that CD80 is a potential therapeutic target for improving the prognosis of patients with LUAD and enhancing the effectiveness of biologically targeted anti-tumor treatments. CXCR3, a receptor for the chemokine CXCL11, demonstrates strong anti-tumor activity *in vivo* (58). Blocking CCR5 to promote the polarization of anti-tumor macrophages has been observed to lead to the regression of metastatic disease and alterations in the TME (59). Our study results indicate that IFIT3 is positively correlated with certain immune molecules such as PDCD1LG2, CD80, CD86, CXCL11, CXCL10, and CCR5 (Figures 9F, H, J). Among these, CXCL11, CXCL10, and CCR5 are chemokines and related receptors for Th1 cells. These findings support the hypothesis that IFIT3 may serve as a potential marker or therapeutic target for malignant tumors.

To delve deeper into the regulatory mechanisms of IFIT3 in malignant tumor progression and immune infiltration, we combined the KEGG results and identified a potential pathway: the JAK3-STAT pathway, which may be associated with IFIT3 (Figure 8C). Activation of the JAK-STAT signaling pathway could suppress cytotoxic T lymphocytes and counteract the anti-tumor effects of PD-1 immune therapy in pancreatic cancer (60). Inhibition of LUAD proliferation, migration, and invasion can be achieved by lowering PYCR1 expression, affecting the JAK/STAT signaling pathway (61). Several studies have reported that the activation of the JAK-STAT signaling pathway can promote cell apoptosis (62, 63). However, the JAK-STAT signaling pathway plays a dual role in the TME, acting as both "anti-tumor" and "pro-tumor" depending on the nature of the response signals. Therefore, we hypothesize that IFIT3 may exert its effects through the JAK-STAT signaling pathway and show a strong positive correlation with immune molecules, thereby playing a role in the regulation of progression and immune infiltration in LUAD.

We comprehensively elucidated the role of IFIT3 in pathway enrichment and immune infiltration within the TME using bioinformatics techniques. Its low expression may serve as an indicator of poor prognosis in LUAD and potentially enhance the effectiveness of immune therapy through the regulation of immune cell infiltration. Therefore, the decreased expression of circ_BBS9 and IFIT3 in LUAD may impact tumor immunity and contribute to tumorigenesis, providing important insights for future immunotherapy research. This also suggests that disease treatment should not only focus on the molecular level but should also be combined with an emphasis on immune infiltration to achieve better therapeutic outcomes. In summary, our data indicates a strong association between IFIT3 and various immune checkpoint molecules and immune activation within the TME. Nevertheless, further validation of IFIT3 as a predictive biomarker for selecting immune checkpoint blockade and the potential utility in treating patients with immunotherapy is required. Consequently, large-scale standardized animal experiments, clinical trials, and additional immunotherapy cohorts and single-cell analyses are necessary, and our team is actively working towards these objectives.

The development and progression of LUAD involve a multifaceted, multistep process primarily steered by aberrant gene expression within cellular signaling pathways. Constructing a high-dimensional immune map that integrates complementary predictive biomarkers becomes paramount for personalized immune therapy, given the intricate interplays among tumors, the tumor microenvironment (TME), and the host's immune responses. Hence, collaborative efforts in the future are imperative to ensure the efficacy of immune therapeutic approaches targeted toward appropriate TMEs at specific intervention junctures. Our study delved into immune-related genes implicated in formulating the LUAD prognosis model, comprehensively analyzing associated immune cells and immune signaling pathways. Despite the comprehensiveness of our research, these conclusions await full validation through *in vitro* or *in vivo* experiments due to inherent limitations. Therefore, further research endeavors are essential to elucidate the precise functions of these pathways, enhancing and confirming the stability of these regulatory networks to solidify their mechanistic underpinnings. We identified that the upregulation of circ_BBS9 impedes the proliferation of lung adenocarcinoma cells and encourages ferroptosis in these cells. Additionally, we established a relationship between the protein IFIT3, which directly interacts with circ_BBS9, and immune infiltration, contributing to the configuration of the immune microenvironment in LUAD. Furthermore, we underscored the potential of circ_BBS9 as a novel biomarker for early diagnosis and treatment, unveiling the direct interplay between circ_BBS9 and IFIT3, which actively shapes the immune microenvironment in LUAD. These investigations provide novel insights into molecular mechanisms and prospective therapeutic targets, holding substantial promise in the diagnosis and treatment landscape of LUAD.

Conclusion

Circ_BBS9 acts as a tumor suppressor in LUAD and may serve as a potential diagnostic biomarker. It may exert its effects by modulating ferroptosis and immune microenvironment through direct interaction with IFIT3 and competitive binding to miR-7150. These findings provide novel insights into LUAD pathogenesis and identify circBBS9 as a promising therapeutic target.

Data availability statement

The datasets presented in this study can be found in online repositories. The names of the repository/repositories and accession number(s) can be found in the article/supplementary material.

Ethics statement

This study was conducted in accordance with the principles outlined in the Declaration of Helsinki and was approved by the Ethics Committee of Jinshan Branch of Shanghai Sixth Peoples Hospital, with approval number jszxyy202205. All patients provided written informed consent prior to their participation in this study. The study adhered to the ethical guidelines and regulations governing research involving human subjects and protected their rights and privacy throughout the investigation. All patient data and information were anonymized and treated with strict confidentiality to ensure compliance with ethical standards.

Author contributions

DP: Conceptualization, Formal analysis, Funding acquisition, Investigation, Methodology, Project administration, Resources, Validation, Writing – original draft, Writing – review & editing. ML: Data curation, Formal analysis, Methodology, Software, Validation, Visualization, Writing – original draft, Writing – review & editing. LL: Investigation, Writing – review & editing. HY: Investigation, Writing – review & editing. DF: Investigation, Writing – review & editing. LC: Investigation, Writing – review & editing. BG: Conceptualization, Formal analysis, Funding acquisition, Investigation, Resources, Supervision, Writing – review & editing.

Funding

This research is supported by the General Program of the Shanghai Jinshan District Health Commission, with the grant number JSKJ-KTMS-2021-12. The principal investigator of the project is DP.

Conflict of interest

The authors declare that the research was conducted in the absence of any commercial or financial relationships that could be construed as a potential conflict of interest.

Publisher's note

References

1. *Current cancer situation in China: good or bad news from the 2018 Global Cancer Statistics?* (2019). Cancer Communications - Wiley Online Library (Accessed October 30, 2023).

2. Migrating into the Tumor: a Roadmap for T Cells: Trends in Cancer . Available online at: https://www.cell.com/trends/cancer/fulltext/S2405-8033(17)30192-9 (Accessed October 30, 2023).

3. Travis WD, Brambilla E, Noguchi M, Nicholson AG, Geisinger KR, Yatabe Y, et al. International association for the study of lung cancer/american thoracic society/european respiratory society international multidisciplinary classification of lung adenocarcinoma. *J Thorac Oncol.* (2011) 6(2):244–85. doi: 10.1097/JTO.0b013e318206a221

4. Deutsch E, Le Péchoux C, Faivre L, Rivera S, Tao Y, Pignon JP, et al. Phase I trial of everolimus in combination with thoracic radiotherapy in non-small-cell lung cancer. *Ann Oncol.* (2015) 26:1223–9. doi: 10.1093/annonc/mdv105

5. *Prognostic Significance of Ground-Glass Opacity Components in 5-Year Survivors With Resected Lung Adenocarcinoma* . SpringerLink (Accessed October 30, 2023).

6. Vitamin D Supplementation and Survival of Patients with Non–small Cell Lung Cancer: A Randomized, Double-Blind, Placebo-Controlled Trial. Clinical Cancer Research | American Association for Cancer Research. Available online at: https://aacrjournals.org/clincancerres/article/24/17/4089/80967/Vitamin-D-Supplementation-and-Survival-of-Patients (Accessed October 30, 2023).

7. CircRNAs in Lung Adenocarcinoma: Diagnosis and Therapy: Ingenta Connect. Available online at: https://www.ingentaconnect.com/content/ben/cgt/2022/00000022/00000001/art00003 (Accessed October 30, 2023).

8. Salzman J, Chen RE, Olsen MN, Wang PL, Brown PO. Cell-type specific features of circular RNA expression. *PloS Genet.* (2013) 9(9):e1003777. doi: 10.1371/journal.pgen.1003777

9. Du WW, Yang W, Li X, Awan FM, Yang Z, Fang L, et al. A circular RNA circ-DNMT1 enhances breast cancer progression by activating autophagy. *Oncogene.* (2018) 37:5829–42. doi: 10.1038/s41388-018-0369-y

10. Du WW, Yang W, Liu E, Yang Z, Dhaliwal P, Yang BB. Foxo3 circular RNA retards cell cycle progression via forming ternary complexes with p21 and CDK2. *Nucleic Acids Res.* (2016) 44:2846–58. doi: 10.1093/nar/gkw027

11. Zhao Y, Zhang C, Tang H, Wu X, Qi Q. Mechanism of RNA circHIPK3 involved in resistance of lung cancer cells to gefitinib. *BioMed Res Int.* (2022) 2022:4541918. doi: 10.1155/2022/4541918

12. Cheng Z, Yu C, Cui S, Wang H, Jin H, Wang C, et al. circTP63 functions as a ceRNA to promote lung squamous cell carcinoma progression by upregulating FOXM1. *Nat Commun.* (2019) 10:3200. doi: 10.1038/s41467-019-11162-4

13. Huang Q, Guo H, Wang S, Ma Y, Chen H, Li H, et al. A novel circular RNA, circXPO1, promotes lung adenocarcinoma progression by interacting with IGF2BP1. *Cell Death Dis.* (2020) 11:1031. doi: 10.1038/s41419-020-03237-8

14. Li B, Zhu L, Lu C, Wang C, Wang H, Jin H, et al. circNDUFB2 inhibits non-small cell lung cancer progression via destabilizing IGF2BPs and activating anti-tumor immunity. *Nat Commun.* (2021) 12:295. doi: 10.1038/s41467-020-20527-z

15. Chen RX, Chen X, Xia LP, Zhang JX, Pan ZZ, Ma XD, et al. N6-methyladenosine modification of circNSUN2 facilitates cytoplasmic export and stabilizes HMGA2 to promote colorectal liver metastasis. *Nat Commun.* (2019) 10:4695. doi: 10.1038/s41467-019-12651-2

16. Du WW, Yang W, Li X, Fang L, Wu N, Li F, et al. The circular RNA circSKA3 binds integrin β1 to induce invadopodium formation enhancing breast cancer invasion. *Mol Ther.* (2020) 28:1287–98. doi: 10.1016/j.ymthe.2020.03.002

17. Chen DL, Sheng H, Zhang DS, Jin Y, Zhao BT, Chen N, et al. The circular RNA circDLG1 promotes gastric cancer progression and anti-PD-1 resistance through the regulation of CXCL12 by sponging miR-141-3p. *Mol Cancer.* (2021) 20(1):166. doi: 10.1186/s12943-021-01475-8

18. Li Y, Chen B, Zhao J, Li Q, Chen S, Guo T, et al. HNRNPL circularizes ARHGAP35 to produce an oncogenic protein. *Adv Sci (Weinh).* (2021) 8:2001701. doi: 10.1002/advs.202001701

19. Dixon SJ, Lemberg KM, Lamprecht MR, Skouta R, Zaitsev EM, Gleason CE, et al. Ferroptosis: an iron-dependent form of nonapoptotic cell death. *Cell*. (2012) 149:1060–72. doi: 10.1016/j.cell.2012.03.042

20. Xie Y, Hou W, Song X, Yu Y, Huang J, Sun X, et al. Ferroptosis: process and function. *Cell Death Differ*. (2016) 23:369–79. doi: 10.1038/cdd.2015.158

21. Badgley MA, Kremer DM, Maurer HC, DelGiorno KE, Lee HJ, Purohit V, et al. Cysteine depletion induces pancreatic tumor ferroptosis in mice. *Science*. (2020) 368:85–9. doi: 10.1126/science.aaw9872

22. Stockwell BR, Jiang X, Gu W. Emerging mechanisms and disease relevance of ferroptosis. *Trends Cell Biol*. (2020) 30:478–90. doi: 10.1016/j.tcb.2020.02.009

23. Angeli JPF, Shah R, Pratt DA, Conrad M. Ferroptosis inhibition: mechanisms and opportunities. *Trends Pharmacol Sci*. (2017) 38:489–98. doi: 10.1016/j.tips.2017.02.005

24. Pohl SÖG, Pervaiz S, Dharmarajan A, Agostino M. Gene expression analysis of heat-shock proteins and redox regulators reveals combinatorial prognostic markers in carcinomas of the gastrointestinal tract. *Redox Biol*. (2019) 25:101060. doi: 10.1016/j.redox.2018.11.018

25. Chen X, Kang R, Kroemer G, Tang D. Broadening horizons: the role of ferroptosis in cancer. *Nat Rev Clin Oncol*. (2021) 18:280–96. doi: 10.1038/s41571-020-00462-0

26. Fang Y, Chen X, Tan Q, Zhou H, Xu J, Gu Q. Inhibiting ferroptosis through disrupting the NCOA4–FTH1 interaction: A new mechanism of action. *ACS Cent Sci*. (2021) 7:980–9. doi: 10.1021/acscentsci.0c01592

27. Torti FM, Torti SV. Regulation of ferritin genes and protein. *Blood*. (2002) 99:3505–16. doi: 10.1182/blood.V99.10.3505

28. Xie B, Guo Y. Molecular mechanism of cell ferroptosis and research progress in regulation of ferroptosis by noncoding RNAs in tumor cells. *Cell Death Discovery*. (2021) 7:101. doi: 10.1038/s41420-021-00483-3

29. Dunn GP, Bruce AT, Ikeda H, Old LJ, Schreiber RD. Cancer immunoediting: from immunosurveillance to tumor escape. *Nat Immunol*. (2002) 3:991–8. doi: 10.1038/ni1102-991

30. Zaynagetdinov R, Stathopoulos GT, Sherrill TP, Cheng DS, McLoed AG, Ausborn JA, et al. Epithelial nuclear factor-κB signaling promotes lung carcinogenesis via recruitment of regulatory T lymphocytes. *Oncogene*. (2012) 31:3164–76. doi: 10.1038/onc.2011.480

31. Shimizu K, Nakata M, Hirami Y, Yukawa T, Maeda A, Tanemoto K. Tumor-infiltrating Foxp3+ regulatory T cells are correlated with cyclooxygenase-2 expression and are associated with recurrence in resected non-small cell lung cancer. *J Thorac Oncol*. (2010) 5:585–90. doi: 10.1097/JTO.0b013e3181d60fd7

32. Srivastava MK, Andersson Å, Zhu L, Harris-White M, Lee JM, Dubinett S, et al. Myeloid suppressor cells and immune modulation in lung cancer. *Immunotherapy*. (2012) 4:291–304. doi: 10.2217/imt.11.178

33. Hinshaw DC, Shevde LA. The tumor microenvironment innately modulates cancer progression. *Cancer Res*. (2019) 79:4557–66. doi: 10.1158/0008-5472.CAN-18-3962

34. Han Y, Wang J, Xu B. Tumor microenvironment subtypes and immune-related signatures for the prognosis of breast cancer. *BioMed Res Int*. (2021) 2021:6650107. doi: 10.1155/2021/6650107

35. Gao Y, Shen M, Shi X. Interaction of dendrimers with the immune system: An insight into cancer nanotheranostics. *VIEW*. (2021) 2:20200120. doi: 10.1002/VIW.20200120

36. Zhu H, Yang C, Yan A, Qiang W, Ruan R, Ma K, et al. Tumor-targeted nano-adjuvants to synergize photomediated immunotherapy enhanced antitumor immunity. *VIEW*. (2023) 4:20220067. doi: 10.1002/VIW.20220067

37. Chen YL, Liu YN, Lin YT, Tsai MF, Wu SG, Chang TH, et al. LncRNA SLCO4A1-AS1 suppresses lung cancer progression by sequestering the TOX4-NTSR1 signaling axis. *J Biomed Science*. (2023) 30:80. doi: 10.1186/s12929-023-00973-9

38. Li T, Fan J, Wang B, Traugh N, Chen Q, Liu JS, et al. TIMER: A web server for comprehensive analysis of tumor-infiltrating immune cells. *Cancer Res*. (2017) 77: e108–10. doi: 10.1158/0008-5472.CAN-17-0307

39. Tang Z, Li C, Kang B, Gao G, Li C, Zhang Z. GEPIA: a web server for cancer and normal gene expression profiling and interactive analyses. *Nucleic Acids Res*. (2017) 45: W98–W102. doi: 10.1093/nar/gkx247

40. Chandrashekar DS, Bashel B, Balasubramanya SAH, Creighton CJ, Ponce-Rodriguez I, Chakravarthi BV, et al. UALCAN: A portal for facilitating tumor subgroup gene expression and survival analyses. *Neoplasia*. (2017) 19:649–58. doi: 10.1016/j.neo.2017.05.002

41. Ru B, Wong CN, Tong Y, Zhong JY, Zhong SS, Wu WC, et al. TISIDB: an integrated repository portal for tumor–immune system interactions. *Wren J Ed Bioinf*. (2019) 35:4200–2. doi: 10.1093/bioinformatics/btz210

42. Guarnerio J, Bezzi M, Jeong JC, Paffenholz SV, Berry K, Naldini MM, et al. Oncogenic role of fusion-circRNAs derived from cancer-associated chromosomal translocations. *Cell*. (2016) 166:1055–6. doi: 10.1016/j.cell.2016.07.035

43. Borran S, Ahmadi G, Rezaei S, Anari MM, Modabberi M, Azarash Z, et al. Circular RNAs: New players in thyroid cancer. *Pathol Res Pract*. (2020) 216:153217. doi: 10.1016/j.prp.2020.153217

44. Xu J, Ji L, Liang Y, Wan Z, Zheng W, Song X, et al. CircRNA-SORE mediates sorafenib resistance in hepatocellular carcinoma by stabilizing YBX1. *Signal Transduct Target Ther*. (2020) 5:298. doi: 10.1038/s41392-020-00375-5

45. Zhang Y, Nguyen TM, Zhang XO, Wang L, Phan T, Clohessy JG, et al. Optimized RNA-targeting CRISPR/Cas13d technology outperforms shRNA in identifying functional circRNAs. *Genome Biol*. (2021) 22:41. doi: 10.1186/s13059-021-02263-9

46. Liu B, Ma H, Liu X, Xing W. CircSCN8A suppresses Malignant progression and induces ferroptosis in non-small cell lung cancer by regulating miR-1290/ACSL4 axis. *Cell Cycle*. (2023) 22:758–76. doi: 10.1080/15384101.2022.2154543

47. Zhou F, Qiao M, Zhou C. The cutting-edge progress of immune-checkpoint blockade in lung cancer. *Cell Mol Immunol*. (2021) 18:279–93. doi: 10.1038/s41423-020-00577-5

48. Bejarano L, Jordão MJC, Joyce JA. Therapeutic targeting of the tumor microenvironment. *Cancer Discovery*. (2021) 11:933–59. doi: 10.1158/2159-8290.CD-20-1808

49. Fridman WH, Pagès F, Sautès-Fridman C, Galon J. The immune contexture in human tumours: impact on clinical outcome. *Nat Rev Cancer*. (2012) 12:298–306. doi: 10.1038/nrc3245

50. Wei J, Barr J, Kong LY, Wang Y, Wu A, Sharma AK, et al. Glioblastoma cancer-initiating cells inhibit T-cell proliferation and effector responses by the signal transducers and activators of transcription 3 pathway. *Mol Cancer Ther*. (2010) 9:67–78. doi: 10.1158/1535-7163.MCT-09-0734

51. Lou Y, Diao L, Cuentas ER, Denning WL, Chen L, Fan YH, et al. Epithelial-mesenchymal transition is associated with a distinct tumor microenvironment including elevation of inflammatory signals and multiple immune checkpoints in lung adenocarcinoma. *Clin Cancer Res*. (2016) 22:3630–42. doi: 10.1158/1078-0432.CCR-15-1434

52. Chen L, Gibbons DL, Goswami S, Cortez MA, Ahn YH, Byers LA, et al. Metastasis is regulated via microRNA-200/ZEB1 axis control of tumour cell PD-L1 expression and intratumoral immunosuppression. *Nat Commun*. (2014) 5:5241. doi: 10.1038/ncomms6241

53. Qu S, Huang C, Zhu T, Wang K, Zhang H, Wang L, et al. OLFML3, as a potential predictor of prognosis and therapeutic target for glioma, is closely related to immune cell infiltration. *VIEW*. (2023) 4:20220052. doi: 10.1002/VIW.20220052

54. Basu A, Ramamoorthi G, Albert G, Gallen C, Beyer A, Snyder C, et al. Differentiation and regulation of TH cells: A balancing act for cancer immunotherapy. *Front Immunol*. (2021) 12:669474. doi: 10.3389/fimmu.2021.669474

55. Aqbi HF, Wallace M, Sappal S, Payne KK, Manjili MH. IFN-γ orchestrates tumor elimination, tumor dormancy, tumor escape, and progression. *J leukocyte Biol*. (2018) 103(6):1219–23. doi: 10.1002/JLB.5MIR0917-351R

56. Bibi F, Naseer MI, Alvi SA, Yasir M, Jiman-Fatani AA, Sawan A, et al. microRNA analysis of gastric cancer patients from Saudi Arabian population. *BMC Genomics*. (2016) 17:751. doi: 10.1186/s12864-016-3090-7

57. Yang Y, Zhou Y, Hou J, Bai C, Li Z, Fan J, et al. Hepatic IFIT3 predicts interferon-α therapeutic response in patients of hepatocellular carcinoma. *Hepatology*. (2017) 66:152. doi: 10.1002/hep.29156

58. Hensbergen PJ, Wijnands PGJTB, Schreurs MWJ, Scheper RJ, Willemze R, Tensen CP. The CXCR3 targeting chemokine CXCL11 has potent antitumor activity *in vivo* involving attraction of CD8+ T lymphocytes but not inhibition of angiogenesis. *J Immunother*. (2005) 28:343–51. doi: 10.1097/01.cji.0000165355.26795.27

59. Halama N, Zoernig I, Berthel A, Kahlert C, Klupp F, Suarez-Carmona M, et al. Tumoral immune cell exploitation in colorectal cancer metastases can be targeted effectively by anti-CCR5 therapy in cancer patients. *Cancer Cell*. (2016) 29:587–601. doi: 10.1016/j.ccell.2016.03.005

60. Lu C, Talukder A, Savage NM, Singh N, Liu K. JAK-STAT-mediated chronic inflammation impairs cytotoxic T lymphocyte activation to decrease anti-PD-1 immunotherapy efficacy in pancreatic cancer. *Oncoimmunology*. (2017) 6:e1291106. doi: 10.1080/2162402X.2017.1291106

61. Gao Y, Luo L, Xie Y, Zhao Y, Yao J, Liu X. PYCR1 knockdown inhibits the proliferation, migration, and invasion by affecting JAK/STAT signaling pathway in lung adenocarcinoma. *Mol Carcinog*. (2020) 59:503–11. doi: 10.1002/mc.23174

62. Philips RL, Wang Y, Cheon H, Kanno Y, Gadina M, Sartorelli V, et al. JAK-STAT pathway at 30: much learned, much more to do. *Cell*. (2022) 185:3857–76. doi: 10.1016/j.cell.2022.09.023

63. Lu F, Zhou J, Chen Q, Zhu J, Zheng X, Fang N, et al. PSMA5 contributes to progression of lung adenocarcinoma in association with the JAK/STAT pathway. *Carcinogenesis*. (2022) 43:624–34. doi: 10.1093/carcin/bgac046

Frontiers in Immunology

Explores novel approaches and diagnoses to treat immune disorders.

The official journal of the International Union of Immunological Societies (IUIS) and the most cited in its field, leading the way for research across basic, translational and clinical immunology.

Discover the latest Research Topics

See more →

Frontiers

Avenue du Tribunal-Fédéral 34
1005 Lausanne, Switzerland
frontiersin.org

Contact us

+41 (0)21 510 17 00
frontiersin.org/about/contact